Preface

The present volume collects the lecture and seminar notes delivered at the Summer School *String Theory: Formal Developments and Applications*, which was held in Cargèse, France from June 21 to July 3, 2010.

The main focus of the school was the interrelations between the fields of superstring theory, cosmology and particle physics, which continue to be the subject of very active research. Much of the recent progress on topical problems in the field was covered, including duality between gravity and gauge theories, strings and cosmology, supersymmetric gauge theory, black hole physics, physics beyond the standard model, and model building for particle physics.

The school was an excellent opportunity for younger researchers to build closer relationships with the lecturers and with each other, be it during the vibrant Gong Show session, under the shade of the Wisdom Tree or gazing at the beautiful Corsican coastline. We hope that these proceedings will further serve in fixing the acquired knowledge, and will become a valuable reference for anyone working in this fascinating domain of physics.

It is a pleasure to extend our warm thanks to the European Science Foundation and CERN within the framework of the ESF Research Conferences Scheme, and the "formation permanente" of the CNRS whose generous funding have allowed this meeting to take place. We also would like to thank all the people who contributed to the organisation of this conference, especially the staff of the Institut d'Études Scientifiques de Cargèse and its director Giovanna Chimini. We also are grateful to Elena Gianolio for her help in organising the school.

Finally, we are very grateful to all the participants of the school for creating a wonderful and stimulating atmosphere, and to the contributors of this volume for their dedication in preparing their notes.

Paris, April 2011
L. Baulieu
J. de Boer
M. R. Douglas
E. Rabinovici
P. Vanhove
P. Windey

Harmony of Scattering Amplitudes: From QCD to Gravity

Zvi Bern*[a] and Harald Ita[a]

[a]Department of Physics and Astronomy
University of California at Los Angeles
Los Angeles, CA 90095-1547, USA

In these lectures we explain a remarkable simplicity in the scattering amplitudes of gravity and gauge theories. We start by summarizing the unitarity method and how it reveals surprising structures in loop amplitudes, and gives us a tool for carrying out state-of-the-art calculations. We review a recently discovered duality between color and kinematics in gauge theories, exposing gravity theories as double copies of gauge theories; these properties have recently been conjectured to hold to all loop orders. We also describe various recent state-of-the-art results obtained with the unitarity method in QCD, supersymmetric gauge theory and supergravity.

1. INTRODUCTION

Recent years have taught us that there is a remarkable simplicity in gauge and gravity scattering amplitudes. A key idea behind these advances has been that new amplitudes can be fully constructed using only on-shell information [1,2]. This avoids unphysical gauge-dependent quantities in intermediate steps, which can obscure important properties of the amplitudes. Studies have uncovered a number of novel unexpected structures in gauge and gravity amplitudes, revealing that they are much simpler than anyone had anticipated. Planar amplitude in maximally supersymmetric gauge theories have an even richer structure. A rather striking example is Witten's observation that amplitudes in massless gauge theories are supported on curves depending on their helicity and loop order [3]. Other examples are the iterative structure leading to an all-loop-order solution of the simplest of the planar amplitudes of $\mathcal{N} = 4$ super-Yang-Mills theory, valid at both weak and strong coupling [4,5], a new symmetry to explain this structure [6,7] and a Grassmannian structure [8]. In these lectures we will not describe these interesting results, which are well discussed in other recent reviews [9].

Instead, here we begin with a brief summary of basic general-purpose tool for carrying out loop-level calculations of scattering amplitudes: the unitarity method. To illustrate its utility we describe a few applications. This includes state-of-the-art predictions of LHC physics (for example, see refs. [10–12]). In particular, the first next-to-leading-order QCD calculation with five final state objects (including jets) [12] was done this way. Other examples which summarize include studies of supersymmetric gauge-theory amplitudes [4,13–15], and their ultraviolet properties in $D > 4$ dimensions [16–18]. It has been used in calculations of $\mathcal{N} = 8$ supergravity amplitudes, demonstrating that they are less divergent in the ultraviolet than had previously been appreciated [19,17,20]. (For other recent discussions of this issue see refs. [21–23].) More generally, the on-shell methods have allowed ever more complex calculations to be carried out. Such calculations in turn reveal an ever richer structure in the scattering amplitudes which can then be used to find improvements in the calculational methods.

An important aspect of the harmony between gauge and gravity theories is that many of the same basic techniques used to carry out calculations for one theory can then be applied to the other theory. But as we shall discuss the relationship goes much deeper, with the detailed multi-loop structure of perturbative gauge and gravity theories intimately intertwined.

*Presenter

Gravity has many similarities with gauge theories. Both are based on the idea of local symmetries and therefore share a number of formal properties. Nevertheless, their structural and dynamical behavior appears to be quite different. Non-abelian gauge theories have a rather different dynamical behavior than gravity. Quantum chromodynamics, for example, exhibits confinement of particles while gravity does not. Moreover, consistent quantum gauge theories have existed for more than a half century, but as yet no satisfactory point-like quantum field theory of gravity has been constructed. The structures of the Lagrangians of the two theories are also rather different: the non-abelian Yang-Mills Lagrangian contains only up to four-point interactions while the Einstein-Hilbert Lagrangian contains infinitely many interactions.

Nevertheless, recent developments [25,26] show that in a precise diagrammatic sense, perturbative gravity is a double copy of gauge theories,

$$\text{gravity} \sim (\text{gauge theory}) \times (\text{gauge theory}). \quad (1)$$

An early version of this property was understood at tree level more than 25 years ago using string theory, via the Kawai-Lewellen-Tye (KLT) relations [27]. These relations hold as well in field theory, as the low-energy limit of string theory. In this limit, the KLT relations for four-, and five-point amplitudes are

$$\begin{aligned} M_4^{\rm tree}(1,2,3,4) &= -is_{12} A_4^{\rm tree}(1,2,3,4) \\ &\quad \times \widetilde{A}_4^{\rm tree}(1,2,4,3)\,, \\ M_5^{\rm tree}(1,2,3,4,5) &= is_{12}s_{34} A_5^{\rm tree}(1,2,3,4,5) \\ &\quad \times \widetilde{A}_5^{\rm tree}(2,1,4,3,5) \\ &\quad + is_{13}s_{24} A_5^{\rm tree}(1,3,2,4,5) \\ &\quad \times \widetilde{A}_5^{\rm tree}(3,1,4,2,5)\,. \end{aligned} \quad (2)$$

Here the M_n's are amplitudes in a gravity theory stripped of couplings, the A_n's and $\widetilde{A}_n$'s are two distinct color-ordered gauge-theory amplitudes and the Mandelstam invariants are $s_{ij} \equiv (k_i + k_j)^2$, with k_i being the outgoing momentum of leg i. The color-ordered gauge-theory amplitudes [28] correspond to the coefficient of color traces with a given ordering of matrices. The gravity states are direct products of gauge-theory states for each external leg. (Explicit formulæ for n-point amplitudes may be found in refs. [29].)

The KLT relations show that gravity and gauge theory are intertwined, but as we shall explain, the heuristic relation (1) is now understood much more precisely. Today we have a simple and direct manifestation of the relation (1), conjectured to extend to all loop orders: the numerators of gravity diagrams are two copies of appropriately arranged gauge-theory diagram numerators. Besides offering a potent tool for carrying out loop calculations in gravity, this remarkable relationship between gravity and gauge theory strongly suggests that they belong together in a unified quantum theory, perhaps along the lines of string theory.

The lecture is organized as follows: In section 2 we give a brief overview of the unitarity method. Then in section 3, we summarize a few nontrivial applications to perturbative QCD, super-Yang-Mills and supergravity. In section 4 we then show a remarkable harmony between gauge and gravity theories, focusing on the double-copy property of gravity scattering amplitudes in terms of gauge-theory ones. Then in section 5 we explain how to arrange the Lagrangian so that they exhibit the double-copy property. Finally in section 6, we give our conclusions and outlook for the future.

2. UNITARITY METHOD

The unitarity method was originally developed in the context of one-loop supersymmetric amplitudes [1], but with further refinements [34–36,14,37,17,18,7], it offers a powerful formalism for any massless theory at any loop order, including non-planar contributions. This method has been reviewed numerous times [38–40], so here we give only a brief summary.

Unitarity has been a basic principle in quantum field theory since its inception. For a description of unitarity during the 1960's, see ref. [41]. However, a variety of difficulties prevented its widespread use as a means of constructing amplitudes, especially after the rise of gauge theories in the 1970's. These difficulties include nonconvergence of dispersion relations and the inapplicability to massless particles. It was also unclear how

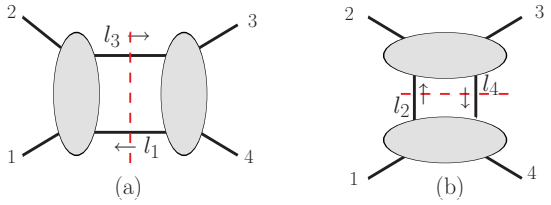

Figure 1. The two-particle cuts of a one-loop four-point amplitude. The exposed intermediate states are placed on shell.

one could fully reconstruct loop amplitudes beyond four points from their unitarity cuts. The unitarity method overcomes these basic difficulties, allowing for the complete construction of loop amplitudes at any loop order. It does so by avoiding dispersion relations, and instead using the existence of an underlying covariant Feynman diagram representations to fully reconstruct amplitudes. By construction the reconstructed Feynman-like integrands have the correct unitarity cuts in all channels.

Over the years there have been a number of important refinements to the unitarity method. Generalized unitarity [41] (where multiple internal lines are placed on shell, subdividing a loop amplitude into more than two pieces) was successfully applied in ref. [35] as a means for greatly simplifying loop calculations. An important more recent development is the use of complex momenta [32] by Britto, Cachazo and Feng [36], leading to the realization that at one-loop in four dimensions, quadruple cuts directly determine the coefficients of all box integrals by freezing the loop integration. Powerful new methods for dealing with triangle and bubble integrals at one-loop, as well as rational terms have also been developed [37,42]. (These have been described in other recent reviews [43].) At higher loops, efficient means of constructing the integrands of amplitudes, including non-planar contributions, have also been devised [14,17,18,44].

A key feature of the unitarity method is that it can construct amplitudes at any loop order directly from on-shell tree amplitudes. It does so from cuts of the form

$$C = \sum_{\text{states}} \prod_j A^{\text{tree}}_{(j)} \tag{3}$$

where the sum over states runs over all physical states that can propagate via the cut lines, which are all placed on shell. The product runs over all tree amplitudes composing the cut. For example, for a one-loop four-point amplitude, the two unitarity cuts shown in fig. 1 are sufficient to reconstruct the complete amplitude. This generalizes to more complicated cases; for example, in fig. 2 various generalized cuts are shown for a three-loop four-point amplitude. This ability to completely reconstruct loop amplitudes from tree amplitudes, allows tree-level simplifications and properties to be carried directly into loop calculations. (This was recently highlighted in a recent review using dual conformal symmetry and BCJ duality as examples [39].)

Although the unitarity method applies just as well to supersymmetric and non-supersymmetric theories, it is usually much simpler to deal with the supersymmetric case because they have a much simpler analytic structure. Indeed, the original application of the unitarity method was to construct one-loop supersymmetric amplitudes with arbitrary numbers of external legs [1]. The better power counting of supersymmetric theories allows all terms in one-loop scattering amplitudes to be readily constructed using cuts evaluated in four dimensions. Naively, this is not allowed because the amplitudes are divergent and need to be regularized. Nevertheless, a more careful study shows that for one-loop supersymmetric amplitudes it gives complete results [1].

For QCD or supersymmetric theories at higher loops, the situation is more complex. For one-loop QCD by using four-dimensional cuts, we can drop certain rational terms in the amplitudes [34]. These terms arise from $\mathcal{O}(\epsilon)$ terms in the integrand hitting ultraviolet poles in ϵ. Such terms can be recaptured by using loop-level on-shell recursion relations allowing the entire calculation to be performed using four-dimensional massless momenta [42]. More generally, by computing in $D = 4 - 2\epsilon$ dimensions, all rational terms are automatically captured and one can fully re-

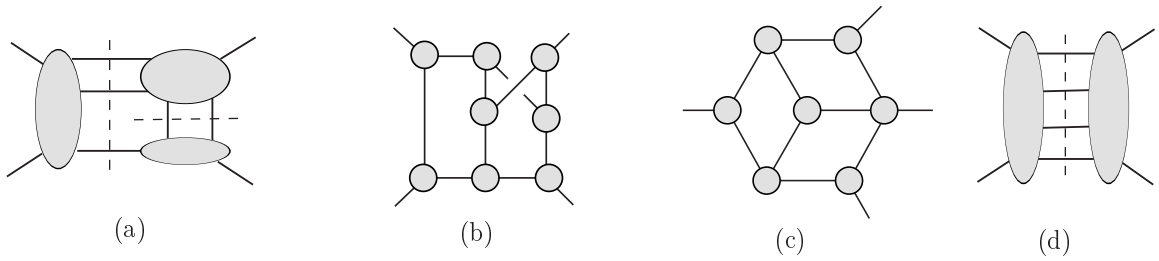

Figure 2. Examples of cuts used to determine the a three-loop four-point amplitude. The cut (a) decomposes the amplitude into a product of tree amplitudes. The cut (b) is a maximal cut and require the loop momenta to be complex momenta. Diagram (c) shows a near-maximal cut and diagram (d) is a four-particle cut. In this figure all exposed intermediate lines are placed on-shell.

construct amplitudes at any loop order [34]. A convenient way to implement this [7,45,39], is via six-dimensional helicity [46,47]. This offers many of the advantages of four-dimensional helicity, but meshes well with regularization of the divergences, in a manner consistent with unitarity.

3. APPLICATIONS OF THE UNITARITY METHOD

An important question is whether the new techniques and undersxtanding has led to any new calculations or applications. In this section we describe two rather different nontrivial applications of the unitarity method. The first of these is an example from collider physics. The second are calculations which illuminate multiloop ultraviolet properties in gauge and gravity theories.

3.1. Applications to QCD

Today the Large Hadron Collider (LHC) is operational and are people eagerly awaiting new results. In many scenarios of new physics, a sharp resonance appear, but in others the first signatures would be slight alterations of various distributions. For many new physics searches the signals are excesses in broader distributions of jets, along with missing energy. In particular, for supersymmetry searches, such multi-parton final states and missing energy are typical. The physics program at the Large Hadron Collider relies, to some extent, on having ever improved theoretical control over modeling of high-energy collisions. A detailed theoretical understanding not only increases the reach in new physics and particle searches, but also provides studies of the fundamental dynamics and properties of particles.

A first step towards a theoretical understanding of QCD is the evaluations of cross sections at leading order (LO) in the strong coupling $\alpha_S(\mu^2)$. Many tools [48] are available to generate predictions at leading order. Some of the methods applied incorporate higher-multiplicity leading-order matrix elements into parton-showering programs [49,50], using matching (or merging) procedures [51].

However, cross sections in QCD can have strong sensitivity to higher-order corrections, motivating the challenging quest for calculating them. Next-to-leading (NLO) order predictions significantly reduce renormalization- and factorization-scale dependence. This becomes more important with increasing jet multiplicity (see e.g. [52]). Fixed-order results at NLO can also be matched to parton showers [53] with the prospect of complete event generation at next to leading order in the strong coupling. Here we will discuss a few parton-level NLO QCD calculations where the new unitarity techniques have had an impact.

NLO cross sections are built from several ingredients: virtual corrections, computed from the in-

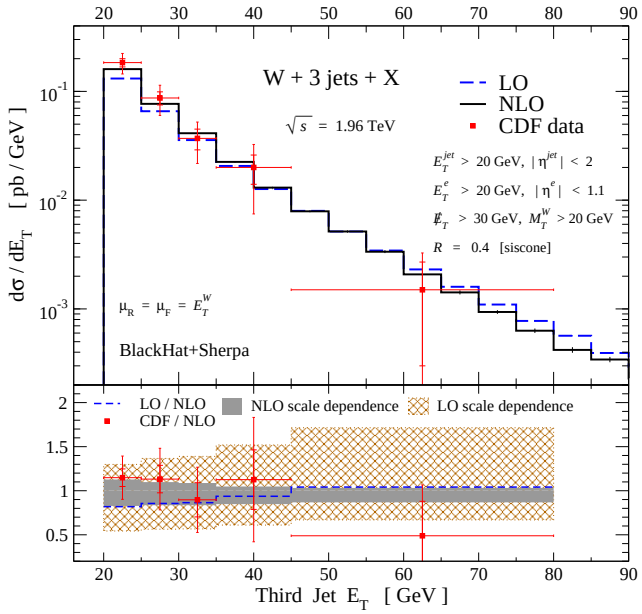

Figure 3. The cross section as a function of the transverse energy of the third jet, for inclusive W + 3-jet production, compared to the NLO prediction. In the upper panel the NLO distribution is the solid (black) histogram, and CDF data points are the (red) points, whose error bars denote the statistical and total uncertainties (excluding the luminosity error). The LO QCD predictions are shown as dashed (blue) lines. The lower panel shows the distribution normalized to the NLO prediction, using the CDF experimental bins (that is, averaging over bins in the upper panel). The scale-dependence bands are shaded (gray) for NLO and cross-hatched (brown) for LO.

terference of tree-level and one-loop amplitudes; real-emission corrections; and a mechanism for isolating and integrating the infrared singularities in the latter. In the past, a bottleneck to these studies was posed by one-loop amplitudes involving six or more partons [52]. On-shell methods, have successfully broken past this bottleneck, by avoiding gauge-noninvariant intermediate steps, and reducing the problem to much smaller elements analogous to tree-level amplitudes. Approaches based on Feynman diagrams have also led to new results with six external partons, exemplified by the NLO cross section for producing $t\bar{t}b\bar{b}$ at hadron colliders [54]. On-shell methods should be especially advantageous for processes involving many external gluons, which often dominate multi-jet final states. Various new results [10–12] already indicate the suitability of these methods for a general-purpose numerical approach to high-multiplicity one-loop amplitudes.

Here we will give an example to illustrate some of the advances of recent years. In particular we will focus on an important class of processes in the search for new physics are vector bosons in association with jets. Processes with Z and W boson in association with jets have a particularly rich phenomenology at the electroweak symmetry breaking scale, being important backgrounds to many searches of new physics, for Higgs physics, and will be important to precision top-quark measurements.

In LO or NLO QCD the jets corresponds to either single partons or pairs of partons (which then

hadronize). In order to point out the key features of NLO QCD predictions we will focus on processes of massive vector-boson production. The state-of-the-art in perturbative QCD for hadron colliders is now reaching parton level next-to-leading order computations with up to five final-state objects. In fact, the only such process to be computed so far is W + 4-jet production [12], using on-shell methods.

A rather nontrivial example of a new result where the unitarity methods has lead to useful phenomenology is W + 3-jet production at the Tevatron. Fig. 3 gives the cross section as a function of the transverse energy of the third most energetic jet, compared against experimental results from the CDF collaboration [55]. Besides showing very good agreement between theory and experiment, within the experimental uncertainties, it also illustrates the genetic feature that NLO results have a much smaller dependence on renormalization and factorization scales than LO results. The NLO scale dependence is shown as the gray band in the lower panel of the figure, while the LO dependence is shown in the cross-hatched region. In each case, the scale dependence is determined by varying the renormalization and factorization scales up and down by a factor of 2, following the traditional prescription. Further details may be found in refs. [10,12].

3.2. Applications to Maximally Supersymmetric Gauge and Gravity Amplitudes

Another arena where the new ideas and methods have had a significant impact is on studies of ultraviolet properties gauge and gravity theories. The theories of choice for studying this at high loop orders are maximally supersymmetric theories, both for their technical simplicity and because supersymmetry tends to mitigate ultraviolet divergences. $\mathcal{N} = 4$ super-Yang-Mills theory was proven to be ultraviolet finite in four dimensions long ago [56]. The ultraviolet behavior of $\mathcal{N} = 8$ supergravity [57] in four dimension is, however, still under study. Below we summarize concrete calculations in maximal super-Yang-Mills theory and supergravity that shed light on this fundamental question. Recent reviews discussing the ultraviolet properties of $\mathcal{N} = 8$ supergravity in more detail are given in refs. [21].

Conventional wisdom holds that it is impossible to construct point-like ultraviolet finite theories of gravity (see *e.g.* refs. [58]). Indeed, simple power-counting arguments point to the difficulty of doing so. In a classic paper, 't Hooft and Veltman showed that gravity coupled to matter generically diverges at one loop in four dimensions [30,31]. Due to the dimensionful nature of the coupling, the divergences cannot be absorbed by a redefinition of the original parameters of the Lagrangian, rendering the theory non-renormalizable. Pure Einstein gravity does not possess a viable counterterm at one loop, delaying the divergence to at least two loops [30,59]. The two-loop divergence of pure Einstein gravity was established by Goroff and Sagnotti and by van de Ven through direct computation [32,33].

Supersymmetry offers a mechanism for delaying the onset of divergences in gravity theories. No supergravity theory can diverge until at least three loops, because the potential three loop counterterm built out of three Riemann tensors cannot be made supersymmetric [58]. This potential counterterm is an R^4 term corresponding to four powers of the Riemann tensor with the indices appropriately contracted, to allow for a supersymmetric completion. Supersymmetry alone cannot delay the ultraviolet divergences in gravity theories because of the increasingly worse divergences at each loop order in gravity theories. This leads to the general question for supergravity theories of whether a given potential counterterms identified by power counting and symmetry arguments is actually present.

Power counting arguments assume that all symmetries and relevant properties are known and accounted for. For the case of $\mathcal{N} = 8$ supergravity we do know that there are unexpected ultraviolet cancellations in the theory to all loop orders [60,61]), though it is still not clear if these are powerful enough to render the theory finite to all loop orders. (These cancellations are related to a well studied property of one-loop $\mathcal{N} = 8$ amplitudes: in four dimensions triangle and bubble integrals drop out of the amplitudes, when expressed in a basis of scalar integral in four dimensions [62].) Some hints also follow from string-

theory dualities [63]. We also know that gravity loop amplitudes are much more closely tied to better behaved gauge-theory amplitudes than had been believed [26]. While these arguments do not offer a proof of finiteness, they do suggest that it would be wise to reexamine the ultraviolet properties of gravity theories. (For other approaches to trying to make quantum field theories of gravity sensible in the ultraviolet see refs. [64].)

Motivated by the hint of high-loop cancellations, explicit cancellations were then carried out in refs. [19,17,20] to directly investigate the ultraviolet properties of $\mathcal{N} = 8$ supergravity. The result of this was to definitively rule out the potential three loop R^4 counterterm in $D = 4$. Although no potential counterterm exists at four loops (because of an "accidental" cancellation similar to the one preventing a pure gravity counterterm at one loop), direct calculation establishes that the four-loop four-point amplitude of $\mathcal{N} = 8$ supergravity has the same power counting in D dimensions as $\mathcal{N} = 4$ super-Yang-Mills theory (which is known to be finite in $D = 4$).

The result of the four loop calculation is that the four-loop four-point amplitude is of the form,

$$A_4 \sim D^8 R^4 \times \text{loop integrals} \tag{4}$$

where the $D^8 R^4$ factor corresponds to 20 powers of momentum in the numerators of the integrals coming out as external momentum. This factors correspond to covariant derivatives contracted to four Riemann tensors in an appropriate way. If we assume that no further ultraviolet cancellations exist, and that no further powers of loop momenta can come out of the integrals as external momenta as the loop order increases, simple power counting shows that in four dimensions the first divergence would occur at seven loops.

Indeed, this is in line with recent comprehensive studies of the potential counterterms of $\mathcal{N} = 8$ supergravity [22], proving that no counterterm compatible with the $E_{7(7)}$ symmetry is available until seven loops. Based on these and other results [23,65,66] a consensus has formed that supersymmetry and the $E_{7(7)}$ symmetry alone cannot prevent divergences in $D = 4$ starting at seven loops and that the theory will likely diverge. There is, however, a more optimistic view [67]. (The previously claimed delay from supersymmetry of potential ultraviolet divergences in $\mathcal{N} = 8$ supergravity until nine loops [68] has been retracted [23].)

Is it possible there are further symmetries or structures that prevent the widely expected seven loop divergences? Powercounting arguments using symmetries to rule out potential counterterms can, of course, never prove the existence of divergences, only that protection against divergences holds to a certain level; if a symmetry or structure is missed then it may turn out the bound is too loose. More generally, the only way we can be certain that the coefficient of a potential counterterm respecting the known symmetries is non-zero is to carry out the explicit calculation to show that the numerical coefficient in front is nonzero.

Today, it is not yet practical to carry out a seven-loop computation. However, a simple way to lower the loop order in which a given potential counterterm can correspond to a divergence is to work in higher dimensions. By raising the dimension $\mathcal{N} = 4$ super-Yang-Mills is no longer ultraviolet finite, allowing this theory to be used as a playground for sharpening our understanding of counterterms in maximally supersymmetric theories [17,69,18]. Explicit calculations [16,14,19,17,20,18] show that at least for four-point amplitudes through four loops, both $\mathcal{N} = 8$ supergravity and $\mathcal{N} = 4$ super-Yang-Mills theory are ultraviolet finite for

$$D < \frac{6}{L} + 4 \qquad (L > 1)\,, \tag{5}$$

where D is the dimension of space-time and L the loop order. (The case of one loop, $L = 1$, is special, with the amplitudes finite for $D < 8$, not $D < 10$.) For $\mathcal{N} = 4$ super-Yang-Mills this bound was proposed in ref. [16] and has been confirmed in ref. [70] using superspace techniques. Explicit computations summarized below demonstrate this bound is saturated in $\mathcal{N} = 4$ super-Yang-Mills theory through at least four loops [71,16,60]. For $\mathcal{N} = 8$ supergravity we know that the bound holds through four loops and that it is saturated at three loops [16,19,17,20].

The first step for carrying out a loop calcula-

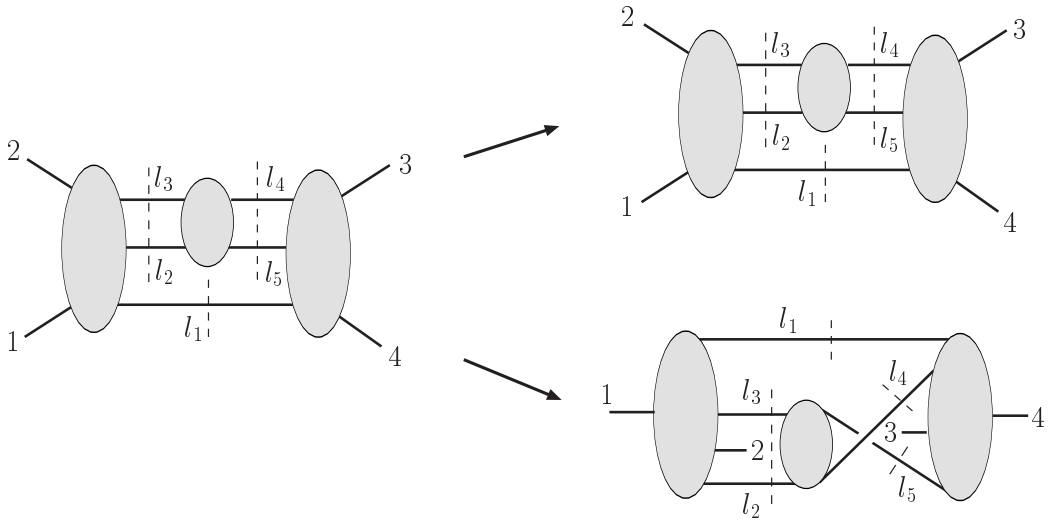

Figure 4. An example of showing how the KLT relations allow us to map gravity cuts into sums over pairs of gauge-theory cuts. Here we display a pair of gauge-theory cuts needed to evaluate the gravity cut on the left side. The remaining pairs are obtained by permuting the external legs $1 \leftrightarrow 2$ and $3 \leftrightarrow 4$.

tion of a gravity scattering amplitude is to first compute the corresponding amplitude in super-Yang-Mills theory. We may obtain $\mathcal{N} = 8$ supergravity amplitudes by considering the amplitudes of $\mathcal{N} = 4$ super-Yang-Mills theory. Following the strategy of refs. [16], by taking unitarity cuts of the gauge-theory amplitude which decompose it into a sum of products of tree amplitudes, we can use the KLT relations to assemble a spanning set[2] of unitarity cuts for the gravity amplitudes using cuts of gauge-theory amplitudes. As an example of how this works, consider the cut for an $\mathcal{N} = 8$ supergravity four-point amplitude shown on the left side of fig. 4,

$$C_{\mathcal{N}=8} = \sum_{\mathcal{N}=8 \text{ states}} M_5^{\text{tree}}(1,2,l_3,l_2,l_1) \times M_4^{\text{tree}}(-l_2,-l_3,l_4,l_5) \times M_5^{\text{tree}}(3,4,-l_1,-l_5,-l_4)\,. \quad (6)$$

The sum runs over all physical states that cross any cut line. The required KLT relations are relabelings of the basic relations in eq. (2). Inserting the relabeled KLT relations into the cut (6), we obtain [17],

$$\begin{aligned} & i\,(l_4+l_5)^2(l_1+k_1)^2(l_3+k_2)^2 \\ & \quad \times (l_4-k_3)^2(l_1-k_4)^2 \\ & \quad \times \Bigg(\sum_{\mathcal{N}=4 \text{ states}} A_5^{\text{tree}}(1,2,l_3,l_2,l_1) \\ & \qquad \times A_4^{\text{tree}}(-l_2,-l_3,l_4,l_5) \\ & \qquad \times A_5^{\text{tree}}(3,4,-l_1,-l_5,-l_4) \Bigg) \\ & \quad \times \Bigg(\sum_{\mathcal{N}=4 \text{ states}} A_5^{\text{tree}}(1,l_1,l_3,2,l_2) \\ & \quad \times A_4^{\text{tree}}(-l_2,-l_3,l_5,l_4) \\ & \quad \times A_5^{\text{tree}}(3,-l_4,-l_1,4,-l_5) \Bigg) \\ & \quad + \{1 \leftrightarrow 2\} + \{3 \leftrightarrow 4\} + \{1 \leftrightarrow 2,\ 3 \leftrightarrow 4\}\,. \end{aligned} \quad (7)$$

The relation is depicted in fig. 4, for one of the

[2] By a spanning set of unitarity cuts, we mean a set of cuts sufficient to construct the complete amplitudes; examples of spanning sets may be found in ref. [18,39].

four terms in the sum over external-leg permutations. One of the gauge-theory cuts is planar, while the second is nonplanar. Remarkably, this equation gives the $\mathcal{N} = 8$ supergravity cut directly in terms of products of two $\mathcal{N} = 4$ super-Yang-Mills cuts and allows us to build the supergravity amplitude using only gauge-theory results. Using this strategy, together with method of maximal cuts [14], the three- and four-loop four-point amplitudes were calculated in refs. [19,17,20].

To determine whether the finiteness bound (5) might hold for $L \geq 5$ will require new information and better tools. The duality between color and kinematics and the double copy structure of gravity [26,40], summarized below in section 4.2, is a promising direction. Using these results we should be able to immediately extract gravity amplitudes from gauge-theory ones, simply by rearranging corresponding gauge-theory amplitudes into a form where they satisfy a duality between color and kinematics [25]. This reorganization is well suited for addressing the issue of the ultraviolet properties of gravity because it converts complicated calculations in quantum gravity directly into much simpler gauge-theory calculations. This may make it possible to go to even higher loop orders than had been previously possible, and finally settle the question of the ultraviolet properties of $\mathcal{N} = 8$ supergravity.

4. EXAMPLES OF SIMPLICITY

In the previous section we noted that there is a strong similarity between gravity and gauge-theory scattering amplitudes. We now make this precise.

4.1. A Comparison of Gravity To Gauge Theory

It is useful to start by comparing gravity to gauge theory using off-shell Feynman diagrammatic methods. The Feynman rules are generated starting from the Einstein-Hilbert and Yang-Mills Lagrangians,

$$\mathcal{L}_{\rm YM} = -\frac{1}{4} F^a_{\mu\nu} F^{a\,\mu\nu}\,, \qquad \mathcal{L}_{\rm EH} = \frac{2}{\kappa^2}\sqrt{-g}R\,. \tag{8}$$

From the Feynman diagrammatic points of view these two Lagrangians have some rather different properties. As illustrated in figs. 5 and 6, with standard gauge choices gauge theories have three- and four-point interactions, while gravity has an infinite number of contact interactions. Perhaps more striking than the infinite number of interactions is the remarkably complexity of these interactions.

To be more concrete consider the three-gluon vertex in Feynman gauge,

$$V^{abc}_{3\mu,\nu,\sigma}(k_1,k_2,k_3) = g f^{abc}\Big[(k_1-k_2)_\sigma \eta_{\mu\nu} + \text{cyclic}\Big]\,, \tag{9}$$

where g is the coupling, f^{abc} the usual group theory structure constants, the $eta_{\mu\nu}$ the flat metric and the k_i the momenta of the vertex. This vertex is relatively simple. We may contrast this to the three-graviton interaction in standard de Donder gauge,

$$\begin{aligned} &G_{3\mu\alpha,\nu\beta,\sigma\gamma}(k_1,k_2,k_3) \\ &\quad = i\frac{\kappa}{2}\Big[-\frac{1}{2}k_1\cdot k_2 \eta_{\mu\alpha}\eta_{\nu\beta}\eta_{\sigma\gamma} \\ &\qquad - \frac{1}{2}P_6(k_{1\nu}k_{1\beta}\eta_{\mu\alpha}\eta_{\sigma\gamma}) \\ &\qquad + \frac{1}{2}k_1\cdot k_2 \eta_{\mu\nu}\eta_{\alpha\beta}\eta_{\sigma\gamma} + \cdots\Big]\,, \end{aligned} \tag{10}$$

where we have displayed the first three terms out of about 100. Here the coupling κ is related to Newton's constant by $\kappa^2 = 32\pi^2 G_N$. In total the vertex has on the order of 100 terms. The precise form of the vertex depends on the gauge, but in general the three vertex is rather a rather involved and unenlightening object. The complete expression can be found in refs. [72,30].

Comparing the vertex in eq. (9) to the one in eq. (10), it is clear that gravity is much more complicated than gauge theory. Moreover, there does not appear to be any simplicity or obvious relation between the gauge and gravity vertices. The former leads to complicated diagrams but the latter is a hopeless mess. One can do somewhat better with special gauge choices and appropriate field redefinitions [33,73], considerably simplifying the Feynman rules. Still, multiloop Feynman

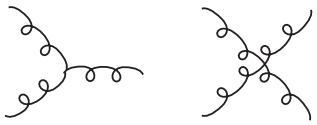

Figure 5. The Feynman rules of gauge theories have three- and four-point vertices.

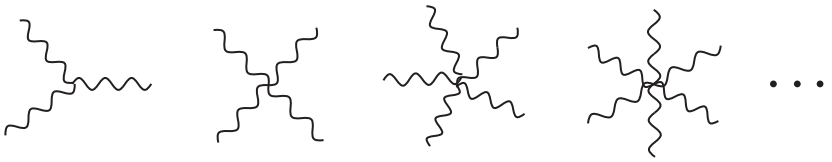

Figure 6. Gravity theories have an infinite number of higher-point contact interactions when using Feynman diagrams.

diagram calculations in (super) gravity extremely difficult, and in many cases out of reach even using the most powerful computers.

Now let us reconsider the same process but using on-shell methods. If we take the three-graviton vertex in eq. (10) and dot the three legs with physical polarizations tensors satisfying the physical state conditions, $k_i^2 = 0$, $\varepsilon_i^{\mu\nu} k_{i\mu} = \varepsilon_i^{\mu\nu} k_{i\nu} = \varepsilon^\mu{}_\mu = 0$, we obtain a greatly simplified vertex,

$$\begin{aligned} G_3(k_1,k_2,k_3) \;=\; & -i\kappa \varepsilon_1^{\mu\alpha} \varepsilon_2^{\nu\beta} \varepsilon_3^{\sigma\gamma} \\ & \times \Big[(k_1)_\sigma \eta_{\mu\nu} + \text{cyclic} \Big] \\ & \times \Big[(k_1)_\gamma \eta_{\alpha\beta} + \text{cyclic} \Big] . \end{aligned} \tag{11}$$

Remarkably, this is just a double copy of the kinematic part of the on-shell Yang-Mills vertex,

$$\begin{aligned} V_3^{abc}(k_1,k_2,k_3) \;=\; & \varepsilon_1^\mu \varepsilon_2^\nu \varepsilon_3^\sigma 2g f^{abc} \Big[(k_1)_\sigma \eta_{\mu\nu} \\ & + \text{cyclic} \Big] , \end{aligned} \tag{12}$$

where the polarization vector satisfies $\varepsilon_i^\mu k_{i\mu} = 0$. To make the comparison, we identify the graviton polarization tensor as a product of gluon polarization vectors, $\varepsilon_i^{\mu\nu} = \varepsilon_i^\mu \times \varepsilon_i^\nu$. Similar considerations allow us to express all three-point vertices in supergravity as products of super-Yang-Mills vertices. Using BCFW recursion [2,74], these three vertices are sufficient to construct any tree-level gauge or gravity amplitude. The unitarity method then allows us to construct any loop amplitude (though expressions valid in $D > 4$ are needed to ensure that no terms are dropped because of regularization issues). In this way the entire gravitational S-matrix is encoded in the three-point vertex (11).

Clearly, there is a rather striking relationship between gravity and gauge theory, but to make it visible we need to keep external states on shell. As we shall see below the double-copy structure in eq. (11) is not accidental, but appears likely to extend to *all* loop orders. As such, it reflects a profound and important property of quantum gravity.

4.2. A Duality Between Color and Kinematics

As a rather striking example of a simple structure in scattering amplitudes, we consider a rather surprising duality between color and kinematics [25,26]. As we discuss below this duality is intimately connected to the double copy relationship between gravity and gauge theory mentioned earlier. In generally, e can write any n-point tree

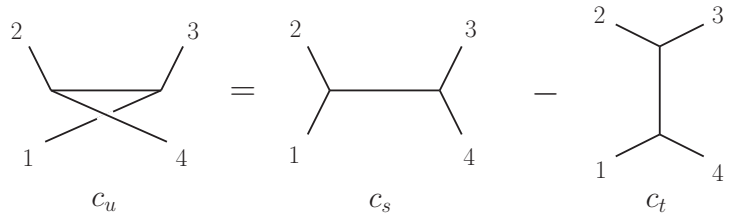

Figure 7. The Jacobi relation for color factors at four points for the three channels labeled by s, t and u. Diagram numerators satisfy the same relations.

level amplitude with all particles in the adjoint representation as,

$$\mathcal{A}_n^{\rm tree}(1,2,3,\ldots,n) = \sum_i \frac{n_i\, c_i}{\prod_{\alpha_i} p_{\alpha_i}^2}\,, \tag{13}$$

where the sum runs over the set of n-point L-loop diagrams with only cubic vertices and we suppressed factors of the coupling constant. These include distinct permutations of external legs. The form (13) can be obtained straightforwardly, for example, from Feynman diagrams, by representing all contact terms as inverse propagators in the kinematic numerators that cancel propagators. We suppress factors of the coupling constant for convenience. The product in the denominator runs over all propagators of each cubic diagram. The c_i are the color factors obtained by dressing every three vertex with an $\tilde{f}^{abc} = i\sqrt{2}f^{abc}$ structure constant, and the n_i are kinematic numerator factors depending on momenta, polarizations and spinors. For supersymmetric amplitudes expressed in superspace, there will also be Grassmann parameters in the numerators.

In general the n_i may be deformed under any shifts, $n_i \to n_i + \Delta_i$, where the Δ_i are arbitrary functions independent of color satisfying the constraint [25,26,75]

$$\sum_i \frac{\Delta_i c_i}{\prod_{\alpha_i} p_{\alpha_i}^2} = 0\,. \tag{14}$$

We may think of these transformation as generalized gauge transformation. Some of the freedom corresponds to gauge transformations in the traditional sense but most does not.

The duality conjectured in ref. [25] requires there to exist such a transformation from any valid representation to one where the numerators satisfy equations in one-to-one correspondence with the Jacobi identity of the color factors,

$$c_i = c_j - c_k \;\Rightarrow\; n_i = n_j - n_k\,. \tag{15}$$

This duality is conjectured to hold to all multiplicity at tree level in a large variety of theories, including supersymmetric extensions of Yang-Mills theory.

At tree level a consequence of this duality is non-trivial relations between the color-ordered partial tree amplitudes of gauge theory [25,76, 77]. The duality has also been studied in string theory [78,79] and from a Lagrangian vantage point [75]. An alternative trace-based representation of the duality (15) was recently given in ref. [80], emphasizing the underlying group theoretic structure of the duality.

Perhaps more remarkable than the duality itself is a related conjecture that once the gauge-theory amplitudes are arranged into a form satisfying the duality (15), corresponding gravity amplitudes can be obtained simply by taking a double copy of gauge-theory numerator factors [25,26],

$$-i\mathcal{M}_n^{\rm tree}(1,2,\ldots,n) = \sum_i \frac{n_i\, \tilde{n}_i}{\prod_{\alpha_i} p_{\alpha_i}^2}\,, \tag{16}$$

where the $\tilde{n}_i$ represent numerator factors of a second gauge-theory amplitude, the sum runs over the same set of diagrams as in eq. (13). We suppressed the gravitational coupling constant in this expression. This is expected to hold in a large class of gravity theories, including theories that

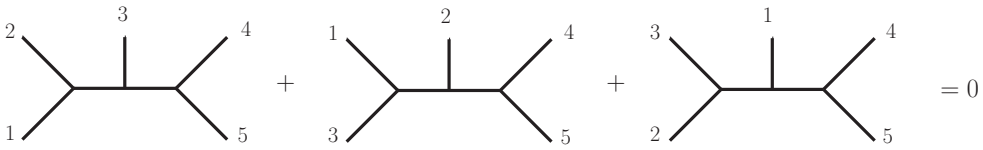

Figure 8. A Jacobi relation at five points. The color factors associated with each diagram automatically satisfy this relation. The duality states that numerators can be rearranged so that they satisfy exactly the same relation.

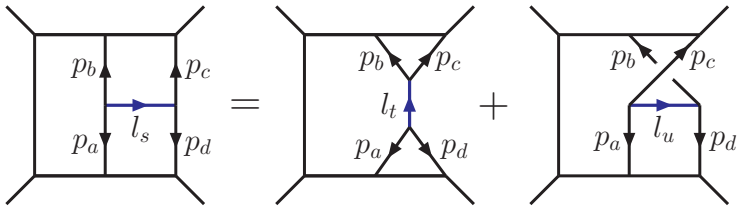

Figure 9. An example of a duality relation satisfied by numerators for diagrams of the three-loop four-point amplitude. Both color factors and numerator factors satisfy these relations.

are the low-energy limits of string theories. At tree level, this double-copy property encodes the KLT relations between gravity and gauge theory [27]. Through use of BCFW recursion [2], the double-copy formula (16) has been proven for pure gravity and for $\mathcal{N} = 8$ supergravity tree amplitudes, under the assumption that the duality (15) holds in the corresponding gauge theories [75].

The above conjectures have been extended to loop level [26], so that at any loop order L,

$$\mathcal{A}_m^{\rm loop} = \sum_j \int \prod_{l=1}^{L} \frac{d^D p_l}{(2\pi)^D} \frac{1}{S_j} \frac{n_j c_j}{\prod_{\alpha_j} p_{\alpha_j}^2} \,,$$

$$\mathcal{M}_m^{\rm loop} = \sum_j \int \prod_{l=1}^{L} \frac{d^D p_l}{(2\pi)^D} \frac{1}{S_j} \frac{n_j \tilde{n}_j}{\prod_{\alpha_j} p_{\alpha_j}^2} \,, \qquad (17)$$

where $\mathcal{A}_n^{\rm loop}$ and $\mathcal{M}_n^{\rm loop}$ are L-loop gauge and gravity amplitudes. As before we removed factors of the coupling constants. The sums now run over all distinct m-point L-loop diagrams with cubic vertices. These include distinct permutations of external legs, and the S_j are the symmetry factors of each diagram. As at tree level, at least one family of numerators (n_j or $\tilde{n}_j$) for gravity must be constrained to satisfy the duality (15). (For pure gravity, extra projectors are needed to obtain loop-level amplitudes from the direct product of two pure Yang-Mills theories.)

This loop-level extension has been tested in the rather nontrivial case of three-loop four-point amplitude of $\mathcal{N} = 4$ super-Yang-Mills theory and $\mathcal{N} = 8$ supergravity [26]. This amplitude has already been studied in some detail in refs. [19,17]. To impose the duality (15) on the amplitude, the duality relation for every propagator in each diagram must be enforced. On any diagram, we can describe any internal line, carrying some momentum l_s, in terms of formal graph vertices $V(p_a, p_b, l_s)$, and $V(-l_s, p_c, p_d)$ where the p_i are the momenta of the other legs attached to l_s, as illustrated on the left side of fig. 9. The duality (15) requires that,

$$\begin{aligned} &n(\{\, V(p_a, p_b, l_s),\, V(-l_s, p_c, p_d),\, \cdots\}) \\ &\quad = n(\{\, V(p_d, p_a, l_t),\, V(-l_t, p_b, p_c),\, \cdots\}) \\ &\qquad + n(\{\, V(p_a, p_c, l_u),\, V(-l_u, p_b, p_d),\, \cdots\}) \,, \end{aligned} \qquad (18)$$

where the ns are the numerators associated with the diagrams specified by the vertices. The omitted vertices are identical in all three diagrams,

and $l_s \equiv (p_c + p_d)$, $l_t \equiv (p_b + p_c)$ and $l_u \equiv (p_b + p_d)$ in the numerator expressions. There is one such equation for every propagator in every diagram. Solving the system of distinct equations enforces the duality conditions (15).

It turns out that imposing the duality completely fixes the form of the amplitude, if all diagrams have the proper power counting of $\mathcal{N} = 4$ super-Yang-Mills, and that all numerators are polynomials in the kinematic invariants once we extract an overall factor the tree amplitude. Moreover, only the 12 diagrams shown in fig. 10 contribute, with the numerator factors given in table 1. These numerator factors give the correct amplitude, as checked against the unitarity cuts in ref. [26].

The fact that this arrangement can be done for the three loop four-point amplitude of $\mathcal{N} = 4$ super-Yang-Mills theory is rather striking, but it is much more surprising that we can immediately obtain $\mathcal{N} = 8$ supergravity results simply by squaring the numerators of each diagram. Indeed, this was confirmed in ref. [26] by comparing against a spanning set of unitarity cuts of the known result for $\mathcal{N} = 8$ supergravity [19,17]. The ability to organize the amplitude into such a form has also been confirmed for the simplest of the two-loop four-point amplitude of QCD [26].

5. A DOUBLE COPY LAGRANGIAN

We now turn to the question of finding a Lagrangian which generates amplitudes with numerators that manifestly satisfy the BCJ duality (15). If a local Lagrangian of this type could be found, it would enable us to construct a corresponding gravity Lagrangian whose squaring relations with Yang-Mills theory are manifest.

The Yang-Mills Lagrangian of the type we seek can differ from the conventional Yang-Mills Lagrangian only by terms that do not affect on the amplitudes. Such a Lagrangian with manifest BCJ duality exists, and differs from the conventional Lagrangian by terms whose sum is identically zero by the color Jacobi identity [75]. Although the added terms sum to zero, they cause the necessary rearrangements in the diagrams so that the duality holds manifestly.

We write the Yang-Mills Lagrangian as

$$\mathcal{L}_{YM} = \mathcal{L} + \mathcal{L}'_5 + \mathcal{L}'_6 + \dots \tag{19}$$

where $\mathcal{L}$ is the conventional Yang-Mills Lagrangian and $\mathcal{L}'_n$, $n > 4$ are the additional terms required so that the duality is satisfied. At four points, the duality holds trivially in any gauge [81,25], so $\mathcal{L}$ by itself will generate diagrams whose numerators satisfy eq. (15). For simplicity we choose Feynman gauge for $\mathcal{L}$. The $\mathcal{L}'_n$ are required to leave scattering amplitudes unchanged, and they must rearrange the numerators of diagrams in a way so that the BCJ duality is satisfied.

By imposing the constraint that the generated five-point diagrams satisfy the BCJ duality (15), we find the Lagrangian,

$$\begin{aligned}\mathcal{L} = &\frac{1}{2} A^a_\mu \Box A^{a\mu} - g f^{a_1 a_2 a_3} \partial_\mu A^{a_1}_\nu A^{a_2 \mu} A^{a_3 \nu} \\ &- \frac{1}{4} g^2 f^{a_1 a_2 b} f^{b a_3 a_4} A^{a_1}_\mu A^{a_2}_\nu A^{a_3 \mu} A^{a_4 \nu}\,, \end{aligned} \tag{20}$$

and

$$\begin{aligned}\mathcal{L}'_5 = &-\frac{1}{2} g^3 f^{a_1 a_2 b} f^{b a_3 c} f^{c a_4 a_5} \\ &\times \Big(\partial_{[\mu} A^{a_1}_{\nu]} A^{a_2}_\rho A^{a_3 \mu} + \partial_{[\mu} A^{a_2}_{\nu]} A^{a_3}_\rho A^{a_1 \mu} \\ &+ \partial_{[\mu} A^{a_3}_{\nu]} A^{a_1}_\rho A^{a_2 \mu} \Big) \frac{1}{\Box} (A^{a_4 \nu} A^{a_5 \rho})\,. \end{aligned} \tag{21}$$

The additional terms in $\mathcal{L}'_5$ are necessarily nonlocal, at least if we want a covariant Lagrangian without auxiliary fields. The numerators n_i are derived from this action by first computing the contribution from the three-point vertices, which gives a set of three-vertex diagrams with unique numerators. Then the contributions from the four- and five-point interaction terms are assigned to the various diagrams with only three-point vertices according to their color factors. Since these terms will contain fewer propagators than those obtained by using only three-point vertices, if we put back all the propagators their contributions to the numerators contain inverse propagators, which cancel some propagators.

As previously mentioned, $\mathcal{L}'_5$ is identically zero by the color Jacobi identity. This can be easily seen after relabeling color indices to obtain,

$$\mathcal{L}'_5 = -\frac{1}{2} g^3 (f^{a_1 a_2 b} f^{b a_3 c} + f^{a_2 a_3 b} f^{b a_1 c}$$

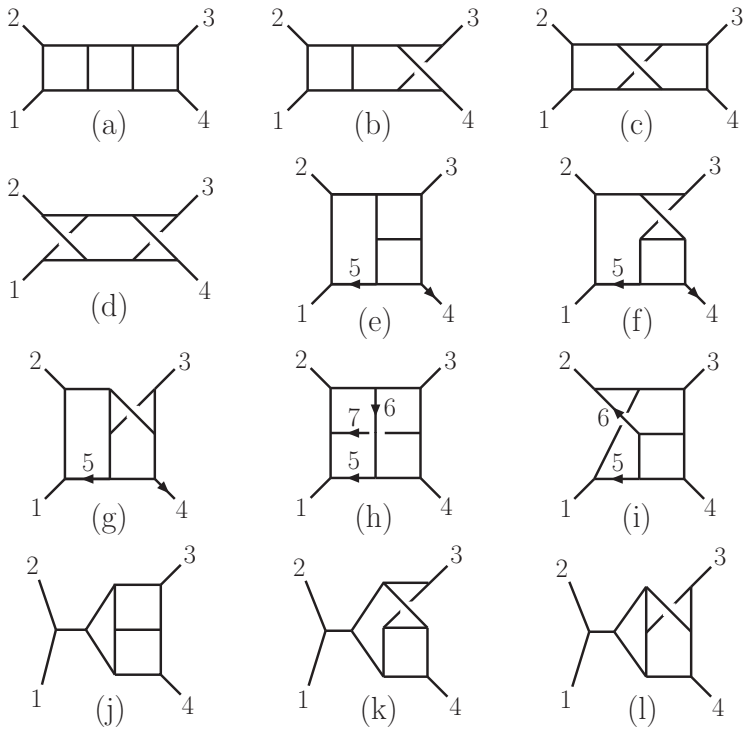

Figure 10. Loop diagrams contributing to the three-loop four-point amplitudes of both $\mathcal{N}=4$ super-Yang-Mills theory and $\mathcal{N}=8$ supergravity. Integrals are specified by combining their propagators with numerator factors given in table 1. The symmetry factor for diagram (d) is 2, and the rest are unity.

$$+ f^{a_3 a_1 b} f^{b a_2 c}) f^{c a_4 a_5} \times \partial_{[\mu} A^{a_1}_{\nu]} A^{a_2}_{\rho} A^{a_3 \mu} \frac{1}{\Box} (A^{a_4 \nu} A^{a_5 \rho}) \,. \quad (22)$$

These terms cause a non-trivial rearrangement amongst the diagrams, although all the added terms must add up to zero by the color Jacobi identity. Nevertheless, they alter the numerators of the individual diagrams such that the duality (15) is satisfied.

It turns out that the set of terms with the desired properties is not unique. Indeed, terms that satisfy the BCJ duality by themselves can also be added. This ambiguity is due to the residual generalized gauge invariance that remains after enforcing the duality identities. The additional terms that can be added to Yang-Mills at five points which preserve the duality (15) are

$$\mathcal{D}_5 = \frac{-\beta}{2} g^3 f^{a_1 a_2 b} f^{b a_3 c} f^{c a_4 a_5} \times \Big(\partial_{(\mu} A^{a_1}_{\nu)} A^{a_2}_{\rho} A^{a_3 \mu} + \partial_{(\mu} A^{a_2}_{\nu)} A^{a_3}_{\rho} A^{a_1 \mu} + \partial_{(\mu} A^{a_3}_{\nu)} A^{a_1}_{\rho} A^{a_2 \mu} \Big) \frac{1}{\Box} (A^{a_4 \nu} A^{a_5 \rho}) \,, \quad (23)$$

where β is an arbitrary parameter. $\mathcal{D}_5$ also vanishes identically by the color Jacobi identity. Since $\mathcal{D}_5$ does not serve to correct lower-point contributions to make the BCJ duality relations hold through five points, we do not need to include it. It does however show that there are multiple Lagrangians with the desired properties.

Table 1
The numerator factors of the integrals $I^{(x)}$ in fig. 10. The first column labels the integral, the second column the relative numerator factor for $\mathcal{N}=4$ super-Yang-Mills theory. The square of this is the relative numerator factor for $\mathcal{N}=8$ supergravity. An overall factor of $stA_4^{\rm tree}$ has been removed, s,t,u are Mandelstam invariants corresponding to $(k_1+k_2)^2,(k_2+k_3)^2,(k_1+k_3)^2$ and $\tau_{ij}=2k_i\cdot l_j$, where k_i and l_j are momenta as labeled in fig. 10.

Integral $I^{(x)}$	$\mathcal{N}=4$ Super-Yang-Mills ($\sqrt{\mathcal{N}=8}$ supergravity) numerator
(a)–(d)	s^2
(e)–(g)	$\big(s\,(-\tau_{35}+\tau_{45}+t)-t\,(\tau_{25}+\tau_{45})+u\,(\tau_{25}+\tau_{35})-s^2\,\big)/3$
(h)	$\big(s\,(2\tau_{15}-\tau_{16}+2\tau_{26}-\tau_{27}+2\tau_{35}+\tau_{36}+\tau_{37}-u)$ $+t\,(\tau_{16}+\tau_{26}-\tau_{37}+2\tau_{36}-2\tau_{15}-2\tau_{27}-2\tau_{35}-3\tau_{17})+s^2\,\big)/3$
(i)	$\big(s\,(-\tau_{25}-\tau_{26}-\tau_{35}+\tau_{36}+\tau_{45}+2t)$ $+t\,(\tau_{26}+\tau_{35}+2\tau_{36}+2\tau_{45}+3\tau_{46})+u\,\tau_{25}+s^2\,\big)/3$
(j)-(l)	$s(t-u)/3$

5.1. A Gravity Lagrangian from Gauge Theory

Now that we have a Lagrangian that gives the desired numerators n_i for gauge theory, we can use it to construct the tree-level gravity Lagrangian by demanding that it gives diagrams whose numerators are a double copy of the gauge-theory numerators, as in eq. (16). However, we need to first bring the Yang-Mills Lagrangian into a cubic form to achieve this. We can do so by introducing an auxiliary field $B^a_{\mu\nu\rho}$ into the Lagrangian. To give the auxiliary fields the same dimensions as the dynamical fields we need to make them propagate. (The propagation is trivial because we recover the original Lagrangian by integrating them out.) At four points this leads to the Lagrangian [75],

$$\begin{aligned}\mathcal{L}_{YM} \;=\; & \frac{1}{2}A^{a\mu}\Box A^a_\mu - B^{a\mu\nu\rho}\Box B^a_{\mu\nu\rho} \\ & - g f^{abc}(\partial_\mu A^a_\nu + \partial^\rho B^a_{\rho\mu\nu})A^{b\mu}A^{c\nu}\,, \end{aligned} \tag{24}$$

where the equation of motion for the auxiliary field $B^a_{\mu\nu\rho}$ becomes

$$\Box B^a_{\mu\nu\rho} = \frac{g}{2} f^{abc}\partial_\mu(A^b_\nu A^c_\rho)\,. \tag{25}$$

Five points becomes more complicated and a new set of auxiliary fields must be introduced to re-express the nonlocal terms into a local and cubic form. The result is [75]

$$\begin{aligned}\mathcal{L}'_5 \;\to\; & Y^{a\mu\nu}\Box X^a_{\mu\nu} + D^{a\mu\nu\rho}_{(3)}\Box C^a_{(3)\,\mu\nu\rho} \\ & + D^{a\mu\nu\rho\sigma}_{(4)}\Box C^a_{(4)\,\mu\nu\rho\sigma} \\ & + g f^{abc}\Big(Y^{a\mu\nu}A^b_\mu A^c_\nu + \partial_\mu D^{a\mu\nu\rho}_{(3)}A^b_\nu A^c_\rho \\ & \qquad - \tfrac{1}{2}\partial_\mu D^{a\mu\nu\rho\sigma}_{(4)}\partial_{[\nu}A^b_{\rho]}A^c_\sigma\Big) \\ & + g f^{abc}X^{a\mu\nu}\Big(\tfrac{1}{2}\partial_\rho C^{b\rho\sigma}_{(3)\ \mu}\partial_{[\sigma}A^c_{\nu]} \\ & \qquad + \partial_\rho C^{b\rho\sigma}_{(4)\ \ \nu[\mu}A^c_{\sigma]}\Big)\,. \end{aligned} \tag{26}$$

From the above Lagrangian we can directly construct a gravity Lagrangian valid through five-points which is manifestly a double copy of the gauge-theory one. At four points we do so by taking two copies of the Lagrangian (24) and identifying the fields as,

$$\begin{aligned} A^\mu\tilde{A}^\nu &\to h^{\mu\nu}\,, \\ A^\mu\tilde{B}^{\nu\rho\sigma} &\to g^{\mu\nu\rho\sigma}\,, \\ B^{\mu\rho\sigma}\tilde{A}^\nu 1 &\to \tilde{g}^{\mu\rho\sigma\nu}\,, \\ B^{\mu\rho\sigma}\tilde{B}^{\nu\tau\lambda} &\to f^{\mu\rho\sigma\nu\tau\lambda}\,, \end{aligned} \tag{27}$$

Here $h_{\mu\nu}$ is the graviton field A^μ and $\tilde{A}^\nu$ gauge fields and all the remaining ones are auxiliary fields. With a similar procedure we can obtain five-point terms in the gravity Lagrangian. Be-

yond this the Lagrangians become more complicated. Such a procedure has not yet been carried out for supergravity, though it should work as well.

We note that above Lagrangians were constructed order by order in perturbation theory. Of course, it would be much better to have a principle for finding all order forms of such Lagrangians.

6. CONCLUSIONS AND OUTLOOK

In these lectures we summarized the unitarity method and some of its applications. We discussed applications to collider physics, and also to the question of ultraviolet properties of maximally supersymmetric gauge and gravity theories in various dimensions. We also illustrated a remarkable harmony between gravity and gauge theories, stemming from a gauge-theory duality between color and kinematics [25,26]. Although the duality remains a conjecture, we can exploit it to guide loop computations, simply by enforcing the duality and verifying the consistency with the unitarity cuts.

There are a number of interesting future directions. The unitarity method offers a general purpose tool for carrying out amplitude calculations in both supersymmetric and non-supersymmetric theories, including their non-planar contributions. In QCD there are many more NLO calculations that need to be carried, especially those involving vector bosons, Higgs bosons, top quarks, in associations with many jets. In particular, a high-priority calculation is for Z bosons in association with four jets. Beyond this is would also be important to merge these types of calculations with parton showering [53].

In $\mathcal{N} = 8$ supergravity, a consensus has formed that the standard symmetries of $\mathcal{N} = 8$ supergravity cannot protect the theory against divergences, starting at seven loops [22] (though there is at least one opinion to the contrary [67]). It would be very interesting to directly check the ultraviolet properties as a function of dimension at five and higher loops. If this can be done it should greatly clarify the ultraviolet behavior of $\mathcal{N} = 8$ supergravity in four dimensions, checking the hypothesis that it may be a an ultraviolet finite theory. The color-kinematic duality and double copy property of gravity, offer a promising avenue for attacking this issue [26,40].

There are also a number of interesting open problems related to the color-kinematics duality. In particular, it would be helpful to carry out further checks of the duality for multiloop processes. More generally an all-orders proof of the duality would be important, especially if it leads to new insight into the group theoretic origins of the duality. We would also like to have Lagrangians whose diagrams satisfy the duality to all orders, and which give gravity Lagrangians as double copies, along the lines described in ref. [75], but constructed in a more systematic fashion. The color-kinematic duality and gravity double-copy structure likely have important non-perturbative implications. In particular, these properties suggest that all classical solutions in gravity theories may be expressible as double copies of classical solutions in gauge theories. The fact that the same kinematic building block appear in gravity and in gauge theories, apparently to all loop orders, is rather striking and may be taken as theoretical evidence of an underlying unification of gauge and gravity theories, perhaps along the lines of string theory.

In summary, the unitarity method is by now a mature formalism for carrying out state-of-the-art loop calculations for phenomenological and theoretical purposes. It has also played an important role in uncovering remarkable structures in scattering amplitudes, including a double copy relationship between gravity and gauge theory. We look forward to many new exciting developments in the coming years.

Acknowledgments

We thank L. J. Dixon, J. J. M. Carrasco, F. Febres Cordero, D. Forde, H. Johansson D. A. Kosower, and R. Roiban for many enlightening discussions and collaboration on work described in this lecture. ZB's work was supported by the US Department of Energy under contract DE-FG03-91ER40662. HI's work is supported by a grant from the US LHC Theory Initiative

through NSF contract PHY–0705682.

REFERENCES

1. Z. Bern, L. J. Dixon, D. C. Dunbar and D. A. Kosower, Nucl. Phys. B **425**, 217 (1994) [hep-ph/9403226]; Nucl. Phys. B **435**, 59 (1995) [hep-ph/9409265].
2. R. Britto, F. Cachazo, B. Feng and E. Witten, Phys. Rev. Lett. **94**, 181602 (2005) [hep-th/0501052].
3. E. Witten, Commun. Math. Phys. **252**, 189 (2004) [arXiv:hep-th/0312171]; R. Roiban, M. Spradlin and A. Volovich, Phys. Rev. D **70**, 026009 (2004) [hep-th/0403190].
4. C. Anastasiou, Z. Bern, L. J. Dixon and D. A. Kosower, Phys. Rev. Lett. **91**, 251602 (2003) [hep-th/0309040]; Z. Bern, L. J. Dixon and V. A. Smirnov, Phys. Rev. D **72**, 085001 (2005) [hep-th/0505205].
5. L. F. Alday and J. Maldacena, JHEP **0706**, 064 (2007) [0705.0303 [hep-th]].
6. J. M. Drummond, J. Henn, V. A. Smirnov and E. Sokatchev, JHEP **0701**, 064 (2007) [hep-th/0607160]; Z. Bern, M. Czakon, L. J. Dixon, D. A. Kosower and V. A. Smirnov, Phys. Rev. D **75**, 085010 (2007) [hep-th/0610248]; J. M. Drummond, G. P. Korchemsky and E. Sokatchev, Nucl. Phys. B **795**, 385 (2008) [0707.0243 [hep-th]]; A. Brandhuber, P. Heslop and G. Travaglini, Nucl. Phys. B **794**, 231 (2008) [0707.1153 [hep-th]]; J. M. Drummond, J. Henn, G. P. Korchemsky and E. Sokatchev, 0808.0491 [hep-th]; J. M. Drummond, J. Henn, G. P. Korchemsky and E. Sokatchev, Nucl. Phys. B **828**, 317 (2010) [0807.1095 [hep-th]]; A. Brandhuber, P. Heslop and G. Travaglini, JHEP **0910**, 063 (2009) [0906.3552 [hep-th]]; A. Brandhuber, P. Heslop and G. Travaglini, Phys. Rev. D **78**, 125005 (2008) [0807.4097 [hep-th]]; S. Caron-Huot and D. O'Connell, 1010.5487 [hep-th]; T. Dennen and Y. t. Huang, 1010.5874 [hep-th].
7. Z. Bern, J. J. Carrasco, T. Dennen, Y. t. Huang and H. Ita, 1010.0494 [hep-th], to appear in Phys. Rev. D.
8. N. Arkani-Hamed, F. Cachazo, C. Cheung and J. Kaplan, JHEP **1003**, 020 (2010) [0907.5418 [hep-th]]; M. Bullimore, L. Mason and D. Skinner, JHEP **1003**, 070 (2010) [0912.0539 [hep-th]].
9. F. Cachazo and P. Svrcek, PoS **RTN2005**, 004 (2005) [hep-th/0504194]. L. F. Alday and R. Roiban, Phys. Rept. **468**, 153 (2008) [0807.1889 [hep-th]]. L. F. Alday and R. Roiban, Acta Phys. Polon. B **39**, 2979 (2008). J. M. Henn, 1103.1016 [hep-th]. A. Brandhuber, B. Spence and G. Travaglini, arXiv:1103.3477 [hep-th].
10. C. F. Berger *et al.*, Phys. Rev. Lett. **102**, 222001 (2009) [0902.2760 [hep-ph]]; Phys. Rev. D **80**, 074036 (2009) [0907.1984 [hep-ph]].
11. R. K. Ellis, K. Melnikov and G. Zanderighi, Phys. Rev. D **80**, 094002 (2009) [0906.1445 [hep-ph]]; C. F. Berger *et al.* [BlackHat Collaboration], Phys. Rev. D **80**, 074036 (2009) [0907.1984 [hep-ph]]; G. Bevilacqua, M. Czakon, C. G. Papadopoulos, R. Pittau and M. Worek, JHEP **0909**, 109 (2009). [0907.4723 [hep-ph]]; K. Melnikov and G. Zanderighi, Phys. Rev. D **81**, 074025 (2010) [0910.3671 [hep-ph]]; G. Bevilacqua, M. Czakon, C. G. Papadopoulos *et al.*, Phys. Rev. Lett. **104**, 162002 (2010). [1002.4009 [hep-ph]]. C. F. Berger *et al.*, Phys. Rev. D **82**, 074002 (2010) [1004.1659 [hep-ph]]; T. Melia, K. Melnikov, R. Rontsch and G. Zanderighi, JHEP **1012**, 053 (2010) [1007.5313 [hep-ph]]; Z. Bern *et al.*, 1103.5445 [hep-ph].
12. C. F. Berger *et al.*, arXiv:1009.2338 [hep-ph].
13. Z.Bern, M. Czakon, L. J. Dixon, D. A. Kosower and V. A. Smirnov, Phys. Rev. D **75**, 085010 (2007) [hep-th/0610248].
14. Z. Bern, J. J. M. Carrasco, H. Johansson and D. A. Kosower, Phys. Rev. D **76**, 125020 (2007) [0705.1864 [hep-th]].
15. F. Cachazo, M. Spradlin and A. Volovich, Phys. Rev. D **74**, 045020 (2006) [hep-th/0602228]; Z. Bern, M. Czakon, D. A. Kosower, R. Roiban and V. A. Smirnov, Phys. Rev. Lett. **97**, 181601 (2006) [hep-th/0604074]; Z. Bern, L. J. Dixon,

D. A. Kosower, R. Roiban, M. Spradlin, C. Vergu and A. Volovich, Phys. Rev. D **78**, 045007 (2008) [0803.1465 [hep-th]]; F. Cachazo, M. Spradlin and A. Volovich, Phys. Rev. D **78**, 105022 (2008) [0805.4832 [hep-th]]; M. Spradlin, A. Volovich and C. Wen, Phys. Rev. D **78**, 085025 (2008) [0808.1054 [hep-th]]; C. Vergu, 0908.2394 [hep-th]; D. A. Kosower, R. Roiban and C. Vergu, Phys. Rev. D **83**, 065018 (2011) [1009.1376 [hep-th]].

16. Z. Bern, L. J. Dixon, D. C. Dunbar, M. Perelstein and J. S. Rozowsky, Nucl. Phys. B **530**, 401 (1998) [hep-th/9802162].
17. Z. Bern, J. J. M. Carrasco, L. J. Dixon, H. Johansson and R. Roiban, Phys. Rev. D **78**, 105019 (2008) [0808.4112 [hep-th]].
18. Z. Bern, J. J. M. Carrasco, L. J. Dixon, H. Johansson and R. Roiban, Phys. Rev. D **82**, 125040 (2010) [1008.3327 [hep-th]].
19. Z. Bern, J. J. Carrasco, L. J. Dixon, H. Johansson, D. A. Kosower and R. Roiban, Phys. Rev. Lett. **98**, 161303 (2007) [hep-th/0702112].
20. Z. Bern, J. J. Carrasco, L. J. Dixon, H. Johansson and R. Roiban, Phys. Rev. Lett. **103**, 081301 (2009) [0905.2326 [hep-th]].
21. Z. Bern, J. J. M. Carrasco and H. Johansson, 0902.3765 [hep-th]; H. Nicolai, Physics, **2**, 70, (2009); R. P. Woodard, Rept. Prog. Phys. **72**, 126002 (2009) 0907.4238 [gr-qc]; L. J. Dixon, 1005.2703 [hep-th]; Z. Bern, J. J. Carrasco, L. Dixon, H. Johansson and R. Roiban, 1103.1848 [hep-th]. H. Elvang, D. Z. Freedman and M. Kiermaier, 1012.3401 [hep-th].
22. G. Bossard, P. S. Howe and K. S. Stelle, 1009.0743 [hep-th]; H. Elvang, D. Z. Freedman and M. Kiermaier, 1003.5018 [hep-th]; N. Beisert, H. Elvang, D. Z. Freedman, M. Kiermaier, A. Morales and S. Stieberger, Phys. Lett. B **694**, 265 (2010) [1009.1643 [hep-th]].
23. M. B. Green, J. G. Russo and P. Vanhove, JHEP **1006**, 075 (2010) [1002.3805 [hep-th]]; P. Vanhove, 1004.1392 [hep-th]; J. Bjornsson and M. B. Green, JHEP **1008**, 132 (2010) [1004.2692 [hep-th]].
24. J. M. Maldacena, Adv. Theor. Math. Phys. **2**, 231 (1998) [Int. J. Theor. Phys. **38**, 1113 (1999)] [hep-th/9711200]; S. S. Gubser, I. R. Klebanov and A. M. Polyakov, Phys. Lett. B **428**, 105 (1998) [hep-th/9802109].
25. Z. Bern, J. J. M. Carrasco and H. Johansson, Phys. Rev. D **78**, 085011 (2008) [arXiv:0805.3993 [hep-ph]].
26. Z. Bern, J. J. M. Carrasco and H. Johansson, Phys. Rev. Lett. **105**, 061602 (2010) [arXiv:1004.0476 [hep-th]].
27. H. Kawai, D. C. Lewellen and S. H. H. Tye, Nucl. Phys. B **269**, 1 (1986); Z. Bern, Living Rev. Rel. **5**, 5 (2002) [gr-qc/0206071].
28. M. L. Mangano and S. J. Parke, Phys. Rept. **200**, 301 (1991); L. J. Dixon, in *QCD & Beyond: Proceedings of TASI '95*, ed. D. E. Soper (World Scientific, 1996) [hep-ph/9601359].
29. Z. Bern, L. J. Dixon, M. Perelstein and J. S. Rozowsky, Nucl. Phys. B **546**, 423 (1999) [hep-th/9811140].
30. G. 't Hooft and M. J. Veltman, *Annales Poincare Phys. Theor.* A **20**, 69 (1974);
31. S. Deser and P. van Nieuwenhuizen, *Phys. Rev.* D **10**, 411 (1974); S. Deser, H. S. Tsao and P. van Nieuwenhuizen, *Phys. Rev.* D **10**, 3337 (1974).
32. M. H. Goroff and A. Sagnotti, Phys. Lett. B **160**, 81 (1985); Nucl. Phys. B **266**, 709 (1986).
33. A. E. M. van de Ven, *Nucl. Phys.* B **378**, 309 (1992).
34. Z. Bern and A. G. Morgan, Nucl. Phys. B **467**, 479 (1996) [hep-ph/9511336]; Z. Bern, L. J. Dixon, D. C. Dunbar and D. A. Kosower, Phys. Lett. B **394**, 105 (1997) [hep-th/9611127]; Z. Bern, L. J. Dixon and D. A. Kosower, JHEP **0001**, 027 (2000) [hep-ph/0001001].
35. Z. Bern, L. J. Dixon and D. A. Kosower, Nucl. Phys. B **513**, 3 (1998) [hep-ph/9708239]; Z. Bern, L. J. Dixon and D. A. Kosower, JHEP **0408**, 012 (2004) [hep-ph/0404293]; Z. Bern, V. Del Duca, L. J. Dixon and D. A. Kosower, Phys. Rev. D **71**, 045006 (2005) [hep-th/0410224].
36. R. Britto, F. Cachazo and B. Feng, Nucl.

Phys. B **725**, 275 (2005) [hep-th/0412103].
37. C. Anastasiou, R. Britto, B. Feng, Z. Kunszt and P. Mastrolia, Phys. Lett. B **645**, 213 (2007) [hep-ph/0609191]; R. Britto and B. Feng, JHEP **0802**, 095 (2008) [0711.4284 [hep-ph]]; R. Britto and B. Feng, Phys. Rev. D **75**, 105006 (2007) [hep-ph/0612089]; G. Ossola, C. G. Papadopoulos and R. Pittau, Nucl. Phys. B **763**, 147 (2007) [hep-ph/0609007]; R. Britto, B. Feng and P. Mastrolia, Phys. Rev. D **78**, 025031 (2008) [0803.1989 [hep-ph]]; D. Forde, Phys. Rev. D **75**, 125019 (2007) [0704.1835 [hep-ph]]; S. D. Badger, JHEP **0901**, 049 (2009) [0806.4600 [hep-ph]].
38. Z. Bern, L. J. Dixon and D. A. Kosower, Ann. Rev. Nucl. Part. Sci. **46**, 109 (1996) [hep-ph/9602280]; Z. Bern, L. J. Dixon and D. A. Kosower, Annals Phys. **322**, 1587 (2007) [0704.2798 [hep-ph]].
39. Z. Bern and Y. t. Huang, 1103.1869 [hep-th].
40. J. J. M. Carrasco and H. Johansson, 1103.3298 [hep-th].
41. R. J. Eden, P. V. Landshoff, D. I. Olive, J. C. Polkinghorne, *The Analytic S Matrix* (Cambridge University Press, 1966).
42. Z. Bern, L. J. Dixon and D. A. Kosower, Phys. Rev. D **71**, 105013 (2005) [hep-th/0501240]; Phys. Rev. D **72**, 125003 (2005) [hep-ph/0505055]; Phys. Rev. D **73**, 065013 (2006) [hep-ph/0507005]; D. Forde and D. A. Kosower, Phys. Rev. D **73**, 065007 (2006) [hep-th/0507292]; Phys. Rev. D **73**, 061701 (2006) [hep-ph/0509358]; C. F. Berger, Z. Bern, L. J. Dixon, D. Forde and D. A. Kosower, Phys. Rev. D **75**, 016006 (2007) [hep-ph/0607014].
43. Z. Bern, L. J. Dixon and D. A. Kosower, Annals Phys. **322**, 1587 (2007) [0704.2798 [hep-ph]]; C. F. Berger and D. Forde, 0912.3534 [hep-ph]; R. Britto, 1012.4493 [hep-th]; H. Ita, to appear in "Scattering Amplitudes in Gauge Theories", special issue of Journal of Physics A, R. Roiban(ed), M. Spradlin(ed), A. Volovich(ed).
44. N. Arkani-Hamed, J. L. Bourjaily, F. Cachazo, S. Caron-Huot and J. Trnka, 1008.2958 [hep-th]; N. Arkani-Hamed, J. L. Bourjaily, F. Cachazo and J. Trnka, 1012.6032 [hep-th].
45. A. Brandhuber, D. Korres, D. Koschade and G. Travaglini, 1010.1515 [hep-th].
46. C. Cheung and D. O'Connell, JHEP **0907**, 075 (2009) [0902.0981 [hep-th]].
47. T. Dennen, Y. t. Huang and W. Siegel, JHEP **1004**, 127 (2010) [0910.2688 [hep-th]].
48. T. Stelzer and W. F. Long, Comput. Phys. Commun. **81**, 357 (1994) [hep-ph/9401258]; J. Alwall *et al.*, JHEP **0709**, 028 (2007) [arXiv:0706.2334 [hep-ph]]; A. Pukhov *et al.*, hep-ph/9908288; M. L. Mangano, M. Moretti, F. Piccinini, R. Pittau and A. D. Polosa, JHEP **0307**, 001 (2003) [hep-ph/0206293]; A. Kanaki and C. G. Papadopoulos, Comput. Phys. Commun. **132**, 306 (2000) [hep-ph/0002082]; A. Cafarella, C. G. Papadopoulos and M. Worek, 0710.2427 [hep-ph].
49. H. U. Bengtsson and T. Sjöstrand, "The Lund Comput. Phys. Commun. **46**, 43 (1987); T. Sjöstrand, P. Eden, C. Friberg, L. Lönnblad, G. Miu, S. Mrenna and E. Norrbin, Comput. Phys. Commun. **135**, 238 (2001) [hep-ph/0010017]; G. Marchesini and B. R. Webber, Cavendish-HEP-87/9; G. Marchesini,*et al.*, Comput. Phys. Commun. **67**, 465 (1992); G. Corcella *et al.*, hep-ph/0210213.
50. T. Gleisberg *et al.*, JHEP **0902**, 007 (2009) [0811.4622 [hep-ph]].
51. S. Catani, F. Krauss, R. Kuhn and B. R. Webber, JHEP **0111**, 063 (2001) [hep-ph/0109231]; M. L. Mangano, M. Moretti, F. Piccinini and M. Treccani, JHEP **0701**, 013 (2007) [hep-ph/0611129]; S. Mrenna and P. Richardson, JHEP **0405**, 040 (2004) [hep-ph/0312274].
52. Z. Bern *et al.*, 0803.0494 [hep-ph].
53. S. Frixione and B.R. Webber, JHEP **0206**, 029 (2002) [hep-ph/0204244]; S. Frixione, P. Nason and B.R. Webber, JHEP **0308**, 007 (2003) [hep-ph/0305252]; S. Frixione, P. Nason and C. Oleari, JHEP **0711**, 070 (2007) [0709.2092 [hep-ph]]; S. Alioli, P. Nason, C. Oleari and E. Re, JHEP **0807**, 060 (2008) [0805.4802 [hep-ph]].
54. A. Bredenstein, A. Denner, S. Dittmaier and S. Pozzorini, JHEP **0808**, 108 (2008)

[0807.1248 [hep-ph]]; "NLO QCD corrections to pp -¿ t anti-t b anti-b + X at the LHC," Phys. Rev. Lett. **103**, 012002 (2009) [0905.0110 [hep-ph]].
55. T. Aaltonen *et al.* [CDF Collaboration], Phys. Rev. D **77**, 011108 (2008) [0711.4044 [hep-ex]].
56. S. Mandelstam, Nucl. Phys. B **213**, 149 (1983); P. S. Howe, K. S. Stelle and P. K. Townsend, Nucl. Phys. B **214**, 519 (1983); L. Brink, O. Lindgren and B. E. W. Nilsson, Phys. Lett. B **123**, 323 (1983).
57. E. Cremmer, B. Julia and J. Scherk, Phys. Lett. B **76**, 409 (1978); E. Cremmer and B. Julia, Phys. Lett. B **80**, 48 (1978); Nucl. Phys. B **159**, 141 (1979).
58. M. T. Grisaru, Phys. Lett. B **66**, 75 (1977); E. T. Tomboulis, Phys. Lett. B **67**, 417 (1977); S. Deser, J. H. Kay and K. S. Stelle, Phys. Rev. Lett. **38**, 527 (1977); S. Ferrara and B. Zumino, Nucl. Phys. B **134**, 301 (1978); P. S. Howe and K. S. Stelle, Phys. Lett. B **137**, 175 (1984). P. S. Howe and K. S. Stelle, Int. J. Mod. Phys. A **4**, 1871 (1989); N. Marcus and A. Sagnotti, Nucl. Phys. B **256**, 77 (1985).
59. R. E. Kallosh, Nucl. Phys. B **78**, 293 (1974); P. van Nieuwenhuizen and C. C. Wu, J. Math. Phys. **18**, 182 (1977).
60. Z. Bern, L. J. Dixon and R. Roiban, Phys. Lett. B **644**, 265 (2007) [hep-th/0611086].
61. Z. Bern, J. J. Carrasco, D. Forde, H. Ita and H. Johansson, Phys. Rev. D **77**, 025010 (2008) [arXiv:0707.1035 [hep-th]].
62. Z. Bern, L. J. Dixon, M. Perelstein and J. S. Rozowsky, Nucl. Phys. B **546**, 423 (1999) [hep-th/9811140]; Z. Bern, N. E. J. Bjerrum-Bohr and D. C. Dunbar, JHEP **0505**, 056 (2005) [hep-th/0501137]; N. E. J. Bjerrum-Bohr, D. C. Dunbar and H. Ita, Phys. Lett. B **621**, 183 (2005) [hep-th/0503102]; N. E. J. Bjerrum-Bohr, D. C. Dunbar, H. Ita, W. B. Perkins and K. Risager, JHEP **0612**, 072 (2006) [hep-th/0610043]; N. E. J. Bjerrum-Bohr and P. Vanhove, JHEP **0804**, 065 (2008) [0802.0868 [hep-th]]; JHEP **0810**, 006 (2008) [0805.3682 [hep-th]]; N. Arkani-Hamed, F. Cachazo and J. Kaplan, JHEP **1009**, 016 (2010) [0808.1446 [hep-th]].
63. G. Chalmers, hep-th/0008162; M. B. Green, J. G. Russo and P. Vanhove, JHEP **0702**, 099 (2007) [hep-th/0610299].
64. S. Weinberg, in *Understanding the Fundamental Constituents of Matter,* ed. A. Zichichi (Plenum Press, New York, 1977); S. Weinberg, in General Relativity, S. W. Hawking and W. Israel (Cambridge University Press, 1979) p. 700; M. Niedermaier and M. Reuter, Living Rev. Rel. **9**, 5 (2006); P. Horava, Phys. Rev. D **79**, 084008 (2009) [0901.3775 [hep-th]].
65. R. Kallosh and P. Ramond, 1006.4684 [hep-th];
66. H. Elvang and M. Kiermaier, JHEP **1010**, 108 (2010) [1007.4813 [hep-th]].
67. R. Kallosh, JHEP **1012**, 009 (2010) [1009.1135 [hep-th]]; R. Kallosh, 1103.4115 [hep-th].
68. M. B. Green, J. G. Russo and P. Vanhove, Phys. Rev. Lett. **98**, 131602 (2007) [hep-th/0611273].
69. G. Bossard, P. S. Howe and K. S. Stelle, Phys. Lett. B **682**, 137 (2009) [0908.3883 [hep-th]]; N. Berkovits, M. B. Green, J. G. Russo and P. Vanhove, JHEP **0911**, 063 (2009) [0908.1923 [hep-th]]; G. Bossard, P. S. Howe, U. Lindstrom, K. S. Stelle and L. Wulff, 1012.3142 [hep-th].
70. P. S. Howe and K. S. Stelle, Phys. Lett. B **554**, 190 (2003) [hep-th/0211279].
71. Z. Bern, J. S. Rozowsky and B. Yan, Phys. Lett. B **401**, 273 (1997) [hep-ph/9702424].

[Deser77]

72. B.S. DeWitt, Phys. Rev. 162:1239 (1967); M. Veltman, in *Les Houches 1975, Proceedings, Methods In Field Theory*, eds. R. Balian and J. Zinn-Justin (North-Holland, Amsterdam, 1976); S. Sannan, Phys. Rev. D34:1749 (1986).
73. Z. Bern and A. K. Grant, Phys. Lett. B **457**, 23 (1999) [hep-th/9904026];
74. J. Bedford, A. Brandhuber, B. J. Spence and G. Travaglini, Nucl. Phys. B **721**, 98 (2005) [hep-th/0502146]; F. Cachazo and P. Svrček, hep-th/0502160; A. Brandhuber, S. McNa-

mara, B. Spence and G. Travaglini, JHEP **0703**, 029 (2007) [hep-th/0701187]; P. Benincasa, C. Boucher-Veronneau and F. Cachazo, JHEP **0711**, 057 (2007) [hep-th/0702032]; P. Benincasa and F. Cachazo, 0705.4305 [hep-th]; N. Arkani-Hamed and J. Kaplan, JHEP **0804**, 076 (2008) [0801.2385 [hep-th]]; A. Hall, Phys. Rev. D **77**, 124004 (2008) [0803.0215 [hep-th]]; C. Cheung, 0808.0504 [hep-th].

75. Z. Bern, T. Dennen, Y. t. Huang and M. Kiermaier, Phys. Rev. D **82**, 065003 (2010) [arXiv:1004.0693 [hep-th]].
76. N. E. J. Bjerrum-Bohr, P. H. Damgaard and P. Vanhove, Phys. Rev. Lett. **103**, 161602 (2009) [0907.1425 [hep-th]]; S. Stieberger, 0907.2211 [hep-th].
77. B. Feng, R. Huang and Y. Jia, 1004.3417 [hep-th].
78. N. E. J. Bjerrum-Bohr, P. H. Damgaard, T. Sondergaard and P. Vanhove, 1003.2403 [hep-th]; C. R. Mafra, 1007.3639 [hep-th].
79. S. H. Henry Tye and Y. Zhang, JHEP **1006**, 071 (2010) [1003.1732 [hep-th]].
80. Z. Bern and T. Dennen, 1103.0312 [hep-th].
81. D. Zhu, Phys. Rev. D **22**, 2266 (1980); C. J. Goebel, F. Halzen and J. P. Leveille, Phys. Rev. D **23**, 2682 (1981).

Holography for strongly coupled media

D. T. Son[a*]

[a]Institute for Nuclear Theory, University of Washington. Seattle, WA 98195-1550, USA

We discuss some recent attempts to apply AdS/CFT correspondence to systems with finite temperature and chemical potential, emphasizing the hydrodynamic aspects. We also discuss the system of nonrelativistic fermions at unitarity, the Schrödinger symmetry and possible directions for constructing a holographic dual of this system. This is the write-up of lectures delivered at Cargese and TASI schools of 2010.

1. Motivation

Many problems of modern theoretical physics are related to strong coupling. One example is the problem of the hot and dense matter in QCD. The creation of hot QCD matter is the goal of relativistic heavy ion experiments, the most recent of which are RHIC and LHC. Although there are ample evidence that some form of matter with strong collective behavior is formed in ultrarelativistic heavy ion collisions, the theoretical problem of finding whether thermal equilibrium is achieved and at which temperature has still not been solved. (The problem can be made very sharp by imagining a world with very small electromagnetic fine structure constant so that nuclei can be very large. Can we make a quark gluon plasma by colliding very large nuclei at very high energy? What is the temperature of the system at thermal equilibration? We still do not have definite answer to these questions.) Assuming that system reaches equilibrium, one can ask questions about the properties of the thermal equilibrium state. While thermodynamics of the QGP at finite temperature and zero chemical potential can be studied by lattice methods, the latter becomes very inefficient in dealing with real time quantities, for example the viscosities. Current lattice methods are also incapable of treating QCD matter at finite chemical potential, a problem that hinders our understanding of the core of neutron stars.

Another example of a strong coupling problem is that of unitarity fermions (unitary Fermi gas). This system is that of nonrelativistic fermion interacting through a short-range potential fine tuned to resonance at threshold (see Section 6 for more discussion). The simplest version of the problem is the Bertsch problem: given a gas of spin-1/2 fermions, interacting with short-range interaction fine tuned to unitarity (defined below in the lectures), what are the properties of the ground state? This problem has became extremely important when it became possible to realize unitarity fermions in atomic trap experiments.

Various other strong coupling problems in condensed matter physics are discussed in Subir Sachdev's lectures in this school. In these lectures, we will describe some points of contact between gauge/gravity duality and the physics of the quark gluon plasma and the unitary Fermi gas.

2. Thermal field theory

There are two main formalisms used in thermal field theory. The first formalism is the Matsubara, Euclidean formalism. It is used in lattice QCD, very convenient for thermodynamic and static quantities (like correlation length), but cannot directly address dynamic, real-time quantities. The second formalism is the real-time, close time path formalism. (For more details, see Ref. [1,2]).

In the Matsubara formalism, the theory is formulated on a Euclidean spacetime, where the time axis is compactified to an interval $0 < \tau <$

*This work is supported, in part, by the DOE grant No. DE-FG02-00ER41132.

$\beta = 1/T$. In the close-time-path formalism, one makes a detour into real time, as in Fig. 1.

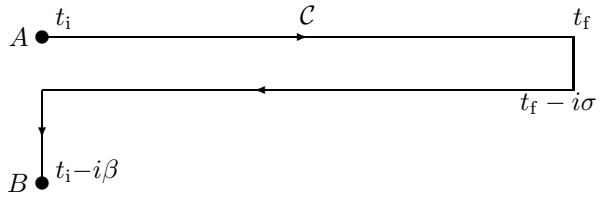

Figure 1. The close time path contour

One can turn on source on the upper and lower parts of the contour, J_1 and J_2. The partition function of field theory now is a functional of both J_1 and J_2, $Z = Z[J_1, J_2]$, and and derivatives of $\log Z$ with respect to J gives a 2×2 matrix propagators G_{ab}, where $a, b = 1, 2$. Changing σ rescales the off-diagonal elements by a trivial factor,

$$G_{12}(\omega, q) = e^{\sigma\omega} G_{12}^{\sigma=0}(\omega, q), \quad (1)$$

$$G_{21}(\omega, q) = e^{-\sigma\omega} G_{21}^{\sigma=0}(\omega, q). \quad (2)$$

For $\sigma = 0$, the propagators G_{ab} include path-ordered, reversed path-ordered, and Wightmann Green's functions. They are related by

$$G_{11} + G_{22} = G_{12} + G_{21}, \quad (3)$$

but the choice $\sigma = \beta/2$ leads to symmetric 2×2 propagator matrix: $G_{12} = G_{21}$. This choice of the σ is most natural for holography, as we will see.

From the point of view of the CTP formalism, putting our system in an external source J corresponds to having, in the $\sigma = 0$ choice of the contour, $J_1 = J_2 = J$. The expectation value of the operator ϕ at a point x on an upper contour is given by an integral over the whole contour, which can be written as

$$\langle \phi_1(x) \rangle = -\int dy\, (G_{11}(x-y)J(y) - G_{12}(x-y)J(y)), \quad \sigma = 0. \quad (4)$$

Define the retarded propagator $G_R = G_{11} - G_{12}$ ($\sigma = 0$). The retarded propagator governs the response of a system to a small external perturbation:

$$\langle \phi(x) \rangle = -\int dy\, G_R(x-y)J(y). \quad (5)$$

On the other hand, for the symmetric choice $\sigma = \beta/2$, $G_R = G_{11} - e^{-\beta\omega/2} G_{12}$.

Normally, the computations of thermal Green's function rely on summing Feynman diagrams. The set of Feynman diagrams that one has to sum in order to compute, say, the viscosity, can be quite complicated [3]. In the low-momentum limit, however, the forms of many correlation functions are simple and are dictated by an effective theory—hydrodynamics.

3. Hydrodynamics

Consider an interacting quantum field theory at finite temperature. One can visualize such a system as a collection of particles (or quasiparticles), moving with random velocities and colliding with each other from time to time. Such a picture is too simplistic for a strongly interacting system (with no discernible quasiparticles) but it does tell us that there is an important length scale in the problem—the mean free path, which is the length which a particle travels before colliding with other particles.

Hydrodynamics can be thought of as an effective theory describing the dynamics of a finite-temperature system at distance scales much larger than the mean free path. By definition the degrees of freedom entering hydrodynamics have to have relaxation time much larger than the mean free time. Such modes include

- Density of conserved quantities. Consider, for example, the QCD plasma, and imagine a perturbation of the system where there is a net excess of charge in a volume with size $L \gg \ell$. If one waits a long time this lump of excess charge will disappear, with the charge now distributing uniformly over the whole volume. However, since charge is conserved, causality implies that the time

scale for this process cannot be smaller than L/c, where c is the speed of light (in fact in many cases the time scale is much bigger than this naive estimate. For example, if the relaxation is due to diffusion, the length scale is $\sim L^2/\ell$).

- Nambu-Goldstone modes. If there is a broken continuous symmetry, Goldstone's theorem dictates that there must be a massless particle at zero temperature. If the symmetry remains broken at a finite temperature, the Nambu-Goldstone mode continuously deforms into a hydrodynamic mode. For example, in superfluid ^{4}He the phase of the condensate φ is a hydrodynamic degree of freedom (the superfluid velocity $\mathbf{v}_s$ is proportional to the gradient of φ: $\mathbf{v}_s = \nabla\varphi/m$).

- Unbroken U(1) gauge fields. At zero temperature, a U(1) gauge field which does not suffers from the Anderson-Higgs mechanism corresponds to a massless photon. At finite temperature, the electric field is screened (Debye screening) but the magnetic field is unscreened and should be included in the hydrodynamic description. An example of such a theory is magnetohydrodynamics, describing for example the interior of the Sun.

In these lectures we will consider only the simplest class of hydrodynamic theories, where the only slow degrees of freedom are the densities of conserved charges. In this case, hydrodynamics is given by the conservation equation,

$$\nabla_\mu T^{\mu\nu} = 0, \tag{6}$$

supplemented by the continuity equation that expresses $T^{\mu\nu}$ in terms of four variables: the local temperature T and the local fluid velocity u^μ:

$$T^{\mu\nu} = (\epsilon + P)u^\mu u^\nu + Pg^{\mu\nu} + \tau^{\mu\nu}, \tag{7}$$

where $\tau^{\mu\nu}$ is the correction containing terms proportional to first derivatives. It is conventional to impose the condition $u_\mu\tau^{\mu\nu} = 0$ which eliminates any ambiguity in the definition of u^μ and T. In this case one has

$$\tau^{\mu\nu} = -\eta P^{\mu\alpha}P^{\nu\beta}(\nabla_\alpha u_\beta + \nabla_\beta u_\alpha) - \zeta P^{\mu\nu}(\nabla\cdot u), \tag{8}$$

where η and ζ are the shear and bulk viscosities, respectively. In a conformal plasma, the stress-energy tensor is traceless, hence $\epsilon = 3P \sim T^4$ and $\zeta = 0$. In such a plasma, the shear viscosity has to scale with the temperature as $\eta \sim T^3$.

3.1. Hydrodynamics and two point functions

From the hydrodynamic equations, one can easily compute the two-point functions of between two components of the stress-energy tensor. According to the general formulas of the linear response theory, the two-point function can be computed by first turning on a weak gravitational perturbation $g_{\mu\nu} = \eta_{\mu\nu} + h_{\mu\nu}$, $h_{\mu\nu} \ll 1$, then measuring the expectation value of the stress-energy tensor $\langle T_{\mu\nu}\rangle$. The two-point function is the coefficient of proportionality between $\langle T_{\mu\nu}\rangle$ and $h_{\mu\nu}$,

$$T_{\mu\nu}(x) \sim \int dy\, \langle T^{\mu\nu}(x)T^{\alpha\beta}(y)\rangle h_{\alpha\beta}(y). \tag{9}$$

On the other hand, when $h_{\mu\nu}$ varies with space and time very slowly, the response of the system can be determined by hydrodynamics. One first generalizes the hydrodynamic equation to curve spacetime. Assuming the system is in thermal equilibrium in the infinite past, and $h_{\mu\nu}$ is nonzero in a finite regime in spacetime, the state of the system can be completely determined.

We can re-derive the well known Kubo's formula in this way. Let us turn on a small metric perturbation whose only nonzero component is h_{xy} which is assumed to be homogeneous in space and is time dependent, $h_{xy} = h_{xy}(t)$. Then by symmetry one can right away determine that the fluid will remain in a state with constant temperature, $T = $ const, and zero spatial velocity $u^\mu = (1, \mathbf{0})$ (a tensor perturbation cannot excite a scalar or vector mode to linear order). Nevertheless, the stress-energy tensor receives a correction

$$T^{xy} = Pg^{xy} - \eta(\nabla_x u_y + \nabla_y u_x) = -Ph_{xy} + 2\eta\Gamma^0_{xy}u_0$$

(10)

proportional to the perturbation. Thus we find the two-point function

$$\langle T^{xy}T^{xy}\rangle = P - i\eta\omega. \tag{11}$$

The real part of this Green's function is a contact term, and depend on the way the two point function is defined; but one cannot get rid of the imaginary part by a redefinition of the Green function. Moreover, the imaginary part gives the value of the viscosity through the Kubo formula:

$$\eta = -\lim_{\omega\to 0}\frac{1}{\omega}\mathrm{Im}\, G_R^{xy,xy}(\omega, \mathbf{0}). \tag{12}$$

4. AdS/CFT prescription for correlation function

4.1. Euclidean Green's function

Let us remind ourselves how the Euclidean Green's function is computed. For simplicity we limit ourselves to the case of an operator of dimension 4, dual to a massless scalar field ϕ. Assuming the action for the scalar field is

$$S = -\frac{K}{2}\int d^5x\,\sqrt{-g}\,g^{\mu\nu}\partial_\mu\phi\partial_\nu\phi. \tag{13}$$

Then the prescription tells us to solve the wave equation

$$\partial_\mu(\sqrt{-g}g^{\mu\nu}\partial_\nu\phi) = 0, \tag{14}$$

with boundary condition $\phi = \phi_0$ at the boundary. The solution, in momentum space, is $\phi(z,k) = \phi_0(k)f_k(z)$, where $f_k(z)$ is the solution to the field equation (at momentum k). We now rewrite S as a boundary action

$$S = \frac{K}{2}\int d^5x\frac{1}{z^3}\phi\phi'. \tag{15}$$

Differentiating the action with respect to the boundary value ϕ_0, we find the two point function to be

$$\langle\phi\phi\rangle_k \sim K\lim_{z\to 0}\frac{f_k'}{z^3}. \tag{16}$$

The boundary condition at the boundary needs to be supplemented by the boundary condition in the IR. At zero temperature, we require $\phi(z)$ to vanish as $z\to 0$. At finite temperature, spacetime is capped off at some $z = z_0$. We require the field to be regular at the horizon; in the case of the scalar, $\phi'(z_0) = 0$. The solution to the field equation is then unique, and the AdS/CFT prescription well defined.

4.2. Real-time Green's function

In real-time, the formulation of the AdS/CFT prescription is more subtle. The AdS/CFT rules are best formulated using the whole Penrose diagram of the black hole.

In the Poincare metric the AdS black hole looks like

$$ds^2 = -\frac{r^2}{R^2}(-f dt^2 + d\mathbf{x}^2) + \frac{R^2}{r^2 f}dr^2, \tag{17}$$

where $f = 1 - r_0^4/r^4$. The metric can be extended pass the horizon, one recovered four quadrants in the following Penrose diagram,

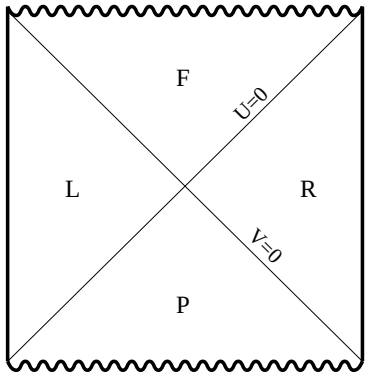

Figure 2. Penrose diagram of AdS black hole

Let us remind ourselves how it is done. Near the horizon, we expand $r = r_0 + \rho$. The (t, r) part of the metric can be rewritten as

$$ds^2 = 4\pi T\rho\left(-dt^2 + \frac{1}{(4\pi T)^2}\frac{d\rho^2}{\rho^2}\right), \tag{18}$$

where $T = r_0/\pi R^2$. This can be rewritten as $ds^2 = e^{4\pi T r_*}(-dt^2 + dr_*^2)$ where $r_* =$

$(4\pi T)^{-1}\ln\rho$. Finally, we introduce Kruskal's coordinates

$$U = -e^{-2\pi T(t-r_*)}, \tag{19}$$

$$V = e^{2\pi T(t+r_*)}, \tag{20}$$

and metric is $ds^2 = -dUdV$. The Poincare coordinates cover only $U<0$, $V>0$ part quadrant of the diagram. There is another copy with the same metric, corresponding to the $U>0$, $V<0$ part. There are two boundaries.

The extension of the AdS/CFT duality was suggested by Maldacena [4], and then explicitly considered in Ref. [5]. The idea is that the two boundaries correspond to two horizontal parts of the close time path contour. The AdS/CFT prescription is then identifies the logarithm partition function of the thermal field theory, with sources J_1 and J_2 on the two parts of the contour, with the classical action of a configuration where the bulk field ϕ reaches the values J_1 and J_2 on the right and left boundaries, respectively.

In addition, one should also put boundaries conditions near the horizon. The choice of the boundary condition should be that when the bulk field ϕ is considered as function of the complex Kruskal coordinates U and V, it is analytic in the U upper half plane and V lower half plane.

The solution to the linearized field equation can be written in terms of the mode function $f_k(r)$, defined as the radial profile of a solution to the wave equation with momentum k, and is incoming wave at the horizon. One can write the solution down separately in the right and left quadrants,

$$\begin{aligned}\phi(k,r)|_R &= \left((n+1)f_k^*(r_R) - n f_k(r_R)\right)\phi_1(k)\\ &+ \sqrt{n(n+1)}\left(f_k(r_R) - f_k^*(r_R)\right)\phi_2(k),\end{aligned} \tag{21}$$

$$\begin{aligned}\phi(k,r)|_L &= \sqrt{n(n+1)}\left(f_k^*(r_L) - f_k(r_L)\right)\phi_1(k)\\ &+ \left((n+1)f_k(r_L) - n f_k^*(r_L)\right)\phi_2(k).\end{aligned} \tag{22}$$

Here $n = (e^{\omega/T}-1)^{-1}$ is the Fermi-Dirac distribution function at frequency ω. Substituting the solution into the quadratic action, using the boundary form of the on-shell action,

$$\begin{aligned}&\frac{K}{2}\int_R \sqrt{-g}g^{rr}\phi(-k,r)\partial_r\phi(k,r)\frac{d^4k}{(2\pi)^4}\\ &-\frac{K}{2}\int_L \sqrt{-g}g^{rr}\phi(-k,r)\partial_r\phi(k,r)\frac{d^4k}{(2\pi)^4}\end{aligned} \tag{23}$$

(where K is a normalization factor) and differentiate it, one obtains the CTP propagators. Taking the appropriate linear combination of G_{11} and G_{12} we then find the retarded Green function,

$$G_R(k) = -K\sqrt{-g}\, g^{rr} f_k(r)\partial_r f_k^*(r)|_{r\to\infty}. \tag{24}$$

This formula coincides with the prescription first proposed in Ref. [6]. We now use this formula to compute the shear viscosity of the $\mathcal{N}=4$ plasma.

4.3. Viscosity

Let us compute the a two-point function. We assume the momentum to be $q=(\omega,0,0,q)$, and we compute the two-point function T^{xy}, we consider gravitation perturbation with the only perturbation being $h_{xy}(t,z)$. One can show that the quadratic action of h_{xy} is that of a minimally coupled theory when written in terms of $\phi = g^{xx}h_{xy}$:

$$\begin{aligned}S &= \frac{1}{2\kappa_{10}^2}\int d^{10}x\,\sqrt{-g}\,(R-2\Lambda)\\ &= -\frac{V(S^5)}{4\kappa_1 0^2}\int d^5x\,\sqrt{-g}\,g^{\mu\nu}\partial_\mu\phi\partial_\nu\phi.\end{aligned} \tag{25}$$

We now the write down the mode equation

$$\left(\frac{f(z)}{z^3}f_k'\right)' + \left(\frac{\omega^2}{z^3 f} - \frac{q^2}{z^3}\right)f_k(z) = 0. \tag{26}$$

The solution to this equation is

$$f_k(z) = \left(1-\frac{z}{z_0}\right)^{-i\omega/4\pi T}. \tag{27}$$

Inserting the solution into the formula for G_R, we find the imaginary part of the retarded propagator,

$$\mathrm{Im}\, G_R(k) = -\frac{V(S^5)}{2\kappa_{10}^2}\frac{R^3}{z_0^3}i\omega. \tag{28}$$

To compute the real part of G_R one needs to be more careful with holographic renormalization. But we can already read out the viscosity from $\mathrm{Im}\, G_R$,

$$\eta = \frac{V(S^5)}{2\kappa_{10}^2}\frac{R^3}{z_0^3}\,. \tag{29}$$

This can be compared with the entropy density,

$$s = \frac{S}{V} = V(S^5)\frac{R^3}{z_0^3}\frac{2\pi}{\kappa_{10}^2}\,, \tag{30}$$

and we find that $\eta/s = 1/4\pi$. This is the common feature of all theories with gravitational dual [7].

5. Fluid-gravity correspondence: Diffusion

There is an alternative method to compute the kinetic coefficients. This method, sometimes called fluid-gravity correspondence, allows one to see directly the emergence of the *nonlinear* hydrodynamic equations from the field equations in the bulk [8]. The approach is thus complementary to standard AdS/CFT method based on the calculations of correlation functions.

We will illustrate the technique of fluid-gravity correspondence on a very simple example where the higher-dimensional theory is an abelian gauge theory in a black hole background,

$$S = -\frac{1}{4g_{\rm YM}^2}\int d^{d+1}x\, F_{\mu\nu}F^{\mu\nu}. \tag{31}$$

The background is chosen to be

$$ds^2 = r^2(-f(r)dt^2 + d\mathbf{x}^2) + \frac{dr^2}{r^2 f(r)}\,, \tag{32}$$

where $f(r)$ is a function that vanishes at the horizon, $f(r_0) = 0$ and tends to 1 at the AdS boundary, $f(\infty) = 1$. This is the usual back hole (black brane) background.

We are interested in solution to Maxwell's equations which satisfies outgoing wave boundary conditions. To enforce the incoming-wave boundary condition, it is more convenient to use the incoming Eddington-Fikelstein coordinates,

$$ds^2 = -r^2 f dv^2 + 2dv\, dr + r^2 d\mathbf{x}^2. \tag{33}$$

The usefulness of the Eddington-Fikelstein coordinates is that regularity at the horizon in these coordinates correspond to incoming wave boundary conditions in the usual coordinates. We go on to construct such a solution. The Maxwell equations are

$$\partial_r(r^d F_{vr}) + r^{d+2}\partial_i F_{ir} = 0, \tag{34}$$

$$r^d\partial_v F_{rv} + r^{d-2}\partial_i F_{iv} + f r^d \partial_i F_{ir} = 0, \tag{35}$$

$$\partial_r(r^{d-2}F_{vi}) + \partial_r(f r^d F_{ri}) + r^{d-2}\partial_v F_{ri} + r^{d-4}\partial_j F_{ji} = 0. \tag{36}$$

We start from gauge field of a charged black hole,

$$A_0 = \frac{q}{r^{d-1}}\,. \tag{37}$$

This is a one-parameter family of solutions to the Maxwell equations, parameterized by the charge density q. It describes a state in the field theory with a constant charge density in complete thermal equilibrium. Note that the solution is translationally invariant in all field-theory directions, t and $\mathbf{x}$.

What happens if we make q a function of the space and time? As one can easily verify, now the configuration (37) is not an exact solution to the Maxwell equation. However, when q varies slowly in space and time, one should be able to still find the solution by expanding it in powers of $\partial_t q$ and $\partial_x q$, which are small parameters. This is exactly the strategy that we will follow.

First we need to settle on a power counting scheme. Anticipating the end result to be a diffusion equation $\partial_t\rho = D\nabla^2\rho$, we shall treat $\partial_i q$ as $O(\epsilon)$ and $\partial_t q$ as $O(\epsilon^2)$, where ϵ is small. We then expand the solutions, using the gauge $A_r = 0$,

$$A_v(r,x) = \frac{q(x)}{r^{d-2}} + A_v^{(1)}, \qquad A_i = A_i^{(1)}. \tag{38}$$

We can demand that $A_0^{(1)}$ falls off faster than $r^{-(d-2)}$ at large r. Otherwise, one can redefine $q(x)$ to absorb any $r^{-(d-2)}$ piece in $A_0^{(1)}$. Consistency requires that we treat $A_v^{(1)}$ as a quantity of order ϵ^2 and $A_i^{(1)} \sim \epsilon$

Substituting the ansatz in the the Maxwell

equations, collecting terms with the same smallness in ϵ, we find

$$\partial_r(r^d\partial_r A_v^{(1)}) + r^{d+2}\partial_i\partial_r A_i^{(1)} = 0, \tag{39}$$

$$(d-1)\partial_v q + fr^d\partial_i\partial_r A_i^{(1)} - \frac{1}{r}\partial_i^2 q = 0, \tag{40}$$

$$-\partial_r\left(\frac{\partial_i q}{r}\right) + \partial_r(fr^d\partial_r A_i) = 0. \tag{41}$$

Integrating the last equation, we find

$$\partial_r A_i^{(1)} = \frac{C}{fr^d} + \frac{\partial_i q}{fr^{d+q}}\,, \tag{42}$$

where C is an x-dependent integration constant. Both terms in the right hand side have pole at the horizon $r = r_0$, and regularity at the horizon requires that the singularities cancel out between the two terms. Therefore we find

$$C = -r_0\partial_i q. \tag{43}$$

Integrating once more, we then can find A_i. Actually for our purposes, we just need to know the asymptotic behavior of A_i at large r,

$$A_i = \frac{r_0}{d-1}\frac{\partial_i q}{r^{d-1}} + O(r^{-d}). \tag{44}$$

We can now substitute A_i into the second equation of (39), taking the large r limit and derive the following equation for q:

$$\partial_v q - \frac{r_0}{d-1}\nabla^2 q = 0, \tag{45}$$

which is nothing but the diffusion equation. Thus we have found a more general solution to the Maxwell equation which is parameterized by solutions to the diffusion equation. Maxwell equation in the background of black brane metric reduces to the diffusion equation in the long-wavelength limit.

6. Nonrelativistic conformal invariance

Fermions interacting through a unitarity interaction form a simplest nonrelativistic strongly interacting system. This system is beautiful because of its simplicity and universality. It has attracted enormous attention since being realized in cold atom experiments.

Let us first define fermions at unitarity. Consider two nonrelativistic particles, interacting through a potential,

$$H = \frac{\mathbf{p}_1^2}{2} + \frac{\mathbf{p}_2^2}{2} + V(|\mathbf{x}_1 - \mathbf{x}_2|). \tag{46}$$

For simplicity, we can consider V of the form of a square well potential, with size r_0 and depth $-V_0$: $V(r < r_0) = -V_0$ and $V(r > r_0) = 0$. If the potential is shallow, it does not have any bound state; but if it is deep enough it may have one, two, or more bound states. There is a critical value of $V_0 \sim r_0^{-2}$ at which the potential starts to have exactly one bound state. We tune V_0 to be exactly this value.

Then we take the range of interaction r_0 to zero, keeping V_0 always tuned to the critical value (in other words, keeping $V_0 r_0^2$ fixed). This limit is called the unitary limit, and the system of fermions interacting with this interaction the unitary Fermi gas.

The stability of such a system is not a trivial issue. It is relatively easy to see that for bosons, and for fermions of three or more different species, the finite-density system is not stable. This fact is related to the so-called Efimov effect: in the limit of zero range interaction, the Hamiltonian is unbounded from below (there is an infinite number of bound states, the lowest of which has an energy determined by the UV cutoff of the theory—the range of the potential).

6.1. Quantum mechanics formulation: boundary condition

The quantum quantum mechanics of unitary fermions can be formulated in a way which gets rid of the interaction potential completely. Let us start with the case of two particles, one spin-up with coordinate $\mathbf{x}$, and another spin-down with coordinate $\mathbf{y}$. Neglecting the center of mass motion, the Schrödinger equation has the form

$$\frac{\partial^2}{\partial\mathbf{r}^2}\Psi(\mathbf{r}) + V(r)\Psi(\mathbf{r}) = -E\Psi(\mathbf{r}). \tag{47}$$

In the limit of zero range, the potential $V(r)$ is zero at any nonzero r. In the limit of $\mathbf{r} \to 0$, the right hand side can be neglected ($E \ll r^{-2}$), and we have the Laplace equation $\nabla_{\mathbf{r}}^2\Psi = 0$. Now

it is known that the Laplace equation has two independent solutions, 1 and r^{-1}. The behavior of the wavefunction at small r is, in general,

$$\Psi(\mathbf{r}) = \frac{C}{r} + C_1 + O(r), \tag{48}$$

where C and C_1 are some numbers. In the usual problem of free particles, the wavefunction is assumed to be regular at $r = 0$, which means $C = 0$. On the other hand, from the mathematical point of view one can impose a general boundary condition

$$\Psi(\mathbf{r}) \sim \left(\frac{1}{r} - \frac{1}{a}\right), \tag{49}$$

with any value of a ($a = 0$ corresponding to free particles). Physically a is obtained by solving the zero-energy Schrödinger equation inside the potential $r < r_0$ and then match it to the solution to the Laplace equation outside the potential $r > r_0$; a therefore characterizes low-energy scatterings and is called the scattering length. The fine-tuning of the potential corresponds to the limit $a \to \infty$.

For the case of a general number of particles, the Hamiltonian is the sum of the kinetic terms of all particles,

$$H = \sum_i \frac{\mathbf{p}_i^2}{2m} = -\frac{1}{2m}\sum_i \frac{\partial^2}{\partial \mathbf{x}_i^2} \tag{50}$$

(where i numerates all particles) but the Hilbert space is nontrivial: the wave function of a system, $\Psi(\mathbf{x}_1, \ldots, \mathbf{x}_N; y_1, \ldots, \mathbf{y}_N)$ satisfies the following condition when one spin-up and one spin-down particles approach each other,

$$\Psi(\mathbf{x}_1, \ldots, \mathbf{x}_N; y_1, \ldots, \mathbf{y}_M) \to \frac{C}{|\mathbf{x}_i - y_j|} + O(1) + O(|\mathbf{x}_i - y_j|), \tag{51}$$

where $\mathbf{x}_i$ and $\mathbf{y}_j$ are the coordinates of the spin-up particles and spin-down particles, respectively. The Hamiltonian is trivial, but the nontriviality of the problem is in the Hilbert space.

For example, we can put a spin-up and a spin-down fermion in a harmonic potential. The Hamiltonian is now

$$H = \frac{1}{2}(\mathbf{p}_1^2 + p_2^2) + \frac{1}{2}\omega^2(\mathbf{x}_1^2 + \mathbf{x}_2^2). \tag{52}$$

The problem can be solved exactly even when the interaction between particles is unitary. The ground state is

$$\Psi(\mathbf{x}_1, \mathbf{x}_2) \sim \frac{e^{-\omega(|\mathbf{x}_1|^2 + |\mathbf{x}_2|^2)/2}}{|\mathbf{x}_1 - \mathbf{x}_2|}, \tag{53}$$

and the ground state energy is $E = 2\omega$. This is lower than the ground state energy in the case of a 3ω, in consistency with the attractiveness of the interaction.

The two-particle problem is special because it can be solved analytically. For three particles in a harmonic potentials, the energy levels are also known exactly (they are solutions to a trigonometric equation). For four particles and more (unless they have the same spin), the many-body problem cannot be solved exactly.

6.2. Symmetries of unitary fermions

A general nonrelativistic system is invariant under translation (in space and time), rotation, and Galilean boosts. In addition, the conserved mass (particle number) corresponds to a phase symmetry, $\psi \to e^{i\alpha}\psi$. These symmetries are enhanced to a new symmetry group called the Schrödinger group. The Schrödinger group contains two new symmetries

- Dilatation: $t \to \lambda^2 t$, $\mathbf{x} \to \lambda \mathbf{x}$,
- Proper conformal transformation: $t = t/(1 - \lambda t)$, $\mathbf{x} \to \mathbf{x}/(1 - \lambda t)$.

Saying that a theory theories has these symmetries means that if one has a solution to the time-dependent Schrödinger equation, $\Psi(t, \mathbf{x}_i)$, then one can generate new solutions. For example, the solution obtained by dilatation is

$$\Psi'(t, \mathbf{x}) = \lambda^{3N/2}\Psi(\lambda^2 t, \lambda x) \tag{54}$$

(the prefactor is to keep the normalization of Ψ). It is obvious that if Ψ solve the free Schrödinger equation, then Ψ' also does. More nontrivially, the boundary condition at short distances for unitary particle is preserved under dilatation. Similarly, the proper conformal transformation corresponds to the following family of new solutions,

$$\Psi'(t, \mathbf{x}) = C(t, \mathbf{x})\Psi\left(\frac{t}{1 - \lambda t}, \frac{\mathbf{x}}{1 - \lambda t}\right). \tag{55}$$

We leave the determination of $C(t, \mathbf{x})$ to the reader.

In the theory of unitarity fermions, the dilatation operator D and the proper conformal transformation C can be expressed in terms of the operators creating and annihilating a particle,

$$D = -\frac{i}{2}\int d\mathbf{x}, \mathbf{x}\cdot(\psi^\dagger\nabla\psi - \nabla\psi^\dagger\psi),$$
$$C = \frac{1}{2}\int d\mathbf{x}, \mathbf{x}^2\psi^\dagger(\mathbf{x})\psi(\mathbf{x}). \quad (56)$$

One can check that the operators D, C and the Hamiltonian H form a close SO(2,1) subalgebra of the Schrödinger algebra,

$$[D,\, C] = -2iC, \quad [D,\, H] = 2iH, \quad [C,\, H] = iD. \quad (57)$$

The full Schrödinger algebra can be found in Ref. [9].

6.3. Local operators

The local operators (for example ψ, $\psi^\dagger$, or $\psi^\dagger\psi$) depend on time t and space $\mathbf{x}$. Its commutators with time and space rotation are completely defined. The local operators can be classified by particle number by taking it commutator with the particle number operator $M = \int d^{\mathbf{x}}, \psi^\dagger\psi$. For example ψ has particle number -1 while for $\psi^\dagger$ it is $+1$. Each operator can be associated with a dimension by

$$[D,\, O(0)] = i\Delta_O O(0). \quad (58)$$

For example, $\Delta_\psi = 3/2$ ($d/2$ in d spatial dimensions). One example of a nontrivial composite operator is obtained when one tries to construct the product of two annihilation operators of particles with different spins, $\psi_\uparrow\psi_\downarrow$. We know that the matrix element of $\psi_\uparrow(\mathbf{x})\psi_\downarrow(\mathbf{y})$ between a two-body state and vacuum is just the wave function,

$$\langle 0|\psi_\uparrow(\mathbf{x})\psi_\downarrow(\mathbf{y})|\Psi\rangle = \Psi(\mathbf{x}, \mathbf{y}). \quad (59)$$

The problem is that when we tries to take $\mathbf{x} \to \mathbf{y}$ to have a local operator $\psi_\uparrow\psi_\downarrow$, the matrix element diverges due to the boundary condition at $\mathbf{x} \to \mathbf{y}$. On the other hand, one can define the following operator

$$O_2(\mathbf{x}) = \lim_{\mathbf{y}\to\mathbf{x}} 4\pi|\mathbf{x} - \mathbf{y}|\psi_\uparrow(\mathbf{x})\psi_\downarrow(\mathbf{y}), \quad (60)$$

which has finite matrix elements between states in the Hamiltonian. Another way to write the equation above is

$$\psi_\uparrow(\mathbf{x})\psi_\downarrow(\mathbf{y}) = \frac{O_2(x)}{4\pi|\mathbf{x} - y|} + \cdots, \quad (61)$$

which has the form of an operator product expansion for unitarity fermions. Operator product expansions have been applied very recently for unitarity fermions; as in particle physics they are most useful at short distances. The operator $O_2^\dagger O_2$ has a special role: its expectation value is called in the literature the Tan's parameter, or the contact.

As in relativistic CFTs, one can introduce the notion of primary and descendant operators. Primary operators are called those which commute, at zero coordinates, with Galilean boosts and the proper conformal transformation: $[K_i,\, O(0)] = [C,\, O(0)] = 0$. By taking derivatives with respect to coordinates and time, descendants are obtained.

The SO(2,1) commutators are important to prove what we call the operator-state correspondence for systems with Schrödinger symmetry. Namely, a primary operator, which does not annihilate the vacuum (or its Hermitian conjugate does not annihilate the vacuum) can be put into correspondence with an eigenstate of the system of a few particles in a harmonic potential [9]. This statement can be proven by first noticing (recall the form of the operator C in Eq. (56) that the Hamiltonian in a harmonic potential can be written as

$$H_{\rm osc} = H + \omega^2 C. \quad (62)$$

Then for an primary operator O, one can construct a state $\Psi_O\rangle$ as follows,

$$|\Psi_O\rangle = e^{-H/\omega}O^\dagger(0)|0\rangle. \quad (63)$$

Physically, first we use $O^\dagger$ to create a state which is localized at the origin of coordinates, and then evolve that state in imaginary time using the free-space Hamiltonian during a time $1/\omega$. The resulting state, whose wavefunction is a Gaussian-type wavepacket, can be shown, by using the SO(2,1)

commutators, to be an eigenstate of the Hamiltonian $H_{\rm osc}$ with energy 2ω.

This operator-state correspondence can be illustrated explicitly in a few example. The operator ψ has dimension 3/2, which matches with the ground state energy of a single particle in an isotropic harmonic potential, $3\omega/2$. The operator O_2 has dimension 2, and corresponds to the ground state of a system of one spin up and one spin down particle in a harmonic potential, whose energy was shown above to be 2ω.

6.4. Schrödinger space

If one wants to move in the direction of constructing a gravitational dual of the unitarity fermions, it seems reasonable to start by asking the question: what is the space-time that realizes the Schrödinger symmetry? (Recall that in the original Maldacena's duality, the symmetry of $AdS_5 \times S^5$ space matches with the symmetry of the quantum field theory). An example of such a space was constructed in Refs. [10,11]. The space has *two* extra dimensions compared to one extra dimensions in standard holography. The metric is

$$ds^2 = -\frac{2(dx^+)^2}{z^4} + \frac{-2dx^+dx^- + dx^i dx^i + dz^2}{z^2}. \tag{64}$$

One can check that this spacetime has realizes all generators of the Schrödinger algebra as Killing vectors. In particular, the total mass and the proper conformal transformation are

$$\begin{aligned} &M : x^- \to x^- + a, \\ &C : z \to (1-ax^+)z, \quad x^i \to (1-ax^+)x^i, \\ &\quad x^+ \to (1-ax^+)x^+, x^- \to x^- - \frac{a}{2}(x^i x^i + z^2). \end{aligned} \tag{65}$$

One can see that the translational symmetry along the direction x^- realizes the conservation of mass in the nonrelativistic theory. The simplest action which gives rise to the Schrödinger spacetime is that of Einstein gravity with negative cosmological constant, coupled to a massive gauge field with a suitably chosen mass,

Subsequently the five-dimensional Schrödinger spacetime (corresponding to two spatial directions in field theory) have been constructed in string theory. As by-product of the construction, one also found black hole solutions, which describe a medium with finite chemical potential and temperature. One might think that these solutions may be the first holographic model for the unitarity Fermi gas. Unfortunately, closer inspection reveals a serious undesirable feature: the equation of state of the black hole is $P(T,\mu) \sim \frac{T^4}{\mu^2}$, which has the correct scaling behavior but is more restrictive than required. The more general equation of state is

$$P(T,\mu) = \mu^2 F(T/\mu), \tag{66}$$

where the function F is not constrained. This is in contrast to the situation in relativistic holography, where fitting the equation of state of QCD is not really a problem in the bottom-up approach.

It seems that one should try to devise a more general way to realize Schrödinger symmetry. Attempts in this direction are being made. At the more general level, one should not expect the gravity dual of unitarity fermions to be a classical theory due to the lack of a large N parameter. One can generalize the unitarity fermions to a many-favor theory with Sp($2N$) vector symmetry. This theory is trivial to solve; at large N the BCS theory becomes exact. The situation is very similar to the relativistic O(N) vector model. One can hope that there is a nonrelativistic high-spin theory that is dual to the Sp($2N$) version of unitary fermions, similar to the case of the O(N) model [12]. As far as I know, to date no serious attempt has been made to uncover such a theory.

7. Summary

In these lectures we have considered some applications of gauge/gravity duality to systems with finite temperature and chemical potential. We have left out some very important applications of gauge gravity duality, most notably jet quenching and heavy quark energy loss.

I thank the organizers of the Cargese and TASI schools for inviting me to give these lectures.

REFERENCES

1. J. I. Kapusta and C. Gale, *Finite-temperature field theory: Principles and applications,* (Cambridge University Press, Cambridge, UK, 2006)
2. M. Le Bellac, "Thermal field theory," (Cambridge University Press, Cambridge, UK, 2000)
3. S. Jeon and L. G. Yaffe, Phys. Rev. D **53**, 5799 (1996) [arXiv:hep-ph/9512263].
4. J. M. Maldacena, JHEP **0304**, 021 (2003) [arXiv:hep-th/0106112].
5. C. P. Herzog and D. T. Son, JHEP **0303**, 046 (2003) [arXiv:hep-th/0212072].
6. D. T. Son and A. O. Starinets, JHEP **0209**, 042 (2002) [arXiv:hep-th/0205051].
7. P. Kovtun, D. T. Son and A. O. Starinets, Phys. Rev. Lett. **94**, 111601 (2005) [arXiv:hep-th/0405231].
8. S. Bhattacharyya, V. E. Hubeny, S. Minwalla and M. Rangamani, JHEP **0802**, 045 (2008) [arXiv:0712.2456 [hep-th]].
9. Y. Nishida and D. T. Son, Phys. Rev. D **76**, 086004 (2007) [arXiv:0706.3746 [hep-th]].
10. D. T. Son, Phys. Rev. D **78**, 046003 (2008) [arXiv:0804.3972 [hep-th]].
11. K. Balasubramanian and J. McGreevy, Phys. Rev. Lett. **101**, 061601 (2008) [arXiv:0804.4053 [hep-th]].
12. I. R. Klebanov and A. M. Polyakov, Phys. Lett. B **550**, 213 (2002) [arXiv:hep-th/0210114].

Lectures on 4d $\mathcal{N} = 1$ susy gauge theories

Ken Intriligator[a]

[a]UCSD Physics Department, 9500 Gilman Dr, La Jolla CA, 92093 USA

This is a very brief introduction to phases of gauge theories, SQCD, Seiberg duality, dynamical susy breaking, and recent related topics.

1. Introduction and generalities

We'll here give a concise introduction to the dynamics of supersymmetric gauge theories. The presentation is heavily influenced by my review articles with Nati Seiberg [1,2]; look there for more details and references. Some related recent topics are briefly mentioned as well.

4d $N = 1$ susy lagrangians have terms $\mathcal{L}_{micro} = \mathcal{L}_D^{micro} + \mathcal{L}_F^{micro}$, called D and F terms if they involve $\int d^4\theta$ or $\int d^2\theta$, respectively. The former include the matter kinetic terms,

$$\mathcal{L}_D^{micro} \supset \int d^4\theta Z_{Q_i} Q_i^\dagger e^{T_{r_i} V} Q_i \qquad (1)$$

Q_i are the matter chiral superfields in representation r_i of the gauge group, and V is the vector (gauge) multiplet. The gauge kinetic terms and matter interactions are given by F-terms:

$$\mathcal{L}_F^{micro} = \int d^2\theta (2\pi i \tau) S + \int d^2\theta W_{tree}(Q_i) + h.c.. \qquad (2)$$

The gauge field kinetic term is written in terms of the "glueball" chiral superfield $S \equiv -TrW_\alpha W^\alpha/32\pi^2$, where $W_\alpha = -\frac{1}{4}\bar{D}\bar{D}e^{-V}D_\alpha e^V = -i\lambda_\alpha(y) + D(y)\theta_\alpha - i(\sigma^\mu\bar{\sigma}^\nu)_\alpha^\beta\theta_\beta F_{\mu\nu}(y) + \theta^2\partial_{\alpha\dot{\alpha}}\bar{\lambda}^{\dot{\alpha}}$, with λ_α the gaugino. See e.g. [3] for the notation.

D terms get quantum corrections, both in perturbation theory and non-perturbatively, hence the renormalization factor Z_{Q_i} in the matter kinetic terms. Quantum corrections to the F terms, on the other hand, are tightly constrained by susy, as they must preserve holomorphy in the chiral superfields. The couplings in F terms are complex, and quantum corrections must preserve holomorphy in them as well. This is the power of holomorphy (see [4]), which can be used to obtain exact results about F-term quantities, like superpotenitals. Holomorphy in superpotential couplings follows from the fact that they could have been replaced with expectation values of background chiral superfields.

As an illustrative example, susy combines the gauge coupling and theta angle into the holomorphic quantity $\tau = \frac{\theta}{2\pi} + 4\pi i/g_h^2$ in eqn. 2. It immediately follows that the beta function for this holomorphic gauge coupling must be one-loop exact: the RG running must preserve holomorphy, $2\pi i\dot{\tau} = i\dot{\theta} + 16\pi^2 g^{-3}\beta_{g_h} = f(\tau) = -b_0$, and a constant is the only holomorphic function $f(\tau)$ compatible with $\dot{\theta} = 0$. (Modulo the possibility of instanton corrections in a partially broken UV group, as happens on the Coulomb branch of $\mathcal{N} = 2$ susy theories, but we won't discuss that here.) Integrating the one-loop exact beta function leads to

$$e^{2\pi i\tau(\mu)} = e^{i\theta - 8\pi^2/g_h^2(\mu)} = \left(\frac{\Lambda}{\mu}\right)^{b_0}, \qquad (3)$$

where Λ is the holomorphic dynamical scale.

The 1-loop exact β_{g_h} leads to the well-studied issue of the multiplet of anomalies, seen also from the fact that susy relates the scale anomaly to that of the $U(1)_R$ current, which is 1-loop exact by the ABJ anomaly argument (see below). This led to a famous puzzle, since direct computation reveals that the physical coupling has a non-zero 2-loop beta function. Considering this issue led NSVZ to their exact expression for the beta function [5]. The basic point is that physical couplings, like g, differ from the holomor-

phic couplings, like g_h, by rescalings associated with absorbing the wavefunction renormalization Z_{Q_i} factors. Such rescalings should not be done if we want to use holomorphy arguments (holomorphic chiral superfields should not be contaminated with non-holomorphic quantities like Z_{Q_i}), but they still need to be accounted for, at the end of the day, in physical quantities.

The above lagrangian description can be in terms of the microscopic degrees of freedom of an asymptotically (UV) free gauge theory. Integrating out the UV modes, in principle, leads to the low-energy effective field theory, for the light degrees of freedom. This is the "dual" theory. These DOF can be IR free (e.g. the pions and their chiral lagrangian nonlinear sigma model, $SU(N_f) \times SU(N_f)/SU(N_f)$). Another possibility, long thought to be exotic, is that the low-energy theory might be in the conformal window, where it RG flows to an interacting, scale invariant CFT.

Starting from a susy theory, we can consider a low energy effective theory that's also supersymmetric. (Supersymmetry can be spontaneously broken at low energy, as we'll discuss, but we'll just consider the theory above any susy breaking scale). For simplicity, let's consider the case where the low-energy theory doesn't include IR free gauge fields:

$$\mathcal{L}_{eff} = \int d^4\theta K(\Phi^I, \bar{\Phi}^{\bar{J}}) + W_{eff}(\Phi) + h.c., \quad (4)$$

where the Φ^I are some composites of the original fields, e.g. mesons and baryons. Upon integrating out the auxiliary fields, this gives a sigma model with Kähler metric $g_{I\bar{J}} = \partial^2 K/\partial\Phi^I\partial\bar{\Phi}^{\bar{J}}$: $\mathcal{L}_{scalar} = g_{I\bar{J}}\partial_\mu\Phi^I\partial^\mu\bar{\Phi}^{\bar{J}} - g^{I\bar{J}}W_I\bar{W}_{\bar{J}}$.

Typically, there is no practical way to directly derive the low-energy effective theory – but sometimes one can conjecture / guess about what the IR degrees of freedom and their interactions are, and do non-trivial checks that constraints are satisfied. In particular, when there are global symmetries there are the 't Hooft anomaly matching conditions, as we'll review. This gives insight into the correct IR d.o.f, and thereby some basic information about the Kahler potential: the associated metric should be canonical, up to higher dimension operator corrections, in terms of the correct d.o.f..

Let's recall aspects of anomalies, which in 4d come from triangle diagrams. At the vertices of the triangle are currents, either global or gauge, or equivalently the associated gauge fields. Anomalies only get contributions from massless fermions (or massless scalars, via WZW terms, when the symmetry is spontaneously broken) running in the loop, and are hence topologically robust. For the case of $(\text{Gauge})^3$, any non-zero anomaly is a sickness; such a theory cannot be cured unless additional matter is added, to cancel the anomaly. The case $(\text{Global})(\text{Gauge})^2$ is the ABJ anomaly (since it's proportional to TrT, it's only for $U(1)$ factors) merely means that the global symmetry is explicitly violated by instantons; it's related to the index of the Dirac operator. Such a broken global symmetry can still be used: as with any broken symmetry, it leads to selection rules upon assigning appropriate charge to the appropriate symmetry breaking order parameter, which in this case is Λ.

Finally, consider the case $(\text{Global})^3$, where all three global symmetries are free of ABJ anomalies. These quantities are the 't Hooft anomalies, which 't Hooft argued (first at lectures here!) must be RG invariant, like an index. So they can be computed in particular at either end of a RG flow, and the two results must agree. When any 't Hooft anomalies are non-zero, the theory must retain some massless d.o.f. even in the IR, to reproduce the non-zero 't Hooft anomaly.

Gauge theories have various possible IR phases; let's mention three possibilities:

(a) Mass gap. Examples $\mathcal{N} = 0$ YM, $\mathcal{N} = 1$ SYM, and $\mathcal{N} = 1$ SQCD with all massive flavors. These theories can have a mass gap because they all have no non-trivial 't Hooft anomalies, e.g. $\mathcal{N} = 1$ SYM has a classical $U(1)_R$ symmetry that's broken by the ABJ anomaly: the instanton in the gauge group G has $2T_2(G)$ (for $SU(N_c)$ it's $2N_c$) gaugino fermion zero modes, explicitly breaking $U(1)_R \to Z_{2T_2(G)}$, so there's no continuous symmetry. (There is a 't Hooft anomaly matching condition for discrete symmetries, but it's considerably weaker).

In the susy cases, as we'll illustrate below,

we can use holomorphy etc. to write down $W_{exact}(g_p)$ to determine $\langle\Phi_p\rangle$.

(b) IR free phase. Here there are massless, IR free d.o.f., which are some composites of the UV fields. An example is ordinary QCD with N_f massless quarks, in the range where there's chiral symmetry breaking. In susy theories, there's also the phenomenon of IR free composite $SU(N_f - N_c)$ gauge fields for SQCD in the free magnetic range. In these cases, 't Hooft anomaly matching can be used as a check.

(c) CFT phase, which occurs when the theory has sufficient massless matter. For example, in non-susy $SU(N_c)$ QCD, there is a conformal window if there are N_f massless flavors, for N_f in some range $N_f^* < N_f < \frac{11}{2}N_c$. The upper boundary is for asymptotic freedom, and fixed points near this upper bound are weakly coupled. (The lower bound N_f^* for the non-supersymmetric case is currently being actively studied and debated by lattice gauge theorists, see e.g. [11].) For SQCD the lower boundary conformal window is known from Seiberg duality [6]: $\frac{3}{2}N_c < N_f < 3N_c$.

Another topic that we'll briefly discuss is dynamical supersymmetry breaking. If susy exists in Nature, it must be broken, and it's most interesting if it's spontaneously broken. More generally, any soft supersymmetry breaking can be written in terms of spurions, thinking about there being background superfields with non-zero θ component expectation values, which spontaneously break supersymmetry. Because soft breaking can be considered to be spontaneous (whether or not it actually is), the theory is still constrained by the broken symmetry. In eqns. 1 and 2, sfermion soft-masses are given by $m_Q^2 = -Z_Q|_{\theta^4}/Z_Q$, gaugino masses are given by $m_\lambda = \tau|_{\theta^2}/\tau$, and there can be susy breaking A terms given by $A_Q = Z_Q|_{\theta^2}/Z_Q$. See e.g. the review [7] and references therein for more details.

Global susy implies $V \geq 0$, with $V = 0$ for susy vacua and $V > 0$ for (perhaps metastable) susy breaking vacua; the vacuum energy is an order parameter for susy breaking. (One can add a negative constant, e.g. to cancel the cosmological constant, in SUGRA, since there $V_{sugra} = e^{K/M_p^2}(g^{i\bar{j}}D_iW\bar{D}_{\bar{j}}\overline{W} - 3M_p^{-2}|W|^2)$ where $D_iW = W_i + M_p^{-2}K_iW$; we'll here ignore sugra, and take $M_p \to \infty$.) There is *dynamical susy breaking* (DSB) if the susy breaking is generated by dimensional transmutation. This can naturally yield large hierarchies $M_s \sim \Lambda \sim M_{cutoff}e^{-c/g^2} \ll M_{cutoff}$. Since it's a vacuum effect, DSB should be looked for in the low-energy effective theory.

2. SQCD

Our main example is $\mathcal{N} = 1$ SQCD, with gauge group $SU(N_c)$ and N_f flavors of matter chiral superfields Q in the fundamental of $SU(N_c)$, and $\widetilde{Q}$ in the anti-fundamental of $SU(N_c)$. We make a table with their global symmetry charges, which we'll now briefly explain (see [6,1,2] for more details). The global symmetries in the table are ABJ (i.e. (global)(gauge)^2) anomaly free except for $U(1)_A$. Writing the ABJ anomaly as $\partial_\mu j^\mu = cF\widetilde{F}$, the coefficient c can be read off from the anomaly triangle diagram, or equivalently from the index of the Dirac operator in an instanton background, $\Delta(\text{charge}) = c\int F\widetilde{F}$. In other words, the instanton leads to a 't Hooft vertex interaction associated with the fermion zero modes, $\sim \overline{\Lambda}^{3N_c-N_f}\lambda^{2N_c}\psi^{N_f}\widetilde{\psi}^{N_f}$, which should be neutral under an anomaly free symmetry. The particular $U(1)_R$ charge of the matter in the table is determined by this anomaly free condition (recall that, under an R-symmetry, the supercharge has $R(Q_\alpha) = -1$, so gauginos have $R(\lambda) = 1$ and for a chiral superfield, $\Phi = \phi + \theta\psi + \theta^2F$, $R(\psi) = R(\phi) - 1$ and $R(F) = R(\phi) - 2$). The anomalous $U(1)_A$ is explicitly broken by the instanton, but we can treat it as being spontaneously broken by assigning charge to the parameter $\Lambda^{3N_c-N_f}$, thought of as a background chiral superfield, as indicated in the table. Similarly, the mass m explicitly breaks $SU(N_f)_{L,R}$ and $U(1)_R$ and $U(1)_A$, but we can treat this as spontaneous breaking by assigning m charges as in the table, thinking of m as a background chiral superfield.

We can form the gauge invariant composite chiral superfields $M_{f\widetilde{g}} = Q_f\widetilde{Q}_{\widetilde{g}}$. For $N_f > N_c$, we can also form baryons $B \sim Q^{N_c}$, which is fully antisymmetric in the omitted flavor indices. We consider the theory for $W_{tree} = TrmM$, and initially consider the theory for vanishing masses m.

Table 1
Some fields and charges in SQCD

Field	$SU(N_f)_{L,R}$	$U(1)_B$	$U(1)_R$	$U(1)_A$
Q	fund, 1	$1/N_c$	$1-\frac{N_c}{N_f}$	1
$\widetilde{Q}$	1, fund	$-1/N_c$	$1-\frac{N_c}{N_f}$	1
$M=Q\widetilde{Q}$	fund, fund	0	$2\left(1-\frac{N_c}{N_f}\right)$	2
W	1,1	0	2	0
m	$\overline{\text{fund}, \text{fund}}$	0	$2\frac{N_c}{N_f}$	-2
$\Lambda^{3N_c-N_f}$	1,1	0	0	$2N_f$
q	$\overline{\text{fund}}, 1$	$1/\widetilde{N}_c$	$1-\frac{\widetilde{N}_c}{N_f}$	-1

Classically, there is then a moduli space of susy vacua, $\mathcal{M}_{cl}=\{\langle Q\rangle,\langle\widetilde{Q}\rangle|D^a=0\}/(\text{gauge transformations})$. By a general theorem (in geometric invariant theory), $\mathcal{M}_{cl}$ is also given by the space of gauge invariant chiral superfield composites, modulo classical relations. For $N_f<N_c$, $\mathcal{M}\cong C^{N_f^2}$, while for $N_f\geq N_c$ $\mathcal{M}_{cl}$ is a conically singular space, with $dim_C(\mathcal{M}_{cl})=2N_fN_c-(N_c^2-1)$. The classical interpretation is that the singularity is resolved upon including the massless "W-bosons" there.

Now consider the quantum theory. First consider $N_f=0$. This theory has a mass gap and chiral symmetry breaking. Classically there is a $U(1)_R$ symmetry, which is broken by the instanton (the anomaly) to Z_{2N_c}, since $\langle S^{N_c}\rangle=\Lambda^{3N_c}$. The Z_{2N_c} chiral symmetry is then spontaneously broken to Z_2, as $\langle S\rangle=(\Lambda^{3N_c})^{1/N_c}$; these are the N_c susy vacua counted by the Witten index, $Tr(-1)^F=N_c$. Can think of $\log\Lambda^{3N_c}\sim g^{-2}$ as the source coupling linearly to the operator S, and write down the 1PI effective action, with $W_{eff}=N_c(\Lambda^{3N_c})^{1/N_c}$, whose derivative w.r.t. $\log\Lambda^{3N_c-N_f}$ gives $\langle S\rangle$, see [8,9] for more details.

Now consider SQCD with N_f massive flavors. Initially take $m>\Lambda$, noting that holomorphic objects can be easily analytically continued in the holomorphic mass m. Below the scale m, we can integrate out the massive flavors and get SYM, so we can use the above results to see that there are N_c susy vacua with mass gap. Matching the running holomorphic coupling $g_h(\mu)$, yields $\Lambda^{3N_c-N_f}\det m=\Lambda_{low}^{3N_c}$. Then gaugino condensation generates

$$W_{low}=N_c(\Lambda_{low}^{3N_c})^{1/N_c}=(\det m\Lambda^{3N_c-N_f})^{1/N_c}. \quad (5)$$

This can be regarded as the 1PI effective action for the source m of the field M. Then the $m\leftrightarrow M$ Legendre transform yields

$$W_{1PI}=(N_c-N_f)\left(\frac{\Lambda^{3N_c-N_f}}{\det M}\right)^{1/(N_c-N_f)}. \quad (6)$$

This works for any N_f for $m\neq 0$, even $N_f>N_c$ where it superficially doesn't make sense (Seiberg duality gives it a sensible meaning).

Now consider $m=0$. For the susy vacua (since the energy is zero) we can vary m/Λ without encountering any phase transitions, since it's a complex quantity we can avoid any singular points in the complex plane and there can't be any phase transition walls. For $N_f<N_c$ the above superpotential is dynamically generated by instantons or gaugino condensation, and leads to a runaway vacuum. The runaway properly satisfies the condition that $V_{dyn}\to 0$ for $M\to\infty$ (asymptotic freedom ensures that the quantum effects go away when the gauge group is Higgsed far in the UV).

On the other hand, for $m=0$ and $N_f\geq N_c$, we get $W_{dyn}=0$: there is a quantum moduli space of susy vacua. The reason for $W_{dyn}=0$ is because the symmetries require that any dynamical superpotential must depend on M as in eqn. 6, but this is incompatible with the condition that $V_{dyn}\to 0$ for $M\to\infty$, unless the coefficient of W_{dyn} is zero. The classical moduli space is given by expectation values of the mesons and baryons, subject to

some constraints $C(M, B, \widetilde{B}) = 0$. These spaces are singular, because we can solve $C = dC = 0$ at the origin. For $N_f = N_c$ the classical constraint $C = \det M - B\widetilde{B} = 0$ is smoothed out by an instanton to $\det M - B\widetilde{B} = \Lambda^{2N_c}$ [10]. On the other hand for $N_f \neq N_c$ the symmetries don't allow any modification of the classical constraints. To see that, consider the anomalous R-symmetry $U(1)_X$, under which all squarks have $X(\phi) = 0$, which is a valid symmetry if we account for its anomaly by assigning (consider again the 't Hooft vertex) $X(\Lambda^{3N_c - N_f}) = 2(N_c - N_f)$. There is no $U(1)_X$ compatible way for Λ to enter into a modification of $C_{class}(\phi) = 0$ for $N_f \neq N_c$, so $C_{quant} = C_{class}$ and $\mathcal{M}_{quant} = \mathcal{M}_{class}$. Since this space is singular, there must be new d.o.f. at the origin.

These new d.o.f. are given by the Seiberg dual [6], whose gauge group is $SU(\widetilde{N}_c)$, for $\widetilde{N}_c \equiv N_f - N_c$, with $W_{tree} = \Phi q \widetilde{q}$. Here $\Phi \sim M/\Lambda$. The interpretation of the duality has 2 cases: (1) For $N_c < N_f < \frac{3}{2}N_c$ the dual theory is IR free. In this range the original electric theory flows in the IR to the IR free magnetic dual; that is the low-energy effective theory. (2) For $\frac{3}{2}N_c < N_f < 3N_c$, both theories are AF. They flow to the same SCFT in the IR. This is the conformal window.

This duality is part of the multi-interconnected web of dualities in field theory and string theory. Let's mention several of the original, highly non-trivial consistency checks. First, the theories have the same global symmetries, with charges compatible with the map $\Phi \sim M/\Lambda$. The chiral rings of the theories match, including their global charges (baryons are mapped to baryons, and glueballs to glueballs). The many 't Hooft anomalies match; this is a fun exercise to verify, and very convincing (any global symmetry can be at each triangle vertex, to illustrate it consider $SU(N_f)_L^2 U(1)_R$, which in the electric theory gets contributions from the fields Q, giving $N_c \cdot (-\frac{N_c}{N_f})$, and in the magnetic dual gets contributions from Φ and q, giving $N_f \cdot (1 - 2\frac{N_c}{N_f}) + \widetilde{N}_c \cdot (-\frac{\widetilde{N}_c}{N_f})$). The deformations and moduli spaces of the dual theories match (classical properties on one side map to non-perturbative quantum effects in the dual). In particular, we mentioned that $W_{dyn} = 0$ for $N_f > N_c$ massless flavors, but nevertheless the 1PI superpotential W_{dyn} must be generated upon adding $W_{tree} = TrmM$; this works thanks to gaugino condensation in the magnetic dual. See [6,1] for more details.

3. Dynamical susy breaking

As mentioned in the intro, to naturalize hierarchy problems, e.g. $m_W \ll m_{GUT}, m_{pl}$, we are interested in spontaneous susy breaking, where the susy breaking scale is given by $V_{min} = M_s^4$ with $M_s \sim \Lambda$. Susy breaking is non-generic, and difficult to achieve. Metastable susy breaking on the other hand seems generic. As we'll now discuss, there are also additional, phenomenological reasons to consider it.

It is difficult to construct potentially realistic theories of dynamical susy breaking. One general challenge is the R-symmetry problem [12]: a theory with generic superpotential has spontaneous susy breaking iff there is a $U(1)_R$ symmetry. The reason is that the conditions for a susy vacuum, $\partial_i W(X_i)$ are n equations for n variables $X_{i=1\ldots n}$, so generically there is a solution, i.e. a susy vacuum, which is what we're now trying to avoid. A non-R global symmetry doesn't help: there are then say $n-1$ independent equations for $n-1$ independent variables, so still generically solutions. On the other hand, an R symmetry helps: writing $W(X_i) = X_n^{2/r_n} f(t_j \equiv X_j / X_n^{r_j/r_n})$, for $j = 1 \ldots n-1$, the equations $W_i = 0$ now generically nave no solution, because they're n equations for $n-1$ variables t_j. So generic superpotentials spontaneously break susy if, and only if, there is an unbroken R-symmetry.

But an unbroken R-symmetry is bad for phenomenology: it forbids majorana gaugino masses. (Though we won't discuss it here, some models have a different way around this issue: let the gaugino get a Dirac mass, by paring it up with the fermion from an adjoint chiral superfield. See e.g. [13] and the earlier references cited therein.) So we'd like to break the R-symmetry. Purely spontaneous R-breaking is also bad: it leads to unobserved R-axion, which would be a problematically massless Goldstone boson if the R-breaking were entirely spontaneous. We can give the R-axion a mass by introducing explicit breaking. (An ex-

ample of this occurs with SUGRA, see [14].)

We're thus led to consider small explicit R-breaking, associated with some parameter $\epsilon \ll 1$. Now, as we discussed in [15], metastable susy breaking is generically compulsory. The point is that, for $\epsilon = 0$, there is an R-symmetry, and so no susy vacua. There will be a susy breaking vacuum at some finite values of $\langle X \rangle$. Turning on ϵ will not disturb this susy breaking vacuum much. On the other hand, for $\epsilon \neq 0$ there is no R-symmetry, so there must be a susy vacuum, which must run off to infinity when $\epsilon \to 0$, i.e. $\langle X \rangle_{susy} \sim 1/\epsilon^p$ for $p > 0$. The susy-breaking vacuum is now a false vacuum, but the susy breaking vacuum is far away for $\epsilon \ll 1$. The false vacuum decays by nucleating a bubble of true vacuum (with $X = X_{susy}$), like boiling, and as discussed in E. Rabinovici's lecture. Since the vacua are widely separated (and rather degenerate), the decay is parametrically suppressed for $\epsilon \ll 1$, with probability $\sim e^{-S_{bounce}} \sim e^{-1/\epsilon^p} \ll 1$. There is thus a potentially non-empty window of ϵ: it should be small enough for the susy breaking vacuum to be long-lived, but big enough to allow for realistic gaugino (and R-axion) masses; it depends on the example whether or not these conditions are compatible.

Let's discuss some simple examples. Consider first $K_{eff}(X, \bar{X})$ and $W_{eff} = \sum_{p=1}^{n} g_p X^p$. Susy is spontaneously broken if K_{eff} is regular and $n = 1$; for $n > 1$, there are $n - 1$ susy vacua. For $K = X\bar{X}$ and $W = fX$, there is a pseudo-moduli space of susy breaking vacua, with ψ_X the massless goldsino. For F-term susy breaking, the goldstino is part of a chiral superfield, and its superpartner tends to be a pseudomodulus. Taking $K = X\bar{X} - c(X\bar{X})/M^2$, the goldstino superpartner is stabilized at the origin and gets a mass; the goldstino of course remains massless. There is an R-symmetry, and if $\langle X \rangle = 0$ it is not spontaneously broken, whereas if $\langle X \rangle = 0$ it is spontaneously broken and there is a massless R-axion. Adding $\Delta W = \epsilon X^2$ explicitly breaks $U(1)_R$, and there can then be metastable susy breaking.

Next example, the O'R model: $W = \frac{1}{2} h X \phi_1^2 + m\phi_1\phi_2 + fX$, which has a $U(1)_R$ symmetry, with $R[X] = R[\phi_2] = 2$, and $R[\phi_1] = 0$. Susy is spontaneously broken at tree level, with $\langle X \rangle$ the classical pseudomodulus that's the superparter of the goldstino. It's lifted at 1-loop by $V_{CW} = \frac{1}{64\pi^2} \mathrm{Str}(\mathcal{M}^4 \log \frac{\mathcal{M}^2}{M^2_{cutoff}})$, which gives $\langle X \rangle = 0$, so the R-symmetry is not spontaneously broken. We can explicitly break the unwanted R-symmetry by adding $\Delta W = \frac{1}{2}\epsilon m \phi_2^2$. As expected, there is now metastable susy breaking, with a faraway susy vacuum at $\langle X \rangle_{susy} = m/h\epsilon$ [16,15].

Our last example is metastable DSB in SQCD [17] with $W_{tree} = mM$ in the free magnetic phase, taking $m \ll \Lambda$. The theory can be reliably analyzed in the IR free magnetic dual, where $W = \mathrm{Tr}(\Phi q \widetilde{q} - f\Phi)$, with $f = \Lambda m$, which breaks susy by the rank condition. There is a compact moduli space of susy breaking vacua with $\langle M \rangle = 0$ and $\langle q \rangle \neq 0$. This is metastable DSB since there are the N_c susy vacua with $\langle M \rangle \neq 0$ far away (need $\epsilon = m/\Lambda \ll 1$). There is an accidental, approximate R-symmetry, explicitly violated by instantons, consistent with the above comments about explicit breaking of an approximate R-symmetry and metastable DSB. This $U(1)_R$ is not spontaneously broken in the susy breaking vacuum. (Note that we can't take N_f in the conformal window: the metastable susy breaking vacua wouldn't be long-lived.) Many variants and applications of this susy breaking mechanism have been explored in the literature.

4. Aspects of SCFTs and recent topics

In the remaining time, we'll briefly mention a few aspects of 4d SCFTs. There are several possible phenomenology applications of CFTs or nearly CFTs, e.g. (1) Walking technicolor: imagine flowing near a CFT (where the RG running is slowed to walking), and then away; could help separate scales, relax problematic technicolor relations. (2) Suppressing flavor anarchy [18]: try to generate flavor hierarchies from RG running with different anomalous dimensions of different generations. (3) Sequestering, e.g. [19]: try to suppress FCNC problematic Kähler potential operators via enhanced anomalous dimensions. (4) Unparticles [20]: consider phenomenology of $\mathcal{O}_{SM}\mathcal{O}_{CFT}/M^{4-\Delta_{SM}-\Delta_{CFT}}$ interaction. (5) Helping / extending gauge mediation, see e.g.[21,22] for discussion of how large anomalous

dimensions could help alleviate the $\mu/B\mu$ problem of gauge mediation.

The observables of a CFT are the operators, their dimensions, and their correlation functions. Unitarity implies that gauge invariant operator's dimensions satisfy $\Delta \geq j_1 + j_2 + 2 - \delta_{j_1 j_2, 0}$, where the unitarity bound for scalars, $j_1 = j_2 = 0$, is saturated for free fields (see [23] for a recent, physical derivation).

In supersymmetric theories, there is a superconformal $U(1)_R$ symmetry which is in the same supermultiplet as the stress-energy tensor. This will be discussed much more in Zohar Komargodski's lecture and lecture notes. For CFTs, it's enough to just consider the FZ multiplet $\mathcal{T}_{\alpha\dot{\alpha}}$, which contains the stress-energy tensor $T_{\mu\nu}$, supercurrents $S_{\alpha\mu}$ and $\bar{S}_{\dot{\alpha}\mu}$, and a global $U(1)_R$ current j^R_μ: $\mathcal{T}_\mu = j^R_\mu + \theta^\alpha S_{\alpha\mu} + \ldots + (\bar{\theta}\theta)^\nu T_{\mu\nu} + \ldots$. Conservation of the energy tensor and supercurrents is written in superspace as $\bar{D}^{\dot{\alpha}} \mathcal{T}_{\alpha\dot{\alpha}} = D_\alpha X$ where X is a chiral superfield. The F-component of X is related to the lack of scale invariance, and the lack of conservation of the $U(1)_R$ current: $\frac{2}{3} T^\mu_\mu + i\partial^\mu j^R_\mu = X|_{\theta^2}$; in a superconformal theory, $X = 0$.

The holomorphic relation between the dilatation and R-current implies a corresponding relation for the charges of chiral superfields: $\Delta(Q_i) \equiv 1 + \frac{1}{2}\gamma_i(g) = \frac{3}{2} R(Q_i)$, where we'll interpret the RHS as renormalization group running R-charges when the theory is running between RG fixed points. Holomorphy links (non)conservation of the dilatation current to that of the $U(1)_R$ current, and there can be non-conservation contributions both at tree-level, and from anomalies. Matching the ABJ anomaly to the imaginary part of the LHS of eqn. (2) gives the anomaly contribution $X \supset -\frac{1}{16\pi^2} \mathrm{Tr}(RG^2) \mathrm{TrW}^2$. Using holomorphy to link the real and imaginary parts of eqns (2) and (3) gives the multiplet of anomalies $\beta(g^{-2}) = -\frac{3}{2} \frac{1}{16\pi^2} \mathrm{Tr}(RG^2)$ which leads to the puzzle mentioned above: it suggests a 1-loop exact beta function. This puzzle was discussed in many papers, with many proposed resolutions, the most fruitful and inspirational being that of Shifman and Vainshtein and co, which ties in with the NSVZ [5] exact beta function: using $R_i = \frac{2}{3} + \frac{1}{3}\gamma_i$ gives $\beta(g^{-2}) = -\frac{1}{32\pi^2} f_{scheme}(g^2)(3T_2(G) - \sum_i T_2(r_i)(1 - \gamma_i(g^2)))$. The beta function for superpotential couplings is also related to their R-violation, as $W = h\mathcal{O}$ leads to $\beta_h = \frac{3}{2} h(R(\mathcal{O}) - 2)$. We'll now focus on the RG fixed points, where the R-symmetry is conserved.

Again, chiral superfield operators have $R(\Phi) = \frac{2}{3}\Delta(\Phi)$. So chiral, spin 0, gauge invariant operators have the unitarity bound $R \geq \frac{2}{3}$, which is saturated for free fields. If this bound is naively violated, some operator is actually a free-field. As an example, consider SQCD in the conformal window. The superconformal $U(1)_R$ symmetry is uniquely determined to be the anomaly free $U(1)_R$ in the SQCD table. Note that the gauge invariant chiral operators satisfy the unitarity bound. The meson saturates the bound at $N_f = \frac{3}{2} N_c$ showing that it is a free-field there; indeed, the entire theory is IR free magnetic there, as seen from the Seiberg dual.

Let's now mention the 4d conformal anomalies a and c. In 2d, we have $T(z)T(w) = \frac{1}{2} c (z - w)^{-4} + 2T(w)(z - w)^{-2} + \ldots$, and the central charge c (which is positive for unitary theories) is related to the conformal anomaly on a curved space, $\langle T^\mu_\mu \rangle_g = cR$, and also counts the number of d.o.f.. In 4d, the conformal anomaly is $\langle T^\mu_\mu \rangle = a(\mathrm{Euler}) + c(\mathrm{Weyl})^2$. The terms on the RHS are two combinations of the Riemann tensor squared; the Euler term is the topological Euler characteristic density, and the Weyl tensor vanishes in a conformally flat background.

(Aside: holographic theories with Einstein action have $a = c$. Adding R^2 terms, can get $a \neq c$.)

In a supersymmetric theory, a and c can be related to the superconformal $U(1)_R$ 't Hooft anomalies [24], which follows from the susy relation between $T_{\mu\nu}$ and j^μ_R: adding background $U(1)_R$ gauge field and curvature, $X \supset \frac{c}{32\pi^2} \mathcal{W}^2 - \frac{a}{32\pi^2} \Xi$, and then holomorphy in X relates $\langle \partial_\mu j^\mu_R \rangle_A$ to $\langle T^\mu_\mu \rangle_g$, where A is a background coupling to j^μ_R, related by susy to the background metric coupled to $T_{\mu\nu}$. The result is

$$a = \frac{3}{32}(3\mathrm{Tr}R^3 - \mathrm{Tr}R), \quad c = \frac{1}{32}(9\mathrm{Tr}R^3 - 5\mathrm{Tr}R). \quad (7)$$

As an example, the SCFT obtained from SQCD in the conformal window has a and c given by these expressions, with $\mathrm{Tr}R = -N_c^2 -$

1 and $\mathrm{Tr}R^3 = N_c^2 - 1 - 2N_c^4 N_f^{-2}$. Mention a-maximization [25]: among all possible R-symmetries, the exact superconformal R-symmetry is that which locally maximizes $a(R) = \frac{3}{32}(3\mathrm{Tr}R^3 - \mathrm{Tr}R)$ w.r.t. R.

Hofman and Maldacena [26] have argued that a/c is bounded both above and below, by the free vector and matter values. Their argument is to conjecture that the correlation functions of the energy flux operators, $\mathcal{E}(\widehat{n}) = \int dt r^2 n^i T_i^0(t, r\vec{n})|_{r\to\infty}$ should be non-negative. For the case of $\mathcal{N} = 1$ supersymmetric theories, they find (where $\widehat{\epsilon}$ and $\widehat{n}$ are unit vectors)

$$\langle J_R \cdot \epsilon | \mathcal{E}(\widehat{n}) | J_R \cdot \epsilon \rangle = 1 + 3\frac{c-a}{c}(\widehat{\epsilon}\cdot\widehat{n}^2 - \frac{1}{3}), \quad (8)$$

$$\langle T \cdot \epsilon | \mathcal{E}(\widehat{n}) | T \cdot \epsilon \rangle = 1 + 6\frac{c-a}{c}(\frac{\epsilon_{ij}^* \epsilon_{il} n_j n_l}{\epsilon_{ij}^* \epsilon_{ij}} - \frac{1}{3}), (9)$$

where J_R is the superconformal $U(1)_R$ symmetry, T is the stress-energy tensor. The conjectured non-negativity of the RHSs then implies

$$\frac{3}{2} \geq \frac{a}{c} \geq \frac{1}{2}. \quad (10)$$

(similarly, for $\mathcal{N} = 0$ theories it's $\frac{31}{18} \geq \frac{a}{c} \geq \frac{1}{3}$, and for $\mathcal{N} = 2$ theories, it's $\frac{5}{4} \geq \frac{a}{c} \geq \frac{1}{2}$). The upper limit is always saturated by a free vector field, and the lower limit is saturated by a free matter field. The inequalities have been verified to be comfortably satisfied in every example checked.

Note from eqns (8) and (9) that the energy flux is peaked in the direction $\widehat{n}$ parallel to the polarization if $c - a > 0$. Most SCFTs indeed have $c - a > 0$ (i.e. $\mathrm{Tr}R < 0$), e.g. Banks-Zaks type weakly coupled theories, at the top of the conformal window, always do. Looking for examples with $c < a$, two examples come to mind: the $SU(2)$ theory with $I = 3/2$ matter [27] and $SO(N_c)$ with a symmetric tensor [28]. These examples are curious for another reason: they have non-trivial 't Hooft anomaly matching compatible with being IR free, which seems to be a misleading coincidence as we believe that they're instead SCFTs. Also, we cannot be completely sure if $a > c$, if there are unseen accidental symmetries.

As another topic, let's mention flavor currents and their correlation functions. Susy puts flavor currents j_μ in supermultiplets $\mathcal{J}_I = J_I + \theta_\alpha j_{\alpha I} + \theta\bar{\sigma}^\mu\theta j_{\mu I} + \ldots$, with $D^2\mathcal{J} = \bar{D}^2\mathcal{J} = 0$ giving current conservation (I labels the flavor current). The currents have 2-point functions

$$\langle j_{\mu I}(x) j_{\nu J}(0)\rangle = (\eta_{\mu\nu}\partial^2 - \partial_\mu\partial_\nu)\frac{C_{1,IJ}(x^2M^2)}{16\pi^4 x^4},$$

where the 1 subscript is for spin 1. The 2-point functions of the other component, $\langle JJ\rangle$, $\langle j_\alpha \bar{j}_{\dot\alpha}\rangle$, are similarly given by functions $C_{0,IJ}$ and $C_{\frac{1}{2},IJ}$. If susy is unbroken, these functions are all equal.

For SCFTs, $C_{1,IJ} = \tau_{IJ} = -3\mathrm{Tr}RF_IF_J$ is a constant. The two-point function of the flavor currents with the $T_{\alpha\dot\alpha}$ multiplet vanishes, so the 2-point function of flavor currents with the superconformal R-current vanishes, $\tau_{IR} = 0$. This implies that the exact superconformal R-symmetry is uniquely determined (in any spacetime dimension) by the condition that it minimizes τ_{RR} among all possible R-symmetries [29].

In [30], general gauge mediation is defined and the visible sector gaugino and sfermion soft masses are related to the hidden, susy-breaking sector's current 2-point functions [31]

$$m_{gaugino} = \frac{g^2}{4}\int d^4x \langle Q^2(J(x)J(0))\rangle,$$

$$m_{sf}^2 = -\frac{g^4 c_2(r)}{128\pi^2}\int d^4x \log(x^2M^2)\langle Q^4(J(x)J(0))\rangle,$$

which vanishes if susy is unbroken, since then the supercharges Q annihilate the vacuum. From a bottom-up perspective, the hidden sector and their correlators are of course not known. But the above expressions are still predictive, as they yield a subspace of the full soft-breaking parameter space of the MSSM and extensions; that will be explored at the LHC.

Acknowledgments: This was a fantastic, stimulating school. I'd like to congratulate the organizers, and thank them for inviting me, and for the hospitality. My research was supported in part by UCSD grant DOE-FG03-97ER40546.

REFERENCES

1. K. A. Intriligator, N. Seiberg, "Lectures on supersymmetric gauge theories and electric -

magnetic duality," Nucl. Phys. Proc. Suppl. **45BC**, 1-28 (1996). [hep-th/9509066].
2. K. A. Intriligator, N. Seiberg, "Lectures on Supersymmetry Breaking," Class. Quant. Grav. **24**, S741-S772 (2007). [hep-ph/0702069].
3. J. Wess, J. Bagger, "Supersymmetry and supergravity," Princeton, USA: Univ. Pr. (1992) 259 p.
4. N. Seiberg, "The Power of holomorphy: Exact results in 4-D SUSY field theories,"
5. V. A. Novikov, M. A. Shifman, A. I. Vainshtein *et al.*, "Exact Gell-Mann-Low Function of Supersymmetric Yang-Mills Theories from Instanton Calculus," Nucl. Phys. **B229**, 381 (1983).
6. N. Seiberg, "Electric - magnetic duality in supersymmetric nonAbelian gauge theories," Nucl. Phys. **B435** (1995) 129-146. [hep-th/9411149].
7. G. F. Giudice, R. Rattazzi, "Theories with gauge mediated supersymmetry breaking," Phys. Rept. **322**, 419-499 (1999). [hep-ph/9801271].
8. K. A. Intriligator, R. G. Leigh, N. Seiberg, "Exact superpotentials in four-dimensions," Phys. Rev. **D50**, 1092-1104 (1994). [hep-th/9403198].
9. K. A. Intriligator, "'Integrating in' and exact superpotentials in 4-d," Phys. Lett. **B336**, 409-414 (1994). [hep-th/9407106].
10. N. Seiberg, "Exact results on the space of vacua of four-dimensional SUSY gauge theories," Phys. Rev. **D49**, 6857-6863 (1994). [hep-th/9402044].
11. Z. Fodor, K. Holland, J. Kuti *et al.*, "Chiral symmetry breaking in nearly conformal gauge theories," PoS **LAT2009**, 055 (2009). [arXiv:0911.2463 [hep-lat]].
12. A. E. Nelson, N. Seiberg, "R symmetry breaking versus supersymmetry breaking," Nucl. Phys. **B416**, 46-62 (1994). [hep-ph/9309299].
13. S. D. L. Amigo, A. E. Blechman, P. J. Fox, E. Poppitz, "R-symmetric gauge mediation," JHEP **0901**, 018 (2009). [arXiv:0809.1112 [hep-ph]].
14. J. Bagger, E. Poppitz, L. Randall, "The R axion from dynamical supersymmetry breaking," Nucl. Phys. **B426**, 3-18 (1994). [hep-ph/9405345].
15. K. A. Intriligator, N. Seiberg, D. Shih, "Supersymmetry breaking, R-symmetry breaking and metastable vacua," JHEP **0707**, 017 (2007). [hep-th/0703281].
16. M. Dine, J. L. Feng, E. Silverstein, "Retrofitting O'Raifeartaigh models with dynamical scales," Phys. Rev. **D74**, 095012 (2006). [hep-th/0608159].
17. K. A. Intriligator, N. Seiberg, D. Shih, "Dynamical SUSY breaking in meta-stable vacua," JHEP **0604**, 021 (2006). [hep-th/0602239].
18. A. E. Nelson, M. J. Strassler, "Suppressing flavor anarchy," JHEP **0009**, 030 (2000). [hep-ph/0006251]..
19. M. A. Luty and R. Sundrum, "Supersymmetry breaking and composite extra dimensions," Phys. Rev. D **65**, 066004 (2002) [arXiv:hep-th/0105137].
20. H. Georgi, "Unparticle Physics," Phys. Rev. Lett. **98**, 221601 (2007) [arXiv:hep-ph/0703260].
21. T. S. Roy and M. Schmaltz, "A hidden solution to the μ/B_μ problem in gauge mediation," Phys. Rev. D **77**, 095008 (2008) [arXiv:0708.3593 [hep-ph]].
22. H. Murayama, Y. Nomura and D. Poland, "More Visible Effects of the Hidden Sector," Phys. Rev. D **77**, 015005 (2008) [arXiv:0709.0775 [hep-ph]].
23. B. Grinstein, K. A. Intriligator, I. Z. Rothstein, "Comments on Unparticles," Phys. Lett. **B662**, 367-374 (2008). [arXiv:0801.1140 [hep-ph]].
24. D. Anselmi, D. Z. Freedman, M. T. Grisaru *et al.*, "Nonperturbative formulas for central functions of supersymmetric gauge theories," Nucl. Phys. **B526**, 543-571 (1998). [hep-th/9708042].
25. K. A. Intriligator, B. Wecht, "The Exact superconformal R symmetry maximizes a," Nucl. Phys. **B667**, 183-200 (2003). [hep-th/0304128]..
26. D. M. Hofman, J. Maldacena, "Conformal collider physics: Energy and charge correlations," JHEP **0805**, 012 (2008).

[arXiv:0803.1467 [hep-th]].
27. K. A. Intriligator, N. Seiberg, S. H. Shenker, "Proposal for a simple model of dynamical SUSY breaking," Phys. Lett. **B342**, 152-154 (1995). [hep-ph/9410203].
28. J. H. Brodie, P. L. Cho, K. A. Intriligator, "Misleading anomaly matchings?," Phys. Lett. **B429**, 319-326 (1998). [hep-th/9802092].
29. E. Barnes, E. Gorbatov, K. A. Intriligator, M. Sudano, J. Wright, "The Exact superconformal R-symmetry minimizes tau(RR)," Nucl. Phys. **B730**, 210-222 (2005). [hep-th/0507137].
30. P. Meade, N. Seiberg, D. Shih, "General Gauge Mediation," Prog. Theor. Phys. Suppl. **177**, 143-158 (2009). [arXiv:0801.3278 [hep-ph]].
31. M. Buican, P. Meade, N. Seiberg, D. Shih, "Exploring General Gauge Mediation," JHEP **0903**, 016 (2009). [arXiv:0812.3668 [hep-ph]].

Aspects of Supersymmetry and its Breaking

Thomas T. Dumitrescu[a*] and Zohar Komargodski[b†]

[a]Department of Physics, Princeton University,
Princeton, New Jersey, 08544, USA

[b]School of Natural Sciences, Institute for Advanced Study,
Princeton, New Jersey, 08540, USA

We describe some basic aspects of supersymmetric field theories, emphasizing the structure of various supersymmetry multiplets. In particular, we discuss supercurrents – multiplets which contain the supersymmetry current and the energy-momentum tensor – and explain how they can be used to constrain the dynamics of supersymmetric field theories, supersymmetry breaking, and supergravity.

1. Supersymmetric Theories

1.1. Supermultiplets and Superfields

A four-dimensional theory possesses $\mathcal{N} = 1$ supersymmetry (SUSY) if it contains a conserved spin-$\frac{1}{2}$ charge Q_α which satisfies the anti-commutation relation

$$\{Q_\alpha, \bar{Q}_{\dot{\alpha}}\} = 2\sigma^\mu_{\alpha\dot{\alpha}} P_\mu \ . \tag{1}$$

Here $\bar{Q}_{\dot{\alpha}}$ is the Hermitian conjugate of Q_α. (We will use bars throughout to denote Hermitian conjugation.) Unless otherwise stated, we follow the conventions of [1]. In local quantum field theories, the basic objects of interest are well-defined local operators. In SUSY field theories all such operators must be embedded in multiplets of the supersymmetry algebra, or *supermultiplets*. Conserved currents furnish an important class of local operators. Of particular interest is the supersymmetry current $S_{\alpha\mu}$, which satisfies

$$\partial^\mu S_{\alpha\mu} = 0 \ , \qquad Q_\alpha = \int d^3x \, S_\alpha{}^0 \ . \tag{2}$$

*T.D. is supported by a DOE Fellowship in High Energy Theory, NSF grant PHY-0756966, and a Centennial Fellowship from Princeton University.

†Z.K. is supported by DOE grant DE-FG02-90ER40542. Any opinions, findings, and conclusions or recommendations expressed in this material are those of the authors and do not necessarily reflect the views of the National Science Foundation.

In this review we will describe some basic aspects of SUSY field theories, emphasizing the structure of various supermultiplets – especially those containing the supersymmetry current. In particular, we will show how these supercurrents can be used to study the dynamics of supersymmetric field theories, SUSY-breaking, and supergravity.

We begin by recalling basic facts about supermultiplets and superfields. A set of bosonic and fermionic operators $\{\mathcal{O}_i^B(x)\}$ and $\{\mathcal{O}_i^F(x)\}$ furnishes a supermultiplet if these operators satisfy commutation relations of the schematic form

$$\begin{aligned} \big[Q_\alpha, \mathcal{O}_i^B(x)\big] &\sim \mathcal{O}_j^F(x) + \partial\mathcal{O}_k^F(x) + \cdots \ , \\ \big\{Q_\alpha, \mathcal{O}_i^F(x)\big\} &\sim \mathcal{O}_j^B(x) + \partial\mathcal{O}_k^B(x) + \cdots \ , \end{aligned} \tag{3}$$

and likewise for the $\bar{Q}_{\dot{\alpha}}$ commutators, such that the SUSY algebra (1) is satisfied. It is straightforward to show that a supermultiplet must contain equally many independent bosonic and fermionic operators (see, for instance, [2]).

It is always possible (and very convenient) to embed the component fields $\mathcal{O}_i^{B,F}(x)$ of a supermultiplet in a superfield $S(x, \theta, \bar{\theta})$. Here θ_α is an anti-commuting superspace coordinate. (For now we suppress any Lorentz indices carried by S.) The component fields are identified with the x-dependent coefficients when $S(x, \theta, \bar{\theta})$ is expanded as a power series in $\theta, \bar{\theta}$. The commutation rela-

tions (3) are succinctly encoded in the formula

$$\left[\xi Q + \bar{\xi}\bar{Q}, S\right] = i\left(\xi \mathcal{Q} + \bar{\xi}\bar{\mathcal{Q}}\right) S \ , \tag{4}$$

which is the defining property of a superfield.[3] Here ξ_α is an arbitrary Grassmann parameter and $\mathcal{Q}_\alpha, \bar{\mathcal{Q}}_{\dot{\alpha}}$ are the superspace differential operators

$$\begin{aligned} \mathcal{Q}_\alpha &= \frac{\partial}{\partial\theta^\alpha} - i\sigma^\mu_{\alpha\dot{\alpha}}\bar{\theta}^{\dot{\alpha}}\partial_\mu \ , \\ \bar{\mathcal{Q}}_{\dot{\alpha}} &= -\frac{\partial}{\partial\bar{\theta}^{\dot{\alpha}}} + i\sigma^\mu_{\alpha\dot{\alpha}}\partial_\mu \ . \end{aligned} \tag{5}$$

Conversely, the defining property (4) implies that the components of any superfield furnish a supermultiplet. Thus, supermultiplets and superfields are in one-to-one correspondence, and we will treat them synonymously.

To see this in a little more detail, consider the component expansion of a general scalar superfield:

$$S(x,\theta,\bar{\theta}) = C(x) + i\theta^\alpha\psi_\alpha(x) + \cdots + \theta^2\bar{\theta}^2 D(x) \ . \tag{6}$$

As explained above, the defining property (4) determines the commutation relations of the supercharges $Q_\alpha, \bar{Q}_{\dot{\alpha}}$ with the component fields. These commutators show that the supercharges act as raising operators for the component fields.[4] This has two important consequences:

- The superfield $S(x,\theta,\bar{\theta})$ can be constructed from its bottom component $C(x)$ by applying the supercharges. Thus, any local operator can be embedded in the bottom component of a superfield. However, it is *not* always possible to embed an operator in a higher component. This will play a crucial role in our analysis of various supercurrents.

- The SUSY variation of the top component $D(x)$ of any superfield is always a total derivative. This fact will enable us to write supersymmetric Lagrangians.

[3] The factor of i in (4) is necessary for Hermiticity in Minkowski space.

[4] For instance, $[Q_\alpha, C] = -\psi_\alpha$.

A general superfield does not furnish an irreducible representation of supersymmetry. To reduce a supermultiplet, we impose supersymmetric constraints. This is most conveniently done in terms of the superspace differential operators

$$\begin{aligned} D_\alpha &= \frac{\partial}{\partial\theta^\alpha} + i\sigma^\mu_{\alpha\dot{\alpha}}\bar{\theta}^{\dot{\alpha}}\partial_\mu \ , \\ \bar{D}_{\dot{\alpha}} &= -\frac{\partial}{\partial\bar{\theta}^{\dot{\alpha}}} - i\sigma^\mu_{\alpha\dot{\alpha}}\partial_\mu \ . \end{aligned} \tag{7}$$

These anti-commute with the supersymmetry generators $\mathcal{Q}_\alpha, \bar{\mathcal{Q}}_{\dot{\alpha}}$, and thus map superfields to superfields. Hence, any constraint written in terms of $D_\alpha, \bar{D}_{\dot{\alpha}}$ is automatically supersymmetric. We are now ready to begin exploring various important supermultiplets.

1.2. Chiral Multiplets and Lagrangians

The most familiar representation of supersymmetry is the chiral multiplet. It is the basic building block which enables us to write SUSY Lagrangians describing only scalars and fermions. The bottom component of a chiral multiplet is annihilated by $\bar{Q}_{\dot{\alpha}}$. For example, the bottom component $\phi(x)$ of a scalar chiral multiplet satisfies

$$\left[\bar{Q}_{\dot{\alpha}}, \phi(x)\right] = 0 \ . \tag{8}$$

The multiplet obtained from $\phi(x)$ by acting with the supercharges is organized in a superfield which satisfies the constraint $\bar{D}_{\dot{\alpha}}\Phi = 0$. This constraint can be solved in components:

$$\Phi = \phi(y) + \sqrt{2}\theta\psi(y) + \theta^2 F(y) \ , \tag{9}$$

where $y^\mu = x^\mu + \theta\sigma^\mu\bar{\theta}$. We immediately note two key properties of chiral superfields:

- Any function which depends on the chiral superfields Φ^i, but not their complex conjugates, is again a chiral superfield. Such a function is said to be holomorphic in the Φ^i.

- The SUSY variation of $F(x)$ is a total derivative.

From (9) we see that Φ contains a complex scalar ϕ, a Weyl fermion ψ_α, and another complex scalar F which will turn out to be a non-propagating auxilliary field. Among other things,

F ensures that the chiral multiplet has four (real) bosonic degrees of freedom to match the four fermionic degrees of freedom coming from ψ_α. We will abbreviate this by saying that Φ is a $4+4$ multiplet. As advertised, Φ has exactly the right field content to describe a theory of scalars and fermions, and we would like to write a Lagrangian for such a theory.

Up to total derivatives, a SUSY Lagrangian $\mathscr{L}$ must be a real scalar whose variation under supersymmetry is a total derivative. We can thus take

$$\mathscr{L} = D + F + \bar{F} \ , \tag{10}$$

where D is the top component of a real scalar superfield $K = \bar{K}$ and F is the θ^2-component of a chiral superfield W. This ensures that $\mathscr{L}$ is real and supersymmetric. For reasons that will be explained below, K is known as the Kähler potential, and W is called the superpotential. A particularly simple choice is to take $K = \bar{\Phi}\Phi$ and $W = 0$. It is standard to pick out different components of a superfield using Grassmann integration. For example, we can use $\int d^4\theta$ to pick out the top component of a superfield, or $\int d^2\theta$ to pick out the θ^2 component. We thus write

$$\mathscr{L} = \int d^4\theta \, \bar{\Phi}\Phi \ , \tag{11}$$

up to total derivatives. In components:

$$\mathscr{L} = -\partial^\mu \bar{\phi} \partial_\mu \phi + i \partial_\mu \psi \sigma^\mu \bar{\psi} + \bar{F} F \ . \tag{12}$$

This describes a free complex scalar ϕ, a free Weyl fermion ψ_α, and a non-propagating auxiliary field F. In this example F vanishes by its equations of motion. Because the choice $K = \bar{\Phi}\Phi$ gives rise to the usual kinetic terms for ϕ and ψ_α, it is called a canonical Kähler potential.

This trivial free theory can be readily generalized: consider N chiral superfields Φ^i and consider the Lagrangian

$$\mathscr{L} = \int d^4\theta \, K(\Phi, \bar{\Phi}) \ , \tag{13}$$

where the Kähler potential K may now be a complicated real function of the Φ^i and their complex conjugates. (The superpotential W is still taken to vanish.) After solving for the auxiliary fields F^i, which are now non-zero, the component Lagrangian takes the form

$$\begin{aligned} \mathscr{L} = & -g_{i\bar{j}} \left(\phi, \bar{\phi}\right) \partial_\mu \bar{\phi}^{\bar{j}} \partial^\mu \phi^i + i g_{i\bar{j}} \, \partial_\mu \psi^i \sigma^\mu \bar{\psi}^{\bar{j}} \\ & + i g_{i\bar{j}} \Gamma^i_{kl} \left(\partial_\mu \phi^k\right) \psi^l \sigma^\mu \bar{\psi}^{\bar{j}} + \frac{1}{4} R_{i\bar{j}k\bar{l}} \, \psi^i \psi^k \, \bar{\psi}^{\bar{j}} \bar{\psi}^{\bar{l}} \end{aligned} \tag{14}$$

This theory is known as the supersymmetric non-linear σ-model. The bosonic part is an ordinary σ-model, whose target space is an N complex dimensional manifold with metric $g_{i\bar{j}}$. Since the Lagrangian (14) does not have a potential term, any point ϕ^i on the target manifold is a supersymmetric vacuum. (Recall that it follows from the SUSY algebra (1) that supersymmetric vacua have zero energy; vacua with positive energy spontaneously break SUSY.) In supersymmetric theories, it is customary to refer to such manifolds of vacua as moduli spaces. As usual, the scalars ϕ^i should be thought of as coordinates on the target space. This is consistent with the fact that the theory is invariant under holomorphic field redefinitions of the form

$$\Phi'^i = f^i(\Phi^j) \ . \tag{15}$$

Such field redefinitions can be thought of as coordinate changes on the target manifold under which the metric transforms in the usual tensorial way.

In the supersymmetric σ-model, the metric is determined by the Kähler potential:

$$g_{i\bar{j}} = \partial_i \partial_{\bar{j}} K \ . \tag{16}$$

Thus, the target space is a Kähler manifold. Note that $g_{i\bar{j}}$ must be positive definite so that the kinetic terms in (14) have the correct sign required by unitarity. The fermions couple to the geometry of this Kähler manifold through the connection Γ^i_{jk} and the curvature tensor $R_{i\bar{j}k\bar{l}}$, which depend on the metric and its derivatives. Under a coordinate chage (15) the fermions transform as $\psi'^i = \frac{\partial \phi'^i}{\partial \phi_j} \psi^j$. They can thus be identified with vectors in the tangent space of the target manifold.

The dynamics of the non-linear σ-model is unchanged under redefinitions of the Kähler poten-

tial which take the form

$$K'(\Phi,\bar{\Phi}) = K(\Phi,\bar{\Phi}) + F(\Phi) + \bar{F}(\bar{\Phi}) \ , \qquad (17)$$

for some holomorphic function F of the Φ^i. This is known as a Kähler transformation. Such a transformation only changes the Lagrangian by a total derivative. This is because $F(\Phi^i)$ is chiral so that its top component is a total derivative. Alternatively, we see from (16) that the metric $g_{i\bar{j}}$ is unaffected by Kähler transformations, so that the component Lagrangian (14) is also unchanged.

It is important to note that while we are always free to perform Kähler transformations, there are situations in which we are forced to do so. This is the case whenever the target manifold has nontrivial topology and must be covered with several patches which make it impossible to consistently define a single-valued Kähler potential. In this case we are forced to use different Kähler potentials in different patches. These Kähler potentials must be related by a Kähler transformation whenever two patches overlap.

As an example of a supersymmetric σ-model which illustrates this point, we consider a single chiral superfield Φ with Kähler potential

$$K = f_\pi^2 \log\left(1 + |\Phi|^2\right) \ . \qquad (18)$$

In this normalization Φ is dimensionless, while the constant f_π has dimensions of mass.[5] The metric is $g_{\phi\bar{\phi}} = \frac{f_\pi^2}{(1+|\phi|^2)^2}$, which we recognize as the familiar round metric on the two-sphere with radius $\sim f_\pi$. The coordinate values $\phi = 0$ and $\phi = \infty$ correspond to antipodal points. As we explained above, the moduli space of SUSY vacua is just the two-sphere itself. This theory is usually referred to as the $\mathbb{CP}^1$-model. The Kähler potential (18) gives rise to the Fubini-Study metric on $\mathbb{CP}^1$, which is nothing but the round metric on the two-sphere.

To describe the point at infinity, we must perform a change of variables $\Phi \to 1/\Phi$. This induces a Kähler transformation (17) with $F(\Phi) = f_\pi^2 \log(\Phi)$. It is, in fact, impossible to cover the two-sphere (or, as we will later explain, any other compact manifold) with patches in such a way that K is a globally well-defined scalar.

So far we have only discussed theories without a superpotential W, such as the SUSY σ-model (13). These theories did not have any scalar potential. The simplest example with a superpotential is a single chiral superfield Φ with canonical Kähler potential and with superpotential $W = \frac{1}{2}m\Phi^2$. After integrating out the auxiliary field F, this leads to the component Lagrangian

$$\begin{aligned}\mathscr{L} = &- \partial^\mu\bar{\phi}\partial_\mu\phi - |m|^2|\phi|^2 + i\partial_\mu\psi\sigma^\mu\bar{\psi} \\ &- \frac{1}{2}m\psi^2 - \frac{1}{2}m^*\bar{\psi}^2 \ . \end{aligned} \qquad (19)$$

Thus, ϕ and ψ both acquire a mass $|m|$.

More generally, we can take the SUSY σ-model (13) and add a superpotential $W(\Phi^i)$. Since W must be chiral, it must be holomorphic in the Φ^i. The resulting theory is called a Wess-Zumino model:

$$\mathscr{L} = \int d^4\theta\, K(\Phi,\bar{\Phi}) + \int d^2\theta\, W(\Phi) + \text{c.c.} \ . \qquad (20)$$

After integrating out the auxiliary fields, this adds to the component Lagrangian (14) of the σ-model a scalar potential and Yukawa-type interactions:

$$\begin{aligned}\mathscr{L} \supset &- g^{i\bar{j}}\partial_i W \partial_{\bar{j}}\bar{W} \\ &- \frac{1}{2}\left(\left(\partial_i\partial_j W - \Gamma^k_{ij}\partial_k W\right)\psi^i\psi^j + \text{c.c.}\right) \ . \end{aligned} \qquad (21)$$

The vacua of this theory are given by the minima of the scalar potential which appears in the first line of (21). Since supersymmetric vacua have zero energy and the metric $g_{i\bar{j}}$ is positive definite, the space of SUSY vacua is specified by the N complex equations $\partial_i W = 0$ in the N complex unknowns ϕ^i. This implies that without any further structure Wess-Zumino models generally have SUSY vacua. In section 3, we will explore some simple theories whose vacua spontaneously break supersymmetry.

1.3. Vector Multiplets and Gauge Theories

In this section we will describe the vector multiplet, which will enable us to write Lagrangians

[5] This notation is due to the fact that f_π is the analogue of the pion decay constant in the chiral Lagrangian for QCD. Our example (18) describes the coset manifold $SU(2)/U(1) = \mathbb{CP}^1$.

for supersymmetric gauge theories. For simplicity we will limit ourselves to the Abelian case. A vector multiplet is a real superfield $V = \bar{V}$, subject to the gauge transformations

$$V \to V + i\left(\Lambda - \bar{\Lambda}\right) \ , \tag{22}$$

where Λ is a chiral superfield. These gauge transformations allow us to fix Wess-Zumino gauge in which the low-lying components of V vanish:

$$V = -\left(\theta\sigma^\mu\bar{\theta}\right) A_\mu + i\theta^2\bar{\theta}\bar{\lambda} - i\bar{\theta}^2\theta\lambda + \frac{1}{2}\theta^2\bar{\theta}^2 D \ . \tag{23}$$

Here A_μ is a real gauge field, the Weyl fermion λ_α is its gaugino superpartner, and D is a real scalar auxiliary field. The residual gauge freedom which remains in Wess-Zumino gauge just consists of ordinary gauge-transformations for A_μ.

To capture the gauge-invariant information in V, we can define the superfield

$$W_\alpha = -\frac{1}{4}\bar{D}^2 D_\alpha V \ , \tag{24}$$

which is invariant under (22). From this definition, we immediately see that W_α satisfies the constraints

$$\bar{D}_{\dot{\alpha}} W_\alpha = 0 \ , \qquad D^\alpha W_\alpha = \bar{D}_{\dot{\alpha}} \bar{W}^{\dot{\alpha}} \ . \tag{25}$$

In components:

$$W_\alpha = -i\lambda_\alpha(y) + \theta_\beta\Big(\delta_\alpha{}^\beta D(y) - i(\sigma^{\mu\nu})_\alpha{}^\beta F_{\mu\nu}(y)\Big) + \theta^2\sigma^\mu_{\alpha\dot{\alpha}}\partial_\mu\bar{\lambda}^{\dot{\alpha}}(y) \ , \tag{26}$$

where the closed, real two-form $F_{\mu\nu} = \partial_\mu A_\nu - \partial_\nu A_\mu$ is the field strength of A_μ. We therefor refer to W_α as a field strength superfield. We see that W_α is a $4+4$ multiplet, corresponding to the $4+4$ gauge-invariant degrees of freedom in V.

For future reference, we note that any spinor superfield W_α which satisfies the constraints (25) has the component expansion (26) for some closed, real two-form $F_{\mu\nu}$. Locally, we can always express such a two-form as $F_{\mu\nu} = \partial_\mu A_\nu - \partial_\nu A_\mu$ for some vector A_μ, and we can consequently write W_α as in (24) for some vector superfield V. However, in general A_μ and V are not well-defined: they may undergo gauge-transformations.

The superfield W_α has exactly the right field content to write supersymmetric kinetic terms for the gauge field and the gaugino. Since W_α is chiral, we can take

$$\begin{aligned}\mathscr{L} &= \frac{1}{4e^2}\int d^2\theta\, W^\alpha W_\alpha + \text{c.c.} \\ &= -\frac{1}{4e^2}F^{\mu\nu}F_{\mu\nu} + \frac{i}{e^2}\partial_\mu\lambda\sigma^\mu\bar{\lambda} + \frac{1}{2e^2}D^2 \ .\end{aligned} \tag{27}$$

Here e is the gauge coupling. In this simple free theory the auxiliary field D vanishes by its equations of motion.

In Abelian gauge theories, it is possible to add a so-called Fayet-Iliopoulos (FI) term to the Lagrangian:

$$\mathscr{L}_{\text{FI}} = \xi\int d^4\theta V \ . \tag{28}$$

Here the FI-parameter ξ is real. The FI-term is gauge invariant because the top-component of a chiral superfield is a total derivative. Note that the gauge-invariance of the FI-term resembles the invariance of the Wess-Zumino Lagrangian (20) under Kähler transformations. This connection will resurface in later sections.

2. Global Symmetries

2.1. Global Current Supermultiplets

In local quantum field theories, the Noether theorem guarantees that each continuous global symmetry gives rise to a conserved current j^μ satisfying

$$\partial^\mu j_\mu = 0 \ , \qquad Q = \int d^3x\, j^0 \ . \tag{29}$$

Here Q is the conserved charge corresponding to j^μ. In this review, we will not discuss R-symmetries, so that Q is just an ordinary global symmetry.[6] In SUSY theories, we must embed j^μ in some supermultiplet. In order to decide what constraints this superfield will satisfy, we are guided by the following two observations:

[6] An R-symmetry is a global symmetry which does not commute with SUSY: $[R, Q_\alpha] = -Q_\alpha$.

- Because Q is an ordinary global symmetry charge, it commutes with SUSY, $[Q_\alpha, Q] = 0$. This implies the current algebra

$$[Q_\alpha, j_\mu] = (\text{S.T.}) \ . \tag{30}$$

  The right-hand-side of this equation is conserved when acting with ∂^μ on both sides, and it is a total space-derivative when $\mu = 0$ so that it integrates to zero; it is known as a Schwinger Term (S.T.).

- We expect j^μ to be the highest spin component in its supermultiplet. If this is not the case, we could not gauge j^μ without introducing higher-spin gauge fields. This is not expected to be consistent in rigid field theories without gravity.

We thus posit that j^μ is embedded in a real, scalar superfield $\mathcal{J}$ which schematically takes the form

$$\mathcal{J} = J + i\theta j - i\bar{\theta}\bar{j} + \left(\theta\sigma^\mu\bar{\theta}\right)(j_\mu + \cdots) + \cdots \ . \tag{31}$$

Here J is a real scalar, and j_α is a Weyl fermion. The dots are terms which are not uniquely fixed by the requirements outlined above. Different choices of Schwinger terms in (30) terms lead to different ways of completing the multiplet. Although there is a constructive way of writing the most general solution, we will not follow this approach here. Instead, we will simply write down a set of constraints for $\mathcal{J}$ and explore the resulting component structure.

Conventionally, the global current supermultiplet $\mathcal{J}$ is taken to satisfy

$$D^2\mathcal{J} = \bar{D}^2\mathcal{J} = 0 \ . \tag{32}$$

A real superfield obeying these constraints is called a linear multiplet. In components, such a multiplet takes the form

$$\begin{aligned}\mathcal{J} = {} & J + i\theta j - i\bar{\theta}\bar{j} + \left(\theta\sigma^\mu\bar{\theta}\right) j_\mu \\ & + \frac{1}{2}\theta^2\bar{\theta}\bar{\sigma}^\mu\partial_\mu j - \frac{1}{2}\bar{\theta}^2\theta\sigma^\mu\partial_\mu\bar{j} - \frac{1}{4}\theta^2\bar{\theta}^2\partial^2 J \ ,\end{aligned} \tag{33}$$

where j_μ is the conserved vector current. We immediately see that $\mathcal{J}$ contains no higher-spin components. Moreover, we can use (4) on (33) to extract the commutation relation

$$[Q_\alpha, j_\mu] = -2i(\sigma_{\mu\nu})_\alpha{}^\beta\partial^\nu j_\beta \ , \tag{34}$$

whose right-hand-side is indeed a pure Schwinger term. Having familiarized ourself with the structure of the global current multiplet (33), we can now explore how it arises in theories with global symmetries.

We begin by revisiting the free theory of a chiral superfield (11), which is invariant under $U(1)$ phase rotations of Φ. This corresponds to the invariance of the component theory (12) under $U(1)$ phase rotations of ϕ, ψ_α and F. The equation of motion $D^2\Phi = 0$ implies that $\mathcal{J} = \bar{\Phi}\Phi$ is a linear multiplet, which in the normalization of (33) contains the conserved vector current

$$j_\mu = i\left(\bar{\phi}\partial_\mu\phi - \partial_\mu\bar{\phi}\phi\right) + \bar{\psi}\bar{\sigma}_\mu\psi \ . \tag{35}$$

This is the usual $U(1)$ phase current which gives charge $+1$ to ϕ and ψ_α.[7]

More generally, we can consider continuous global symmetries of the SUSY σ-model (13). Assume that this theory is invariant under the infinitesimal global symmetry transformation

$$\delta\Phi^i = \varepsilon^{(a)}X^{(a)i}(\Phi) \ . \tag{36}$$

Here the $X^{(a)i}$ are holomorphic in the Φ^i and the $\varepsilon^{(a)}$ are infinitesimal real parameters; we will use indices $a, b, \ldots$ to label different global symmetries. The transformation (36) must leave the metric $g_{i\bar{j}}$ invariant.[8] However, the Lagrangian (13) may pick up a Kähler transformation:

$$\delta\mathscr{L} = \int d^4\theta\,\varepsilon^{(a)}\left(F^{(a)}(\Phi) + \bar{F}^{(a)}(\bar{\Phi})\right) \ , \tag{37}$$

where the functions $F^{(a)}$ are holomorphic in the Φ^i. This only changes the Lagrangian by a total derivative.

[7] In our convention, an operator $\mathcal{O}$ has charge q under the symmetry generated by Q if it satisfies $[Q, \mathcal{O}] = q\mathcal{O}$.

[8] Geometrically, this means that the $X^{(a)i}$ are the components of holomorphic Killing vector fields $X^{(a)} = X^{(a)i}\partial_i$.

To find the conserved currents corresponding to the symmetries (36), we perform the superspace analog of the usual Noether procedure: replace each infinitesimal transformation parameter $\varepsilon^{(a)}$ with an arbitrary infinitesimal chiral superfield $\Lambda^{(a)}$. (The fact that the $\Lambda^{(a)}$ are chiral ensures that the variations of the chiral superfields Φ^i are still chiral.) To linear order in the $\Lambda^{(a)}$, the change in the Lagrangian must now take the form

$$\delta\mathscr{L} = \int d^4\theta\, \Lambda^{(a)} \left(F^{(a)} - i\mathcal{J}^{(a)}\right) + \text{c.c.} \ , \qquad (38)$$

for some real superfields $\mathcal{J}^{(a)}$. Note that (38) reduces to (37) if we set $\Lambda^{(a)} = \varepsilon^{(a)}$. However, using the explicit form (36) of the infinitesimal transformation with $\varepsilon^{(a)}$ replaced by $\Lambda^{(a)}$, we can also write the change in the Lagrangian as

$$\delta\mathscr{L} = \int d^4\theta\, \Lambda^{(a)} X^{(a)i} \partial_i K + \text{c.c.} \ . \qquad (39)$$

Since (38) and (39) must agree for all chiral superfields $\Lambda^{(a)}$, we can identify the Noether currents

$$\mathcal{J}^{(a)} = iX^{(a)i}\partial_i K - iF^{(a)} \ . \qquad (40)$$

These are guaranteed to be real and conserved, as can be checked using the sigma model equations of motion $D^2\partial_{\bar{i}}K = 0$. Note that the Noether currents (40) depend on the functions $F^{(a)}$ which appear in the Kähler transformation (37). This is not surprising: when the Lagrangian changes by a total derivative under a symmetry transformation, then the Noether current acquires an additional piece.

Such a situation can arise even in the trivial theory (11). This theory has a shift symmetry $\delta\Phi = \varepsilon$ under which the Lagrangian undergoes a Kähler transformation with $F = \Phi$. By (40), the Noether current for this symmetry is given by

$$\mathcal{J} = i(\bar{\Phi} - \Phi) \ . \qquad (41)$$

An interesting complication occurs if we compactify the target space of this model to a cylinder by identifying $\Phi \sim \Phi + i$. As we go around the cylinder once, the bottom component of $\mathcal{J}$ shifts by a constant. It is thus not a good operator in the theory. In this case, we cannot embed the vector current corresponding to the shift symmetry in the linear multiplet $\mathcal{J}$. This also means that we cannot gauge the shift symmetry in the usual way (see subsection 2.2). This difficutly can be overcome by embedding j_μ in a different multiplet which is well-defined. (The details of this procedure are beyond the scope of this review.) Conceptually, this situation has an exact analogue for multiplets containing the supersymmetry current $S_{\alpha\mu}$ and the energy-momentum tensor $T_{\mu\nu}$, to be discussed in detail below.

2.2. Gauging Global Symmetries

In order to couple matter to a gauge field A_μ, we add to the Lagrangian a term

$$\delta\mathscr{L} \sim j_\mu A^\mu + \cdots \ . \qquad (42)$$

Here j_μ is a conserved matter current, so that this interaction is invariant under gauge transformations of A_μ. If the current j_μ itself transforms under gauge transformations, then (42) contains additional terms (represented by the dots) with higher powers of A_μ to ensure gauge invariance. They will not be important for us, and we will not discuss them.

In SUSY theories, the analogue of (42) is given by the coupling

$$\delta\mathscr{L} = \int d^4\theta \mathcal{J} V \ , \qquad (43)$$

where $\mathcal{J}$ is a linear multiplet and V is a vector multiplet. Since $D^2\mathcal{J} = 0$, this interaction term is invariant under gauge transformations (22) of V. In addition to the term in (42), the interaction (43) contains Yukawa-type interactions for the gaugino λ_α, as well as a coupling of the bottom component J of $\mathcal{J}$ to the auxiliary field D of the vector multiplet V. When D is integrated out, it gives rise to a new contribution to the scalar potential:

$$V_D = \frac{e^2}{8}\left(J + \xi\right)^2 \ , \qquad (44)$$

where e is the gauge coupling and ξ is an FI-term, which may be present. We refer to (44) as a D-term potential, since it arises from integrating out

the D-component of a vector multiplet. This is to be contrasted with the scalar potentials discussed at the end of subsection 1.2, which were the result of integrating out the F-components of chiral superfields. These are known as F-term potentials.

As a simple example, which will reappear in later sections, consider a theory of two chiral superfields $\Phi_{1,2}$ with canonical Kähler potential and charge $+1$ under $U(1)$ phase rotations.[9] The corresponding conserved current is given by

$$\mathcal{J} = \bar{\Phi}_1\Phi_1 + \bar{\Phi}_2\Phi_2 \ . \tag{45}$$

This gives rise to the D-term potential

$$V_D = \frac{e^2}{8}\left(|\phi_1|^2 + |\phi_2|^2 + \xi\right)^2 \ . \tag{46}$$

If $\xi > 0$, then the vacuum energy is positive: there are no SUSY vacua. If $\xi < 0$, then the moduli space of vacua is given by the three-sphere $|\phi_1|^2 + |\phi_2|^2 = -\xi$ modulo $U(1)$ gauge transformations acting on $\phi_{1,2}$, which is nothing but $\mathbb{CP}^1$. The corresponding low-energy theory describing the massless moduli is the $\mathbb{CP}^1$-model, which we introduced at the end of subsection 1.2.

For future use, we now briefly describe how to gauge a general global symmetry of the non-linear σ-model. As in the examples above, we simply add to the Lagrangian (13) a term

$$\mathscr{L}' = \int d^4\theta\, \mathcal{J}^{(a)}V^{(a)} \ . \tag{47}$$

Here the $\mathcal{J}^{(a)}$ are the Noether currents (40). Under a gauge-transformation with chiral gauge parameter $\Lambda^{(a)}$, the vector fields transform in the usual way, while the change in the σ-model Lagrangian $\mathscr{L}$ is given in (38). The complete Lagrangian is now gauge-invariant up to total derivatives:

$$\delta\left(\mathscr{L} + \mathscr{L}'\right) = \int d^4\theta\, \Lambda^{(a)}F^{(a)} + \text{c.c.} + \cdots \ , \tag{48}$$

where the dots represent unimportant higher-order terms and the $F^{(a)}$ are the holomorphic functions which appear in the Kähler transformation (37). The D-term scalar potential in this theory is given by

$$V_D = \frac{1}{8}\sum_a g_a^2\left(J^{(a)}\right)^2 \ . \tag{49}$$

Here the g_a are the gauge coupling constants which arise from the kinetic terms of the different $V^{(a)}$, and the $J^{(a)}$ are the bottom components of the Noether currents $\mathcal{J}^{(a)}$.

3. SUSY-Breaking

3.1. Simple Examples

If supersymmetry is to play any role in describing nature, then it must be spontaneously broken. As we already mentioned, SUSY is spontaneously broken if the vacuum energy is positive. Moreover, broken supersymmetry always leads to a massless fermion, the Goldstino, which is the exact analogue of the Goldstone bosons which appear when ordinary global symmetries are spontaneously broken. We will now explore a few simple examples which break SUSY at tree-level.

The simplest SUSY-breaking theory consists of one chiral superfield Φ with a linear term in the superpotential

$$\mathscr{L} = \int d^4\theta\, \bar{\Phi}\Phi + \int d^2\theta\, f\Phi + \text{c.c.} \ . \tag{50}$$

The scalar potential in this theory is simply a constant $V = |f|^2$. Thus, the spectrum consists of a massless fermion ψ_α – the Goldstino – and a massless scalar ϕ. Since there is no potential for ϕ, the theory has infinitely many SUSY-breaking vacua with nonzero energy $|f|^2$, and since the theory is free these vacua are not lifted.

We can make this model more interesting by adding an additional term to the Kähler potential:

$$\mathscr{L} = \int d^4\theta\, \left(\bar{\Phi}\Phi - \frac{1}{4\Lambda^2}\bar{\Phi}^2\Phi^2\right) + \int d^2\theta\, f\Phi + \text{c.c.} \ . \tag{51}$$

[9] The fact that this theory is quantum mechanically anomalous will not be important for us.

This is an effective theory below the high cutoff scale Λ. The scalar potential is now given by

$$V = \frac{|f|^2}{1 - \frac{1}{\Lambda^2}|\phi|^2} = |f|^2 \left(1 + \frac{|\phi|^2}{\Lambda^2} + \cdots\right) \ . \quad (52)$$

Now there is a single SUSY-breaking vacuum at $\phi = 0$. The boson ϕ has acquired a mass $|f|^2/\Lambda^2$, while the massless fermion ψ_α is again identified with the Goldstino.

The model (51) is not renormalizable. The simplest non-trivial, renormalizable model of spontaneous SUSY-breaking is the O'Raifeartaigh model [3]. The model has three chiral superfields $X, \Phi, \tilde{\Phi}$ with canonical Kähler potential and superpotential

$$W = X\Phi^2 + m\Phi\tilde{\Phi} + fX \ . \quad (53)$$

The conditions for the existence of a SUSY vacuum are $\phi = 0$, $\phi^2 = f$, and $m\tilde{\phi} = 2x\phi$, where we denote by $x, \phi, \tilde{\phi}$ the bottom components of $X, \Phi, \tilde{\Phi}$. Clearly these conditions are inconsistent and there is no supersymmetric vacuum. By studying minima of the full scalar potential V, we see that the theory has a SUSY-breaking vacuum with energy $V = |f|^2$ at $\phi = \tilde{\phi} = 0$. (This vacuum is only stable if $2|f| < |m|^2$; if this is not the case, the structure of the vacuum is somewhat different, but SUSY is still broken.) For $\phi = 0$, the scalar potential is independent of x. The field x is thus massless and can take on any vacuum expectation value. Just like the trivial theory (50), the O'Raifeartaigh model thus has infinitely many SUSY-breaking vacua at tree level. (This is a very general property of such theories [4,5].) However, unlike the previous theory which was free, it is now possible for radiative corrections to lift this vacuum degeneracy: x becomes massive and is stabilized at the origin by the one-loop correction to the scalar potential:

$$V^{(1)} \sim \frac{1}{16\pi^2}\frac{|f|^2}{m^2}|x|^2 + \cdots \ . \quad (54)$$

Note that after integrating out the heavy fields $\Phi, \tilde{\Phi}$ of mass $\sim m$, the low-energy dynamics of X is governed by an effective theory of the form (51) with the cutoff given by $\Lambda \sim m$.

In the three examples above SUSY was broken because the vacuum energy was positive due to non-vanishing F-terms coming from chiral superfields. It is also possible to break supersymmetry through non-vanishing D-terms coming from vector superfields. The prototypical such example is the FI-model:

$$\mathscr{L} = \frac{1}{4e^2}\int d^2\theta\, W^\alpha W_\alpha + \text{c.c.} + \int \xi d^4\theta\, V \ . \quad (55)$$

This model is free, but has a vacuum energy $V = e^2\xi^2/8$. The free gauge field is necessarily massles, while the massless gaugino is the Goldstino.

3.2. Comments on Dynamical SUSY-Breaking

Unlike other symmetries, the spontaneous breaking of supersymmetry is highly constrained. It is a consequence of powerful non-renormalization theorems [6,7] that *supersymmetric vacua cannot be lifted by radiative corrections*: if there is a SUSY vacuum in the classical theory, then it cannot disappear in perturbation theory. Thus SUSY can only be broken in two ways:

- The classical theory has no SUSY vacua. In this case we say that it breaks SUSY at tree-level.
- The classical theory has SUSY vacua, but they are lifted by non-perturbative effects. This is known as dynamical SUSY-breaking.

All theories discussed in the previous subsection break SUSY at tree-level. As was emphasized by Witten [8], such models are unappealing because they force us to introduce dimensionful parameters by hand so that we still have to explain the large hierarchy between the electroweak scale and the Planck or GUT scale.

On the other hand, the option of dynamical SUSY-breaking is very appealing. The scale $\sqrt{f}$ of supersymmetry breaking can now arise through dimensional transmutation

$$\sqrt{f} \sim \Lambda_{UV}\ e^{-\frac{8\pi^2}{g^2}} \ , \quad (56)$$

with $g \lesssim 1$ an asymtotically free gauge coupling, and thus $\sqrt{f}$ can naturally be exponentially

smaller than the cutoff Λ_{UV}. This might explain why the weak scale is so much smaller than the Planck or GUT scale. We should thus be studying theories with strong dynamics in the IR which can trigger SUSY-breaking. This is a vast subject (see [9] and references therein), and we will restrict ourselves to a few general comments.

Roughly speaking, dynamical theories fall into three classes:

- Theories in which supersymmetry breaking is triggered by non-perturbative effects, but the vacuum is in the semiclassical regime.
- Theories in which the vacuum is in the strongly-coupled regime of the original degrees of freedom, but can still be analyzed via Seiberg duality [10].
- Strongly coupled theories in which little can be said about the vacuum, but for which there are convincing (usually indirect) arguments that SUSY is broken.

The first two types of models are referred to as calculable. At low energies, they are described by Wess-Zumino models, possibly with IR-free gauge fields and effective FI-terms. By studying such models we may hope to shed light on the dynamics of interesting dynamical models.

In the next section we will continue our study of interesting supermultiplets. We will then explain how these multiplets can be used to constrain the dynamics and low-energy behavior of various theories – both with and without SUSY breaking.

4. Supercurrents

4.1. The Ferrara-Zumino Multiplet

Four-dimensional theories with $\mathcal{N} = 1$ supersymmetry possess a conserved supersymmetry current $S_{\alpha\mu}$ satisfying (2). Just like any other well-defined local operator, we have to embed $S_{\alpha\mu}$ in some multiplet. In order to write down sensible constraints for such a supercurrent multiplet, we are guided by the following two observations:

- The SUSY-algebra (1) gives rise to the current algebra

$$\{\bar{Q}_{\dot\alpha}, S_{\alpha\nu}\} = 2\sigma^{\mu}_{\alpha\dot\alpha} T_{\mu\nu} + (\text{S.T.}) \ , \tag{57}$$

where (S.T.) are Schwinger Terms, and $T_{\mu\nu}$ is a conserved, symmetric energy momentum tensor:

$$\partial^{\nu} T_{\mu\nu} = 0 \ , \qquad P_{\mu} = \int d^3x \, T_{\mu}{}^{0} \ . \tag{58}$$

The supersymmetry currrent and the energy-momentum tensor must thus belong to the same supermultiplet – a supercurrent.

- We expect $T_{\mu\nu}$ to be the highest spin component in the supercurrent multiplet. If this is not the case, then it might be problematic to couple the theory to supergravity.

We conclude that the supersymmetry current and the energy-momentum tensor are embedded in a real vector superfield $\mathcal{J}_{\mu}$ which schematically takes the form

$$\begin{aligned} \mathcal{J}_{\mu} = & \, j_{\mu} - i\theta \left(S_{\mu} + \cdots\right) + i\bar\theta \left(\bar{S}_{\mu} + \cdots\right) \\ & + \left(\theta\sigma^{\nu}\bar\theta\right)\left(2T_{\nu\mu} + \cdots\right) + \cdots \ . \end{aligned} \tag{59}$$

The real vector j_{μ} is generally not conserved. As in the case of the global current multiplet, the dots are terms which are not uniquely fixed by the requirements outlined above, and different choices of Schwinger terms in in (57) give rise to different ways of completing the multiplet. Again we will not discuss the constructive approach to writing the most general solution [11]. Instead, we will begin by exploring the most conventional set of constraints for the supercurrent multiplet, only amending them when we are forced to do so.

The simplest and most widely known supercurrent is called the Ferrara-Zumino (FZ) multiplet [12]. It is defined by the equations[10]

$$\bar{D}^{\dot\alpha} \mathcal{J}_{\alpha\dot\alpha} = D_{\alpha} X \ , \qquad \bar{D}_{\dot\alpha} X = 0 \ . \tag{60}$$

[10] Our convention for switching between vectors and bispinors is $\ell_{\alpha\dot\alpha} = -2\sigma^{\mu}_{\alpha\dot\alpha}\ell_{\mu}$, $\ell_{\mu} = \frac{1}{4}\bar\sigma^{\dot\alpha\alpha}_{\mu}\ell_{\alpha\dot\alpha}$.

In components, the FZ-multiplet takes the form

$$\begin{aligned}\mathcal{J}_\mu &= j_\mu - i\theta\left(S_\mu + \frac{1}{3}\sigma_\mu\bar\sigma^\nu S_\nu\right) + \frac{i}{2}\theta^2\partial_\mu\bar x \\ &+ i\bar\theta\left(\bar S_\mu + \frac{1}{3}\bar\sigma_\mu\sigma^\nu\bar S_\nu\right) - \frac{i}{2}\bar\theta^2\partial_\mu x \\ &+ \left(\theta\sigma^\nu\bar\theta\right)\left(2T_{\mu\nu} - \frac{2}{3}\eta_{\mu\nu}T - \frac{1}{2}\varepsilon_{\nu\mu\rho\sigma}\partial^\rho j^\sigma\right) \\ &+ \cdots \ . \end{aligned} \tag{61}$$

Here $T = T^\lambda{}_\lambda$ is the trace of the energy-momentum tensor. The higher components of $\mathcal{J}_{\alpha\dot\alpha}$ only contain derivatives of components which we have already displayed. The chiral superfield X takes the form

$$X = x(y) + \sqrt{2}\theta\psi(y) + \theta^2 F(y) \ , \tag{62}$$

with

$$\begin{aligned}\psi &= \frac{i\sqrt{2}}{3}\sigma^\mu_{\alpha\dot\alpha}\bar S^{\dot\alpha}_\mu \ , \\ F &= \frac{2}{3}T + i\partial^\mu j_\mu \ . \end{aligned} \tag{63}$$

We see that the FZ-multiplet contains $12 = 2\,[x] + 4\,[j_\mu] + 6\,[T_{\mu\nu}]$ independent bosonic components, which match the 12 fermionic components of $S_{\alpha\mu}$. Thus, the FZ-multiplet is a $12+12$ multiplet. It is straightforward to check that the explicit component expressions (61) and (62) lead to a SUSY current algebra of the form (57):

$$\begin{aligned}\{\bar Q_{\dot\alpha}, S_{\alpha\mu}\} = \sigma^\nu_{\alpha\dot\alpha}\Big(&2T_{\nu\mu} + i\partial_\nu j_\mu \\ &- i\eta_{\mu\nu}\partial^\lambda j_\lambda - \frac{1}{2}\varepsilon_{\nu\mu\rho\lambda}\partial^\rho j^\lambda\Big) \ . \end{aligned} \tag{64}$$

When X vanishes, then we see from (63) that the energy-momentum tensor is traceless, and that j_μ is now a conserved current. In this case, the theory is superconformal and the FZ-multiplet only has $8+8$ components.

As the simplest example, we again consider the free theory (11) of a single chiral superfield Φ. Using the superspace equation of motion $D^2\Phi = 0$ it is straightforward to check that the multiplet

$$\mathcal{J}_{\alpha\dot\alpha} = 2D_\alpha\Phi\bar D_{\dot\alpha}\bar\Phi - \frac{2}{3}[D_\alpha, \bar D_{\dot\alpha}]\bar\Phi\Phi \tag{65}$$

satisfies

$$\bar D^{\dot\alpha}\mathcal{J}_{\alpha\dot\alpha} = 0 \ . \tag{66}$$

As expected, the FZ-multiplet reduces to the superconformal multiplet for the free scalar. By expanding Φ in components and comparing with (61), we see that the energy-momentum tensor embedded in $\mathcal{J}_{\alpha\dot\alpha}$ reads

$$\begin{aligned}T_{\mu\nu} &= \partial_\mu\bar\phi\partial_\nu\phi + (\mu\leftrightarrow\nu) - \eta_{\mu\nu}\partial^\lambda\bar\phi\partial_\lambda\phi \\ &\quad - \frac{1}{3}\left(\partial_\mu\partial_\nu - \eta_{\mu\nu}\partial^2\right)|\phi|^2 + (\text{fermions}) \ . \end{aligned} \tag{67}$$

The first line is the familiar energy-momentum tensor for a free, massless scalar. The second line is an improvement term: it is automatically conserved (without using the equations of motion), and it does not affect the conserved charge P_μ because setting $\nu = 0$ turns it into a total space derivative. We are free to add these kind of improvement terms to any conserved current. In this case the constraint $\bar D^{\dot\alpha}\mathcal{J}_{\alpha\dot\alpha} = 0$ fixes the improvement term in a particular way: it guarantees that $T_{\mu\nu}$ is traceless. The relation between supersymmetric constraints and improvement terms will play a pivotal role in what follows.

More generally, we can consider the Wess-Zumino model (20). Using the equations of motion $\bar D^2\partial_i K = 4\partial_i W$, we can check that

$$\begin{aligned}\mathcal{J}_{\alpha\dot\alpha} &= 2g_{i\bar\jmath}D_\alpha\Phi^i\bar D_{\dot\alpha}\bar\Phi^{\bar\jmath} - \frac{2}{3}[D_\alpha, \bar D_{\dot\alpha}]K \ , \\ X &= 4W - \frac{1}{3}\bar D^2 K \end{aligned} \tag{68}$$

satisfy the defining equation (60) of the FZ-multiplet. We will make use of this formula on several occasions.

Finally, the FZ-multiplet for the FI-model (55) readily follows from the equation of motion $D^\alpha W_\alpha = e^2\xi$. It is given by:

$$\begin{aligned}\mathcal{J}_{\alpha\dot\alpha} &= -\frac{4}{e^2}W_\alpha\bar W_{\dot\alpha} - \frac{2}{3}\xi[D_\alpha, \bar D_{\dot\alpha}]V \ , \\ X &= -\frac{\xi}{3}\bar D^2 V \ . \end{aligned} \tag{69}$$

It is similarly straightforward to obtain the FZ-multiplet for gauge theories coupled to matter (we

will not write down the most general expression here).

Looking at (55) we make an unsettling observation: in the presence of an FI-term ξ, neither $\mathcal{J}_{\alpha\dot{\alpha}}$ nor X are invariant under the usual gauge-transformation $\delta V = i(\Lambda - \bar{\Lambda})$, with Λ chiral [13]. (This conclusion is not changed by the inclusion of matter.) Thus, the FZ-multiplet is not gauge-invariant, and consequently its components are not well-defined operators. From this, we might mistakenly conclude that models with FI-terms are inherently ill-defined, because they do not have a well-defined supersymmetry current or energy-momentum tensor.

To see why this is not so, we examine the gauge non-invariance of the FZ-multiplet (69) in more detail. Under a gauge transformation, this multiplet transforms as follows:

$$\begin{aligned} \delta\mathcal{J}_{\alpha\dot{\alpha}} &= -\frac{2}{3}\xi\partial_{\alpha\dot{\alpha}}\left(\Lambda + \bar{\Lambda}\right) \ , \\ \delta X &= \frac{i}{3}\xi\bar{D}^2\bar{\Lambda} \ . \end{aligned} \tag{70}$$

By expanding these expressions in components and comparing with (61), we see that the bottom component $j_\mu \sim \xi A_\mu + (\text{fermions})$ explicitly depends on the gauge field A_μ and is simply not gauge-invariant. However, the gauge non-invariance of the energy-momentum tensor takes the special form

$$\delta T_{\mu\nu} = \frac{2}{3}\xi\left(\partial_\mu\partial_\nu - \eta_{\mu\nu}\partial^2\right)\mathrm{Im}\Lambda| \ , \tag{71}$$

where $\Lambda|$ denotes the bottom component of the superfield Λ. We see that the transformation of $T_{\mu\nu}$ in (70) is a pure improvement term. As we explained above, this means that it is automatically conserved and does not affect the conserved charged P_μ. Completely analogously, it can be checked that the supersymmetry current $S_{\alpha\mu}$ also only shifts by a pure improvement term. The FI-model thus has well-defined, gauge-invariant operators P_μ, Q_α, which make it a well-defined supersymmetric field theory.

How, then, do we interpret the fact that the supersymmetry current and the energy-momentum tensor embedded in the FZ-multiplet (61) are not gauge-invariant and do not exist as well-defined operators? The answer is that $S_{\alpha\mu}$ and $T_{\mu\nu}$ are not unique; they are only defined up to improvement terms. Different choices of improvement terms lead to different local currents, but do not affect the corresponding charges. It is usually possible to chose the improvement terms in such a way that the currents are well-defined operators. However, a problem could arise when attempting to embed these operators into supermultiplets. In this case there may be a clash between the existence of certain supermultiplets and the requirement that these multiplets be gauge invariant. This is precisely what happens in the FI-model: forcing $S_{\alpha\mu}$ and $T_{\mu\nu}$ into an FZ-multiplet requires us to pick gauge non-invariant improvement terms. Conversely, it is possible to pick gauge-invariant improvement terms for $S_{\alpha\mu}$ and $T_{\mu\nu}$, but this makes it impossible to embed these operators into an FZ-multiplet. In this case it is necessary (and possible) to find different supermultiplets into which we can embed gauge-invariant choices for $S_{\alpha\mu}$ and $T_{\mu\nu}$. Such multiplets will be discussed in section 6.

In light of the preceding discussion, we are led to carefully reconsider the existence of the FZ-multiplet (68) for the Wess-Zumino model. We see that the Kähler potential K formally appears in the same way as the vector field V in the FZ-multiplet for the FI-model. Morover, Kähler transformations of K are take the same form as gauge-transformations of V. We conclude that the FZ-multiplet of the Wess-Zumino model is not invariant under Kähler transformations. Again, these Kähler transformations only change the supersymmetry current and the energy-momentum tensor by improvement terms.

However, unlike gauge transformations, Kähler transformations are not an absolute necessity. It often does not matter if the multiplet transforms under Kähler transformations. The only become essential when the target space $\mathcal{M}$ of the sigma model needs to be covered with several patches and Kähler transformations are needed to switch between the patches. This happens, for instance, in the $\mathbb{CP}^1$ model described in subsection 1.2. In such theories, the FZ-multiplet is not a well-defined operator. Equivalent ways of describing the target space of the theory result in energy-

momentum tensors which differ by improvement terms, even though they should be identical, and likewise for the supersymmetry currents. In other words, there is no unambiguous way of fixing these operators.

We would like to understand the precise mathematical conditions under which the FZ-multiplet for Wess-Zumino models is well-defined. From the metric $g_{i\bar{j}}$ we can construct the Kähler form

$$\omega = i g_{i\bar{j}} d\phi^i \wedge d\bar{\phi}^{\bar{j}} \ . \tag{72}$$

Since $g_{i\bar{j}}$ is locally derived from a Kähler potential, ω is closed: $d\omega = 0$. In every patch we can thus find a one-form $\mathcal{A}$ such that $\omega = d\mathcal{A}$. Locally, this Kähler connection is given by $\mathcal{A} \sim i\partial_i K d\phi^i + \text{c.c.}$. In general, ω is not exact and the Kähler connection $\mathcal{A}$ is not globally well-defined. The obstruction to the global existence of $\mathcal{A}$ is measured by the cohomology class $[\omega] \in H^2(\mathcal{M})$. If ω vanishes in $H^2(\mathcal{M})$, then $\mathcal{A}$ is globally well-defined and thus a good operator the theory.

The bottom component of (68) is given by

$$j_\mu = \frac{2i}{3}\partial_i K \partial_\mu \phi^i + \text{c.c.} - \frac{1}{3} g_{i\bar{j}} \bar{\psi}^{\bar{j}} \bar{\sigma}_\mu \psi^i \ . \tag{73}$$

While the fermionic piece only depends on the metric and is thus invariant under Kähler transformations, we recognize the bosonic piece as the pull-back to space-time of the Kähler connection $\mathcal{A}$. This is is well-defined only if ω is exact and vanishes in $H^2(\mathcal{M})$. If this condition is not satisfied, then j_μ is not a good local operator in the theory, since it depends on the choice of patch in target space. In this case, the entire FZ-multiplet (68) is not well-defined [14].

As a special case, note that the Kähler form of a compact manifold can never be exact. If this were the case, then the volume form $\omega^{\dim(\mathcal{M})/2}$ would also be exact and thus integrate to zero on the compact manifold; this is a contradiction. Thus, a Wess-Zumino model with compact target manifold, such as the $\mathbb{CP}^1$-model (18), cannot have a well-defined FZ-multiplet.

In this section we have explored the FZ-multiplet, in which the supersymmetry current and the energy-momentum tensor are conventionally embedded. This multiplet exists in the vast majority of SUSY theories, including asymptotically free gauge theories, such as supersymmetric QCD (SQCD). As far as we know, the FZ-multiplet only fails to exist when one of the following conditions holds:

- Some $U(1)$ gauge group has an FI-term.
- The target-space has non-trivial topology, so that the Kähler form is not exact.

In the first case, the FZ-multiplet is not gauge-invariant, while in the second case it is not globally well-defined. These insights will enable us to derive exact results about the dynamics of SUSY field theories, SUSY-breaking, and supergravity.

4.2. Consequences for SUSY Theories

It is a general fact about quantum field theory that operator equations are invariant under renormalization group (RG) flow as long as the operators involved are well-defined and gauge-invariant. This means that if some operator relation holds in the UV (where field theories are usually defined), then it continues to hold along the entire RG-flow. Applying this reasoning to the FZ-multiplet immediately leads to constraints on the RG-flow of supersymmetric field theories.

Consider a supersymmetric field theory which has no FI-terms in the UV. This means that this theory has a well-defined, gauge invariant FZ-multiplet. This multiplet must therefore persist along the entire RG-flow. We conclude that FI-terms cannot be generated along the flow; this is true at any order in perturbation theory and even non-perturbatively. For instance, it might happen that the theory flows through a regime with strong dynamics, and that a $U(1)$ gauge symmetry emerges in some weakly-coupled dual description. In this case the gauge-invariance of the FZ-multiplet prevents this emergent $U(1)$ gauge theory from having an FI-term. It is even possible to argue that if an FI-term is present in the UV, then its value is not renormalized. Other derivations of these results can be found in [15–18].

Completely analogously, let us consider a theory which has a well-defined, gauge-invariant FZ-multiplet in the UV. For example, we could consider an ordinary SUSY gauge theory, with

canonical Kähler potential for the matter fields and no FI-terms. At low energies, such field theories are often described by a weakly-coupled σ-model (perhaps with IR-free gauge fields). It is expected that this will happen whenever the field theory has a strong coupling scale Λ, below which it is described by massless moduli. Since this theory has a well-defined FZ-multiplet in the UV, and this multiplet persists along the entire RG-flow, we conclude that the low-energy σ-model must have have an exact Kähler form ω. This severely constrains the quantum moduli space of the low-energy theory: the integral $\int \omega \wedge \omega \wedge \cdots$ over any compact, even-dimensional cycle must vanish. As we already explained in the previous subsection, the means in particular that the moduli space cannot be compact (of course, it can be a set of points). It is particularly interesting to test this theorem in SQCD with the same number of colors and flavors. In this case the topology of the modul-space changes under RG-flow and becomes non-trivial in the IR [19]. However, in accordance with the general result above, the Kähler form of this deformed quantum moduli space is exact.

The formal similarity between the two theorems described above is not coincidental. On the one hand, they are both consequences of the RG-invariance of the FZ-multiplet. On the other hand, it may be that if a theory does not have an FZ-multiplet in the UV due to the presence of an FI-term, it may flow to a σ-model which fails to have an FZ-multiplet because its target space has a non-exact Kähler form.

The simplest example of this phenomenon is the theory discussed at the end of subsection 2.2. In the UV, this theory starts out as an abelian gauge theory with an FI-term ξ and two chiral matter fields of charge $+1$. When $\xi < 0$, it follows from the scalar potential (46) that the low-energy theory which describes the moduli space of SUSY-vacua is given by the $\mathbb{CP}^1$-model, whose target space is compact.

5. Applications to SUSY-Breaking

In this section we will consider two applications of the FZ-multiplet to SUSY-breaking. The first application rests on the relation of the FZ-multiplet to the Goldstino. This will enable us to derive exact results about such SUSY-breaking theories. It will also lead to a useful formalism for writing Lagrangians with non-linearly realized supersymmetry. The second application concerns the interplay of F-terms and D-terms in SUSY-breaking theories. We show under very broad assumptions that there can be no SUSY-breaking vacua (even meta-stable ones) in which the D-terms are parametrically larger than the F-terms.

5.1. The FZ-Multiplet and the Goldstino

A universal prediction of spontaneous SUSY-breaking is the existence of a massless Weyl fermion, the Goldstino G_α. We will not do justice to the extensive literature on the Goldstino. Most of the references can be found in [20], which is also the main reference for this subsection.

When a global symmetry is spontaneously broken, the corresponding conserved charge is not a well-defined operator because its correlation functions are IR divergent. As a result, the physical states of the theory are not in linear representations of the symmetry. However, the conserved current and even commutators of local operators with the conserved charge do exist. In contrast to the states, the local operators do in fact furnish a linear representation of the symmetry. These statements carry over without modification when supersymmetry is spontaneously broken in infinite volume: the supercharge Q_α does not exist, but the supersymmtry current and (anti-) commutators with Q_α do exist. (When SUSY is spontaneously broken in finite volume, even Q_α exists.) This means that operators still reside in supermultiplets, and that we can use the formalism of superspace and superfields without modification.

Recall the defining equation (60) of the FZ-multiplet:

$$\bar{D}^{\dot{\alpha}} \mathcal{J}_{\alpha\dot{\alpha}} = D_\alpha X \ , \tag{74}$$

where X is chiral. In this subsection we will only discuss theories which admit a well-defined, gauge-invariant FZ-multiplet. This multiplet requires the existence of a complex scalar x, the bottom component of X, which is a well-defined operator in the theory. If we are given a micro-

scopic description of the theory in the UV, we can express x in terms of elementary fields.

The chiral superfield X can be consistently followed along the RG-flow down to the IR, even when SUSY is spontaneously broken. We can see this in the simplest SUSY-breaking model (50), which only has a single chiral superfield Φ. In this theory, the F-term is non-zero, but ϕ and ψ_α are free, massless fields. As was discussed in subsection 3.1, we identify ψ_α with the Goldstino G_α. Since this theory is a Wess-Zumino model with $K = \bar{\Phi}\Phi$ and $W = f\Phi$, we find from (20) that $X = \frac{8}{3}f\Phi$. In this simple example, the operator X is thus proportional to Φ, so that the θ-component of X is proportional to the Goldstino.

More generally, standard arguments about symmetry breaking show that when supersymmetry is spontaneously broken, the low-energy supersymmetry current is expressed in terms of the Goldstino G_α as

$$S_{\alpha\mu} = \sqrt{2} f \sigma_{\mu\alpha\dot{\alpha}} \bar{G}^{\dot{\alpha}} + f' (\sigma_{\mu\nu})_\alpha{}^\beta \partial^\nu G_\beta + \cdots \ , \quad (75)$$

for some constants f and f'. Note that the term with f' is an improvement term and can be ignored. We see that at low energies, the spin-$\frac{3}{2}$ component of the supersymmetry current essentially decouples, while the spin-$\frac{1}{2}$ component is proportional to the Goldstino. Since we know from (63) that the θ-component of X is given by the spin-$\frac{1}{2}$ projection of $S_{\alpha\mu}$, we again conclude that at long distance the θ-component of X is proportional to the Goldstino.

In the trivial example of a free chiral superfield Φ, the lowest component x of the superfield X is proportional to the free scalar ϕ. In general, the low-energy Goldstino is not accompanied by a massless scalar. Then, the bosonic operator x cannot create a-one particle state. Instead, the simplest bosonic state it can create contains two Goldstinos. When supersymmetry is broken in finite volume, the states in the Hilbert space are in linear supersymmetry multiplets. The supersymmetric partner of a one Goldstino state $\bar{Q}_{\dot{\alpha}}|0\rangle$ is a two Goldstino state $\bar{Q}_{\dot{1}}\bar{Q}_{\dot{2}}|0\rangle$. At infinite volume the supercharge does not exist and the zero momentum Goldstino state is not normalizable. However, the finite volume intuition is still valid. The operator ψ_ϕ creates a one Goldstino state and its superpartner $\phi \sim x$ creates a two-Goldstino state.

We denote this non-linear superfield which contains the Goldstino bilinear in the bottom component X_{NL}, and x_{NL} denotes the bottom component itself. Consistency of this superfield under supersymmetry transformations (which, again, are legal even if SUSY is spontaneously broken) fixes it to take the form

$$X_{NL} = \frac{G^2}{2F} + \sqrt{2}\theta G + \theta^2 F \ , \quad (76)$$

where all the fields are functions of y^μ. Clearly, (76) satisfies the interesting operator identity

$$X_{NL}^2 = 0 \ . \quad (77)$$

(Other realizations of nonlinear supersymmetry can be found, for example, in [21,22])

We conclude that the Goldstino resides in a chiral superfield X_{NL} which satisfies $X_{NL}^2 = 0$. Furthermore, this chiral superfield is the IR limit of the microscopic superfield X. Surprisingly, this result is true both for F-term and for D-term breaking because it relies only on the existence of the chiral operator X. (The only exception is the situation with pure D-term breaking which occurs when a tree-level FI-term is present for an unbroken $U(1)$ gauge theory. In this case the operator X is not gauge invariant and we do not discuss it here.[11] Thus, our discussion is applicable in all the interesting models of dynamical SUSY breaking.

We will momentarily see that this identification of the low-energy limit of the operator X, which exists in all field theories we are interested in, allows us to derive some non-perturbative results.

It is instructive to compare the situation here with the theory of ordinary Goldstone bosons like pions. Clearly, the decay constant f here is analogous to the decay constant f_π of pion physics. Both of them are well defined. However, in pion

[11] However, our discussion does apply in the Higgs phase of the FI-model [23], where the low-energy limit of X can be rendered gauge invariant by dressing it with fields that obtain expectation values.

physics the order parameter $\langle\psi\psi\rangle$ for chiral symmetry breaking does not have a universal definition with a precise normalization (it suffers from wavefunction renormalization). In our case the order parameter for supersymmetry breaking is the energy-momentum tensor which resides in the same multiplet as the supersymmetry current. Hence, it has a well-defined normalization. Therefore, our X is completely well-defined. Correspondingly, the operator $\psi\psi$ of pion physics acts as an interpolating field for pions, but its normalization is not meaningful. In our case X is used both as an order parameter for supersymmetry breaking and as an interpolating field for Goldstinos with well-defined normalization.

The analogy with pion physics also clarifies the meaning of our constraint (77). It arises from removing the massless scalar in X. This is analogous to describing pion physics by starting with a linear sigma model with a σ-field. Removing the σ-field is implemented by imposing a constraint $UU^\dagger = 1$, which is analogous to our $X_{NL}^2 = 0$.

Since in every microscopic theory we can identify X in the ultraviolet, and if SUSY is spontaneously broken we also know its universal low-energy limit, we can calculate various correlation functions of operators at large separations even in strongly coupled models. Hence even "incalculable" models of SUSY breaking (like the $SU(5)$ theory of [24] or the $SO(10)$ theory of [25]) have a solvable sector at long distances. The operator x interpolates between the vacuum and a state with two Goldstinos, with a universal normalization. This is because at long distances the leading behavior of x is proportional to that of G^2. Therefore,

$$\lim_{|\mathbf{r}|\to\infty} \langle x(\mathbf{r})\bar{x}(0)\rangle = \left(\frac{4}{3\pi^2}\right)^2 \frac{1}{|\mathbf{r}|^6} \ . \tag{78}$$

This is independent of the details of the microscopic theory and its coupling constants. In a similar fashion we can calculate the long distance limit of any correlation function of x and $\bar{x}$.

This idea can be pushed further and many more non-perturbative results of this form can be obtained. In fact, a pretty rich set of exact results on SUSY-breaking theories arises with interesting underlying mathematical structure, but we will not elaborate on this any further here.

We will now explain how to use X_{NL} to write supersymmetric effective Lagrangians. We start without including derivatives. At that level, the most general supersymmetric Lagrangian subject to the constraint $X_{NL}^2 = 0$ is

$$\int d^4\theta\, \bar{X}_{NL} X_{NL} + \int d^2\theta\, f X_{NL} + \text{c.c.} \ , \tag{79}$$

where without loss of generality we take f to be real. This looks like the free chiral multiplet except that the superfield is constrained. This constraint removes the massless scalar field and introduces nonlinearities.

More explicitly, the constraint can be solved as in (76). Substituting this in (79), we derive the component Lagrangian

$$i\partial_\mu \bar{G}\bar{\sigma}^\mu G + \bar{F}F + \frac{\bar{G}^2}{2\bar{F}}\partial^2\left(\frac{G^2}{2F}\right) + (fF + \text{c.c.}) \ . \tag{80}$$

The equations of motion of the auxiliary fields $F, \bar{F}$ can be solved and upon substituting this back in the component Lagrangian we find

$$\begin{aligned}\mathcal{L} = &-f^2 + i\partial_\mu \bar{G}\bar{\sigma}^\mu G + \tfrac{1}{4f^2}\bar{G}^2\partial^2 G^2 \\ &-\tfrac{1}{16f^6} G^2\bar{G}^2\partial^2 G^2 \partial^2 \bar{G}^2 \ .\end{aligned} \tag{81}$$

This is equivalent to the Akulov-Volkov Lagrangian [26]. (See also [27–29].) Here we have given a fully off-shell supersymmetric description of this theory.

The real advantage of this approach is the simplifications in writing higher derivative corrections to (79) and, more interestingly, couplings to possibly light matter fields (such as MSSM fields, Goldstone bosons, 't Hooft fermions etc.). Indeed such problems are easily solved in this formalism since we have an off-shell description and so we can use all the familiar superspace techniques for writing Lagrangians (the number of allowed operators is smaller because of the various constraints).

This toolbox can be put to use in many possible contexts and some recent examples include [30–37]

The last thing we would like to demonstrate before closing this subsection is the way the nilpotent equation (77) arises from the dynamics in a simple example. In order to remove the massless scalar we include a non-canonical Kähler potential

$$K = \bar{\Phi}\Phi - \frac{c}{M^2}\bar{\Phi}^2\Phi^2 \ , \tag{82}$$

and

$$W = f\Phi \ . \tag{83}$$

Here c is a dimensionless positive number of order one. Such a theory can arise as the low-energy Lagrangian below some scale M after neglecting higher order terms in $\frac{1}{M}$. (For example, the low-energy limit of the standard O'Raifeartaigh model looks like (82).) It is valid for

$$\sqrt{f} \ll E \ll M \ . \tag{84}$$

Let us integrate out the massive bosons. Remembering that the Lagrangian contains interaction terms of the form $-\frac{c}{M^2}\left|2\phi F_\phi - \psi^2\right|^2$, the zero-momentum equation of motion of ϕ sets it to

$$\phi = \frac{\psi^2}{2F_\phi} \ . \tag{85}$$

Note that it is independent of c, or in other words, it is independent of the details of the high energy physics (this is an example of our universality).

Upon substituting (85) back into Φ, we discover that in the $\Phi^2 = 0$. Hence, it satisfies the same constraint as X_{NL}. To make the relation more precise, we can go through a careful calculation of the supercurrent. The main point, however, is that the nilpotentcy equation arises from integrating out heavy degrees of freedom.

5.2. Restrictions on Large D-Terms

In subsection 3.1 we encountered several simple models of F-term and D-term SUSY-breaking. While models with FI-terms lead to many tree-level examples of D-term SUSY-breaking, most known calculable models of dynamical supersymmetry breaking are predominately F-term driven. We would like to understand whether this has to hold in general, or whether there are in fact dynamical models with large D-terms. In this subsection, we will show that such models do not exist: under broad assumptions, the D-terms are necessarily parametrically smaller than the F-terms [36].

To get an intuitive picture, we can loosely identify D-term breaking with the presence of FI-terms. In dynamical models, one usually starts with a well-behaved, asymptotically-free gauge theory without FI-terms in the UV. Since such theories has a well-defined FZ-multiplet, the discussion of subsection 4.2 show that they cannot acquire FI-terms at low energies. Roughly speaking, the absence of low-energy FI-terms implies the absence of large D-terms.

We can make this intuitive picture precise by using the tools we have developed so far. Since we are interested in calculable models with parametrically small F-terms, we consider theories in which the low-energy dynamics responsible for SUSY-breaking is described by a σ-model (13) and the F-terms are set to zero in first approximation. In addition, we will include IR-free gauge fields by gauging some global symmetries of the σ-model. If the D-term potential which results from this gauging leads to SUSY-breaking vacua (even meta-stable ones), then these putative vacua will have parametrically large D-terms which are larger than the F-terms by inverse powers of the small, IR-free gauge couplings. We will now show that such vacua do not exist in theories which have a well-defined, gauge-invariant FZ-multiplet. (Therefore they cannot exist in interesting dynamical models.)

As was discussed at the end of subsection 2.2, the Lagrangian for the gauged σ-model is given by making the substitution

$$K \to K + \mathcal{J}^{(a)}V^{(a)} \ , \tag{86}$$

and including conventional kinetic terms for the gauge fields. By making an identical substitution in expression (68) for the FZ-multiplet of the σ-model, we see that a gauge-transformation (48) changes this new FZ-multiplet $\mathcal{J}_{\alpha\dot{\alpha}}$ by an amount

$$\delta\mathcal{J}_{\alpha\dot{\alpha}} \sim i\partial_{\alpha\dot{\alpha}}\Lambda^{(a)}F^{(a)} + \text{c.c.} \ . \tag{87}$$

Since we assumed that the UV theory had a well-defined FZ-multiplet, the same must be true for the low-energy gauged σ-model. Thus, all functions $F^{(a)}$ must vanish. The Noether currents $\mathcal{J}^{(a)}$ now take the simple form

$$\mathcal{J}^{(a)} = iX^{(a)i}\partial_i K \ . \tag{88}$$

Using this expression, it is straightforward to check that the D-term potential (49) of the gauged σ-model satisfies the identity

$$V_D = \frac{1}{2}g^{i\bar{j}}\partial_i K \partial_{\bar{j}} V_D \ . \tag{89}$$

This identity immediately implies that a critical point of the potential can only occur when $V_D = 0$. In other words, every critical point must be a supersymmetric minimum and this D-term potential does not admit SUSY-breaking vacua – not even metastable ones.

The argument we have given above explains the absence of dynamical models with parametrically large D-terms. It is, however, possible to build models of dynamical SUSY-breaking with comparable D-terms and F-terms (see [36] and references therein).

6. More Supercurrent Multiplets

We have seen that there are well-defined supersymmetric field theories which do not admit an FZ-multiplet. In these theories, we must search for other, well-defined supercurrent multiplets into which the energy-momentum tensor and the supersymmetry current can be embedded. Note that the existence of such alternative multiplets has no effect on the results we extracted in previous sections, which were based on the existence of a well-defined FZ-multiplet.

There is indeed a supercurrent multiplet $\mathcal{S}_{\alpha\dot{\alpha}}$ which exists in theories with FI-terms or non-exact Kähler form, which do not admit an FZ-multiplet. This supercurrent multiplet satisfies the defining equations

$$\begin{aligned} &\bar{D}^{\dot{\alpha}}\mathcal{S}_{\alpha\dot{\alpha}} = D_\alpha X + \chi_\alpha \ , \qquad \bar{D}_{\dot{\alpha}} X = 0 \ , \\ &\bar{D}_{\dot{\alpha}}\chi_\alpha = 0 \ , \qquad D^\alpha \chi_\alpha = \bar{D}_{\dot{\alpha}}\bar{\chi}^{\dot{\alpha}} \ . \end{aligned} \tag{90}$$

Note that X appears exactly as in the FZ-multiplet, while χ_α satisfies the same constraints as the field-strength superfield W_α discussed in subsection 1.3. In components, the $\mathcal{S}$-multiplet takes the form

$$\begin{aligned} \mathcal{S}_\mu &= j_\mu - i\theta\left(S_\mu - \frac{i}{\sqrt{2}}\sigma_\mu\bar{\psi}\right) + \frac{i}{2}\theta^2\partial_\mu\bar{x} \\ &+ i\bar{\theta}\left(\bar{S}_\mu - \frac{i}{\sqrt{2}}\bar{\sigma}_\mu\psi\right) - \frac{i}{2}\bar{\theta}^2\partial_\mu x + \left(\theta\sigma^\nu\bar{\theta}\right)\Big(2T_{\mu\nu} \\ &- \eta_{\mu\nu}Z + \frac{1}{2}\epsilon_{\mu\nu\rho\sigma}\partial^\rho j^\sigma + \frac{1}{8}\epsilon_{\mu\nu\rho\sigma}F^{\rho\sigma}\Big) + \dots \ . \end{aligned} \tag{91}$$

The chiral superfields X and χ_α are given by

$$\begin{aligned} X &= x(y) + \sqrt{2}\theta\psi(y) + \theta^2\left(Z(y) + i\partial^\nu j_\nu(y)\right) \ , \\ \chi_\alpha &= -i\lambda_\alpha(y) + \theta_\beta\left(\delta_\alpha{}^\beta D(y) - i(\sigma^{\mu\nu})_\alpha{}^\beta F_{\mu\nu}(y)\right) \\ &+ \theta^2\sigma^\nu_{\alpha\dot{\alpha}}\partial_\nu\bar{\lambda}^{\dot{\alpha}}(y) \ , \end{aligned} \tag{92}$$

with

$$\begin{aligned} D &= -4T + 6Z \ , \\ \lambda &= 2\sigma^\mu\bar{S}_\mu + 3i\sqrt{2}\psi \ . \end{aligned} \tag{93}$$

As before, the operator j_μ is not in general conserved, while the supersymmetry current $S_{\alpha\mu}$ and the symmetric energy-momentum tensor $T_{\mu\nu}$ are conserved. The $\mathcal{S}$-multiplet has 4+4 more degrees of freedom than the FZ-multiplet. They consists of the real scalar Z, the closed, real two-form $F_{\mu\nu}$ and the Weyl fermion ψ_α. The $\mathcal{S}$-multiplet is thus a $16+16$ multiplet.[12]

As in the case of the FZ-multiplet, the component expressions (91)and (92) lead to a SUSY current algebra of the form (57):

$$\begin{aligned} \{\bar{Q}_{\dot{\alpha}}, S_{\alpha\mu}\} = \sigma^\nu_{\alpha\dot{\alpha}}\Big(&2T_{\mu\nu} - \frac{1}{8}\epsilon_{\nu\mu\rho\sigma}F^{\rho\sigma} + i\partial_\nu j_\mu \\ &- i\eta_{\nu\mu}\partial^\rho j_\rho - \frac{1}{2}\epsilon_{\nu\mu\rho\sigma}\partial^\rho j^\sigma\Big) \ . \end{aligned} \tag{94}$$

However, the Schwinger Terms are now mor complicated. The supersymmetry algebra (1) follows

[12] Setting $X = 0$ in the $\mathcal{S}$-multiplet results in the so-called $\mathcal{R}$-multiplet. It is a $12+12$ multiplet whose bottom component j_μ is a conserved R-current. We will not discuss the $\mathcal{R}$-multiplet in this review, although we will occasionally refer to it in passing.

provided that $\int d^3x\, F_{ij}$ vanishes for all spatial indices i, j.

All known supersymmetric field theories admit a well-defined $\mathcal{S}$-multiplet.[13] Those theories which do not have FI-terms or non-exact Kähler form also admit a well-defined FZ-multiplet.[14] For instance, consider a Wess-Zumino model with arbitrary K and W. If the Kähler form is not exact, then the FZ-multiplet does not exist. However, the $\mathcal{S}$-multiplet exists, and takes the form

$$\mathcal{S}_{\alpha\dot\alpha} = 2g_{i\bar j} D_\alpha \Phi^i \bar D_{\dot\alpha} \bar\Phi^{\bar j} \ , \tag{95}$$

with $X = 4W$ and $\chi_\alpha = \bar D^2 D_\alpha K$.

The existence of the $\mathcal{S}$-multiplet in theories without an FZ-multiplet has important consequences for supergravity theories. In the next section we will explain how to construct supergravity starting from the supercurrent, and this will lead to additional applications.

7. Elements of Linearized Supergravity and Constraints on Moduli

In this section we study the couplings of supercurrent multiplets to supergravity theories. We are only interested in linearized supergravity, namely the leading order in $\frac{1}{M_p}$. This approximate analysis is sufficient to derive several general results.

This approach to supergravity is taken, for example, in [2]. We begin with a review of the coupling of the FZ-multiplet to supergravity. We then explain the coupling of the $\mathcal{S}$-multiplet to supergravity.[15]

7.1. Gauging the FZ-Multiplet

We start by reviewing the coupling of the FZ-multiplet to linearized gravity. The FZ-multiplet contains a conserved energy-momentum tensor and supercurrent and can therefore be coupled to supergravity. The supergravity multiplet is embedded in a real vector superfield $H_{\alpha\dot\alpha}$. The $\theta\bar\theta$ component of $H_{\alpha\dot\alpha}$ contains the metric field, $h_{\mu\nu}$, a two form field $B_{\mu\nu}$, and a real scalar. The coupling of gravity to matter is dictated at leading order by

$$\int d^4\theta\, \mathcal{J}_{\alpha\dot\alpha} H^{\alpha\dot\alpha} \ . \tag{96}$$

We should impose gauge invariance, namely, the invariance under coordinate transformations and local supersymmetry transformations. The gauge parameters are embedded in a complex superfield L_α, which so far obey no constraints. We assign a transformation law to the supergravity fields of the form

$$H'_{\alpha\dot\alpha} = H_{\alpha\dot\alpha} + D_\alpha \bar L_{\dot\alpha} - \bar D_{\dot\alpha} L_\alpha \ . \tag{97}$$

where $\bar L_{\dot\alpha}$ is the complex conjugate of L_α, and thus this maintains the reality condition.

Requiring that (96) be invariant under these coordinate transformations, we get a constraint on the superfield L_α. Indeed, invariance requires that

$$0 = \int d^4\theta\, \bar D^{\dot\alpha} \mathcal{J}_{\alpha\dot\alpha} L^\alpha = \int d^4\theta\, X D^\alpha L_\alpha \ . \tag{98}$$

Since X is an unconstrained chiral superfield we get the complex equation

$$\bar D^2 D^\alpha L_\alpha = 0 \ . \tag{99}$$

The analog of the Wess-Zumino gauge is that the lowest components of H_μ vanish, i.e.

$$H_\mu\big| = H_\mu\big|_\theta = H_\mu\big|_{\bar\theta} = 0 \ , \tag{100}$$

as well as the fact that $H_\mu\big|_{\theta\sigma^\nu\bar\theta}$ is symmetric in μ and ν.

There is also some residual gauge freedom:

- $H_\mu\big|_{\theta^2}$ can be shifted by any complex divergenceless vector. This leaves only one complex degree of freedom, $\partial^\mu H_\mu\big|_{\theta^2}$.
- The metric field $h_{\mu\nu}$ transforms as

  $$\delta h_{\mu\nu} = \partial_\nu \xi_\mu + \partial_\mu \xi_\nu \ , \tag{101}$$

  where ξ_μ is a real vector.

[13] There are, however, theories in which $D_\alpha X$ is well-defined, but X itself is not.

[14] R-symmetric theories always admit a well-defined $\mathcal{R}$-multiplet.

[15] The case of the $\mathcal{R}$-multiplet is very similar but will not be discussed in detail because gravitational theories with global symmetries do not seem to be relevant according to our current understanding of quantum gravity.

- The gravitino transforms as

$$\delta\Psi_{\mu\alpha} = \partial_\mu \omega_\alpha \ . \tag{102}$$

In this Wess-Zumino gauge the components containing the gravitino and metric take the form

$$H_\mu\big|_{\theta\sigma^\nu\bar\theta} = h_{\mu\nu} - \eta_{\mu\nu} h \ , \tag{103}$$

and

$$H_\mu\big|_{\bar\theta^2\theta} = \Psi_{\mu\alpha} + \sigma_\mu\bar\sigma^\rho\Psi_\rho \ . \tag{104}$$

The top component of H_μ is a vector field which survives in the Wess-Zumino gauge. The bosonic off-shell degrees of freedom in H_μ consist of the complex scalar $\partial^\mu H_\mu\big|_{\theta^2}$, six real degrees of freedom in the graviton and the four real degrees of freedom in the top component of H_μ, for a total of 12 off-shell bosons. For the fermions, we have only the gravitino. It has $16-4=12$ off-shell degrees of freedom. This is the old minimal multiplet of supergravity [38–40]. This is in accordance with the 12 degrees of freedom in the FZ-multiplet.

A simple consistency check is to verify the leading couplings of the graviton and gravitino to matter. Recalling the formula for $\mathcal{J}_{\alpha\dot\alpha}$ (61) we find

$$\mathscr{L} \sim h_{\mu\nu} T^{\mu\nu} \ , \tag{105}$$

as expected. Similarly, for the coupling of the gravitino to matter we get

$$\begin{aligned}\mathscr{L} &\sim \epsilon^{\alpha\beta}\left(\Psi_\mu + \sigma_\mu\bar\sigma^\rho\Psi_\rho\right)_\alpha \left(S^\mu + \tfrac{1}{3}\sigma^\mu\bar\sigma^\rho S_\rho\right)_\beta \\ &= \Psi_{\mu\alpha} S^{\alpha\mu} \ .\end{aligned} \tag{106}$$

The last ingredient is the kinetic term for the graviton and gravitino. We begin by constructing a real superfield $E^{FZ}_{\alpha\dot\alpha}$ by covariantly differentiating $H_{\alpha\dot\alpha}$

$$\begin{aligned}E^{FZ}_{\alpha\dot\beta} &= \bar D_{\dot\tau} D^2 \bar D^{\dot\tau} H_{\alpha\dot\beta} + \bar D_{\dot\tau} D^2 \bar D_{\dot\beta} H^{\dot\tau}_\alpha \\ &\quad + D^\gamma \bar D^2 D_\alpha H_{\gamma\dot\beta} - 2\partial_{\alpha\dot\beta}\partial^{\gamma\dot\tau} H_{\gamma\dot\tau} \ .\end{aligned} \tag{107}$$

The reader can easily check that this expression is real. It is equivalent to a different-looking expression in [41]. The gauge transformations (97) act as

$$E'^{FZ}_{\alpha\dot\beta} = E^{FZ}_{\alpha\dot\beta} + [D_\alpha, \bar D_{\dot\beta}]\left(D^2\bar D_{\dot\alpha}\bar L^{\dot\alpha} + \bar D^2 D^\beta L_\beta\right) \ . \tag{108}$$

We see that $E^{FZ}_{\alpha\dot\beta}$ is invariant if (99) is imposed.

The superfield $E^{FZ}_{\alpha\dot\beta}$ satisfies another important algebraic equation

$$\bar D^{\dot\beta} E^{FZ}_{\alpha\dot\beta} = D_\alpha\left(\bar D^2 [D^\gamma, \bar D^{\dot\tau}] H_{\gamma\dot\tau}\right) \ . \tag{109}$$

Here, the expression in parenthesis is chiral. Note the similarity of the equation above to the defining property of the FZ-multiplet itself (60). The fact that E^{FZ} is invariant and satisfies an equation identical to the supercurrent superfield guarantees that the Lagrangian

$$\mathscr{L}_{\rm kin} \sim M_P^2 \int d^4\theta\, H^\mu E^{FZ}_\mu \tag{110}$$

is invariant. This contains in components the linearized Einstein and Rarita-Schwinger terms. The six additional supergauge-invariant bosons, $\partial^\mu H_\mu\big|_{\theta^2}$, $H_\mu\big|_{\theta^4}$ are auxiliary fields which are easily integrated out yielding $\partial^\mu H_\mu\big|_{\theta^2} \sim ix$, $H_\mu\big|_{\theta^4} \sim j_\mu$ where x and j_μ are the matter operators in the supercurrent multiplet.

We conclude that theories which have a well-defined FZ-multiplet can be coupled to supergravity in this fashion. The coupling to supergravity adds to the original theory a propagating graviton and gravitino. No other propagating fields are present in theory other than the original ones and the graviton and gravitino. This is important to remember in order to appreciate the point we will make soon. Note that if the FZ multiplet is not well defined (for example if it is not gauge invariant or if it is not globally well defined) the procedure above of constructing minimal supergravity cannot be carried out.[16]

7.2. Supergravity from the $\mathcal{S}$-Multiplet

We emphasized in the previous sections that various supersymmetric field theories do not have

[16] If there is no FZ-multiplet but there is an R-symmetry, we can construct the $\mathcal{R}$-multiplet and couple it to supergravity. For example, a free supersymmetric $U(1)$ theory with an FI-term can be coupled to supergravity in this fashion. For more comments on this case see also [42,43]. This procedure, however, gives rise to a supergravity theory with a continuous global R-symmetry.

an FZ-multiplet and the energy-momentum tensor and the supersymmetry current must be embedded in a larger multiplet $\mathcal{S}_{\alpha\dot\alpha}$. In such a case the construction of the previous subsection cannot be accomplished and the only possible supergravity theory is the one in which the $\mathcal{S}_{\alpha\dot\alpha}$ is gauged.

In this section we analyze this theory and as in the previous subsection, we limit ourselves to the analysis of the linearized theory. Since we have already understood how to do such things in the previous sections, we will be somewhat briefer now.

We begin from the coupling to matter

$$\int d^4\theta\, \mathcal{S}_{\alpha\dot\alpha} H^{\alpha\dot\alpha} \ . \tag{111}$$

For this to be invariant under (97), we need to impose the constraints

$$\bar D^2 D^\alpha L_\alpha = 0 \ , \qquad \bar D_{\dot\alpha} D^2 \bar L^{\dot\alpha} = D_\alpha \bar D^2 L^\alpha \ . \tag{112}$$

The first of them already appeared in the gauging of the FZ-multiplet but the second one is new. Since L_α is more constrained here than in the previous subsection, we will find more gauge invariant degrees of freedom. Some of them will even propagate.

Using an arbitrary L_α subject to these constraints we can choose the Wess-Zumino gauge

$$H_\mu\big| = H_\mu\big|_\theta = H_\mu\big|_{\bar\theta} = 0 \ . \tag{113}$$

The residual gauge transformations allow us to transform $H_\mu\big|_{\theta^2}$ by any divergence-less vector so we remain with one complex gauge invariant operator $\partial^\mu H_\mu\big|_{\theta^2}$. Another important residual transformation is

$$\delta H_\mu\big|_{\theta\sigma^\nu\bar\theta} + \delta H_\nu\big|_{\theta\sigma^\mu\bar\theta} = \partial_\mu\xi_\nu + \partial_\nu\xi_\mu \ , \tag{114}$$

with $\partial^\nu\xi_\nu = 0$. This means that the trace part of this symmetric tensor is invariant under the residual symmetries and therefore, the $\theta\bar\theta$ component contains the usual graviton but also an additional invariant scalar. The antisymmetric piece enjoys the usual gauge transformation of a two-form

$$\delta B_{\mu\nu} = \partial_\nu\omega_\nu - \partial_\nu\omega_\mu \ . \tag{115}$$

We also note that the top component of H_μ is invariant. Thus, we see that we have 16 off-shell bosonic degrees of freedom. The fermion is in the $\theta^2\bar\theta$ component (and its complex conjugate). It has residual gauge symmetry

$$\delta\Psi_{\mu\alpha} = i\partial_\mu\omega_\alpha \ , \qquad \sigma^\mu_{\alpha\dot\alpha}\partial_\mu\bar\omega^{\dot\alpha} = 0 \ . \tag{116}$$

Since ω_α satisfies the Dirac equation it cannot be used to set any further components to zero. Therefore, our theory includes a gravitino as well as an additional Weyl fermion. Thus, we have 16 off-shell fermionic degrees of freedom.

We conclude that the theory has $16+16$ fields. This is in accord with the $16+16$ operators in the multiplet $\mathcal{S}_{\alpha\dot\alpha}$. This supergravity multiplet has been recognized in the supergravity literature [44–46].

It is easy to construct a kinetic term; in fact $E^{FZ}_{\alpha\dot\beta}$ defined in (107) is still invariant because the set of transformations here is smaller than when the FZ-multiplet is gauged. However, this theory has another invariant. It is easy to see that $[D^\beta, \bar D^{\dot\beta}]H_{\beta\dot\beta}$ is invariant. We can use this observation to write an invariant kinetic term

$$\int d^4\theta\, \left([D,\bar D]H\right)^2 \ , \tag{117}$$

in addition to the one we have already included in the discussion of the FZ-multiplet.

To summarize, we find that this theory admits two independent kinetic terms. Thus there is one free real parameter r, and the most general kinetic term is

$$\int d^4\theta \left(H^{\alpha\dot\alpha} E^{FZ}_{\alpha\dot\alpha} + \frac{1}{2r} H^{\alpha\dot\alpha}[D_\alpha, \bar D_{\dot\alpha}][D^\beta, \bar D^{\dot\beta}] H_{\beta\dot\beta} \right) . \tag{118}$$

Our goal now is to identify the on-shell degrees of freedom in this theory and study their couplings to matter fields. There are many ways to do this, here we will choose a somewhat peculiar way that will make some very important facts transparent. We enlarge the gauge symmetry, relaxing either one of the two constraints (112) or both, and add compensator fields.

In order to contrast the situation with that in the previous subsection we choose to keep the first constraint in (112) and relax the second one by adding a chiral compensator field λ_α which transforms as

$$\delta\lambda_\alpha = \frac{3}{2}\bar{D}^2 L_\alpha \ . \tag{119}$$

First, the non-invariance of the coupling to matter $\int d^4\theta\, H^{\alpha\dot\alpha}\mathcal{S}_{\alpha\dot\alpha}$ can be corrected by a adding to the Lagrangian the term $-\frac{1}{6}\int d^2\theta\,\lambda^\alpha\chi_\alpha + \text{c.c.}$. Next, we move to the kinetic terms (118). The first term is invariant, but the second term is not. This is easily fixed by adding more terms to the Lagrangian. We end up with the invariant Lagrangian

$$\begin{aligned}\mathscr{L} = &\int d^4\theta\big(H^{\alpha\dot\alpha}E^{FZ}_{\alpha\dot\alpha} + \frac{1}{2r}H^{\alpha\dot\alpha}[D_\alpha,\bar{D}_{\dot\alpha}]\big([D,\bar{D}]H\big)\\ &+ H^{\alpha\dot\alpha}\mathcal{S}_{\alpha\dot\alpha}\big) - \big(\frac{1}{6}\int d^2\theta\lambda^\alpha\chi_\alpha + \text{c.c.}\big)\\ &- \frac{1}{r}\int d^4\theta\bigg(\big(D^\gamma\lambda_\gamma + \bar{D}_{\dot\gamma}\bar\lambda^{\dot\gamma}\big)[D,\bar{D}]H\\ &- \frac{1}{2}\big(D^\gamma\lambda_\gamma + \bar{D}_{\dot\gamma}\bar\lambda^{\dot\gamma}\big)^2\bigg)\ .\end{aligned} \tag{120}$$

The first term in the second line corrects the non-invariance of the coupling to matter and the other two terms fix the transformations of the kinetic terms.

In order to read out the spectrum we denote $G = D^\gamma\lambda_\gamma + \bar{D}_{\dot\gamma}\bar\lambda^{\dot\gamma}$ which is a real linear superfield (i.e. it satisfies $D^2G = 0$). We also express $\chi_\alpha = -\frac{3}{2}\bar{D}^2 D_\alpha U$, with a real U. We should remember that this U might not be well-defined; e.g. it might not be globally well-defined or might not be gauge invariant. In fact, the need of gauging the $\mathcal{S}$-multiplet arises precisely when this U is not well-defined. The Lagrangian above becomes

$$\begin{aligned}\mathscr{L} = &\int d^4\theta\big(H^{\alpha\dot\alpha}E^{FZ}_{\alpha\dot\alpha} + \tfrac{1}{2r}H^{\alpha\dot\alpha}[D_\alpha,\bar{D}_{\dot\alpha}][D,\bar{D}]H\\ &+H^{\alpha\dot\alpha}\mathcal{S}_{\alpha\dot\alpha}\big)\\ &-\tfrac{1}{r}\int d^4\theta\bigg(G\big([D,\bar{D}]H - rU\big) - \tfrac{1}{2}G^2\bigg)\ .\end{aligned} \tag{121}$$

Now we can dualize G. This is done by viewing it as an arbitrary real superfield and imposing the constraint $D^2G = 0$ by a Lagrange multiplier term $\int d^4\theta\,\big(\Phi+\bar\Phi\big)\,G$ where Φ is a chiral superfield. This makes it easy to integrate out G using its equation of motion $G = r^2\,\big(\Phi+\bar\Phi\big) + r^2U + [D,\bar{D}]H$ to find the Lagrangian

$$\begin{aligned}\mathscr{L} = \int d^4\theta\bigg(&H^{\alpha\dot\alpha}E^{FZ}_{\alpha\dot\alpha} + \big(\Phi+\bar\Phi+U\big)[D,\bar{D}]H\\ &-\tfrac{r}{2}\big(\Phi+\bar\Phi+U\big)^2 + H^{\alpha\dot\alpha}\mathcal{S}_{\alpha\dot\alpha}\bigg)\ .\end{aligned} \tag{122}$$

In this presentation the theory looks like a standard supergravity theory based on the FZ-multiplet which is coupled to a matter system which includes the original matter as well as the chiral superfield Φ. This is consistent with the counting of degrees of freedom ($4+4$ degrees of freedom in addition to ordinary supergravity) and with the identification of the 16/16 supergravity as an ordinary supergravity coupled to a chiral superfield. Note that even though the new superfield Φ originated from the gravity multiplet, its couplings are not completely determined. At the linear order we have freedom in the dimensionless parameter r and we expect additional freedom at higher orders.

The linear multiplet G, or equivalently the chiral superfield Φ, are easily recognized as the dilaton multiplet in string theory. There the graviton and the gravitino are accompanied by a dilaton, a two-form field and a fermion (dilatino). These are the degrees of freedom in G. After a duality transformation this multiplet turns into a chiral superfield Φ. Furthermore, as in string models, the second term in (122) mixes the dilaton and the trace of the linearized graviton h^μ_μ. Both this term and the term quadratic in Φ lead to the dilaton kinetic term.

As we mentioned above, the need for the multiplet $\mathcal{S}_{\alpha\dot\alpha}$ arises when the operator U is not a good operator in the theory. In this case the current $\mathcal{J}_{\alpha\dot\alpha}$ does not exist. The couplings in (122) explain how the chiral field Φ fixes this problem. Even though U is not a good operator, $\hat{U} = \Phi + \bar\Phi + U$ is a good operator. If U is not gauge invariant, Φ transforms under gauge transformations such that $\hat{U}$ is gauge invariant. And if U is not globally well-defined because it undergoes Kähler transformations, Φ has simi-

lar Kähler transformations such that $\hat{U}$ is well-defined.

The result of this discussion can be presented in two different ways. First, as we did here, we started with a rigid theory without an FZ-multiplet and we had to gauge the $\mathcal{S}$-multiplet. This has led us to the Lagrangian (122). Alternatively, we could add the chiral superfield Φ to the original rigid theory such that the combined theory does have an FZ-multiplet. Then, this new rigid theory can be coupled to standard supergravity by gauging the FZ-multiplet.

Our discussion makes it clear that if we want to couple the theory to supergravity, the additional chiral superfield Φ is not an option – it must be added, and it is propagating.

7.3. Summary and Constraints on Moduli

Of particular interest to us in this section was the coupling of theories without an FZ-multiplet to supergravity. Here we have limited ourselves to supersymmetric field theories in which all dimensionful parameters are fixed and we have studied the limit $M_p \to \infty$. We have not studied theories in which the matter couplings depend on M_p. These have been recently discussed in [47–51] but we will not elaborate on such "intrinsically gravitational" theories here.

In case where the FZ-multiplet does not exist, we have to gauge the $\mathcal{S}$-multiplet. The upshot of the analysis of this gauging is the following. We add to the rigid theory a chiral superfield Φ whose couplings are such that the combined system including Φ has an FZ-multiplet. This determines some but not all of the couplings of Φ to the matter fields. In the case of the FI-term Φ Higgses the symmetry and in the case of nontrivial target space geometry of the rigid theory it creates a larger total space in which the topology is simpler. Now that we have an FZ-multiplet we can simply gauge it using standard supergravity techniques. In particular, at the linearized level the couplings of Φ depend on only one free parameter: the normalization of its kinetic term.

Our results fit nicely with the many known examples of string vacua. We see that the ubiquity of moduli in string theory is a result of low energy consistency conditions in supergravity. As we emphasized above, the chiral superfield Φ is similar to the dilaton superfield in four dimensional supersymmetric string vacua. We often have field theory limits without an FZ-multiplet. For example, we can have a theory on a brane with an FI-term. The field theory limit does not have an FZ-multiplet and correspondingly, $U \sim \xi V$ is not gauge invariant. This problem is fixed, as in (122), by coupling the matter theory to Φ which is not gauge invariant (note the similarity to the way this is realized in string theory [52]). Similarly, we often consider field theory limits with a target space whose Kähler form is not exact. This happens, for instance, on D3-branes at a point in a Calabi-Yau manifold. If the latter is non-compact we find a supersymmetric field theory on the brane which typically does not have an FZ-multiplet because U is not globally well-defined. Coupling this system to supergravity corresponds to making M_p finite. In this case this is achieved by making the Calabi-Yau compact. Then in addition to the graviton, various moduli of the Calabi-Yau space become dynamical. They include fields like our Φ which couple as in (122), thus avoiding the problems with the FZ-multiplet and making the supergravity theory consistent.

This discussion has direct implications for moduli stabilization. It is often desirable to stabilize some moduli at energies above the supersymmetry breaking scale. In this case we have to make sure that the resulting supergravity theory is still consistent. In particular, it is impossible to stabilize Φ in a supersymmetric way and be left with a low energy theory without an FZ-multiplet.

For example, if the low energy theory includes a $U(1)$ gauge field with an FI-term, this term must be Φ dependent. Furthermore, if the mass of Φ is above the scale of supersymmetry breaking, it must be the same as the mass of the gauge field it Higgses. Consequently, there is no regime in which it is meaningful to say that there is an FI-term. Similar comments hold for theories with a compact target space. It is impossible to stabilize the Kähler moduli while allowing moduli for the positions of branes to remain massless without supersymmetry breaking.

The comments above have applications to

many popular string constructions including D-inflation, flux compactifications, and sequestering.

REFERENCES

1. J. Wess and J. Bagger, "Supersymmetry and supergravity," *Princeton, USA: Univ. Pr. (1992) 259 p*
2. S. Weinberg, "The quantum theory of fields. Vol. 3: Supersymmetry," Cambridge, UK: Univ. Pr. (2000) 419 p.
3. L. O'Raifeartaigh, "Spontaneous Symmetry Breaking For Chiral Scalar Superfields," Nucl. Phys. B **96**, 331 (1975).
4. S. Ray, "Some properties of meta-stable supersymmetry-breaking vacua in Wess-Zumino models," Phys. Lett. B **642**, 137 (2006) [arXiv:hep-th/0607172].
5. Z. Komargodski, D. Shih, "Notes on SUSY and R-Symmetry Breaking in Wess-Zumino Models," JHEP **0904**, 093 (2009). [arXiv:0902.0030 [hep-th]].
6. M. T. Grisaru, W. Siegel, M. Rocek, "Improved Methods for Supergraphs," Nucl. Phys. **B159**, 429 (1979).
7. N. Seiberg, "Naturalness versus supersymmetric nonrenormalization theorems," Phys. Lett. **B318**, 469-475 (1993). [hep-ph/9309335].
8. E. Witten, "Dynamical Breaking of Supersymmetry," Nucl. Phys. **B188**, 513 (1981).
9. K. A. Intriligator, N. Seiberg, "Lectures on Supersymmetry Breaking," Class. Quant. Grav. **24**, S741-S772 (2007). [hep-ph/0702069].
10. N. Seiberg, "Electric - magnetic duality in supersymmetric nonAbelian gauge theories," Nucl. Phys. **B435**, 129-146 (1995). [hep-th/9411149].
11. T. T. Dumitrescu, to appear.
12. S. Ferrara, B. Zumino, "Transformation Properties of the Supercurrent," Nucl. Phys. **B87**, 207 (1975).
13. Z. Komargodski, N. Seiberg, "Comments on the Fayet-Iliopoulos Term in Field Theory and Supergravity," JHEP **0906**, 007 (2009). [arXiv:0904.1159 [hep-th]].
14. Z. Komargodski, N. Seiberg, "Comments on Supercurrent Multiplets, Supersymmetric Field Theories and Supergravity," JHEP **1007**, 017 (2010). [arXiv:1002.2228 [hep-th]].
15. W. Fischler, H. P. Nilles, J. Polchinski *et al.*, "Vanishing Renormalization of the D Term in Supersymmetric U(1) Theories," Phys. Rev. Lett. **47**, 757 (1981).
16. M. A. Shifman, A. I. Vainshtein, "Solution of the Anomaly Puzzle in SUSY Gauge Theories and the Wilson Operator Expansion," Nucl. Phys. **B277**, 456 (1986).
17. M. Dine, "Fields, Strings and Duality: TASI 96," eds. C. Efthimiou and B. Greene (World Scientific, Sigapore, 1997).
18. S. Weinberg, "Nonrenormalization theorems in nonrenormalizable theories," Phys. Rev. Lett. **80**, 3702-3705 (1998). [hep-th/9803099].
19. N. Seiberg, "Exact results on the space of vacua of four-dimensional SUSY gauge theories," Phys. Rev. **D49**, 6857-6863 (1994). [hep-th/9402044].
20. Z. Komargodski, N. Seiberg, "From Linear SUSY to Constrained Superfields," JHEP **0909**, 066 (2009). [arXiv:0907.2441 [hep-th]].
21. M. Rocek, "Linearizing the Volkov-Akulov Model," Phys. Rev. Lett. **41**, 451-453 (1978).
22. S. Samuel, J. Wess, "A Superfield Formulation Of The Nonlinear Realization Of Supersymmetry And Its Coupling To Supergravity," Nucl. Phys. **B221**, 153 (1983).
23. P. Fayet, J. Iliopoulos, "Spontaneously Broken Supergauge Symmetries and Goldstone Spinors," Phys. Lett. **B51**, 461-464 (1974).
24. I. Affleck, M. Dine, N. Seiberg, "Dynamical Supersymmetry Breaking In Chiral Theories," Phys. Lett. **B137**, 187 (1984).
25. I. Affleck, M. Dine, N. Seiberg, "Exponential Hierarchy From Dynamical Supersymmetry Breaking," Phys. Lett. **B140**, 59 (1984).
26. D. V. Volkov, V. P. Akulov, "Is the Neutrino a Goldstone Particle?," Phys. Lett. **B46**, 109-110 (1973).
27. H. Luo, M. Luo, L. Wang, "The Goldstino Field in Linear and Nonlinear Realizations of Supersymmetry," Phys. Lett. **B685**, 338-340 (2010). [arXiv:0911.2836 [hep-th]].
28. A. A. Zheltukhin, "On equivalence of the

Komargodski-Seiberg action to the Volkov-Akulov action," [arXiv:1009.2166 [hep-th]].
29. S. M. Kuzenko, S. J. Tyler, "Relating the Komargodski-Seiberg and Akulov-Volkov actions: Exact nonlinear field redefinition," [arXiv:1009.3298 [hep-th]].
30. M. Dine, G. Festuccia, Z. Komargodski, "A Bound on the Superpotential," JHEP **1003**, 011 (2010). [arXiv:0910.2527 [hep-th]].
31. L. Alvarez-Gaume, C. Gomez, R. Jimenez, "Minimal Inflation," Phys. Lett. **B690**, 68-72 (2010). [arXiv:1001.0010 [hep-th]].
32. C. Cheung, Y. Nomura, J. Thaler, "Goldstini," JHEP **1003**, 073 (2010). [arXiv:1002.1967 [hep-ph]].
33. I. Antoniadis, M. Buican, "Goldstinos, Supercurrents and Metastable SUSY Breaking in N=2 Supersymmetric Gauge Theories," [arXiv:1005.3012 [hep-th]].
34. I. Antoniadis, E. Dudas, D. M. Ghilencea *et al.*, "Non-linear MSSM," Nucl. Phys. **B841**, 157-177 (2010). [arXiv:1006.1662 [hep-ph]].
35. N. Craig, J. March-Russell, M. McCullough, "The Goldstini Variations," JHEP **1010**, 095 (2010). [arXiv:1007.1239 [hep-ph]].
36. T. T. Dumitrescu, Z. Komargodski and M. Sudano, "Global Symmetries and D-Terms in Supersymmetric Field Theories," arXiv:1007.5352 [hep-th].
37. H. -C. Cheng, W. -C. Huang, I. Low *et al.*, "Goldstini as the decaying dark matter," [arXiv:1012.5300 [hep-ph]].
38. K. S. Stelle, P. C. West, "Minimal Auxiliary Fields for Supergravity," Phys. Lett. **B74**, 330 (1978).
39. S. Ferrara, P. van Nieuwenhuizen, "The Auxiliary Fields of Supergravity," Phys. Lett. **B74**, 333 (1978).
40. E. S. Fradkin, M. A. Vasiliev, "S Matrix For Theories That Admit Closure Of The Algebra With The Aid Of Auxiliary Fields: The Auxiliary Fields In Supergravity," Lett. Nuovo Cim. **22**, 651 (1978).
41. S. Ferrara, B. Zumino, "Structure of Conformal Supergravity," Nucl. Phys. **B134**, 301 (1978).
42. K. R. Dienes, B. Thomas, "On the Inconsistency of Fayet-Iliopoulos Terms in Supergravity Theories," Phys. Rev. **D81**, 065023 (2010). [arXiv:0911.0677 [hep-th]].
43. S. M. Kuzenko, "The Fayet-Iliopoulos term and nonlinear self-duality," Phys. Rev. **D81**, 085036 (2010). [arXiv:0911.5190 [hep-th]].
44. G. Girardi, R. Grimm, M. Muller *et al.*, "Antisymmetric Tensor Gauge Potential In Curved Superspace And A (16+16) Supergravity Multiplet," Phys. Lett. **B147**, 81 (1984).
45. W. Lang, J. Louis, B. A. Ovrut, "(16+16) Supergravity Coupled To Matter: The Low-energy Limit Of The Superstring," Phys. Lett. **B158**, 40 (1985).
46. W. Siegel, "16/16 Supergravity," Class. Quant. Grav. **3**, L47-L48 (1986).
47. E. Witten, J. Bagger, "Quantization of Newton's Constant in Certain Supergravity Theories," Phys. Lett. **B115**, 202 (1982).
48. N. Seiberg, "Modifying the Sum Over Topological Sectors and Constraints on Supergravity," JHEP **1007**, 070 (2010). [arXiv:1005.0002 [hep-th]].
49. J. Distler, E. Sharpe, "Quantization of Fayet-Iliopoulos Parameters in Supergravity," [arXiv:1008.0419 [hep-th]].
50. T. Banks, N. Seiberg, "Symmetries and Strings in Field Theory and Gravity," [arXiv:1011.5120 [hep-th]].
51. S. Hellerman, E. Sharpe, "Sums over topological sectors and quantization of Fayet-Iliopoulos parameters," [arXiv:1012.5999 [hep-th]].
52. M. Dine, N. Seiberg, E. Witten, "Fayet-Iliopoulos Terms in String Theory," Nucl. Phys. **B289**, 589 (1987).

Darboux coordinates, Yang-Yang functional, and gauge theory

N. Nekrasov[a,b*,c†], A. Rosly[b,d] and S. Shatashvili[a‡e,f]

[a]IHES, 35 route de Chartres
91440 Bures-sur-Yvette, FRANCE

[b]ITEP, Bol. Cheremushkinskaya 25
117259 Moscow, RUSSIA

[c]Simons Center for Geometry and Physics, Stony Brook University, Stony Brook NY 11794 USA

[d]Laboratory of Algebraic Geometry, SU-HSE, 7 Vavilova Str.,
117312 Moscow, RUSSIA

[e]Hamilton Mathematics Institute, Trinity College Dublin
Dublin 2, IRELAND

[f]School of Mathematics, Trinity College Dublin
Dublin 2, IRELAND

The moduli space of SL_2 flat connections on a punctured Riemann surface Σ with the fixed conjugacy classes of the monodromies around the punctures is endowed with a system of holomorphic Darboux coordinates, in which the generating function of the variety of SL_2-opers is identified with the universal part of the effective twisted superpotential of the Gaiotto type four dimensional $\mathcal{N} = 2$ supersymmetric theory subject to the two-dimensional Ω-deformation. This allows to give a definition of the Yang-Yang functionals for the quantum Hitchin system in terms of the classical geometry of the moduli space of local systems for the dual gauge group, and connect it to the instanton counting of the four dimensional gauge theories, in the rank one case.

1. Introduction

The exact relation between the microscopic definition of a quantum field theory and its low energy behavior is the major research subject. In the context of the supersymmetric gauge theories in four and two dimensions this relation touches upon some unexpected domains of the mathematical physics, such as the theory of classical and quantum integrable systems, and, in particular, the celebrated Bethe ansatz.

1.1. Bethe ansatz

Bethe ansatz is a useful technique for finding the spectra of the quantum integrable systems, such as the spin chains or the many-body systems, or even the 1+1 dimensional quantum field theories, see [1].

Generally speaking, the ansatz consists in finding a set of states $\mathbf{\Psi}(\lambda_1, \ldots, \lambda_N)$ which are characterized using some algebraic structure, or in terms of some functional equations, or otherwise. The physical meaning of the parameters $\lambda_1, \ldots, \lambda_N$ may differ from context to context, yet often they are the quasi-momenta of the quasi-free constituents.

The condition that $\mathbf{\Psi}(\lambda_1, \ldots, \lambda_N)$ actually belongs to the (Hilbert) space of states of the model, and it is the joint eigenstate of all the commuting Hamiltonians translates to the set of N equations on the quasimomenta $\lambda_1, \ldots, \lambda_N$ which, remark-

*On leave of absence
†On leave of absence
‡IHES Louis Michel Chair

ably, have the potential:

$$\frac{\partial Y(\lambda)}{\partial \lambda_k} = 2\pi i n_k, \qquad k = 1, \dots N \tag{1}$$

The function $Y(\lambda)$ is often analytic multivalued. We call it the Yang-Yang function, since C.N Yang and C.P. Yang used it for the analysis of the non-linear Schrödinger model [2] (see also [3]).

As an illustration, consider the simplest spin chain, the $SU(2)$ Heisenberg magnet, with L spin sites. It can be solved with the help of the algebraic Bethe ansatz, where the eigenstate of all the commuting Hamiltonians is found in the form of the N "quasiparticles"

$$B(\lambda_1)B(\lambda_2)\dots B(\lambda_N)|\mathrm{vac}\rangle \tag{2}$$

where the quasimomenta λ_k solve the equation (1) with the function

$$Y(\lambda) = \sum_{i=1}^{N} L\varpi_{\frac{1}{2}}(\lambda_i) + \sum_{i<j}^{N} \varpi_1(\lambda_i - \lambda_j) \tag{3}$$

where $\varpi_s(\lambda)$ is a certain special function whose explicit form is known:

$$\varpi_s(\lambda) = (\lambda + is)\log(\lambda + is) - (\lambda - is)\log(\lambda - is) \tag{4}$$

and $B(\lambda)$ is the creation operator (see [4] for details) of the quasiparticle of quasimomentum λ. The eigenvalues of all the commuting Hamiltonians are written in terms of the solutions to (1). In addition, the function $Y(\lambda)$, its derivatives with respect to the parameters, or its Hessian enter in the explicit expressions for the norms of the Bethe vectors (2), the correlation functions of local operators (see e. g. [5] and the references there). Thus the function $Y(\lambda)$ plays a central role in the concise formulation of the solution of the quantum system.

The universality of (1) is so far an experimental fact about the world of the quantum integrability. It has been a somewhat puzzling (and therefore for a long time abandonded) question as to what is the meaning of the function $Y(\lambda)$, why is the spectrum of the quantum problem described by what looks like a classical equation (1)? why does the function $Y(\lambda)$ look like a classical action of some classical mechanical system?

The goal of this paper is to elucidate this point. We shall show (in the restricted class of integrable systems) that one can indeed associate to the quantum integrable system a classical mechanical model, i.e. a symplectic manifold and a Lagrangian submanifold, and that the function $Y(\lambda)$ is identified with the generating function of this submanifold, in the appropriate Darboux coordinates. Thus we give a geometric definition of the Yang-Yang function for a large class of quantum integrable systems.

1.2. Gauge theories and quantum integrability

It turns out that quantum gauge theories are the way to understand the correspondence between the quantum integrability and classical symplectic geometry.

In [6] a connection between a quantum integrable system, the N-particle sector of the nonlinear Schrödinger theory, and a topologically twisted two dimensional gauge theory, was observed. The coupling constant of the quantum integrable system maps to the equivariant parameter, the twisted mass of the gauge theory, i.e. to the bulk coupling. In [7], [8] this subject was revived, by showing that the observation of [6] can be interpreted as the statement that the 2-observable [9] of the topological gauge theory of [6] descends from the Yang-Yang function [2] of the system of N non-relativistic particles on a circle with the δ-function pairwise potential (equivalent to the N-particle sector of the nonlinear Schrödinger system). Together with the earlier work on the relation between the quantum integrable many-body and spin systems of the Calogero-Moser-Sutherland type, harmonic analysis, and the topological gauge theories in various spacetime dimensions [10], [11], [12], [13] (where the strength of the interaction on the quantum system side corresponds to the parameters of the line defects on the gauge theory side) this strongly suggested that the connection between the gauge theory, the representation theory, and the quantum integrable systems is universal.

In all these cases the spectrum of the observables in gauge theory maps to the spectrum of quantum Hamiltonians on the integrable theory side.

Eventually in [14], [15], [16] the precise form of the Bethe/Gauge correspondence was formulated:

The supersymmetric vacua of the gauge theories with the two dimensional $\mathcal{N} = 2$ super-Poincare invariance, with the generic twisted masses and the superpotential, are the stationary states (the common eigenstates of the commuting Hamiltonians) of some quantum integrable system. The commuting Hamiltonians are the generators of the twisted chiral ring of the gauge theory. The quasimomenta of Bethe particles are the special coordinates on quasiclassical moduli space of vacua (the genericity assumption on the masses and superpotential implies this is a Coulomb branch). The Yang-Yang functional, generating the Bethe equations of the quantum system, is the effective twisted superpotential of the gauge theory. Thus, Bethe equations single out the supersymmetric vacua of the gauge theory.

This correspondence was checked for a large class of spin systems including the *XXX*, *XXZ*, *XYZ* spin chains for all spin groups and impurities, and for some quantum algebraic integrable systems as the elliptic Calogero-Moser, its relativistic version and limits such as the periodic Toda chain.

The gauge theories with the two dimensional super-Poincare invariance need not be two dimensional. In fact, in [17] the four dimensional theories with four dimensional super-Poincare invariance subject to the Ω-deformation in two dimensions were studied, leading to the quantum integrable systems whose classical limits are the Seiberg-Witten integrable systems [18], [19], [20], [21] describing the moduli space of vacua of the original four dimensional $\mathcal{N} = 2$ supersymmetric theory. The Ω-background in quantum field theory was introduced in [22], the idea is based on the earlier work [23], [24]. Its partition function, $\mathcal{Z}$-function, plays an important role in what follows.

1.3. Gauge theories from six dimensions

This paper will study a limited set of four dimensional $\mathcal{N} = 2$ gauge theories, namely those which can be engineered by taking the six dimensional (0,2) superconformal theory (discovered in [25], [26]) and compactifying it with a partial twist on a Riemann surface.

The resulting theory can be analyzed in several ways. One the one hand, by assuming the size of Σ negligible one deals with the four dimensional superconformal theory with $\mathcal{N} = 2$ supersymmetry. The enhancement of the $\mathcal{N} = 2$ supersymmetry to the superconformal symmetry is clear from the superconformal symmetry of the six dimensional $(0, 2)$ theory.

Indeed, consider first the compactification of the six dimensional theory on a finite size Riemann surface Σ, with the metric g_2. Let the metric on the four dimensional spacetime X^4 be g_4. The Lagrangian of the theory on X^4 depends on g_2.

If the six dimensional theory were a gauge theory to begin with, then the resulting four dimensional theory would have had the gauge coupling $\mathbf{g}_6$ depending on the symplectic, i.e. Kähler, moduli of Σ, e.g. $\mathbf{g}_4^{-2} = \mathbf{g}_6^{-2}\mathrm{Area}_\Sigma$, where

$$\mathrm{Area}_\Sigma = \int_\Sigma \sqrt{\det(g_2)} \tag{5}$$

However the $(0, 2)$ theory in six dimensions is not a gauge theory, and the relation between the couplings in four dimensions and the geometry of Σ is subtle. To begin with, one gets not one, but several gauge group factors, depending on the topology of Σ, and their couplings remain finite even when $\mathrm{Area}_\Sigma \to 0$. The couplings are determined by the complex structure of Σ, determined by the conformal class $[g_2]$ of g_2.

The conformal transformation of the four dimensional metric on X^4

$$g_4 \mapsto l^2 g_4 \tag{6}$$

lifts to the conformal transformation of the six dimensional metric

$$g_6 = g_2 \oplus g_4 \mapsto l^2 g_6 = l^2 g_2 \oplus l^2 g_4 \tag{7}$$

on $\Sigma \times X^4$. If Σ has a finite size metric, then the resulting six dimensional metric in the right hand

side of (7) gives rise to a different metric on Σ. However, in the limit of vanishing area of Σ the difference is negligible, hence the theory, in this limit, becomes conformal in the four dimensional sense.

It is not trivial to identify what this theory is, in four dimensional terms, e.g. describe the matter content and the Lagrangian.

When Σ is a two-torus, one can use the string duality dictionary to conclude that this theory is the $\mathcal{N} = 4$ super-Yang-Mills theory, whose gauge group is determined by the type of the six dimensional superconformal theory we started with. In particular, for the A_1 theory in six dimensions we get the $SU(2)$ theory in four dimensions. When Σ is a genus g Riemann surface, Gaiotto argues [27] one gets the $\mathcal{N} = 2$ super-Yang-Mills with the gauge group $SU(2)^{3g-3}$ with $2g - 2$ hypermultiplets transforming in the tri-fundamental representations of some triples of $SU(2)$'s out of the total $3g - 3$ factors. The precise assignment of these triplets is not unique, it is encoded in the trivalent graph describing the maximal degeneration of the complex structure of Σ. In particular, the complexified gauge couplings of the $SU(2)$ groups are identified with the usual asymptotic complex structure moduli corresponding to the pinched handles on the degenerate Riemann surface. In [27] more general theories, corresponding to the genus g complex curves with n punctures and some local data, assigning a complex number ν_k to the puncture z_k, were proposed. In particular, the celebrated $\mathcal{N} = 2$ $SU(2)$ theory with $N_f = 4$ fundamental hypermultiplets corresponds to the genus 0 curve, a sphere, with 4 punctures. The one-dimensional moduli space $\overline{\mathcal{M}}_{0,4} \approx \mathbf{CP}^1$ of complex structures of the 4-punctured sphere parametrizes the gauge coupling of the $SU(2)$ gauge group. Remarkably, this theory already exhibits the non-trivial S-duality of the $\mathcal{N} = 2$ theory. There are three points of the maximal degeneration in $\overline{\mathcal{M}}_{0,4}$. In the neighborhood of each point one identifies the gauge theory with the $SU(2)$ theory with four fundamental hypers, however, the relation between the gauge couplings and the matter multiplet masses in the three respective weak coupling regions is nontrivial – these are not the same gauge groups and not the same matter multiplets, as has been already observed in [28] at the level of the Seiberg-Witten curves. In particular, the triality exchanging the representations of the global $SO(8)$ symmetry group is identified in [27] with the modular group of $\mathcal{M}_{0,4}$.

1.4. The Ω-background

Any $\mathcal{N} = 2$ supersymmetric theory in four dimensions can be subject to the Ω-deformation. This is achieved in three steps: i) given the four dimensional theory T_4 find a six dimensional $\mathcal{N} = 1$ supersymmetric gauge theory T_6, whose dimensional reduction yields T_4; ii) compactify T_6 on a manifold X^6 which is an $\mathbf{R}^4$ vector bundle over the two-torus $\mathbf{T}^2$, of area r^2 with a flat $Spin(4) = SU(2)_+ \times SU(2)_-$ connection, whose holonomies around the two non-contractible cycles are $(e^{\frac{ir}{2}\mathrm{Re}(\varepsilon_1+\varepsilon_2)\sigma_3}, e^{\frac{ir}{2}\mathrm{Re}(\varepsilon_1-\varepsilon_2)\sigma_3})$ and $(e^{\frac{ir}{2}\mathrm{Im}(\varepsilon_1+\varepsilon_2)\sigma_3}, e^{\frac{ir}{2}\mathrm{Im}(\varepsilon_1-\varepsilon_2)\sigma_3})$, respectively. In addition, embed the $SU(2)_+$ part of the flat connection into the R-symmetry $SU(2)$ of the six dimensional theory; iii) take the limit $r \to 0$ while keeping the complex numbers $\varepsilon_1, \varepsilon_2$ finite. In this way we get the Ω-deformed theory on $\mathbf{R}^4$. The parameters $\varepsilon_1, \varepsilon_2$ first appeared as the equivariant parameters in the integrals over the instanton and D-brane moduli spaces in [6], [29].

The embedding of $SU(2)_+$ into the R-symmetry group is not unique when there are matter multiplets, as one can also embed $SU(2)_+$ in the global symmetry group. In other words, the masses of the four dimensional matter multiplets can be shifted by the multiples of $\varepsilon_1 + \varepsilon_2$.

Also, one can formulate the Ω-deformed theories on more general four-manifolds X^4, it suffices to have a $U(1)$, or $U(1) \times U(1)$ isometry (it should also be possible to extend this definition to the manifolds with $U(1)$-invariant conformal structure, but we shall not discuss this here). The idea is to use the X^4 bundle over $\mathbf{T}^2$ at the step ii.) of the procedure above, twisted by the elements of the symmetry group of X^4, which tend to identity as $r \to 0$.

In technical terms, this procedure amounts to replacing the adjoint scalar σ in the $\mathcal{N} = 2$ four

dimensional vector multiplet by the operator:

$$\sigma \mapsto \sigma + \varepsilon_1 \nabla_{\varphi_1} + \varepsilon_2 \nabla_{\varphi_2} \tag{8}$$

where ∂_{φ_1} and ∂_{φ_2} are the two vector fields on X^4 generating the $U(1) \times U(1)$ action.

In this paper, as in [17], we shall be interested in a particular case of the Ω-deformation, where $\varepsilon_2 = 0$. In this case the four dimensional $\mathcal{N} = 2$ super-Poincare invariance is reduced to the two dimensional $\mathcal{N} = 2$ super-Poincare. The parameter $\varepsilon_1 = \hbar$ is identified, in the spirit of [14], [16] with the Planck constant of a quantum integrable system, obtained by the quantization of the Seiberg-Witten integrable system corresponding to T_4.

One can think about this correspondence as a simplified version of the M-theory/string theory correspondence [30], in a sense that the Planck constant of one theory is mapped to the geometric parameter of the other.

1.5. Two dimensional flat connections and higher dimensional gauge theory

The moduli space $\mathcal{M}_{g,n;\nu}$ of flat connections (or, which is the same, local systems) with the gauge group G, on a genus g Riemann surface Σ with a finite number n of punctures, with the prescribed conjugacy classes ν of the monodromies around the punctures, is a frequent player in the studies of two, and three dimensional gauge theories, such as the Yang-Mills theory in two dimensions [31], [9], and the Chern-Simons theory in three dimensions [32]. In this context the case of a compact group G is the most natural.

In the attempts to describe the two [33], [34], [35], [36] or three [37] dimensional quantum gravity using the formalism of vierbeins and spin connections the non-compact gauge groups, such as $SL(2, \mathbf{R})$ or $SL(2, \mathbf{C})$, become important.

Despite some progress [38], [39] along these lines the satisfactory gauge theory construction of the quantum gravity theory is still missing [40].

Recently, the moduli spaces of flat connections $\mathcal{M}_{g,n;\nu}$ on a Riemann surface Σ, with or without punctures, with the complex gauge groups, such as $SL(2, \mathbf{C})$ or $PGL(2, \mathbf{C})$ became ubiquitous in the study of the four dimensional $\mathcal{N} = 2$ supersymmetric gauge theories, obtained by the compactification of the six dimensional $(0, 2)$-superconformal theory of the A_1 type, on a Riemann surface Σ. In what follows we shall often use a shorter notation $\mathcal{M}_\Sigma^{loc}$ or $\mathcal{M}^{loc}$ for $\mathcal{M}_{g,n;\nu}$.

A simple way of seeing the role of $\mathcal{M}_\Sigma^{loc}$ is to compactify the theory on a circle $\mathbf{S}^1_{R_a}$, of radius R_a. On the one hand, the analysis of [41] shows that the effective description of the resulting theory is the three dimensional $\mathcal{N} = 4$ supersymmetric sigma model on a manifold $M_{\rm tot}$ which is the total space of the Seiberg-Witten fibration over the moduli space of vacua of the four dimensional theory, in other words, the complex phase space of the Seiberg-Witten integrable system. On the other hand, remembering the six dimensional (0,2) origin of the theory in four dimensions, changing the order of compactification on Σ and $\mathbf{S}^1_R$ we arrive at the picture where the five dimensional maximally supersymmetric Yang-Mills theory with the gauge group $SU(2)$ (for the general A,D,E type (0,2) theory one gets the A,D,E type Lie group as the gauge group), and the five dimensional coupling

$$\mathbf{g}_5^2 = R_a$$

(so that the Yang-Mills instantons, which are the solitons of the $4 + 1$ dimensional theory, could be identified with the Kaluza-Klein modes of the six dimensional theory), is further compactified with a partial twist on Σ. The partial twist makes two out of five adjoint scalars in the vector multiplet a one-form on Σ valued in the adjoint bundle.

In the limit of vanishing size of Σ we arrive at the three dimensional theory which is clearly the sigma model on the moduli space of the minimal energy configurations, which are the complex connections, $\mathcal{A} = A + i\phi$, which are flat, $\mathcal{F} = d\mathcal{A} + \mathcal{A} \wedge \mathcal{A} = 0$, which are also D-flat, $D_A^* \phi = 0$, considered modulo gauge transformations. The D-flatness condition and the compact gauge transformations together can be traded for the invariance under the complex gauge transformations. Thus, we end up with the sigma model on the moduli space $\mathcal{M}_\Sigma^{loc}$ of complex flat connections on Σ, also known as the $G_{\mathbf{C}}$-local systems. The kinetic term of this sigma model is proportional to $\frac{1}{\mathbf{g}_5^2} = \frac{1}{R_a}$, thus we are led to the conclusion, as in [41], that the Kähler class of the metric

on $\mathcal{M}$ as seen by the effective action is proportional to $\frac{1}{R_a}$. The arguments of [41] involve the electric-magnetic duality, and this is the way to relate the two points of view we just reviewed.

1.6. The hyperkähler structure

The two descriptions of the effective target space above are consistent. They just exhibit different complex structures on the same manifold. The target space of the $\mathcal{N} = 4$ sigma model in three dimensions has to be a hyperkähler manifold. For the theories we consider this manifold is the moduli space $\mathcal{M}_H$ of solutions of Hitchin's equations [42]:

$$\begin{array}{c} D_z\phi_{\bar z} = 0,\, D_{\bar z}\phi_z = 0, \\ F_{z\bar z} + [\phi_z, \phi_{\bar z}] = 0 \end{array} \tag{9}$$

which is indeed hyperkähler (see [43] for the detailed review of its properties). In the complex structure (which is conventionally denoted by I) where the components $A_{\bar z}, \phi_z$ of the gauge field and the twisted scalar are holomorphic, the space $\mathcal{M}_H$ has the structure of the algebraic integrable system [44], with the base being the space of holomorphic differentials of degrees $d_1, d_2, \ldots, d_r$, for $r = rk(G)$, $P_i(\phi_z) \in H^0(\Sigma, K_\Sigma^{d_i})$ for the degree d_i invariant polynomials on $Lie(G)$, and the fiber being a (complement to a divisor in a) Jacobian of the spectral curve $\mathcal{C} \subset T^*\Sigma$, defined by the equation (for $G = SU(N)$, for other Lie groups see the review [45])

$$\mathrm{Det}(\phi_z - \lambda) = 0$$

In the complex structure J, where the holomorphic coordinates are the components

$$\mathcal{A}_z = A_z + i\phi_z, \qquad \mathcal{A}_{\bar z} = A_{\bar z} + i\phi_{\bar z},$$

M_H is identified (up to the usual stability issues) with the moduli space of the complex $G_{\mathbf{C}}$-flat connections. Finally, $K = IJ$, and the K-holomorphic coordinates are

$$A_z + \phi_z, \qquad A_{\bar z} - \phi_{\bar z}$$

The complex structure J is natural, if one thinks of the three dimensional theory as coming from the compactification of the six dimensional $\mathcal{N} = 1$ gauge theory on a three manifold $\Sigma \times \mathbf{S}^1_{r'}$, in the limit $r' \to \infty$.

To say that $\mathcal{M}_H$ is hyperkähler means that there exists the whole two-sphere of complex structures,

$$\mathcal{I} = aI + bJ + cK, \quad \mathcal{I}^2 = -1,$$

for any (a, b, c), s.t. $a^2 + b^2 + c^2 = 1$, and the two-sphere of the corresponding Kähler forms,

$$\omega_{\mathcal{I}} = a\omega_I + b\omega_J + c\omega_K \tag{10}$$

where

$$\omega_I = \int_\Sigma \mathrm{tr}\ (\delta A \wedge \delta A - \delta\phi \wedge \delta\phi) \tag{11}$$

$$\omega_J = \int_\Sigma \mathrm{tr}\ (\delta A \wedge *\delta\phi) \tag{12}$$

$$\omega_K = \int_\Sigma \mathrm{tr}\ (\delta A \wedge \delta\phi) \tag{13}$$

For the compact Σ the form ω_I realizes a non-trivial cohomology class of $\mathcal{M}_H$, while ω_J and ω_K are cohomologically trivial. We shall normalize the forms (10) in such a way that ω_I realizes the integral cohomology class, the restriction of ω_I onto the subvariety Bun_G where $\phi = 0$ is, up to the $(2\pi i)$ multiple, the curvature of the canonical Hermitian connection on the determinant line bundle L over Bun_G:

$$[\omega_I]\Big|_{\mathrm{Bun}_G} = c_1\,(L) \tag{14}$$

If the Riemann surface Σ has $n > 0$ punctures, then all three symplectic forms $\omega_{I,J,K}$ on the moduli space of the solutions to Hitchin's equations with the sources are, in general, cohomologically non-trivial.

1.7. From $\mathcal{N} = 2$ 4d gauge theory to 2d $\mathcal{N} = (4, 4)$ sigma model

We can further compactify the theory on a circle $\mathbf{S}^1_{R_b}$. On the one hand, this gives a two dimensional $\mathcal{N} = (4, 4)$ sigma model with the same target space M_H, whose Kähler class is proportional to R_b/R_a. More generally, if we start with the $(0, 2)$ theory and compactify it on $E_\rho \times \Sigma$, where

E_ρ is the elliptic curve with the complex modulus ρ, we would get the two dimensional sigma model on M_H with the complexified Kähler class

$$[\varpi] = \rho[\omega_I] \tag{15}$$

The two dimensional $\mathcal{N} = 2$ sigma model can be topologically twisted to define an A model, which depends on the symplectic structure of the target space, or to define a B model, which depends on the complex structure of the target space. The $\mathcal{N} = (2,2)$ theory can be twisted in an asymmetric manner, so that the left- and the right- chirality worldsheet one-form fermions would transform into the $\bar\partial$-derivatives of the worldsheet bosons which are holomorphic in the target space in two different complex structures (I_+, I_-) (there are also the generalizations involving the generalized complex structures but we shall not need them, see the discussion and the references in [43]).

1.8. Ω-deformation as the boundary condition

In topology, the G-equivariant cohomology of a space Y with the free G-action is the ordinary cohomology of the quotient space Y/G. As a module over $H^*(BG)$ (which is a polynomial ring) this is a pure torsion, and so, upon localization becomes trivial.

Similarly, the Ω-deformation of the gauge theory living on a spacetime X^4 with the free acting $U(1) \times U(1)$ isometry is can be undone by a field redefinition, and a redefinition of the couplings, as explained, for $X^4 = T^2 \times B^2$, in [46]. On the other hand, as we reviewed in the previous section, the four dimensional gauge theory compactified on T^2, reduces, at low energy, to the sigma model on the total space of the Seiberg-Witten fibration. The relation (15) gets modified, as the effective Kähler parameter ρ and the effective complex structure parameter τ (the asymptotic gauge coupling) get mixed with the parameters $\varepsilon_1, \varepsilon_2$ of the Ω-deformation.

If $U(1) \times U(1)$ acts on the four-manifold X^4 with the fixed points, then the transformation mapping the gauge theory to the sigma model is valid approximately, outside the fixed locus. We can view the worldsheet $B^2 = X^4/T^2$ of the sigma model as a two-manifold with corners, perhaps non-compact, and replace the effects of the Ω-deformation, which cannot be removed near the boundary ∂B^2, by some boundary conditions, i.e. the branes in the sigma model.

It is argued in [46] that at the smooth connected component of the boundary ∂B^2 the corresponding brane can be interpreted as a (A, B, A) brane, which, depending on the duality frame, is either the so-called canonical coisotropic brane (the cc-brane $\mathcal{B}^{cc}$, for short), or a particular complex (in the complex structure J) Lagrangian (with respect to ω_I and ω_K) brane, known as the brane of opers $\mathcal{B}_{\mathcal{O}_\tau}$, in the case of the $SU(2)$ Hitchin moduli space $\mathcal{M}_H$. This brane depends on the complex structure τ of the Riemann surface Σ, while the topological field theory, in which it is BRST invariant, does not.

The components at infinity $\partial B^2_\infty = \overline{B}^2 \backslash B^2$ also come with some boundary conditions, both in the gauge theory, and in the effective sigma model. It was argued in [46] that the corresponding branes $\mathcal{B}^\infty_\gamma$ also correspond to the middle-dimensional complex Lagrangians $\mathcal{L}_\gamma$ of the (A, B, A)-type, which, unlike $\mathcal{O}_\tau$, are defined in topological terms (i.e. these do not depend on the complex structure of Σ), yet may depend on some combinatorial data γ.

From now on we shall be discussing the Gaiotto theories of A_1 type. To describe the branes $\mathcal{B}^{cc}, \mathcal{B}_{\mathcal{O}_\tau}, \mathcal{B}^\infty_\gamma$ in more detail we need to discuss the geometry of the moduli space of flat connections.

1.9. Two two dimensional theories

Suppose we study the four dimensional theory on the manifold $X^4 = C^2 \times \mathbf{S}^1 \times \mathbf{R}^1$, where C^2 is topologically a disk, with the cigar metric:

$$ds^2_{C^2} = dr^2 + f(r) d\varphi_1^2 \tag{16}$$

Where $f(r) \sim r^2$ for $r \to 0$ and $f(r) \sim R^2$, for $r \to \infty$, for some constant R. Let φ_2 be the angular coordinate on the second $\mathbf{S}^1$. The base B^2 is, in this case, the half-plane $\mathbf{R}_+ \times \mathbf{R}$. Suppose we turn on the Ω-deformation corresponding to the isometry rotating C^2, i.e. the isometry generated by $\partial/\partial\varphi_1$.

On the one hand, we can relate this theory to the sigma model with the worldsheet B^2, as in

[46]. The sigma model brane corresponding to the boundary $r = 0$ is $\mathcal{B}^{cc}$ or its T-dual $\mathcal{B}_{\mathcal{O}_\tau}$. The other "boundary", at $r \to \infty$, leads to some asymptotic boundary condition, which we view as the brane $\mathcal{B}^{\infty}$, or $\mathcal{B}^{\infty}_{\gamma}$ if we want to specify the type γ of the boundary conditions. We shall call this viewpoint the theory T_{rt}

On the other hand, we can view this theory as a two dimensional $\mathcal{N} = (2,2)$ gauge theory with the worldsheet $\mathbf{S}^1 \times \mathbf{R}^1$, with an infinite number of fields, as in [17]. The Ω-deformation corresponds, in this two dimensional language, to turning on the twisted mass ε, corresponding to the global symmetry $U(1)$, which is the rotation of C^2. We shall call this two dimensional theory the theory T_{2t}.

The two dimensional theory has at low energies (in the sense of the theory on $\mathbf{S}^1 \times \mathbf{R}^1$) a description of the sigma model on the complexified Cartan subalgebra $\mathbf{t_C}$ of the gauge group, with the effective twisted superpotential $\tilde{\mathcal{W}}^{\rm eff}(\sigma; \tau; m, \varepsilon)$. Here σ denotes the flat coordinates on $\mathbf{t_C}$, τ denotes the four dimensional complexified gauge couplings, which are identified, for the Gaiotto A_1 theories, with the complex moduli of Σ in a suitable parametrization, m denotes the masses of the matter multiplets in four dimensions, and finally ε is the parameter of the Ω-background which is viewed as the two dimensional twisted mass. This superpotential can be split as a sum of two contributions: a contribution of the fixed point in C^2 and a contribution of the boundary at infinity:

$$\tilde{\mathcal{W}}^{\rm eff}(\sigma, \tau, m, \varepsilon, \gamma) = \varepsilon \left(\mathcal{W}_{\mathcal{O}_\tau}(\sigma/\varepsilon, m/\varepsilon) - \mathcal{W}_{\infty}(\sigma/\varepsilon, m/\varepsilon, \gamma) \right) \tag{17}$$

The contribution $\mathcal{W}_{\mathcal{O}_\tau}(\sigma/\varepsilon; m/\varepsilon)$ of the fixed point is computed from the asymptotics of the $\mathcal{Z}$-function as follows [17]:

$$\mathcal{W}_{\mathcal{O}_\tau}(\alpha, \nu) = \frac{1}{\varepsilon} {\rm Lim}_{\varepsilon_2 \to 0}\ \varepsilon_2 {\rm log} \mathcal{Z}(\alpha\varepsilon, \tau, \nu\varepsilon; \varepsilon, \varepsilon_2) \tag{18}$$

The left hand side is independent of ε, as follows from the asymptotic conformal invariance of the gauge theory under consideration.

The contribution of the region at infinity $\mathcal{W}_{\infty}(\alpha; \nu, \gamma)$ is independent of τ. This is demonstrated by observing [22] that the gauge theory subject to the Ω-deformation is extremely weakly coupled far away from the fixed points of the action of the isometry involved in the Ω-background. So we do not expect anything interesting to come from the bulk, however, if we cut the cigar C^2 at some finite value of r to have an infrared regulator, then we may expect some effective three dimensional supersymmetric gauge theory to live on the product of the circle at infinity $\mathbf{S}^1_{\infty}$ and the cylinder $\mathbf{S}^1 \times \mathbf{R}^1$, in analogy with the analysis of [47], [48]. Compared to the situation studied there we have half the supersymmetry, so the three dimensional theory has only four supercharges, and upon compactification on $\mathbf{S}^1_{\infty}$ generates a twisted superpotential, of the form studied in [14],[15]

$$\mathcal{W}_{\infty}(\alpha; \nu, \gamma) \sim \sum_{\ell} Li_2(e^{\ell(\alpha, \nu)}) \tag{19}$$

where the sum is over the charged matter fields, and ℓ is the linear function of the gauge multiplet scalar vevs and the masses. The degrees of freedom living at $\mathbf{S}^1_{\infty}$ depend on some combinatorial data γ which we shall make more explicit later, but we shall not attempt to identify the boundary theory and the corresponding superpotential more precisely. Instead, we focus on $\mathcal{W}_{\mathcal{O}_\tau}$.

1.10. Twisted superpotential as the generating function

Our main conjecture is as follows:

The effective twisted superpotential of the theory on $\mathbf{S}^1 \times \mathbf{R}^1$ obtained by localizing at the fixed point in C^2 is essentially the difference of the generating functions of the Lagrangian subvarieties $\mathcal{O}_\tau$ and $\mathcal{L}_\gamma$ in $\mathcal{M}^{loc}$, defined with respect to the appropriate Darboux coordinate system on $\mathcal{M}^{loc}$. The supersymmetric vacua of the theory T_{2t} correspond to the intersection points $v \in \mathcal{O}_\tau \cap \mathcal{L}_\gamma$, which are also the vacua of the theory T_{rt} subject to the appropriate D-brane boundary conditions.

This statement can be viewed as the improvement on the result of A. Beilinson and V. Drin-

feld. They show in [49] that upon the holomorphic quantization of the Hitchin system for the group G the spectrum (in the sense of commutative algebra) of twisted differential operators, e.g. the abstract quantum commuting Hamiltonians, identifies canonically with $\mathcal{O}_\tau$ for the dual group ${}^LG$. In this paper we will concentrate on

$$G = PGL(2,C),\ {}^LG = SL(2,C)\ .$$

Our point is that in the Darboux coordinate system (α,β) the generating function $\mathcal{W}_{\mathcal{O}_\tau}(\alpha,\nu)$ of the variety of opers,

$$\beta = \frac{\partial \mathcal{W}_{\mathcal{O}_\tau}(\alpha,\nu)}{\partial\alpha} \tag{20}$$

is essentially the Yang-Yang function of the quantum Hitchin system. More precisely, the Yang-Yang function $\mathcal{Y}(\alpha,\nu,\tau,\gamma)$ of the quantum Hitchin system depends on the complex structure τ of Σ (as does the Hitchin's integrable system) and on the choice of the "real slice", which defines the space of states $\mathcal{H}_\gamma$. Our claim is:

$$\mathcal{Y}(\alpha,\nu,\tau;\gamma) = \mathcal{W}_{\mathcal{O}_\tau}(\alpha,\nu) - \mathcal{W}_\gamma(\alpha,\nu) \tag{21}$$

i.e. up to a τ-independent piece the twisted superpotential $\mathcal{W}_{\mathcal{O}_\tau}(\alpha,\nu)$ computed by the four dimensional instanton calculus (18) is the Yang-Yang function. Indeed, the coordinates (α,β) are defined up to $2\pi i\mathbf{Z}$, so the *Bethe* equation

$$\frac{\partial\mathcal{Y}(\alpha,\nu,\tau,\gamma)}{\partial\alpha_k} = 2\pi i n_k,\ n_k \in \mathbf{Z} \tag{22}$$

determines the spectrum

$$E_k(\vec{n}) = \frac{\partial\mathcal{Y}(\alpha,\nu,\tau,\gamma)}{\partial\tau_k} \tag{23}$$

of the quantum Hitchin system. Let us clarify the meaning of (23). The classical Hamiltonians of the A_1 type Hitchin system are the quadratic differentials with the second order poles at the punctures, with the prescribed leading singularity. More precisely, given a basis $\mu^z_{(k)\bar{z}}$, $k = 1,\ldots,3g-3+n$, of the Beltrami differentials which correspond to the variations of the complex structure of the punctured Σ,

$$\mu^z_{(k)\bar{z}} \leftrightarrow \frac{\partial}{\partial\tau_k} \tag{24}$$

we compute:

$$H_k = \int_\Sigma \mu^z_{(k)\bar{z}}\mathrm{Tr}\phi_z^2 \tag{25}$$

Upon the deformation quantization H_k become the elements of the noncommutative ring (one has to talk about the sheaf of D-modules to actually see the noncommutative algebras, since the globally defined objects form a commutative subalgebra, [49]), whose spectrum we wish to determine. One has to specify the space of states on which we represent both the noncommutative algebra and its commutative subalgebra of the quantum integrals of motion. This is done (indirectly) by picking up a Lagrangian submanifold $\mathcal{L}_\gamma$. At the moment it is hard to make this construction explicit, since it involves the T-duality along the fibers of the Hitchin fibration. See [50],[46] for more details. The formula (23) actually makes sense even without specifying the space of states. It reflects the canonical identification [49] of the spectrum of the commutative algebra of the quantized Hitchin's Hamiltonians (the twisted differential operators on Bun_G) with the variety of opers. Indeed, $\mathcal{O}_\tau$ is a Lagrangian submanifold in $\mathcal{M}^{loc}$. As we vary the complex structure τ infinitesimally, the corresponding variation of the Lagrangian submanifold is described by a closed one-form defined on $\mathcal{O}_\tau$, i.e. a holomorphic function, since the variety of opers is simply-connected. This function can be computed locally using the Hamilton-Jacobi equation which gives (23) in the "static gauge" where to view the deformation of $\mathcal{O}_\tau$ while keeping α, the "Lagrangian half of the monodromy data", fixed.

Let us conclude with a few comments. In the context of the quantum integrable systems the Yang-Yang function is defined as a potential for Bethe equations, which is unique up to a constant which could be function of the parameters of the system, such as the complex structure parameters τ in our case. This ambiguity can be partly fixed by requiring that the derivatives of the Yang-Yang function with respect to the parameters τ_k correspond to the suitably normalized operators Φ_k, forming a basis in the space of quantum integrals of motion.

The eigenvalue $E_k(\vec{n})$ in (23) is calculated on

the solutions of (22) and depends on the discrete parameters $\vec{n}$. Obviously, the ambiguity we referred to above does not affect the differences $E_k(\vec{n}) - E_k(\vec{n}')$ of levels.

We would like to stress that both Eqs. (22), (23) make sense for any choice of the Darboux coordinates on $\mathcal{M}^{loc}$, as they express in coordinates two geometric facts: i) The eigenstates of the quantum system correspond to the intersection points v of two Lagrangian submanifolds in $\mathcal{M}^{loc}$; ii) the eigenvalues of the quantum Hamiltonians are the functions on the variety of opers which generate its deformations corresponding to the variations of the complex structure of Σ, evaluated at the intersection points v. In this sense the equations Eqs. (22), (23) (which for the genus zero case were formally written in [51]) do not determine the Yang-Yang function $\mathcal{Y}(\alpha, \tau, \nu, \gamma)$.

However, once both α and β coordinates are fixed, the Yang-Yang function is determined by the Lagrangian submanifolds $\mathcal{O}_\tau$ and $\mathcal{L}_\gamma$, and the claim that the τ-dependent piece coincides with the localized four dimensional gauge theory twisted superpotential (18) becomes quite nontrivial. It would not be true if instead of our (α, β) coordinates one took, e.g., Fock-Goncharov coordinates [52], which are used in [53] with much success.

2. Geometry of the moduli space of flat connections

Recall that we use the notations $\mathcal{M}_{g,n;\nu}$, $\mathcal{M}^{loc}_\Sigma$ or $\mathcal{M}^{loc}$ interchangeably.

2.1. Moduli of flat connections: explicit description

The moduli space $\mathcal{M}_{g,n;\nu}$ of flat connections is the space of equivalence classes of the homomorphisms of the fundamental group of the n-punctured genus g surface to the gauge group G, with the condition that the conjugacy class $[\mathrm{g}_k]$ of the image of the simple loop g_k surrounding the k'th puncture lands in a particular conjugacy class in G, which we label by ν_k. In case $G = SL(2, \mathbf{C})$ we view ν_k as a complex number modulo the action of the affine Weyl group which flips the sign of ν_k and shifts it by an integer. The invariant is the trace $m_k \in \mathbf{C}$ of the monodromy g_k around the puncture z_k:

$$m_k = 2\cos(2\pi\nu_k) = \mathrm{tr}(\mathrm{g}_k) \tag{26}$$

To be more precise we shall study the moduli space of flat G connections on a surface Σ with n small disks removed. This moduli space can be identified, very simply, with the space of $(2g + n)$-tuples of the elements of G, $(\mathbf{a}_1, \mathbf{b}_1, \ldots, \mathbf{a}_g, \mathbf{b}_g; \mathrm{g}_1, \ldots, \mathrm{g}_n)$, obeying:

$$\mathrm{g}_n \mathrm{g}_{n-1} \ldots \mathrm{g}_2 \mathrm{g}_1 \prod_{l=1}^{g} \mathbf{a}_l \mathbf{b}_l \mathbf{a}_l^{-1} \mathbf{b}_l^{-1} = 1 \tag{27}$$

considered up to a simultaneous conjugation:

$$(\mathbf{a}_1, \mathbf{b}_1, \ldots, \mathbf{a}_g, \mathbf{b}_g; \mathrm{g}_1, \ldots, \mathrm{g}_n) \sim \tag{28}$$
$$(h^{-1}\mathbf{a}_1 h, h^{-1}\mathbf{b}_1 h, \ldots, h^{-1}\mathbf{a}_g h, h^{-1}\mathbf{b}_g h;$$
$$h^{-1}\mathrm{g}_1 h, \ldots, h^{-1}\mathrm{g}_n h),$$

for any $h \in G$, and with the fixed conjugacy classes, which for $G = SL(2, \mathbf{C})$ reads as $\mathrm{tr}(\mathrm{g}_k) = 2\cos(2\pi\nu_k)$.

This identification depends upon the choice of the generators of the fundamental group of the complement $\Sigma \backslash \{z_1, \ldots, z_n\}$, as in the Fig. 1: From now we assume $(\nu_1, \ldots, \nu_n)$ which allows us to think of the space of functions on $\mathcal{M}_{g,n;\nu}$ as of the polynomial ring generated by the traces of monodromies around the noncontractible loops. This could be viewed as a definition of the $\mathcal{M}_{g,n;\nu}$ as of an affine variery.

Alternatively, one could choose a subset of stable points. This choice depends, in turn, on the n-tuple of real numbers $r_1, \ldots, r_n$. To implement this procedure properly one needs to use the full set of Hitchin's equations [42] with the delta function sources (see, e.g. [12], [54], [55], [56], [57], [58]). We shall not discuss this any further.

2.2. The symplectic form

The moduli space of flat connections on a compact Riemann surface is a symplectic manifold [31], with the symplectic form written on the space of all connections as:

$$\Omega = \int_\Sigma \mathrm{Tr}\, \delta A \wedge \delta A \tag{29}$$

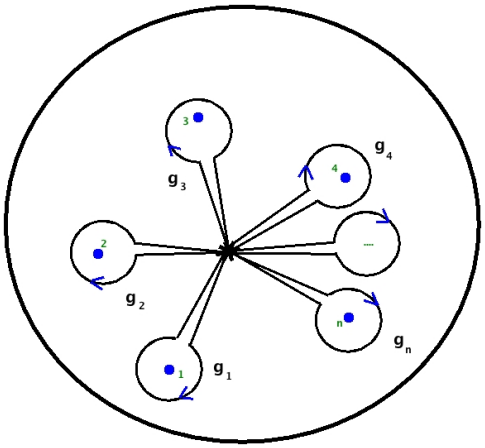

Figure 1. Generators of $\pi_1\left(\mathbf{S}^2\backslash\{z_1,\ldots,z_n\}\right)$

When one studies the moduli of flat connections on a surface with boundaries, one may use the Poisson description. Also, in the finite dimensional description of the moduli space, e.g. as in (27) one can realize the Poisson structure on the moduli space as descending from that on the space of graph connections, [59],[60], [61]. Alternatively, one may use the formalism of [52] to describe the symplectic form and some set of Darboux coordinates (which are different from the coordinates (α,β) which we introduce below!) associated with the triangulations of Σ with marked points (this formalism works if there is at least one puncture). See also [62], [63], [64], [65].

Using any of the formalisms above, or even the basic formula (29) which defines the Poisson structure on the space of all connections one deduces that the Poisson bracket of the Wilson loops in the fundamental representation is given by the "skein-relations" [63], [64]:

$$\left\{\mathrm{tr}P\mathrm{exp}\oint_{\gamma_1}\mathcal{A},\ \mathrm{tr}P\mathrm{exp}\oint_{\gamma_2}\mathcal{A}\right\}= \tag{30}$$

$$\frac{1}{2}\sum_{x\in\gamma_1\cap\gamma_2}\left(\mathrm{tr}P\mathrm{exp}\oint_{\gamma^+_{x,1,2}}\mathcal{A}-\mathrm{tr}P\mathrm{exp}\oint_{\gamma^-_{x,1,2}}\mathcal{A}\right)$$

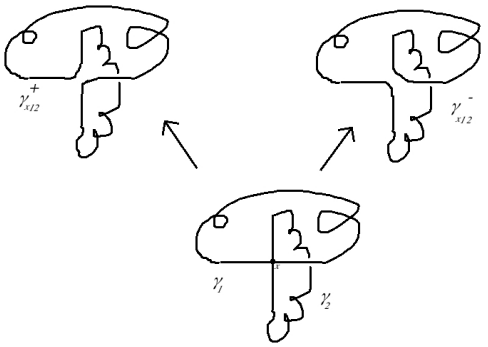

Figure 2. The intersecting loops γ_1, γ_2 and the simple loops $\gamma^{\pm}_{x,1,2}$

where the loops $\gamma^{\pm}_{x,1,2}$ are obtained by removing a small neighborhood of the intersection point x and replacing it by two arcs making a single loop, as in the Fig.2:

2.2.1. The case of a sphere with four punctures

Let us study first the case of $g=0, n=4$ in some detail. Let $\nu=(\nu_1,\nu_2,\nu_3,\nu_4)$. The moduli space $\mathcal{M}_{0,4;\nu}$ has the complex dimension two:

$$\mathcal{M}_{0,4;\nu}=$$

$$\left\{(\mathrm{g}_1,\mathrm{g}_2,\mathrm{g}_3)\in G^{\times 3}\ \middle|\ \begin{array}{c}\mathrm{tr}(\mathrm{g}_i)=m_i,\ i=1,2,3\\ \mathrm{tr}(\mathrm{g}_3\mathrm{g}_2\mathrm{g}_1)=m_4\end{array}\right\}\Big/G \tag{31}$$

where G acts by simultaneous conjugation $(\mathrm{g}_1,\mathrm{g}_2,\mathrm{g}_3)\ \mapsto\ \left(h^{-1}\mathrm{g}_1h,h^{-1}\mathrm{g}_2h,h^{-1}\mathrm{g}_3h\right)$. The generators of the coordinate ring of $\mathcal{M}_{0,4;\nu}$ can be taken to be:

$$\begin{array}{l}A=m_{12}=\mathrm{tr}(\mathrm{g}_1\mathrm{g}_2),\\ B=m_{23}=\mathrm{tr}(\mathrm{g}_2\mathrm{g}_3),\\ C=m_{13}=\mathrm{tr}(\mathrm{g}_1\mathrm{g}_3)\end{array} \tag{32}$$

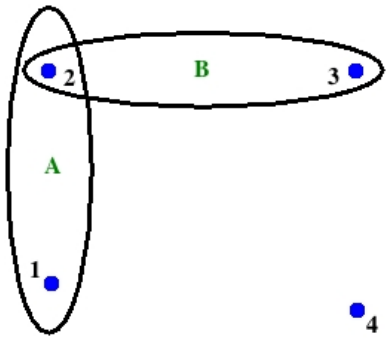

Figure 3. The A and B loops

with one polynomial relation (which is easy to verify)

$$\begin{aligned} &W_{0,4}(A,B,C)=0,\\ &W_{0,4}=ABC+A^2+B^2+C^2-4\\ &\qquad -A(m_3m_4+m_1m_2)\\ &\qquad -B(m_1m_4+m_2m_3)\\ &\qquad -C(m_1m_3+m_2m_4)\\ &+m_1^2+m_2^2+m_3^2+m_4^2+m_1m_2m_3m_4 \end{aligned} \tag{33}$$

The application of the rule (30) to the loops drawn around the pairs of points z_1, z_2 and z_2, z_3, respectively, as in the Fig.3: gives rise to the difference of two loops,

$$\{A,B\}=C^+-C^-$$

drawn on Fig. 4, which can be expressed via A, B, and C as follows:

$$C^+=\mathrm{tr}(\mathrm{g}_2^{-1}\mathrm{g}_1\mathrm{g}_2\mathrm{g}_3)= \tag{34}$$

$$-C-AB+m_1m_3+m_2m_4,$$

$$C^-=C$$

and also as the derivative of $W_{0,4}$:

$$\{A,B\}=\frac{\partial W_{0,4}}{\partial C} \tag{35}$$

In arriving at (34) we used the following identity

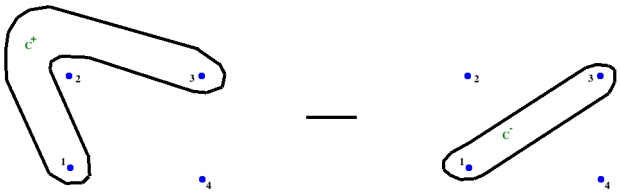

Figure 4. The C^+ and C^- loops

for the $SL(2)$ matrices:

$$\mathrm{tr}(g)\mathrm{tr}(h)=\mathrm{tr}(gh)+\mathrm{tr}(gh^{-1}) \tag{36}$$

which can also be expressed graphically: for any $x\in\gamma_1\cap\gamma_2$:

$$\mathrm{tr}P\mathrm{exp}\oint_{\gamma_1}\mathcal{A}\times\mathrm{tr}P\mathrm{exp}\oint_{\gamma_2}\mathcal{A}=$$

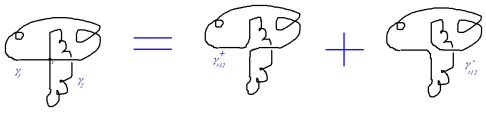

$$\mathrm{tr}P\mathrm{exp}\oint_{\gamma^+_{x12}}\mathcal{A}+\mathrm{tr}P\mathrm{exp}\oint_{\gamma^-_{x12}}\mathcal{A}$$

We can parametrize A, B, C with the help of the Darboux coordinates on $\mathcal{M}_{0,4;\nu}$, (α,β), i.e. $\{\alpha,\beta\}=1$,

$$\begin{aligned} &A=e^{\alpha}+e^{-\alpha},\\ &B(A^2-4)+2(m_2m_3+m_1m_4)-A(m_1m_3+m_2m_4)\\ &\qquad=(e^{\beta}+e^{-\beta})\sqrt{c_{12}(A)c_{34}(A)},\\ &(2C+AB-m_1m_3-m_2m_4)\left(e^{\alpha}-e^{-\alpha}\right)=\\ &\qquad=\left(e^{\beta}-e^{-\beta}\right)\sqrt{c_{12}(A)c_{34}(A)} \end{aligned} \tag{37}$$

where

$$c_{ij}(A)=A^2+m_i^2+m_j^2-Am_im_j-4$$

2.2.2. The case of a torus with one puncture

Now consider the case $g=1$, $n=1$. The moduli space is:

$\mathcal{M}_{1,1;\nu}=$

$$\left\{(\mathrm{g},\mathrm{h}) \in G^{\times 2} \;\middle|\; \mathrm{tr}(\mathrm{ghg}^{-1}\mathrm{h}^{-1}) = m\right\} \Big/ G \quad (38)$$

and it can be coordinatized by

$$A = \mathrm{tr}(\mathrm{g}),\ B = \mathrm{tr}(\mathrm{h}),\ C = \mathrm{tr}(\mathrm{gh}), \quad (39)$$

which obey the relation

$$\begin{aligned} W_{1,1}(A,B,C) &= 0 \\ W_{1,1} &= A^2 + B^2 + C^2 - ABC - m - 2 \end{aligned} \quad (40)$$

and the Poisson bracket of, e.g. A and B is easily computed to be

$$\{A, B\} = C - \frac{1}{2}AB \quad (41)$$

Now the local coordinates α, β, on $\mathcal{M}_{1,1;\nu}$, s.t.

$$\begin{aligned} A &= e^{\alpha} + e^{-\alpha}\,, \\ B &= \left(e^{\beta/2} + e^{-\beta/2}\right)\sqrt{\frac{A^2 - m - 2}{A^2 - 4}} \\ C &= \left(e^{\alpha+\beta/2} + e^{-\alpha-\beta/2}\right)\sqrt{\frac{A^2 - m - 2}{A^2 - 4}} \end{aligned} \quad (42)$$

are the Darboux coordinates for (41). Incidentally, the coordinates α, β in (42) are the coordinate and momentum in the two-body relativistic Calogero-Moser system with the coupling constant ν, the so-called Rujsenaars-Schneider system, whose Hamiltonian is B, see [11].

2.2.3. The braid and modular group actions

The set of generators $A, B, C, \ldots$ of the ring of polynomial functions on $\mathcal{M}^{loc}$ depends on the choice of the generators of the fundamental group of the (punctured) surface Σ, and so do the coordinates α, β defined by (37), (42). For example, in the genus one case, the monodromies (g, h) are defined with respect to some choice of the A and B cycles. An equally good choice is, e.g. $(\mathrm{g}, \mathrm{hg}^n)$, for any $n \in \mathbf{Z}$. The corresponding (α, β) coordinates transform to $(\alpha, \beta \pm 2n\alpha)$. There are analogous formulae in the genus zero case. We shall discuss them below.

3. The Darboux coordinates

In this section we describe the coordinate system on the moduli space $\mathcal{M}_{g,n;\nu}$ of flat $SL_2(\mathbf{C})$ connections on the punctured Riemann surface with the fixed conjugacy classes of the monodromies around the punctures.

3.1. The coordinate charts from the pant decomposition

We cover $\mathcal{M}_{g,n;\nu}$ by the coordinate charts $\mathcal{U}_\Gamma$ labelled by the points $\Gamma \in \overline{\mathcal{M}}_{g,n}$ in the Deligne-Mumford moduli stack of stable curves of genus g with n punctures, corresponding to the maximally degenerate Riemann surfaces. These points are in one-to-one correspondence with the trivalent graphs Γ with $b_1(\Gamma) = g$ with n tails. Such a graph has $3g - 3 + n$ internal edges (the edge is called internal if neither of its endpoints is a tail), and $2g - 2 + n$ internal (i.e. trivalent) vertices. This data is equivalent to a choice of the pant decomposition of Σ.

To each internal edge e we assign a pair (α_e, β_e) of complex numbers, with some discrete identifications. The edge e corresponds to a simple loop γ_e on Σ which gets contracted at the degeneration of the complex structure, corresponding to Γ. The holonomy around this loop determines α_e (up to the obvious indeterminancy):

$$\mathrm{tr} P\exp \oint_{\gamma_e} \mathcal{A} = e^{\alpha_e} + e^{-\alpha_e} \quad (43)$$

The rule of computing the dual coordinate β_e is the following. There are two situations: the two endpoints of the edge e are disctinct, in which case we call e *the genus* 0 *edge*, or the two endpoints coincide, in which case we call e *the genus* 1 *edge*. Each of the two endpoints of the genus 0 edge e has two other edges emanating, some of them could be tails, some of them could be identical, see the Figs. 5. By cutting open the simple loops on Σ corresponding to the edges emanating out of the two end-points of e, we get a sphere with four holes, which is cut out of Σ. Let us enumerate these holes, so that the two holes on the one end are 1 and 2, and the other two are 3 and 4. The flat connection on Σ restricts to the flat connection on the four-holed sphere, and defines the invariant functions, A, B, C, as in (32). Then, α and β defined by (37) are the α_e and β_e, corresponding to the edge e. We could have mislabeled the two edges emanating from one end of

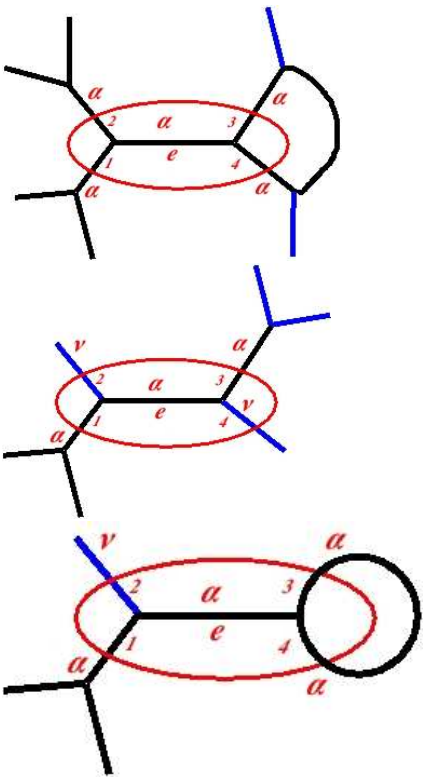

Figure 5. The genus 0 edges

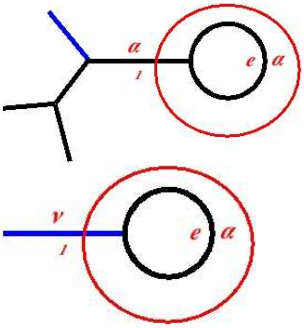

Figure 6. The genus 1 edges

e. This would have replaced β_e by $\beta_e \pm \alpha_e$.

For the genus 1 edge the situation is similar, except that there is only one simple loop to cut, which extracts out of Σ a one-holed torus. The restriction of flat connection onto this torus defines the invariant functions A, B and C as in (39). Then, using (42) we define the (α_e, β_e) pair for the local genus 1 edge.

3.1.1. A little bit of geometry

In this section we shall review some standard facts about the geometry of symplectic surfaces, the complexification of the Euclidean and Lobachevsky geometries, and the spaces of polygons.

We shall construct a complex version of the spherical and hyperbolic geometry of polygons in $M^3 = \mathbf{S}^3$ or $M^3 = \mathbf{H}^3$. It turns out that the Darboux coordinates α and β of the previous considerations can be viewed as describing the geometry of quadrangles in the $M^3_{\mathbf{C}} \approx G$. The justification for the somewhat involved analysis of the simple geometry is that the generalization of the Darboux coordinates for $n > 4$ turns out to describe the n-gons in G.

Let us view the group G as the affine hypersurface in the four dimensional complex vector space $V = \mathbf{C}^4 = \mathrm{Mat}_2(\mathbf{C})$ of the 2×2 complex matrices. We endow V with the complex metric:

$$\langle X, Y\rangle = \frac{1}{2}\left(\mathrm{tr}(XY) - \mathrm{tr}X\mathrm{tr}Y\right) \tag{44}$$

which is clearly invariant under the action of the group $G \times G$:

$$X \mapsto (g_L, g_R)\cdot X = g_L X g_R^{-1} \tag{45}$$

The group G is realized as a hypersurface:

$$\langle g, g\rangle = 1 \;\Leftrightarrow\; g \in G \tag{46}$$

The metric (44) induces a complex metric on G:

$$ds^2_G = \frac{1}{2}\mathrm{tr}dg^2 - \frac{1}{2}(\mathrm{tr}dg)^2 = -\frac{1}{2}\mathrm{tr}\left(g^{-1}dg\right)^2 \tag{47}$$

where we used the identity in $G \subset \mathrm{Mat}_{2\times 2}(\mathbf{C})$:

$$g + g^{-1} = \mathrm{tr}g \cdot 1 \tag{48}$$

The volume form $dg_{11}dg_{12}dg_{21}dg_{22}$ on V induces the volume form $\mathrm{vol}_G = \frac{1}{8\pi^2}\mathrm{tr}\left(g^{-1}dg\right)^3$ on G which is normalized so as to have a period 1 on the compact three-cycle $\mathbf{S}^3 \subset G$.

Given four elements $\mathrm{g}_1, \mathrm{g}_2, \mathrm{g}_3, \mathrm{g}_4 \in G$, which obey $\mathrm{g}_4\mathrm{g}_3\mathrm{g}_2\mathrm{g}_1 = 1$, we construct the complexified analogue of the hyperbolic tetrahedron Δ (see the Figure) . The vertices of Δ are the points: $(v_1 = 1, v_2 = \mathrm{g}_1, v_3 = \mathrm{g}_2\mathrm{g}_1, v_4 = \mathrm{g}_3\mathrm{g}_2\mathrm{g}_1)$. Let us introduce the Gram matrix of Δ:

$$\mathcal{C} = \|c_{ij}\|_{i,j=1\ldots4}, \qquad c_{ij} = c_{ji} = \langle v_i, v_j\rangle \quad (49)$$

We shall assume this matrix non-degenerate, $\mathrm{Det}(\mathcal{C}) \neq 0$. This implies that the vectors $v_1, \ldots, v_4$ are linearly independent. In particular, since $\langle v_i, v_i\rangle = 1$ for any i, we have that $c_{ij} \neq \pm 1$ for any $i \neq j$. Let us introduce the (hyperbolic) angle α_{ij}, via

$$\cosh(\alpha_{ij}) = c_{ij} \quad (50)$$

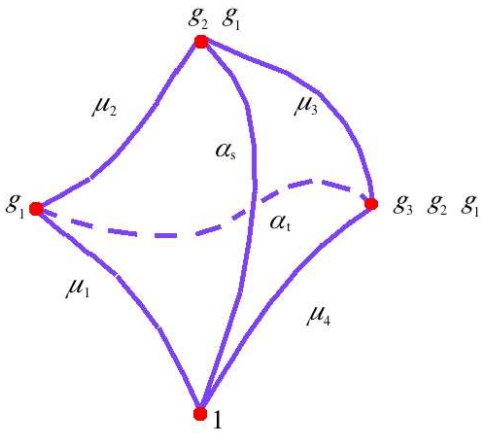

The choice of α_{ij} given c_{ij} is of course not unique, even up to a shift by $2\pi i\mathbf{Z}$. To fix the choice of α_{ij} as a unique element in $\mathbf{C}/2\pi i\mathbf{Z}$, one can pick $s_{ij} = \sinh(\alpha_{ij})$ in addition to c_{ij}. The edge e_{ij} connecting the vertices v_i and v_j is the intersection of the two dimensional complex plane $E_{ij} = \mathrm{Span}(v_i, v_j) \subset V$ and G:

$$e_{ij} = E_{ij} \cap G =$$

$$\{t_1 v_i + t_2 v_j \,|\, t_1^2 + t_2^2 + 2t_1t_2c_{ij} = 1,\, t_1, t_2 \in \mathbf{C}\} \quad (51)$$

We can identify e_{ij} with a copy of $\mathbf{C}^\times$, using the explicit parametrization: for $z \in \mathbf{C}^\times$,

$$t_1 = \frac{e^{2\alpha_{ij}} - z^2}{z(e^{2\alpha_{ij}} - 1)} \quad (52)$$

$$t_2 = \frac{e^{\alpha_{ij}}(z^2 - 1)}{z(e^{2\alpha_{ij}} - 1)}$$

The metric (47) restricts to e_{ij}, as

$$ds^2_{e_{ij}} = -\left(\frac{dz}{z}\right)^2 . \quad (53)$$

Thus, on e_{ij}, the complex metric (53) is a square of a $(1,0)$-differential $ds = idz/z$. The "length" of the edge l_{ij} is the period of ds along the one-chain connecting the vertices v_i and v_j, which in the z-coordinate is a path $\mathcal{C}_{ij}$ connecting the points 1 and $e^{\alpha_{ij}}$.

$$\int_{\mathcal{C}_{ij}} ds = \alpha_{ij} \bmod 2\pi i\mathbf{Z} \quad (54)$$

The face f_{ijk} of the the tetrahedron, with the vertices v_i, v_j, v_k, is the intersection of the three complex dimensional vector space $F_{ijk} = \mathrm{Span}(v_i, v_j, v_k) \subset V$ and G:

$$f_{ijk} = F_{ijk} \cap G =$$

$$\{\; t_1 v_i + t_2 v_j + t_3 v_k \,|\, t_1, t_2, t_3 \in \mathbf{C}, \quad (55)$$

$$t_1^2 + t_2^2 + t_3^2 + 2t_1t_2c_{ij} + 2t_1t_3c_{ik} + 2t_2t_3c_{jk} = 1\,\}$$

The manifold f_{ijk} is diffeomorphic to $T^*\mathbf{S}^2$. Given two faces, f_{ijk} and f_{jkl}, with the common edge l_{jk}, we define the angle β_{il} between them, as the angle between the planes F_{ijk} and F_{jkl}. The latter is defined as the angle between the normal lines, n_{ijk} and n_{jkl}, once a coorientation of the faces f_{ijk} and f_{jkl} is picked. Let us explain what it is.

The normal line n to a three-dimensional vector subspace $F \subset V$ is defined as the one-dimensional complex line in V, $n \subset V$, orthogonal, in the sense of the metric (44), to F: for any $f \in F$, $\langle f, n\rangle = 0$. There are two vectors of unit norm in n, which differ by a sign. A choice of one of these two unit norm vectors is the choice of the coorientation of F in V. We shall denote the unit norm vector in n by the same letter n.

Once the coorientation is fixed, the angle is defined via:

$$\cosh(\beta_{il}) = \langle n_{ijk}, n_{jkl} \rangle \tag{56}$$

A change of coorientation of one of the two planes changes the angle β to $\pi i - \beta$. This ambiguity is in addition to the ambiguity $\beta \mapsto -\beta$, and $\beta \mapsto \beta + 2\pi i k$, $k \in \mathbf{Z}$.

Let us now make the following useful observation (cf. [66]): Let ${}^L\mathcal{C}$ be the matrix of the hyperbolic cosines of the dihedral angles β_{ij}:

$${}^L\mathcal{C} = \|\cosh(\beta_{ij})\|_{i,j=1}^4 \tag{57}$$

Then:

$${}^L\mathcal{C} = \frac{1}{\sqrt{\mathcal{C}_d^\vee}}\, \mathcal{C}^\vee \, \frac{1}{\sqrt{\mathcal{C}_d^\vee}} \tag{58}$$

where $\mathcal{C}^\vee = \mathrm{Det}(\mathcal{C})\mathcal{C}^{-1}$ is the matrix of the minors of $\mathcal{C}$, and $\mathcal{C}_d^\vee$ is its diagonal part, e.g.

$$\cosh(\beta_{ij}) = \frac{\mathcal{C}_{ij}^\vee}{\sqrt{\mathcal{C}_{ii}^\vee \mathcal{C}_{jj}^\vee}} \tag{59}$$

The coorientation ambiguity in the definition of the β angles is the reason for the square root ambiguity in (59). To demonstrate (59) let us note that the vectors

$$v_i^\vee = \sum_{j=1}^4 \mathcal{C}_{ij}^\vee v_j \tag{60}$$

obey

$$\langle v_i^\vee, v_k \rangle = \mathrm{Det}(\mathcal{C})\delta_{ik} \tag{61}$$

and

$$\langle v_i^\vee, v_j^\vee \rangle = \mathrm{Det}(\mathcal{C})\mathcal{C}_{ij}^\vee \tag{62}$$

Therefore, we can choose the normal vectors to be

$$n_{ijk} = \varepsilon_{ijkl} \frac{v_l^\vee}{\sqrt{\mathrm{Det}(\mathcal{C})\mathcal{C}_{ll}^\vee}} \tag{63}$$

from which (59) follows immediately.

We can interpret the matrix ${}^L\mathcal{C}$ as the Gram matrix of the dual tetrahedron

$${}^L\Delta \quad \subset \quad {}^LG = PGL(2, \mathbf{C})$$

whose vertices are the normals to the faces of Δ up to a choice of orientation. Now let us return to the study of the moduli space $\mathcal{M}_{0,4;\vec{\nu}}$. We assign to every point in a finite cover of $\mathcal{M}_{0,4;\nu}$ a tetrahedron (perhaps, degenerate) in G, up to the action of the group $G \times G$ of the isometries of the metric (44). The vertices of the tetrahedron can be chosen to be:

$$(v_1, v_2, v_3, v_4) = (1, \mathrm{g}_1, \mathrm{g}_2\mathrm{g}_1, \mathrm{g}_3\mathrm{g}_2\mathrm{g}_1) \tag{64}$$

The corresponding Gram matrix is readily computed:

$$\mathcal{C} = \frac{1}{2}\begin{pmatrix} 2 & m_1 & A & m_4 \\ m_1 & 2 & m_2 & B \\ A & m_2 & 2 & m_3 \\ m_4 & B & m_3 & 2 \end{pmatrix} \tag{65}$$

which gives

$$\begin{aligned} -4\mathcal{C}_{22}^\vee = c_{34}(A),\ -4\mathcal{C}_{44}^\vee = c_{12}(A), \\ 8\mathcal{C}_{24}^\vee = B(A^2-4) - A(m_1m_3 + m_2m_4) \\ +2(m_2m_3 + m_1m_4) \end{aligned} \tag{66}$$

3.1.2. The Darboux coordinates for $\mathcal{M}_{0,4;\nu}$

We are now in position to state the definition of our coordinates in the case of the 4-punctured sphere. There are three points of the maximal degeneration of the complex structure which correspond to the s, t, and u channel tree scattering graphs. These degenerations collide the points $1-2, 3-4$, the points $1-4, 2-3$ and the points $1-3, 2-4$, respectively, see the Fig. 7. We cover the moduli space of flat connections by three coordinate charts. Each chart $\mathcal{U}_i$ has the coordinates (α_i, β_i), where $i = s, t, u$. The relation of (α_s, β_s), and (α_t, β_t) coordinates to the flat connection on the 4-punctured sphere with the basic holonomies $\mathrm{g}_{1,2,3}$ is depicted in the Fig. 8. The coordinates (α_u, β_u) are obtained by applying the modular group action:

$$(\mathrm{g}_1, \mathrm{g}_2, \mathrm{g}_3) \mapsto \left(\mathrm{g}_2, \mathrm{g}_2\mathrm{g}_1\mathrm{g}_2^{-1}, \mathrm{g}_3\right) \tag{67}$$

which maps the tetrahedron with the vertices $(1, \mathrm{g}_1, \mathrm{g}_2\mathrm{g}_1, \mathrm{g}_3\mathrm{g}_2\mathrm{g}_1)$ to the tetrahedron with the vertices $(1, \mathrm{g}_2, \mathrm{g}_2\mathrm{g}_1, \mathrm{g}_3\mathrm{g}_2\mathrm{g}_1)$.

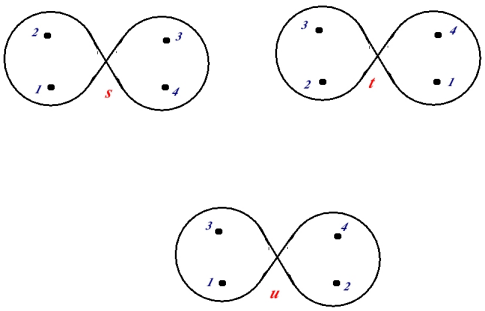

Figure 7. The degeneration points in $\overline{\mathcal{M}}_{0,4}$

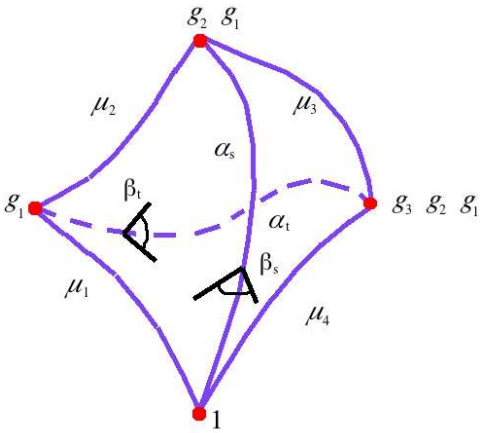

Figure 8. The (α_s, β_s) and (α_t, β_t) coordinates

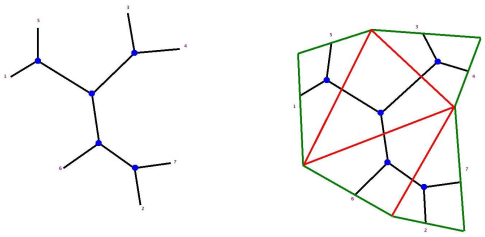

Figure 9. From the tree graph to the polygon triangulated by the diagonals

3.1.3. The Darboux coordinates for $\mathcal{M}_{0,n;\nu}$ are defined analogously, and can be given a geometric interpretation in terms of the geometry of a polygon with the vertices $(1, \mathrm{g}_1, \mathrm{g}_2\mathrm{g}_1, \ldots, \mathrm{g}_{n-1}\mathrm{g}_{n-2}\ldots\mathrm{g}_2\mathrm{g}_1)$ which is cut by $n-3$ diagonals onto $n-2$ (complexified hyperbolic or spherical) triangles. The coordinate α_i, $i = 1, \ldots, n-3$ is the hyperbolic length of the diagonal d_i, while the coordinate β_i is the dihedral angle between the two adjacent triangles, which share the common edge d_i, see Fig. 9 for the case of $n = 7$.

3.1.4. The coordinate transformations

It is interesting to look at the coordinate transformations which glue our coordinate systems on the overlaps $\mathcal{U}_\Gamma \cap \mathcal{U}_{\Gamma'}$. It suffices to discuss the overlaps where the two graphs Γ and Γ' differ in exactly one genus 0 edge, or in exactly one genus 1 edge. In the first case the basic transformation is $(\alpha_s, \beta_s) \mapsto (\alpha_t, \beta_t)$ in the case of $\mathcal{M}_{0,4;\nu}$. Recall that the canonical transformations, i.e. the transformations preserving the symplectic form, are generated by a function, the so-called generating function: $\mathcal{S}_{0,4}(\alpha_s, \alpha_t; \vec{\nu})$, such that:

$$\beta_s = \frac{\partial \mathcal{S}_{0,4}}{\partial \alpha_s}\,, \quad \beta_t = \frac{\partial \mathcal{S}_{0,4}}{\partial \alpha_t} \tag{68}$$

Using the formulae of [67] one can easily derive that $\mathcal{S}_{0,4}(\alpha_s, \alpha_t, \nu_1, \nu_2, \nu_3, \nu_4)$ is the hyperbolic volume of the tetrahedron ${}^L\Delta$, which is dual to the tetrahedron Δ (Fig. 8) whose edges have the lengths

$$\alpha_s, \alpha_t, \mu_1, \mu_2, \mu_3, \mu_4\ .$$

where $\mu_k = 2\pi i \nu_k$. The explicit formula can be derived using [66] (see also [67], [68], [69], [70]): Let

$$\begin{aligned}
\mathcal{V}_1 &= \alpha_s + \mu_1 + \mu_2 \\
\mathcal{V}_2 &= \alpha_s + \mu_3 + \mu_4 \\
\mathcal{V}_3 &= \alpha_t + \mu_1 + \mu_4 \\
\mathcal{V}_4 &= \alpha_t + \mu_2 + \mu_3 \\
\mathcal{H}_1 &= \mu_1 + \mu_2 + \mu_3 + \mu_4 \\
\mathcal{H}_2 &= \alpha_s + \alpha_t + \mu_1 + \mu_3 \\
\mathcal{H}_3 &= \alpha_s + \alpha_t + \mu_2 + \mu_4 \\
\mathcal{H}_4 &= 0
\end{aligned}$$

Then:

$$\begin{aligned}
&\mathcal{S}_{0,4}(\alpha_s, \alpha_t, \vec{\nu}) = \\
&\sum_{a=1}^{4} \left[Li_2\left(w_+ e^{\mathcal{V}_a}\right) - Li_2\left(w_- e^{\mathcal{V}_a}\right) \right. \\
&\left. - Li_2\left(w_+ e^{\mathcal{H}_a}\right) + Li_2\left(w_- e^{\mathcal{H}_a}\right) \right]
\end{aligned} \tag{69}$$

where $w_\pm$ are the two different roots of the (quadratic in w) equation:

$$\prod_{a=1}^{4} (1 - w e^{\mathcal{V}_a}) = \prod_{a=1}^{4} (1 - w e^{\mathcal{H}_a}) \tag{70}$$

For the genus 1 edge the formalism is similar and we shall not present it here.

3.1.5. The Hamiltonian flows and bending

Fix Γ and consider the Hamiltonian flows generated by the Poisson-commuting functions $A_e = e^{\alpha_e} + e^{-\alpha_e}$, for all edges e. These flows generate a complexified integrable system. Its real slices include the Fenchel-Nielsen twistings on the Teichmüller space and Goldman flows [65] on the moduli space of $SU(2)$ flat connections.

In our coordinates the flow generated by α_e acts very simply: β_e is shifted while $\alpha_{e'}$'s and $\beta_{e'}$ for $e' \neq e$ are unchanged. It is amusing to see the action of this flow on the monodromy data of a flat connection $\mathcal{A}$. We shall do it for the $g = 0, n = 4$ case.

Thus, let us take α as a Hamiltonian, and let us try to find out what is the Hamiltonian flow $\mathcal{U}_t$ generated by it. Of course, in the (α, β) coordinates this is trivial: $\mathcal{U}_t : (\alpha, \beta) \mapsto (\alpha, \beta + t)$. Let us calculate the effect of this transformation on the flat connection $\mathcal{A}$, which we parametrize by the gauge equivalence class of the triple $(\mathrm{g}_1, \mathrm{g}_2, \mathrm{g}_3, \mathrm{g}_4)$, with $\mathrm{g}_4\mathrm{g}_3\mathrm{g}_2\mathrm{g}_1 = 1$. We claim:

$$\mathcal{U}_t : (\mathrm{g}_1, \mathrm{g}_2, \mathrm{g}_3, \mathrm{g}_4) \mapsto (\mathrm{g}_1, \mathrm{g}_2, e^{-tJ}\mathrm{g}_3 e^{tJ}, e^{-tJ}\mathrm{g}_4 e^{tJ}) \tag{71}$$

where we have introduced a normalized Lie algebra element J, a traceless 2×2 matrix with the eigenvalues $\pm\frac{1}{2}$, $\mathrm{tr} J = 0$, $\mathrm{tr} J^2 = \frac{1}{2}$, such that:

$$\mathrm{g}_2\mathrm{g}_1 = e^{2\alpha J} \ . \tag{72}$$

Indeed, let

$$B_t = \mathrm{tr}(\mathrm{g}_2 e^{-tJ}\mathrm{g}_3 e^{tJ}) \tag{73}$$

Using the identity for the SL_2 matrices:

$$e^{2t\alpha J} = \frac{\sinh(1-t)\alpha}{\sinh\alpha} + \frac{\sinh t\alpha}{\sinh\alpha}\, e^{2\alpha J} \ .$$

we can easily compute:

$$\begin{aligned}
B_t(A^2 - 4) + 2\,(m_2 m_3 + m_1 m_4) - \\
A\,(m_1 m_3 + m_2 m_4) = \\
2\cosh(\beta + t)\sqrt{c_{12}(A) c_{34}(A)}
\end{aligned}$$

which establishes (71).

In the general $g = 0$ case, the Hamiltonian flow generated by α_e corresponding to the edge e, and the corresponding diagonal d_e (as in the Fig. 9), has a very simple geometric interpretation (modulo the complexification): one simply bends the hyperbolic n-gon along the diagonal d_e. The angle of bending corresponding to $\mathcal{U}_t$ is equal to t. This is a complexified version of the constructions in [63], [71], [72], [73].

4. The brane of opers

In this section we study briefly the so-called brane of opers in the sigma model with the target space $\mathcal{M}_\Sigma^{loc}$. This is a (A, B, A) type D-brane

$\mathcal{B}_{\mathcal{O}_\tau}$, which corresponds to the J-complex Ω_J-Lagrangian submanifold $\mathcal{O}_\tau \subset \mathcal{M}^{loc}_\Sigma$, described in [74]. In fact, locally $\mathcal{M}^{loc}$ is foliated by the varieties of SL_2-opers for different complex structures on Σ, as expressed by the local identification of the moduli space of flat SL_2-connections with the moduli space of projective structures [75], see also [36], [76].

Roughly speaking, a flat connection $\mathcal{A} = \mathcal{A}_z dz + \mathcal{A}_{\bar z} d\bar z$ is a G-oper, if the gauge equivalence class of $\bar A = \mathcal{A}_{\bar z} d\bar z$ defines a particular holomorphic G-bundle on Σ, which is determined by the complex structure of Σ. For $G = SL_2(\mathbf{C})$ this bundle is such that the associated rank two vector bundle is the (unique up to isomorphism) nontrivial extension of the bundle $K_\Sigma^{-1/2}$ by $K_\Sigma^{1/2}$.

Locally an SL_2-oper is a second order (meromorphic) differential operator $\mathcal{D} = -\partial^2 + T(z)$ which acts on the $(-\frac{1}{2})$-differentials.

If we fix for convenience some reference complex structure on Σ, with the local coordinates $(w, \bar w)$, and describe the generic complex structure with the help of the Beltrami differential $\mu = \mu^w_{\bar w} d\bar w \partial_w$, then

$$A_{\bar w} - \mu A_w = \begin{pmatrix} -\frac{1}{2}\partial\mu & 0 \\ -\frac{1}{2}\partial^2\mu & \frac{1}{2}\partial\mu \end{pmatrix},\ A_w = \begin{pmatrix} 0 & 1 \\ \tilde T & 0 \end{pmatrix} \tag{74}$$

where $\tilde T$ obeys the following compatibility condition

$$\left(\bar\partial - \mu\partial - 2\partial\mu\right)\tilde T = -\frac{1}{2}\partial^3\mu \tag{75}$$

The notion of a G-oper was in general given for a Riemann surface with punctures, where the opers may develop certain poles [74]. In this paper we study only the case of regular singularities. It means at any puncture, T has at most the second order pole.

In the case of $G = SL_2(\mathbf{C})$ the space of opers for varying complex structure of Σ is the open subset in the moduli space of flat G-connections [75].

4.1. The SL_2-opers in genus zero

In the case of the genus zero surface with n marked points the SL_2-oper can be identified with the second order differential operator (the projective connection) of the form:

$$\mathcal{D} = -\partial_z^2 + T(z)$$
$$T(z) = \sum_{a=1}^n \frac{\Delta_a}{(z-x_a)^2} + \frac{\epsilon_a}{z-x_a} \tag{76}$$

where the *accessory parameters* ϵ_a obey

$$\sum_{a=1}^n \epsilon_a = 0$$
$$\sum_{a=1}^n \left(x_a\epsilon_a + \Delta_a\right) = 0 \tag{77}$$
$$\sum_{a=1}^n \left(x_a^2\epsilon_a + 2x_a\Delta_a\right) = 0$$

in order for (76) be non-singular at $z = \infty$. Actually, an open set in the space of all SL_2-flat connections on the n-punctured sphere can be parametrized by the space of n-tuples $(x_a, \epsilon_a)_{a=1}^n$ obeying (77) modulo the diagonal PGL_2-action

$$(x_a, \epsilon_a)_{a=1}^n \mapsto$$
$$\left(\frac{Ax_a + B}{Cx_a + D},\ \epsilon_a(Cx_a+D)^2 + 2C(Cx_a+D)\Delta_a\right)_{a=1}^n$$

The oper (76) defines a point in $\mathcal{M}_{0,n;\nu}$ when

$$\Delta_a = \nu_a(\nu_a - 1)\,,\ a = 1, \dots n \tag{78}$$

The correspondence (24,25) $\partial_{\tau_k} \leftrightarrow H_k$ between the variations of the complex moduli of Σ and the functions on the variety of opers $\mathcal{O}_\tau$ is provided, in this case, by the one-form

$$\delta = \sum_a \epsilon_a dx_a \tag{79}$$

Once a global coordinate z on the sphere is fixed, e.g. by requiring three out of n punctures to be at $0, 1, \infty$, the one-form δ becomes well-defined in the tangent space to $\mathcal{M}_{0,n}$.

4.2. The SL_2-opers in genus one

We can also describe quite explicitly the space of opers on an elliptic curve E_τ with regular singularities at the points $x_1, \dots, x_n \in E_\tau$:

$$\mathcal{D} = -\partial_z^2 + T(z)$$
$$T(z) = u + \sum_{a=1}^n \Delta_a \wp(z - x_a) + \epsilon_a \zeta(z - x_a) \tag{80}$$

where $\sum_a \epsilon_a = 0$, u is a constant, and we used the Weierstrass ζ and $\wp = \zeta'$ functions. The correspondence $\partial_{\tau_k} \leftrightarrow H_k$ is now represented by the one-form

$$\delta = \sum_a \epsilon_a dx_a + u d\tau \tag{81}$$

4.3. The opers on degenerate curves

For practical purposes it is useful to study the regular opers on a smooth curve with punctures whose complex structure approaches that of a maximally degenerate stable curve. As we discussed above, such maximal degeneration can be encoded in a trivalent graph Γ with n tails and g loops. Each internal vertex corresponds to a three-holed sphere, each internal edge corresponds to a double point (a pinched handle). A complex structure close to the maximally degenerate one, corresponding to Γ, is parametrized by assigning the complex numbers q_e, $|q_e| \ll 1$ to the internal edges.

The oper $\mathcal{D}$ on Σ which is close to Γ can be approximated by the following data: the hypergeometric oper on every trivalent vertex:

$$T(z_v) = \frac{\Delta_1}{z_v^2} + \frac{\Delta_2}{(z_v-1)^2} + \frac{\Delta_3 - \Delta_1 - \Delta_2}{z_v(z_v-1)} \tag{82}$$

where z_v is a coordinate on the three-punctured sphere corresponding to the vertex v; and the glueing of the local coordinates across the edges:

$$z_{v_1(e)} z_{v_2(e)} = q_e \tag{83}$$

where we assume that on the two spheres $v_1(e)$ and $v_2(e)$ the double point corresponding to e is at the points $z = 0$ on each component. Given the internal vertex v let e_1, e_2, e_3 be the three emanating edges. Let them correspond to the points $z_v = 0, z_v = 1, z_v = \infty$, respectively. Then,

$$\Delta_k = \eta_k (\eta_k - 1) \tag{84}$$

where $\eta_k = \frac{\alpha_{e_k}}{2\pi i} + \delta_k$ if e_k is an internal edge, and $\eta_k = \nu_i$ if e_k is the i'th tail, $\delta_{1,3} = \frac{1}{2}$, $\delta_2 = 0$. This shift is due to the fact that $\mathcal{D}$ acts on the $(-1/2)$-differentials

$$\Psi_v = \psi(z_v) dz_v^{-\frac{1}{2}}$$

4.4. Comparison with the four dimensional gauge theory

In the perturbative limit, where the Riemann surface Σ approaches one of the maximally degenerate complex structures $\tau \to \tau_*$ the $\mathcal{Z}$-function simplifies, and (18) can be calculated rather explicitly [81]:

$$\begin{aligned} \mathcal{W}_{\mathcal{O}_\tau}(\alpha, \nu) = \sum_e \left(\frac{\tau_e}{2} \alpha_e^2 + \Upsilon(2\alpha_e) \right) \\ - \sum_v \Upsilon\Big(\sum_{e \ni v} \pm \alpha_e \Big) \end{aligned} \tag{85}$$

where Υ is a special function, whose derivative gives the logarithm of the Γ-function:

$$\begin{aligned} \Upsilon'(x) &= \log\left(\frac{\Gamma(x+\varepsilon)}{\Gamma(-x+\varepsilon)} \right) \\ \Upsilon(x) &= \frac{d}{ds}\Big|_{s=0} \frac{\mu^s}{\Gamma(s)} \int_0^\infty \frac{dt}{t^2} \frac{t^s}{1 - e^{-t\varepsilon}} e^{-tx} \end{aligned} \tag{86}$$

In order to compare this gauge theory result with the generating function of the variety of opers corresponding to our system of Darboux coordinates (α, β) we approximate the oper on the nearly degenerate curve by the collection of the hypergeometric opers on the three-holed spheres corresponding to the internal vertices v of the degeneration graph Γ, insert the transition matrices

$$\begin{pmatrix} q_e^{\alpha_e} & 0 \\ 0 & q_e^{-\alpha_e} \end{pmatrix} \tag{87}$$

at the double points, which correspond to the edges e, and use the standard transition matrices for the solutions of the hypergeometric equation, to compute the monodromy matrices $\mathrm{g}_1, \mathrm{g}_2, \mathrm{g}_3, \mathrm{g}_4$ for each genus zero edge, and the matrices g, h for each genus one edge.

One can also include the $e^{2\pi i \tau_e}$-corrections by the usual quantum mechanical perturbation theory and verify the agreement with the instanton calculations on the gauge theory side. We have performed these checks for low instanton numbers for the two basic cases: $SU(2)$ $N_f = 4$ theory (which corresponds to $\mathcal{M}_{0,4}$) and for the $SU(2)$ $\mathcal{N} = 2^*$ theory (which corresponds to $\mathcal{M}_{1,1}$).

4.5. The topological brane

The study of the separation of variables (proposed by E. Sklyanin [82]) for the quantum Gaudin system, which is essentially the genus zero case of the Hitchin system, suggests the following definition of this second brane. We assume that the ν_k parameters are generic (and definitely not half-integral, as in [83]).

Then we define a subvariety $\mathcal{L}_\gamma$ for any pair $\gamma = (\Gamma, or)$ which consists of the degeneration graph Γ together with the choice of orientation or. For the oriented edge e we define the source $s(e)$ and the target $t(e)$ vertices in the obvious way.

The definition of $\mathcal{L}_\gamma$ is the following: *For every internal genus zero egde e we require α_e to be equal to the sum of $\pm\alpha_e$'s or $\pm\nu_k$'s (the sign depends on the orientation) corresponding to the two other edges which enter $s(e)$*

$$\alpha_e = \sum_{e', t(e')=s(e)} \eta_{e'} - \sum_{e', s(e')=s(e)} \eta_{e'}$$

where, as before $\eta_e = \alpha_e \pm \delta_e$ if e is an internal edge, and $\eta_e = \nu_k$ if e is the k'th tail.

In the coordinate patch $\mathcal{U}_{\Gamma'}$ the variety $\mathcal{L}_\gamma$ is described by the generating function, which is a sum of dilogarithms, as follows from (69).

5. Further directions and discussion

In this paper we have introduced a system of holomorphic Darboux coordinates α, β on the moduli space $\mathcal{M}_\Sigma^{loc}$ of flat $SL_2(\mathbf{C})$-connections on a punctured Riemann surface with fixed conjugacy classes of the monodromies around the punctures. The main claim about this coordinate system is the identification of the generating function of the variety $\mathcal{O}_\tau$ of SL_2-opers with the effective twisted superpotential of the four dimensional A_1 type Gaiotto theory corresponding to Σ, subject to the two dimensional Ω-deformation.

We also expressed the Yang-Yang function of the quantum Hitchin system, using our coordinate system, as a difference of the generating functions of the variety of opers $\mathcal{O}_\tau$, and the second Lagrangian submanifold $\mathcal{L}_\gamma$, which determines the space of states of the quantum Hitchin system. We presented a proposal for the construction of $\mathcal{L}_\gamma$ in the genus zero case. We would like to stress that the Yang-Yang function we are talking about here is different from the Yang-Yang functions of the finite dimensional Gaudin model or spin chains, which can be derived by taking a critical level limit of the free field representation of the current algebra conformal blocks [77], [78], [79], [80], as explained in [14], [15], [16].

The generating function $\mathcal{W}_{\mathcal{O}_\tau}$ also has other applications. For example, it can be identified with the classical conformal block of the Liouville theory [84], which makes the relation to the four dimensional gauge theory natural in view of the conjecture [85]. It also provides the "holomorphic part" of the classical Liouville action, which is discussed in [33], [34], [86], [36], [87].

Since the variety of opers is well-understood for all Lie groups G, it is urgent to generalize our Darboux coordinates for the case of general G. This would allow us to compute the effective twisted superpotentials of the exotic theories which do not have a Lagrangian description (a general A, D, E type $(0, 2)$ theory compactified on a Riemann surface and subject to the Ω-deformation).

In order to characterize the conformal blocks of Liouville and Toda conformal theories, using the [85] relation, we need to turn on the generic Ω-deformation, with both $\varepsilon_1, \varepsilon_2$ non-vanishing. It was argued that this would effectively quantize the algebras of holomorphic functions on $\mathcal{M}_\Sigma^{loc}(G)$ and $\mathcal{M}_\Sigma^{loc}({}^LG)$, with the deformation quantization parameters $\hbar = \varepsilon_2/\varepsilon_1$ and $1/\hbar = \varepsilon_1/\varepsilon_2$, respectively. The $\mathcal{Z}$-function is then a vector in the representation of $\mathcal{A}_G^\hbar \times \mathcal{A}_{{}^LG}^{1/\hbar}$, which corresponds, quasiclassically, to $\mathcal{O}_\tau$. To find this vector seems like an extremely important problem. For the recent discussion of related problems see [38], [88], [51], [46].

6. Acknowledgements

We are grateful to V. Fock, E. Frenkel, A. Gerasimov, Yu. Neretin, F. Smirnov for valuable discussions. Research of NN was partly supported by FASI RF 14.740.11.0347 that of AR was partly supported by RFBR-09-02-00393, FASI RF 14.740.11.0347, RFBR-09-

01-93106-NCNIL-a, and RF Government Grant-11.G34.31.0023, that of SS by SFI grant 08/RFP/MTH1546 and by ESF grant ITGP. Part of the research was done while AR visited IHES in the summer of 2010. NN also thanks Ilya Khrzhanovsky for the opportunity to carry out some of the research on the project at the "DAU" Institute in Kharkiv, Ukraine, and to D. Kaledin and A. Losev for discussions.

The main conjecture about the generating function of the variety of opers was announced by one of the authors at the Simons Center workshop on "Perspectives, Open Problems & Applications of Quantum Liouville Theory" (Mar 29-Apr 2, 2010). The results of this paper were also reported at various seminars and conferences, in particular, at the Institut Henri Poincare, at the conferences "Symmetry, Duality, and Cinema" (Jun 2010) and "Advances in string theory, wall crossing, and quaternion-Kähler geometry" (Aug 30 - Sept 3, 2010), at the Cargese Summer School "String Theory: Formal Developments and Applications" (Jun 21-Jul 3, 2010) at the IAS (Princeton) seminar (Oct 29, 2010), at the DESY conference "From Sigma Models to Four-dimensional QFT", (Nov 29 - Dec 3, 2010), at the Hebrew Univeristy of Jerusalem IAS 15th Midrasha Mathematicae on Derived Categories of Algebro-Geometric Origin and Integrable systems" (Dec 19 - 24, 2010). We thank all the organizers and the audiences for the fruitful atmosphere and stimulating questions.

REFERENCES

1. L. D. Faddeev, "The Bethe Ansatz," SFB-288-70 (1993);
2. C. N. Yang and C. P. Yang, J. Math. Phys. **10**, 1115 (1969).
3. C. N. Yang and C. P. Yang, Phys. Rev. **150**, 321 (1966).
4. L. D. Faddeev, E. K. Sklyanin and L. A. Takhtajan, Theor. Math. Phys. **40**, 688 (1980) [Teor. Mat. Fiz. **40**, 194 (1979)].
5. M. Jimbo, T. Miwa, F. Smirnov, "Hidden Grassmann Structure in the XXZ Model III: Introducing Matsubara direction," arXiv:0811.0439, J.Phys. **A** 42 (2009) 304018
6. G. W. Moore, N. Nekrasov and S. Shatashvili, "Integrating over Higgs branches," Commun. Math. Phys. **209**, 97 (2000) [arXiv:hep-th/9712241].
7. A. A. Gerasimov and S. L. Shatashvili, "Higgs bundles, gauge theories and quantum groups," Commun. Math. Phys. **277**, 323 (2008) [arXiv:hep-th/0609024].
8. A. A. Gerasimov and S. L. Shatashvili, "Two-dimensional Gauge Theories and Quantum Integrable Systems," arXiv:0711.1472 [hep-th].
9. E. Witten, "Two dimensional gauge theory revisited", arXiv:hep-th/9204083
10. A. Gorsky and N. Nekrasov, "Quantum integrable systems of particles as gauge theories," Theor. Math. Phys. **100**, 874 (1994) [Teor. Mat. Fiz. **100**, 97 (1994)].
11. A. Gorsky and N. Nekrasov, "Relativistic Calogero-Moser Model As Gauged WZW Theory," Nucl. Phys. B **436**, 582 (1995) [arXiv:hep-th/9401017].
12. A. Gorsky and N. Nekrasov, "Elliptic Calogero-Moser System From Two-Dimensional Current Algebra," arXiv:hep-th/9401021.
13. A. Gorsky and N. Nekrasov, "Hamiltonian systems of Calogero type and two-dimensional Yang-Mills theory," Nucl. Phys. B **414**, 213 (1994) [arXiv:hep-th/9304047].
14. N. A. Nekrasov and S. L. Shatashvili, "Supersymmetric vacua and Bethe ansatz," Nucl. Phys. Proc. Suppl. **192-193**, 91 (2009) [arXiv:0901.4744 [hep-th]].
15. N. Nekrasov and S. Shatashvili, "Bethe Ansatz And Supersymmetric Vacua," AIP Conf. Proc. **1134**, 154 (2009).
16. N. A. Nekrasov and S. L. Shatashvili, "Quantum integrability and supersymmetric vacua," Prog. Theor. Phys. Suppl. **177**, 105 (2009) [arXiv:0901.4748 [hep-th]].
17. N. A. Nekrasov and S. L. Shatashvili, "Quantization of Integrable Systems and Four Dimensional Gauge Theories," arXiv:0908.4052 [hep-th].
18. A. Gorsky, I. Krichever, A. Marshakov, A. Mironov, A. Morozov, "Integrability and Seiberg-Witten exact solution," Phys. Lett.

B355, 466-474 (1995). [hep-th/9505035].
19. E. Martinec and N. Warner, "Integrable systems and supersymmetric gauge theory", "Nucl.Phys.B459:97-112,1996, arXiv:hep-th/9509161
20. R. Donagi, E. Witten, "Supersymmetric Yang-Mills theory and integrable systems," Nucl. Phys. **B460**, 299-334 (1996). [hep-th/9510101].
21. R. Y. Donagi, "Seiberg-Witten integrable systems," [alg-geom/9705010].
22. N. A. Nekrasov, "Seiberg-Witten Prepotential From Instanton Counting," Adv. Theor. Math. Phys. **7**, 831 (2004) [arXiv:hep-th/0206161].
23. A. Losev, N. Nekrasov and S. L. Shatashvili, "Testing Seiberg-Witten solution," In Cargese 1997, *Strings, branes and dualities*, pp. 359-372, [arXiv:hep-th/9801061].
24. A. Losev, N. Nekrasov and S. L. Shatashvili, "Issues in topological gauge theory," Nucl. Phys. B **534**, 549 (1998) [arXiv:hep-th/9711108].
25. E. Witten, "Some comments on string dynamics," arXiv:hep-th/9507121.
26. A. Strominger, "Open p-branes," Phys. Lett. B **383**, 44 (1996) [arXiv:hep-th/9512059].
27. D. Gaiotto, "N=2 dualities," arXiv:0904.2715 [hep-th].
28. N. Seiberg and E. Witten, "Monopoles, duality and chiral symmetry breaking in N=2 supersymmetric Nucl. Phys. B **431**, 484 (1994) [arXiv:hep-th/9408099].
29. G. W. Moore, N. Nekrasov and S. Shatashvili, "D-particle bound states and generalized instantons," Commun. Math. Phys. **209**, 77 (2000) [arXiv:hep-th/9803265].
30. E. Witten, "String theory dynamics in various dimensions," Nucl. Phys. B **443**, 85 (1995) [arXiv:hep-th/9503124].
31. M. Atiyah, R. Bott, "The Yang-Mills Equations Over Riemann Surfaces", Phil. Trans. R.Soc. London A **308**, 523-615 (1982)
32. E. Witten, "Quantum field theory and the Jones polynomial," Commun. Math. Phys., 121 (1989) 351
33. A.M. Polyakov, "Quantum Gravity in Two-Dimensions," Mod. Phys. Lett.**A2** (1987) 893.
34. A. Alekseev and S. L. Shatashvili, Nucl. Phys. B **323**, 719 (1989).
35. E. Verlinde, H. Verlinde, "A solution of two dimensional topological quantum gravity", PUPT-1176, IASSNS-HEP-90/40, April 1990
36. H. Verlinde, Nucl. Phys. **B**337 (1990) 652
37. E. Witten, "(2+1)-Dimensional Gravity as an Exactly Soluble System," Nucl. Phys. B **311**, 46 (1988).
38. L. Chekhov and V. V. Fock, "A quantum Teichmüller space," Theor. Math. Phys. **120**, 1245 (1999) [Teor. Mat. Fiz. **120**, 511 (1999)] [arXiv:math/9908165].
39. L. O. Chekhov and V. V. Fock, "Observables in 3D gravity and geodesic algebras," Czech. J. Phys. **50**, 1201 (2000).
40. E. Witten, "Three-Dimensional Gravity Revisited," arXiv:0706.3359 [hep-th].
41. N. Seiberg and E. Witten, "Gauge dynamics and compactification to three dimensions," arXiv:hep-th/9607163.
42. N. Hitchin, "The self-duality equations on a Riemann surface," Proc. London Math. Soc. (3) **55** (1987) 59–126
43. A. Kapustin and E. Witten, "Electric-magnetic duality and the geometric Langlands program," arXiv:hep-th/0604151.
44. N. Hitchin, "Stable bundles and integrable systems," Duke Math. J. **54** (1987) 91–114
45. R. Donagi, "Spectral Covers," arXiv:alg-geom/9505009
46. N. Nekrasov and E. Witten, "The Omega Deformation, Branes, Integrability, and Liouville Theory," JHEP **1009**, 092 (2010) [arXiv:1002.0888 [hep-th]].
47. D. Gaiotto, E. Witten, "S-Duality Of Boundary Conditions in N = 4 Super Yang-Mills Theory," arXiv:0807.3720v1 [hep-th]
48. D. Gaiotto, E. Witten, "Supersymmetric Boundary Conditions in N = 4 Super Yang-Mills Theory," arXiv:0804.2902v1 [hep-th]
49. A. Beilinson, V. Drinfeld, "Quantization of Hitchin's integrable system and Hecke eigensheaves", preprint
50. S. Gukov, E. Witten, "Branes And Quantization," arXiv:0809.0305v2 [hep-th]
51. J. Teschner, "Quantization of the Hitchin

moduli spaces, Liouville theory, and the geometric Langlands correspondence I", arXiv:1005.2846v2 [hep-th]
52. V. Fock, A. Goncharov, "Moduli spaces of local systems and higher Teichmller theory", Publ. Math. Inst. Hautes Études Sci. No. 103 (2006), 1-211.
53. D. Gaiotto, G. W. Moore and A. Neitzke, "Wall-crossing, Hitchin Systems, and the WKB Approximation," arXiv:0907.3987 [hep-th].
54. N. Nekrasov, "Holomorphic bundles and many body systems," Commun. Math. Phys. **180**, 587 (1996) [arXiv:hep-th/9503157].
55. R. Donagi, E. Markman, "Spectral curves, algebraically completely integrable Hamiltonian systems, and moduli of bundles," [alg-geom/9507017].
56. A. Kapustin and S. Sethi, "The Higgs branch of impurity theories," Adv. Theor. Math. Phys. **2**, 571 (1998) [arXiv:hep-th/9804027].
57. E. Markman, "Spectral curves and integrable systems", Compositio Math. 93 (1994), no. 3, 255-290
58. A. Gorsky, N. Nekrasov and V. Rubtsov, "Hilbert schemes, separated variables, and D-branes," Commun. Math. Phys. **222**, 299 (2001) [arXiv:hep-th/9901089].
59. V. V. Fock and A. A. Rosly, "Poisson structure on moduli of flat connections on Riemann surfaces and r-matrix," preprint ITEP-72-92 (1992), AMS Transl. **191**, 67 (1999) [arXiv:math/9802054].
60. V. V. Fock and A. A. Rosly, "Flat connections and polyubles," Theor. Math. Phys. **95**, 526 (1993) [Teor. Mat. Fiz. **95**, 228 (1993)].
61. V. V. Fock and A. A. Rosly, "Moduli space of flat connections as a Poisson manifold," Int. J. Mod. Phys. B **11**, 3195 (1997).
62. W. Goldman, "The symplectic nature of the fundamental group on surfaces," Adv. Math. **54**, 200-225 (1984)
63. W. Goldman, "Invariant functions on Lie groups and Hamiltonian flows of surface group representations," Invent. math. 85, 263-302 (1986)
64. V.G. Turaev, "Skein quantization of Poisson algebras of loops on surfaces", Ann. Sci. École Norm. Sup. (4) 24 (1991), no. 6, 635704
65. A. N. Tyurin, "Quantization, Classical and Quantum FIeld Theory and Theta Functions", CRM monograph series, Vol. 21, AMS , 2003.
66. D.A. Derevnin, A.D. Mednykh, A formula for the volume of a hyperbolic tetrahedron, Russ. Math. Surv. **60** (2), (2005) 346-348
67. L. Schläfli, "Theorie der vielfachen Kontinuität", In: Gesammelte mathematishe Abhandlungen, Basel: Birkhäuser, 1950.
68. N. I. Lobatschefskij, "Imaginäre Geometrie und ihre Anwendung auf einige Integrale", Deutsche äubersetzung von H.Liebmann, Leipzig: Teubner, 1904.
69. Yu. Cho, H. Kim, "On the volume formula for hyperbolic tetrahedra", Discrete and Computational Geometry, 22, 1999, p.347-366.
70. J. Milnor, "The Schläfli differential equality" in Collected Papers. I. Geometry (Publish or Perish, Houston, TX, 1994), pp. 281-295.
71. M. Kapovich, J. J. Millson, T. Treloar, arXiv:math/9907143
72. A.A. Klyachko, "Spatial polygons and stable configurations of points in the projective line," Algebraic geometry and its applications (Yaroslavl, 1992), 6784, Aspects Math., E25, Vieweg, Braunschweig, 1994.
73. P. Foth, "Polygons in Minkowski space and Gelfand-Tsetlin for pseudounitary groups," arXiv:math/0703525
74. A. Beilinson, V. Drinfeld, "Opers", math.AG/0501398
75. A. Bilal, I. Kogan, V. Fock, "On the origin of W-algebras," CERN-TH.5965/90
76. A. Gerasimov, A. Levin and A. Marshakov, "On W gravity in two-dimensions," Nucl. Phys. B **360**, 537 (1991).
77. A. Gerasimov, A. Morozov, M. Olshanetsky, A. Marshakov and S. L. Shatashvili, "Wess-Zumino-Witten model as a theory of free fields," Int. J. Mod. Phys. A **5**, 2495 (1990), preprints ITEP-89-64, ITEP-89-70, ITEP-89-72, ITEP-89-74, April 1989
78. A.Varchenko, V.Schechtman, "Integral Representations of N-Point Conformal Correlators in the WZW Model," Bonn, Max-Planck Institute (1989), 1-22.

79. N. Reshetikhin and A. Varchenko, "Quasi-classical asymptotics of solutions to the KZ equations," arXiv:hep-th/9402126.
80. G. Felder and A. Varchenko, arXiv:hep-th/9511120.
81. N. Nekrasov, V. Pestun, to appear
82. E. Sklyanin, J. Sov. Math. 47 (1989) 2473-2488
83. B. Feigin, E. Frenkel and N. Reshetikhin, "Gaudin model, Bethe ansatz and correlation functions at the critical level," Commun. Math. Phys. **166**, 27 (1994) [arXiv:hep-th/9402022].
84. A. B. Zamolodchikov and A. B. Zamolodchikov, "Structure constants and conformal bootstrap in Liouville field theory", Nucl. Phys. B477 (1996) 577, hep-th/9506136
85. L. F. Alday, D. Gaiotto and Y. Tachikawa, "Liouville Correlation Functions from Four-dimensional Gauge Theories," Lett. Math. Phys. **91**, 167 (2010) [arXiv:0906.3219 [hep-th]].
86. L.A. Takhtajan, P.G. Zograf, "On Liouville equation, accessory parameters and the geometry of Teichmuller space for Riemann surface of genus 0", Math. USSR Sbornik **60** (1988) 143
87. E. Aldrovandi, L.A. Takhtajan, "Generating Functional in CFT on Riemann Surfaces II: Homological Aspects", arXiv:math/0006147
88. L. F. Alday, D. Gaiotto, S. Gukov, Y. Tachikawa and H. Verlinde, JHEP **1001**, 113 (2010) [arXiv:0909.0945 [hep-th]].

Time-dependent AdS/CFT correspondence and the Quark-Gluon plasma

Alice Bernamonti[a*] and Robi Peschanski[b †]

[a] Theoretische Natuurkunde, Vrije Universiteit Brussel, and International Solvay Institutes
Pleinlaan 2, B-1050 Brussels, Belgium

[b] Institut de Physique Théorique, CEA, and CNRS (URA 2306), 91191 Gif/Yvette Cedex, France

Experiments on high-energy heavy-ion collisions reveal the formation and some intriguing properties of the Quark-Gluon Plasma (QGP), a new phase of matter predicted by Quantum Chromodynamics (QCD), the quantum field theory of strong interactions. The phenomenological success of relativistic hydrodynamic simulations with remarkably weak shear viscosity, modeling QGP as an almost *perfect fluid*, are in favor of the occurrence of a strongly-coupled QGP expanding and cooling during the reaction. A derivation of these features in QCD at strong coupling is still lacking and represents a very intricate theoretical challenge. As a quite unique modern tool to relate these dynamical features to a microscopic gauge field theory at strong coupling, time-dependent realizations of the AdS/CFT correspondence provide a fruitful way to study these properties in a realistic kinematic configuration. Relating a 4-dimensional Yang-Mills gauge theory with four supersymmetries (which is a conformal field theory, CFT_4) with gravity in Anti-de Sitter space in five dimensions (AdS_5), the AdS/CFT correspondence provides a useful "laboratory" to study yet unknown strong coupling properties of QCD. Besides the interest of revealing new aspects of the AdS/CFT correspondence in a dynamical set-up, the application to plasma formation leads to non trivial theoretical properties, as we will discuss in the lectures. The highlights of the present lectures are:

1. Emergence of an (almost) perfect hydrodynamic fluid at late proper-times after the collision.
2. Duality between an expanding 4-dimensional plasma and a black hole moving radially in the bulk.
3. Intimate link between conformal hydrodynamics and Einstein's equations in the asymptotically AdS_5 space.
4. Possibility of studying the far-from-equilibrium stage of a gauge field theory at early collisional proper-times.

1. Heavy-Ion reactions and the QGP

One of the most striking lessons one may draw [1,2] from experiments on heavy-ion collisions at high energy (*e.g.* at the RHIC accelerator) is that fluid hydrodynamics seems to be relevant for understanding the dynamics of the reaction (see, for instance, the reviews [2]). Indeed, the elliptic flow [3] describing the anisotropy of the low transverse momentum particles produced in a collision at non zero impact parameter implies the existence of a collective flow of particles. It agrees with the picture of an hydrodynamical pressure gradient due to the initial eccentricity in the collision[3]. Moreover, the hydrodynamic simulations which are successful to describe this elliptic flow are consistent with an almost "perfect fluid" behavior, *i.e.* a small *viscosity over entropy ratio* η/s [5]. This ratio is particularly interesting since it depends mainly on fundamental features of the fluid, being in particular independent of the particle density (see later, eq.(1)).

The validity of an hydrodynamical description assuming a quasi-perfect fluid behavior has been nicely anticipated by Bjorken[4] in Ref.[8]. The so-called *Bjorken flow* is based on the approxima-

*Aspirant FWO; Alice.Bernamonti@vub.ac.be
†robi.peschanski@cea.fr

[3]Note that a preliminary analysis of recent LHC data on the elliptic flow at the Alice detector seems to confirm the validity of the hydrodynamic approach [4].

[4]The introduction of hydrodynamics in the description of high-energy hadronic collisions has been originally proposed by Landau [6], assuming "full stopping" initial conditions which result in a non boost-invariant solution or *Landau flow* (see [7] for a unified description of Bjorken and Landau flows). However "full stopping" initial conditions do not seem to agree with present day data.

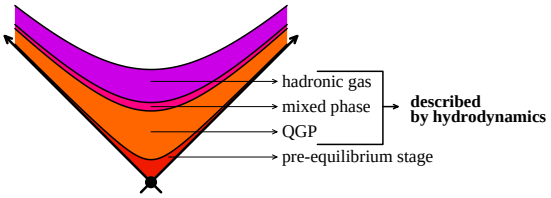

Figure 1. *Description of QGP formation in heavy ion collisions.* The kinematic landscape is defined by $\tau = \sqrt{x_0^2 - x_1^2}$; $\eta = \frac{1}{2}\log\frac{x_0+x_1}{x_0-x_1}$; $x_T = \{x_2, x_3\}$. The coordinates along the light-cone are $x_0 \pm x_1$, the transverse ones are $\{x_2, x_3\}$ and τ is the proper time, while η is called the "space-time rapidity".

tion of an intermediate stage of the reaction process consisting in a boost-invariant quark-gluon plasma (QGP) behaving as a relativistically expanding fluid. It is formed after a (strikingly rapid) thermalization period and finally decays into hadrons. A schematic description of the process in light-cone kinematics is shown in Fig.1. Boost-invariance can be justified in the central region of the collision since the observed distribution of particles is flat, in agreement with the prediction of hydrodynamic boost-invariance, where (space-time) fluid and (energy-momentum) particle rapidities are proven to be equal [8] (see later the discussion in section 3).

The Bjorken flow was instrumental for deriving and predicting many qualitative and even semi-quantitative features of the quark-gluon plasma formation in heavy-ion reactions. It was later confirmed and developed through numerical simulations where various effects have been included, up to the full 4-dimensional structure of the hydrodynamic flow. However, since hydrodynamics is an effective mean-field approach, it says only little on the relation with the microscopic gauge field theory, *i.e.*, in the present case, Quantum Chromodynamics (QCD). Some important questions remain unsolved, such as the reason why the fluid behaves like a (almost) perfect fluid, what is the small amount of viscosity it may require, why and how fast thermalization proceeds, etc...

The problem is made even more difficult by the strong coupling regime of QCD, which is very probably required, since a perturbative description leads in general to high η/s ratio. In fact, large collision cross-sections with transversally cut-off momenta are required in order to explain a small macroscopic shear viscosity. The mean free path and the average transverse momentum induced by the gauge field medium should be small, in order to damp the nearby force transversal to the flow measuring shear viscosity. In a classical physics context, one may write

$$\frac{\eta}{s} = \frac{\rho_{part} \times \lambda_{free} \times \bar{p}_{av}}{\rho_{part} \times k_B} \quad \left[\geq \frac{1}{4\pi} \frac{\hbar}{k_B} \right] \ , \qquad (1)$$

where ρ_{part}, (*resp.* $\bar{p}_{av}$) is the particle density, (*resp.* average transverse momentum) and λ_{free} the mean free-path. Both small mean free-path and low average transverse momentum are expected in the non-perturbative regime of QCD and more generally from a gauge theory at strong coupling. We also quote in formula (1) the AdS/CFT value [9] $1/4\pi$ in terms of the fundamental constants' ratio $\hbar/k_B$, corresponding to the large coupling limit of the conformal field theory. This AdS/CFT ratio appears to be very small compared to all known non-relativistic fluids, as suggested by the inequality between square brackets. Indeed, the AdS/CFT value has been proposed as an absolute theoretical lower bound [10]. A discussion is in progress to fully confirm this statement or to find counter-examples in microscopic theories (see [11] and references therein).

In any case, a very small phenomenological viscosity ratio is confirmed; not meaning that viscosity effects should be neglected . Observations on the elliptic flow primarily, and other observables, allow one to give estimates of η/s which are within range of the AdS/CFT value (see, *e.g.* [4,5]).

It is thus interesting to use our modern (while still in progress) knowledge of non-perturbative methods in quantum field theory to fill the gap between the macroscopic and microscopic descriptions of the quark-gluon plasma produced in heavy-ion collisions. Lattice gauge theory methods are very useful to analyze the static proper-

ties of the quark-gluon plasma, but they are still unable to describe the plasma in collision.

Hence we are led to rely upon the new tools offered by the Gauge/Gravity correspondence and in particular on the most studied and well-known of its realizations, namely the AdS/CFT duality [12] between $\mathcal{N} = 4$ supersymmetric Yang-Mills theory and type IIB superstring in the large N_c approximation. The properties of the gauge theory in (physical) Minkowski space in 3+1 dimensions are in one-to-one relation with properties of the bulk theory, in the 10D target space of strings. For our applications, strong coupling features will be related by duality to the geometric structure of the 5D metric with Minkowski boundary, which is built on top of vacuum AdS. At weak coupling, the physical space corresponds to the world-volume of a stack of infinitely many ($N_c \to \infty$) joint D3-branes. Note that the overall consistency of the correspondence scheme will be required, even if only geometrical properties will be used in practice.

One should be aware, when using AdS/CFT tools, that there does not yet exist a gravity dual construction for QCD. Also, the relation between perturbative (weak-coupling) and non-perturbative (strong-coupling) aspects of QCD are left over in the correspondence, which conveniently describes the strong coupling regime of gauge theories uniquely. However, the nice feature of the quark-gluon plasma is that it is a deconfined phase of QCD, characterized by collective degrees of freedom. Thus one may expect to get useful information from AdS/CFT. This has already been proved in the description of static geometries, by the evaluation of η/s [9]. Other aspects of the QGP can be studied via the duality, in a static plasma configuration at fixed temperature.

Our specific aim and the subject of the present lectures is the investigation of the Gauge/Gravity duality in a dynamical *time-dependent* setting using the AdS/CFT correspondence. The goal is to describe a collision process in a strongly coupled gauge theory, including in particular the cooling of temperature accompanying the proper-time evolution of the fluid.

In section 2, we introduce the theoretical tool of holographic renormalization and apply it, as a warm-up exercise, to a static uniform plasma. Sections 3 and 4 present, respectively, the late and early proper-time analysis of the plasma evolution, with particular emphasis on boost-invariant flows.

2. AdS/CFT and strong gauge interactions

In the previous section, we mentioned the ubiquity of hydrodynamic methods in the description of QGP produced at RHIC. Yet, despite their success in describing the data, we have to keep in mind that they are used as a phenomenological model, without a real derivation from gauge theory. This is understandable, since almost perfect fluid hydrodynamics is intrinsically a strong coupling phenomenon, for which one lacks a purely gauge theoretical method.[5]

On the other hand, there exists a wide class of gauge theories, which can be studied analytically at strong coupling. These are superconformal field theories with gravity duals. In the unifying context of string theory, using the AdS/CFT correspondence, one is able to map gauge theory dynamics (CFT) at strong coupling and large number of colors into solving Einstein's equations in asymptotically anti-de Sitter space (AdS). The theories with gravity duals can differ substantially from real world QCD at zero temperature. The best known example of such theories - $\mathcal{N} = 4$ super Yang-Mills (SYM) - is a superconformal field theory with matter in the adjoint representation of the gauge group SU(N_c). Because of the conformal symmetry at the quantum level this theory does not exhibit confinement. On the other hand, differences between $\mathcal{N} = 4$ SYM and QCD are less significant above QCD's critical temperature, when quarks and gluons are in the deconfined phase. Moreover, it was observed on the lattice that QCD exhibits a quasi-conformal trend [14] in a range of temperatures $T > 300$ MeV. There the equation of state is reasonably approximated by the conformal relation $\epsilon = 3p$, corresponding to a traceless energy-momentum tensor. The

[5] Lattice QCD methods do not work well here, as this would require analytical continuation to Minkowski signature which is nontrivial in this context [13].

above observations, together with experimental results suggesting that QGP is a strongly coupled medium, are an incentive to use the AdS/CFT correspondence as a tool to get insight into non-perturbative dynamics.

2.1. AdS/CFT correspondence

We will now describe how to set up an AdS/CFT computation for determining the space-time behavior of the gauge field plasma corresponding to a Bjorken boost-invariant flow. The problem is formulated in terms of the proper-time evolution of the matter energy-momentum tensor on the CFT boundary [15]. This method does not make any underlying assumption about local equilibrium or hydrodynamical behavior. We will indeed obtain the hydrodynamic expansion as a generic consequence of the late time behavior of the expanding and strongly coupled plasma.

Suppose we consider some macroscopic state of the plasma characterized by a space-time profile of the energy-momentum tensor

$$T_{\mu\nu}(x^\rho) \ , \quad \mu,\nu,\rho = \{0,\cdots,3\} \ . \tag{2}$$

Then, since the AdS/CFT correspondence asserts an exact equivalence between gauge and string theories, such a state should have its counterpart on the gravity side of the correspondence. Typically, it will be given by a modification of the geometry of the original $AdS_5 \times S^5$ metric. This follows from the fact that operators in the gauge theory correspond to fields in supergravity (or string theory). When we consider a state with a nonzero expectation value of an operator, the dual gravity background will have the corresponding field modified from its 'vacuum' value. In the case of the energy-momentum tensor, the corresponding field is just the 5D metric. One then has to assume that the geometry is well defined, *i.e.* it is free from naked singularities - singularities not hidden by an event horizon -. This principle selects the allowed physical space-time profiles of the gauge theory energy-momentum tensor. Thus this becomes the main dynamical mechanism for selecting the appropriate strongly coupled gauge theory from the dual Einstein equations. In practice, the geometry will be obtained from a "holographic renormalization" procedure starting from the boundary. The boundary conditions serve as initial conditions for the construction of the bulk features, the fifth dimension acting as a renormalization scale. Let us describe in detail this construction.

2.2. Holographic renormalization

The Gauge/Gravity duality can be described as an "holographic" correspondence between the 4-dimensional physical space where the gauge theory lives and the 5-dimensional space where the supergravity (weak curvature) approximation of the 10-dimensional string theory is valid. It means qualitatively that the whole information should be the same on both sides of the correspondence, despite the difference in dimensionality. In practice, this notion of "holography" has a precise realization in terms of the "holographic renormalization" program [16]. Let us illustrate the holographic renormalization by simple examples, which will in fact be sufficient for the applications we have in mind.

Suppose that, when considering the presence of matter on the 4-dimensional physical space, our corresponding 5-dimensional geometry is parameterized by

$$ds^2 = \frac{g_{\mu\nu}(x^\rho,z)dx^\mu dx^\nu + dz^2}{z^2} \equiv g^{5D}_{\alpha\beta}dx^\alpha dx^\beta, \tag{3}$$

where we adopt the Fefferman-Graham definition [17] of the 5D metric. The flat case $g_{\mu\nu} = \eta_{\mu\nu}$ parametrizes AdS_5 in Poincaré coordinates. The conformal boundary of space-time is at $z=0$.

Considering the general metric (3) from the point-of-view of the AdS/CFT correspondence, the following questions are in order:

i) What are the constraints imposed on $g_{\mu\nu}(x^\rho,z)$?

ii) What is the corresponding energy-momentum profile $\langle T_{\mu\nu}(x^\rho)\rangle$?

The metric (3) has to be a solution of 5D Einstein's equation with negative cosmological con-

stant[6]

$$R_{\alpha\beta} = \frac{1}{2} g_{\alpha\beta} \left(R - 12 \right) \ . \tag{4}$$

The expectation value of the energy momentum tensor may be recovered by expanding the metric near the boundary $z=0$. The "holographic renormalization" procedure [16], for a Minkowskian boundary metric, gives[7]

$$g_{\mu\nu}(x^\rho, z) = \eta_{\mu\nu} + z^4 g^{(4)}_{\mu\nu}(x^\rho) + \dots \ , \tag{5}$$

and

$$\langle T_{\mu\nu}(x^\rho) \rangle = \frac{N_c^2}{2\pi^2} \cdot g^{(4)}_{\mu\nu}(x^\rho) \ . \tag{6}$$

The relations (5,6) can be used in two ways. Firstly, given a solution of Einstein's equations, we may read off the corresponding gauge theoretical energy-momentum tensor. Secondly, given a traceless and conserved energy-momentum profile, one may integrate Einstein's equations into the bulk in order to obtain the dual geometry[8]. Then the criterion of non singularity of the geometry will determine the allowed space-time evolution of the plasma. Let us note that this formulation is in fact quite far from a conventional initial value problem.

2.3. Example: static uniform plasma

Before moving to the case of an expanding plasma, it is convenient to consider the simple situation of a static uniform plasma with a constant energy-momentum tensor. This will provide a useful exercise introducing the main tools for further applications.

[6]One can show that such solutions lift to 10D solutions of ten dimensional type IIB supergravity. The effective 5D negative cosmological constant comes from the 5-form field in 10D supergravity.

[7]In principle, in (5) also additional logarithmic terms appear (see [16]). They are absent in all the cases we are going to examine.

[8]This can be done order by order in z^2, which is a near-boundary expansion. However potential singularities are hidden deep in the bulk, thus this power series needs to be resummed.

Starting from a constant diagonal energy-momentum tensor

$$T_{\mu\nu} = \begin{pmatrix} \epsilon & 0 & 0 & 0 \\ 0 & p_\parallel & 0 & 0 \\ 0 & 0 & p_\perp & 0 \\ 0 & 0 & 0 & p_\perp \end{pmatrix} , \tag{7}$$

with $p_\parallel = p_\perp$ and energy density and pressure related by $\epsilon = 3p$, one has to solve the 5D Einstein's equations for an Ansatz

$$ds^2 = \frac{-e^{a(z)} dt^2 + e^{b(z)} d\vec{x}^2 + dz^2}{z^2} \tag{8}$$

obeying the above-mentioned boundary conditions (5,6). Inserting (8) into the Einstein's equations (4) and splitting them into components, one gets

$$\begin{aligned} R_{11} &\Rightarrow -8a' + za'^2 - 6b' + 3za'b' + 2za'' = 0 \ , \\ R_{55} &\Rightarrow -2a' + za'^2 - 6b' + 3zb'^2 + 2z(a'' + 3b'') = 0 \ , \\ R_{22} &\Rightarrow -2a' - 12b' + za'b' + 3zb'^2 + 2zb'' = 0 \ . \end{aligned}$$

Then

$$R_{11} - R_{55} \Rightarrow a' = \frac{zb'^2 + 2zb''}{zb' - 2} \, , \tag{9}$$

while combining it with the expression from R_{22} for a' gives

$$-3b'^2 + zb'^2 + zb'' = 0 \, . \tag{10}$$

From those last two equations, it is easy to obtain independent equations for $a(z)$ and $b(z)$ and their solutions. With appropriate normalizations at $z=0$, one gets

$$\begin{aligned} b &\equiv \log\left(1 + \frac{z^4}{z_0^4}\right) \\ a &\equiv 2\log\left(1 - \frac{z^4}{z_0^4}\right) - \log\left(1 + \frac{z^4}{z_0^4}\right) \ , \end{aligned} \tag{11}$$

where z_0 is the integration constant. Hence, Einstein's equations can be exactly solved analytically in this case and we find [15] that the exact dual geometry of such a system is

$$ds^2 = -\frac{\left(1 - \frac{z^4}{z_0^4}\right)^2}{\left(1 + \frac{z^4}{z_0^4}\right)} \frac{dt^2}{z^2} + \left(1 + \frac{z^4}{z_0^4}\right) \frac{d\vec{x}^2}{z^2} + \frac{dz^2}{z^2} . \tag{12}$$

This metric may look at first glance unfamiliar, but a change of coordinates

$$\tilde{z} \equiv \frac{z}{\sqrt{1+\frac{z^4}{z_0^4}}} \tag{13}$$

transforms it to the standard metric form of the AdS-Schwarzschild static black hole[9]

$$\tilde{z}^2 ds^2 = -\left(1-\frac{\tilde{z}^4}{\tilde{z}_0^4}\right) dt^2 + d\vec{x}^2 + \frac{1}{1-\frac{\tilde{z}^4}{\tilde{z}_0^4}} d\tilde{z}^2, \tag{14}$$

with $\tilde{z}_0 = z_0/\sqrt{2}$ being the location of the horizon. Before we proceed further, let us note here one crucial thing: the fact that the dual geometry of a gauge theory system with constant energy density is a black hole was *not* an assumption, but rather an outcome of a computation.

The Hawking temperature

$$T = \frac{1}{\pi \tilde{z}_0} \equiv \frac{\sqrt{2}}{\pi z_0} \tag{15}$$

is then identified with the gauge theory temperature, and the entropy with the Bekenstein-Hawking black hole entropy

$$S = \frac{N_c^2}{2\pi \tilde{z}_0^3} = \frac{\pi^2}{2} N_c^2 T^3 \tag{16}$$

which is 3/4 of the entropy at zero coupling. This identification between the black hole characteristics and the equilibrium thermodynamics of the plasma reveals a striking correspondence between the near-horizon and boundary properties of the gauge/gravity system.

To finish our discussion of the static black hole, we note that the Fefferman-Graham coordinates cover only the part of space-time lying outside of the horizon. It will appear useful to introduce different coordinates allowing one to go inside the horizon, such as the Eddington-Finkelstein's coordinate system. Through the time coordinate redefinition

$$u \equiv t - \frac{1}{4}\tilde{z}_0 \left(2 \arctan \frac{\tilde{z}}{\tilde{z}_0} + \log \frac{\tilde{z}_0 + \tilde{z}}{\tilde{z}_0 - \tilde{z}}\right) , \tag{17}$$

the metric (14) becomes:

$$\tilde{z}^2 ds^2 = -\left(1-\frac{\tilde{z}^4}{\tilde{z}_0^4}\right) du^2 + d\vec{x}^2 + 2 du d\tilde{z} \, . \tag{18}$$

Now the metric is well defined at $\tilde{z} = \tilde{z}_0$ and the horizon can be smoothly crossed. Note that the time coordinate gets an infinite shift near the horizon, here being harmless, but which reveals to be quite subtle for the time-dependent backgrounds we will consider now.

3. AdS/CFT and late time quark-gluon plasma flow

In this part, we describe applications of the methods introduced in section 2 to the analysis of plasma dynamics in strongly coupled gauge theories. The time dependence of the system introduces considerable computational difficulties and it is in general a hard task to achieve a detailed quantitative description of the plasma evolution. Nevertheless, significant information on the dynamics can be extracted working in simplified and symmetric, but realistic setups. We shall consider specific regimes of the problem in exam, but some general lessons can still be drawn about the highly nonlinear regime of the plasma expansion.

Throughout the next sections we will model the products of heavy-ion collisions with a $\mathcal{N}=4$ SYM plasma at finite temperature. We mainly focus on the results obtained in Ref. [15] concerning the late proper-time behavior of the quark-gluon plasma. Recent and detailed reviews on the subject are also Refs. [19] and [20] .

The structure of the sections is organized in the following way. In section 3.1 we review briefly the "Bjorken flow" description of the central rapidity region of heavy-ion collisions. This serves as an introduction to section 3.2, where we present the gauge theory setup which has been used in [15] to model the products of heavy-ion reactions. The description is in fact inspired by the hydrodynamic description of heavy-ion collisions by Bjorken [8] and based on the central assumption of boost invariance. This hypothesis seems experimentally to be valid in the central rapidity region of the heavy-ion collision process. In section 3.3, we review the computation of the holo-

[9] The identification of the metric (12) as the dual of a static fluid at fixed temperature has previously been made in [18] using the approach 'from bulk to boundary'. This is the reverse way w.r.t. holographic renormalization which proceeds 'from boundary to bulk'. The interest of holographic renormalization is that it allows a construction of the dual geometry starting only from 4-dimensional physical data.

graphic dual geometry of the plasma system in the asymptotic limit of large proper-time. The properties of this class of time-dependent space-times are investigated in section 3.4. The requirement of the absence of naked singularities in the bulk selects uniquely the gravity dual of a perfect fluid. This non-singular solution can be interpreted as a black hole moving off from the AdS boundary in the radial direction, as a function of proper-time. We conclude with sections 3.5 and 3.6, where we present attempts of going beyond the assumptions of perfect hydrodynamics and boost invariance.

3.1. Hydrodynamic Bjorken flow

The introduction of relativistic hydrodynamics in the description of high-energy hadronic reactions is due to Landau in a remarkable premonitory paper [6]. However, the experimental evidence of a connection between heavy-ion collisions and relativistic hydrodynamics has been first modeled by Bjorken in [8]. In this description, boost-invariance of the plasma arises as an outcome of the assumption of hydrodynamics, in a semi-classical approximation where the fluid follows ballistic trajectories or, in other terms, the momentum-space rapidity is equal to the space-time one (see Fig.2). The model is therefore well suited to parametrize the central region of ultra-relativistic collisions, for which the particle distribution is nearly flat as a function of rapidity.

In this section, we review a number of aspects of this picture. The summary is intended to be useful in the follow-up to motivate the assumptions of the AdS/CFT models we discuss and to interpret the physical results we obtain.

For the discussion that follows, it is convenient to parametrize flat four-dimensional space-time of coordinates $(t, x_1, x_\perp)$, where $x_\perp = (x_2, x_3)$, in terms of the light-cone coordinates $(x^+, x^-, x_\perp)$. The latter are defined by $x^\pm \equiv t \pm x_1$, in which the flat space-time metric reads

$$ds^2 = -dx^+ dx^- + dx_\perp^2 \,. \tag{19}$$

The proper-time τ and space-time rapidity η of the fluid are related to the light-cone coordinates by $x^\pm \equiv \tau\, e^{\pm\eta}$.

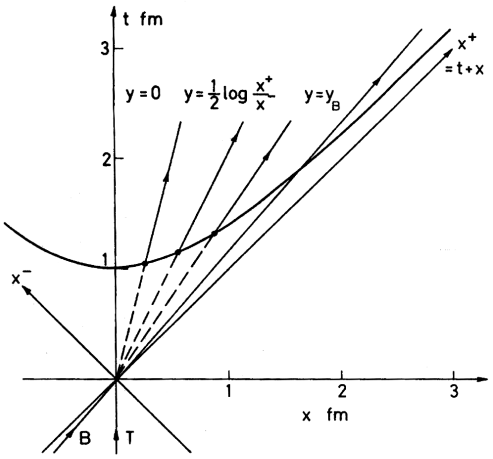

Fig.1

Figure 2. Semi-classical fluid trajectories: the In-Out cascade. The rapidity y is equal to the space-time rapidity $\eta = \frac{1}{2}\log\frac{x^+}{x^-}$.

In the first stages of the collision, a rather dense interacting medium is created and the individual partonic or hadronic degrees of freedom can be neglected to a good approximation. This observation justifies the treatment of the medium as a fluid and, moreover, allows the assumption of local equilibrium. In the simplest perfect fluid approximation, the energy-momentum tensor reads

$$T^{\mu\nu} = (\epsilon + p) u^\mu u^\nu - p\, \eta^{\mu\nu} \,, \tag{20}$$

where ϵ, p and u^μ are the energy density, pressure and 4-velocity of the fluid, respectively; while $\eta^{\mu\nu}$ is the flat metric of expression (19). We further assume an equation of state of the form

$$\epsilon = g\, p \,, \tag{21}$$

where $1/\sqrt{g}$ is the sound velocity of the liquid. In the case of a conformal theory, the traceless condition $T^\mu_\mu = 0$ implies $g = 3$ in four dimensions. The continuity equation $\partial_\mu T^{\mu\nu} = 0$ for a perfect fluid of energy density and pressure related by (21) reduces to two equations

$$
\begin{aligned}
g\partial_+(\ln p) &= -\frac{(1+g)^2}{2}\partial_+ p - \frac{g^2-1}{2}e^{-2y}\partial_- y \\
g\partial_-(\ln p) &= \frac{(1+g)^2}{2}\partial_- p - \frac{g^2-1}{2}e^{2y}\partial_+ y \quad (22)
\end{aligned}
$$

for the pressure and the rapidity

$$
y \equiv \frac{1}{2}\ln\left(\frac{\epsilon+p}{\epsilon-p}\right) \tag{23}
$$

of the fluid. The other thermodynamical quantities can be derived from the equation of state (21) and the standard thermodynamical identities

$$
p+\epsilon = Ts\,, \qquad d\epsilon = Tds\,, \tag{24}
$$

where T and s are the temperature and entropy density of the fluid and we have assumed, for simplicity, vanishing chemical potential.

The result is

$$
p = \frac{\epsilon}{g} = p_0\, T^{g+1}\,, \quad s = s_0\, T^g \propto p^{\frac{g}{g+1}}\,, \tag{25}
$$

for constant p_0 and s_0.

The key observation is that the expansion of the fluid can be described by a semi-classical picture. In fact, the high occupation numbers of the system allow to assume that the fluid components follow quasi-classical trajectories in spacetime, here straight-line trajectories starting at the origin (see Fig.2), and given by

$$
y = \eta\,. \tag{26}
$$

Plugging the Ansatz (26) into (22), one obtains

$$
g\partial_+(\ln p) = -\frac{1+g}{2x^+}\,, \quad g\partial_-(\ln p) = -\frac{1+g}{2x^-}\,, \tag{27}
$$

from which it easily follows

$$
\ln\frac{p}{p_0} = \frac{1+g}{2}\log x^+x^- \;\Rightarrow\; p(\tau) = \frac{p_0}{\tau^{\frac{1+g}{g}}}\,. \tag{28}
$$

The simple Ansatz (26) thus leads to a boost-invariant system. Such a physical description is suitable to model the central rapidity region of highly relativistic heavy-ion collisions, where a central plateau in the distribution of particles is detected.

Specifically, in the perfect fluid four-dimensional case, the behavior is

$$
p(\tau) = \frac{\epsilon(\tau)}{3} = \frac{p_0}{\tau^{\frac{4}{3}}} \sim T^{\,4}(\tau)\,, \quad s \sim T^3(\tau)\,. \tag{29}
$$

Note that the entropy density verifies $s = s_0\tau^{-1}$. Hence the total entropy S per unit of rapidity (and transverse area) is constant [8] (as expected from a perfect fluid) since

$$
dS \equiv \int s\, d^3x = s\tau \int d^2x_\perp dy\,. \tag{30}
$$

3.2. Boost-invariant flow

Inspired by Bjorken's analysis, the methods provided by the AdS/CFT correspondence have been applied to study the dynamics of boost-invariant strongly interacting gauge theory matter in [15]. There are technical reasons for making this symmetry assumption, due to the complication of the Einstein's equations in the gravity dual. On a more theoretical level, using the $\mathcal{N} = 4$ SYM theory as a substitute to QCD seems at first sight highly problematic. Moreover, experimentally the assumption of boost invariance is not optimal, since the observed multiplicity distribution of particles in heavy-ion collisions is rapidity-flat only in the central region. In terms of the hydrodynamic modelization, this means that the entropy is rapidity-independent, and thus obeying boost-invariance, only in the same region.

All these warning remarks have to be certainly taken into account, when using the AdS/CFT correspondence in a physical context. However, there are convincing arguments to show that for appropriate observables and by using AdS/CFT methods, one obtains a first fruitful approach to the behavior of QCD at strong coupling. From a phenomenological point-of-view, boost-invariance is widely used in modeling the relativistic heavy-ion collisions at RHIC in the central region of rapidity, where the hydrodynamic approach seems successful in describing the data and the occurrence of the quark-gluon plasma. Moreover, this plasma is a non-confining phase of QCD for which no specific hadronic scale seems to be relevant. In a more theoretical language, in this regime QCD appears to be nearly conformal. The above argu-

ments suggest that it is reasonable to apply boost-invariance, at least in a first approximation, and to study the dynamics of the $\mathcal{N} = 4$ SYM plasma under consideration.

In a boost-invariant setup, it is natural to parametrize the flat four-dimensional boundary in terms of the coordinates $(\tau, \eta, x_\perp)$, where τ is the proper-time, η the space-time rapidity and $x_\perp = (x_2, x_3)$ denotes the transverse directions. We already introduced these coordinates in the previous section, but it is worth being more explicit here. In terms of the Minkowski coordinates $(t, x_1, x_\perp)$, the definition of τ and η reads

$$t = \tau \cosh \eta \,, \qquad x_1 = \tau \sinh \eta \,, \tag{31}$$

and the metric has the form

$$ds^2 = -d\tau^2 + \tau^2 d\eta^2 + dx_\perp^2 \,. \tag{32}$$

For simplicity, further assume independence on the transverse coordinates $x_\perp$, corresponding to the limit of infinitely large nuclei colliding.

The energy-momentum tensor $T_{\mu\nu}$ of the gauge theory can then be written in diagonal form and has only three non-vanishing components: $T_{\tau\tau}$, $T_{\eta\eta}$ and $T_{x_2x_2} = T_{x_3x_3}$, which depend on proper-time. The conservation condition $D_\nu T^{\mu\nu} = 0$ and, since we are dealing with a conformal theory, the tracelessness condition $T^\mu_\mu = 0$ further restrict the form of the energy-momentum tensor. It can be shown that all components can be expressed in terms of a single function $\epsilon = \epsilon(\tau)$:

$$T_{\mu\nu} = \text{diag}\left(\epsilon, -\tau^2(\tau\epsilon' + \epsilon), \epsilon + \frac{\tau\epsilon'}{2}, \epsilon + \frac{\tau\epsilon'}{2}\right) . \tag{33}$$

The function $\epsilon(\tau)$ can be interpreted as the energy density of the plasma at mid-rapidity (*i.e.* at $x_1 = 0$) as a function of proper-time. The last kinematic constraint on the stress-energy tensor is the positive energy condition. For any time-like vector t^μ, the energy density in the reference frame whose time-like direction is specified by t^μ should be non-negative

$$T_{\mu\nu} t^\mu t^\nu \geq 0 \,. \tag{34}$$

For the Ansatz (33), it implies

$$\epsilon(\tau) \geq 0 \,, \quad \epsilon'(\tau) \leq 0 \,, \quad \tau\epsilon'(\tau) \geq -4\,\epsilon(\tau) \,. \tag{35}$$

The explicit expression of ϵ specifies the dynamics of the theory and it is the information we aim to determine through the AdS/CFT correspondence.

In the following, we restrict the analysis to the class of gauge theories whose late proper-time evolution is specified by a power-law parameter s, such that

$$\epsilon(\tau) \propto \frac{1}{\tau^s} \,. \tag{36}$$

The positive energy condition (34) fixes the range of possible powers s to $0 \leq s \leq 4$.

Notice that the family of gauge theories described by (36), includes a number of cases of physical interest. If the longitudinal pressure $T_{\eta\eta}$ vanishes, see (33), the plasma is in a *free streaming* phase which is expected to be well suited to the case of a weakly coupled plasma [21]. Solving for ϵ in (33) leads to $\epsilon(\tau) \propto \tau^{-1}$. If the gauge theory plasma behaves, instead, as a perfect fluid, the energy-momentum tensor has to be of the form (20) with $\epsilon = 3\,p$. Under the assumption of boost invariance, $u^\mu = (1, 0, 0, 0)$ and the comparison with (33) leads to the Bjorken solution of section 3.1: $\epsilon(\tau) \propto \tau^{-4/3}$. The case $\epsilon(\tau) \propto \tau^0$ is also of interest, it describes a fully anisotropic medium with negative longitudinal pressure $p_\parallel \equiv T_{\eta\eta}/\tau^2 = -\epsilon = -p_\perp$ that might be relevant for the early times dynamics at strong coupling, as advocated in [22]. As we shall see in section 4, the status of early times dynamics in the AdS/CFT correspondence seems to be more complex.

While we will deal in detail with the dual description of the early-time flow in the following, in the present part we restrict the analysis to the range $0 < s < 4$. In what follows, we will determine which, if any, of the above behaviors is relevant for the description of the large proper-time evolution.

3.3. Large proper-time behavior of the gravity dual

In this section, following the procedure of holographic renormalization introduced in section 2.2, we repeat the construction of [15] of the dual geometries to the boost invariant gauge theories with energy densities of the form (36). Since

the bulk metric shares the same symmetries of the plasma system, the most general Ansatz in Fefferman-Graham coordinates reads

$$\begin{aligned} z^2 ds^2 &= -e^{a(\tau,z)} d\tau^2 + \tau^2 e^{b(\tau,z)} d\eta^2 \\ &\quad + e^{c(\tau,z)} dx_\perp^2 + dz^2 \,. \end{aligned} \tag{37}$$

According to the holographic dictionary, to determine the metric components $a(\tau,z)$, $b(\tau,z)$ and $c(\tau,z)$, Recalling Einstein equations with a negative cosmological constant

$$R_{\alpha\beta} = \frac{1}{2} g_{\alpha\beta}(R-12) \tag{38}$$

one has to solve them in a power series expansion in the radial coordinate z. The indices α,β in (38) denote the bulk coordinates $(\tau,z,\eta,x_\perp)$ and the metric components are subject to the boundary conditions

$$a(\tau,z) = -z^4\epsilon(\tau) + z^6 a_6(\tau) + z^8 a_8(\tau) + \dots \tag{39}$$

around $z=0$ and similar ones for $b(\tau,z)$ and $c(\tau,z)$. By studying the explicit form of the Fefferman-Graham expansion, it can be shown that the large τ asymptotics of the exact solutions can be obtained analytically (see [15] for the details of the computation). In fact, introducing the scaling variable

$$v = \frac{z}{\tau^{\frac{s}{4}}} \,, \tag{40}$$

the exact solutions have an expansion of the form

$$a(\tau,z) = a(v) + \mathcal{O}\left(\frac{1}{\tau^\alpha}\right) \,, \tag{41}$$

for some positive power α. The asymptotic equations, obtained from (38) taking the limit $\tau\to\infty$, while keeping v fixed, can then be solved exactly. The solution is

$$\begin{aligned} a(v) &= A(v) - 2m(v) \\ b(v) &= A(v) + (2s-2)m(v) \\ c(v) &= A(v) + (2-s)m(v) \end{aligned} \tag{42}$$

where

$$\begin{aligned} A(v) &= \frac{1}{2}\ln\left(1-\Delta^2(s)v^8\right) \\ m(v) &= \frac{1}{4\Delta(s)}\ln\frac{1+\Delta(s)v^4}{1-\Delta(s)v^4} \\ \Delta(s) &= \sqrt{\frac{3\,s^2-8s+8}{24}} \,. \end{aligned} \tag{43}$$

3.4. Selection of the perfect fluid

Let us now examine in more detail the geometry we obtained. The dual asymptotic metric of the boost-invariant plasma has a potential singularity for $v=\Delta^{-1/4}(s)$, where the argument of the logarithm in (43) vanishes.

As usual, to distinguish a physical singularity from a coordinate one, it is sufficient to construct a scalar invariant formed out of the Riemann tensor which diverges at the singularity location. While the curvature scalar is everywhere regular, the simplest non-trivial scalar that can be considered is the square of the Riemann tensor (or Kretschmann scalar)

$$\mathfrak{R}^2 \equiv R^{\alpha\beta\gamma\delta} R_{\alpha\beta\gamma\delta} \,. \tag{44}$$

In the asymptotic limit $\tau\to\infty$ with v fixed, the general structure of this expression becomes

$$\mathfrak{R}^2 = \frac{N(v,s)}{\left(1-\Delta^2(s)v^8\right)^4} + \mathcal{O}\left(\frac{1}{\tau^\beta}\right) \,, \tag{45}$$

for a positive β. The explicit expression of the numerator $N(v,s)$ is quite complicated and can be found in [15]. For generic s, the above asymptotic expression for $\mathfrak{R}^2$ diverges at $v=\Delta^{-1/4}(s)$ and the singularity is a physical naked one. It turns out that only for $s=4/3$ the fourth order pole of the denominator gets cancelled by an identical contribution in the numerator leaving a bounded scalar invariant. Only the physical singularity in the dual geometry of a perfect fluid (which will be found at $z=\infty$, see later on) can be hidden behind an event horizon.

The above analysis suggests a criterion to select the profile $\epsilon(\tau)$ in (33). The proposal of [15] is that a physical boundary energy-momentum tensor has to be dual to a geometry satisfying the cosmic censorship. It then turns out that the requirement of the absence of naked singularity in the bulk uniquely selects perfect hydrodynamics as the large proper-time dynamics of the strongly coupled plasma.

The scaling variable (40) and the energy density for a perfect relativistic fluid are

$$v = \frac{z}{\tau^{\frac{1}{3}}} \,, \quad \epsilon(\tau) = \frac{e_0}{\tau^{\frac{4}{3}}} \,, \tag{46}$$

where we have reinstated a dimensionful parameter e_0 in ϵ. In this case, the metric coefficients

simplify considerably and the asymptotic geometry can be written in the compact Fefferman-Graham form

$$z^2 ds^2 = -\frac{\left(1-\frac{e_0}{3}\frac{z^4}{\tau^{4/3}}\right)^2}{1+\frac{e_0}{3}\frac{z^4}{\tau^{4/3}}}\,d\tau^2 + dz^2 + \left(1+\frac{e_0}{3}\frac{z^4}{\tau^{4/3}}\right)\left(\tau^2 dy^2 + dx_\perp^2\right) . \quad (47)$$

This geometry is analogous to the static AdS black brane solution of section 2.2 and thus the potential singularity is indeed a coordinate one. Here, however, the horizon position depends on proper-time

$$z_0 = \left(\frac{3}{e_0}\right)^{\frac{1}{4}} \tau^{\frac{1}{3}} . \quad (48)$$

Although a precise notion of temperature and entropy still lacks in a dynamical setup, in order to obtain a qualitative estimate one could naively generalize the static formula to infer

$$T = \frac{\sqrt{2}}{\pi z_0} = \left(\frac{e_0}{3}\right)^{\frac{1}{4}} \frac{\sqrt{2}}{\pi \tau^{\frac{1}{3}}} \quad (49)$$

for the temperature and the total entropy $S \propto s\tau = const.$, see (30). Observe that these estimates are in agreement with the "Bjorken flow" expressions of equation (29). Since the temperature of the black hole coincides with the one of the plasma, the gravity dual of the plasma cooling off during expansion is in terms of a black hole which moves off in the radial direction of the bulk, from the boundary towards the interior. A similar picture had already been qualitatively proposed in [23].

3.5. In-flow viscosity and relaxation time

It should be stressed that the results of section 3.4 were obtained in the scaling limit. The gravity dual selects perfect hydrodynamics only in the strict asymptotic limit of infinite proper-time. Indeed, as shown for instance in [19] and [20], it is straightforward to repeat the computation of the square of the Riemann tensor up to the first subleading corrections in the metric and check that it is always singular for perfect fluid dynamics. The evaluation of $\mathfrak{R}^2$ leads to

$$\mathfrak{R}^2 = R_0(v) + \frac{1}{\tau^{\frac{4}{3}}} R_2(v) , \quad (50)$$

where $R_0(v)$ is finite, but $R_2(v)$ develops a 4^{th} order singularity. From the gravity side, it is then clear that the energy density in (46) needs to be corrected. It turns out that these corrections are due to viscous hydrodynamics, but it is instructive to see how the result arises using purely AdS/CFT methods. Assume that

$$\epsilon(\tau) = \frac{1}{\tau^{\frac{4}{3}}}\left(1-\frac{2\eta_0}{\tau^r}\right) \quad (51)$$

for a generic positive exponent r. Solving Einstein's equations with this boundary condition and computing the Kretschmann scalar yields a result of the form

$$\mathfrak{R}^2 = R_0(v) + \frac{1}{\tau^r} R_1(v) + \frac{1}{\tau^{2r}} \tilde{R}_2(v) + \frac{1}{\tau^{\frac{4}{3}}} R_2(v) , \quad (52)$$

where the last two terms are always singular. To obtain a bounded Kretschmann scalar, the only possibility is to make those two terms proportional to each other and therefore to set $r = 2/3$. This is exactly the scaling of a viscosity correction to Bjorken hydrodynamics with shear viscosity $\eta = \eta_0/\tau$ (which follows from $\eta \propto T^3$ in the $\mathcal{N} = 4$ SYM case). Moreover, in [24] it has been shown that, to implement the cancellation of the potentially singular terms, the coefficient η_0 has to be tuned to $\eta_0 = 2^{-1/2}3^{-3/4}$. This specific value corresponds to a shear viscosity to entropy ratio

$$\frac{\eta}{s} = \frac{1}{4\pi} . \quad (53)$$

It is remarkable that the above result, obtained in a non-linear and dynamical setup coincides with the shear viscosity value obtained in [9], studying the response of a static plasma at fixed temperature to small perturbations.

The procedure can be further generalized to higher orders to compute the other hydrodynamics coefficients. In general, the metric components $a(\tau, z)$, $b(\tau, z)$ and $c(\tau, z)$ in (37) have an expansion of the form

$$a(\tau, z) = \sum_n a_n(v) \frac{1}{\tau^{\frac{2n}{3}}} , \quad (54)$$

while the one of the curvature invariant is

$$\mathfrak{R}^2 = \sum_n R_n \frac{1}{\mathcal{T}^{\frac{4n}{3}}} \,. \tag{55}$$

The 2^{nd} order formalism is obtained truncating the sums above at $n = 3$ and has been worked out in [25] (with a correction given in Ref.[26], see further on). It results into a relaxation time

$$\tau_r = \frac{2 - \ln 2}{2\pi T} \,, \tag{56}$$

which is about thirty times shorter than the one estimated on the basis of Boltzmann's kinetic theory. The value (56) has been corrected by matching the results for the Bjorken flow of Ref.[25] with the full second-order formalism for hydrodynamics in conformal field theories at finite temperature derived in [26].

Surprisingly, at this order, a new feature arises, namely the presence of a leftover logarithmic singularity in the expansion of $\mathfrak{R}^2$. In [25], it has been argued that such a divergence could be cured considering the coupling of a dilaton to the bulk metric. A non vanishing dilaton profile turns on, on the gauge theory side, a non-zero expectation value of $\mathrm{Tr}F^2$, meaning that electric and magnetic modes are no longer equilibrated. The tuning of the dilaton field to achieve a non-singular Kretschmann scalar, leads to a negative expectation value $\langle \mathrm{Tr}F^2 \rangle < 0$, implying that electric modes dominate.

However, the logarithmic divergences that arise at NNLO in the energy density expansion, have been considered more extensively in [27] and [28] (see also [29] and [30]). The conclusion is that the logarithmic singularity origins in a pathology of the Fefferman-Graham coordinates. There exists in fact a singular transformation to Eddington-Finkelstein coordinates, which yields a regular and smooth metric from the boundary up to the standard black brane singularity. In this coordinate system, the late proper-time expansions of curvature invariants is regular at the horizon. In order to proceed to higher orders, one would then have to perform the analysis in Eddington-Finkelstein coordinates.

3.6. Duality beyond boost-invariance

The efficacy of the approach that we presented in the previous sections resides in that no assumption about the dynamics of the plasma has to be made. It is the gravity dual analysis alone that selects the physically relevant evolution. However, in order to solve the full system of Einstein's equations one is in general constrained to work in highly symmetric setups and in specific regimes of interest. In particular, it is very hard to relax the assumption of boost invariance of the gauge theory matter. Significant progress in this direction has been achieved through a different approach in [31], where it has been shown in general how hydrodynamics arises from the gravity side.

The starting point of the analysis is the five-dimensional static AdS black brane which is dual to a strongly coupled plasma at rest (*i.e.* with flow vector $u^\mu = (1, 0, 0, 0)$) and at temperature T. In incoming Eddington-Finkelstein coordinates, the metric reads

$$\begin{aligned} ds^2 &= -r^2 \left[1 - \left(\frac{T}{\pi r} \right)^4 \right] dv^2 + 2\, dv dr \\ &\quad + r^2 \eta_{ij}\, dx^i dx^j \,, \end{aligned} \tag{57}$$

where the coordinate r is related to the radial coordinate z by $r = 1/z$. The conformal boundary of space-time is at $r = \infty$ and the horizon at $r = T/\pi$. This choice of the coordinate system is consistent with the comments of the end of section 3.5; these coordinates are well defined on the horizon and extend all the way from the boundary to the black brane singularity.

By performing a boost, one can obtain the dual geometry to a uniformly moving plasma with 4-velocity u^μ

$$\begin{aligned} ds^2 &= -r^2 \left[1 - \left(\frac{T}{\pi r} \right)^4 \right] u_\mu u_\nu\, dx^\mu dx^\nu \\ &\quad - 2 u_\mu\, dx^\mu dr + r^2 (\eta_{\mu\nu} + u_\mu u_\nu) dx^\mu dx^\nu \,. \end{aligned} \tag{58}$$

The main idea of [31] is to promote T and u^μ to be slowly varying functions of the boundary Minkowski coordinates. In this way, the geometry ceases to be an exact solution of Einstein's equations because of the appearance of gradients of the temperature and of the velocity. The metric

(58) can be corrected order by order in a derivative expansion. The integration constants that arise at each order can be fixed requiring regularity of the metric at the horizon. The energy-momentum tensor of the plasma can then be read off from the corrected geometry and it is expressed, as the metric itself, in terms of T, u^μ and their derivatives. Explicit results have been worked out up to second order and read

$$T^{\mu\nu} = \frac{1}{16\pi G_5}\Bigg[(\pi T)^4(\eta^{\mu\nu}+4u^\mu u^\nu) - 2(\pi T)^3\sigma^{\mu\nu} + (\pi T^2)\Bigg(\log 2\, T^{\mu\nu}_{2a} + (2-\log 2)\left(\frac{1}{3}\,T^{\mu\nu}_{2c}+T^{\mu\nu}_{2d}+T^{\mu\nu}_{2e}\right)\Bigg)\Bigg], \tag{59}$$

where G_5 is the five dimensional Newton's constant and the rather lengthy expressions of the quantities $\sigma^{\mu\nu}$, $T^{\mu\nu}_{2a}$, etc. can be found in the original paper [31]. The first term in $T^{\mu\nu}$ is simply the perfect fluid energy-momentum tensor, the second term involves the shear viscosity, while the third is the contribution of second order hydrodynamics.

The conservation equation $\partial_\mu T^{\mu\nu}=0$ is equivalent, by definition, to the relativistic Navier-Stokes equation. Therefore, the dual geometry of every solution of the hydrodynamic equations is given by (58) plus correction terms up to the same order in the gradient expansion.

We should note, however, that this construction is adequate exclusively for near the equilibrium setups. Starting from the boosted black brane metric, in fact, one implicitly assumes the existence of a hydrodynamical description, in terms of flow velocity and energy density. As we explain in section 4, when dealing with processes that do not admit such a description, as the early stages of heavy-ion collisions, one has to recur to different methods.

4. AdS/CFT and early time quark-gluon plasma flow

One of the main theoretical challenges of the physics of quark-gluon plasma is to describe its thermalization process.

The plasma is created in the initial stages of heavy-ion collisions, during which the system is certainly out-of-equilibrium. However, simulations based on the RHIC data suggest that an hydrodynamical description becomes reliable at times < 1 fm/c after the collision event [32–34]. Perturbative QCD calculations [33,35,36] lead to a much longer thermalization time $\tau_{therm} \gtrsim 2.5$ fm/c, pointing in the direction of a strongly coupled scenario. As we saw, holographic methods are, up to now, one of the few tools of investigation available in this context, as well as a very promising one.

In this section, we describe some steps forwards towards a description of the thermalization process of QGP, modeled by a strongly coupled $\mathcal{N}=4$ SYM plasma at finite temperature. Since it is a developing subject on a settled theoretical question dealing with far-from-equilibrium dynamics at strong coupling, we will discuss three different approaches.

i) In section 4.1, we presents estimates of the thermalization response-time computed through the quasi-normal modes of small perturbations away from the thermal background. This explores the information one can get on thermalization and isotropization from *linearized* solutions, coupling non-hydrodynamic perturbations to a moving black hole background.

ii) Section 4.2 is devoted to the discussion of the fully *non-linear* thermalization dynamics of a boost-invariant plasma, evolving from an anisotropic out-of-equilibrium early stage towards the hydrodynamic regime. The results point towards a dependence on initial conditions but also to the indication of a fast (if not complete) isotropization as characteristic of strongly coupled dynamics.

iii) In section 4.3 we mention the results obtained in modeling the Lorentz-contracted relativistic nuclei of a heavy-ion collision through initial shock waves and look for a solution of the dual gravitational field after the collision. This provides a realistic scenario, at least from the kinematic point of view.

A warning is to remind the following unsolved problem. The preferred phenomenological sce-

nario for the QGP formation starts from initial conditions which may be dominated by weak QCD coupling, due to the high density of partons in a fast boosted nucleus. Hence the problem remains open to describe on a microscopic basis the transition from a far-from-equilibrium weakly coupled system towards a hydrodynamic one at strong coupling. At least the AdS/CFT correspondence allows to make a few first (and quite unique at present) steps on the understanding of strongly coupled dynamics.

4.1. Thermalization response-time

4.1.1. Quasi-normal modes

The quasi-normal modes of a black hole describe the response of the system after a small perturbation. Since the field that sources the perturbation can fall into the black hole or radiate to infinity, the modes of oscillations decay, their frequencies being complex. The geometry therefore undergoes damped oscillations that produce an exponential decay of the perturbation. The frequencies and damping of these oscillations are entirely fixed by the black hole, and are independent of the initial perturbation. For black holes in asymptotically flat space-times, the exponential decay of the quasi-normal modes is followed by a power-law decrease [37]. The decay is instead purely exponential in the case of black holes in AdS [38].

In the AdS/CFT framework, perturbing a static black hole in AdS corresponds to perturbing the approximately thermal dual state, and the decay of the perturbations describes relaxation back to thermal equilibrium. Computing the quasi-normal modes of the equations of motion linearized around the background allows therefore to estimate the thermalization response-time of the strongly coupled dual gauge theory after a small deviation from equilibrium.

The behavior of quasi-normal modes should be contrasted with the one of hydrodynamical excitations that go to zero at small transverse momentum and have a slower power-law decay. In the static case, for instance, both quasi-normal modes and viscosity calculation correspond to poles of specific retarded propagators, respectively for a scalar and metric deformation, through Fourier transform in the time variable. However, in the limit of zero transverse momentum, the poles corresponding to the viscosity case vanish. The "non-hydrodynamic" nature of the scalar quasi-normal modes allows instead to obtain a finite thermalization response-time in this limit.

The quasi-normal modes analysis has been carried out in [39] for black holes in four, five and seven dimensional global AdS and perturbations produced by a minimally coupled scalar field excitation. See also [40–42] for later developments. In asymptotically AdS space times, quasi-normal modes are defined as solutions of the wave equation that are purely ingoing near the horizon and vanish at the boundary. For a minimally coupled scalar perturbation, they are obtained solving the wave equation for a massless scalar field $\nabla^2\Phi = 0$ in the gravitational background, with absorbing boundary conditions at the horizon $z = z_0$ and Dirichlet conditions at the boundary $z = 0$. One writes

$$\nabla^2\Phi \equiv \frac{1}{\sqrt{-g}}\partial_\alpha\left(\sqrt{-g}g^{\alpha\beta}\partial_\beta\Phi\right) = 0 \tag{60}$$

for the standard covariant coupling of the scalar field Φ to the background metric $g^{\alpha\beta}$ of determinant g.

4.1.2. Static black hole

Since the main example throughout the notes is $\mathcal{N} = 4$ SYM in four-dimensional Minkowski space, in the following we refer the results obtained in the case of a static planar black hole in AdS_5. To facilitate the comparison with the results of [43] discussed later in the section, we work in Fefferman-Graham coordinates.

Recall that in these coordinates, see (12), the metric of a five-dimensional black brane reads

$$ds^2 = -\frac{\left(1-\frac{z^4}{z_0^4}\right)^2}{\left(1+\frac{z^4}{z_0^4}\right)}\frac{dt^2}{z^2} + \left(1+\frac{z^4}{z_0^4}\right)\frac{d\vec{x}^2}{z^2} + \frac{dz^2}{z^2}. \tag{61}$$

where $(t, \vec{x})$ are the boundary coordinates, z is the AdS radius and z_0 is the location of the event horizon in the bulk.

In the case of the static metric (61), Eq.(60)

writes

$$- \quad \frac{1}{z^3}\frac{\left(1-\frac{z^4}{z_0^4}\right)^2}{1+\frac{z^4}{z_0^4}}\,\partial_t^2\Phi(t,z) + \quad \partial_z\left[\frac{1}{z^3}\left(1-\frac{z^8}{z_0^8}\right)\partial_z\Phi(t,z)\right]=0\,. \tag{62}$$

Using the separation of variables

$$\Phi(t,z)=e^{i\omega t}\;\phi(z)\,, \tag{63}$$

the wave equation (62) leads to a Heun equation in the bulk variable [40]

$$\phi'' \quad + \quad \frac{1-\tilde{z}^2}{\tilde{z}(1-\tilde{z})(2-\tilde{z})}\phi' + \frac{(z_0\omega)^2}{8\tilde{z}(1-\tilde{z})(2-\tilde{z})}\phi=0 \tag{64}$$

where $\tilde{z}\equiv(1-(z/z_0)^2)^2/(1+(z/z_0)^4)$, $z_0=\sqrt{2}(\pi T)^{-1}$, *cf.* (15), and the prime denotes the derivative with respect to $\tilde{z}$.

The quasi-normal modes analysis then proceeds through a combination of analytic and numerical methods (see [39] for details). Note that quasi-normal modes appear also as poles in the complex frequency plane of the Fourier transform in time t of the retarded Green's function (see *e.g.* [44]).

Interestingly enough, for a homogeneous scalar excitation, the dominant decay mode at large time is given by a quasi-normal mode whose frequency acquires a non zero imaginary part and thus corresponds to a minimal exponential decay mode with temperature. Technically, by matching Eq.(64) with a Shrödinger equation

$$\partial_{z^*}^2\phi(z^*)+\;\frac{\sqrt{8}\;e^{12z^*}}{\sinh^{3/2}(8z^*)}\Big(\frac{\omega}{\pi T}\Big)^2\,\phi(z^*)=0 \tag{65}$$

through the change of variable

$$z\to z^*\equiv\frac{1}{4}\;[\tanh^{-1}(z^4/z_0^4)]^4,$$

one gets quantized "energy states". The dominant exponential decay mode, corresponds to the state with minimal energy in the Shrödinger equation (65). Denoting ω_k the eigenvalues of Eq. (65), one finds

$$\frac{\omega_k}{\pi T}=a_k-ib_k\,, \tag{66}$$

and

$$\cdots>b_k>\cdots>b_1=2.74667\,, \tag{67}$$

where T denotes both the plasma and black brane temperature. The corresponding response timescale is thus given by the first eigenvalue ω_1 and leads to $\tau_{resp}=1/\Im m\omega_1\sim 0.116/T$.

4.1.3. Moving black hole

A similar analysis was carried out in [43] for a black hole moving away in the radial bulk direction. This geometry was discussed in section 3.4 and is the gravity dual of a boost-invariant expanding perfect fluid in $\mathcal{N}=4$ SYM at large proper-time. Knowledge of the quasi-normal modes of this black hole gives an estimate of the *thermalization response-time* of the strongly coupled gauge theory, that is the relaxation time after a perturbation of the local thermal equilibrium due to the coupling to a scalar field.

The background geometry describing a black hole moving off from the boundary in the z direction was given in (48). In terms of the scaling variable $v=z\tau^{-1/3}$, it writes

$$z^2ds^2 \quad = \quad -\frac{(1-v^4)^2}{(1+v^4)}d\tau^2+ +(1+v^4)(\tau^2dy^2+dx_\perp^2)+dz^2\,. \tag{68}$$

Consider now the wave equation of a canonically coupled scalar field Φ in the boost-invariant setting. In the scaling limit $v=$const and $\tau\to\infty$, the corresponding Klein-Gordon equation (60) is now expressed in terms of the two variables τ and z. Through the change of variables $(\tau,z)\to(\tau,v)$, so that

$$\partial_z\to\tau^{-\frac{1}{3}}\partial_v\,,\quad \partial_\tau\to\partial_\tau-\frac{1}{3}\tau^{-\frac{4}{3}}\partial_v\,, \tag{69}$$

and neglecting the non diagonal terms in the large τ expansion, one gets

$$- \quad \frac{1}{v^3}\frac{(1+v^4)^2}{1-v^4}\partial_\tau^2\Phi(\tau,v) + \quad \tau^{-\frac{2}{3}}\;\partial_v\left(\frac{1}{v^3}(1-v^8)\partial_v\Phi(\tau,v)\right)=0\;, \tag{70}$$

which is similar to (62) but with a τ-dependent coefficient. Performing the separation of variables

$$\Phi(\tau, z) = f(\tau)\phi(v)\,, \tag{71}$$

it reduces to two decoupled equations

$$\partial_\tau^2 f(\tau) + \hat{\omega}^2 \tau^{-\frac{2}{3}} f(\tau) \quad = 0 \tag{72}$$

$$\partial_v \left[\frac{(1-v^8)}{v^3}\partial_v \phi(v)\right] + \hat{\omega}^2 \frac{(1-v^4)^2}{v^3(1+v^4)}\ \phi(v) = 0\,. \tag{73}$$

where we introduced an *a priori* arbitrary parameter $\hat{\omega}$, whose allowed values will be fixed by the (quantized) solutions of (73).

Equation (72) is solved by linear combinations of the Bessel functions

$$\sqrt{\tau} J_{\pm\frac{3}{4}}\left(\frac{3}{2}\hat{\omega}\tau^{\frac{2}{3}}\right)\,, \tag{74}$$

with relevant large τ behavior

$$f(\tau) \sim \tau^{\frac{1}{6}} e^{\frac{3}{2} i(\hat{\omega}_1)\tau^{\frac{2}{3}}} \tag{75}$$

where $\Im m\ \hat{\omega}_1 = 2.74667$ is the same as in (67). Indeed, the equation in the v variable (73) is formally identical to the Heun equation (64) of the static black hole and therefore leads to the same numerical values for the quasi-normal modes and frequencies. However, the variables v and τ of (71) are different from the variables z and t relevant in the static case. Moreover, the proper-time dependence (75) has a non trivial scaling compared to the plane wave dependence of the static solution.

Noting that the moving horizon is at $z_0 = \left(\frac{3}{e_0}\right)^{\frac{1}{4}} \tau^{\frac{1}{3}} = \frac{\sqrt{2}}{\pi T}$, *cf.* (48,49), it was suggested in [43], that this result could be understood in terms of an adiabatic approximation of the expanding case, with locally fixed temperature. Indeed,

$$|f(\tau)| \sim e^{-\frac{3}{2}\Im m(\hat{\omega}_1)\ \tau^{\frac{2}{3}}} \sim e^{-\pi b_1 T \tau}\ , \tag{76}$$

where $\omega_1 = \pi T(a_1 - i b_1)$ is the dominant decay mode in the static case (67).

Plugging in the numerical value of the dominant decay mode (67) in (75) leads to a damping factor of the form

$$\exp\left(-\frac{3}{2}\cdot 2.7466 \cdot \tau^{\frac{2}{3}}\right) \sim e^{-8.3 T\tau}\ . \tag{77}$$

The above results were extended in [41] to include also vector and tensor quasi-normal modes.

In the limits to which this analysis can be considered quantitatively relevant for the thermalization in heavy-ion reactions, the fast decay modes of frequency (67) damp out to $1/e$ of their original amplitude in a time no greater than

$$\tau_{resp}\Big|_{T=T_{peak}} = \frac{0.116}{T}\Big|_{T=T_{peak}} \approx 0.08 \text{ fm/c}\,, \tag{78}$$

for a typical initial peak gauge theory temperature $T_{peak} \approx 300$ MeV, which is commonly considered as reasonable in phenomenology. Given the highly anisotropic momentum space distribution expected in the early stages of a RHIC collision, one tentatively estimates a certain finite number n of e-foldings of the "response thermalization process" have to elapse before hydrodynamic approximations can be used. The estimated thermalization time becomes

$$\tau_{therm} \sim n \times \tau_{resp}\Big|_{T=T_{peak}}\,, \tag{79}$$

leading to $\tau_{therm} \approx 0.3$ fm/c following the guess of [41] of about $n = 4$ iterations. The above estimate compares in order of magnitude with the simulations predictions on real experiments. Nevertheless, it should be clear that it is extrapolated from the quasi-normal modes analysis, that, by definition, only applies to the late-time stages of the whole thermalization process. Moreover, the thermalization response time has been obtained in a linearized approximation around the black hole background through AdS/CFT methods.

As a final remark on this response time studies, it is worth noting that the same properties are valid for quasi-normal modes dominating the transverse space diagonalization of the metric after a non diagonal perturbation. Let us indeed introduce a non diagonal transverse component g_{x_1,x_2} using its contravariant expression

$$g^{x_1}_{x_2}(z,\tau) \equiv \frac{z^2}{1+v^4} g_{x_1 x_2}\ . \tag{80}$$

It verifies (with $g^{x_1}_{x_2}(z,\tau) = f(\tau)\ g^{x_1}_{x_2}(v)$) the same equations (72,73); such as

$$\partial_v\left(\frac{1}{v^3}(1-v^8)\partial_v g^{x_1}_{x_2}(v)\right) + \frac{\hat{\omega}^2}{v^3}\frac{(1+v^4)^2}{1-v^4} g^{x_1}_{x_2}(v) = 0\ . \tag{81}$$

In some sense, isotropization and thermalization response-times are equal at large proper-times. We now will turn to the study of the non-linear problem of isotropization and thermalization when starting from far-from-equilibrium initial conditions.

4.2. Thermalization of boost-invariant plasma

In the present section we describe three different approaches to the study of the thermalization process of a strongly coupled boost-invariant plasma. The analysis are to be intended as complementary and point towards a fast isotropization/thermalization. However, as we shall discuss, this represents only an early stage for a full understanding of far-from-equilibrium dynamics leading to the QGP formation.

4.2.1. Solution with "full anisotropy"

One of the first holographic estimates of the isotropization/thermalization time of the quark-gluon plasma appeared in [22]. The setup of this analysis is similar to the one considered in [15], but with differences which we will comment at the end of this subsection.

The starting proposal of the paper is that Bjorken hydrodynamics at late times can be singled out, in the holographic renormalization program, relaxing the assumptions to only require that the metric tensor is a real and single-valued function of the coordinates everywhere in the bulk, without imposing any constraint on the curvature invariants. Applying the same strategy to early time dynamics [22] leads to infer the existence of a solution corresponding to the fully anisotropic case with constant energy density ϵ. In the notation of section 3.2, it corresponds to the solution with $s = 0$ in equation (36), and thus to "full anisotropy" at initial time, namely $\varepsilon = p_\perp = -p_\parallel$. The system is initially anisotropic, with negative longitudinal pressure, and is expected to evolve at late times to ideal Bjorken hydrodynamics, with longitudinal and transverse pressure components equal and positive. Isotropization must take place at some intermediate proper-time.

Assuming a smooth transition between full anisotropy and full isotropy, the isotropization time τ_{iso} can be estimated matching the small and large proper-time regimes. In [22], this proper-time was defined as the crossing value of the branch-point singularities of the two regimes, leading to

$$\tau_{iso} = \left(\frac{3N_c^2}{2\pi^2 e_0} \right)^{\frac{3}{8}} . \tag{82}$$

Here e_0 is the same dimensionfull parameter that appeared in (46) in the late proper-time behavior $\epsilon(\tau) = e_0 \tau^{-4/3}$.

Phenomenologically, to obtain a rough estimate of the isotropization time (82), one can extrapolate the realistic evaluations of RHIC to the supersymmetric case under consideration. The hydrodynamical simulations for central $Au+Au$ collisions with $\sqrt{s} = 200$ GeV yield the energy density $\epsilon = 15$ GeV/fm^3 at the proper-time $\tau = 0.6$ fm/c. Plugging in the corresponding value of e_0 in (82) and setting $N=3$, in [22] it was obtained $\tau_{iso} \approx 0.3$ fm/c.

Ref.[22] thus points towards a small value of the thermalization time. However, the analysis relies on the assumption of a rapid and smooth interpolation between the initial fluid conditions and the late time regime. A full solution of that transition remains necessary, as we shall discuss now, either by starting from given initial conditions or by a general study of the non-linear gravitational solution in the bulk of the AdS space.

4.2.2. Far-from-equilibrium forcing dynamics

A way to prepare an out-of-equilibrium state is to turn on, in the ground state of a system, a time-dependent perturbation of the background fields. For instance, one can introduce a time-dependent deformation of the boundary geometry with compact support. From an holographic perspective, this acts as a source of gravitational radiation in the bulk, leading to gravitational collapse and inevitably to black hole formation. After the perturbation is turned off, the geometry relaxes to a smooth and slowly varying form. In the dual theory, the latter process describes relaxation of the non-hydrodynamic degrees of freedom towards perfect fluid-dynamics.

This approach has been taken in [45] (following previous analysis [46]) to study the thermalization process of a boost-invariant $\mathcal{N} = 4$ SYM plasma.

The familiar Ansatz of two-dimensional spatial homogeneity, $O(2)$ rotational invariance in the transverse plane (defined by $x_\perp$) and boost-invariance in the longitudinal direction ($x_\parallel = x_1$) has been considered in [45]. This setup has the advantage of allowing the comparison with the late proper-time results of [15]. Since the late hydrodynamic evolution is nearly isotropic, it is especially interesting to generate a high anisotropy in the initial non-equilibrium state.

To get some intuition on the process, we borrow Fig.3 from [45]. The figure depicts a space-time diagram of the field theory evolution. The system starts out at proper-time $\tau = 0$ in the ground state. At $\tau = \tau_i$, the four-dimensional boundary geometry starts to deform in the vicinity of $x_\parallel = 0$ and the perturbation acts until time τ_f, propagating in the $\pm x_\parallel$ directions at speeds asymptotically approaching the speed of light. The relevant space-time region is I in red. At $\tau = \tau_f$, the field theory is out-of-equilibrium and significantly anisotropic. It relaxes towards local equilibrium and hydrodynamics in region II in yellow. After time τ_*, region III in green, the system is well approximated by a perfect fluid behavior. Deriving the thermalization time of the plasma amounts to the computation of the proper-time τ_* in the diagram.

In [45], the deformation of the boundary geometry was taken to be produced by a time-dependent shear

$$ds^2 = -d\tau^2 + e^{\gamma(\tau)} d\vec{x}_\perp + \tau^2 e^{-2\gamma(\tau)} dy^2 \,. \qquad (83)$$

Here

$$\gamma(\tau) = c\,\Theta\left[\delta(\tau)\right]\delta(\tau)^6 e^{-\frac{1}{\delta(\tau)}} \,, \qquad (84)$$

with

$$\delta(\tau) = 1 - \frac{(\tau - \tau_0)^2}{\Delta^2} \,; \qquad (85)$$

c is a constant characterizing the amplitude of the perturbation and Θ is the unit step function. The deformation acts during the time interval (τ_i, τ_f), with endpoints $\tau_i \equiv \tau_0 - \Delta$ and $\tau_f \equiv \tau_0 + \Delta$.

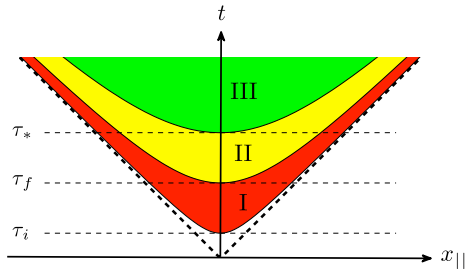

Figure 3. Space-time diagram of the field theory plasma evolution. The metric deformation is turned on in the time interval (τ_i, τ_f). At τ_* hydrodynamics sets in. Figure from [45].

Choosing $\tau_0 \equiv 5/4\,\Delta$, the geometry is flat at $\tau = 0$. All quantities will be measured in units where $\Delta = 1$, so that $\tau_i = 1/4$ and $\tau_f = 9/4$.

The most general bulk Ansatz consistent with diffeomorphism and spatial 3D translational invariance, together with $O(2)$ rotation invariance, is

$$\begin{aligned} ds^2 = -A d\tau^2 \;&+\; \Sigma^2 \left[e^B d\vec{x}_\perp^2 + e^{-2B} dy^2\right] \\ &+\; 2dr d\tau \,, \end{aligned} \qquad (86)$$

where A, B and Σ are all functions of the bulk radial coordinates r and τ only. The coordinate r is related to the previously used z, by $r = 1/z$. Notice that here τ and r are generalized infalling Eddington-Finkelstein coordinates.

Einstein's equations, subject to the boundary conditions that the boundary metric $g_{\mu\nu}(x)$ coincides with (83), can be solved numerically. The boundary stress-energy tensor can be computed through

$$T^{\mu\nu}(x) = \frac{2}{\sqrt{-g(x)}} \frac{\delta S_G}{\delta g_{\mu\nu}} \,, \qquad (87)$$

where S_G denotes the gravitational action. The time-dependence of the energy density, longitudinal and transverse pressures then follows from (see [16])

$$T^\mu_\nu = \frac{N_c^2}{2\pi^2} \mathrm{diag}(-\epsilon, p_\parallel, p_\perp, p_\perp) \,. \qquad (88)$$

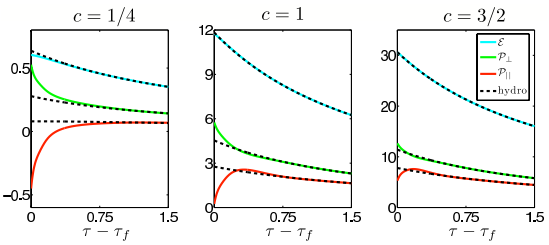

Figure 4. Energy density (blue top curve), transverse pressure (green middle line) and longitudinal pressure (red bottom), divided by $N_c^2/2\pi^2$, as a function of time for $c = 1/4$, $c = 1$ and $c = 3/2$. The dashed black lines show the second order viscous hydrodynamic approximation to the different stress tensor components.

The numerical solution explicitly shows the formation of an event and apparent horizon, which build up in the bulk and merge at late times. At asymptotically late times, the metric settles down to the moving black hole dual of the perfect fluid (48).

The transition from the far-from-equilibrium behavior to near-local-equilibrium hydrodynamics is found to be regulated by the relative importance of the exponentially decaying non-hydrodynamic degrees of freedom in comparison to the slowly relaxing hydrodynamic modes. This is in contrast with the naive expectation that hydrodynamic should set in at the time at which higher order terms in the hydrodynamic expansion become comparable to lower order terms.

A quantification of the results is provided in figure Fig.4, which was presented in [45]. The energy density (ϵ), transverse and longitudinal pressures ($p_\perp$ and $p_\parallel$) are plotted for different values of c, as a function of time, starting at $\tau = \tau_f$. On top of the numerical data are represented the hydrodynamic approximations. The plots show a significant anisotropy, even at late times, where hydrodynamics applies. For all values of c, the transverse pressure approaches the longitudinal pressure from above. This statement can be checked by perturbative computations of the first order viscous corrections. As the value of c increases, the system gets closer to equilibrium at τ_f. Indeed, for larger c, the perturbation does more work on the geometry and the system reaches a higher temperature. In a conformal theory, as $\mathcal{N} = 4$ SYM is, the relaxation time of the non-hydrodynamic degrees of freedom must scale inversely with the temperature. For $c \to \infty$, the system will always be close to local equilibrium and isotropic already at τ_f.

The thermalization time τ_* was defined in [45] as the time beyond which the stress tensor agrees with the hydrodynamic approximation within 10%. In all the analyzed cases, the relevant dynamics, from the production of the plasma to his relaxation to near to local equilibrium, takes place over a time $\tau_* - \tau_i \lesssim 2/T_*$, where T_* denotes the local temperature at the onset of the hydrodynamic regime.

4.2.3. General approach to the early-time flow

In this section we discuss the results obtained in [47], where an analysis of the early time expansion of the boost-invariant flow has been carried out on the lines of [15]. We refer the reader back to section 3.2 for the setup and the basic assumptions.

The idea of the approach is the same as for the large proper-time regime discussed in sections 3.3 and 3.4. In the following, we describe how to holographically reconstruct the dual geometry to a plasma configuration with stress-energy tensor (33) at early proper-times. This is accomplished solving Einstein's equations in a power series expansion starting from the conformal boundary of space-time and subject to the appropriate boundary conditions.

In the late times case, the structure of Einstein's equations naturally led to the introduction of a scaling variable and to a remarkable simplification of the computations. It turns out that it is not possible in general to apply the same procedure to the small τ regime. In what follows we schematically reproduce the main steps of the computation and point out the complications encountered in [47].

We recall that the most general Ansatz for the

bulk metric consistent with the plasma symmetries is

$$z^2 ds^2 = -e^{a(\tau,z)} d\tau^2 + \tau^2 e^{b(\tau,z)} dy^2 + e^{c(\tau,z)} d\vec{x}_\perp^2 + dz^2 \,. \quad (89)$$

Solving Einstein's equations (38)

$$R_{\alpha\beta} = \frac{1}{2} g_{\alpha\beta}(R - 12) \quad (90)$$

in a power series expansion in the bulk coordinate z, together with the boundary conditions (39)

$$a(\tau, z) = -z^4 \epsilon(\tau) + z^6 a_6(\tau) + z^8 a_8(\tau) + \dots \quad (91)$$

allows to fix the metric components $a(\tau, z)$, $b(\tau, z)$ and $c(\tau, z)$ order by order in the z expansion.

Analyzing the structure of the early-time expansion of the equations, in [47] it was concluded that a scaling variable does not exist in general in the $\tau \to 0$ limit. As we shall see, the solution of [22] is not unique. One has to analyze the full solution at $\tau \sim 0$.

From a physical point of view, it is natural to expect that the initial conditions should play a crucial role at early times. On the gauge theory side, the initial state can be prepared in a multitude of ways and therefore its early-time behavior cannot be expected to be universal. This contrasts the late time dynamics which, under the specific symmetry assumptions under consideration, is governed by a single temperature scale. The dissipative effects which act during the plasma evolution wash out the differences due to the initial conditions leading to a hierarchy of terms and to a single scale governing the large time expansion of the energy density.

In the absence of a scaling argument, one can still determine the small τ behavior of the energy density $\epsilon(\tau)$ assuming that at $\tau = 0$ the initial condition is regular. This assumption does not need to be a priori relevant for realistic heavy-ion collisions, but it is in any case an interesting analysis in its own. It implies in fact a finite limit of $\epsilon(\tau)$ as $\tau \to 0$, consistent with the $s = 0$ behavior found in [22]. Moreover, it restricts the expansion of the energy density to be only in even powers of the proper-time

$$\epsilon(\tau) = \epsilon_0 + \epsilon_2 \tau^2 + \epsilon_4 \tau^4 + \dots \quad (92)$$

The coefficients ϵ_{2n} are uniquely determined, through Einstein's equations, in terms of the coefficients of the initial condition for the metric

$$a_0(z) \equiv a(\tau = 0, z) \quad (93)$$

and similarly for the other components.

The admissible initial conditions are given by the constraint equations contained in the full set of Einstein's equations. These imply $a_0(z) = b_0(z)$. Defining

$$v(z^2) \equiv \frac{1}{4z} a_0'(z) = \frac{1}{4z} b_0'(z) \quad (94)$$

$$w(z^2) \equiv \frac{1}{4z} c_0'(z) \,, \quad (95)$$

the remaining constraint reads

$$v' + w' + v^2 + w^2 = 0 \,, \quad (96)$$

where the prime denotes the z^2-derivative. It is easy to see that there does not exist an anywhere bounded solution of the constraint equation. Integration of (96) gives

$$0 = \int_0^\infty (v' + w') dz^2 + \int_0^\infty (v^2 + w^2) dz^2 = \int_0^\infty (v^2 + w^2) dz^2 \,, \quad (97)$$

since the first integral vanishes because of the boundary conditions. The only regular solution is vacuum AdS_5 with $v = w = 0$. Therefore, at any time, including $\tau = 0$, the metrics of interest are singular.

The requirement imposed in [47] of the absence of curvature singularities (other than the one at $z = \infty$) is thus a very powerful tool to select the allowed initial conditions. The coordinate singularity that is then left at all times in the bulk might signal the presence of a dynamical horizon, although this interesting statement requires further investigation.

A bonus that follows from the simplicity of (96) is that it can be solved analytically. One neat example of a solution to the initial value constraint, satisfying the non-singularity requirement, reads

$$a_0(z) = b_0(z) = 2 \ln \cos a z^2 \,, \quad c_0(z) = 2 \ln \cosh a z^2 \,, \quad (98)$$

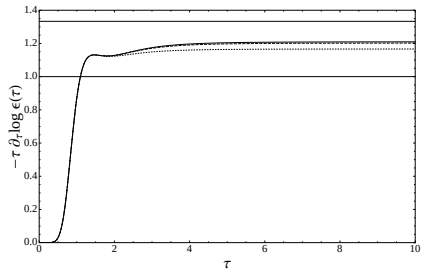

Figure 5. Padé approximation of the effective power $s_{eff}(\tau)$ in the energy density for expansions up to order τ^{64} (dotted line), τ^{80} (dashed line), τ^{96} (solid line) and initial conditions (98). The two horizontal lines denote $s = 1$ (free streaming scenario) and $s = 4/3$ (perfect fluid case).

for a generic constant a. The details of a larger number of allowed initial conditions can be found in [47]. Some of them are also mentioned in the following.

Given the class of acceptable initial conditions, one then needs to solve Einstein's equations with these initial data to obtain the profile $\epsilon(\tau)$. In the absence of a scaling variable, the solution has to be exact and the ideal treatment of the equations should be numerical. This analysis is in progress [48].

In a primary exam, an analytic analysis was pursued in [47] where the equations were solved in a power series in z and τ for specific initial conditions. The limit of this approach is that the power series for the energy density has a finite radius of convergence necessitating the use of as a resummation scheme, such as Padé approximation.

The system evolves from an early time dynamics governed by the initial conditions to an hydrodynamical regime at late times. One way to quantify this transition is through the exam of the effective exponent of the power-law dependence of the energy density

$$s_{eff}(\tau) \equiv -\tau \frac{d}{d\tau} \ln \epsilon(\tau)\,. \tag{99}$$

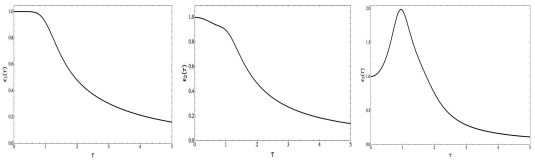

Figure 6. Padé resumed profiles for $\epsilon(\tau)$ for the initial conditions $v + w = \tanh(z^2) - \tan(z^2)$, $v + w = \tanh(z^2 + z^8/6) - \tan(z^2)$ and $v + w = 2/3z^6(1 + z^2/2)/(z^2 - 1)$, respectively.

In Fig.5, this effective power is plotted as a function of τ for the initial conditions (98). The plot is taken from [47]. The different curves correspond to different cuts in the Padé approximation. All profiles start out at zero, clearly cross the line $s = 1$ denoting the free streaming scenario, and move upwards towards $s = 4/3$, which corresponds to the perfect fluid flow. However, to be sure that the profile indeed reaches $s = 4/3$, a numerical solutions is required.

One can also perform the Padé approximation assuming the late time exponent $s = 4/3$. The profiles of $\epsilon(\tau)$ obtained in this way are plotted in Fig.6 for a set of initial conditions (plots taken from [47]). The energy densities differ in the initial stages of the evolution, whereas in the late-time regime they seem to approach local equilibrium.

Recall that the positivity condition $T_{\mu\nu}t^\mu t^\nu \geq 0$ implied $-4\epsilon/\tau \leq \epsilon' \leq 0$ (see eq. (35)). In the third plot of Fig.6, a temporary violation of the positive energy condition is observed. Such a transient behavior may appear for a quantum-driven process (see *e.g.* the discussion in [49], quoting field-theoretical results [50].).

An alternative way to describe the transition to hydrodynamics is through the relative difference between the longitudinal and transverse pressures defined as

$$\Delta p(\tau) = 1 - \frac{p_\parallel(\tau)}{p_\perp(\tau)}\,. \tag{100}$$

When the quantity $\Delta p(\tau)$ approaches zero, it signals isotropization indicating local equilibrium,

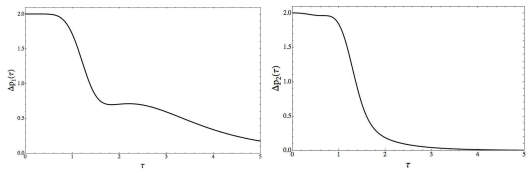

Figure 7. Relative difference in pressures $\Delta p(\tau) = 1 - p_\parallel/p_\perp$ for the initial conditions $v+w = \tanh(z^2) - \tan(z^2)$ and $v+w = \tanh(z^2 + z^8/6) - \tan(z^2)$, respectively. The profiles exhibit a rapid fall-off at $\tau \sim \mathcal{O}(1)$, but the first profile does not reach yet complete isotropization.

while a value of order one indicates a situation close to a free streaming scenario. Fig.7 appears in [47] and shows the relative difference of pressures (100) for a couple of initial conditions. It is interesting to observe that both profiles exhibit a rapid fall-off on a scale $\tau \sim \mathcal{O}(1)$. In the first profile however, isotropization remains incomplete until $\tau \sim \mathcal{O}(5)$. It is interesting to note that figures 6 and 7 are consistent with the full anisotropy solution at *very small* proper-times but show a variety of behavior in the whole of the early proper-time region.

These results point towards a fast isotropization, which could however remain incomplete for some time. The convergence to the hydrodynamic regime remains an open problem. In the coming more systematic numerical study [48] the stability of the Padé approximation has been shown reliable to a larger proper-time interval through non trivial reparametrization of the metric. A more general proof of the transition to the hydrodynamic regime, filling the gap between early-time and late-time behavior is still lacking. Some progress has been made, as we shall see now, starting from specific *shock wave* initial conditions mimicking the initial ultra-relativistic colliding heavy-ions.

4.3. Shock wave initial conditions

An interesting way to model ultra-relativistically boosted large nuclei is through gauge theory shock waves. In this context, by shock wave we mean a plane shell of matter moving at the speed of light. The gravity dual of a boundary shock wave has been first constructed in [15] and later applied to various analysis, such as in attempts to describe holographically deep inelastic scattering or heavy-ion reactions through shock waves collisions.

In terms of the light-cone coordinates $x^\pm \equiv t \pm y$, an ultra relativistic source extended in the transverse direction (a model for an incident heavy ion with large transverse size) and moving along the direction x^+ has an energy-momentum tensor

$$T_{--} \equiv F(x^-) \sim \mu\, \delta(x^-)\,. \tag{101}$$

The last term represents more specifically a shock wave, *i.e.* a shell with vanishing thickness and transverse energy density μ. It may be more concretely represented by a Gaussian centered at $x^- = 0$.

For arbitrary profile $F(x^-)$, the dual background to this configuration reads

$$z^2 ds^2 = -dx^- dx^+ + z^4 F(x^-) dx^{-2} + d\vec{x}_\perp^2 + dz^2, \tag{102}$$

where $F(x^-) = \langle T_{--} \rangle$, and is an exact solution[10] to Einstein equations [15].

These solutions constitute the starting point towards solving the problem of shock waves collisions. Shock waves having a very small thickness along the collision axis and localized in the transverse directions qualitatively resemble the highly Lorentz-contracted nuclei in a heavy-ion collision. Fig.8 appeared in [52] and depicts the space-time picture of ultra-relativistic heavy-ion collisions in the center of mass frame. In the AdS/CFT language, the collision of shock waves in $\mathcal{N} = 4$ SYM translates into colliding gravitational shock waves in the bulk.

Several deserving attempts, both analytical and numerical, have been made to solve this problem [49,52–60], but the full understanding of the transition to the hydrodynamic regime is still an active subject of research. Let us discuss some of these angles of attack.

[10] Note that the solution (102) has been provided a generalization to profiles $F = F(x^-, \vec{x}_\perp, z)$ in [51].

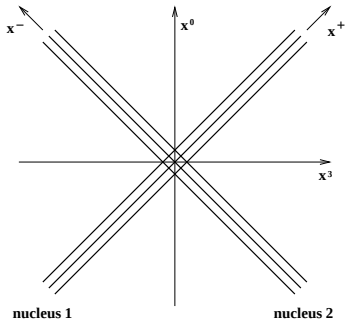

Figure 8. Space-time diagram of the collision of two ultra-relativistic nuclei in the center of mass frame.

The collision of two singular shock waves moving in the directions $x^{\pm}$ on the boundary of a five-dimensional AdS space was studied in [49]. The pre-collision line element is given by the superposition of two metrics of the form (102), with delta-function Ansatz $F(x^{\pm}) \sim \delta(x^{\pm})$. Solving Einstein's equations in a power series expansion in the proper-time allows to extract the expression of the energy-momentum tensor right after the collision. In [49], it was observed that the latter quantity is not boost-invariant in the sense of Bjorken. Boost-invariance could be eventually re-established at later times, at which the expansion breaks down. A crude estimate of the thermalization time in this simple model leads to $\tau_{therm} \sim \mu^{-\frac{1}{3}}$. The non-trivial dimensionless factor in the above relation is $\mathcal{O}(1)$.

In [52], it was observed that the metric of a single shock wave, moving along the light cone, can be computed exactly in first order perturbation theory. The only diagram contributing represents a single graviton exchange between the source nucleus at the AdS boundary and the location in the bulk where the metric is measured. The metric after the collision in the forward light cone can then be constructed perturbatively through an expansion in graviton exchanges. This computation was carried out at tree level in [52] and up to NNLO in [53], where the technique was applied to proton-nucleus collisions.

The analysis of the holographic stress-energy tensor leads to the strong prediction of full nuclear stopping of the two nuclei shortly after the collision. This happens after a time of the order of the inverse typical transverse momentum scale, independently of the energy density. This behavior was interpreted in [52] as signaling black hole creation in the bulk. If the two nuclei stop completely, the strong interactions exerted between them are likely to thermalize the system, eventually leading to Landau hydrodynamics at late times [6]. This non boost-invariant solution is not expected to satisfy the phenomenological constraints, even if the description of multiplicities seems to be valid.

In [52,53] it was pointed out that weak interactions are expected to be determinant in the very early stages of the collision [61]. Since a realistic model should take them into account, and in absence of a dual description incorporating weak coupling aspects of QCD, it was proposed to mimic these effects through net zero-energy unphysical shock waves with profiles $F(x^{\pm}) \sim \delta'(x^{\pm})$. The resulting energy density of the strongly coupled medium starts out as a constant at early proper time, in agreement with the results of [22].

The above analytic approaches have the limit of not being able to address the non-linearity of the thermalization process. A numerical treatment of the full problem appeared in [62], after these lectures were given.[11] The main advantage of solving the initial value problem numerically is that it is more likely to properly describe the transition between the early and late time behaviors.

Ref. [62] considered the collision of two planar sheets in $\mathcal{N} = 4$ SYM propagating towards each other at the speed of light, with finite energy density, finite thickness and Gaussian profile

$$F(x^{\pm}) = \frac{\mu^3}{\sqrt{2\pi\omega^2}} e^{-\left(x^{\pm}/\omega\sqrt{2}\right)^2} . \qquad (103)$$

The equivalent gravitational problem is the collision of two planar shock waves which are reg-

[11] Other recent papers related to our lectures are quoted in Refs.[63–65].

ular, non-singular, source-less solutions to Einstein's equations. The collision leads to horizon formation in the bulk and the numerical integration was stopped in [62] at the apparent horizon location.

The energy density of the collision products is found to be peaked around two receding maxima which move outwards at less than the speed of light. Setting the width in (103) to $\omega = 0.75/\mu$, the application of this model to the RHIC collisions leads to $\mu \sim 2.3$ GeV. The total time required for thermalization, from when the Gaussian shock waves start to overlap significantly until the onset of hydrodynamics, is estimated to be $\Delta v_{tot} \sim 4/\mu \sim 0.35$ fm/c (v denotes time in ingoing Eddington-Finkelstein coordinates). This timescale is consistent with the results of [45].

Acknowledgements

A.B. would like to thank the lecturers, organizers and participants of the Cargèse Summer School for providing an active environment for lively and valuable discussions. The research of A.B. is supported by the Belgian Federal Science Policy Office through the Interuniversity Attraction Pole IAP VI/11 and by FWO-Vlaanderen through project G011410N. R.P. would like to mention the continuously inspiring collaboration with Romuald Janik on the research subject of these lectures. He also thanks the organizers for the invitation and the participants for the stimulating and friendly atmosphere of the Cargèse summer school. We thank Rudolf Baier for reminding the relevant Ref.[26].

REFERENCES

1. E. V. Shuryak, "What RHIC experiments and theory tell us about properties of quark-gluon plasma?," Nucl. Phys. A **750**, 64 (2005).
2. P. F. Kolb and U. W. Heinz, "Hydrodynamic description of ultrarelativistic heavy-ion collisions." Invited review for 'Quark Gluon Plasma 3'. Editors: R.C. Hwa and X.N. Wang, World Scientific, Singapore. (In Hwa, R.C. (ed.) et al.: "Quark gluon plasma" 634-714.;
   P. Huovinen and P. V. Ruuskanen, "Hydrodynamic Models for Heavy Ion Collisions," Ann. Rev. Nucl. Part. Sci. **56**, 163 (2006);
   J. Y. Ollitrault, "Relativistic hydrodynamics," Eur. J. Phys. **29**, 275 (2008);
   T. Hirano, N. van der Kolk and A. Bilandzic, "Hydrodynamics and Flow," Lect. Notes Phys. **785**, 139 (2010).
3. J. Y. Ollitrault, "Anisotropy As A Signature Of Transverse Collective Flow," Phys. Rev. D **46**, 229 (1992).
4. M. Luzum, "Elliptic flow at LHC: Comparing heavy ion data to viscous hydrodynamic prediction," arXiv:1011.5173 [nucl-th].
5. M. Luzum and P. Romatschke, "Conformal Relativistic Viscous Hydrodynamics: Applications to RHIC results at sqrt($s_N N$) = 200 GeV," Phys. Rev. C **78**, 034915 (2008) [Erratum-ibid. C **79**, 039903 (2009)].
6. L. D. Landau, "On the multiparticle production in high-energy collisions," Izv. Akad. Nauk Ser. Fiz. **17**, 51 (1953) (in Russian). [English translation: *Collected Papers of L. D. Landau, edited by D. ter Haar (Gordon and Breach, New-York, 1968)*].
7. A. Bialas, R. A. Janik and R. B. Peschanski, "Unified description of Bjorken and Landau 1+1 hydrodynamics," Phys. Rev. C **76**, 054901 (2007).
8. J. D. Bjorken, "Highly Relativistic Nucleus-Nucleus Collisions: The Central Rapidity Region," Phys. Rev. D **27** (1983) 140.
9. G. Policastro, D. T. Son and A. O. Starinets, "The shear viscosity of strongly coupled N = 4 supersymmetric Yang-Mills plasma," Phys. Rev. Lett. **87**, 081601 (2001).
10. P. Kovtun, D. T. Son and A. O. Starinets, "Viscosity in strongly interacting quantum field theories from black hole physics," Phys. Rev. Lett. **94**, 111601 (2005).
11. R. C. Myers, M. F. Paulos, A. Sinha, "Holographic Hydrodynamics with a Chemical Potential," JHEP **0906** (2009) 006.
12. J. M. Maldacena, "The large N limit of superconformal field theories and supergravity," Adv. Theor. Math. Phys. **2**, 231 (1998) [Int. J. Theor. Phys. **38**, 1113 (1999)];
    S. S. Gubser, I. R. Klebanov and

A. M. Polyakov, "Gauge theory correlators from non-critical string theory," Phys. Lett. B **428**, 105 (1998);
E. Witten, "Anti-de Sitter space and holography," Adv. Theor. Math. Phys. **2**, 253 (1998).
13. See, however, for an early AdS/CFT application with analytic continuation to Minkowski: R. A. Janik and R. B. Peschanski, "High energy scattering and the AdS/CFT correspondence," Nucl. Phys. B **565**, 193 (2000).
14. A. Bazavov *et al.*, "Equation of state and QCD transition at finite temperature," Phys. Rev. D **80**, 014504 (2009).
15. R. A. Janik and R. B. Peschanski, "Asymptotic perfect fluid dynamics as a consequence of AdS/CFT," Phys. Rev. D **73**, 045013 (2006), "Gauge / gravity duality and thermalization of a boost-invariant perfect fluid," Phys. Rev. D **74**, 046007 (2006).
16. V. Balasubramanian, P. Kraus, "A Stress tensor for Anti-de Sitter gravity," Commun. Math. Phys. **208** (1999) 413-428;
S. de Haro, S. N. Solodukhin and K. Skenderis, "Holographic reconstruction of space time and renormalization in the AdS/CFT correspondence," Commun. Math. Phys. **217**, 595 (2001);
K. Skenderis, "Lecture notes on holographic renormalization," Class. Quant. Grav. **19**, 5849 (2002).
17. C. Fefferman and C.R. Graham, "Conformal Invariants," in *Elie Cartan et les Mathématiques d'aujourd'hui*, Astérisque (1985) 95.
18. V. Balasubramanian, J. de Boer and D. Minic, "Mass, entropy and holography in asymptotically de Sitter spaces," Phys. Rev. D **65**, 123508 (2002);
R. C. Myers, "Stress tensors and Casimir energies in the AdS/CFT correspondence," Phys. Rev. D **60**, 046002 (1999).
19. M. P. Heller, R. A. Janik and R. Peschanski, "Hydrodynamic Flow of the Quark-Gluon Plasma and Gauge/Gravity Correspondence," Acta Phys. Polon. B **39** (2008) 3183.
20. R. A. Janik, "The dynamics of quark-gluon plasma and AdS/CFT," arXiv:1003.3291 [hep-th].
21. Y. V. Kovchegov, "Can thermalization in heavy ion collisions be described by QCD diagrams?," Nucl. Phys. A **762**, 298 (2005).
22. Y. V. Kovchegov and A. Taliotis, "Early time dynamics in heavy ion collisions from AdS/CFT correspondence," Phys. Rev. C **76** (2007) 014905.
23. E. Shuryak, S. J. Sin and I. Zahed, "A Gravity Dual of RHIC Collisions," J. Korean Phys. Soc. **50** (2007) 384 [arXiv:hep-th/0511199].
24. R. A. Janik, "Viscous plasma evolution from gravity using AdS/CFT," Phys. Rev. Lett. **98** (2007) 022302.
25. M. P. Heller and R. A. Janik, "Viscous hydrodynamics relaxation time from AdS/CFT," Phys. Rev. D **76** (2007) 025027.
26. R. Baier, P. Romatschke, D. T. Son, A. O. Starinets and M. A. Stephanov, "Relativistic viscous hydrodynamics, conformal invariance, and holography," JHEP **0804**, 100 (2008).
27. P. Benincasa, A. Buchel, M. P. Heller and R. A. Janik, "On the supergravity description of boost invariant conformal plasma at strong coupling," Phys. Rev. D **77** (2008) 046006.
28. M. P. Heller, P. Surowka, R. Loganayagam, M. Spalinski and S. E. Vazquez, "Consistent Holographic Description Of Boost-Invariant Plasma," Phys. Rev. Lett. **102** (2009) 041601.
29. S. Kinoshita, S. Mukohyama, S. Nakamura and K. y. Oda, "A Holographic Dual of Bjorken Flow," Prog. Theor. Phys. **121** (2009) 121.
30. S. Kinoshita, S. Mukohyama, S. Nakamura and K. y. Oda, "Consistent Anti-de Sitter-Space/Conformal-Field-Theory Dual for a Time-Dependent Finite Temperature System," Phys. Rev. Lett. **102** (2009) 031601.
31. S. Bhattacharyya, V. E. Hubeny, S. Minwalla and M. Rangamani, "Nonlinear Fluid Dynamics from Gravity," JHEP **0802** (2008) 045.
32. U. W. Heinz, "Thermalization at RHIC," AIP Conf. Proc. **739** (2005) 163.
33. P. B. Arnold, J. Lenaghan, G. D. Moore and L. G. Yaffe, "Apparent thermalization due to

plasma instabilities in quark gluon plasma," Phys. Rev. Lett. **94** (2005) 072302.
34. K. Adcox *et al.* [PHENIX Collaboration], "Formation of dense partonic matter in relativistic nucleus nucleus collisions at RHIC: Experimental evaluation by the PHENIX collaboration," Nucl. Phys. A **757** (2005) 184.
35. R. Baier, A. H. Mueller, D. Schiff and D. T. Son, "'Bottom-up' thermalization in heavy ion collisions," Phys. Lett. B **502** (2001) 51.
36. D. Molnar and M. Gyulassy, "Saturation of elliptic flow at RHIC: Results from the covariant elastic parton cascade model MPC," Nucl. Phys. A **697** (2002) 495 [Erratum-ibid. A **703** (2002) 893].
37. R. H. Price, "Nonspherical perturbations of relativistic gravitational collapse. 1. Scalar and gravitational perturbations," Phys. Rev. **D5** (1972) 2419-2438.
38. E. S. C. Ching, P. T. Leung, W. M. Suen *et al.*, "Wave propagation in gravitational systems: Late time behavior," Phys. Rev. **D52** (1995) 2118-2132.
39. G. T. Horowitz and V. E. Hubeny, "Quasinormal modes of AdS black holes and the approach to thermal equilibrium," Phys. Rev. D **62** (2000) 024027.
40. A. O. Starinets, "Quasinormal modes of near extremal black branes," Phys. Rev. D **66** (2002) 124013.
41. J. J. Friess, S. S. Gubser, G. Michalogiorgakis and S. S. Pufu, "Expanding plasmas and quasinormal modes of anti-de Sitter black holes," JHEP **0704** (2007) 080.
42. N. Iqbal and H. Liu, "Universality of the hydrodynamic limit in AdS/CFT and the membrane paradigm," Phys. Rev. D **79** (2009) 025023.
43. R. A. Janik and R. B. Peschanski, "Gauge / gravity duality and thermalization of a boost-invariant perfect fluid," Phys. Rev. D **74** (2006) 046007.
44. D. T. Son and A. O. Starinets, "Viscosity, Black Holes, and Quantum Field Theory," Ann. Rev. Nucl. Part. Sci. **57**, 95 (2007).
45. P. M. Chesler and L. G. Yaffe, "Boost invariant flow, black hole formation, and far-from-equilibrium dynamics in N = 4 supersymmetric Yang-Mills theory," Phys. Rev. D **82** (2010) 026006.
46. P. M. Chesler and L. G. Yaffe, "Horizon formation and far-from-equilibrium isotropization in supersymmetric Yang-Mills plasma," Phys. Rev. Lett. **102** (2009) 211601.
47. G. Beuf, M. P. Heller, R. A. Janik and R. Peschanski, "Boost-invariant early time dynamics from AdS/CFT," JHEP **0910** (2009) 043.
48. M. P. Heller, R. A. Janik and P. Witaszczyk, to appear.
49. D. Grumiller and P. Romatschke, "On the collision of two shock waves in AdS5," JHEP **0808**, 027 (2008).
50. H. Epstein, V. Glaser and A. Jaffe, "Nonpositivity of energy density in Quantized field theories," Nuovo Cim. **36** (1965) 1016;
M. Visser, "Scale anomalies imply violation of the averaged null energy condition," Phys. Lett. B **349**, 443 (1995) [arXiv:gr-qc/9409043].
51. G. Beuf, "Gravity dual of N=4 SYM theory with fast moving sources," Phys. Lett. B **686** (2010) 55.
52. J. L. Albacete, Y. V. Kovchegov, A. Taliotis, "Modeling Heavy Ion Collisions in AdS/CFT," JHEP **0807** (2008) 100.
53. J. L. Albacete, Y. V. Kovchegov, A. Taliotis, "Asymmetric Collision of Two Shock Waves in AdS(5)," JHEP **0905** (2009) 060.
54. K. Kang, H. Nastase, "High energy QCD from Planckian scattering in AdS and the Froissart bound," Phys. Rev. **D72** (2005) 106003.
55. S. S. Gubser, S. S. Pufu, A. Yarom, "Shock waves from heavy-quark mesons in AdS/CFT," JHEP **0807** (2008) 108.
56. S. S. Gubser, S. S. Pufu, A. Yarom, "Entropy production in collisions of gravitational shock waves and of heavy ions," Phys. Rev. **D78** (2008) 066014.
57. L. Alvarez-Gaume, C. Gomez, A. Sabio Vera *et al.*, "Critical formation of trapped surfaces in the collision of gravitational shock waves," JHEP **0902** (2009) 009.
58. S. Lin, E. Shuryak, "Grazing Collisions of

Gravitational Shock Waves and Entropy Production in Heavy Ion Collision," Phys. Rev. **D79** (2009) 124015.
59. S. S. Gubser, S. S. Pufu, A. Yarom, "Off-center collisions in AdS(5) with applications to multiplicity estimates in heavy-ion collisions," JHEP **0911** (2009) 050.
60. Y. V. Kovchegov, S. Lin, "Toward Thermalization in Heavy Ion Collisions at Strong Coupling," JHEP **1003** (2010) 057.
61. E. Iancu and R. Venugopalan, "The color glass condensate and high energy scattering in QCD," arXiv:hep-ph/0303204, "QGP3", Eds. R.C. Hwa and X.N.Wang, World Scientific. In Hwa, R.C. (ed.) et al.: "Quark gluon plasma" 249-3363, for a review and references.
62. P. M. Chesler and L. G. Yaffe, "Holography and colliding gravitational shock waves in asymptotically AdS_5 spacetime," Phys. Rev. Lett. **106**, 021601 (2011).
63. T. Kalaydzhyan and I. Kirsch, "Holographic dual of a boost-invariant plasma with chemical potential," arXiv:1012.1966 [hep-th].
64. K. Hashimoto, N. Iizuka and T. Oka, "Rapid Thermalization by Baryon Injection in Gauge/Gravity Duality," arXiv:1012.4463 [hep-th].
65. V. Balasubramanian *et al.*, "Thermalization of Strongly Coupled Field Theories," arXiv:1012.4753 [hep-th].

Holography of AdS vacuum bubbles

J.LF. Barbon[a] and E. Rabinovici[b]

[a]Instituto de Física Teórica IFT UAM/CSIC,
Cantoblanco, Madrid 28049, Spain

[b]Racah Institute of Physics, The Hebrew University,
Jerusalem 91904, Israel

We consider the fate of AdS vacua connected by tunneling events. A precise holographic dual of thin-walled Coleman–de Luccia bounces is proposed in terms of Fubini instantons in an unstable CFT. This proposal is backed by several qualitative and quantitative checks, including the precise calculation of the instanton action appearing in evaluating the decay rate. Big crunches manifest themselves as time dependent processes which reach the boundary of field space in a finite time. The infinite energy difference involved is identified on the boundary and highlights the ill-defined nature of the bulk setup. We propose a qualitative scenario in which the crunch is resolved by stabilizing the CFT, so that all attempts at crunching always end up shielded from the boundary by the formation of black hole horizons. In all these well defined bulk processes the configurations have the same asymptotics and are finite energy excitations.

1. INTRODUCTION

The presence of certain types of singularities in classical gravity as well as the presence and properties of black objects presents serious challenges to any contender for a more complete description of general coordinate invariant systems. The uncovering of the Quantum Field Theory (QFT) holographic duals of Anti-de Sitter (AdS) string backgrounds has been a big step in providing a non perturbative definition of string theory [2]. In some cases the more accessible properties of QFT could be used to test and verify if certain challenges are indeed resolved by string theory. For example the potential black hole information paradox was articulated for the case of black holes in AdS. Known properties of QFT have shown that in this case the non perturbative definition of string theory has removed the sting out of the argument for a paradox.

This tool has the potential of becoming a double edged sword as it may turn out that it can be used to demonstrate that physics around a certain string background corresponds to an ill defined QFT. As there is no court of appeal available after a non perturbative definition this would mean that string theory failed to resolve the challenge. However before drawing drastic conclusions one should verify that indeed string theory was under the obligation to resolve that particular challenge. Not all challenges need to be met. In particular if the string background is derived for a set of repulsive branes there is no need to search for a static solution, if a bulk configuration has an infinite amount of energy on a certain Cauchy surface there is neither need nor possibility to save it from forming a big crunch singularity.

It is this latter issue of the big crunch on which we focus in these lectures. The AdS/CFT correspondence is an arena which is both rather well defined and also well suited to address aspects of the decay of metastable states which may lead to a crunch. We study how big crunches manifest themselves in the boundary holographic description and utilize the QFT knowledge to learn how these configurations can be inoculated and stabilized. This provides a class of configurations which may seem to be leading to a big crunch but do avoid it. In the process of studying this problem we are led to develop a dictionary between the physics of boundary QFTs which have metastable

states and bulk theories of gravity which have potentially metastable states. For some earlier discussions on similar issues see [29,19,30,32,28].

Coleman and de Luccia (CdL) have studied the decay of (non supersymmetric) metastable scalar field states in the presence of gravity [3]. They have set up the general formalism and studied decays to and from a zero cosmological constant state. They have shown that in the thin-wall approximation decays from a potentially metastable zero cosmological constant state to a lower, negative energy AdS state, may either not occur at all or may be on the verge of a big crunch. The first situation occurs when the surface tension of the bubble wall driving the decay is large enough relative to the difference in vacuum energy between the two states. The second situation will generically result, not in the decay into the lower AdS state, but lead instead to a big crunch once small perturbations are admitted.

This result remains essentially unchanged when one considers the properties of a potential decay among two different negative energy AdS states. As in AdS space the volume and surface scale in the same way as a function of a length scale, the parameters of the potential predetermine if the decay via bubble formation and expansion is energetically possible. The case when the decay is allowed leads essentially to a big crunch. Considering the difficulties to define a local concept of energy in general coordinate invariant systems, it is not obvious how to decide upon the basis of a bulk calculation alone if a big crunch is acceptable or needs to be resolved. An infinite amount of energy on a given Cauchy surface should lead to an acceptable big crunch. It is in terms of the boundary CFT that the question is better posed and if the big crunch in the bulk is acceptable then one would expect that identifying its QFT dual would reveal an ill defined, incurable system. We indeed uncover the dual QFT of the CdL bubble and it shows an unbounded potential. Moreover the metastable state reaches an infinite distance in field space in a finite time.

Our results are obtained after rewriting the standard defect treatment [13,8–10,20,12] of thin-walled bubbles in terms of a theory of branes, defined by effective tension and charge parameters. This presentation of the thin-wall approximation to the bubble dynamics has the advantage of suggesting the appropriate dual descriptions in an AdS/CFT framework. As a concrete result, we present an explicit duality relationship between spherical CdL bubbles in AdS and non-gravitational bubbles that mediate the decay through a barrier which is unbounded from below and conformal. This duality goes as far as matching exactly the instanton action for Fubini-type configurations in a critical scalar field theory [23] and the WKB exponent for the nucleation probability in the brane description of bubble dynamics, for a certain range of the parameters. This calculation exhibits a remarkable matching of non supersymmetric quantities.

The next stage is to stabilize the system on the duality side which is most transparent, i.e in the QFT framework. We suggest how to do so and this results in a QFT which has stable and metastable vacuum states. This system itself is the subject of the original Coleman's treatment of the fate of a false vacuum in a QFT. We suggest a system where a potential but finite energy big crunch is indeed stopped on its tracks. The dual bulk configuration has hybrid features of a CdL bubble whose expansion is interrupted and of a domain wall.

This result has bearing on the issues raised in particular by Banks [4]. Our regularized analysis incorporates a natural feature of any finite-energy QFT state, namely that it looks like the vacuum when probed at very high energies. According to the UV/IR relation of AdS/CFT, this in turn implies that both bulk configurations must be identical near the boundary of AdS. In particular, they must share the same value of the asymptotic cosmological constant. Hence, the standard CdL transitions with a lower vacuum energy bubble reaching the boundary cannot correspond to quantum transitions with finite energy exchanges in the QFT. In fact, the true vacuum configuration of any regularized decay also has the asymptotics of the vacuum corresponding to the higher energy AdS vacuum, although it has transient features of the lower AdS geometry in a finite region of bulk spacetime. The extent of that region is determined by the regulator. The endpoint of

the configuration formed in its interior is a black hole which has swept under the protection of its horizon all the evidence of the potential crunch.

The lecture is organized as follows. In section 2 we review the defect approach to thin-walled bubbles in AdS spacetimes, and rephrase it in terms of a brane-type action for the shells representing the walls. In section 3 we show how the formalism based on brane dynamics can be used to compute decay rates in thermally excited situations in either of the two vacua separated by the bubble wall. In section 4 we match these results to an effective Conformal Field Theory (CFT) Lagrangian model, and present our statement regarding the dual of CdL bubbles. In section 5 we study the regularization of the ensuing bulk crunches by a stable UV potential in the CFT, and discuss the bulk interpretation of the decay endpoints resulting from this regularization of the problem. We also suggest a very schematic 5-d effective potential appropriate for these considerations. We conclude by section 6.

These lectures follow closely our paper [1] which contains a slightly more complete account of the details.

2. Thin-walled bubbles in AdS

Let us consider the simplest possible model of a 'landscape' in the form of a single scalar field with potential $U(\chi)$, coupled to gravity in $d+1 > 3$ spacetime dimensions. The potential is assumed to have two locally stable vacua of negative energy densities $U_- < U_+ < 0$. The corresponding Anti–de Sitter (AdS) cosmological constants in $d+1$ spacetime dimensions, $\lambda_\pm = -1/R_\pm^2$, are related to the energy densities by

$$U_\pm = \frac{d(d-1)\lambda_\pm}{16\pi G} \ ,$$

where $R_\pm$ are the curvature radii of the two AdS's. The vacuum closer to zero energy density, χ_+, corresponds to an AdS 'closer' to flat space over a larger distance scale.

We can introduce a certain amount of excitation in the system by adding Schwarzschild terms

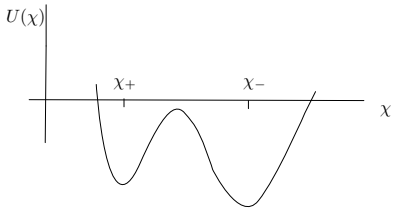

Figure 1. A scalar field model that reproduces two classical AdS vacua with negative cosmological constant proportional to $U_\pm = U(\chi_\pm) < 0$.

of effective mass parameters

$$\mu_\pm = \frac{16\pi G M_\pm}{(d-1)v} \ , \tag{1}$$

where $v = |\mathbf{S}^{d-1}|$ denotes the volume of the angular $(d-1)$-dimensional sphere. Hence, the $\mathrm{AdS}_\pm$ asymptotic metrics in $d+1$ spacetime dimensions read (in global coordinates)

$$ds_\pm^2 = -f_\pm(r)dt_\pm^2 + \frac{dr^2}{f_\pm(r)} + r^2\, d\Omega_{d-1}^2 \ , \tag{2}$$

with

$$f_\pm(r) = 1 - \lambda_\pm\, r^2 - \frac{\mu_\pm}{r^{d-2}} \ . \tag{3}$$

According to the basic rules of AdS/CFT (cf. [2]), a global AdS background admits a dual nonperturbative description in terms of a CFT with an effective number of degrees of freedom $N_{\mathrm{eff}} \sim R^{d-1}/G$, where R is the curvature radius of AdS. The CFT is defined on the manifold $\mathbf{R} \times \mathbf{S}^{d-1}$, with the first factor representing the time coordinate, and the spatial sphere of radius R introducing a spectral gap of order $1/R$. Hence, the model $U(\chi)$ provides us with two candidate quantum systems, associated to the two conformal field theories dual to $\mathrm{AdS}_\pm$.

In the thin-wall approximation, one may consider configurations of bubbles of one metric immersed on the other, separated by a spherical wall whose thickness is negligible compared to its size. A bubble of the high vacuum (+) leaving the low vacuum (−) outside is the situation studied by

Guth and Fahri (GF) in [7]. The Coleman–de Luccia (CdL) situation corresponds to a bubble of the low vacuum (−) surrounded by the high vacuum (+) outside it.

The total ADM mass of the CdL bubble, measured with respect to the AdS_+ vacuum, is given by M_+. If the interior of the bubble is an AdS_- space with some internal M_- excitation (such as a black hole at the center), then we refer to the ADM mass of the shell forming the bubble wall, as $\omega = M_+ - M_-$, a quantity which may be either positive or negative. On the other hand, we shall restrict the $AdS_\pm$ mass parameters to be non-negative, $M_\pm \geq 0$ so that no naked singularities occur in the geometry.

The conditions for the quantum nucleation of an AdS_- bubble inside an AdS_+ vacuum were studied in the original reference [3] applying the thin-wall approximation to the χ field theory coupled to gravity. Here, we shall follow the analysis of [12] to describe the bubbles directly as defects in general relativity, whereby all the details of the potential function $U(\chi)$ are folded into two parameters, given by the surface tension of the bubble, and the difference $\Delta U = U_+ - U_-$ of vacuum energies.[1] This approach has the advantage of including all nonlinear relativistic effects in the motion of the bubbles, and the disadvantage that it is fundamentally tied to the 'thin' aspect of the walls from the beginning.

The thin-wall approximation was revealed, already in the original paper [3], as inadequate to understand the long-time evolution of the system, in particular it misses the generic occurrence of crunch cosmological singularities as a result of the back-reaction from the detailed scalar field dynamics during the phase of bubble growth. Despite this caveat, we will show that the physical singularity associated to the crunch can be identified within the thin-wall approximation in AdS spaces and, when combined with the AdS/CFT dictionary, conveniently interpreted in terms of the dual CFT.

[1] Notice that local maxima of $U(\chi)$ may still be good metastable vacua provided the effective mass gap controlled by $d^2U/d\chi^2$ is below the BF bound [5].

2.1. Junction Dynamics

We describe the bubble wall as a shell characterized solely by the surface tension, i.e. the energy-momentum tensor is

$$T^{ab}\big|_{\rm shell} = -\sigma\, h^{ab} \ , \tag{4}$$

where h_{ab} is the induced metric at the bubble wall and σ is the surface tension.

The energy of the bubble of radius r, measured with respect to the AdS_+ vacuum, is estimated in order of magnitude as built from a surface term of order $\sigma\, r^{d-1}$ and a (negative) volume term of order $-\Delta U\, r^d = -(U_+ - U_-)\, r^d$, when the bubble is small ($r \ll R_-$) and of order $-\Delta U\, R_-\, r^{d-1}$ when the bubble is large in units of the AdS_- radius. This energy function has a potential barrier which a zero-energy shell can tunnel through, emerging at the turning point $\bar r \sim \sigma/\Delta U$ for $\sigma \ll \Delta U R_-$. In the opposite regime of large tension, $\sigma \gg \Delta U R_-$, the energy function is monotonically increasing and no tunneling occurs. The low-tension turning point and the tunneling action diverge as $\sigma/\Delta U R_-$ approaches a critical value of $\mathcal{O}(1)$.

In more detail, the dynamics of the wall is determined by the junction conditions [13]

$$\Delta K_{ab} - h_{ab}\, \Delta K = -8\pi G\, T_{ab}\big|_{\rm shell} \ , \tag{5}$$

where ΔK_{ab} is the jump in extrinsic curvature at the shell (exterior minus interior), and $\Delta K = h^{ab}\Delta K_{ab}$. Using the explicit form of the energy-momentum tensor (4) we can rewrite this equation as

$$\Delta K^a_b = -\kappa\, \delta^a_b \ , \tag{6}$$

where we have defined the related tension parameter

$$\kappa = \frac{8\pi G}{d-1}\,\sigma \ .$$

Computing the extrinsic curvature for the case of a spherical shell of induced metric

$$ds^2\big|_{\rm shell} = -d\tau^2 + r(\tau)^2\, d\Omega^2_{d-1} \ , \tag{7}$$

one finds

$$\left[\left(\frac{dr}{d\tau}\right)^2 + f_-(r)\right]^{\frac{1}{2}} - \left[\left(\frac{dr}{d\tau}\right)^2 + f_+(r)\right]^{\frac{1}{2}} = \kappa\, r(\tau)$$

for the equation determining the shell's trajectory $r(\tau)$ as a function of its proper time. Squaring this equation one can picture the dynamics in the form of a zero-energy motion in an effective non-relativistic potential problem [12]:

$$\left(\frac{dr}{d\tau}\right)^2 + U_{\rm eff}(r) = 0 \,, \tag{8}$$

where

$$U_{\rm eff}(r) = f_+(r) - \left(\frac{\kappa^2 r^2 + f_+(r) - f_-(r)}{2\kappa r}\right)^2 \,. \tag{9}$$

Expanding out the terms in the potential we may rewrite it in the form presented in ref. [12],

$$U_{\rm eff}(r) = 1 - A\, r^2 - \frac{B}{r^{d-2}} - \frac{C}{r^{2d-2}} \,. \tag{10}$$

The coefficient A controls the large r behavior of the bubbles and depends just on 'vacuum' quantities, $\lambda_\pm$ and κ. The coefficient C is always positive and proportional to $(\Delta\mu)^2$, the squared mass of the shell, and controls the small r motion of the bubbles, while B depends linearly on the mass parameters $\mu_\pm$ and determines the transient behavior at intermediate radii. This potential problem describes the motion of thin-walled bubbles for any value of $\lambda_\pm$, including positive values appropriate for de Sitter type bubbles. Those were studied extensively in [20,12,21].

In either GF or CdL cases, one usually thinks of a quantum nucleation of a bubble at radius $\bar{r}$ at $\tau = 0$, and subsequent classical evolution past this point. Hence, the nucleated bubble is an initial condition for normal classical evolution for $\tau > 0$. It is useful to consider situations in which the $\tau > 0$ solution is reflected back to $\tau < 0$ and thus look at time-symmetric solutions. The bubbles that come out of tunneling correspond then to the turning points of the classical motion for time-symmetric solutions.

The CdL situation described above corresponds to $\mu_\pm = 0$, leading to a very simple quadratic potential, $U_{\rm eff}(r) = 1 - A\, r^2$. There are turning points only in the case that $A > 0$, and all trajectories come from $r = \infty$, hit the turning point at $\tau = 0$ and then go off to infinity again (the CdL discussion would correspond to the $\tau \geq 0$ half of this). The condition for $A > 0$ is that κ be *outside* the interval $[\kappa_c, \kappa_c']$ with

$$\kappa_c = \frac{1}{R_-} - \frac{1}{R_+} \,, \qquad \kappa_c' = \frac{1}{R_-} + \frac{1}{R_+} \,. \tag{11}$$

The turning point (equal to the nucleation size of CdL) satisfies

$$\bar{r}^2 = \frac{1}{A} = \frac{4\kappa^2}{(\kappa^2 - \kappa_c^2)(\kappa^2 - \kappa_c'^2)} \,, \tag{12}$$

so that $\bar{r} \to \infty$ as $\kappa \to \kappa_c$. This agrees with the CdL analysis. However, the existence of turning points for $\kappa > \kappa_c'$, not anticipated in the original CdL analysis, is an unphysical feature of the equation (8), which is obtained by squaring the true equations of motion in order to get rid of non-linear terms in $dr/d\tau$. Filtering out the physical solutions of (8) requires the computation of the extrinsic curvature and the explicit verification of the correct signs in equation (5) (cf. [8,20,12]). The sorting of these subtleties, as well as a convenient starting point to discuss nucleation rates, is most conveniently done in a brane-action form of the shell dynamics, as we introduce in the next subsection.

2.2. Bubble walls as branes

In order to relate the mechanics of the shell to physical quantities defined in the dual QFT, it is useful to recast the proper-time dependence into asymptotic time dependence, t_+, because this is the time variable with a direct physical interpretation on the UV definition of the QFT side. We thus transform

$$\frac{dr}{d\tau} = \frac{dt}{d\tau}\,\dot{r}$$

where $\dot{r} = dr/dt$. In what follows, we shall denote $t = t_+$ and $f = f_+$, and we make a choice of units so that $R_+ = 1$.

We compute $dt/d\tau$ by matching the exterior metric ds_+^2 in (2) at the shell locus $r = r(\tau)$, to the induced metric at the shell (7), to find

$$\frac{dt}{d\tau} = \sqrt{\frac{1}{f(r)} + \frac{(dr/d\tau)^2}{f(r)^2}} \,.$$

Plugging this expression back into (8) we find the equivalent potential problem in terms of asymp-

totic time, expressed again as the zero-energy motion

$$\dot{r}^2 + V_{\rm eff}(r) = 0 \,, \tag{13}$$

with

$$V_{\rm eff}(r) = f(r)^2 \left[\frac{f(r)}{f(r) - U_{\rm eff}(r)} - 1 \right] \,. \tag{14}$$

Using the form (9) of $U_{\rm eff}$ we give an explicit expression for $V_{\rm eff}$ as

$$V_{\rm eff}(r) = f(r)^2 \left[\frac{\sigma^2\, v^2\, r^{2d-2}\, f(r)}{(q\, v\, r^d + \omega)^2} - 1 \right] \,, \tag{15}$$

where we have defined

$$q = (d-1)\frac{\Delta\lambda - \kappa^2}{16\pi G} \,, \qquad \Delta\lambda = \lambda_+ - \lambda_- \,, \tag{16}$$

and ω is the ADM mass of the shell, related to the difference in mass parameters $\Delta\mu = \mu_+ - \mu_-$ by the standard formula

$$\omega = M_+ - M_- = \frac{(d-1)\, v}{16\pi G}\Delta\mu \,.$$

The particular presentation of $V_{\rm eff}$ in (14), based on the parameters q, σ and ω, finds its rationale in the fact that (13) follows from a brane-type action of the form

$$\begin{aligned} I &= \int dt\, L \qquad\qquad (17) \\ &= -\sigma v \int dt r^{d-1} \sqrt{f(r) - \frac{\dot{r}^2}{f(r)}} + qv \int dt r^d, \end{aligned}$$

where ω emerges naturally as the canonical energy

$$\omega = \dot{r}\, p_r - L = \dot{r}\, \frac{\partial L}{\partial \dot{r}} - L \tag{18}$$

associated with this Lagrangian,

$$\omega = \frac{\sigma\, v\, r^{d-1}\, f(r)}{\sqrt{f(r) - \frac{\dot{r}^2}{f(r)}}} - q\, v\, r^d \,.$$

Squaring this equation and solving for $\dot{r}^{\,2}$ we readily obtain (15).

The brane nature is rendered more explicit when considering the spherical geometry of the shell and the induced metric, i.e. we can rewrite the action in the form

$$I = -\sigma \int_{\mathcal{W}} \sqrt{-\det(h_{ab})} + q \int_{\mathcal{W}} C_d \,, \tag{19}$$

where $\mathcal{W}$ is the worldvolume of the shell, h_{ab} its induced metric, and C_d a d-form defined by

$$C_d = r^d\, dt \wedge dv \,,$$

up to a closed form. [2] The exterior derivative of C_d is proportional to the volume form of AdS, $dC_d = (d)\, r^{d-1}\, dr \wedge dt \wedge dv$, with dv the volume form of $\mathbf{S}^{d-1}$. In this way we can rewrite the effective charge coupling in (19) as a volume integral over a $(d+1)$-dimensional manifold having $\mathcal{W}$ as one boundary component, i.e. the charge coupling is of Wess–Zumino type.[3]

It is interesting to dissect the form of the effective brane charge q, by writing it in terms of primitive dynamical quantities

$$q = q_0 - \frac{4\pi G}{d-1}\,\sigma^2 \,,$$

where

$$q_0 = (d-1)\frac{\Delta\lambda}{16\pi G} = \frac{\Delta U}{d} \,,$$

is the effective charge in the absence of gravitation, i.e. in the $G \to 0$ limit. It is proportional to the vacuum energy difference, elucidating the nature of the Wess–Zumino term in (19) as a purely volume contribution to the energy. It is however peculiar to find that q_0 is renormalized additively by a 'surface' term, proportional to σ^2. In fact, this term can be interpreted as a 'surface binding energy' of the shell, and always has a volume scaling. In Newtonian terms, the effective mass of the shell is $\sigma v r^{d-1}$, and the associated gravitational self energy is proportional to $G(\sigma v r^{d-1})^2/r^{d-2} \sim G\sigma^2 r^d$, thus mimicking a volume term.

[2] The ambiguity by a closed form translates into boundary terms in the action (19), such as different additive normalizations of the energy ω. The conventions adopted here are those that ensure the ADM relation $\omega = M_+ - M_-$.

[3] For a similar incarnation of effective branes in more general situations of strong gravitational dynamics see [34].

2.3. Qualitative Dynamics

In going from (17) to (13) and (15) we must take the square of (18). In this process, some information about signs is lost, so that the set of solutions to (13) is actually larger than the physical set of trajectories determined by (17). We can resolve the ambiguity by looking at the explicit form of (18):

$$\omega + q\,v\,r^d = \frac{\sigma\,v\,r^{d-1}\,f(r)}{\sqrt{f(r) - \frac{\dot{r}^2}{f(r)}}}\ .$$

The positivity of the right hand side translates into the following rule: given the location of the pole of (15), $r_\omega = (-\omega/qv)^{1/d}$, we can only find positive charge branes ($q > 0$) propagating to the right of the pole, and negative-charge branes ($q < 0$) propagating to the left of the pole. In terms of bulk variables the constraint $\omega + q\,v\,r^d > 0$ is equivalent to the inequality

$$(\Delta\lambda - \kappa^2)\,r + \frac{\Delta\mu}{r^{d-1}} > 0\ ,$$

which in particular implies that only branes with $\Delta\lambda > \kappa^2$ can propagate to asymptotically large radii. Since we are precisely interested in CdL bubbles that are able to reach the boundary, we henceforth concentrate on the case $\Delta\lambda > \kappa^2$ in what follows.

Shells bounding bubbles of the GF type, with AdS$_-$ on the asymptotic region, will be called *antibranes*. Their effective potential with respect to the asymptotic time, t_- in this case, is obtained from (15) by setting $f = f_-$ and switching the $+$ and $-$ labels, which in turn implies that the effective charge is negative for antibranes. As a consequence, no bubble leaving AdS$_-$ in its exterior can ever hit $r = \infty$. [4]

We may also use the *interior* time t_+ to describe the dynamics of the antibranes. In this case one finds exactly the same potential (15) as for branes, with effective values of charge $\bar{q} = -q$ and canonical energy $\bar{\omega} = -\omega$. Again, we have the rule that branes propagate to the right of the pole, and antibranes do so to the left of the pole. Hence, we conclude that $V_{\rm eff}(r)$ in (15) describes at the same time trajectoires of branes (in 'exterior' time) and antibranes (for which t_+ is the 'interior' time).

These considerations show that trajectories fall into different topological classes. We either have shells that bounce off a turning point and go to infinity, or we have shells that bounce off a turning point and go to smaller radii, falling into a black hole. In this last case the bubble can be either of GF or CdL type.

The effective potential $V_{\rm eff}(r)$ in (15) describes bubbles of AdS$_-$ embedded in AdS$_+$, in terms of the exterior time t_+. Since this coordinate is only defined outside horizons of the AdS$_+$ patch, we define the physical region for the trajectories described by $V_{\rm eff}(r)$ to be $r \geq r_0$, where $r_0(M_+)$ stands for any black hole horizon upon which the shell may impinge. For purely vacuum bubbles, the physical region is just $r \geq 0$.

For shell energies $\omega > \omega_0 \equiv -q\,v\,r_0$ the pole in the potential $r_\omega = (-\omega/qv)^{1/d}$ is outside the physical region. On the other hand, for $\omega < \omega_0$ the pole is located in the physical region, $r_\omega > r_0$. In this case the potential describes two types of objects. Brane trajectories (bubbles of AdS$_-$ inside AdS$_+$) take place in the asymptotic (large r) region $r > r_\omega$, and antibrane trajectories (bubbles of AdS$_+$ inside AdS$_-$) are restricted to the region 'below' the pole, $r < r_\omega$. The occurrence of poles in our brane effective potentials is a genuinely relativistic property, which can be found in more mundane situations, such as an electron in a constant electric field, with Lagrangian

$$L_e = -m_e\sqrt{1 - \dot{x}^2} + e\,\mathcal{E}\,x\ .$$

Performing the canonical analysis for this system we find an effective potential description $\dot{x}^2 + V_{\rm e}(x) = 0$, with

$$V_{\rm e}(x) = \frac{m_e^2}{(\omega + e\,\mathcal{E}\,x)^2} - 1\ , \qquad (20)$$

with evident similarities to our brane potentials, including the rule that electrons propagate in the region $x > -\omega/e\mathcal{E}$ and positrons do so in the region $x < -\omega/e\mathcal{E}$. The two turning points at

[4] This fact would pull the rug under any attempt one might consider of sending antibranes as protective measures to collide with runaway branes stopping them on their way to crunch on the boundary.

$x_\pm = -\omega/e\mathcal{E} \pm m_e/e\mathcal{E}$ are interpreted semiclassically as the nucleation positions of e^+e^- pairs in a Schwinger decay process of the electric field.

By analogy with the e^+e^- situation we may contemplate 'brane-antibrane' pairs obtained by a superposition of the solutions discussed above. Namely a bubble of AdS_+ vacuum oscillating inside a bubble of AdS_-, which is itself immersed in the AdS_+ vacuum. Such a configuration could arise if AdS_+ chose to decay by nucleating a 'thick shell' made of AdS_-, rather than a spherical bubble of AdS_-. This configuration is topologically equivalent to a superposition of smaller AdS_- bubbles disposed off center, making the AdS_- shell. This suggests that these configurations are not dynamically important in themselves, since they can be constructed from the more elementary spherical bubbles.

2.4. The CdL potential

We can now go back to the basic CdL situation, corresponding to $\omega = 0$ and $f(r) = 1 + r^2$. The resulting potential is

$$V_{\rm eff}(r)\big|_{\rm vac} = (1+r^2)^2 \left[\frac{\sigma^2}{q^2}\frac{1+r^2}{r^2} - 1\right] .$$

It diverges as $r \to 0$ as $(\sigma/q)^2/r^2$, and it is asymptotic to

$$\left[(\sigma/q)^2 - 1\right]\, r^4 + 3\left[(\sigma/q)^2 - 1\right]\, r^2 + r^2 \qquad (21)$$

as $r \to \infty$. The last term, scaling as r^2, is of geometrical origin. It is proportional to the world-volume curvature of the brane, changing sign for negatively-curved world-volumes (see [14] for a study of this sort). The condition for the existence of vacuum tunneling transitions is that the tension be smaller than the charge in appropriate units, i.e. $\sigma < |q|$. We note that

$$\frac{q^2 - \sigma^2}{\sigma^2} = \frac{(\kappa^2 - \kappa_c^2)(\kappa^2 - \kappa_c'^2)}{4\kappa^2} ,$$

so that the $\sigma < |q|$ condition is equivalent to the previously stated condition that κ be outside the interval $[\kappa_c, \kappa_c']$.

When $\sigma = |q|$ we have a marginal situation where the leading terms in volume and surface energies cancel one another. In fact, for a flat world-volume, corresponding to $f(r) = r^2$, the potential vanishes altogether and we get back a familiar 'no-force' condition on the brane signaling a situation of marginal stability.

Restoring arbitrary units, we have $\sigma = |q|\, R_+$ which gives

$$\Delta U = \frac{4\pi d}{d-1}\, G\, \sigma^2$$

in the $R_+ \to \infty$ limit. This was identified in [3] as the condition of marginal stability of Minkowski spacetime, and later interpreted as a supersymmetric relation in the case that the theory admits a supersymmetric embedding (see [15–17]). Hence, we interpret $|q| \le \sigma$ as a BPS bound if the brane is to be understood as a (possibly non-supersymmetric) excitation over a supersymmetric vacuum.

We conclude that nonperturbative instabilities require violation of the BPS bound for the shell, with implicit supersymmetry breakdown. In this case, the turning point, obtained from $V_{\rm eff}(\bar r) = 0$, is given by

$$\bar r = \frac{\sigma/|q|}{\sqrt{1 - \sigma^2/q^2}} = \frac{\alpha}{\sqrt{1-\alpha^2}} ,$$

and indeed we find $\bar r \to \infty$ as $|q| \to \sigma$. We denote $\alpha = \sigma/|q|$ the parameter characterizing the 'degree of violation' of the bound.

From this one can find whether a running away bubble ever hits the boundary of AdS in finite asymptotic time, or 'boundary QFT time'. The hit time from nucleation at $\bar r$ is

$$t_{\rm hit} = \int_{\bar r}^{\infty} \frac{dr}{\dot r} = \int_{\bar r}^{\infty} \frac{dr}{\sqrt{-V_{\rm eff}(r)}} . \qquad (22)$$

Using the asymptotics (21), we find $t_{\rm hit} \sim (1 + \bar r^2)/\bar r$ in units of R_+. Hence, the bubble hits the boundary in finite time and in doing so its 'kinetic energy', $\dot r^2$ diverges. [5] This is a first indication, within the thin wall approximation, of the existence of a singularity at $t_{\rm hit}$. In fact, as already studied in the original CdL paper, the analysis beyond the thin-wall approximation reveals that the dynamics of scalar fields forces the interior of the bubble to crunch in finite time.

[5] Notice that the 'proper hit time' $\tau_{\rm hit}$ is infinite, because $U_{\rm eff}(r) \to -r^2/\bar r^2$ as $r \to \infty$, a gentle fall.

2.5. Potential Galore

We may now classify the qualitative form of the effective potentials as a function of the parameters. We shall restrict ourselves to the interesting case of $\alpha < 1$ and to non-negative mass parameters $M_\pm \geq 0$ to avoid naked singularities. [6] This still leaves the mass of the shell $\omega = M_+ - M_-$ as a free parameter in the interval $[-\infty, M_+]$.

As mentioned above, shell energies above the critical value $\omega_0 = -q\, v\, r_0(M_+)$ yield potentials without poles in the physical region. Conversely, at very negative shell energies, $\omega < \omega_0$, the pole moves into the physical region. For any $\omega \neq \omega_0$ we have $V_{\rm eff}(r_0) = V'_{\rm eff}(r_0) = 0$, where the prime denotes derivative with respect to r. Furthermore the second derivative $V''_{\rm eff}(r_0) < 0$, so that the horizon is a local maximum of the potential, which further vanishes there. It follows that the vicinity of the horizon is an allowed region for brane (or antibrane) propagation. For $\omega < \omega_0$ there are antibranes that oscillate between the horizon and a turning point $\bar{r}'$ 'below' the pole, i.e. in the region $r_0 < r < \bar{r}'$ with $\bar{r}' < r_\omega$. Brane trajectories exist in the asymptotic region $\bar{r} < r < \infty$.

For the critical value of the energy, $\omega = \omega_0$, the potential still vanishes at the horizon, but the first derivative $V'_{\rm eff}(r_0) > 0$. Hence, there is a barrier extending from the horizon up to the large r turning point, of order $\bar{r}$.

For $\omega > \omega_0$ there are no poles in the physical region, and thus no antibrane trajectories either. Branes propagating in the vicinity of the horizon encounter a finite potential barrier for $\omega < \omega_s$, where ω_s is the 'sphaleron' energy, for which the potential barrier degenerates to a single point. For $\omega \gg \omega_s$ there is no barrier at all and the brane trajectories lay on the interval $r_0 < r < \infty$.

3. Decay rates

One advantage of the brane picture for bubble nucleation is the existence of an action principle, in the form of (17), which allows us to compute the rates for nucleation of spherical bubbles by using the standard quantum mechanical WKB approximation (see [11] for a related but slightly different treatment).

The WKB ansatz for the wave function of a spherical brane is of the form

$$\Psi_{\rm WKB}(t,r) \sim \exp\left(-i\omega t + i\int^r p_{r'}\, dr'\right) \ ,$$

at energy ω, where $p_r = \partial L/\partial \dot{r}$, and the probability of barrier penetration in the leading exponential approximation is given by

$$P_{\rm WKB} \sim \exp\left(-2\,{\rm Im}\, W(\omega)\right) \ ,$$

where $W = I + \omega t$, with I the action (17). The imaginary part in the classically forbidden region can be captured by the analytic continuation to the Euclidean signature $t = -it_E$ and we find ${\rm Im}\, W(\omega) = W_E = I_E - \omega t_E$, with I_E the Euclidean action

$$\begin{aligned} I_E &= \int dt_E\, L_E \qquad (23)\\ &= v\int dt_E \left[\sigma\, r^{d-1}\sqrt{f(r) + \frac{\dot{r}_E^2}{f(r)}} - q\, r^d\right] \ . \end{aligned}$$

In terms of the canonical momentum $(p_r)_E = \partial L_E/\partial \dot{r}_E$ we can write $W_E = \int dr\, (p_r)_E$. Finally, Euclidean trajectories correspond to motion in the effective problem

$$\dot{r}_E^2 - V_{\rm eff}(r) = 0 \ , \qquad (24)$$

which results form the real-time problem by a formal switch of the sign of the potential. Using this equation in the formula for the Euclidean action, we find the convenient expression

$$\begin{aligned} 2W_E(\omega) &= 2\int_{\bar{r}'}^{\bar{r}} dr\, (p_r)_E \qquad (25)\\ &= 2qv\int_{\bar{r}'}^{\bar{r}} \frac{dr}{f(r)}\sqrt{\alpha^2\, r^{2d-2} f(r) - (r^d - r_\omega^d)^2} \ , \end{aligned}$$

where the turning points in the integral are defined by the positivity of the square root argument, and $r_\omega^d = -\omega/qv$ is the location of the pole in the potential. This is a general formula for any value of the bubble parameters, including cases where the pole falls in the integration

[6] Potentials with $\alpha > 1$ have no instabilities and the marginal BPS-saturated case, $\alpha = 1$ is controlled by subleading curvature terms, cf. [14]

region, $\bar{r}' < r_\omega < \bar{r}$. The exponential WKB factor (25) is integrable across the pole and in this case it determines the rate of nucleation of brane/antibrane pairs, in a generalization of the Schwinger mechanism.[7]

The total nucleation rate of shells centered at $r = 0$ takes the form

$$\Gamma = \int_{\omega_{\rm min}}^{\omega_{\rm max}} d\omega \, P_{\rm WKB}(\omega) \ , \qquad (26)$$

where the limits in the integral correspond to the maximum and minimum possible energies of the shells. For the case $\alpha < 1$, which is the subject of main interest here, the effective potential is unbounded from below and shells of arbitrarily negative energy can always propagate at sufficiently large radius, i.e. $\omega_{\rm min} = -\infty$. On the other hand, we require $M_\pm \geq 0$ in order to avoid a naked singularities in the interior of the $\mathrm{AdS}_\pm$ bubbles, so that $\omega_{\rm max} = M_+$.

Shells with $\omega < \omega_0 = -q\,v\,r_0^d$ see an effective potential with a pole above the horizon. As stated before, this corresponds to Schwinger-like processes in which a concentric brane/antibrane pair is nucleated above the horizon. For very negative values of ω, the WKB exponent scales as $2W_E \propto qv(-\omega/qv)^{\frac{d-1}{d}}$, so that the nucleation of very large branes is suppressed. As ω approaches ω_0 from below, the pole in the effective potential narrows down and makes a smaller and smaller contribution to the $\omega = \omega_0$ barrier. Hence, we conclude that the contribution to (26) coming from Schwinger-like processes is dominated by the endpoint and we may discard it when computing in the leading exponential approximation.

The tunneling rate for pair production approaches continuously that of single bubble nucleation. This is a reflection of the non-topological character of spherical bubbles on global AdS, i.e. they can continuously shrink to zero size and disappear.

3.1. Vacuum AdS decay

In the CdL case, for a zero-mass bubble, $M_+ = 0$, bounded by a zero-mass shell, $\omega = 0$, we have $\bar{r}' = 0$ and $f(r) = 1 + r^2$. The general expression for the tunneling exponent (25) reduces to [8]

$$2W_E = 2\,q\,v\,\frac{\bar{r}^{d+1}}{\sqrt{1+\bar{r}^2}} \int_0^1 dx \frac{x^{\,d-1}}{1+\bar{r}^2 x^2} \sqrt{1-x^2} \ .$$

This integral can be evaluated explicitly in terms of beta and hypergeometric functions as

$$2W_E = 2q\,v\,B(\tfrac{3}{2},\tfrac{d}{2})\,\frac{\bar{r}^{\,d+1}}{\sqrt{1+\bar{r}^{\,2}}}\,F\left[1,\tfrac{d}{2},\tfrac{d+3}{2},-\bar{r}^{\,2}\right] \ .$$

For small bubbles, $\bar{r} \ll 1$, we have

$$2W_E\Big|_{\bar{r}\ll 1} \approx q\,v\,B(\tfrac{3}{2},\tfrac{d}{2})\,\bar{r}^{\,d+1} \ .$$

In this limit, corresponding to $\alpha \ll 1$, the charge parameter scales as

$$q \longrightarrow \frac{(d-1)\Delta\lambda}{16\pi G} = \frac{\Delta U}{d} \ ,$$

and we obtain the bubble nucleation amplitude in the limit of weak gravity, with semiclassical suppression exponent

$$2W_E\Big|_{\bar{r}\ll 1} \approx v\,B(\tfrac{3}{2},\tfrac{d}{2})\,\left(\frac{d}{\Delta U}\right)^d \sigma^{d+1} \ ,$$

which agrees with the known factor of $27\pi^2\sigma^4/2(\Delta U)^3$ in the four-dimensional case.

For large bubbles, where the background curvature effects are felt strongly, we obtain

$$2W_E\Big|_{\bar{r}\gg 1} \approx q\,v\,B(\tfrac{3}{2},\tfrac{d-2}{2})\,\bar{r}^{\,d-2} \ , \qquad (27)$$

a form that will be used later in the matching to the dual CFT.

The same results can be obtained in an explicitly $O(d+1)$-invariant formalism, more akin to the original presentation of [3].

3.2. Decay of excited states

For excited initial states, with $M_+ > 0$, we can think of the branes as thermally emitted by the black hole horizon at $r = r_0$, with a basic rate

[7] For the e^+e^- potential (20), equation (25) gives the expected exponent $2W_E = 2\int_{x_-}^{x_+} dx\sqrt{m_e^2 - (e\mathcal{E}x)^2} = \pi m_e^2/e\mathcal{E}$ controlling the Schwinger effect amplitude.

[8] Notice that we take the initial tunneling condition at $\bar{r}' = 0$ despite the pole at the origin of the zero-temperature potential $V_{\rm eff}(r)$, since the barrier is still integrable. It can be regularized by introducing a small horizon radius, $r_0 > 0$ and taking the limit $r_0 \to 0$ at the end.

governed by Hawking's formula, proportional to $\exp(-\beta\omega)$, [9] with $\beta(M_+) = 1/T(M_+)$ the inverse Hawking temperature associated to the mass M_+. This basic input rate is further convoluted with the potential barriers that the branes may encounter outside the horizon, i.e. we have the 'grey-body' spectral formula for the total rate

$$\Gamma(M_+) \sim \int_{\omega_0}^{M_+} d\omega\, e^{-\beta\omega} e^{-2W_E(\omega)} \ , \qquad (28)$$

where $\omega_0 = -q\, v\, r_0^d$ is the minimum emission energy of branes by the horizon. If the barrier is present, we may approximate this integral by its value at the saddle point to obtain the usual result (cf. [33])

$$\Gamma(\beta) \propto \exp\left(-I_E(\beta)\right) \ ,$$

where $I_E(\beta)$ is the Euclidean action evaluated over periodic Euclidean solutions of (24) with period $\beta(M_+)$.

For high enough excitation energy M_+ the barrier in the potential disappears and all branes with negative energy $\omega_0 < \omega < 0$ are emitted without exponential suppression, in which case the formula (28) does not apply. In this situation the decay rate is just like that of a Schwarzschild black hole, i.e. it is given by the natural time scale of the black hole, $\Gamma(M_+) \sim T(M_+)$. The critical excitation energy beyond which the barrier disappears altogether corresponds to a vanishing sphaleron energy, $\omega_s = 0$, and can be computed by solving $V_{\rm eff}(\bar{r}_c) = V'_{\rm eff}(\bar{r}_c) = 0$ for $\omega = 0$, resulting in a critical radius $\bar{r}_c^2 = (d-2)\alpha^2/d(1-\alpha^2) = (d-2)\bar{r}^{\,2}/d$. So the barrier is not present for

$$\mu_+ \geq \frac{2}{d}\left(\frac{d-2}{d}\right)^{\frac{d-2}{2}} \bar{r}^{\,d-2} \ .$$

This results conforms to standard intuition about metastable state decays, namely the barrier would become ineffective if we start with a sufficiently large energy M_+ above the metastable 'vacuum' (pure AdS_+).

[9] At the semiclassical level we are insensitive to the effects of quantum statistics. More generally, we may approximate the Hawking rate by the detailed balance formula $\exp(\Delta S)$, with ΔS the entropy jump in the emission process. Such a generalization may induce chemical potential terms associated to conserved charges.

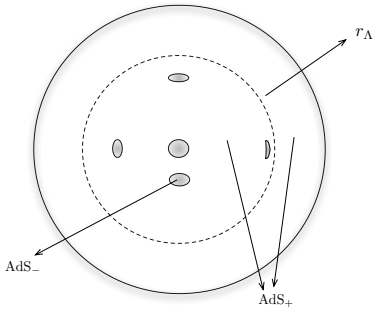

Figure 2. Picture of the nucleation process within a sphere of radius r_Λ. Bubbles of AdS_- grow inside AdS_+ and have size $\bar{r} \ll r_\Lambda$ at birth. In the coordinates chosen, only the central bubble looks spherical, although they are all approximately spherical. Most of the bubbles are nucleated in the vicinity of $r = r_\Lambda$ since most of the volume is concentrated there. In QFT terms, these are the 'smaller' bubbles, according to the UV/IR dictionary. The bulk volume term implies a UV divergence of the rate.

3.3. Measure

Going back to the vacuum transition, with $\omega = 0$ and $f(r) = 1 + r^2$, we may now give an estimate of the preexponential factor. A detailed computation would involve examining the one-loop fluctuation determinant, including its zero (and negative) modes, around the classical Euclidean configuration. We can, however, give an estimate based on the symmetries of the problem. Since AdS is a homogeneous space, the rate of nucleation picks a volume degeneracy factor from integration over bubble position inside AdS_+ with Euclidean metric

$$ds^2 = (1+r^2)\, dt_E^2 + \frac{dr^2}{1+r^2} + r^2\, d\Omega_{d-1}^2 \ .$$

Working within a cutoff radius r_Λ, we have a factor of $\Delta t\, m_*\, (m_*\, r_\Lambda)^d$ in the rate, with m_* a microphysical mass scale that arises in the computation of the one-loop functional determinants in the bulk. [10] In vacuum decay problems, m_* is

[10] This homogeneity property of the AdS background implies that the leading decay process is still given by vac-

usually governed by the gap of the metastable state, i.e. $m_* \sim 1/R_+ = 1$. Hence, we conclude that the decay rate is afflicted by a volume divergence. [11]

As long as we are interested in the local bulk physics, we can just define the decay rate per unit time and unit volume, obtaining $m_*^{d+1} \exp(-2W_E)$. On the other hand, anticipating the field-theory interpretation through the AdS/CFT dictionary, we may also consider the decay rate per unit time and unit volume of the conformal boundary $\mathbf{R} \times \mathbf{S}^{d-1}$, which diverges as $m_*^{d+1} (r_\Lambda)^d$, as always in units $R_+ = 1$. This radial divergence will be interpreted as a UV divergence in the CFT.

4. Matching to a boundary CFT picture

The description of the shell dynamics in terms of a brane action is appropriate for the matching to more detailed specifications of the theory, where the bulk theory is actually a string theory, and defects are identified as particular D-branes in the spectrum. The simplest case is the basic blueprint for holography, namely the duality between type IIB string theory on $\mathrm{AdS}_5 \times \mathbf{S}^5$ with N units of Ramond–Ramond flux and four-dimensional maximally supersymmetric $SU(N)$ Yang–Mills theory.

A pattern of gauge symmetry breaking of the form $SU(N) \to SU(N-1) \times U(1)$ is described in the bulk by the dynamics of a probe D3-brane. The brane action is identified with the effective action of the $SU(N)$ gauge theory, evaluated over configurations of the adjoint scalar fied Φ of the form

$$\Phi = \mathrm{diag}(0, 0, \ldots, \phi) \,, \tag{29}$$

i.e. we have an effective Lagrangian for ϕ, after we use the UV/IR map $\phi \sim r$, having integrated out all the 'unhiggsed' $SU(N-1)$ degrees of freedom. In the bulk AdS description, crossing a D3-brane amounts to a jump of one unit of Ramond–Ramond flux through the $\mathbf{S}^5$ factor, which in turn produces a small change in the effective five-dimensional AdS cosmological constant. Hence, we have all the ingredients to interpret spherical D3-brane probes as shells bounding bubbles that mediate transitions between AdS vacua of different curvature radius. We may as well consider a simple generalization in which n D3-branes, with $n \ll N$, are bundled into a bubble wall with $SU(n)$ internal degrees of freedom.

More generally, given an AdS/CFT model constructed from a decoupling limit of N branes, the number of microscopic degrees of freedom (central charge) scales as $N_{\text{eff}} \sim N^a$, with a a rational number of $\mathcal{O}(1)$ (for example, for gauge theories we have $a = 2$ and for M2-branes we have $a = 3/2$.) It is related to Newton's constant and the curvature radius by $N_{\text{eff}} = N^a \sim R_+^{d-2}/G$. If we imagine that the AdS_- region is obtained from the AdS_+ configuration by the removal of n constituent branes (or n units of the corresponding flux in some extra compact manifold) then we have

$$\begin{aligned} \frac{R_+ - R_-}{R_+ + R_-} &\sim \frac{N^{\frac{a}{d-1}} - (N-n)^{\frac{a}{d-1}}}{N^{\frac{a}{d-1}} + (N-n)^{\frac{a}{d-1}}} \\ &\sim \frac{a}{2(d-1)} \frac{n}{N} \,. \end{aligned} \tag{30}$$

Since $n \ll N$ for the 'thin brane' picture to make sense, this quantity is always small throughout our discussion, quite independently of whether the bubbles are close to BPS saturation or not, and we shall set $n = 1$ and $1 \ll N < \infty$ in what follows. In particular, for order of magnitude estimates, we can consider an average value of the curvature radius $R \sim R_- \sim R_+ = 1$. It is interesting to notice that the large N gauge theory model provides a 'mini-landscape', with $\mathcal{O}(N)$ quasi-degenerate vacua.

Using the relation between N_{eff} and G, together with (30), we find the scalings

$$q \sim N^a \left(\frac{1}{N} - \kappa^2 \right) \sim N^{a-1} - \alpha^2 q^2 \,,$$

where we have used $R_+ = 1$ and $\sigma = \alpha\, q$. From these expressions we can extract the scaling of q

uum CdL bubbles even in the presence of a black hole, since vacuum bubbles nucleated far from the black hole are approximately described by the zero-temperature effective potential.

[11] The importance of this fact was emphasized to us in early 2009 by Daniel Harlow. See [44] and also [35] for similar remarks in a different context.

and σ as a function of N. In the physical situation $\alpha^2/N \ll 1$ we find $q \sim N^{a-1}$, obtaining back the usual scaling $q \sim 1/g_s \sim N$ in the standard case of $\mathcal{N} = 4$, $SU(N)$ SYM theory. More detailed comparisons of the effective charge q, as defined in (16), would require taking into account $\mathcal{O}(1/N)$ jumps of the five-dimensional Newton's constant across a D3-brane in the $AdS_5 \times \mathbf{S}^5$ model, while (16) is an effective $(d+1)$-dimensional description, incorporating just vacuum energy jumps.

4.1. The canonical frame near the boundary

In order to compare the brane motion in the bulk with standard presentations of CFT degrees of freedom it is convenient to rewrite the brane effective action in terms of a canonical variable with a standard Lagrangian at low velocities, i.e. we perform the field redefinition $r(t) \to \phi(t)$ so that

$$I = v \int dt \left(\tfrac{1}{2} \dot{\phi}^2 - V_s(\phi) + \mathcal{O}(\dot{\phi}^4) \right) , \qquad (31)$$

where $V_s(\phi)$ is the 'static' potential, defined by $\omega|_{\dot{r}=0} = v\, V_s(r)$. [12] Expanding (17) to quadratic order in $\dot{r}$ and matching to (31) we find the map between the radial variable r and the canonical brane field as

$$\begin{aligned} \phi &= \sqrt{\sigma} \int_0^r dr' \frac{(r')^{\frac{d-1}{2}}}{f(r')^{3/4}} \\ &= \frac{2\sqrt{\sigma}}{d-2}\, r^{\frac{d-2}{2}} \left(1 + \mathcal{O}(r^{-2})\right) , \end{aligned} \qquad (32)$$

whereas the static potential is given by

$$V_s(\phi) = \sigma\, r^{d-1} \sqrt{f(r)} - q\, r^d , \qquad (33)$$

with r solved in terms of ϕ by inverting (32). In the large ϕ region, it reads

$$V_s\big|_{\phi\to\infty} = \frac{(d-2)^2}{8}\, \phi^2 - \lambda\, \phi^{\frac{2d}{d-2}} + \ldots , \qquad (34)$$

where

$$\lambda = \left(\frac{d-2}{2} \right)^{\frac{2d}{d-2}} \frac{1}{\sigma^{\frac{2}{d-2}}} \frac{q-\sigma}{\sigma} . \qquad (35)$$

[12] This is the rigid spherical brane case of more general field redefinitions that may be found in [18]

The first term in (34) gives the conformal coupling

$$\frac{d-2}{8(d-1)}\, \mathcal{R}\, \phi^2$$

to the background curvature of the boundary $\mathbf{S}^{d-1} \times \mathbf{R}$, and the second term is a standard marginal operator in d spacetime dimensions. Notice that the potential is asymptotically unbounded below whenever $\sigma < q$, i.e. precisely when the BPS bound is violated.

The $1/r$ corrections to both the field-theory Lagrangian (35) and the field redefinition (32) are proportional to powers of the background curvature $\mathcal{R}$, which breaks spontaneously the conformal symmetry. In the limit of a flat boundary, $\mathcal{R} \to 0$, both (32) and (35) are given by a single monomial.

We can check this identification by obtaining (32) directly from the microscopic brane picture. Let the field ϕ be normalized canonically in the D3-brane world-volume action, so that we have $r/2\pi\alpha' = g_{\rm YM}\phi$ for the mass of a 'W-boson' constructed from a stretched string. Here α' is the type IIB string Regge slope parameter and $g^2_{\rm YM} = 2\pi g_s$ is the world-volume Yang–Mills coupling in terms of the string coupling constant g_s. Using the fact that the BPS tension of the D3-brane is $\sigma = ((2\pi)^3 g_s \alpha'^2)^{-1}$ we find perfect agreement with the rule expressed in (32) for $d = 4$.

The identification (35) in the D3-brane theory allows us to trace the effective coupling λ back to the SYM Lagrangian. In this case $\lambda \sim (1-\alpha)/N$ and the operator $-\lambda\,\phi^4$ can be obtained from a standard single-trace quartic operator $-\frac{1-\alpha}{N}\,\mathrm{Tr}\,\Phi^4 + \ldots$, evaluated along (29), (we use canonical normalization of the adjoint scalar fields.) On the other hand, we shall obviate details about the R-symmetry structure of the operators or, equivalently, the localization of D3-branes on the $\mathbf{S}^5$ or analogous 'internal Einstein manifolds'.

4.2. The large-brane CFT and the Fubini Instanton

Our discussion so far indicates that standard CdL bubbles can be associated to branes, at least to the extent that the thin-wall approximation

is applicable to the shells bounding the bubbles. Using the asymptotic map (32) between the collective coordinate of the shell and a canonical field in the d-dimensional CFT, we find that the CdL dynamics of (large) spherical shells in AdS_{d+1} is described by nonperturbative bubble nucleation effects of a conformal d-dimensional Lagrangian of the form

$$\mathcal{L}_d = -\frac{1}{2}\,(\partial\phi)^2 - \frac{d-2}{8(d-1)}\,\mathcal{R}\,\phi^2 + \lambda\,\phi^{\frac{d}{\Delta}}\ , \qquad (36)$$

where $\mathcal{R}$ is the Ricci scalar of the d-dimensional CFT spacetime and we denote

$$\Delta = \frac{d-2}{2}$$

the mass dimension of the scalar field. The effective coupling of the marginal scalar operator is given by (35), [13]

$$\lambda = \Delta^{d/\Delta}\,\sigma^{-\frac{1}{\Delta}}\,\frac{q-\sigma}{\sigma} \sim \left(\frac{1}{N^{a-1}}\right)^{\frac{1}{\Delta}}\,\frac{1-\alpha}{\alpha^{\frac{d}{2\Delta}}}\ . \qquad (37)$$

Hence, the violation of the BPS bound for the bulk branes, $\alpha < 1$, is equivalent to $\lambda > 0$, namely the condition of *instability* of the CFT potential at large values of the field. Notice that this detailed map with the particular interactions in (36) and (37) is actually asymptotic in the sense that it was derived for bubbles of large size, $\bar{r} \gg 1$, in units of the AdS_+ radius (cf. (32). In principle, one may extend the analysis to general $\bar{r}$ in units of R_+, at the expense of keeping all terms in the power expansions of (32) and (33).

Classical solutions of (36) with different values of the constant background curvature, $\mathcal{R}$, can be related by conformal transformations. In particular, the explicit map

$$dt_E^2 + d\Omega_{d-1}^2 = \frac{1}{u^2}\,\left(du^2 + u^2\,d\Omega_{d-1}^2\right)\ , \qquad (38)$$

with $|x| = u = \exp(t_E)$, expresses the conformal equivalence of the Hamiltonian manifold $\mathbf{R}\times\mathbf{S}^{d-1}$ with the flat hyperplane $\mathbf{R}^d$. Using this map we can profit from the knowledge of instanton solutions of the massless theory, defined on $\mathbf{R}^d$. Such instantons are Euclidean versions of field configurations discussed by Fubini in [23] (see also [24] for a review) and take the form

$$\phi_{\mathrm{inst}}(x) = \sqrt{\frac{2}{\lambda}}\,\frac{\rho}{|x|^2+\rho^2}\ , \qquad (39)$$

in the four-dimensional case, where $|x|$ is the Euclidean length on $\mathbf{R}^4$ and ρ is an arbitrary length scale that characterizes the 'size' of the instanton, with action $S_{\mathrm{inst}} = 2\pi^2/3\lambda$. The similarity to Yang–Mills instantons is clear from the explicit formula (39) and, like in the gauge theory case, they *do not* have thin walls, despite being characterized by a size parameter. [14] These instantons mediate the decay of the classical $\phi = 0$ state by nucleation at $t = 0$ of bubbles

$$\phi_{\mathrm{bubble}}(\vec{x}, t=0) = \sqrt{\frac{2}{\lambda}}\,\frac{\rho}{\vec{x}^{\,2}+\rho^2}$$

of size ρ and field value $\phi_0 \sim 1/\sqrt{\lambda\rho^2}$ at the center, that subsequently expand in an asymptotically null trajectory. Notice that the energy barrier inducing the metastability of the $\phi = 0$ configuration is supported just by kinetic terms in the massless model.

All these considerations can be generalized to arbitrary $d > 2$ dimensions. The instanton solution on $\mathbf{R}^d$ with size ρ and position x_0 parameters is now given by

$$\phi_{\mathrm{inst}}(x) = \left(\frac{2}{\lambda}\right)^{\Delta/2}\,\left(\frac{\Delta\,\rho}{|x-x_0|^2+\rho^2}\right)^{\Delta}\ , \qquad (40)$$

and the resulting instanton action

$$\begin{aligned} S_{\mathrm{inst}} &= \int_{\mathbf{R}^d}\left(\tfrac{1}{2}(\partial\phi_{\mathrm{inst}})^2 - \lambda\,(\phi_{\mathrm{inst}})^{d/\Delta}\right) \qquad (41)\\ &= \frac{2^{d/2}\Delta^d\,v}{\lambda^{\Delta}}\int_0^\infty ds\,\frac{s^{d-1}(s^2-1)}{(s^2+1)^d}\ , \end{aligned}$$

where, as before, $v = |\mathbf{S}^{d-1}|$.

[13] It is quite interesting to note that the scaling of λ with N is the same, equal to $1/N$, in all three 'canonical' constructions of CFTs from parallel branes, namely D3, M2 and M5 branes.

[14] We shall refer to these Euclidean configurations as 'Fubini instantons', despite the fact that they are actually bounces (i.e. having one negative eigen-mode). In particular, these solutions are used as approximations to false vacuum bounces in situations where the thin-wall approximation is not applicable, cf. [25].

We can evaluate the integral in terms of special functions as follows. We first split the s^2-1 term in the numerator of (41) and work out each integral separately with the change of variables $s \to (1+s^2)^{-1}$, resulting in integral representations of beta functions, to finally find

$$S_{\rm inst} = \frac{c}{\lambda^\Delta} \ , \qquad \text{with} \quad c = \frac{v}{2^\Delta}\Delta^d\, B(\tfrac{3}{2},\tfrac{d-2}{2}) \ . \quad (42)$$

Alternatively, the same action can be computed by using a stereographic projection to map the $\mathbf{R}^d$ problem into the same problem on $\mathbf{S}^d$, with curvature scalar $\mathcal{R} = d(d-1)$. In this case, a constant solution of the Euclidean equations of motion is $\bar\phi = (\Delta^2/2\lambda)^{\Delta/2}$, with action

$$S_{\rm inst} = |\mathbf{S}^d| \left(\frac{d(d-2)}{8}\bar\phi^{\,2} - \lambda\,\bar\phi^{\,\frac{2d}{d-2}} \right) = \frac{c}{\lambda^\Delta} \ ,$$

where we have used the explicit formula for the spheres' volume, $|\mathbf{S}^{d-1}| = 2\pi^{d/2}/\Gamma(d/2)$.

In order to compare these instantons to our CdL bubbles in the bulk, we can apply the conformal transformation (38) to (40) and obtain the corresponding instanton fields on $\mathbf{R}\times\mathbf{S}^{d-1}$. For general values of x_0 one gets a complicated expression, representing an instanton field partially localized on the sphere. A simpler configuration is obtained for $x_0 = 0$, with the form

$$\begin{aligned} \tilde\phi_{\rm inst}(t_E,\Omega) &= u^\Delta\,\phi_{\rm inst}(u) \\ &= \left(\frac{\Delta^2}{2\lambda}\right)^{\Delta/2} (\cosh((t_E - t_\rho))^{-\Delta} \ , \end{aligned}$$

where $t_\rho = \log\rho$ acquires the interpretation of Euclidean time location rather than size, since the resulting instanton on $\mathbf{R}\times\mathbf{S}^{d-1}$ is constant on the sphere with value $\bar\phi = (\Delta^2/2\lambda)^{\Delta/2}$ at the time-symmetric point.

4.3. A detailed bulk/boundary matching

We check the duality of Fubini instantons with bulk CdL bounces in three stages. First, we notice that the field value of the instanton, $\bar\phi$, exactly matches the nucleation radius of the CdL bubble, $\bar r$, according to the map (32) in the $\alpha \to 1^-$ limit. This follows by direct inspection of (32), using the formula (37) in the mentioned limit. Second, we are able to exactly match the instanton action (42) to the previously computed tunneling rate exponent $2W_E$, again in the $\alpha \to 1^-$ limit in (27).

To see this, use

$$q\,\bar r^{\,d-2} = q\left(\frac{\alpha^2}{1-\alpha^2}\right)^\Delta \longrightarrow \frac{\Delta^d}{(2\lambda)^\Delta}$$

to finally obtain

$$2W_E \longrightarrow q\,v\,\bar r^{\,d-2}\,B(\tfrac{3}{2},\tfrac{d-2}{2}) \longrightarrow \frac{c}{\lambda^\Delta} \ ,$$

with the same constant, c, previously evaluated in (42). The precise matching of the leading exponential rate of nucleation is quite remarkable, since no supersymmetry can be summoned to explain the precise agreement. The required bubbles *must* violate the BPS bound in order to have a nonzero nucleation rate. In turn, this means that the vacua in question have to break supersymmetry.

The third check involves the measure over the instanton moduli space. In the single-instanton sector, conformal invariance fixes the instanton measure completely implying a rate proportional to (in $\mathbf{R}^d$ variables)

$$d^d x_0\,\frac{d\rho}{\rho^{d+1}}\exp\left(-c/\lambda^\Delta\right) \ . \quad (43)$$

Postponing for the time being the question of convergence of (43), we notice that the same expression can be reproduced in the bulk description. Any two instanton configurations in the CFT can be obtained from one another by a conformal transformation (such as translations and dilatations in the form of (40)). Therefore, having successfully matched particular instanton configurations which are uniform on $\mathbf{S}^{d-1}$ or $\mathbf{S}^d$, we are guaranteed a complete matching throughout the whole moduli space, since the conformal group is realized as an isometry group of AdS in the bulk description.

We have presented the discussion of spherical bubbles in section 2 in a particular coordinate system with explicit $U(1)\times O(d)$ isometries, adapted to the boundary CFT geometry $\mathbf{R}\times\mathbf{S}^{d-1}$ with the first factor representing the time direction. Hence, bubbles centered at $r=0$ represent

homogeneous configurations on the CFT spatial sphere. However, the bulk AdS spacetime is completely homogeneous, so that bubbles of the same proper size (controlled by $\bar{r}$) will nucleate homogeneously throughout AdS_{d+1} with uniform probability per unit AdS volume. A bubble nucleating 'off center' with respect to the $O(d)$-symmetric frame, say centered around the point with coordinates (r_b, Ω_b), represents an inhomogeneous configuration on the CFTs' $\mathbf{S}^{d-1}$ spatial sphere.

We can actually exhibit the form (43) of the measure by going to a boundary of the instanton moduli space corresponding to $r_b \gg 1$. In this limit, the standard UV/IR relation of AdS/CFT applies, and such CdL bounce will be interpreted as a Fubini instanton centered around (t_b, Ω_b) and with a 'boundary size' given by $\rho \sim 1/r_b$. This relation implies that bulk and boundary single-instanton measures are actually equal

$$\begin{aligned} & dt_b \, d\Omega_b \, dr_b \, r_b^{d-1} \, \exp\left(-2W_E\right) \qquad (44) \\ \approx \quad & d^d x_0 \, \frac{d\rho}{\rho^{d+1}} \, \exp\left(-c/\lambda^{\Delta}\right) \, , \end{aligned}$$

in the $r_b \sim \rho^{-1} \gg 1$ region of the moduli space, since small instantons do not distinguish $\mathbf{R} \times \mathbf{S}^{d-1}$ from $\mathbf{R}^d$. It would be interesting to extend the quantitative bulk/boundary checks to the value of the negative eigenvalue for quadratic fluctuations around the bounce solutions.

The singularity of the measure (44) at $\rho = 0$ leads to a divergent rate in the dilute-instanton approximation, a characteristic feature of CFTs. In the bulk description, the singularity has a simple interpretation from integrating the nucleation point of the bubble over the infinite volume of AdS. This singularity may be cured by fermion zero modes, forcing potentially divergent amplitudes to vanish, a mechanism at work in supersymmetric CFTs. If the UV fixed point is replaced by an asymptotically free theory the UV divergence may be turned into an IR 'large instanton' divergence, as happens for example in Yang–Mills theories. A safer possibility is to contemplate a modification of the UV behavior that effectively cuts off the zero-size region of instanton moduli space. For instantons mediating vacuum decay, the natural UV modification involves then a *stabilization* of the theory.

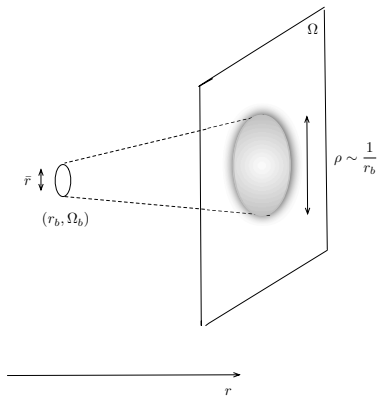

Figure 3. A bulk CdL bubble of size $\bar{r}$ and sitting at the point (r_b, Ω_b), with $r_b \gg 1$, is dual to a Fubini bubble of size $\rho \sim 1/r_b$ on the boundary theory, centered around Ω_b.

We shall see in the next section that the divergence of the decay rate is related to the crunch singularity that ensues when considering the classical evolution after nucleation.

5. Remarks on crunches and their regularization

Having identified a fairly precise duality between CdL bounces and Fubini instantons in an unstable CFT, we may now consider the fate of the nucleated bubbles as they grow towards the boundary of AdS. As explained above, these zero-energy bubbles reach the boundary of AdS in finite asymptotic time, and $dr/dt \sim d\phi/dt$ diverges in the process. This is interpreted in the dual CFT as the roll down in a potential of an unstable marginal operator.

The precise value of the time elapsed between nucleation and the arrival at the boundary does depend on the nucleation point r_b. The UV/IR correspondence translates this r_b dependence into the size parameter of the CFT bubble, $\rho \sim 1/r_b$, and to the central value of the field, via the relation $\phi_0 \sim 1/\sqrt{\lambda \rho^2}$. This makes contact with the results of [26], where it was found that the time to roll down a conformally invariant poten-

tial was only a function of the starting point ϕ_0. Working on $\mathbf{S}^3 \times \mathbf{R}$, the minimal value of ϕ_0 is $\bar{\phi} = (\Delta^2/2\lambda)^{\Delta/2}$, which translates into $\bar{r}$ with the use of (32) giving the maximal hit time computed in (22), corresponding to a 'centered' bubble nucleation.

The diverging kinetic energy of the rolling scalar field triggers an UV singularity which betrays the presence of a crunch singularity in the bulk. In fact, the structure of this crunch singularity is quite intrincate. The volume extensivity of the decay rate implies that an expanding bubble is bound to collide with an infinite number of other bubbles on its way to the boundary, and moreover do so in a *finite* time. Each collision will release energy in the form of radiation and make the approach to the crunch a rather complicated foam-like process. In the dual CFT picture we see that smaller and smaller Fubini bubbles are created at a conformally invariant rate, bubbles within bubbles with a fractal-like structure of field strenghts. [15]

The fact that the QFT Hamiltonian following from (36) is unbounded below means that this complicated decay process has no identifiable 'endpoint' in a nonperturbative sense, i.e. in the QFT space of states, and thus there is no clear suggestion as to how the 'crunch' should be treated in the boundary QFT. [16]

A natural definition from the physical point of view is to modify the UV behavior of (36) in such a way that the theory is ultimately stable, albeit with a large tunable hierarchy between the stabilization mechanism and the instability described by (36). In such a set up we can give a description of the endpoint and see what became of the crunch. Equivalently, we can see how the regularized model develops a 'crunching' behavior as the UV regularization is removed. Previous work along these lines includes [19]. Here, we shall address this question emphasizing the requirement of having a well defined exact CFT description of the far UV behavior of the model.

[15] For a recent numerical evaluation of a similar process, in the context of the so-called 'spinodal' transition, see for example [27].

[16] However, somewhat formal proposals have been advanced in [32].

5.1. A quantum quench

Let us denote by Φ the collection of fields in the QFT, including the brane collective coordinate ϕ. Consider a QFT potential $\mathcal{V}(\Phi)$ with the property that, when restricted to the ϕ direction in field space, it shows the qualitative features of the $V(\phi)$ potential depicted in figure 4. This potential supports tunneling phenomena, where the field value of the maximal-size bubbles is $\bar{\phi}$, and we assume the slope at $\phi > \bar{\phi}$ to be approximately conformal, so that the decay of the semiclassical state at $\phi = 0$ proceeds by nucleation of Fubini-type bubbles. Conformal symmetry is broken by $\mathcal{O}(1)$ effects at the scale $\phi_w \gg \bar{\phi}$, where the potential is stabilized with a net drop of potential energy $\Delta V = V(0) - V(\phi_w) = V(\bar{\phi}) - V(\phi_w)$. Thus, we assume that the region $0 < \phi \ll \phi_w$ is described by (36) and controlled by conformal invariance. We also assume that at $\phi \gg \phi_w$ the potential ultimately retains the conformal properties, being dominated by a stable marginal operator i.e. $V(\phi \to \infty) \to +\phi^{d/\Delta}$.

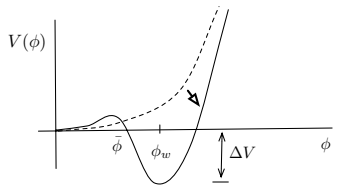

Figure 4. QFT potential with tunneling phenomena. Maximal size bubbles are nucleated with typical energy scale $\bar{\phi}$ and the stabilization scale at ϕ_w may be set at a hierarchically larger energy. The metastable state dual to AdS_+ may be prepared at $t = 0$ as the vacuum of the stable conformal potential in dashed lines. The evolution of this state past $t = 0$ (the quantum quench indicated by an arrow) will proceed by nonperturbative bubble nucleation. These bubbles will be of Fubini type provided the unstable section of potential, for $0 < \phi < \phi_w$, is approximately conformal and well described by (36).

Rather than describing the metastable state by the $\phi = 0$ configuration, we can think more broadly in terms of a wave functional $\Psi_+[\Phi]$ for all CFT degrees of freedom, whose restriction to the ϕ direction in field space is assumed to be well peaked around $\phi = 0$. The basic hypothesis of the AdS/CFT correspondence is that this state admits a semiclassical description in the large N limit in terms of weakly coupled gravity on a background X_+ whose geometrical symmetries encode the quantum symmetries of $\Psi_+[\Phi]$. In particular, if $\Psi_+[\Phi]$ is conformally invariant, X_+ is isometric to AdS, and we denote it by AdS_+.

We can specify the X_+ state more graphically by means of a 'quantum quench'. Let us consider a CFT with an exactly marginal potential $\mathcal{V}_+(\Phi)$ whose projection in the ϕ direction is the operator $+\phi^{d/\Delta}$. The ground state of this theory is a conformally invariant state that we denote $\Psi_+[\Phi]$, with a dual description given by the AdS_+ background. The quantum quench consists of the sudden change of the potential $\mathcal{V}_+(\Phi) \to \mathcal{V}(\Phi)$ at time $t = 0$, as shown in figure 4. After the quantum quench, the AdS_+ state is no longer stationary in the deformed CFT with potential $\mathcal{V}(\Phi)$, and will decay, in this case nonperturbatively via bubble nucleation.

An elementary event of bubble nucleation is described by the discrete jump $X_+ \to X_*$, where X_* is a new background with a bubble, which subsequently evolves perturbatively. The long-time limit of X_* should be generically described as the dual of a locally thermalized state with energy ΔV, measured with reference to the absolute ground state $\Psi_w[\Phi]$ of the QFT defined by $\mathcal{V}(\Phi)$, after the quantum quench. The detailed description of the decay of $\Psi_+[\Phi]$ is necessarily very complex, as it involves multiple bubble nucleation and subsequent dissipation and collision of bubbles, but the basic elements of the process can be understood in the terms just described.

The quantum quench construction is just a formal device to identify initial states with particular properties, in this case the conformal nature of the initial AdS_+ state. For our purposes, the important property of this procedure is the bounded nature of the potential deformation $\mathcal{V}_+ \to \mathcal{V}$, which has 'compact support' in field space, namely the two potentials have the same UV asymptotics. This ensures that the ground state of the new potential, denoted $\Psi_w[\Phi]$, has the same UV asymptotic behavior as $\Psi_+[\Phi]$, and moreover the two states differ only by a finite amount of energy. On general grounds, all normalizable states of the CFT with finite energy will share this property, namely they all look like the vacuum when probed at very short distances. As an immediate corollary of this statement, the bulk background X_w, dual to the new ground state $\Psi_w[\Phi]$, will have the same asymptotics as X_+, namely it must approach AdS_+ near the boundary.

This simple argument, using basic facts about quantum field theory and the AdS/CFT correspondence, shows that no finite-energy state can ever change its boundary asymptotics as a result of a decay process. By *finite energy* we of course mean the energy measured with respect to the true ground state of the theory.[17] In particular, the $\mathrm{AdS}_+ \to \mathrm{AdS}_-$ transitions suggested by the evolution of CdL bubbles are only possible to the extent that they represent *infinite* energy falls, as in the unstable model (36). Thus, this embedding of the problem into a well-defined AdS/CFT model puts into perspective the occurrence of crunches in the final state.

In the following sections we describe a qualitative scenario for a CFT stabilization and its effects on the crunching problem, using the bulk effective brane description. Then in section 5.4 we discuss some possible routes towards the detailed construction of the potential $V(\phi)$ of figure 4 in concrete AdS/CFT examples.

5.2. A bulky stabilization

The general remarks in the previous section indicate that any successful stabilization of the CFT will incorporate an energy scale ϕ_w, with a bulk radial scale counterpart $r_w \sim (\phi_w/\sqrt{\sigma})^{\frac{2}{d-2}}$, beyond which no bubble nucleation takes place

[17] This true ground state, X_w, has negative ADM energy when measured with respect to that of AdS_+, thus violating the corresponding positive energy theorem [6]. This is possible by evading the required energy condition, since $U(\chi)$ can attain negative values below U_+ in the bulk gravity Lagrangian, precisely for those configurations with (non-supersymmetric) AdS_- bubbles.

and moreover bubbles nucleated at lower scales are stopped in their rolling towards the UV. [18]

We can devise a simple bulk model that incorporates these features by assuming that r_w is the location of a bulk domain wall for the effective brane tension. Namely we have $\sigma < q$ for $r < r_w$ and $\sigma > q$ for $r > r_w$. Equivalently, we have $\kappa < \kappa_c$ for $r < r_w$ and $\kappa > \kappa_c$ for $r > r_w$.

The effective brane potential for this situation can be obtained by simply patching the low and high tension potentials across the domain wall location, namely we define $V_{\rm eff}(r) = V_{\rm eff}(r)_{\sigma<|q|}$ for $r < r_w$, and $V_{\rm eff}(r) = V_{\rm eff}(r)_{\sigma>|q|} + \Delta_w$ for $r > r_w$, with the constant Δ_w defined by $\Delta_w = V_{\rm eff}(r_w)_{\sigma<|q|} - V_{\rm eff}(r_w)_{\sigma>|q|}$, to ensure that $V_{\rm eff}$ is continuous at r_w.

We may ask if the 'tension domain wall' envisaged here admits a simple five-dimensional supergravity incarnation, a sort of 'toy landscape' description in terms of an effective potential. A minimal qualitative model would involve a potential for two scalar fields $U(\chi, \sigma)$, with χ controlling the value of the cosmological constant and σ a dilaton-like field determining the tension of branes. A potential with four local minima, with the form of Fig. 5, would do the job provided it supports domain walls, located at $r = r_w$, separating two regions with tensions $\sigma_\pm$, where $\sigma_- < q$ and $\sigma_+ > q$. In addition, the transitions $\chi_+ \to \chi_-$ should correspond to dynamical bubbles if occurring on a region $\sigma = \sigma_-$ and to static domain walls for the case $\sigma = \sigma_+$. This can be achieved if the vacuum energy differences satisfy $U(\chi_+, \sigma_-) - U(\chi_-, \sigma_-) > U(\chi_+, \sigma_+) - U(\chi_-, \sigma_+)$, so that the corresponding shells violate the BPS bound in the σ_- region but satisfy it in the large tension region σ_+.

In this model, the homogeneous vacua $(\chi_\pm, \sigma_+)$ are stable, protected by the high tension of the branes they support. The lower homogeneous vacuum, (χ_-, σ_-) is also stable because it does not have other vacua to decay into. On the other hand the homogeneous AdS_+ background (χ_+, σ_-) is unstable towards nucleation of bubbles of the (χ_-, σ_-) vacuum, giving the standard

[18] This strategy of making the asymptotic geometry 'safe' was used to good effect in other problems of AdS stabilization (cf. for example [36]).

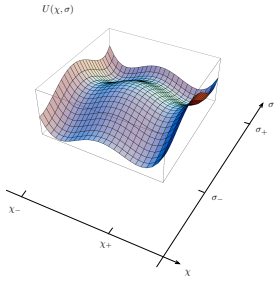

Figure 5. Schematic potential supporting a domain wall for the value of the shell tensions and vacuum bubbles. CdL bubbles correspond to transitions $(\chi_+, \sigma_-) \to (\chi_-, \sigma_-)$. On the other hand, the vacua (χ_+, σ_+) and (χ_-, σ_+) are approximately degenerate, so that no expanding bubbles can exist in a region with $\sigma = \sigma_+$. The regularized background in the text implies considering a combination of CdL bubbles and a static domain wall effecting the transition $\sigma_- \to \sigma_+$ at $r = r_w$.

CdL decay process ending in a crunch. The regularized background with bubble instabilities corresponds to a domain-wall spacetime which looks like the vacuum (χ_+, σ_-) for $r < r_w$, and like the vacuum (χ_+, σ_+) for $r > r_w$. Hence, bubbles cannot form in the $r > r_w$ region, but the decay of the (χ_+, σ_-) region of the vacuum proceeds as before. Being a compact domain of the original spacetime, we do not expect any naked singularities to emerge in this case.

5.3. Endpoints

Bubbles nucleated at $\bar{r} \ll r_w$ will start oscillating around r_w and eventually lose their energy into radiation, by settling down to the absolute minimum at $r = r_w$. As the oscillating bubble wall loses energy to radiation, gradually the mass parameter of the interior solution, μ_-, begins to increase. Hence, the dissipation of oscillation energy into radiation leads to $\Delta\mu < 0$ and accordingly to $\omega < 0$ for the slowing-down brane. The effect on $V_{\rm eff}$ is to gradually lift the minimum at $r = r_w$ and bring, at the same time, the pole of the potential into the physical region of positive radii. As the turning point $\bar{r}$ increases, the

static brane with no oscillation energy left corresponds to the situation where $V_{\rm eff}\,(r_w)=0$, which happens at a negative critical value of the energy $-\omega_r$, given by

$$-\omega_r = V_s(r_w) = -q\,v\,(r_w)^d + \sigma\,v\,(r_w)^{d-1}\,\sqrt{f(r_w)}\;,$$

where $V_s(r)$ is the static potential defined in (33). Since we assume $r_w \gg 1$, this 'reheating' energy, released in the damping of the brane oscillations, is of order $\omega_r \sim (q-\sigma)\,v\,(r_w)^d = q\,v\,(1-\alpha)\,(r_w)^d \sim \eta\,N_{\rm eff}\,(r_w)^d$, with $\eta=(1-\alpha)/N$. We can interpret this energy as a fraction $1/N$ of the plasma energy at effective temperature $T_w \sim r_w$, with a further suppression by the saturation factor $1-\alpha$.

More generally, using the map between the brane static potential and the CFT potential in the saturation limit, $1-\alpha \ll 1$, we obtain

$$\omega_r \sim \lambda\,(\phi_w)^{\frac{2d}{d-2}} \sim |V\,(\phi_w)| = \Delta V\;,$$

showing that ω_r is also the 'reheating' energy in QFT terms.

The bubble nucleation rate scales again as $(r_\Lambda)^d$, with the cutoff replaced by the stabilization scale, $r_\Lambda \sim \Lambda \sim (\phi_w/\sqrt{\sigma}\,)^{\frac{2}{d-2}}$, which breaks conformal invariance and renders the instanton measure well defined. In particular, notice that $\sigma > q$ for $r > r_w$, which precludes the nucleation of any brane in this region.

The picture presented so far, where the false vacuum energy is released by dissipation of a coherent oscillation of a single bubble, is necessarily simplistic, since we know that the dominant process of AdS_+ to AdS_- conversion involves copious bubble collisions, particularly for the case $\bar{r} \ll r_w$. This means that most of the bubbles will release part of their kinetic energy in collision-induced radiation while they are still falling, far from the minimum at r_w. In other words, each individual bubble will contribute less to the reheating, but there will be many bubbles colliding and eventually contributing to a locally thermalized state with a reheating energy $\omega_r \sim |V\,(\phi_w)|$.

The final form of the bulk endpoint configuration depends on the value of the parameters. For $\eta\,r_w^d \gg 1$ the reheating energy is above the threshold for the large AdS black hole, so the radiation will collapse into a large AdS black hole with radius $r_s \sim \eta^{1/d}\,r_w \ll r_w$. On the other hand, if η is so small that $\eta\,r_w^d \ll 1$ the interior black hole will be small in units of the AdS curvature radius and we see that in either case the resulting black hole is well-contained inside the sphere of radius r_w. In fact, when η is too small, it is entropically favorable for the system to settle into a graviton radiation gas. This happens for released energies below the threshold $\omega_r \ll (N_{\rm eff}\,)^{\frac{d+1}{2d-1}}$, again in units of $R_+=1$. The corresponding bound on η for the pure radiation endpoint is $\eta \ll (N_{\rm eff}\,)^{\frac{2-d}{2d-1}}$.

For a fixed value of η, removing the regularization by sending $r_w \to \infty$ in units of R_+ puts us eventually in the regime $\eta\,r_w^d \gg 1$, i.e. the endpoint is a large AdS black hole of ever growing horizon radius. The black hole is always well-contained inside the sphere of radius r_w, unless we push the parameters to extreme limits, $\eta \sim 1$, in which case the black hole has radius of order r_w. In either case, the crunch singularity inside the black hole can be seen as a regularized version of the boundary crunch singularity that develops in the strict $r_w=\infty$ situation.

What was discussed so far is the expected endpoint of evolution for a system with just two 'levels', given by the two $\mathrm{AdS}_\pm$ solutions. In explicit CFT realizations, the large N limit actually puts at our disposal $\mathcal{O}(N)$ metastable vacua obtained by gradually removing constituents branes from the initial AdS_+ background. Hence, as progressive nucleation of ever more curved AdS bubbles proceeds, the final curvature of the AdS_- cores becomes eventually of order one, and a geometrical picture breaks down, together with the single-field description based on the ϕ collective coordinate. The internal metric for $r < r_w$ having curvature of order one, the threshold at r_w is akin to a 'wall', likely to be interpreted as a mass gap and a trivial IR limit of the theory. Hence, we expect the final endpoint to be a thermal excitation of a massive phase. It would be interesting to elucidate the fate of the global and gauge symmetries, as the branes 'pile up' at $r=r_w$, depending on the dynamics on the extra dimensions, such as

the $\mathbf{S}^5$ of the basic AdS/CFT example.

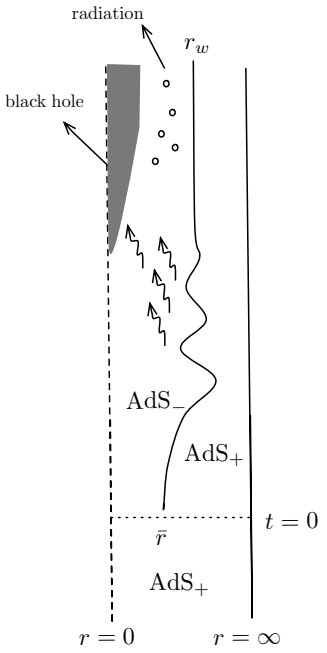

Figure 6. Picture in global coordinates showing the nucleation and relaxation of a bubble centered at $r = 0$. The bubble with AdS_- inside is nucleated at $t = 0$ to enter a damped oscillation, relaxing at $r = r_w$ after the excess energy is radiated away, and finally ending in a radiation equilibrium state which may collapse into a black hole depending on the energetics. The detailed process of the thermalization is actually dominated by a chaotic foam of bubble collisions, rather than this simple picture of single-bubble relaxation.

5.4. Toy models of potential stabilization

In this section we conclude with some speculations about possible realizations of the stabilization scenario described above. Since the key to the bulk description studied in this lecture is the existence of a conformally invariant barrier $-\lambda\,\phi^{d/\Delta}$, a natural stabilization would involve adding an irrelevant operator with a high scale M and *positive* coefficient (cf. [30,19]). One may imagine engineering the physics at this threshold in such a way that the leading operators below the scale M are a stable irrelevant operator and an unstable marginal operator, i.e. $-\lambda\,\phi^{d/\Delta}+\phi^{d/\Delta+\delta}/M^{\delta}$, with $\delta > 0$. This potential produces a stabilization scale at $\phi_w \sim M\,\lambda^{1/\delta}$.

This has the difficulty of leaving the UV definition of the theory undetermined, and thus removes the justification for the use of AdS_+ as an initial state. Therefore, such a strategy (see e.g. the last example in [30]) must be taken to completion by specifying the detailed physics at the scale M in such a way that the theory flows to an UV fixed point above M and indeed generates the required pattern of signs for the effective operators below M. If these conditions are met, we can associate the UV fixed point above M with the AdS_+ state. The detailed geometrical implementation of the stabilization would involve a moderate hierarchy between the minimum of the potential r_w and the transition to AdS_+ geometry at $r \sim r_M > r_w$. This makes the model more complicated, but on the other hand all of the qualitative features discussed in this section would be realized.

A more self-contained strategy of stabilization can be envisaged by adjusting CFT perturbations using finite-N effects. Let us concentrate on the 'template' model of $\mathcal{N} = 4$ SYM in four dimensions with gauge group $SU(N)$. We have seen in section 4.1 that the operator ϕ^4 can be generated with a coefficient of $O(1/N)$ from the canonically normalized gauge invariant operator $\frac{1}{N}\mathrm{Tr}\;\Phi^4$. The same operator ϕ^4 may be generated by projecting the double-trace operator $\frac{1}{N^2}\left(\mathrm{Tr}\,\Phi^2\right)^2$, now with a coefficient of $\mathcal{O}(1/N^2)$ (we again assume canonical normalization of the Φ matrix field.) Let us then consider a perturbation of the SYM Lagrangian specified by

$$\begin{aligned}\mathcal{L} &= \mathcal{L}_{\mathrm{SYM}} - \frac{g_1(\mu)}{N}\left(\mathrm{Tr}\,\Phi^4 + \ldots\right) \\ &+ \frac{g_2(\mu)}{N^2}\left(\left(\mathrm{Tr}\,\Phi^2\right)^2 + \ldots\right)\,,\end{aligned} \tag{45}$$

where $g_1(\mu)$ and $g_2(\mu)$ are both positive at a conventional renormalization scale μ. The dots stand for extra terms, such as contributions from

fermion fields or the detailed $SO(6)$ structure. In particular, we can choose the single-trace operator to be a supersymmetric F-term deformation with generic coupling, which lifts the Coulomb phase of the SYM theory (cf. [31]) and thus serves as a good stabilization operator in the UV. The double-trace operator breaks supersymmetry and the running of $g_2(\mu)$ breaks conformal symmetry to one-loop order. The effective coupling being unstable, it is actually asymptotically free, i.e. we have $g_2(\mu) = c/b_0 \log(\mu/\Lambda_{\rm IR})$, where $b_0 > 0$ is the leading beta-function coefficient of the coupling g_2/c, and $\Lambda_{\rm IR}$ the strong infrared scale. We may further assume $\Lambda_{\rm IR} < 1$, in units of R_+, in order for the leading logarithmic running to be a good approximation down to the mass gap scale $1/R_+ = 1$.

On further evaluating (45) along the $U(1)$ direction $\Phi = \mathrm{diag}\,(0, 0, \ldots, \phi)$, using $\mu = \phi$ as the renormalization scale, we obtain the effective potential

$$V(\phi) = \frac{g_1}{N}\,\phi^4 - \frac{c\,\phi^4}{N^2\,b_0\,\log(\phi/\Lambda_{\rm IR})}\ , \qquad (46)$$

with $c = 2\pi^2/3$ and $b_0 = 3$ at one-loop order. This potential has the required qualitative features with a stabilization scale of order

$$\phi_w \sim \Lambda_{\rm IR}\,\exp\left(\frac{c}{b_0\,N\,g_1}\right)\ .$$

This expression is corrected at next to leading order both from the renormalization of g_2 and the running of $g_1(\mu)$, which starts once the mixing with the double-trace operator is taken into account. The asymptotic freedom of g_2 suggests that these running effects on g_1 are negligible at large ϕ.

We can now make contact with the notations of section 4. The stabilizing F-term has a coupling with the natural order of magnitude in the large N limit, i.e. $g_1 = \mathcal{O}(1)$ as $N \to \infty$. On the other hand, the double-trace operator has a coefficient of order g_2/N^2 with $g_2 = \mathcal{O}(1)$. Since the natural scale of the ϕ^4 operator is $(1-\alpha)/N$, according to (37), we must set $1 - \alpha \sim g_2/N$ in order to match the potentials. Therefore, we conclude that this stabilization method can only work if implemented at large, but *finite* values of N.

The conformal symmetry of the unstable section of the potential (46) is spoiled by the logarithmic running of the double-trace coupling. The main consequence regarding the theory of Fubini instantons is the expected lifting of the instanton moduli space, namely the measure for small instantons (43) gets replaced by

$$\begin{aligned} & d^4x_0\,\frac{d\rho}{\rho^5}\,\exp\left(-2\pi^2N^2/3g_2(\rho)\right) \\ = \quad & d^4x_0\,\frac{d\rho}{\rho^5}\,\left(\rho\Lambda_{\rm IR}\right)^{b_0\,N^2}\ . \end{aligned}$$

At large, but finite N, the small instanton singularity has been tamed, much as in the Yang–Mills theory, and replaced by a large-instanton divergence, which in our case is cured by the 'small volume' assumption $R_+\Lambda_{\rm IR} < 1$.

The structure outlined here is based on perturbative intuition, but the main ingredients should hold at strong 't Hooft coupling, if the double-trace perturbation is implemented along the lines of [22], which in particular preserves the one-loop form of the running for the double-trace coupling. The analysis of D3-brane probes in [28] and [31] is indeed compatible with our picture.

A given CFT is associated to a particular set of backgrounds with a given asymptotic behavior. On the other hand, solutions of the 'supergravity potential' $U(\sigma, \chi)$, with different asymptotic cosmological constant are not in general related by well-defined tunneling transitions. Hence, it would seem that the landscape is 'agnostic', i.e. it will by itself allow many different CFT models to describe different modes of decay which, from the point of view of the effective potential $U(\chi, \sigma)$, look roughly on the same footing. So, regularized models in which the decay process occurs inside a fixed Hilbert space do exist, but the same landscape potential *also* contains the decay modes which take place inside the Hilbert space of sick CFT duals.

6. Discussion

The issues tackled in these lectures are rather challenging. They touch upon the resolution of

gravitational singularities in string theory and the very nature of the so called 'landscape' [37]. In retrospect the authors need to separate what was well known and/or self-evident from the new insights that were gained in this work. This task can be no less demanding. The topics themselves have been examined in the past, in particular, as we have already mentioned, this is true of the idea that the big crunch singularity is in some way or another related to an instability in a boundary field theory. In this work we have set up and studied these questions in the AdS/CFT framework, an arena in which one has somewhat more control. The basic strategy was to obtain the dual holographic formulation, allowing us to be more precise in formulating the issues involved, as well as finding ways to resolve various instabilities. After that was done one needed to return to the less familiar bulk part and uncover where the medicine offered on the boundary leads to in the original bulk problem. We recall several of the important results.

In the issue of a big crunch we have used the observation of Coleman and de Luccia that in some region of parameter space the decay of a false vacuum in AdS space leads to a crunch. We have essentially derived the CFT dual of the background which is a CdL bubble. The result is a CFT on the boundary which has no ground state in those cases for which a tunneling can occur and is stable otherwise. We have related the parameters of the bulk theory with those of the boundary one, checking that the presentation of the dual theory is faithful. The most striking of these checks was obtained by successfully reinterpreting the basic physics of the AdS decay, as described by the work of Coleman and de Luccia, in terms of analogous instanton processes in unstable CFTs. The duality involves a precise correspondence of the leading decay rate on both sides, including the detailed identity of the CdL bounce action and the QFT instanton action. This was shown in the limit in which the unstable potential is weakly coupled. This precise matching is quite intriguing on its own, since the required semiclassical objects only exist in situations where supersymmetry is broken; perhaps conformal symmetry is the 'éminence grise' behind this phenomenon.

We then discussed the main implications of this result first for the interpretation and then for the possible 'resolution' of the ensuing crunch singularity. When faced with a crunch singularity one may expect the nonperturbative stringy resolution to either smooth it out, or rather reveal it as an ill-posed question. In the second case one can still blame the initial state as being unphysical, or the exact Hamiltonian for being ill defined.

In our case we find that metastable AdS backgrounds can indeed admit dual descriptions as time-dependent solutions of an unstable Hamiltonian with no ground state. However, once the CFT was found one could also say that the initial state was unphysical, having infinite energy with respect to the 'true' ground state. This infinite energy does not reveal itself as the ADM mass of the original AdS_+ spacetime but rather, to make sense of the energetics we must regularize the system so that the dual QFT does have a stable ground state, controlled by a threshold energy scale ϕ_w, or the corresponding radial scale r_w in the bulk. When this is done we find that no finite-energy decay process can change the asymptotics of the initial AdS_+ spacetime, which stays protected for $r > r_w$. This result addresses the concerns raised by T. Banks on the interpretation of these decays [4].

We then conclude by drawing in bold strokes the endpoint of the decay: a locally thermalized state that results from the 'reheating' of the oscillating bubbles by dissipation and collision. In bulk terms, this is a black hole which stays well-contained in the region $r < r_w$ and harbors all the reheating energy. Hence, we see that the crunch, if it exists, is safely cloaked behind a black hole horizon. In the limit where we remove the regularization, $r_w \to \infty$, we obtain the previous cosmological crunch as the black hole grows to infinite size, engulfing the whole background manifold validating yet again the picture we suggested for the unregularized decay.

We have went further and attempted to draw a five dimensional caricature of the resolved decay. This involved a domain wall in which the parameters allowed decay in one region of space but not in the other. For this we needed to allow the participation of several fields in the low

energy effective theory.

This leads to some final comments on the landscape. We have started by recalling that in the presence of gravity when one exhibits an effective potential what one sees is not always what one gets. What would look as local maxima or meta stable minima, had the potential described a field in a QFT with the presence of gravity, are in fact stable. Moreover when one considers the potential with four minima we recalled above we have found that the landscape is what we called 'agnostic'. The same low energy potential allows both well defined and ill defined CFT's to represent various decays, the effective action is not a very useful diagnostic of which is which, one needs a more extensive analysis to be able to do that. However the bottom line is that some are well defined and show embryo big crunch features, as much as the theory will allow. Several months after these lectures were delivered there was additional progress in investigating these issues (cf. [45,43,42])

Acknowledgements:

The work of J.L.F. Barbón was partially supported by MEC and FEDER under a grant FPA2009-07908, the Spanish Consolider-Ingenio 2010 Programme CPAN (CSD2007-00042) and Comunidad Autónoma de Madrid under grant HEPHACOS S2009/ESP-1473. The work of E. Rabinovici was partially supported by the Humbodlt foundation, a DIP grant H, 52, the Einstein Center at the Hebrew University, the American-Israeli Bi-National Science Foundation and the Israel Science Foundation Center of Excellence.

REFERENCES

1. J. L. F. Barbon and E. Rabinovici, "Holography of AdS vacuum bubbles," JHEP **1004**, 123 (2010) [arXiv:1003.4966 [hep-th]].
2. J. M. Maldacena, "The large N limit of superconformal field theories and supergravity," Adv. Theor. Math. Phys. **2**, 231 (1998) [Int. J. Theor. Phys. **38**, 1113 (1999)] [arXiv:hep-th/9711200]. S. S. Gubser, I. R. Klebanov and A. M. Polyakov, "Gauge theory correlators from non-critical string theory," Phys. Lett. B **428**, 105 (1998) [arXiv:hep-th/9802109]. E. Witten, "Anti-de Sitter space and holography," Adv. Theor. Math. Phys. **2**, 253 (1998) [arXiv:hep-th/9802150].
3. S. R. Coleman and F. De Luccia, "Gravitational Effects On And Of Vacuum Decay," Phys. Rev. D **21**, 3305 (1980).
4. T. Banks, "Heretics of the false vacuum: Gravitational effects on and of vacuum decay. II," arXiv:hep-th/0211160. T. Banks, "Landskepticism or why effective potentials don't count string models," arXiv:hep-th/0412129.
5. P. Breitenlohner and D. Z. Freedman, "Stability In Gauged Extended Supergravity," Annals Phys. **144**, 249 (1982).
   P. Breitenlohner and D. Z. Freedman, "Positive Energy In Anti-De Sitter Backgrounds And Gauged Extended Supergravity," Phys. Lett. B **115**, 197 (1982).
6. L. F. Abbott and S. Deser, "Stability Of Gravity With A Cosmological Constant," Nucl. Phys. B **195**, 76 (1982).
7. E. Farhi and A. H. Guth, "An Obstacle to Creating a Universe in the Laboratory," Phys. Lett. B **183**, 149 (1987). E. Farhi, A. H. Guth and J. Guven, "Is it Possible to Create a Universe in the Laboratory by Quantum Tunneling?." Nucl. Phys. B **339**, 417 (1990).
8. S. K. Blau, E. I. Guendelman and A. H. Guth, "The Dynamics of False Vacuum Bubbles," Phys. Rev. D **35**, 1747 (1987).
9. V. A. Berezin, V. A. Kuzmin and I. I. Tkachev, "Thin Wall Vacuum Domains Evolution," Phys. Lett. B **120**, 91 (1983). V. A. Berezin, V. A. Kuzmin and I. I. Tkachev, "Dynamics of Bubbles in General Relativity," Phys. Rev. D **36**, 2919 (1987).
10. A. Aurilia, G. Denardo, F. Legovini and E. Spallucci, "Vacuum Tension Effects On The Evolution Of Domain Walls In The Early Universe," Nucl. Phys. B **252**, 523 (1985).
11. V. A. Berezin, V. A. Kuzmin and I. I. Tkachev, "O(3) invariant processes at false vacuum decay in general relativity," Int. J. Mod. Phys. A **5**, 4639 (1990).
12. B. Freivogel, V. E. Hubeny, A. Maloney,

R. C. Myers, M. Rangamani and S. Shenker, "Inflation in AdS/CFT," JHEP **0603**, 007 (2006) [arXiv:hep-th/0510046].
13. W. Israel, "Singular hypersurfaces and thin shells in general relativity," Nuovo Cim. B **44S10**, 1 (1966) [Erratum-ibid. B **48**, 463 (1967 NUCIA,B44,1.1966)].
14. J. L. F. Barbon and J. Martinez-Magan, "Spontaneous fragmentation of topological black holes," JHEP **1008**, 031 (2010) [arXiv:1005.4439 [hep-th]].
15. S. Weinberg, "Does Gravitation Resolve The Ambiguity Among Supersymmetry Vacua?," Phys. Rev. Lett. **48**, 1776 (1982).
16. M. Cvetic, S. Griffies , S-J. Rey, "Static domain walls in N=1 supergravity", Nucl. Phys. B**381**, 301-328 (1992), [arXiv:hep-th/9201007]. M. Cvetic, S. Griffies, Soo-Jong Rey, "Nonperturbative stability of supergravity and superstring vacua", Nucl Phys. B**389**, 3-24 (1993) [arXiv:hep-th/9206004]. M. Cvetic, F. Quevedo, S-J. Rey, "Stringy domain walls and target space modular invariance." Phys. Rev. Lett. **67**,1836-1839 (1991).
17. A. Ceresole, G. Dall'Agata, A. Giryavets, R. Kallosh and A. D. Linde, "Domain walls, near-BPS bubbles, and probabilities in the landscape," Phys. Rev. D **74**, 086010 (2006) [arXiv:hep-th/0605266]. M. Dine, G. Festuccia and A. Morisse, "The Fate of Nearly Supersymmetric Vacua," JHEP **0909**, 013 (2009) [arXiv:0901.1169 [hep-th]]. M. Dine, G. Festuccia, A. Morisse and K. van den Broek, "Metastable Domains of the Landscape," JHEP **0806**, 014 (2008) [arXiv:0712.1397 [hep-th]]. P. Narayan and S. P. Trivedi, "On The Stability Of Non-Supersymmetric AdS Vacua," arXiv:1002.4498 [Unknown].
18. N. Seiberg and E. Witten, "The D1/D5 system and singular CFT," JHEP **9904**, 017 (1999) [arXiv:hep-th/9903224].
19. T. Hertog and G. T. Horowitz, "Holographic description of AdS cosmologies," JHEP **0504**, 005 (2005) [arXiv:hep-th/0503071].
20. G. L. Alberghi, D. A. Lowe and M. Trodden, "Charged false vacuum bubbles and the AdS/CFT correspondence," JHEP **9907**, 020 (1999) [arXiv:hep-th/9906047].
21. David A. Lowe, "Some comments on embedding inflation in the AdS/CFT correspondence," Phys. Rev. D**77**, 066003 (2008) arXiv:0710.3564 [hep-th].
22. E. Witten, "Multi-trace operators, boundary conditions, and AdS/CFT correspondence," arXiv:hep-th/0112258. M. Berkooz, A. Sever and A. Shomer, "Double-trace deformations, boundary conditions and spacetime singularities," JHEP **0205**, 034 (2002) [arXiv:hep-th/0112264].
23. S. Fubini, "A New Approach To Conformal Invariant Field Theories," Nuovo Cim. A **34**, 521 (1976).
24. J. Zinn-Justin, "Quantum Field Theory and Critical Phenomena", Clarendon Press, Oxford 1996.
25. A. D. Linde, "Particle Physics and Inflationary Cosmology," arXiv:hep-th/0503203.
26. V. Asnin, E. Rabinovici and M. Smolkin, "On rolling, tunneling and decaying in some large N vector models," JHEP **0908**, 001 (2009) [arXiv:0905.3526 [hep-th]].
27. J. Garcia-Bellido, M. Garcia Perez and A. Gonzalez-Arroyo, "Symmetry breaking and false vacuum decay after hybrid inflation," Phys. Rev. D **67**, 103501 (2003) [arXiv:hep-ph/0208228].
28. A. Bernamonti and B. Craps, "D-Brane Potentials from Multi-Trace Deformations in AdS/CFT," JHEP **0908**, 112 (2009) [arXiv:0907.0889 [hep-th]].
29. T. Hertog and G. T. Horowitz, "Towards a big crunch dual," JHEP **0407**, 073 (2004) [arXiv:hep-th/0406134].
30. S. Elitzur, A. Giveon, M. Porrati and E. Rabinovici, "Multitrace deformations of vector and adjoint theories and their holographic duals," JHEP **0602**, 006 (2006) [arXiv:hep-th/0511061]. *ibid* Nucl. Phys. Proc. Suppl. **171**, 231 (2007).
31. O. Aharony, B. Kol and S. Yankielowicz, "On exactly marginal deformations of N = 4 SYM and type IIB supergravity on AdS(5) x S**5," JHEP **0206**, 039 (2002) [arXiv:hep-th/0205090].
32. B. Craps, T. Hertog and N. Turok, "Quan-

tum Resolution of Cosmological Singularities using AdS/CFT," arXiv:0712.4180 [hep-th]. N. Turok, B. Craps and T. Hertog, "From Big Crunch to Big Bang with AdS/CFT," arXiv:0711.1824 [hep-th].
33. I. Affleck, "Quantum Statistical Metastability," Phys. Rev. Lett. **46**, 388 (1981).
34. M. M. Caldarelli, O. J. C. Dias, R. Emparan and D. Klemm, "Black Holes as Lumps of Fluid," JHEP **0904**, 024 (2009) [arXiv:0811.2381 [hep-th]]. R. Emparan, T. Harmark, V. Niarchos and N. A. Obers, "Blackfolds," Phys. Rev. Lett. **102**, 191301 (2009) [arXiv:0902.0427 [hep-th]]; "Essentials of Blackfold Dynamics," arXiv:0910.1601 [Unknown]; "New Horizons for Black Holes and Branes," arXiv:0912.2352 [Unknown].
35. G. T. Horowitz, J. Orgera and J. Polchinski, "Nonperturbative Instability of AdS_5 x S^5/Z_k," Phys. Rev. D **77**, 024004 (2008) [arXiv:0709.4262 [hep-th]].
36. J. L. F. Barbon and E. Rabinovici, "Closed-string tachyons and the Hagedorn transition in AdS space," JHEP **0203**, 057 (2002) [arXiv:hep-th/0112173]; "Remarks on black hole instabilities and closed string tachyons," Found. Phys. **33**, 145 (2003) [arXiv:hep-th/0211212].
37. L. Susskind, "The anthropic landscape of string theory," arXiv:hep-th/0302219.
38. J. L. F. Barbon and E. Rabinovici, "Remarks on black hole instabilities and closed string tachyons," Found. Phys. **33**, 145 (2003) [arXiv:hep-th/0211212].
39. S. de Haro and A. C. Petkou, "Instantons and conformal holography," JHEP **0612**, 076 (2006) [arXiv:hep-th/0606276].
40. S. de Haro, I. Papadimitriou and A. C. Petkou, "Conformally coupled scalars, instantons and vacuum instability in AdS(4)," Phys. Rev. Lett. **98**, 231601 (2007) [arXiv:hep-th/0611315].
41. I. Papadimitriou, "Multi-Trace Deformations in AdS/CFT: Exploring the Vacuum Structure of the Deformed CFT," JHEP **0705**, 075 (2007) [arXiv:hep-th/0703152].
42. J. L. F. Barbon and E. Rabinovici, "AdS Crunches, CFT Falls And Cosmological Complementarity," arXiv:1102.3015 [hep-th].
43. D. Harlow and L. Susskind, "Crunches, Hats, and a Conjecture," arXiv:1012.5302 [hep-th].
44. D. Harlow, "Metastability in Anti de Sitter Space," arXiv:1003.5909 [hep-th].
45. J. Maldacena, "Vacuum decay into Anti de Sitter space," arXiv:1012.0274 [hep-th].

Black Hole Microstate Counting and its Macroscopic Counterpart

Ipsita Mandal and Ashoke Sen[a]

[a]Harish-Chandra Research Institute
Chhatnag Road, Jhusi, Allahabad 211019, India

We survey recent results on the exact dyon spectrum in a class of $\mathcal{N} = 4$ supersymmetric string theories, and discuss how the results can be understood from the macroscopic viewpoint using AdS_2/CFT_1 correspondence. The comparison between the microscopic and the macroscopic results includes power suppressed corrections to the entropy, the sign of the index, logarithmic corrections and also the twisted index measuring the distribution of discrete quantum numbers among the microstates.

(Based on lectures given by A.S. at the 12th Marcel Grossmann Meeting On General Relativity, 12-18 Jul 2009, Paris, France; CERN Winter School on Supergravity, Strings, and Gauge Theory, 25-29 January 2010; String Theory: Formal Developments And Applications, 21 Jun - 3 Jul 2010, Cargese, France, and notes taken by I.M. at the Cargese school.)

1. Introduction

Black holes are classical solutions of the equations of motion of general theory of relativity. Each black hole is surrounded by an event horizon that acts as a one way membrane. Nothing, including light, can escape a black hole horizon. Thus classically the horizon of a black hole behaves as a perfect black body at zero temperature.

This picture undergoes a dramatic modification in quantum theory [1–4]. There a black hole behaves as a thermodynamic system with definite temperature, entropy etc. In particular, the temperature and the Bekenstein-Hawking entropy of a black hole is given by the simple formulæ:

$$T = \frac{\kappa}{2\pi}, \qquad S_{BH} = \frac{A}{4\,G_N}, \tag{1}$$

where κ is the surface gravity – acceleration due to gravity at the horizon of the black hole (measured by an observer at infinity), A is the area of the event horizon and G_N is the Newton's gravitational constant. We have set $\hbar = c = k_B = 1$.

Now, for ordinary objects, the entropy of a system has a microscopic interpretation. If we fix the macroscopic parameters (*e.g.* total electric charge, energy etc.) and count the number of quantum states (dubbed microstates), each of which has the same charge, energy etc., then we can define the microscopic (statistical) entropy as:

$$S_{micro} = \ln\, d_{micro}\,, \tag{2}$$

where d_{micro} is the number of such microstates. This naturally leads to the question whether the entropy of a black hole has a similar statistical interpretation. As pointed out by Hawking, answering this question in the affirmative is essential for any consistent theory of quantum gravity as otherwise it leads to violation of the laws of quantum mechanics.

In order to investigate the statistical origin of black hole entropy, we need a quantum theory of gravity. Since string theory gives a framework for studying classical and quantum properties of black holes, we shall carry out our investigation in string theory. Now, even though there is a unique string (M)-theory, it can exist in many different stable and metastable phases. Without knowing precisely which phase of string theory describes the part of the universe we live in, we cannot directly compare string theory to experiments. However, there are some issues like those involving black hole thermodynamics, which are universal, and hence can be addressed in any phase of string theory. We shall make use of this freedom to study these issues in a special class of

phases of string theory with a large amount of unbroken supersymmetry. Since these phases have Bose-Fermi degenerate spectrum of states, they do not describe the observed world. Nevertheless they contain black hole solutions and hence can be used to study issues involving black hole thermodynamics.

Many aspects of black hole thermodynamics have been studied in string theory, but we shall focus our attention on one particular aspect: entropy of the black hole in the zero temperature limit (i.e., supersymmetric, extremal black holes). The advantage of studying such a black hole is that it is a stable state of the theory. The general strategy is as follows[5,6]:

1. Identify a supersymmetric black hole carrying a certain set of electric charges $\{Q_i\}$ and magnetic charges $\{P_i\}$, and calculate its entropy $S_{BH}(Q,P)$ using the Bekenstein-Hawking formula.[1]

2. Identify the supersymmetric quantum states in string theory carrying the same set of charges. These can include not only the fundamental strings but also other objects in string theory which are required for consistency of the theory (*e.g.* D-branes, Kaluza-Klein monopoles). We then calculate the number $d_{micro}(Q,P)$ of these states.

3. Compare $S_{micro} \equiv \ln d_{micro}(Q,P)$ with $S_{BH}(Q,P)$.

For a class of supersymmetric extremal black holes in type IIB string theory on $K3 \times S^1$, Strominger and Vafa[6] computed the Bekenstein-Hawking entropy via (1) and found agreement with the statistical entropy defined in (2). This agreement is quite remarkable since it relates a geometric quantity in black hole space-time to a counting problem that does not make any direct reference to black holes. At the same time, one should keep in mind that the Bekenstein-Hawking formula is an approximate formula that holds in classical general theory of relativity. While string theory gives a theory of gravity that reduces to Einstein's theory when gravity is weak, there are corrections.[2] Thus the Bekenstein-Hawking formula for the entropy works well only when gravity at the horizon is weak. Typically this requires the charges to be large. Similarly, the computation of d_{micro} in [6] was also carried out in the limit of large charges, so that instead of having to carry out an exact counting of states, one can use some appropriate asymptotic formula to compute it. Thus the agreement between S_{BH} and S_{micro}, seen in [6], can be regarded as an agreement in the limit of large size.

This leads to the following question: For ordinary systems, thermodynamics provides an accurate description only in the limit of large volume. Is the situation with black holes similar, i.e., do they only capture the information about the system in the limit of large charge and mass? Or, could it be that the relation $A/4G_N = \ln d_{micro}$ is an approximation to an exact result? Our goal will be to argue for the second possibility by giving an exact formula to which the above is an approximation.

In order to address this issue, we have to work on two fronts:

1. Count the number of microstates to greater accuracy.

2. Calculate the black hole entropy to greater accuracy.

We can then compare the two to see if they agree beyond the large charge limit. In these lectures we shall describe the progress on both fronts.

Note that on the gravity side we shall not try to identify the individual microstates – this is the goal of the fuzzball program [7]. Our approach will be to find a systematic procedure that allows us to compute the total number of states in the ensemble from the gravity side without having to identify the individual microstates. More

[1] Since we are considering a generic phase of string theory, it may have more that one Maxwell field and hence multiple charges.

[2] In string theory, even at classical level, we have higher derivative (α') corrections. This is because strings are not point objects. So even at classical level, there will be corrections to the Bekenstein-Hawking formula. Besides this, there will also be quantum corrections.

generally, we would like to find an algorithm for computing the trace of various observables in this ensemble from the gravity side.

We end this section by giving a summary of the progress, which will be reviewed in detail in the rest of these lecture notes:

1. **Progress in microscopic counting:** In a wide class of phases of string theory with 16 or more unbroken supercharges, one now has a complete understanding of the microscopic 'degeneracies' of supersymmetric black holes [8–53]. Typically, such theories have multiple Maxwell fields and the black hole is characterized by multiple electric and magnetic charges, collectively denoted by (Q, P). It turns out that for a wide class of charge vectors (all charge vectors in some cases), $d_{micro}(Q, P)$ in these theories can be explicitly computed and can be expressed as Fourier expansion coefficients of some functions with remarkable symmetry properties. This provides us with the 'experimental data' to be explained by a 'theory of black holes', giving a powerful tool for checking the internal consistency of string theory. Needless to say, in the large charge limit, these degeneracies agree with the exponential of the Bekenstein-Hawking entropy of black holes carrying the same set of charges. Our goal will be to see how far the agreement can be pushed beyond the large charge limit.

2. **Progress in black hole entropy computation:** On the macroscopic side, we would like to ask whether we can find an exact formula for the black hole entropy that can be compared with $\ln d_{micro}(Q, P)$. This will require us to take into account

   (a) stringy (α') corrections, and

   (b) quantum (g_s) corrections.

   We shall describe an approach to finding such a general formula for black hole entropy using AdS_2/CFT_1 correspondence. We shall then apply this general formalism to the specific case of supersymmetric black holes in $\mathcal{N} = 4$ supersymmetric string theories, and compare the results with the microscopic answer.

2. Microstate counting

In this section we shall survey the known results on the counting of quarter-BPS dyons in $\mathcal{N} = 4$ supersymmetric string theories.

2.1. The role of index

The counting of microstates is always done in a region of the moduli space where gravity is weak and hence the states do not form a black hole. In order to be able to compare it with the black hole entropy, we must focus on quantities which do not change as we change the coupling from small to large value. So we need an appropriate index which is protected by supersymmetry, and at the same time does not vanish identically when evaluated on the microstates of interest. The relevant index in $D = 4$ turns out to be the helicity trace index [54,55].

Suppose we have a BPS state that breaks $4n$ supersymmetries. Then there will be $4n$ fermion zero modes (goldstinos) on the world-line of the state. Quantization of these zero modes will produce Bose-Fermi degenerate states. Thus the usual Witten index $Tr(-1)^F$, which measures the difference between the number of bosonic and fermionic states, will receive vanishing contribution from these states. To remedy this situation, we define a new index called the helicity trace index:

$$\begin{aligned} B_{2n} &= \frac{1}{(2n)!}\, Tr\{(-1)^F (2h)^{2n}\} \\ &= \frac{1}{(2n)!} Tr\{(-1)^{2h} (2h)^{2n}\}\,, \end{aligned} \tag{3}$$

where h is the third component of the angular momentum in the rest frame. The trace is taken over states carrying a fixed set of charges. For every pair of fermion zero modes, $Tr\{(-1)^F(2h)\}$ gives a non-vanishing result i, leading to a non-zero contribution $(-1)^n$ to B_{2n}. On the other hand, any state that breaks more than $4n$ supersymmetries, will have more then $2n$ pairs of fermion zero modes and will give vanishing contribution to this trace. In particular, non-BPS states will

not contribute, and the index will be protected from corrections as we vary the moduli (except at the walls of marginal stability [56–60], which will be discussed in §2.4).

Quarter-BPS black holes in $\mathcal{N}=4$ supersymmetric string theories preserve four of the sixteen supersymmetries, and hence break twelve supersymmetries. Thus the relevant helicity trace index is B_6. We shall now describe the microscopic results for B_6 in a class of $\mathcal{N}=4$ supersymmetric string theories. However, we must keep in mind that, since on the microscopic side we compute an index, on the black hole side also we must compute an index. Otherwise we cannot compare the results of microscopic and macroscopic computations. We will show in §3.7 how can we use black hole entropy to compute the index B_6 on the black hole side.

2.2. Microstate counting in heterotic string theory on T^6

The simplest example of an $\mathcal{N}=4$ supersymmetric string theory is heterotic string theory on T^6 (or equivalently type IIA or IIB string theory on $K3\times T^2$, as they are related by duality transformations). This theory has 28 U(1) gauge fields arising from the Cartan generators of the $E_8\times E_8$ (or $SO(32)$) gauge group, and the components of the metric and the 2-form field along the six internal directions. Thus a generic charged state is characterized by 28 dimensional electric charge vector Q and 28 dimensional magnetic charge vector P. Under the $O(6,22;\,\mathbb{Z})$ T-duality symmetry of the theory, the charges Q and P transform as vectors. This allows us to define T-duality invariant bilinears in the charges[3]: Q^2, P^2, $Q\cdot P$.

Our goal is to compute the index $B_6(Q,P)$. The computation is done in the dual frame: type IIB on $K3\times S^1\times\widetilde{S}^1$, where S^1 and $\widetilde{S}^1$ represent two circles which are not factored metrically.[4] In this frame, we compute B_6 for a rotating D1-D5-p system[61] in Kaluza-Klein (KK) monopole (or equivalently Taub-NUT) background. More specifically, we take a system containing [10]

1. one KK monopole along $\widetilde{S}^1$;
2. one D5-brane wrapped on $K3\times S^1$;
3. $(\widetilde{Q}_1+1)$ D1-branes wrapped on S^1;
4. $-n$ units of momentum along S^1;
5. J units of momentum along $\widetilde{S}^1$.

The momentum along $\widetilde{S}^1$ appears as an angular momentum at the center of the Taub-NUT space [62]. Thus, macroscopically, the system describes a rotating BMPV black hole [63] at the center of the Taub-NUT space [10]. In the weak coupling limit, the dynamics is given by that of a system of decoupled harmonic oscillators, and an exact computation of B_6 is possible. The result is then expressed in terms of the T-duality invariant bilinears Q^2, P^2, $Q\cdot P$ in the original heterotic frame, using the fact that the system described above has

$$Q^2=2n,\qquad P^2=2\widetilde{Q}_1,\qquad Q\cdot P=J\,. \tag{4}$$

If Q^2, P^2 and $Q\cdot P$ were the only T-duality invariants, i.e., if any two dyons with the same Q^2, P^2 and $Q\cdot P$ had been related to each other by a T-duality transformation, then the result for $B_6(Q,P)$ for the specific system described above will give the result for all dyons in the theory. However it turns out that this is not quite correct. Nevertheless, any charge vector satisfying the condition[22]

$$\gcd\{Q_iP_j-Q_jP_i\,,\quad 1\le i,j\le 28\}=1\,, \tag{5}$$

can be related to the above system by a T-duality transformation[31]. Thus the formula we quote below is valid only for this special class of charges. We shall briefly comment on the other charge vectors in §2.5.

Let us denote by $B_6(\widetilde{Q}_1,n,J)$ the sixth helicity trace associated with the system described above. We define the partition function as:

$$Z(\rho,\sigma,v)=\sum_{\widetilde{Q}_1,n,J}(-1)^J\,B_6\;e^{2\pi i(\widetilde{Q}_1\rho+n\sigma+Jv)}\,. \tag{6}$$

[3]Note that these bilinears are not positive definite as $O(6,22;\,\mathbf{Z})$-invariant matrices have both positive and negative eigenvalues.

[4]The problem with carrying out this computation in heterotic frame is that there the system will contain $NS5$-branes, and the coupling constant diverges at the core of these branes.

The computation of Z proceeds as follows. In the weakly coupled type IIB description, the low energy dynamics of the system is described by three weakly interacting pieces:

1. The closed string excitations around the KK monopole.

2. The dynamics of the D1-D5 center of mass coordinate in the KK monopole background.

3. The motion of the D1 branes along $K3$.

The dyon partition function is obtained as the product of the partition functions of these three subsystems [17].[5] The analysis can be simplified by taking the size of S^1 to be large compared to other dimensions, so that we can regard each subsystem as a 1+1 dimensional CFT. Since BPS condition forces the modes carrying positive momentum along S^1 (right-moving modes) to be frozen into their ground state, only left-moving modes can be excited. We shall now describe the contribution to Z from each subsystem.

First consider the fields describing the dynamics of KK monopole. These include

1. 3 left-moving and 3 right-moving bosons arising from its motion in the 3 transverse directions;

2. 2 left-moving and 2 right-moving bosons arising from the components of 2-form fields along the harmonic 2-form in Taub-NUT space [64,65];

3. 19 left-moving and 3 right-moving bosons, arising from the components of the 4-form field along the wedge product of the harmonic 2-form on Taub-NUT and a harmonic 2-form on $K3$;

4. 8 right-moving goldstino fermions associated with the eight supersymmetries which are broken by the KK monopole.

Since the right-moving modes are frozen into their ground state, the contribution to the partition function from the KK-monopole dynamics, after separating out the contribution from fermion zero modes which go into the helicity trace, is equal to that of 24 left-moving bosons [17]:

$$Z_{KK} = e^{-2\pi i\sigma} \prod_{n=1}^{\infty} \left\{(1-e^{2\pi i n\sigma})^{-24}\right\} . \tag{7}$$

The overall factor of $e^{-2\pi i\sigma}$ is a reflection of the fact that the ground state of the Kaluza-Klein monopole carries a net momentum of 1 along S^1.

The dynamics of the D1-D5 center of mass motion in the KK monopole background is described by a supersymmetric sigma model with Taub-NUT space as the target space. By taking the size of the Taub-NUT space to be large, we can take the oscillator modes to be those of a free field theory, but the zero mode dynamics is described by a supersymmetric quantum mechanics problem. The contribution is found to be [17]

$$\begin{aligned} Z_{CM} \;=\; & e^{-2\pi iv} \prod_{n=1}^{\infty} \{(e^{\pi iv}-e^{\pi iv})^{-2}(1-e^{2\pi i n\sigma})^4 \\ & (1-e^{2\pi i(n\sigma+v)})^{-2}(1-e^{2\pi i(n\sigma-v)})^{-2}\} . \end{aligned} \tag{8}$$

The third component comprises D1-brane motion along $K3$. This can be computed as outlined below [66]:

1. First consider a single D1-brane, wrapped k times along S^1 and carrying fixed momenta along S^1 and $\widetilde{S}^1$. The dynamics of this system is described by a supersymmetric sigma model with target space $K3$. The number of states of this system can be counted by the standard method of going to the orbifold limit. After removing a trivial degeneracy factor associated with fermion zero mode quantization, the net number of bosonic minus fermionic states, carrying momentum $-l$ along S^1 and j along $\widetilde{S}^1$, is given by

[5] A factor of $(-1)^{J+1}$ in (6) was missed in [17]. The $(-1)^J$ factor arises because in five dimensions, at the center of the KK monopole, we have $(-1)^F = (-1)^{J+2h}$ instead of $(-1)^{2h}$ [13]. An overall factor of -1, which has been absorbed in the definition of B_6 in (6), arises from the partition function of the quantum mechanics describing the D1-D5-brane motion in the KK monopole background[28]. A detailed derivation of many of the results given in this section has been reviewed in [28].

$c(4lk-j^2)$, where $c(n)$ is defined as:

$$F(\tau,z) \equiv 8\Big\{\frac{\vartheta_2(\tau,z)^2}{\vartheta_2(\tau,0)^2}+\frac{\vartheta_3(\tau,z)^2}{\vartheta_3(\tau,0)^2} +\frac{\vartheta_4(\tau,z)^2}{\vartheta_4(\tau,0)^2}\Big\}, \quad (9)$$

$$F(\tau,z) \equiv \sum_{j\in\mathbf{Z},n} c(4n-j^2)e^{2\pi i(n\tau+zj)}. \quad (10)$$

Physically, $c(4n-j^2)$ counts the number of BPS states in the supersymmetric sigma model with target space $K3$ with $L_0=n$ and $\mathcal{J}_3=j/2$, where $\mathcal{J}_3$ denotes the third component of the $SU(2)$ R-symmetry current.

2. A generic state contains multiple D1-branes of this type, carrying different amounts of winding along S^1 and different momenta along S^1 and $\widetilde{S}^1$. The total number of states can be determined from the result of step 1 by simple combinatorics.

The net contribution to the partition function from D1-brane motion along $K3$ is [66]:

$$Z_{D1} = e^{-2\pi i\rho}\prod_{\substack{l,j,k\in Z\\ k>0,l\geq 0}}\Big\{1-e^{2\pi i(l\sigma+k\rho+jv)}\Big\}^{-c_{lkj}}, \quad (11)$$

where $c_{lkj}\equiv c(4lk-j^2)$.

After taking the product of the component partition functions (7), (8) and (11), we get [17]

$$Z = \prod_{\substack{l,j,k\in Z\\ k\geq 0,l\geq 0,j<0 \text{ for } k=l=0}}\Big\{1-e^{2\pi i(l\sigma+k\rho+jv)}\Big\}^{-c_{lkj}} \times e^{-2\pi i(\rho+\sigma+v)}, \quad (12)$$

where we have used the explicit values of $c(u)$ to express the contribution from (7) and (8) in terms of $c(n)$. Indeed these two factors give the $k=0$ term in (12). Eq.(12) can be expressed as

$$Z(\rho,\sigma,v)=1/\Phi_{10}(\rho,\sigma,v)\,. \quad (13)$$

Here Φ_{10} is a well known function, known as the weight 10 Igusa cusp form of $Sp(2,\mathbf{Z})$[67,68].[6] The formula for Z given above was conjectured in [8].

Eq.(6) can be inverted to express $B_6(\widetilde{Q}_1,n,J)$ as

$$B_6(\widetilde{Q}_1,n,J) = \int d\rho d\sigma dv\, e^{-2\pi i(\widetilde{Q}_1\rho+n\sigma+Jv)}\,Z \times (-1)^J. \quad (14)$$

We shall express this in a more duality invariant notation using (4):

$$B_6(Q,P) = \int d\rho d\sigma dv\, e^{-\pi i(P^2\rho+Q^2\sigma+2Q\cdot Pv)}\,Z \times (-1)^{Q\cdot P}\,. \quad (15)$$

2.3. Asymptotic expansion

In order to compare (15) with the black hole entropy, we need to find its behaviour for large Q^2, P^2, $Q.P$. It turns out that this is controlled by the behaviour of Z at its poles, which in turn are at the zeroes of Φ_{10} [8]. The location of the zeroes of Φ_{10} as well as the behaviour of Φ_{10} around these zeroes can be determined using its modular properties. We perform one of the three integrals using the residue theorem, picking up contributions from various poles. The leading contribution comes from the pole at [8]

$$(\rho\sigma-v^2)+v=0\,. \quad (16)$$

After picking up the residue at this pole, we are left with a two dimensional integral:

$$-B_6(Q,P)\simeq\int\frac{d^2\tau}{\tau_2^2}\,e^{F(Q^2,P^2,Q.P,\tau_1,\tau_2)}\,, \quad (17)$$

where (τ_1,τ_2) parametrize the locus of the zeroes of Φ_{10} at (16) in the (ρ,σ,v) space and

$$F = \frac{\pi}{2\tau_2}(Q-\tau P)\cdot(Q-\bar\tau P)$$

[6] $Sp(2,\mathbf{Z})$ includes the $SL(2,\mathbf{Z})$ S-duality group, but it is a much bigger group than the S-duality group of string theory. Thus it is not completely understood why Z has $Sp(2,\mathbf{Z})$ symmetry (see [12,20,43] for some attempts in this direction). In fact, this property of Z comes out at the very end after combining the results from the individual subsystems. But once we arrive at this final form, these symmetries can be conveniently used to analyse the asymptotic behaviour of Z.

$$-24\ln\eta(\tau)-24\ln\eta(-\bar\tau)-12\ln(2\tau_2)$$
$$+\ln\{26+\frac{\pi}{\tau_2}(Q-\tau P)\cdot(Q-\bar\tau P)\}. \quad (18)$$

We evaluate this integral by the saddle point method. We expand F around its extremum and carry out the integral using perturbation theory. If we consider a limit in which we scale all the charges by some large parameter Λ, then the perturbation expansion around the saddle point generates a series in inverse power of Λ^2, with the leading semi-classical result being of order Λ^2.

Applying the above procedure, first of all we find that, for large charges, $-B_6(Q,P)$ is positive [28] (i.e., $B_6(Q,P)$ is negative). Furthermore [9, 69]:

$$\begin{aligned}\ln|B_6(Q,P)| &= \pi\sqrt{Q^2P^2-(Q.P)^2}\\ &\quad -\phi\left(\frac{Q.P}{P^2},\frac{\sqrt{Q^2P^2-(Q.P)^2}}{P^2}\right)\\ &\quad +\mathcal{O}\left(\frac{1}{Q^2,P^2,Q.P}\right), \qquad (19)\end{aligned}$$

where

$$\begin{aligned}\phi(\tau_1,\tau_2) &\equiv 12\ln\tau_2+24\ln\eta(\tau_1+i\tau_2)\\ &\quad +24\ln\eta(-\tau_1+i\tau_2). \qquad (20)\end{aligned}$$

The first term, $\pi\sqrt{Q^2P^2-(Q\cdot P)^2}$, is indeed the Bekenstein-Hawking entropy of the black hole [70–72]. The macroscopic origin of the other terms will be discussed in §3.4.

2.4. Walls of marginal stability

Our result for the D1-D5-KK monopole system was derived for weakly coupled type IIB string theory. However, as we move around in the moduli space, we may hit walls of marginal stability, at which the quarter-BPS dyon under consideration becomes unstable against decay into a pair of half-BPS dyons. At these walls, the index jumps, and hence we cannot trust our formula on the other side of the wall. It turns out, however, that with the help of S-duality, we can always bring the moduli to a domain where the type IIB theory is in the weakly coupled domain and we can trust our original formula. The net outcome of this analysis is that, in different domains, the index is given by the formula:

$$\begin{aligned}B_6(Q,P) &= \int_C d\rho d\sigma dv\, e^{-\pi i(P^2\rho+Q^2\sigma+2Q.Pv)}/\Phi_{10}\\ &\quad\times\ (-1)^{Q.P}, \qquad (21)\end{aligned}$$

where C denotes the choice of 'contour' that picks a 3 real dimensional subspace of integration in the 3 complex dimensional space:

$$\begin{aligned}&Im(\rho)=M_1,\quad Im(\sigma)=M_2,\quad Im(v)=M_3,\\ &0\le Re(\rho),Re(\sigma),Re(v)\le 1. \qquad (22)\end{aligned}$$

The three real numbers (M_1,M_2,M_3), which specify the choice of the contour C, depend on the domain in the moduli space where we compute the index [21,22,25]. For example in the weak coupling limit of type IIB string theory, for the system we have analyzed, we have $M_1,M_2>>1$, $1<<|M_3|<<M_1,M_2$ and the sign of M_3 is positive or negative depending on whether the angle between S^1 and $\widetilde{S}^1$ is larger or smaller than $\pi/2$ [17,19]. The jumps in the index, across the walls of marginal stability, are encoded in the residues at the poles in Z that we encounter while deforming the contour corresponding to one domain to the contour corresponding to the other domain. There is a precise correspondence between different walls of marginal stability and different poles of Z. For the decay $(Q,P)\Rightarrow(Q,0)+(0,P)$, the associated wall is at $v=0$ [17–19,21,22]. This, together with the S-duality invariance of the theory, tells us that for the wall associated with the decay

$$\begin{aligned}(Q,P) &\Rightarrow (\alpha Q+\beta P,\gamma Q+\delta P)\\ &\quad +((1-\alpha)Q-\beta P,-\gamma Q+(1-\delta)P), \qquad (23)\end{aligned}$$

the corresponding pole is at

$$\gamma\rho-\beta\sigma+(\alpha-\delta)v=0. \qquad (24)$$

A precise formula giving (M_1,M_2,M_3) in terms of the moduli and charges can be found in [25]. We should keep in mind, however, that the result is independent of (M_1,M_2,M_3) as long as changing them does not make the contour cross a pole.

On the black hole (macroscopic) side, these jumps correspond to (dis-)appearance of two-centered black holes as we cross walls of marginal

stability. There is a precise match between the B_6 index of 2-centered black holes carrying charges given on the right hand side of (23), and the change in $B_6(Q,P)$ computed from the residues at the poles (24) [24,25].

In this context, we would like to mention that the changes in the index across the walls of marginal stability are subleading, as these give corrections which grow as exponentials of single power of the charges. This is related to the fact that only decays of a 1/4-BPS dyon into half-BPS dyons contribute to the wall crossing in an $\mathcal{N}=4$ supersymmetric string theory [26,38,48]. However the contribution from the multi-centered solutions can become significant when we study dyons in $\mathcal{N}=2$ supersymmetric string theories [60].

2.5. Other duality orbits

We have already said that the results given above are valid for a subset of dyons satisfying the condition (5). These can be related via duality transformation to the D1-D5-p-KK system analyzed here. But we would like to see if we can say something about the dyons which are outside these duality orbits, i.e., which have[22]

$$\gcd\{Q_iP_j - Q_jP_i\,, \quad 1\le i,j\le 28\} = r\,, \qquad (25)$$

for some integer $r>1$. These dyons can be related to a system of IIB on $K3\times S^1\times \widetilde{S}^1$ with [22,31,32]

1. 1 KK monopole along $\widetilde{S}^1$,
2. r D5-branes wrapped on $K3\times S^1$,
3. $(\widetilde{Q}_1+1)\,r$ D1-branes wrapped on S^1,
4. $-n$ units of momentum along S^1,
5. rJ units of momentum along $\widetilde{S}^1$.

If we can compute the B_6 index for these dyons, we can use this to compute the B_6 index of any other dyon. This has not yet been done from first principles, but a guess has been made by requiring that wall crossing is controlled by the residues at the poles of the partition function as in the $r=1$ case. In the domain of the moduli space where 2-centered black holes are absent, the proposal for the B_6 index for these dyons is [35]

$$\sum_{s|r} s\, B_6\left(\widetilde{Q}_1\frac{r}{s}, n, J\frac{r}{s}\right)\,, \qquad (26)$$

where $B_6(\widetilde{Q}_1,n,J)$ is the function defined in (14). An effective string model for arriving at this result has been suggested in [37], but this has not been derived completely from first principles. Note that for large charges, the contribution from the $s>1$ terms grow as $\exp(\pi\sqrt{Q^2P^2-(Q\cdot P)^2}/s)$ and hence are exponentially suppressed compared to the leading $s=1$ term. Thus the result for the index reduces to that for the $r=1$ case up to exponentially suppressed corrections.

2.6. Generalization I: Twisted index

Let us take type IIB theory on $K3\times S^1\times\widetilde{S}^1$. On special subspaces of the moduli space of $K3$, we encounter enhanced discrete symmetries which preserve the holomorphic (2,0)-form on $K3$ [73,74]. Thus these symmetries commute with supersymmetry. Let us work on such a subspace of the moduli space with a $\mathbb{Z}_N$ discrete symmetry generated by g. In this subspace, we can define a twisted index:

$$B_6^g = \frac{1}{6!}Tr\{(-1)^F(2h)^6 g\}\,. \qquad (27)$$

This can be calculated using the same method described earlier by keeping track of the g quantum numbers of the various modes contributing to the partition function. The final result takes the form [51]:

$$\begin{aligned} B_6^g(Q,P) \;&=\; \int_C d\rho d\sigma dv\, e^{-\pi i(P^2\rho+Q^2\sigma+2Q.Pv)}\, Z^g \\ &\quad\times\;\; (-1)^{Q.P}, \end{aligned} \qquad (28)$$

where the functions Z^g are known explicitly. They also turn out to have nice modular properties and poles in the complex (ρ,σ,v) space.[7] As a result, we can find the behaviour of this

[7] General discussion on such modular forms can be found in [75–82].

index for large charges by the same method described earlier. The important difference is that now there are no poles at (24). Instead the poles are at [51]

$$\begin{aligned} & n_2(\rho\sigma - v^2) - m_1\rho + n_1\sigma + m_2 + jv = 0\,, \\ & m_1 n_1 + m_2 n_2 + \frac{1}{4}j^2 = \frac{1}{4}\,, \\ & m_1, n_1, m_2 \in \mathbb{Z}\,, \quad j \in 2\,\mathbb{Z}+1\,, \quad n_2 \in N\,\mathbb{Z}\,. \end{aligned} \tag{29}$$

The leading contribution now comes from the poles at (29) with $n_2 = N$, and the answer in the large charge limit is [51]:

$$\ln|B_g^6(Q,P)| = \pi\sqrt{Q^2P^2-(Q.P)^2}/N + \mathcal{O}(1)\,. \tag{30}$$

A macroscopic explanation of this result will be given in §4.1.

2.7. Generalization II: CHL models

We again start with type IIB string theory on $K3 \times S^1 \times \widetilde{S}^1$ with a $\mathbb{Z}_M$ symmetry generated by $\widetilde{g}$ as described in §2.6, but this time we take an orbifold of this theory by $\widetilde{g}$ accompanied by $2\pi/M$ shift along S^1.[8] This generates a new class of $\mathcal{N}=4$ supersymmetric string theories known as CHL models [83,84]. The orbifold operation removes some of the $U(1)$ gauge fields. Thus, in general, CHL models have $(r+6)$ U(1) gauge fields with $r < 22$, and Q and P are $(r+6)$ dimensional vectors.[9] The precise value of r depends on M, – the order of the orbifold group. The T-duality group is a discrete subgroup of $O(6,r)$ with Q and P transforming as vectors of $O(6,r)$. Thus $O(6,r)$ invariant bilinears Q^2, P^2 and $Q\cdot P$ are T-duality invariants.

In this theory we can take the same D1-D5-KK monopole system as considered earlier since all of these configurations, as well as momenta along S^1 and $\widetilde{S}^1$, are invariant under the orbifold group. The index B_6 in this theory can be calculated in the same way as before, keeping track of the $\widetilde{g}$ quantum numbers of the various modes, and the effect of the orbifold projection. The result of this computation is [17]:

$$\begin{aligned} B_6(Q,P) &= \int_C d\rho d\sigma dv\, e^{-\pi i(P^2\rho + Q^2\sigma + 2Q.Pv)}\, \widetilde{Z}^g \\ &\quad \times \ (-1)^{Q.P}\,, \end{aligned} \tag{31}$$

where $\widetilde{Z}^g(\rho,\sigma,v)$ is yet another new function, also with nice modular properties and poles in the (ρ,σ,v) space. We find that its behaviour for large charges is given by:

$$\begin{aligned} \ln|B_6(Q,P)| &= \pi\sqrt{Q^2P^2-(Q.P)^2} \\ &\quad -\phi\left(\frac{Q.P}{P^2}, \sqrt{\frac{Q^2P^2-(Q.P)^2}{P^2}}\right) \\ &\quad +\mathcal{O}\left(\frac{1}{Q^2,P^2,Q.P}\right)\,, \end{aligned} \tag{32}$$

where

$$\begin{aligned} \phi(\tau_1,\tau_2) &\equiv (k+2)\ln\tau_2 + \ln\ g(\tau_1+i\tau_2) \\ &\quad + \ln\ g(-\tau_1+i\tau_2)\,. \end{aligned} \tag{33}$$

Here k are known numbers and $g(\tau)$ are known functions, depending on the choice of M. This generalizes (19). Furthermore, in each case we have $B_6(Q,P) < 0$. The macroscopic origin of (32) will be explained in §3.4, and the macroscopic explanation of the sign of B_6 will be given in §3.7.

Note that unlike in the case of heterotic string theory on T^6, in this case the duality orbits have not been completely classified. As a result, two vectors with the same values of Q^2, P^2 and $Q\cdot P$ are not necessarily related by a duality transformation. Our result for the index, given in (31), holds only for those charge vectors which can be related by a duality transformation to the specific D1-D5-KK monopole system for which we have carried out our analysis.

2.8. Generalization III: Twisted index in CHL models

Next we consider a special subspace of the moduli space on which type IIB string theory on $K3 \times S^1 \times \widetilde{S}^1$ has a $\mathbb{Z}_M \times \mathbb{Z}_N$ discrete symmetry that commutes with supersymmetry. Let $\widetilde{g}$ and g be the generators of $\mathbb{Z}_M$ and $\mathbb{Z}_N$ respectively. Let us now take an orbifold of this theory

[8] The $\mathbf{Z}_M$ symmetries are chosen from the same set as the $\mathbf{Z}_N$ symmetries of the §2.6, but we are using a different label since in the next section we shall combine the analysis of §2.6 and this subsection.

[9] Since 6 of the U(1) gauge fields represent graviphoton fields, they must exist in all $\mathcal{N}=4$ supersymmetric string theories.

by a $\mathbb{Z}_M$ symmetry generated by $\widetilde{g}$ together with $1/M$ unit of shift along S^1. Here g still generates a symmetry of the theory. We now define:

$$B_6^g = \frac{1}{6!}\, Tr\{(-1)^F (2h)^6 g\}\,. \tag{34}$$

The computation of the above index gives the result [52]

$$\begin{aligned} B_6^g(Q,P) &= \int_C d\rho d\sigma dv\, e^{-\pi i(P^2\rho+Q^2\sigma+2Q.Pv)}\, \widehat{Z}^{g,\widetilde{g}} \\ &\quad (-1)^{Q.P}\,, \end{aligned} \tag{35}$$

where $\widehat{Z}^{g,\widetilde{g}}$ is yet another set of functions, also with nice modular properties and poles in the complex (ρ,σ,v) space. Its behaviour for large charges is found to be

$$\ln|B_6^g(Q,P)| = \pi\sqrt{Q^2P^2-(Q.P)^2}/N + \mathcal{O}(1)\,. \tag{36}$$

A macroscopic explanation of this result will be given in §4.1.

2.9. Generalization IV: Twisted index in type II string compactification

The analysis described above has also been generalized to untwisted and twisted indices in type II string compactifications on T^6 and its asymmetric orbifolds. We shall not describe the analysis here; they can be found in [18,19,51,52]. The general feature of all these models is that a $\mathbb{Z}_N$ twisted index B_6^g grows as

$$\ln|B_6^g(Q,P)| = \pi\sqrt{Q^2P^2-(Q.P)^2}/N + \mathcal{O}(1)\,. \tag{37}$$

This includes the case of $N = 1$, i.e., the untwisted index, for which $\ln|B_6(Q,P)| \simeq \pi\sqrt{Q^2P^2-(Q.P)^2}$. Macroscopic explanation for these results is the same as that for the black holes in heterotic string theories, and hence we shall not discuss these cases separately.

A special mention must be given to the untwisted index in type II string theory on T^6. This theory has $\mathcal{N}=8$ supersymmetry and the black holes with finite area event horizon are 1/8-BPS. Thus the relevant helicity trace index is B_{14}. For states carrying only NS-NS sector charges (and those related to these by duality symmetry), we can again label the charges by a pair of vectors (Q,P), representing the electric and magnetic charges respectively. In the $r=1$ sector defined in (5), the result for this index is known in terms of Fourier coefficeints of an appropriate combination of Jacobi theta function and Dedekind eta function [11,13,36,85]. For large charges, we get [86]

$$\begin{aligned} \ln|B_{14}(Q,P)| &\simeq \pi\sqrt{Q^2P^2-(Q.P)^2} \\ &\quad -2\ln\left[Q^2P^2-(Q.P)^2\right] \\ &\quad +\mathcal{O}(\text{charge}^{-2})\,. \end{aligned} \tag{38}$$

Note that there is a logarithmic correction to the entropy, which was absent in the other cases discussed so far. So far this logarithmic term has not been reproduced from direct macroscopic analysis. Some discussion on this can be found in §4.2.

3. Macroscopic analysis

Our next goal is to

- develop tools for computing the entropy of extremal black holes including stringy and quantum corrections,
- relate this entropy to the helicity trace index,
- apply it to black holes carrying the same charges for which we have computed the microscopic index, and
- compare the macroscopic results with the microscopic results.

In this section, we shall mainly address the first and the second issues, i.e., find a general formula for computing the black hole degeneracy and the helicity trace on the macroscopic side. Some aspects of the third and the fourth issues will be discussed in §3.4, but we postpone the major part of this to §4. Since AdS_2 space will play a crucial role in our analysis, we begin by describing some aspects of AdS_2 space.

3.1. What is AdS_2 ?

Take a three dimensional space labelled by coordinates (x,y,z) and metric

$$ds^2 = dx^2 - dy^2 - dz^2\,. \tag{39}$$

AdS_2 may be regarded as a two dimensional Lorentzian space embedded in this 3-dimensional space via the relation:

$$x^2 - y^2 - z^2 = -a^2\,, \tag{40}$$

where a is some constant giving the radius of AdS_2. Clearly, this space has an SO(2,1) isometry.

Introducing the independent coordinates (η, t) such that

$$x = a\,\sinh\eta\cosh t\,,\; y = a\,\cosh\eta\,,$$
$$z = a\,\sinh\eta\sinh t\,, \tag{41}$$

we can write

$$dx^2 - dy^2 - dz^2 = a^2(d\eta^2 - \sinh^2\eta\, dt^2)\,. \tag{42}$$

Finally, defining

$$r = \cosh\eta\,, \tag{43}$$

the metric for AdS_2 can be expressed as:

$$ds^2 = a^2\left[\frac{dr^2}{r^2-1} - (r^2-1)dt^2\right], \quad r \geq 1\,. \tag{44}$$

Using a change of coordinates, one can show that the apparent singularity at $r = 1$ is a coordinate singularity, and one can continue the space-time beyond $r = 1$ to generate what is known as global AdS_2 space-time. This will not play any direct role in our subsequent discussion.

3.2. Why AdS_2 ?

The reason that AdS_2 plays an important role for extremal black holes is that all known black holes develop an AdS_2 factor in their near horizon geometry in the extremal limit. In particular, the time translation symmetry gets enhanced to the $SO(2,1)$ isometry of AdS_2. We shall illustrate how this happens by considering the example of Reissner-Nordstrom solution in $D = 4$. This is described by the metric

$$\begin{aligned} ds^2 &= -(1-\rho_+/\rho)(1-\rho_-/\rho)d\tau^2 \\ &\quad + \frac{d\rho^2}{(1-\rho_+/\rho)(1-\rho_-/\rho)} \\ &\quad + \rho^2(d\psi^2 + \sin^2\psi d\phi^2)\,. \end{aligned} \tag{45}$$

Here $\rho_\pm$ are parameters determined in terms of the mass and charges carried by the black hole. In the extremal limit, $\rho_- \to \rho_+$. In order to take this limit, we define:

$$2\lambda = \rho_+ - \rho_-, \quad t = \frac{\lambda\,\tau}{\rho_+^2}, \quad r = \frac{2\rho - \rho_+ - \rho_-}{2\lambda}\,, \tag{46}$$

and take $\lambda \to 0$ limit keeping r, t fixed. In this limit, the metric takes the form [87–89]:

$$\begin{aligned} ds^2 &= \rho_+^2\left[-(r^2-1)dt^2 + \frac{dr^2}{r^2-1}\right] \\ &\quad + \rho_+^2(d\psi^2 + \sin^2\psi d\phi^2)\,. \end{aligned} \tag{47}$$

This describes the space $AdS_2 \times S^2$. One can also verify that, in this limit, the near horizon electric and magnetic fields are invariant under the isometries of $AdS_2 \times S^2$.

We will now postulate that *any extremal black hole has an AdS_2 factor / $SO(2,1)$ isometry in the near horizon geometry.* This postulate has been partially proved in [90,91]. The full near horizon geometry takes the form $AdS_2 \times K$, where K is some compact space. K includes not only the compact space on which string theory is compactified (to get a four dimensional theory), but also the angular coordinates (*e.g.* the S^2 factor for spherically symmetric black holes in four dimensions).

3.3. Higher derivative corrections

In string theory, we expect the Bekenstein-Hawking formula for the black hole entropy to receive

- higher derivative corrections arising in classical string theory, and
- quantum corrections.

Of these, the higher derivative corrections are captured by Wald's general formula for black hole entropy in any general coordinate invariant classical theory of gravity [92–95]. Furthermore, this formula takes a very simple prescription for black holes with an AdS_2 factor in the near horizon geometry [96–98]. We shall illustrate this in the context of spherically symmetric black holes in four dimensional theories. In this case, the near horizon geometry has an $AdS_2 \times S^2$ factor. Consider an arbitrary general coordinate invariant theory of gravity coupled to a set of gauge fields

$A^{(i)}_\mu$ and neutral scalar fields $\{\phi_s\}$. The most general form of the near horizon geometry of an extremal black hole, consistent with the symmetry of $AdS_2 \times S^2$, is:

$$\begin{aligned} ds^2 \equiv g_{\mu\nu}dx^\mu dx^\nu = v_1 \left(-(r^2-1)dt^2 + \frac{dr^2}{r^2-1}\right) \\ + v_2 \left(d\psi^2 + \sin^2\psi d\phi^2\right) , \\ \phi_s = u_s \,, \quad F^{(i)}_{rt} = e_i \,, \quad F^{(i)}_{\psi\phi} = \frac{p_i}{4\pi}\sin\psi \,, \end{aligned} \tag{48}$$

where v_1, v_2, $\{u_s\}$, $\{e_i\}$ and $\{p_i\}$ are constants. For this background, the components of the Riemann tensor are given by:

$$\begin{aligned} R_{\alpha\beta\gamma\delta} &= -v_1(g_{\alpha\gamma}\, g_{\beta\delta} - g_{\alpha\delta}\, g_{\beta\gamma}) \,, \\ R_{mnpq} &= v_2(g_{mp}\, g_{nq} - g_{mq}\, g_{np}) \,, \end{aligned} \tag{49}$$

where $\{\alpha,\beta,\gamma,\delta = r,t\}$ and $\{m,n,p,q = \psi,\phi\}$. The covariant derivatives of the Riemann tensor, scalar fields and gauge field strengths vanish.

Let $\sqrt{-\det g}\,\mathcal{L}$ be the Lagrangian density evaluated in the background (48). We define the functions:

$$\begin{aligned} f(\vec{u},\vec{v},\vec{e},\vec{p}) &\equiv \int d\psi\, d\phi\, \sqrt{-\det g}\,\mathcal{L} \,, \\ \mathcal{E}(\vec{u},\vec{v},\vec{e},\vec{q},\vec{p}) &\equiv 2\,\pi\{\, e_i\, q_i - f(\vec{u},\vec{v},\vec{e},\vec{p})\} \,. \end{aligned} \tag{50}$$

Then for an extremal black hole of electric charge $\vec{q}$ and magnetic charge $\vec{p}$, one finds that [96]

1. the values of $\{u_s\}$, $\{e_i\}$, v_1 and v_2 are obtained by extremizing $\mathcal{E}(\vec{u},\vec{v},\vec{e},\vec{q},\vec{p})$ with respect to these variables:

$$\frac{\partial\mathcal{E}}{\partial u_s} = 0 \,, \ \frac{\partial\mathcal{E}}{\partial v_1} = 0 \,, \ \frac{\partial\mathcal{E}}{\partial v_2} = 0 \,, \ \frac{\partial\mathcal{E}}{\partial e_i} = 0 \,; \tag{51}$$

2. the Wald entropy of the black hole is given by

$$S_{BH} = \mathcal{E} \,, \tag{52}$$

at the extremum.

Eqs.(51) follows from the equations of motion and the definition of the electric charge, while (52) follows from Wald's formula for the black hole entropy.

These results provide us with [96–98]

1. an algebraic method for computing the entropy of extremal black holes without solving any differential equation;

2. a proof of the attractor mechanism [99–102], i.e., the black hole entropy is independent of the asymptotic moduli.

However, this approach does not prove the existence of an extremal black hole carrying a given set of charges; it works assuming that the solution exists.

3.4. Quantum corrections: A first look

Next we must address the effect of quantum corrections on the black hole entropy. The first guess would be that we should apply Wald's formula again, but replacing the classical action by the one particle irreducible (1PI) action. This will again give a simple algebraic method for computing the entropy once we compute the 1PI action. However, this prescription is not complete since the 1PI action typically has non-local contribution due to massless states propagating in the loops. In contrast, Wald's formula is valid for theories with local Lagrangian density. This is apparent in (50) where the definition of the function f requires explicit knowledge of the local Lagrangian density $\mathcal{L}$.

Nevertheless, this procedure has been used to compute corrections to black hole entropy from local terms in the 1PI action with significant success [103–112]. If we consider the CHL models obtained by $\mathbb{Z}_N$ orbifold of type IIB on $K3\times S^1\times\widetilde{S}^1$, then at tree level there are no corrections to the black hole entropy from the four derivative terms in the effective action. But at one loop, these theories get corrections proportional to the Gauss-Bonnet term in the 1PI action[113,55]:

$$\begin{aligned} \sqrt{-\det g}\;\Delta\mathcal{L} &= -\frac{\sqrt{-\det g}}{64\pi^2}\,\phi(\tau,\bar\tau)\{R^2 \\ &\quad -4R_{\mu\nu}\,R^{\mu\nu} + R_{\mu\nu\rho\sigma}\,R^{\mu\nu\rho\sigma}\} \,, \end{aligned} \tag{53}$$

where τ is the modulus of the torus $(S^1\times\widetilde{S}^1)$ and ϕ is the same function that appeared in (33). Adding this correction to the supergravity action,

we find that the Wald entropy of a black hole in the CHL model is given by [88]

$$\begin{aligned} S_{BH} &= \pi\sqrt{Q^2P^2-(Q.P)^2} \\ &\quad -\phi\left(\frac{Q.P}{P^2}, \sqrt{\frac{Q^2P^2-(Q.P)^2}{P^2}}\right) \\ &\quad +\mathcal{O}\left(\frac{1}{Q^2, P^2, Q.P}\right), \end{aligned} \tag{54}$$

in exact agreement with the result (32) for $\ln|B_6(Q,P)|$ for large charges.[10]

3.5. Quantum corrections to horizon degeneracy

Let us denote by d_{hor} the degeneracy associated with the horizon of an extremal black hole. We shall now turn to the full quantum computation of d_{hor} from the macroscopic side, and describe a proposal for computing quantum corrected entropy in terms of a path integral of string theory in this near horizon geometry [117,118]. The steps for computing d_{hor} are as follows:

1. Go to the Euclidean formalism by the replacement $t \to -i\theta$ and represent the AdS_2 factor by the metric:

$$\begin{aligned} & ds^2 = v\left((r^2-1)\,d\theta^2 + \frac{dr^2}{r^2-1}\right), \\ & \text{where} \quad 1 \le r < \infty, \quad \theta \equiv \theta + 2\pi\,. \end{aligned} \tag{55}$$

With $r = \cosh\eta = (1+\rho^2)/(1-\rho^2)$ as the change of variable , we get the metric on a unit disk:

$$\begin{aligned} ds^2 &= v\left(\sinh^2\eta\; d\theta^2 + d\eta^2\right) \\ &= \frac{4v}{(1-\rho^2)^2}(d\rho^2 + \rho^2 d\theta^2), \\ \text{where} &\qquad 0 \le \eta < \infty, \quad 0 \le \rho < 1\,. \end{aligned} \tag{56}$$

2. Regularize the infinite volume of AdS_2 by putting a cut-off $r \le r_0 f(\theta)$, for some smooth periodic function $f(\theta)$. This makes the AdS_2 boundary have a finite length L.

3. Define:

$$Z_{AdS_2} \equiv \left\langle \exp[-iq_k \oint d\theta\, A_\theta^{(k)}] \right\rangle, \tag{57}$$

where the symbol $\langle\ \rangle$ denotes the unnormalized path integral over string fields in the Euclidean near horizon background geometry weighted by exp[−Action]. Here $\{q_k\}$ stands for the electric charges carried by the black hole, representing the electric fluxes of the U(1) gauge fields $A^{(k)}$'s through AdS_2. The integral $\oint$ runs over the boundary of the infrared regulated AdS_2.

Note that near the boundary of AdS_2, the θ-independent solution to the Maxwell's equations has the form:

$$A_r = 0, \quad A_\theta = C_1 + C_2 r\,, \tag{58}$$

where C_1 (chemical potential) represents a normalizable mode and C_2 (electric charge) represents a non-normalizable mode. Hence the path integral (57) must be carried out keeping C_2 (charge) fixed and integrating over C_1 (chemical potential).[11] Another way to motivate this is the following: in AdS_2, if we try to add charge/mass, it will destroy the asymptotic boundary conditions as it is a two dimensional spacetime. With this new rule, the first order variation of the action will contain a boundary term besides the terms proportional to the equations of motion. This boundary term must be cancelled by some other term in order to have a well-defined path integral. The boundary term $\exp[-iq_k \oint d\theta\, A_\theta^{(k)}]$ precisely serves this purpose.

4. Now, by AdS_2/CFT_1 correspondence, string theory on $AdS_2 \times K$ must be dual

[10] In fact the original computation involved a more refined version of the 1PI action, where the complete supersymmetric completion of the curvature squared terms in the 1PI action was included in the computation [104–112,114–116]. Surprisingly, the result is the same as in (54). Nevertheless, there can be additional four derivative corrections to the action which could give additional contribution to the entropy to this order. One expects that a suitable non-renormalization theorem will make these additional contributions vanish, but this has not been proven so far.

[11] This is different from the standard rules in higher dimensional space-time where the asymptotic value of the gauge field is held fixed.

to a one dimensional conformal field theory, which we shall call CFT_1, living on the boundary of AdS_2. Furthermore, we must have[12]

$$Z_{AdS_2} = Z_{CFT_1} = Tr(e^{-LH}) \,, \tag{59}$$

where H is the Hamltonian of CFT_1 and L is the length of the boundary circle of the infrared regulated AdS_2. The standard rule of AdS/CFT correspondence also gives us some insight into how to identify the CFT_1, – it must be given by the infrared limit of the quantum mechanics that describes the black hole microstates. Now in all known examples, including the ones discussed in §2, the quantum mechanics describing the dynamics of the microscopic system has a finite gap that separates the ground states from the first excited state.[13] Thus in the infrared limit ($L \to \infty$), only the ground states of this quantum mechanics (in a fixed charge sector) survive, and CFT_1 will consist of a finite number d_0 of degenerate ground states of some energy E_0. This gives, from (59),

$$Z_{AdS_2} = d_0 \, e^{-L\,E_0} \,. \tag{60}$$

This suggests that we define d_{hor} to be the finite part of Z_{AdS_2}, defined by expressing Z_{AdS_2} as

$$Z_{AdS_2} = e^{CL+O(L^{-1})} \times d_{hor} \,, \quad \text{as } L \to \infty \,. \tag{61}$$

Here C is a constant. The above definition of d_{hor} will be called the *quantum entropy function*.

5. Finally we note that, since the AdS_2 path integral is evaluated by keeping fixed the asymptotic value of the electric field (and hence the electric charge for a given action), the AdS_2 path integral computes the entropy in the microcanonical ensemble where all the charges are fixed.

One of the consistency tests this proposal must satisfy is that, in the classical limit, it should reproduce the exponential of the Wald entropy. This can be seen as follows: In the classical limit,

$$\begin{aligned} Z_{AdS_2} &= \exp[-\text{Action} - iq_k \oint d\theta \, A^{(k)}_\theta] \Big|_{classical} \\ &= e^{\int dr d\theta \, \{\sqrt{\det g_{AdS_2}} \mathcal{L}_{AdS_2} - iq_k F^{(k)}_{r\theta}\}} , \end{aligned} \tag{62}$$

where g_{AdS_2} is the metric on AdS_2, and $\mathcal{L}_{AdS_2}$ is the two dimensional Lagrangian density obtained after dimensional reduction on K and is evaluated on the near horizon geometry.[14] Taking the infrared cut-off to be $\eta \le \eta_0$ for simplicity, using the Euclidean version of the near horizon background given in (48), and evaluating the r, θ integral, we get,

$$\begin{aligned} Z_{AdS_2} &= e^{-2\pi\left(q_i e_i - \sqrt{\det g_{AdS_2}}\, \mathcal{L}_{AdS_2}\right)(\cosh\eta_0 - 1)} \\ &= e^{2\pi\left(q_i e_i - \sqrt{\det g_{AdS_2}}\, \mathcal{L}_{AdS_2}\right) + CL + \mathcal{O}(L^{-1})} \\ &= e^{S_{wald} + CL + \mathcal{O}(L^{-1})} \,, \end{aligned} \tag{63}$$

where

$$L = \sqrt{v} \, \sinh\eta_0 \Rightarrow \cosh\eta_0 = L/\sqrt{v} + \mathcal{O}(L^{-1}) \,. \tag{64}$$

The constant C can receive additional corrections from boundary terms in the action which we have ignored. The important point is that these boundary terms do not affect the value of the finite part, and hence d_{hor} is well defined.

This establishes that $d_{hor} = \exp[S_{wald}]$ in the classical limit.

We conclude this section with two comments:

- By choosing the boundary terms appropriately, we could cancel the constant C and reinterprete the full partition function Z_{AdS_2} as d_{hor}. In the dual CFT_1, this corresponds to shifting the ground state energy by adding appropriate counterterms.

[12] We emphasize that here, since the boundary theory is on a circle, its partition function can be given a Hilbert space interpretation. This is not possible in higher dimensional AdS_{d+1} spaces where the boundary theory lives on S^d.

[13] Even though the dynamics was described by a two dimensional CFT, the CFT was compactified on a circle of finite size, and hence had a gap in its spectrum.

[14] Note that the Euclidean action is given by $-\int dr d\theta \sqrt{g_{AdS_2}} \mathcal{L}$, where $\mathcal{L}$ is the analytic continuation of the Lagrangian density for Lorentzian signature.

- Our interpretation of the AdS_2 partition function as the degeneracy associated with the horizon is based on representing Euclidean AdS_2 as a disk with a single boundary. If instead we represent it as a strip with two boundaries, with the help of the standard conformal transformation $\tan\frac{w}{2} = \frac{z-1}{z+1}$, mapping the unit disk in the $z = \rho\, e^{i\theta}$ plane to a strip in the w plane, then we have two copies of CFT_1 living on the two boundaries of the strip, each with degeneracy d_{hor}. Standard argument [119] shows that the Hartle-Hawking state of this system will represent the maximally entangled state between these two copies of the CFT_1, and as a result, d_{hor} can be reinterpreted as the entanglement entropy between the two boundaries in this state. This has been verified explicitly in [120] in the classical limit.

3.6. Hair contribution

In general, the macroscopic degeneracy, denoted by d_{macro}, can have two kinds of contributions [121,122]:

1. From the the degrees of freedom living on the horizon.

2. From the degrees of freedom living outside the horizon (hair) [121,122].[15]

Denoting the degeneracy associated with the horizon degrees of freedom by d_{hor} and those associated with the hair degrees of freedom by d_{hair}, we can write down a general formula for d_{macro}:

$$d_{macro}(\vec{Q}) = \sum_n \sum_{\substack{\{\vec{Q}_i\},\vec{Q}_{hair} \\ \Sigma_{i=1}^n \vec{Q}_i+\vec{Q}_{hair}=\vec{Q}}} \left\{\prod_{i=1}^n d_{hor}(\vec{Q}_i)\right\} \times d_{hair}(\vec{Q}_{hair};\{\vec{Q}_i\})\,. \tag{65}$$

The nth term in the sum represents the contribution from an n-centered black hole, $\vec{Q}_i$ denotes the charge carried by the i-th center and $\vec{Q}_{hair}$ denotes the charges carried by the hair modes.[16] In principle, d_{hair} can be calculated by explicitly identifying and quantizing the hair modes. On the other hand, $d_{hor}(\vec{Q}_i)$ for each center can be computed using the quantum entropy function formalism described in §3.5.

3.7. Degeneracy to index

As discussed before, on the microscopic side we usually compute an index. On the other hand, d_{hor} computes degeneracy. More generally, eq.(65) gives us a general formula for computing the degeneracy on the macroscopic side. Thus this cannot be directly compared with the B_6 index computed on the microscopic side.

We shall now describe a strategy for using d_{hor} to compute the index on the macroscopic side [118,123]. We shall illustrate this for the helicity trace B_n for four dimensional black holes, but it can be generalized to five dimensional black holes as well [124]. For a black hole that breaks $2k$ supercharges, we had defined

$$B_k = \frac{1}{k!}\, Tr\{(-1)^{2h}(2h)^k\}\,, \tag{66}$$

where h is the third component of angular momentum in the rest frame. Since the total contribution to h can be regarded as a sum of the contributions from the horizon and the hair degrees of freedom, we can express B_k as

$$B_{k;macro} = \frac{1}{k!} Tr\{(-1)^{2(h_{hor}+h_{hair})}(2h_{hor}+2h_{hair})^k\},$$

where h_{hor} and h_{hair} denote the contribution to h from the horizon and the hair degrees of freedom respectively.

Now, typically all the fermion zero modes associated with the broken supersymmetries are hair degrees of freedom, since we can generate these zero mode deformations by supersymmetry transformation parameters which go to constant at infinity and vanish below a certain radius. Thus the hair modes contain $2k$ fermion zero modes, and in order that the trace over these zero modes do not

[15] For example, the fermion zero modes associated with the broken supersymmetry generators are always part of the hair modes, since the effect of supersymmetry-breaking by the classical black hole solution can be felt outside the horizon of the black hole.

[16] In this section we shall use $\vec{Q}$ to denote all the electric and all the magnetic charges, as well as the angular momentum.

make the whole trace vanish, we need an insertion of $(2h_{hair})^k$ into the trace. In other words, if we expand the $(2h_{hor}+2h_{hair})^k$ factor in a binomial expansion, then only the $(2h_{hair})^k$ term will contribute. This gives

$$\begin{aligned} B_{k;macro} &= \frac{1}{k!}Tr\{(-1)^{2h_{hor}+2h_{hair}}(2h_{hair})^k\} \\ &= \sum B_{0;hor}\times B_{k;hair}\,. \end{aligned} \tag{67}$$

This can be expanded in the spirit of (65) as

$$\begin{aligned} B_{k;macro}(\vec{Q}) = \sum_n \sum_{\{\vec{Q}_i\},\vec{Q}_{hair}} \left\{\prod_{i=1}^n B_{0;hor}(\vec{Q}_i)\right\} \\ \times B_{k;hair}(\vec{Q}_{hair};\{\vec{Q}_i\}), \\ \text{with the constraint} \quad \sum_{i=1}^n \vec{Q}_i+\vec{Q}_{hair}=\vec{Q}\,. \end{aligned} \tag{68}$$

where now the vector $\vec{Q}$ no longer contains the angular momentum. A further simplification follows from the fact that in four dimensions, only the $h_{hor}=0$ black holes are supersymmetric. This is of course known to be true for a classical black hole, but more generally it follows from the fact that unbroken supersymmetries, together with the $SL(2,R)$ isometry of the near horizon geometry, generate the full $SU(1,1|2)$ supergroup which includes $SU(2)$ as a symmetry group. This implies a spherically symmetric horizon, and hence zero angular momentum since the partition function on AdS_2 computes the entropy in a fixed angular momentum sector (microcanonical ensemble). Thus $B_{0;hor}=Tr_{hor}(1)=d_{hor}$, and we can express (68) as

$$\begin{aligned} B_{k;macro}(\vec{Q}) &= \sum_n \sum_{\substack{\{\vec{Q}_i\},\vec{Q}_{hair}\\ \sum_{i=1}^n \vec{Q}_i+\vec{Q}_{hair}=\vec{Q}}} \prod_{i=1}^n d_{hor}(\vec{Q}_i) \\ &\quad \times B_{k;hair}(\vec{Q}_{hair};\{\vec{Q}_i\})\,. \end{aligned} \tag{69}$$

Most of our analysis involves 1/4-BPS black holes in $\mathcal{N}=4$ supersymmetric string theories in $D=4$ which preserves 4 out of 16 supersymmetries, i.e., such a black hole configuration breaks 12 supersymmetries. Thus the relevant helicity trace index is B_6. In these theories, the contribution from multi-centered black holes is known to be exponentially suppressed [26,38,48]. Furthermore, for single-centered black holes, often the only hair modes are the fermion zero modes. In this case, $\vec{Q}_{hair}=0$. Furthermore, since for each pair of fermion zero modes $Tr\{(-1)^F(2h)\}=i$, we have $B_{6;hair}=i^6=-1$. Thus

$$B_{6;macro}(\vec{Q}) = -d_{hor}(\vec{Q})\,, \tag{70}$$

up to exponentially suppressed contribution from multi-centered black holes. This explains how we can compare the helicity trace index computed in the microscopic theory with d_{hor} computed in the macroscopic theory. Note that since $d_{hor}(\vec{Q})>0$, we get $B_{6;macro}<0$. This agrees with the explicit microscopic results stated above (19) and below (33).

4. Applications of quantum entropy function

Eq.(54) shows how Wald's formula applied to 1PI action can be used to calculate some of the subleading corrections to the black hole entropy, and reproduce the results known from microscopic computation. Since quantum entropy function reduces to the exponential of Wald entropy in the classical limit, we expect that as long as the quantum corrections generate a local contribution to the 1PI action, Wald's formula applied to 1PI action and quantum entropy function will give the same results. In this section, we shall describe how quantum entropy function can be used to compute some other corrections to the entropy which could not be calculated by direct use of Wald's formula.

4.1. Computation of twisted index

Suppose we have a $\mathbb{Z}_N$ symmetry generated by g that commutes with all the supersymmetries of an $\mathcal{N}=4$ supersymmetric string theory. We can then define a twisted index:

$$B_6^g = \frac{1}{6!}Tr\{(-1)^{2h}(2h)^6 g\}\,. \tag{71}$$

In §2.6 and §2.8, we described the results for such indices in a wide variety of $\mathcal{N}=4$ supersymmetric

string theories. We shall now describe how to compute them from the macroscopic side.

We proceed as in §3.7. After separating out the contribution from the hair degrees of freedom, we see that the relevant quantity associated with the horizon is

$$Tr_{hor}\{(-1)^{2h_{hor}}g\} = Tr_{hor}(g)\,, \tag{72}$$

since $h_{hor} = 0$ for a supersymmetric black hole. By following the logic of AdS/CFT correspondence, we find that d_{hor} is now given by the finite part of a twisted partition function

$$Z_g = \left\langle \exp[-iq_k \oint d\theta\, A^{(k)}_\theta] \right\rangle_g\,, \tag{73}$$

where the subscript g denotes that in carrying out the path integral, we are instructed to integrate over field configurations with a g-twisted boundary condition on the fields under $\theta \to \theta + 2\pi$. Other than this, the asymptotic boundary conditions must be identical to that of the attractor geometry since the charges have not changed.

From the Euclidean AdS_2 metric given in (55), we find that the circle at infinity, parametrized by θ, is contractible at the origin $r = 1$. Thus a g-twist under $\theta \to \theta + 2\pi$ is not admissible. Hence we conclude that the $AdS_2 \times S^2$ geometry is not a valid saddle point of the path integral. This however is not the end of the story, since according to the rules of quantum gravity we must sum over all geometries and field configurations keeping fixed the asymptotic boundary conditions. Thus we should investigate if there are other saddle points which could contribute to the path integral. To find out possible candidates, we must keep in mind the following constraints:

1. It must have the same asymptotic geometry as the $AdS_2 \times S^2$ geometry.
2. It must have a g-twist under $\theta \to \theta + 2\pi$.
3. It must preserve sufficient amount of supersymmetries so that integration over the fermion zero modes do not make the integral vanish [125,126].

There are indeed such saddle points in the path integral, constructed as follows [51]:

1. Take the original near horizon geometry of the black hole.
2. Take a $\mathbb{Z}_N$ orbifold of this background with $\mathbb{Z}_N$ generated by the simultaneous action of
   (a) $2\pi/N$ rotation in AdS_2 ($\theta \to \theta + \frac{2\pi}{N}$),
   (b) $2\pi/N$ rotation in S^2 ($\phi \to \phi + \frac{2\pi}{N}$; this is needed for preserving SUSY), and
   (c) g.

To see that this has the same asymptotic geometry as the attractor geometry, we make a rescaling

$$\theta \to \theta/N, \qquad r \to N\, r\,. \tag{74}$$

After this rescaling, the metric takes the form:

$$ds^2 = v\left((r^2 - N^{-2})d\theta^2 + \frac{dr^2}{r^2 - N^{-2}}\right)\,, \tag{75}$$

with the orbifold action given by:

$$\theta \to \theta + 2\pi\,, \qquad \phi \to \phi + 2\pi/N\,, \qquad g\,. \tag{76}$$

For large r, the metric approaches the AdS_2 metric.[17] The g transformation provides us with the correct boundary condition under $\theta \to \theta + 2\pi$. The shift along the ϕ-direction can be regarded as a Wilson line, and hence is an allowed fluctuation in AdS_2. In other words, by a coordinate change $\phi \to \phi + \theta/N$, we can remove the shift in ϕ, but this will generate a constant $g_{\theta\phi}$ at the boundary, which describes a normalizable mode and hence is an allowed fluctuation.

The classical action associated with this orbifold can be obtained by dividing the action associated with the parent geometry by N. Thus the classical action associated with this saddle point, after removing the divergent part proportional to the length of the boundary, is S_{wald}/N. As a result, the contribution to the finite part of the twisted partition function from this saddle point is

$$Z_g^{finite} \sim \exp\left[S_{wald}/N\right]\,. \tag{77}$$

[17] In contrast, we note that for two dimensional flat spacetime, orbifolding not only introduces a conical singularity but also changes the asymptotic spacetime.

This is exactly what we have found in the microscopic analysis of the twisted index in §2.6 and §2.8.

Note that $\exp[S_{wald}/N] << \exp[S_{wald}]$. Thus the $\mathbb{Z}_N$ quantum numbers must be delicately distributed among the microstates of the black hole so that a charge of order unity, averaged over $\exp[S_{wald}]$ number of states, gives a contribution of order $\exp[S_{wald}/N]$. In other words, there is a large cancellation going on among terms of order unity to give this result. Nevertheless we see that black holes are able to capture information about this highly sensitive data.

4.2. Logarithmic corrections to the black hole entropy

As already discussed before, the effect of integrating out the massive mode contribution to Z_{AdS_2} can be regarded as a modification of the effective Lagrangian density, and can be accommodated using Wald's formula. However, for calculating the one loop contribution due to the massless modes, we need to compute directly the determinant of the kinetic operator in the $AdS_2 \times S^2$ background.

Let us consider an example where we have a massless scalar field with the standard kinetic term in the near horizon $AdS_2 \times S^2$ background for a spherically symmetric extremal black hole in $D = 4$. All the eigenvalues and eigenfunctions of $\Box$ on $AdS_2 \times S^2$ can be found explicitly, which can then be used to compute det $\Box$, and hence the one loop contribution to Z_{AdS_2}. The result for the contribution to $\ln d_{hor}$ from this massless scalar is of the form[18] [127]:

$$-\frac{1}{180}\,\ln A\,. \tag{78}$$

For black holes in supergravity/superstring theory, the kinetic operator for fluctuations around the near horizon geometry mixes scalars, vectors and tensors. Thus one needs to diagonalize the kinetic operator, find the determinant, and then compute its contribution to Z_{AdS_2} and hence d_{hor}. For the quarter-BPS black holes in $\mathcal{N} = 4$ supersymmetric theories, one finds that the fluctuations in the matter multiplet fields do not mix with the fluctuations in the gravity multiplet fields to quadratic order [127]. So far the contribution to the one loop determinant from the matter multiplet fields has been calculated. The outcome of such calculation is that all contributions cancel [127]. While this does not lead to a complete computation of logarithmic corrections to the extremal black hole entropy, it already gives us some non-trivial information, namely, that the logarithmic correction to the entropy of quarter-BPS dyons in $\mathcal{N} = 4$ supersymmetric string theories cannot depend on the number of matter multiplets in the theory. This agrees with the microscopic result given in (32), which has no logarithimic correction for any value of r, – the number of matter multiplets in the theory.

One might tend to conclude that the reason for this cancellation is supersymmetry. However, the above system turns out to be a special case, since the microscopic result (38) for 1/8-BPS dyons in $\mathcal{N} = 8$ supersymmetric string theories, which have the same amount of supersymmetry in the near horizon geometry, does have logarithmic correction to its entropy [86]. Thus we expect that the cancellation of logarithmic corrections is not merely a consequence of supersymmetry.

5. Other applications

Quantum entropy function has also been used to explain several other features of the microscopic formula. For example, we see from the microscopic formula (26) that for charge vectors (Q, P) with $r(Q, P) > 1$, there are additional contributions to the B_6 index whose leading term takes the form $\exp\left(\pi\sqrt{Q^2P^2 - (Q \cdot P)^2}/s\right)$, where s is a factor of r. It turns out that precisely for $r(Q, P) > 1$, the functional integral for Z_{AdS_2} receives extra contribution from saddle points obtained by taking a freely acting $\mathbb{Z}_s$ quotient – for $s|r$ – of the original near horizon geometry. The leading semi-classical contribution from such a saddle point is given by $\exp(S_{wald}/s) = \exp\left(\pi\sqrt{Q^2P^2 - (Q \cdot P)^2}/s\right)$, precisely in agreement with the microscopic results[118,86].

For $r = 1$, the result for B_6 for large charges

[18] A different approach to computing logarithmic corrections to extremal black hole entropy can be found in [88].

takes the form of a sum of the contributions from different poles. The leading asymptotic expansion comes from a specific pole and is given by (17). It turns out that the contributions from the other poles have the leading term of the form $\exp\left(\pi\sqrt{Q^2P^2-(Q\cdot P)^2}/N\right)$, for $N\in\mathbb{Z}$, $N>1$. On the other hand, Z_{AdS_2} receives contribution from, besides the original near horizon geometry, its $\mathbb{Z}_N$ orbifolds which do not change the boundary condition at infinity. The leading semi-classical contribution from these saddle points is given by $\exp\left(\pi\sqrt{Q^2P^2-(Q\cdot P)^2}/N\right)$, precisely in correspondence with the leading contribution from the subleading poles in the microscopic formula[46,128].

6. Discussion

All these results provide us with the 'experimental verification' of the theory of extremal black holes, based on Wald's formula and AdS_2/CFT_1 correspondence. The results described here show that quantum gravity in the near horizon geometry contains detailed information about not only the total number of microstates but also finer details (*e.g.* the $\mathbb{Z}_N$ quantum numbers carried by the microstates). Thus, at least for extremal black holes, there seems to be an exact duality between

$$\textit{Gravity description} \;\Leftrightarrow\; \textit{Microscopic description}\,. \tag{79}$$

The gravity description contains as much information as the microscopic description, but in a quite different way.

It is clear from our discussions that whereas the α'-corrections are well-understood through Wald's formalism, we need to understand the g_s corrections better. The quantum entropy function formalism provides us with a tool for investigations in that direction. Eventually we hope to reproduce the complete asymptotic expansion of the microscopic result for $\ln|B_6|$ from the string theory path integral over AdS_2. Our basic tool is the localization of the path integral to a finite dimensional subspace using supersymmetry. This has been pursued to some extent in [126]. In this process, we hope to learn not only about black holes but also about string theory, *e.g.* the rules for carrying out path integral over string fields.

Another useful direction of study is the generalization of these results to $\mathcal{N}=2$ supersymmetric string theories. Some attempts at generalizing the microscopic results of §2 in special $\mathcal{N}=2$ supersymmetric string theories can be found in [129–131].

Acknowledgement: We would like to thank Nabamita Banerjee, Shamik Banerjee, Atish Dabholkar, Justin David, Suvankar Dutta, Dileep Jatkar, Joao Gomes, Rajesh Gopakumar, Rajesh Gupta and Sameer Murthy for collaboration and/or useful discussions. A.S. would like to thank the Perimeter institute, Canada and the Simons Center at Stony Brook for hospitality during the preparation of this manuscript. The work of I.M. was supported in part by DAE project 11-R&D-HRI-5.02-0304 and the grant from the Chaires Internationales de Recherche Blaise Pascal of A.S. The work of A.S. was supported in part by the J. C. Bose fellowship of the Department of Science and Technology, India, the DAE project 11-R&D-HRI-5.02-0304, and by the Chaires Internationales de Recherche Blaise Pascal, France.

REFERENCES

1. S. W. Hawking, Phys. Rev. Lett. **26**, 1344 (1971).
2. J. D. Bekenstein, Phys. Rev. D **7**, 2333 (1973).
3. J. D. Bekenstein, Phys. Rev. D **9**, 3292 (1974).
4. S. W. Hawking, Nature **248**, 30 (1974).
5. A. Sen, Mod. Phys. Lett. A **10**, 2081 (1995) [arXiv:hep-th/9504147].
6. A. Strominger and C. Vafa, Phys. Lett. B **379**, 99 (1996) [arXiv:hep-th/9601029].
7. S. D. Mathur, arXiv:0810.4525 [hep-th], and references therein.
8. R. Dijkgraaf, E. P. Verlinde and H. L. Verlinde, Nucl. Phys. B **484**, 543 (1997) [arXiv:hep-th/9607026].
9. G. Lopes Cardoso, B. de Wit, J. Kappeli and T. Mohaupt, JHEP **0412**, 075 (2004) [arXiv:hep-th/0412287].
10. D. Shih, A. Strominger and X. Yin, JHEP **0610**, 087 (2006) [arXiv:hep-th/0505094].
11. D. Shih, A. Strominger and X. Yin, JHEP **0606**, 037 (2006) [arXiv:hep-th/0506151].

12. D. Gaiotto, arXiv:hep-th/0506249.
13. D. Shih and X. Yin, JHEP **0604**, 034 (2006) [arXiv:hep-th/0508174].
14. D. P. Jatkar and A. Sen, JHEP **0604**, 018 (2006) [arXiv:hep-th/0510147].
15. J. R. David, D. P. Jatkar and A. Sen, JHEP **0606**, 064 (2006) [arXiv:hep-th/0602254].
16. A. Dabholkar and S. Nampuri, JHEP **0711**, 077 (2007) [arXiv:hep-th/0603066].
17. J. R. David and A. Sen, JHEP **0611**, 072 (2006) [arXiv:hep-th/0605210].
18. J. R. David, D. P. Jatkar and A. Sen, JHEP **0611**, 073 (2006) [arXiv:hep-th/0607155].
19. J. R. David, D. P. Jatkar and A. Sen, JHEP **0701**, 016 (2007) [arXiv:hep-th/0609109].
20. A. Dabholkar and D. Gaiotto, JHEP **0712**, 087 (2007) [arXiv:hep-th/0612011]
21. A. Sen, JHEP **0705**, 039 (2007) [arXiv:hep-th/0702141].
22. A. Dabholkar, D. Gaiotto and S. Nampuri, JHEP **0801**, 023 (2008) [arXiv:hep-th/0702150].
23. N. Banerjee, D. P. Jatkar and A. Sen, JHEP **0707**, 024 (2007) [arXiv:0705.1433 [hep-th]].
24. A. Sen, JHEP **0709**, 045 (2007) [arXiv:0705.3874 [hep-th]].
25. M. C. N. Cheng and E. Verlinde, JHEP **0709**, 070 (2007) [arXiv:0706.2363 [hep-th]].
26. A. Sen, JHEP **0710**, 059 (2007) [arXiv:0707.1563 [hep-th]].
27. A. Mukherjee, S. Mukhi and R. Nigam, JHEP **0710**, 037 (2007) [arXiv:0707.3035 [hep-th]].
28. A. Sen, Gen. Rel. Grav. **40**, 2249 (2008) [arXiv:0708.1270 [hep-th]].
29. A. Sen, JHEP **0712**, 019 (2007) [arXiv:0708.3715 [hep-th]].
30. A. Mukherjee, S. Mukhi and R. Nigam, Mod. Phys. Lett. A **24**, 1507 (2009) [arXiv:0710.4533 [hep-th]].
31. S. Banerjee and A. Sen, JHEP **0803**, 022 (2008) [arXiv:0712.0043 [hep-th]].
32. S. Banerjee and A. Sen, JHEP **0804**, 012 (2008) [arXiv:0801.0149 [hep-th]].
33. S. Banerjee, A. Sen and Y. K. Srivastava, JHEP **0805**, 101 (2008) [arXiv:0802.0544 [hep-th]].
34. A. Dabholkar, K. Narayan and S. Nampuri, JHEP **0803**, 026 (2008) [arXiv:0802.0761 [hep-th]].
35. S. Banerjee, A. Sen and Y. K. Srivastava, arXiv:0802.1556 [hep-th].
36. A. Sen, JHEP **0807**, 118 (2008) [arXiv:0803.1014 [hep-th]].
37. A. Dabholkar, J. Gomes and S. Murthy, JHEP **0805**, 098 (2008) [arXiv:0802.1556 [hep-th]].
38. A. Sen, JHEP **0807**, 078 (2008) [arXiv:0803.3857 [hep-th]].
39. M. C. N. Cheng and E. P. Verlinde, SIGMA **4**, 068 (2008) [arXiv:0806.2337 [hep-th]].
40. A. Castro and S. Murthy, JHEP **0906**, 024 (2009) [arXiv:0807.0237 [hep-th]].
41. N. Banerjee, Phys. Rev. D **79**, 081501 (2009) [arXiv:0807.1314 [hep-th]].
42. S. Govindarajan and K. Gopala Krishna, JHEP **0904**, 032 (2009) [arXiv:0807.4451 [hep-th]].
43. S. Banerjee, A. Sen and Y. K. Srivastava, JHEP **0903**, 151 (2009) [arXiv:0808.1746 [hep-th]].
44. S. Mukhi and R. Nigam, JHEP **0812**, 056 (2008) [arXiv:0809.1157 [hep-th]].
45. M. C. N. Cheng and A. Dabholkar, Commun. Num. Theor. Phys. **3**, 59 (2009) [arXiv:0809.4258 [hep-th]].
46. N. Banerjee, D. P. Jatkar and A. Sen, JHEP **0905**, 121 (2009) [arXiv:0810.3472 [hep-th]].
47. M. C. N. Cheng and L. Hollands, JHEP **0904**, 067 (2009) [arXiv:0901.1758 [hep-th]].
48. A. Dabholkar, M. Guica, S. Murthy and S. Nampuri, JHEP **1006**, 007 (2010) [arXiv:0903.2481 [hep-th]].
49. S. Govindarajan and K. Gopala Krishna, JHEP **1005**, 014 (2010) [arXiv:0907.1410 [hep-th]].
50. A. Dabholkar and J. Gomes, JHEP **1003**, 128 (2010) [arXiv:0911.0586 [hep-th]].
51. A. Sen, JHEP **1005**, 028 (2010) [arXiv:0911.1563 [hep-th]].
52. A. Sen, arXiv:1002.3857 [hep-th].
53. S. Govindarajan, arXiv:1006.3472 [hep-th].
54. C. Bachas and E. Kiritsis, Nucl. Phys. Proc. Suppl. **55B**, 194 (1997) [arXiv:hep-th/9611205].
55. A. Gregori, E. Kiritsis, C. Kounnas, N. A. Obers, P. M. Petropoulos and B. Pioline, Nucl. Phys. B **510**, 423 (1998) [arXiv:hep-th/9708062].
56. F. Denef, arXiv:hep-th/0010222.
57. F. Denef, B. R. Greene and M. Raugas, JHEP **0105**, 012 (2001) [arXiv:hep-th/0101135].
58. F. Denef, JHEP **0210**, 023 (2002) [arXiv:hep-th/0206072].
59. B. Bates and F. Denef, arXiv:hep-th/0304094.
60. F. Denef and G. W. Moore, arXiv:hep-

th/0702146.
61. J. C. Breckenridge, R. C. Myers, A. W. Peet and C. Vafa, Phys. Lett. B **391**, 93 (1997) [arXiv:hep-th/9602065].
62. D. Gaiotto, A. Strominger and X. Yin, JHEP **0602**, 024 (2006) [arXiv:hep-th/0503217].
63. J. C. Breckenridge, D. A. Lowe, R. C. Myers, A. W. Peet, A. Strominger and C. Vafa, Phys. Lett. B **381**, 423 (1996) [arXiv:hep-th/9603078].
64. D. Brill, Phys. Rev. B133 (1964) 845.
65. C. N. Pope, Nucl. Phys. B **141**, 432 (1978).
66. R. Dijkgraaf, G. W. Moore, E. P. Verlinde and H. L. Verlinde, Commun. Math. Phys. **185**, 197 (1997) [arXiv:hep-th/9608096].
67. J. Igusa, Amer. J. Math. 84 (1962) 175200.
68. J. Igusa, Amer. J. Math. 86 (1962) 392412.
69. G. Lopes Cardoso, B. de Wit, J. Kappeli and T. Mohaupt, JHEP **0603**, 074 (2006) [arXiv:hep-th/0601108].
70. M. Cvetic and D. Youm, Phys. Rev. D **53**, 584 (1996) [arXiv:hep-th/9507090].
71. M. J. Duff, J. T. Liu and J. Rahmfeld, Nucl. Phys. B **459**, 125 (1996) [arXiv:hep-th/9508094].
72. M. Cvetic and A. A. Tseytlin, Phys. Rev. uffff D **53**, 5619 (1996) [Erratum-ibid. uffff D **55**, 3907 (1997)] [arXiv:hep-th/9512031].
73. S. Chaudhuri and D. A. Lowe, Nucl. Phys. B **459**, 113 (1996) [arXiv:hep-th/9508144].
74. P. S. Aspinwall, Nucl. Phys. Proc. Suppl. **46**, 30 (1996) [arXiv:hep-th/9508154].
75. R. Borcherds, Invent. Math. **120** (1995) 161.
76. V. A. Gritsenko and V. V. Nikulin, Amer. J. Math. **119**, 181 (1997) [arXiv:alg-geom/9504006].
77. T. Ibukiyama, Int. J. Math 2(1) (1991) 1735.
78. S. Hayashida and T. Ibukiyama, Journal of Kyoto Univ 45 (2005).
79. H. Aoki and T. Ibukiyama, International Journal of Mathematics 16 (2005) 249279.
80. M. Eichler and D. Zagier, The theory of jacobi forms, Birkhauser (1985).
81. N. -P. Skoruppa, Mathematics of Computation, **58**, 381 (1992).
82. M. Manickam, B. Ramakrishnan and T. C. Vasudevan, Manuscripta Math., **81**, 161 (1993).
83. S. Chaudhuri, G. Hockney and J. D. Lykken, Phys. Rev. Lett. **75**, 2264 (1995) [arXiv:hep-th/9505054].
84. S. Chaudhuri and J. Polchinski, Phys. Rev. D **52**, 7168 (1995) [arXiv:hep-th/9506048].
85. A. Sen, JHEP **0808**, 037 (2008) [arXiv:0804.0651 [hep-th]].
86. A. Sen, JHEP **1002**, 090 (2010) [arXiv:0908.0039 [hep-th]].
87. O. B. Zaslavsky, Phys. Rev. D **56**, 2188 (1997) [Erratum-ibid. D **59**, 069901 (1999)] [arXiv:gr-qc/9707015].
88. R. B. Mann and S. N. Solodukhin, Nucl. Phys. B **523**, 293 (1998) [arXiv:hep-th/9709064].
89. J. M. Maldacena, J. Michelson and A. Strominger, JHEP **9902**, 011 (1999) [arXiv:hep-th/9812073].
90. H. K. Kunduri, J. Lucietti and H. S. Reall, Class. Quant. Grav. **24**, 4169 (2007) [arXiv:0705.4214 [hep-th]].
91. P. Figueras, H. K. Kunduri, J. Lucietti and M. Rangamani, Phys. Rev. D **78**, 044042 (2008) [arXiv:0803.2998 [hep-th]].
92. R. M. Wald, Phys. Rev. D **48**, 3427 (1993) [arXiv:gr-qc/9307038].
93. T. Jacobson, G. Kang and R. C. Myers, Phys. Rev. D **49**, 6587 (1994) [arXiv:gr-qc/9312023].
94. V. Iyer and R. M. Wald, Phys. Rev. D **50**, 846 (1994) [arXiv:gr-qc/9403028].
95. T. Jacobson, G. Kang and R. C. Myers, arXiv:gr-qc/9502009.
96. A. Sen, JHEP **0509**, 038 (2005) [arXiv:hep-th/0506177].
97. A. Sen, JHEP **0603**, 008 (2006) [arXiv:hep-th/0508042].
98. D. Astefanesei, K. Goldstein, R. P. Jena, A. Sen and S. P. Trivedi, JHEP **0610**, 058 (2006) [arXiv:hep-th/0606244].
99. S. Ferrara, R. Kallosh and A. Strominger, Phys. Rev. D **52**, 5412 (1995) [arXiv:hep-th/9508072].
100. A. Strominger, Phys. Lett. B **383**, 39 (1996) [arXiv:hep-th/9602111].
101. S. Ferrara and R. Kallosh, Phys. Rev. D **54**, 1514 (1996) [arXiv:hep-th/9602136].
102. K. Goldstein, N. Iizuka, R. P. Jena and S. P. Trivedi, Phys. Rev. D **72**, 124021 (2005) [arXiv:hep-th/0507096].
103. J. M. Maldacena, A. Strominger and E. Witten, JHEP **9712**, 002 (1997) [arXiv:hep-th/9711053].
104. K. Behrndt, G. Lopes Cardoso, B. de Wit, D. Lust, T. Mohaupt and W. A. Sabra, Phys. Lett. B **429**, 289 (1998) [arXiv:hep-th/9801081].

105.G. Lopes Cardoso, B. de Wit and T. Mohaupt, Phys. Lett. B **451**, 309 (1999) [arXiv:hep-th/9812082].
106.G. Lopes Cardoso, B. de Wit and T. Mohaupt, Fortsch. Phys. **48**, 49 (2000) [arXiv:hep-th/9904005].
107.G. Lopes Cardoso, B. de Wit and T. Mohaupt, Nucl. Phys. B **567**, 87 (2000) [arXiv:hep-th/9906094].
108.G. Lopes Cardoso, B. de Wit and T. Mohaupt, Class. Quant. Grav. **17**, 1007 (2000) [arXiv:hep-th/9910179].
109.T. Mohaupt, Fortsch. Phys. **49**, 3 (2001) [arXiv:hep-th/0007195].
110.G. Lopes Cardoso, B. de Wit, J. Kappeli and T. Mohaupt, interactions," JHEP **0012**, 019 (2000) [arXiv:hep-th/0009234].
111.G. L. Cardoso, B. de Wit, J. Kappeli and T. Mohaupt, with R**2-interactions," Fortsch. Phys. **49**, 557 (2001) [arXiv:hep-th/0012232].
112.H. Ooguri, A. Strominger and C. Vafa, Phys. Rev. D **70**, 106007 (2004) [arXiv:hep-th/0405146].
113.J. A. Harvey and G. W. Moore, Phys. Rev. D **57**, 2323 (1998) [arXiv:hep-th/9610237].
114.B. Sahoo and A. Sen, JHEP **0609**, 029 (2006) [arXiv:hep-th/0603149].
115.G. L. Cardoso, B. de Wit and S. Mahapatra, JHEP **0703**, 085 (2007) [arXiv:hep-th/0612225].
116.G. L. Cardoso, B. de Wit and S. Mahapatra, JHEP **0902**, 006 (2009) [arXiv:0808.2627 [hep-th]].
117.A. Sen, Int. J. Mod. Phys. A **24**, 4225 (2009) [arXiv:0809.3304 [hep-th]].
118.A. Sen, JHEP **0908**, 068 (2009) [arXiv:0903.1477 [hep-th]].
119.J. M. Maldacena, JHEP **0304**, 021 (2003) [arXiv:hep-th/0106112].
120.T. Azeyanagi, T. Nishioka and T. Takayanagi, Phys. Rev. D **77**, 064005 (2008) [arXiv:0710.2956 [hep-th]].
121.N. Banerjee, I. Mandal and A. Sen, JHEP **0907**, 091 (2009) [arXiv:0901.0359 [hep-th]].
122.D. P. Jatkar, A. Sen and Y. K. Srivastava, JHEP **1002**, 038 (2010) [arXiv:0907.0593 [hep-th]].
123.A. Dabholkar, J. Gomes, S. Murthy and A. Sen, to appear.
124.A. Sen, JHEP **1005**, 097 (2010) [arXiv:0908.3402 [hep-th]].
125.C. Beasley, D. Gaiotto, M. Guica, L. Huang, A. Strominger and X. Yin, arXiv:hep-th/0608021.
126.N. Banerjee, S. Banerjee, R. K. Gupta, I. Mandal and A. Sen, JHEP **1002**, 091 (2010) [arXiv:0905.2686 [hep-th]].
127.S. Banerjee, R. K. Gupta and A. Sen, arXiv:1005.3044 [hep-th].
128.S. Murthy and B. Pioline, JHEP **0909**, 022 (2009) [arXiv:0904.4253 [hep-th]].
129.J. R. David, JHEP **0802**, 025 (2008) [arXiv:0711.1971 [hep-th]].
130.G. L. Cardoso, J. R. David, B. de Wit and S. Mahapatra, JHEP **0812**, 086 (2008) [arXiv:0810.1233 [hep-th]].
131.J. R. David, JHEP **0908**, 054 (2009) [arXiv:0905.4115 [hep-th]].

Standard Model, Higgs Boson(s) and New Physics at the LHC in Run I

Y. Sirois[a*]

[a]Laboratoire Leprince-Ringuet, Ecole Polytechnique, CNRS/IN2P3
91128 Palaiseau, France

A overview of the ATLAS and CMS detectors and first physics results from the 2010 data taking campaign at the LHC collider is presented. Measurements with pp collisions at $\sqrt{s} = 7$ TeV and for integrated luminosities reaching up to about $40\,\mathrm{pb}^{-1}$ are summarized for weak bosons and top quark production, as well as for the search of the Higgs Boson(s), supersymmetry and new interactions at the TeV scale. The physics prospects for the complete Run I from 2010 to 2012 with a few fb^{-1} of luminosity collected per experiment are discussed.

1. INTRODUCTION

The first proton-proton collisions have been delivered at the Large Hadron Collider (LHC) in December 2009, and a record centre-of-mass energy ($\sqrt{s}$) of 7 TeV was attained starting in early spring 2010. This is a turning point for high energy physics, nearly twenty years after a major international workshop in Aachen, where the ambitious LHC project was first discussed, and proto-collaborations formed for two large experiments [1], the ATLAS and CMS experiments. The experiments are expected to collect data at this working point during three years, until fall 2012. This first major physics run (henceforward called Run I) marks the opening of a new era for high energy physics. A period of renewed exploration in unknown territories for the fundamental interactions.

The essential physics motivations for the LHC remain as they were at the origin of the project, some twenty years ago, despite generations of precision measurements and searches at the LEP e^+e^- collider, the HERA ep collider, the Tevatron $p\bar{p}$ collider, and the Babar and Belle B-Factories, where the phenomenology of the $\mathrm{SU}(3)_C \times \mathrm{SU}(2)_L \times \mathrm{U}(1)_Y$ standard model (SM) of strong and electroweak forces has been remarkably confirmed. They stems from the fact that the SM remains incomplete and dissatisfactory. The difficulties with the theoretical description of particle interactions appear today more acute than at any moment in the past history of physics. These are associated with the complexity of the structure of matter, and to the gauge symmetries and the notion of symmetry breaking. The LHC has been designed before and above all to address problems of the latter kind, and in particular to answer questions related to the electroweak symmetry breaking, but progress with the understanding of the structure of matter is also possible.

In this paper, the status and prospects for the proton-proton physics with Run I data in the ATLAS and CMS experiments are reviewed. The collider and the experiments are briefly described in section 2. A comparison of the physics reach between the Tevatron and the LHC experiments is presented in section 3. A selection of first experimental results concerned with a "rediscovery" of the SM at high $\sqrt{s}$, and the understanding of the SM candles are summarized in section 4. The candles will help to guide the steps toward the Higgs boson and possibly into territories beyond the SM. With increasing integrated luminosities, the hunt for the Higgs has been initiated at the LHC by both experiments. Some of the most significant results obtained integrating the 2010 data (Run 1a) are presented in section 5, together with prospectives for the full Run I where 1 to 10 fb^{-1} of data could be collected per

*Adapted from lectures given at the 2010 Cargèse Summer School of physics, "String Theory: Formal Developments and Applications", (June 21- July 3, 2010).

experiment. The high $\sqrt{s}$ could provides access to new physics even at rather modest integrated luminosities, and some the most promising searches are discussed in section 6. Conclusions on the expected highlights for the Run I at the LHC are given in section 7.

2. THE COLLIDER AND THE TWO LARGE EXPERIMENTS

The ATLAS ("A Toroidal LHC Apparatus") [2] and CMS ("Compact Muon Solenoid") [3] detectors are multi-purpose devices with a cylindrical geometry, and forward-backward symmetry along the beam line.

Both experiments have been designed to allow for a good measurement of leptons at very high momenta, offer sufficient transverse or longitudinal granularity to provide a high discrimination of isolated leptons against QCD instrumental background, and provide a nearly 4π solid angle coverage for the measurement of hadronic jets and transverse energy flow. Leptons at very high momenta could originate e.g. from the decay of new resonances at the TeV scale (see section 6). Isolated leptons (or photons) are a crucial ingredient of the signature for important and rare signal events e.g. from the decay of a Higgs boson (section 5). Missing energy is a characteristic of the signature e.g. for the production of supersymmetric matter (section 5).

Above all other considerations, the detailed design of the experiments follows from the choice of the main magnets. The CMS experiment has chosen a solenoid which allows for a compact detector. The solenoid provides field lines parallel to the Z (beam) axis so that charged particles trajectories bend in the transverse plane. The excellent momentum resolution required for TeV muons is made possible via a very high magnetic field and a fine grained tracker. The ATLAS experiment has chosen a toroid which imposes a very large volume. The toroid provides field lines which are circles centered on the Z axis, so that muons bend in a plane defined by the beam axis and the muon position. This provides excellent stand alone momentum resolution for TeV muons, but an internal solenoid is needed for the purpose of vertex reconstruction and additional momentum measurements with a fine grained tracker.

In the central region, one expects the number of particles produced per unit rapidity y in pp collisions to be approximately constant and form a "rapidity plateau". The rapidity y for a particle is defined along the Z direction as $y \equiv 1/2 \ln(E + p_Z)/(E - p_Z) = 1/2 \ln(1 + \beta \cos\theta)/(1 - \beta \cos\theta)$. where $\beta = p/E$ and θ is the polar angle relative to the Z axis. At the LHC for the nominal machine at $\sqrt{s} = 14$ TeV, one expects [4] a rapidity plateau of width $\Delta y \simeq 6$. In pp collisions, most of the particles are produced in the central plateau region but most of the energy will be directed at higher rapidities, in the proton fragmentation regions. Thus, both experiments have equipped the rapidity plateau region with fined grained electromagnetic calorimetry and charged track measurement devices. The fined grained coverage extend up to $|\eta| \approx 3$. The pseudorapidity η is defined as $\eta = 1/2 \ln(1 + \cos\theta)/(1 - \cos\theta) = -\log\tan(\theta/2)$. It corresponds to the rapidity of a particle with zero mass ($\beta = 1$) and is a good approximation for the rapidity when for a particle $m \ll p_T$. The $|\eta|$ of a particle of given p_T is always larger than its true $|y|$. The debris from the proton fragmentation are largely contained for inelastic collisions in the region $|y| \lesssim 5$. Both experiments cover the very forward regions up to $|\eta| \approx 5$ with additional calorimetry.

A three-dimensional representation of the ATLAS detector is shown Fig. 1. The layout comprises a thin superconducting solenoid surrounding inner tracking detectors and three large superconducting toroids supporting a large muon tracker. The inner detectors consist of a silicon pixel device, a silicon microstrip device and a transition radiation tracker, all immersed in the 2 Tesla field from the solenoid. High-granularity liquid-argon (LAr) electromagnetic sampling calorimeters cover the pseudorapidity region $|\eta| < 3.2$. An iron-scintillator tile calorimeter provides coverage over $|\eta| < 1.7$. The end-cap and forward regions, spanning $1.5 < |\eta| < 4.9$, are instrumented with LAr calorimetry for both electromagnetic and hadronic measurements. The muon spectrometer covering $|\eta| < 2.7$ relies on the magnetic deflection of muons

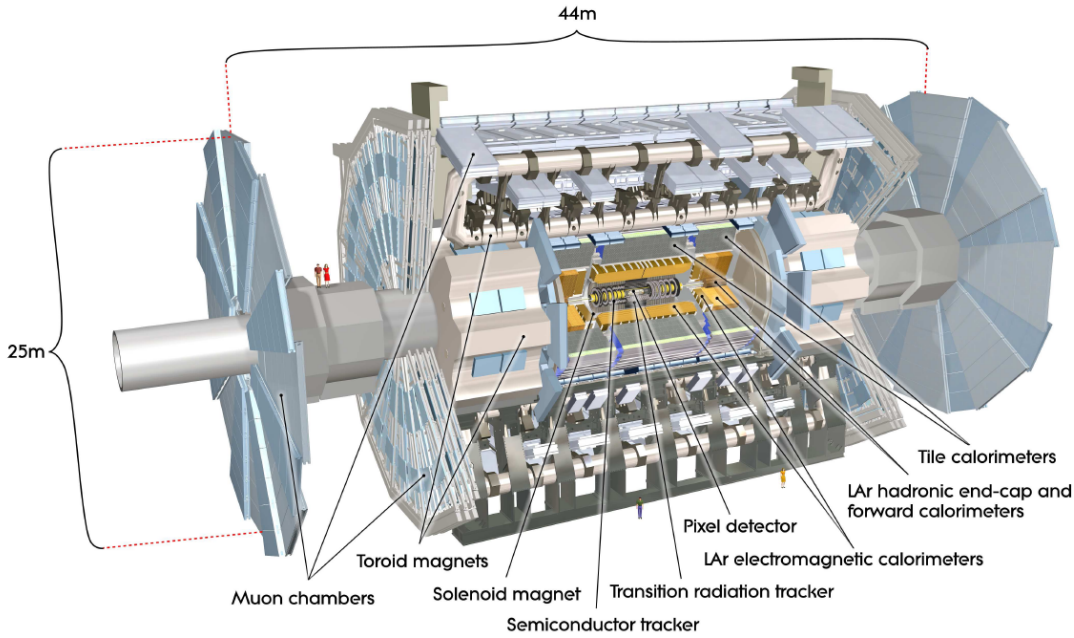

Figure 1. Cut-away three-dimensional view of the ATLAS Detector. The instrument occupies a volume of cylindrical shape of 44 m in length and 25 m in diameter. The overall weight of the detector is approximately 7000 t.

tracks in the air-core toroid magnets, instrumented with separate trigger and high-precision tracking chambers

A three-dimensional representation of the CMS detector is shown Fig. 2. The layout comprises a superconducting solenoid of 6 m internal diameter, providing a uniform magnetic field of 3.8 T. The bore of the solenoid is instrumented with various particle detection systems. The inner tracking system is composed of a pixel detector with three barrel layers at radii between 4.4 and 10.2 cm and a silicon strip tracker with 10 barrel detection layers extending outwards to a radius of 1.1m. Each system is completed by two end caps, extending the acceptance up to $|\eta| < 2.5$. A lead tungstate crystal electromagnetic calorimeter with fine transverse $(\Delta\eta, \Delta\phi)$ granularity and a brass-scintillator hadronic calorimeter surround the tracking volume and cover the region $|\eta| < 3$. The steel return yoke outside the solenoid is in turn instrumented with gas detectors which are used to identify muons in the range $|\eta| < 2.4$. The barrel region is covered by drift tubes and the end-cap region by cathode strip chambers. A calorimeter made of steel absorber and quartz fiber extends to coverage in forward regions up to $|\eta| < 5.0$.

Both experiments have profited from many months of training and analysis with cosmic data [5,6] before the arrival of the first LHC collisions. The first LHC collisions were produced at a proton-proton $\sqrt{s} = 900$ GeV during "pilot" runs and then, after a few weeks, at a record $\sqrt{s} = 2.36$ TeV. The data collected by the two large experiments, ATLAS and CMS during these early runs were essentially used to finalize the commissioning of the detectors and the analysis tools, and to validate the computing and

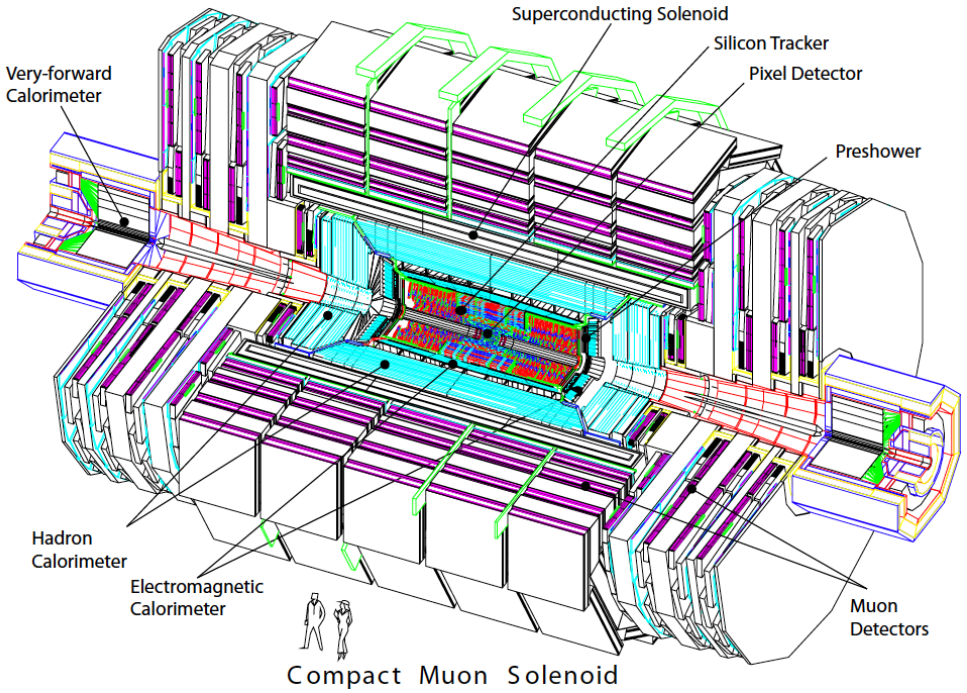

Figure 2. Cut-away perspective view of the CMS Detector. The instrument occupies a volume of cylindrical shape of 21.6 m in length and 14.6 m in diameter, and has a total weight of 12500 t.

data distribution models [7,8]. But the level of readiness of the experiments was such, that first physics results could be produced, in some cases within days or weeks. The first public results concerned basic QCD background properties such as the measurement of the underlying event activity, track multiplicity and transverse momentum flow measurements, or for instance the observation of diffraction in proton-proton collisions. After a short technical stop, the LHC operations have resumed in early spring 2010 at $\sqrt{s} = 7$ TeV, the highest energy compatible with a secured and stable functioning of the collider. Before to start with section 4 a journey through some of the main 2010 results and prospects for the full Run I, it is useful to briefly compare the situation of the Tevatron and the LHC colliders.

3. CROSS SECTIONS, KINEMATICS: FROM TEVATRON TO LHC:

The evolution of the production cross sections for characteristic particles in $p\bar{p}$ and pp collisions [9,10] is shown as a function of $\sqrt{s}$ in Fig. 3. The production cross section for a given massive particle increases faster with $\sqrt{s}$ than the total inclusive $p\bar{p}$ (pp) cross section, and fastest for the heaviest particles. In comparison to the Tevatron, the LHC thus offers a cleaner environment for Z/W electroweak physics. The Z and W production will be used as "candles" at the LHC and are expected to be measured with very small remaining instrumental QCD background. The LHC also brings a very large increase of the top quark and Higgs boson production cross sections. The Higgs boson observation will profit from a lower background from electroweak processes at the LHC. But this observation remains very challenging with an eventual signal (taking into ac-

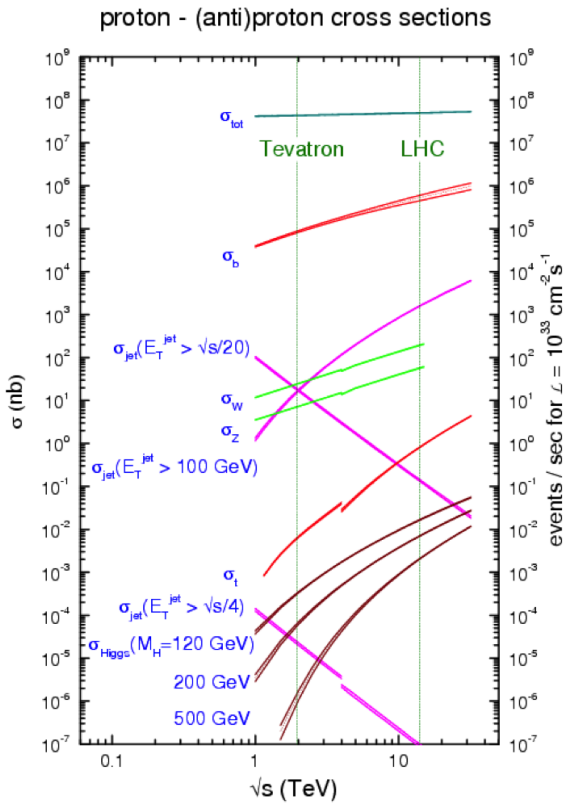

Figure 3. Evolution of the production cross section as a function of $\sqrt{s}$ at $p\bar{p}$ and pp colliders, for inclusive jets and for various massive particles (b- and t-quarks, Z and W bosons, SM Higgs boson) [9].

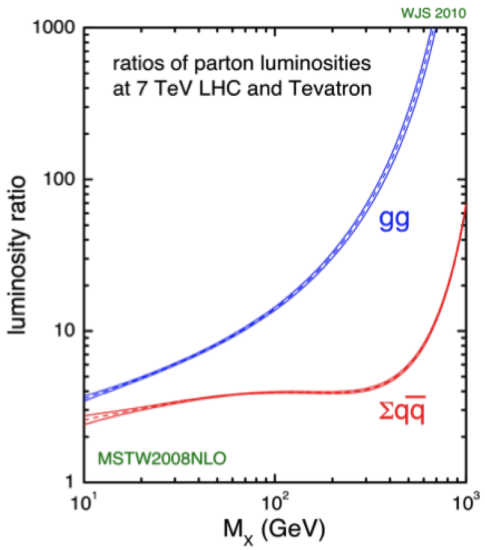

Figure 4. Parton luminosity ratio for gluon-gluon and the sum of quark-antiquark interactions as a function of the energy available to create a mass M_X. The ratio is obtained [10] for 7 TeV pp collisions (LHC Run I) normalized to 1.96 TeV $p\bar{p}$ (Tevatron Run II).

count the Higgs boson decay branching ratio) lying 10^{10} to 10^{13} orders of magnitude below to the inelastic collision rate, depending on the channel. The search for the Higgs implies the usage of state-of-the-art detector and triggering technologies combined with rare decay data reduction and analysis techniques.

The Tevatron $p\bar{p}$ collider and the LHC pp collider provide a broad band of partons (quarks, anti-quarks and gluons) that may participate in the hard collisions. For an hypothetical particle X of given mass M_X produced at a rapidity y in a hard collision between partons, the Bjorken x_1 and x_2, the fraction of the proton longitudinal momenta carried by the participating partons are $x_1 = (M_X/\sqrt{s}) \times e^{+y}$ and $x_2 = (M_X/\sqrt{s}) \times e^{-y}$, and $M_X = \sqrt{x_1 x_2 s}$. Compared to the situation at the Tevatron, the production of particles of a given mass M_X at the LHC thus involves partons at much lower x_i values, where the gluon parton density is increasing rapidly, and this has dramatic consequences. To see this, it is instructive to compare the ratio of the parton luminosities [10,11] in 7 TeV pp collisions over those in 1.96 TeV $p\bar{p}$ collisions as a function of the energy available to create a given mass M_X, i.e. the centre-of-mass energy of the colliding partons. Such a ratio is shown in Fig. 4 for gluon-gluon and quark-antiquark interactions. The gluon density in the proton increases rapidly when probing partons that carry a smaller fraction of the proton momenta, and this translates in a considerable gain in parton luminosities at the LHC for a given M_X. In this respect the LHC can be seen as a "gluon-gluon" collider. For the production

of a Higgs boson via gluon-gluon fusion (see section 5) a gain of a factor of 10 to 15 is obtained in the low mass range $110 \lesssim M_X \lesssim 135$ GeV. For the production of a pair of squarks from supersymmetry, which involves quarks or gluons in the initial state (section 5) the gain factor is > 100, for masses above 300 GeV. The production of a new Z′ gauge boson (section 6) which involves quarks and anti-quarks in the initial state is enhanced by a factor > 50 for masses at the TeV scale.

4. FIRST RESULTS AT THE LHC: STANDARD MODEL CANDLES

W and Z Bosons:

The measurement of inclusive production of W and Z bosons has been an important benchmark at the LHC in 2010. The W and Z production in hadronic collisions occur at leading order through the annihilation process $q\bar{q} \to \mathrm{W/Z}$. The dynamics is controlled by QCD. In contrast to the situation at the Tevatron, the scattering at the LHC involves partons at lower Bjorken x and thus dominantly involves sea quarks and anti-quarks. The inclusive W and Z production also receives a small (<5%) "electroweak" contribution via vector boson fusion.

Early results on inclusive W and Z production were obtained by ATLAS [12] with an integrated luminosity of only $320\,\mathrm{nb}^{-1}$ and by CMS [13] with an integrated luminosity of $2.9\,\mathrm{pb}^{-1}$. Some illustration of the early CMS results are provided in Fig. 5 and 6. The di-electron invariant mass spectrum for the Z selection at the LHC is seen in Fig. 5 to be quasi-background free for masses in the range from 60 to 120 GeV. The total background from QCD instrumental background, di-top production etc. amounts to well below 0.5% of the selected sample. The transverse mass (M_T) spectrum for the W selection is also seen to be remarkably clean. The transverse mass is defined as $M_T = \sqrt{2 p_T \not{E}_T (1 - \cos\Delta\phi)}$, where $\Delta\phi$ is the angle between the missing transverse momentum and the lepton transverse momentum, and $\not{E}_T$ is the missing transverse energy. In the CMS analysis the $\not{E}_T$ is actually measured as the negative of the vector sum of all reconstructed

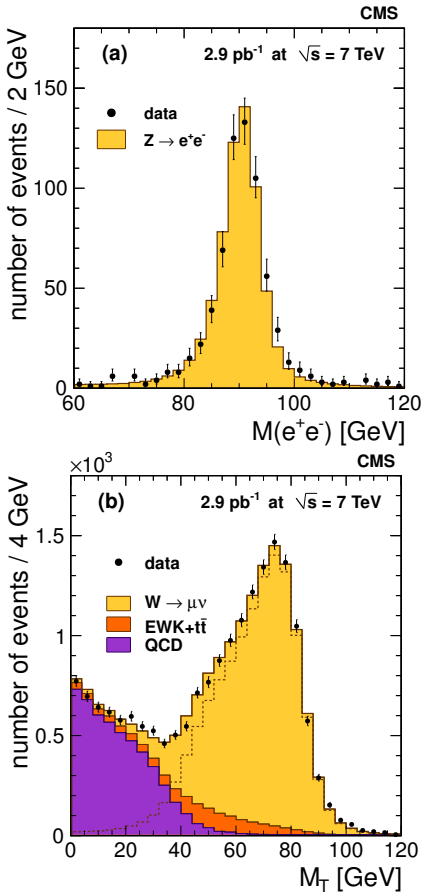

Figure 5. Measurement by CMS at the LHC [13] of *(top)* the Z → *ll* signal mass distribution for a $\mathrm{Z} \to e^+e^-$ sample and *(bottom)* the W → *lν* signal transverse mass distribution for a $\mathrm{W} \to \mu\nu$ sample.

transverse momentum of particles identified with a particle flow algorithm [14]. The increase of the W and Z cross sections with collider energy is seen in Fig. 6 to be as expected by the SM. The measured ratio of the W to Z production cross sections as well as the ratio $R_\pm$ of the W^+ to W^- production cross sections are also seen to be very well predicted. These provide a stringent test of the theory because the systematic uncertainty from the pp luminosity measurement cancels out in the ratio. The ratio $R_\pm > 1$ is a reflection of the structure of the proton and its

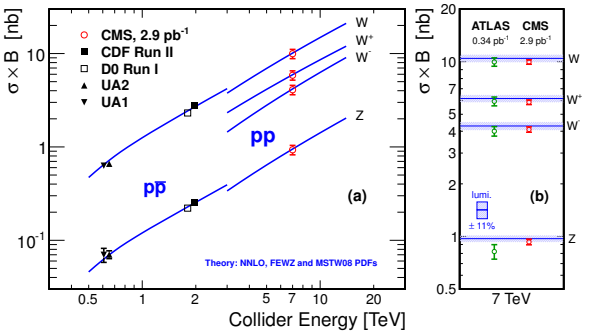

Figure 6. Measurement at the LHC of the W and Z production cross section times branching ratio as a function of $\sqrt{s}$. The results shown correspond to the early 2010 CMS [13] and ATLAS [12] results. They are compared to lower energy results from Tevatron experiments.

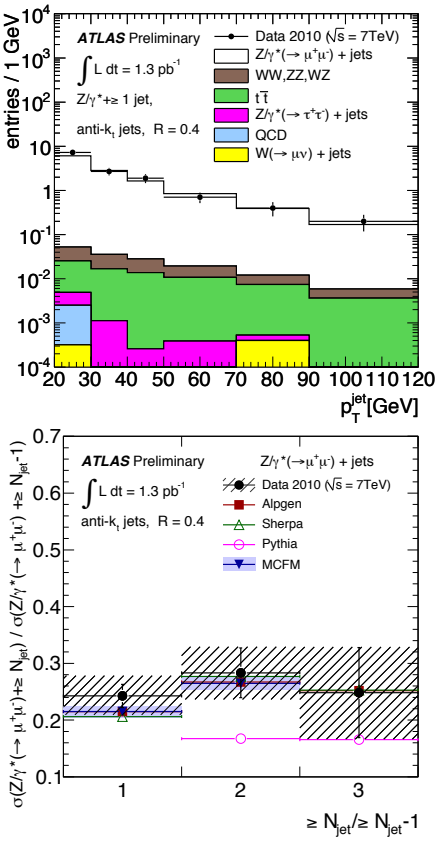

Figure 7. Measurements at the LHC [16] of the $Z/\gamma* \to \mu^+\mu^-$ + jets production for events containing at least one jet with $p_T^{\rm jet} > 20$ GeV; *(top)* leading-jet p_T spectrum; *(bottom)* measured ratio of the cross sections ($\sigma_{Njet}/\sigma_{Njet-1}$).

uud composition in valence quarks. The cross section $\sigma(\mathrm{pp} \to \mathrm{W}X) \times \mathcal{B}(\mathrm{W} \to l\nu)$ is measured to be $\simeq$10 nb, and about 10 times larger than $\sigma(\mathrm{pp} \to \mathrm{Z}X) \times \mathcal{B}(\mathrm{Z} \to ll)$. The CMS results have been very recently updated [15] for the complete 2010 integrated luminosity of $36\,\mathrm{pb}^{-1}$. A good agreement is found between the measurements at the LHC and theoretical predictions computed at the Next-to-next-to-Leading-Order (NNLO) QCD level.

With increasing integrated luminosity in the course of the LHC during in 2010, it became possible to perform measurements of the Z and W production cross sections in association with jets. Results were obtained by the ATLAS collaboration first for W + jets [16], and more recently for Z + jets [17], using $1.3\,\mathrm{pb}^{-1}$ of integrated luminosity. Results on Z + jets are illustrated in Fig. 7. The CMS collaboration has recently presented results [18] using the full 2010 data set of $36\,\mathrm{pb}^{-1}$. The results are found fully consistent between Z + jets and W + jets, and Berends-Giele scaling has been verified for final states with up to 4 jets.

Another important SM electroweak benchmark at the LHC is the observation and first inclusive production cross section for Z boson production in the $\mathrm{Z} \to \tau^+\tau^-$ decay mode. The tau lepton can decay into a purely leptonic final state $\tau_l \to l\nu_l\nu_\tau$ where $l = e, \mu$ or into semihadronic final states. The former are denoted "τ_l" and the latter "τ_h" decays. Establishing a $\mathrm{Z} \to \tau_l\tau_h$ signal is particularly important as a SM candle (and background) for new physics searches relying on tau lepton pair production, such as the searches in the scalar sector of supersymmetric theories (see section 5). Results for the $\mathrm{Z} \to \tau^+\tau^-$ decay mode have been recently presented by the ATLAS [19] for an integrated luminosity of $8.3\,\mathrm{pb}^{-1}$ and CMS [20] collaborations for the full 2010 dataset of $36\,\mathrm{pb}^{-1}$. A rather clean signal is established in both experiments. The cross section

$\sigma(\mathrm{pp} \to \mathrm{Z}X) \times \mathcal{B}(\mathrm{Z} \to \tau^+\tau^-)$ obtained by CMS is of about $\simeq 1\,\mathrm{nb}$ and is measured with precision of about 10%.

Top Quark:
The LHC is a top quark factory. At hadronic colliders, the top quarks are produced primarily via the strong interaction in top-antitop ($t\bar{t}$) pairs. The dominating $t\bar{t}$ production mechanism in pp collisions is via gluon fusion, whereas in contrast in $\mathrm{p\bar{p}}$ collisions at the Tevatron the pairs are predominantly produced through quark-antiquark annihilation. Single top can be produced in hadronic collisions through electroweak processes such as via t-channel exchange of a W boson. This should allow for precision measurements the top quark physical mass m_t (or Yukawa coupling to the Higgs boson) and the CKM mass mixing matrix element $|V_{tb}|$. Improving on the precision already obtained in the Tevatron experiments on the top quark mass will take time. In contrast, a direct measurement of $|V_{tb}|$ could become possible with a precision of $\mathcal{O}(10)\%$ using LHC Run I data. Otherwise, besides m_t and $|V_{tb}|$ which are free parameters of the SM, the top quark quantum numbers are highly constrained by the structure of the theory and the cancellation of triangular anomalies.

The top width is calculable in the SM and found to be ~ 1.5 GeV. The correspondingly very short top quark lifetime of $\sim 0.5 \times 10^{-24}$, a value much smaller than the characteristic QCD time scale of Λ^{-1}_{QCD}, implies that it is expected to decay before top-flavoured hadrons can form. Interesting top quark spin correlation studies are thus made possible in gluon-gluon interactions at the LHC. The top quark physics opens new possibilities for search of physics beyond the SM. One possibility is to look for new top quark decays. With $|V_{tb}| \sim 1$, the top quark is expected to decay with $\sim 100\%$ to Wb. But there is room to search for the decay $t \to \mathrm{H}^+ b$ involving a charged Higgs (see section 5). More generally the top quark could very well turn out to be something else than just another elementary quark, with possibly part or all of it's mass arising from something else than the ordinary Yukawa interaction with the SM Higgs field. Some of the possible consequences will be discussed in section 5. Besides precision measurements and the search for new physics involving the top quark itself, the top quark production at the LHC is an important background for other searches as it is one of the main source (with W and Z production) of isolated high p_T leptons.

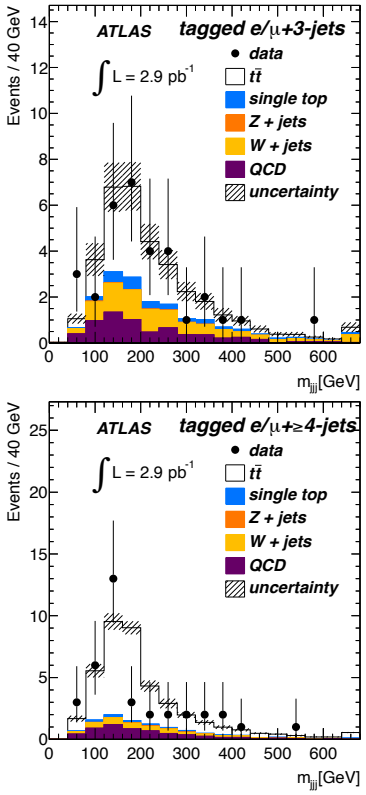

Figure 8. Distribution of the invariant mass measured by ATLAS [22] for the 3-jet combination having the highest p_T in *(top)* the 3-jet and *(bottom)* $\geq$ 4-jet tagged samples. The data points are compared to the sum of all expected contributions. The background uncertainty on the total expectation is represented by the hatched area.

The first top-quark pair production cross sections where measured at the LHC by the CMS [21] and ATLAS [22] experiments with integrated luminosities of only $\simeq 3\,\mathrm{pb}^{-1}$. A good signal to background ratio is obtained [22] with cut-based analysis strategies as illustrated in Fig. 8

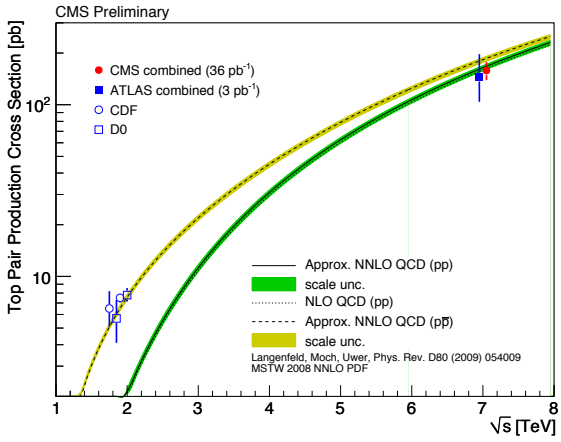

Figure 9. Top-quark pair production cross section as a function of $\sqrt{s}$ measured in $p\bar{p}$ and pp collisions. The CDF and D0 measurements were obtained at $\sqrt{s} = 1.8$ TeV and $\sqrt{s} = 1.96$ TeV [23]. The CMS combined measurement from Ref. [24] is shown as well as the ATLAS measurement from Ref. [22].

for the lepton + jets sample. The top production cross section measurements presented by CMS [24] at early spring 2011 conferences is shown Fig. 9 and compared to ATLAS results and to $p\bar{p}$ collisions results from the Tevatron. The evolution of the cross section with $\sqrt{s}$ is found to be well described by the SM at NLO. Combining various channels, a total cross section of $\sigma_{t\bar{t}} = 158 \pm 19\,\text{pb}$ is measured (including uncertainties on the pp luminosity).

The observation of single top production is difficult at hadronic colliders. The first observation of single top production at the Tevatron was obtained in 2009, more than twenty years after the start of the operation of the $p\bar{p}$ collider. Both the ATLAS [25] and CMS [26] have already performed analysis at the LHC using their full 2010 datasets and a first measurement of the t-channel production cross section has been presented very recently [26]. Such a finding which relies on a complicated final state with a least a lepton, $\not{E}_{\rm T}$, b-quark tagging and jets and makes use of multivariate analysis techniques shows the level of readiness of the LHC experiments for challenging searches such as the eventual search for a Higgs boson at low or intermediate masses.

Di-Bosons:
The measurements of weak di-boson production are the next, and possibly the last, step on the road towards SM Higgs boson production. The WW production has been observed by both the ATLAS [27] and the CMS [28] experiments using their full 2011 datasets. The definitive observation of WZ will require four to five times more data and is expected in spring or early summer 2011. A single event has been observed in the ZZ$\rightarrow$ 4μ channel in 2010 satisfying pre-defined cuts [29] and with a reconstructed 4 lepton invariant mass of $m_{4l} \simeq 202$ GeV. The cross section $\times$ branching ratio for decays with charged lepton ($l = e\mu$) is about ten times smaller for ZZ production than that for WW production. The rate of ZZ* signal events for reconstructed 4 lepton masses $m_{4l} > 100$ GeV is expected to be too low to allow for a background measurement from side-bands at the time of an eventual discovery of the SM Higgs bosons, for a wide range of possible $m_{\rm H}$ ($\simeq m_{4l}$) hypothesis.

5. HIGGS BOSON(S) AND SUPERSYMMETRY: PROSPECTS AND FIRST RESULTS

Electroweak Symmetry Breaking:
A most important unsolved (or unproven) issue for the SM is the question of the origin of particle masses and electroweak symmetry breaking. In the SM, a fundamental scalar field, the so-called Higgs field, is assumed to pervade the universe and to possess, through self-interactions, a non-zero field strength of the ground state. While the electroweak Lagrangian is invariant under gauge symmetry, the non-zero vacuum expectation value for the scalar field induces a breaking of the $\text{SU}(2)_L \times \text{U}(1)_Y$ symmetries which relates the electromagnetic and weak interactions. This "Higgs mechanism" of spontaneous electroweak symmetry breaking (EWSB) provides a mass to the gauge Z^0 and $W^{\pm}$ gauge bosons and leave the photon massless, while preserving the renormalizability of the theory. In the SM, the scalar

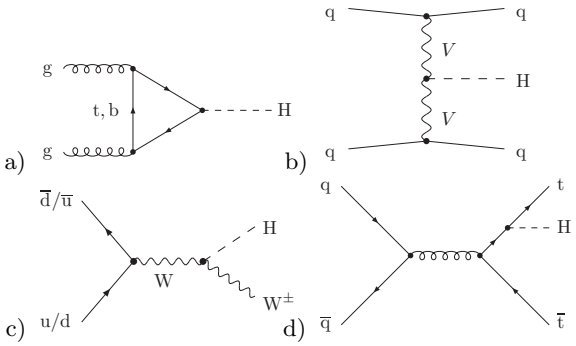

Figure 10. Examples of leading order Feynman diagrams contribution to the production of the SM Higgs boson in hadronic collisions; (a) gluon-gluon fusion $gg \rightarrow$ H through b- and t-quark fermion loops; (b) vector boson fusion WWH or ZZH; (c) Higgs-strahlung WH or ZH; (d) associated production of a Higgs boson and a $t\bar{t}$ pair.

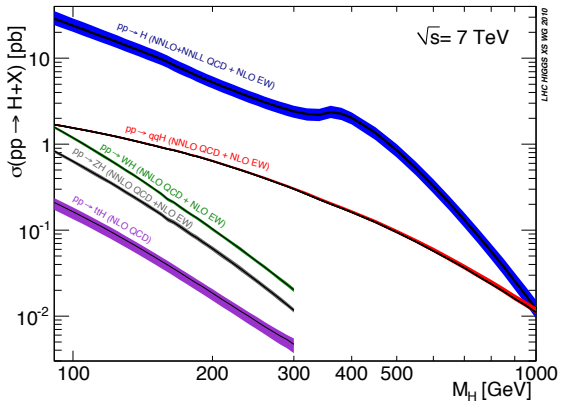

Figure 11. Standard Model Higgs boson production cross section [30] in pp collisions at the LHC at $\sqrt{s} = 7$ TeV.

field transforms as a doublet under $SU(2)_L$ and the EWSB leaves one physical Higgs boson. The mass of the Higgs boson is not provided by the theory. The elementary fermions acquire masses after EWSB through Yukawa interactions (of arbitrary strengths) with the Higgs field. The SM Higgs boson thus couples to elementary fermions in proportion to their mass which are arbitrary parameters in the theory. The existence of a "Higgs mechanism" remains unproven, but he standard EWSB is the only known way to achieve perfect unitarisation of $W_L W_L$ scattering. In absence of the Higgs boson and the WWH coupling, new interactions should appear at the TeV scale to avoid unitarity violations from the $W_L W_L$ scattering amplitudes which grows quadratically with energy.

SM Higgs Boson Production:

The SM Higgs boson production mechanisms in hadronic collisions are illustrated with examples of leading-order (LO) diagrams in Fig. 10. The main production processes are gluon-gluon fusion (ggH), vector boson fusion (VBF H), "Higgstrahlung" (VH) and associated production (e.g. $t\bar{t}$ H). The corresponding production cross sections [30] in pp collisions at the LHC at $\sqrt{s} =$ 7 TeV are shown in Fig. 11.

The gluon-gluon fusion production mechanism (ggH) dominates over the entire mass range allowed by the SM, as can be seen in Fig. 11. It is about seven times larger then the sum of all other contributions. The ggH production in the SM is mediated by triangular quark fermion loops. The dynamics is controlled by the strong interactions. The LO contribution is proportional to α_s^2 where α_s is the strong coupling constant. The higher order QCD corrections are important and they stabilize the cross section when the renormalisation and factorization scales are varied. The NLO contributions increase the LO cross section by 80-100% at the LHC. The strength of the Yukawa couplings g_{ffH} of the Higgs boson to fermions is proportional to the fermion mass m_f, such that the ggH production arises mainly via the mediation of top quark loops.

The sub-leading production mechanism is the VBF Higgs boson production through WWH or ZZH couplings. The LO contribution involves only quarks or antiquarks in the initial state. The higher order QCD corrections are small. The NLO contributions increase the LO cross section by 5-10% at the LHC. In the VBF process, the weak bosons are emitted from a quark from each of the incoming proton. The quarks are deflected and give a characteristic pair of "forward-backward" jet tags that can be exploited by the experiments to suppress background. As

can be seen in Fig. 11, the relative contribution of the VBF mechanism increases with increasing Higgs boson mass hypothesis. At $m_{\rm H} = 110$ GeV, it represents 6.6% of the total "inclusive" (VBF H+ggH) production. This fraction increases to 11.1% at $m_{\rm H} = 300$ GeV.

The VH production mechanism plays a role mostly at low $m_{\rm H}$. The WH production cross section is about 1.8 times larger than the ZH production. Compared to the VBF H contribution, the sum of the WH and ZH contributions is almost as large at $m_{\rm H} = 110$ GeV, but become ten times smaller at $m_{\rm H} = 110$ GeV. The NLO contributions increase the LO cross section for VH production by about 20% at the LHC.

SM Higgs Boson Decay:
The SM Higgs boson decay branching ratios as a function of the Higgs boson mass hypothesis are shown in Fig. 12. The decay H $\to b\bar{b}$ dominates in

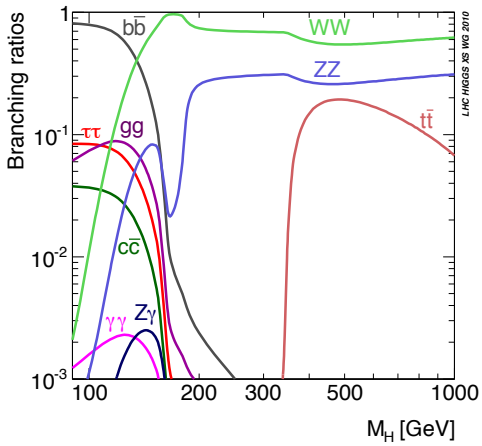

Figure 12. Standard Model Higgs boson decay branching ratios [30] as a function of the Higgs boson mass hypothesis.

the "low mass" range, up to $m_{\rm H} \simeq 135$ GeV. The branching ratio for the decay H $\to \gamma\gamma$ peaks in this low mass range around $m_{\rm H} \simeq 125$ GeV. The decay in electroweak bosons, H $\to$ W$^+$W$^-$ and H $\to$ ZZ represent from 85% to almost 100% of the Higgs boson decays in the "high mass" range beyond $m_{\rm H} \simeq 155$ GeV. The notion of "low" and "high" mass range defined in this way will be useful for the following discussion. The region in between with $135 \lesssim m_{\rm H} \lesssim 155$ GeV, called here the "intermediate mass" range, is covered by many channels. The branching ratio for the decay H $\to$ Zγ peaks around $m_{\rm H} \simeq 145$ GeV. The branching ratio for the decay H $\to$ ZZ becomes larger than that of H $\to \tau\tau$ near the lower edge of the intermediate mass region, namely around $m_{\rm H} \simeq 133$ GeV. The branching ratio for the decay H $\to \gamma\gamma$ remains sizeable ($\geq 0.1\%$) over the full intermediate mass range. The branching ratio for the decay H $\to \tau\tau$ remains above 1% over the full low and intermediate mass ranges. Not visible on Fig. 12 is the branching ratio for the decay H $\to \mu\mu$ which is suppressed by $(m_\mu/m_\tau)^2 \simeq 3.5 \times 10^{-3}$ with respect to that of H $\to \tau\tau$, and thus remains everywhere well below 0.1%.

The mean number of SM Higgs boson events expected for an integrated luminosity of 1 fb^{-1} from the various production mechanisms and the decay branching ratio in some of the leading channels are given for convenience in Table 1 and 2. As can be seen from these tables, the

Table 1
Mean number of Higgs boson events expected in the various production modes for an integrated luminosity of 1 fb^{-1} and for various SM Higgs boson mass ($m_{\rm H}$) hypothesis.

$m_{\rm H}$ GeV	ggH	VBF H	WH	ZH	$t\bar{t}$H
110	19800	1400	875	472	126
120	16600	1270	656	360	97.6
130	14100	1150	501	278	76.6
150	10500	962	300	171	48.7
170	7730	817	188	111	32.2
200	5250	637	103	61	18.5
300	2420	301	20	12	4.7

SM Higgs boson will have been copiously produced at the LHC by the time we arrive to such an integrated luminosity, but only a handful of

Table 2
Decay branching ratio (in %) for the SM Higgs boson.

$m_{\rm H}$ GeV	$b\bar{b}$	$\tau\tau$	$\gamma\gamma$	WW	ZZ
110	74.5	8.03	0.197	4.82	0.44
120	64.9	7.11	0.225	14.3	0.16
130	49.4	5.49	0.226	30.5	4.02
150	15.7	1.79	0.137	69.9	8.28
170	0.79	0.092	0.016	96.5	2.36
200	-	-	-	74.1	25.6
300	-	-	-	69.2	30.7

events are expected to be reconstructed in some of the most spectacular channels. The decay chain $\mathrm{H} \rightarrow \mathrm{ZZ}^{(*)} \rightarrow 4l$ with $l = e, \mu$ constitutes a *golden* channel at the LHC. The branching ratio for the $\mathrm{Z} \rightarrow 2l$ decay is 6.74% so that $\mathcal{B}(\mathrm{H} \rightarrow 4l)/\mathcal{B}(\mathrm{H} \rightarrow \mathrm{ZZ}) \simeq 4.5 \times 10^{-3}$. For a Higgs boson mass below the $2m_{\rm Z}$ threshold, interference contributions become relevant for final states with identical fermions ($4e$ or 4μ). This provides an enhancement of more than 10% at $m_{\rm H} = 120$ GeV. One expects on average from ~ 2.9 events at $m_{\rm H} = 130$ GeV and less than 5 events for any mass value in the low and intermediate range. A maximal number of signal events of ~ 6.8 is expected if $m_{\rm H} = 200$ GeV. For the actual experiments, such numbers must be folded with the acceptance and reconstruction efficiency within acceptance. The reconstruction efficiency scales with ϵ_l^4 where ϵ_l is the reconstruction efficiency (combining particle identification and isolation) for an individual lepton. Preserving the highest reconstruction efficiency at a working point for lepton identification and isolation sufficient to get rid of instrumental background such as Z+jets, $\mathrm{Z}b\bar{b}$ and $t\bar{t}$ is a challenge. The resolution on the reconstructed mass m_{4l} is then the key for a statistical separation of the signal from the electroweak ZZ continuum.

SM Higgs Boson, Prospects and Results: The search for the SM Higgs boson over a wide range of possible mass is one of the first objective for the experiments at the LHC. A combination of the possible Higgs decay channels will be needed to arrive to a full coverage of the allowed SM mass range in Run I. Prospective studies extrapolating from more detailed analysis by the CMS [31] and ATLAS [32] experiments show that $1\mathrm{fb}^{-1}$ of integrated luminosity could be already sufficient to be sensitive to a SM Higgs in the intermediate and high mass range. This is illustrated with the prospective analysis shown in Fig. 13 showing the expected exclusion limits that could be established from a combination of channels.

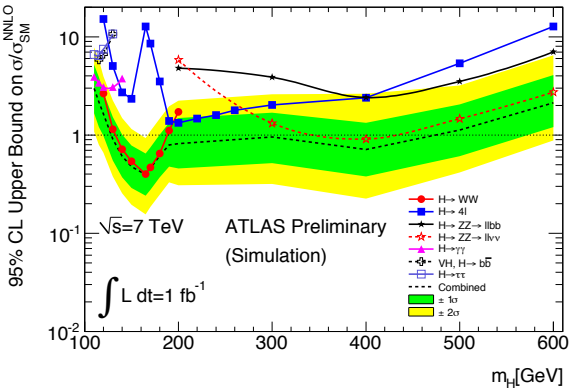

Figure 13. Multiple of the SM Higgs production cross section that can be excluded using $1\mathrm{fb}^{-1}$ of integrated luminosity at $\sqrt{s} = 7$ TeV in the ATLAS experiment [32]. The contribution from each production and decay channel is indicated as well as the combined result.

The H→WW channel is seen to be the most sensitive for an exclusion for masse up to $\sim$ 190 GeV. This situation should remain for as long as the integrated luminosity remains relatively modest (here 1 fb^{-1}). This is because of the small branching ratio in the H→ $\gamma\gamma$ and H→ZZ→ $4l$ which forbids a contribution at low and intermediate masses for such luminosity. The H→ZZ is found to be the most sensitive for an exclusion at masses $\gtrsim 190$ GeV, with the $2l2\nu$ channel bringing a significant contribution at very high masses.

The H→ $\gamma\gamma$ and H→ $4l$ will gain importance in the combination at low $m_{\rm H}$ as soon as the integrated luminosity allows them to open up. This

is illustrated in Fig.14 which shows the expected significance for a discovery for an integrated luminosity of 5 fb^{-1} at $\sqrt{s} = 7$ TeV.

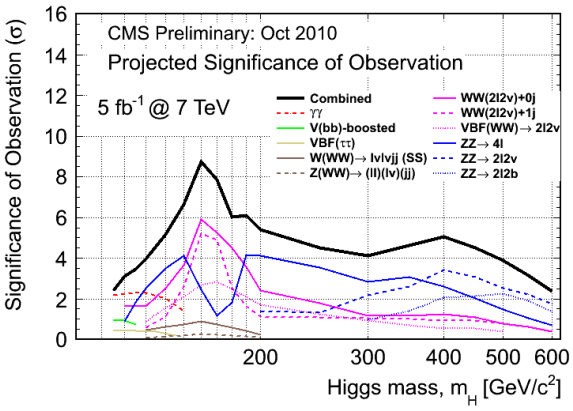

Figure 14. Significance of a SM Higgs boson observation at the LHC for an integrated luminosity of 5 fb^{-1} at a pp centre-of-mass energy of 7 TeV.

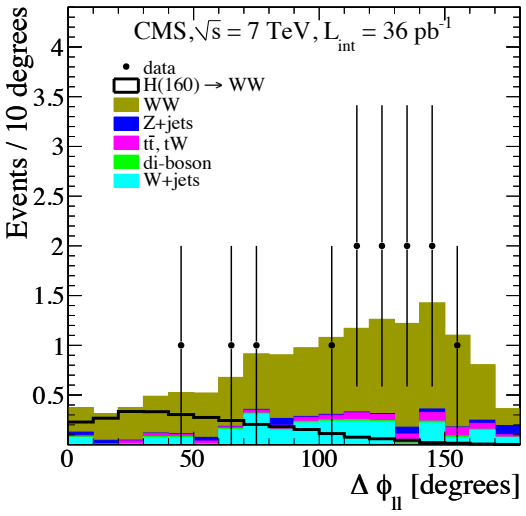

Figure 15. Azimuthal angular separation between the selected charged leptons after WW* selection by CMS [28]. The data points are compared to the mean expectation from the background (staggered histogram) including the contribution from the WW* continuum, and for a SM Higgs boson with $m_{\rm H} = 160\,{\rm GeV/c^2}$.

The H→WW channel is the most powerful channel for exclusion at very low luminosity and this as been exploited by both experiments. Results in this channel from the ATLAS and CMS experiment obtained with the full 2010 datasets are shown in Fig. 15, 16, 17 and 18.

SUSY Higgses, Prospects and Results:
The Higgs boson in the SM suffers from quadratically divergent self-energy corrections at high energies [35]. Numerous extensions to the SM have been proposed to address these divergences. Considerable attention has been given to the related question of the hierarchy of the fundamental interactions when contemplating a grand unification and new physics at some very high energy scale. A most studied family of models are the supersymmetric models. In supersymmetry, a symmetry between fundamental bosons and fermions is postulated which results in a cancellation of the divergences at tree level. This implies the existence of supersymmetric particle partners for ordinary fermions and bosons which will be discussed below. In the Higgs sector, the minimal supersymmetric extension to the standard model (MSSM) requires the presence of two Higgs doublets. This leads to a more complicated Higgs boson sector, with five massive Higgs bosons: a light neutral scalar (h), two charged scalars ($H^{\pm}$), a heavy neutral CP-even state (H) and a neutral CP-odd state (A).

The masses of the MSSM Higgs boson states are specified up to radiative corrections mainly by two parameters, usually taken to be the mass of the pseudoscalar state m_A, and the ratio $\tan\beta$ of the vacuum expectation values for the two Higgs doublets giving mass to the u-like and d-like quarks, $\tan\beta \equiv v_u/v_d$. At large $\tan\beta$ (greater than about 20–30) the couplings of the Higgs bosons to down-type quarks are proportional to $\tan\beta$. As a result the production cross section for two of the three neutral Higgs bosons can be nearly as large as that for electroweak gauge bosons (W,Z) production at a proton-proton collider such as the LHC. Two main production processes contribute to $pp \to \phi + X$, where $\phi = h, H$,

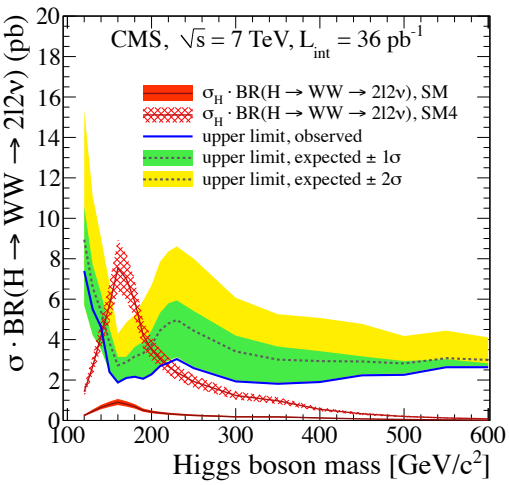

Figure 16. Mean expected and observed upper limits at 95% C.L. on the cross section $\sigma_{\mathrm{H}} \times \mathcal{B}(\mathrm{H} \rightarrow \mathrm{WW}^* \rightarrow 2l2\nu)$ for masses in the range $120-600$ GeV/c^2, as obtained by CMS [28] using multi-variate selection techniques for the event selections and a Bayesian statistical approach. The expected cross sections for the SM and for the SM extended with a fourth-fermion family (SM4) are also presented.

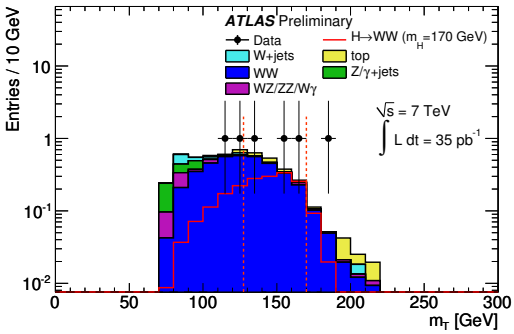

Figure 17. The transverse mass distribution m_{T} in the H + 0jet analysis for the $\mathrm{H} \rightarrow \mathrm{WW}^*$ channel, measured by ATLAS [33] after all selection cuts (except for the cut on m_{T} itself). The optimal signal region lies between the two dotted lines.

or A: gg fusion through a b-quark loop and direct $b\bar{b}$ annihilation from the b parton density in the incoming beam protons.

The results from the CMS experiment [36] are shown in Fig. 19, and 20. Similar results were obtained by the ATLAS experiment [37]. The $\mathrm{H} \rightarrow \tau\tau$ is one of the promising decay channel, but not the only one, studied in the context of SUSY theories at the LHC. Of course the situation and the essential phenomenology could turn out to be very different if non-minimal models are realized.

Higgs bosons in 2HDM Models:
The extended Higgs sector of minimal supersymmetric (mSUSY) theories can be effectively matched to a particular type of two Higgs doublet-model (2HDM). The 2HDMs, with two doublet of Higgs fields having the same quantum numbers, are the simplest extension of the SM that are compatible with gauge invariance. As for the SM, the 2HDM allow for a perfect unitarization of $\mathrm{W}_L\mathrm{W}_L$ scattering. The masses relations and couplings of the five physical Higgs bosons in the most general 2HDM can vary significantly from the mSUSY models, and this could have important consequences for the LHC.

In a generic 2HDM, the expressions for the vector boson masses coincide with the ones in the SM if $v_1^2 + v_2^2 = v^2$ where v_1 and v_2 are the vacuum expectation values (VEVs) corresponding to each of the doublets, and v is the VEV of the Higgs doublet for the SM. The HZZ and HWW couplings are controlled by two angles, β which is defined as usual via $\tan\beta = v_2/v_2$, and α the mixing angle in the neutral Higgs sector. In terms of α and β, the couplings of the h^0 and H^0 to the vector bosons are necessarily suppressed with respect to the SM Higgs boson couplings and one has: $g_{\mathrm{h^0VV}} = \sin(\beta-\alpha) \times g_{\mathrm{HVV}}$ and $g_{\mathrm{H^0VV}} = \cos(\beta-\alpha) \times g_{\mathrm{HVV}}$, such that the sum rule $g^2_{\mathrm{h^0VV}} + g^2_{\mathrm{H^0VV}} = g^2_{\mathrm{HVV}}$ is verified. A consequence is that if the HVV coupling vanishes for one of the CP-even neutral Higgs bosons, either h^0 or H^0, such that it decouples from vector bosons at tree level, then the Higgs coupling of the other neutral Higgs bosons is SM-like. This has been considered a "natural" scenario in mSUSY theories in which $\cos(\beta-\alpha) \sim 0$ might be expected such that $g_{\mathrm{h^0VV}}$ saturates the sum rule and is

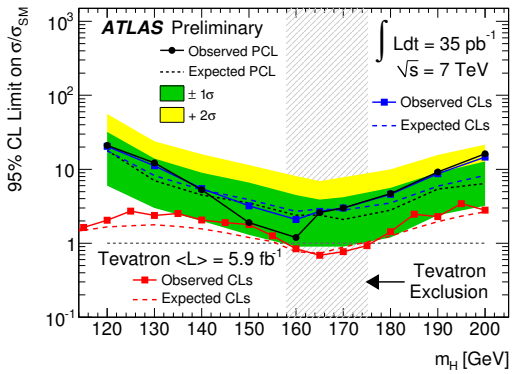

Figure 18. Upper limit at 95% C.L. on the expected signal rate for $\sigma_{\mathrm{H}} \times \mathcal{B}(\mathrm{H} \to \mathrm{WW}^* \to 2l2\nu)$ expressed as a multiple of the SM rate. The results from ATLAS [33]. are shown for two different statistical methods and compared to previous results obtained in Tevatron experiments [34].

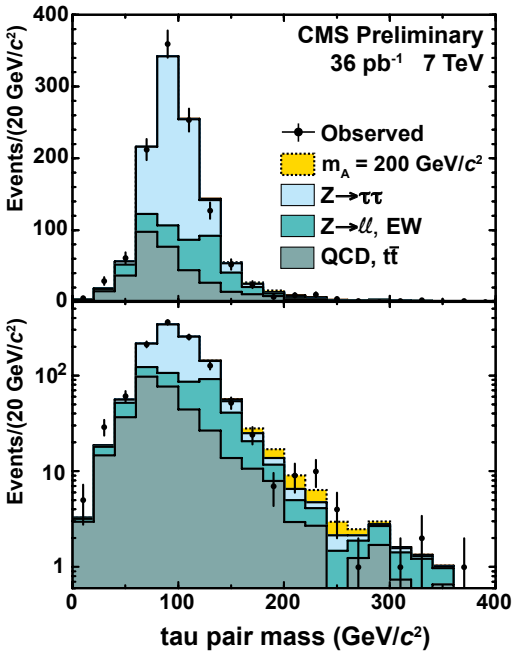

Figure 19. Reconstructed tau invariant mass distribution for the sum of the $e\tau_h, \mu\tau_h$ and $e\mu$ final states, measured by CMS [36]. The observed distribution (data points) is compared to the sum of the expected background (shaded histogram), and a contribution from a Higgs boson signal with $m_A = 200\,\mathrm{GeV/c^2}$ with a normalization corresponding to the upper bound at 95% C.L. on $\sigma_{\mathrm{H}} \times B(\mathrm{H} \to \tau\tau)$.

SM-like while the $g_{\mathrm{H^0VV}}$ is highly suppressed.

More generally in a 2HDM, the h^0 can be made SM-like while the other Higgs bosons are much heavier and decouple from known particles. There is also the possibility for different fermions to acquire their mass from different doublets, allowing the implementation of a hierarchy of couplings e.g. between the d-like quarks such as the bottom quark and u-like quarks such as the top quark. The 2HDM thus allows for a variety of configurations with Yukawa couplings enhanced or suppressed with respect to the SM that could have dramatic consequences for the phenomenology at the LHC. The case where both Higgs doublets couple with the up and down sectors lead to flavour changing neutral currents (FCNC) and are called 2HDM of type III. In general, to avoid unwanted flavour changing neutral currents (FCNC) mediated at tree level by Higgs boson exchange, it is sufficient that all fermions of a given electric charge couple to no more than one Higgs doublet [40]. Models where one doublet couples to d-like quarks and the other to u-like quarks are called 2HDM of type II. The Higgs sector of the MSSM belongs to this class.

In a 2HDM of type I, only one Higgs doublet couples to fermions but the couplings nevertheless differ from SM-like couplings because of mixing. For $\alpha = 0$, the coupling of the h^0 are maximal (for a given $\tan\beta$) and the H^0 is decoupled (at tree level) from fermions. For $\alpha = \pi/2$, a similar situation occurs but with the role of the h^0 and H^0 interchanged. Thus, the h^0 (H^0) becomes *fermiophobic* for $\alpha = \pi/2$ ($\alpha = 0$). For a fermiophobic Higgs boson, the $gg\mathrm{h}^0$ production is suppressed, and one is left with WW h^0 and Vh^0 production, with $\mathrm{h}^0 \to \gamma\gamma$ as the main decay mode (via a virtual loop of W bosons) for the observation of a low mass Higgs boson. A search for the $\mathrm{h}^0 \to \gamma\gamma$ in a fermiophobic 2HDM model will be performed at the LHC during Run I.

The leptonic and quarkonic sectors could very

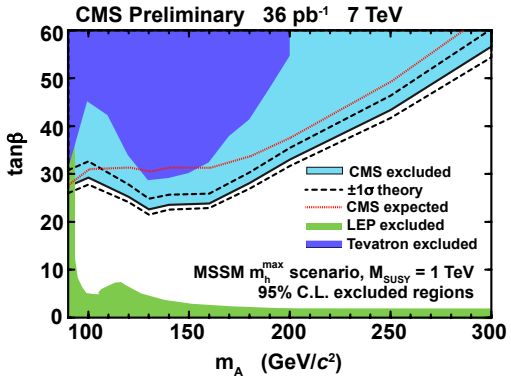

Figure 20. Region of the $\tan\beta$ vs m_A parameter space excluded at 95% C.L., in the context of the MSSM $m_h^{(\max)}$ scenario, by CMS [36]. The result is compared to exclusion regions previously established in LEP [38] and Tevatron [39] experiments.

well be organized in a non-symmetric manner within a 2HDM. The leptons and the quarks need not be getting their mass from the same Higgs doublet. It is possible to have the lepton mass to originate from one doublet while the quark masses (or only u-like or d-like quarks) originate from the other doublet. In this way, the h^0 can be made *chromophobic*. The phenomenology of chromophobic Higgs at the LHC is very interesting and should be studied in detail during Run I. As for a fermiophobic Higgs boson, a chromophobic Higgs boson is only produced via vector boson fusion or Higgstrahlung. But the main decay channel at low mass is now the $h^0 \to \tau\tau$ while the $h^0 \to \gamma\gamma$ still contributes. For a reasonable range of $\tan\beta$ and $\sin(\alpha-\beta)$ values, an enhancement of more than a factor 10 is possible with respect to the situation with the SM, for the VBF Higgs boson production followed by a decay in di-taus [41].

The dominance of the VBF Higgs boson production for a discovery of the Higgs boson at low mass, with $h^0 \to \tau\tau$ (or $h^0 \to \gamma\gamma$) as main observation channels, is a feature of different types of models beyond the SM. One could imagine that the vector bosons, the leptons, and the light quarks receive their mass through a SM-like mechanism but that the mass of the heavy quarks in the third generation have a partly, or completely, different origin. Such a situation is a feature of some models with top-quark condensation such as discussed in Ref. [42].

Supersymmetric Matter:

SUSY was mentioned above in the context of the EWSB, as a mean to stabilize the Higgs boson mass at the electroweak scale, and possibly explain the hierarchy between that scale and the GUT or Planck scale. But the importance of SUSY goes far beyond this role in the Higgs sector. SUSY generalizes the four-dimensional space-time translation and rotation symmetries to include mixing with internal quantum dimensions. It is a symmetry between boson and fermion fields. It predicts the existence of new particles, the "super-partners" of each of the ordinary elementary fermions and bosons. To each ordinary fermion, the constituents of matter, must correspond bosonic SUSY partners, the sfermions (sleptons and squarks). To each boson, the mediators of interactions and the Higgs bosons, correspond fermionic SUSY partners, the gauginos and higgsinos.

To avoid unwanted lepton or baryon number violating interactions caused by the exchange of squarks or sleptons, the R-Parity ($R_{\rm p}$) is introduced as a discrete symmetry [43]. It distinguishes ordinary particles ($R_{\rm p} = +1$) from the super-particles ($R_{\rm p} = -1$) and is defined as $R_{\rm p} = (-1)^{3B+L+2S}$ where S is the spin, B the baryon number and L the lepton number. Assuming a strict conservation of $R_{\rm p}$ in all physics processes, the lightest supersymmetric particle (LSP) is stable and a natural candidate for dark matter. The escape of the LSP leads to a characteristic $\not{E}_{\rm T}$ signature in the final state for the SUSY searches at colliders.

Supersymmetry theory and phenomenology as well as the experimental searches at colliders have been a very fertile area of activity in high energy physics for many decades. Searches at colliders have been guided in particular by the MSSM, the archetype of SUSY models which realizes a extension of the SM which is minimal in fields and couplings, and with a parametrization of the (unspecified) underlying SUSY-Breaking theory. The un-

derlying physics (e.g. at some Grand Unification scale) generally introduces relations among the SUSY parameters. This the case of minimal Supergravity (mSUGRA) which incorporates gravity and where this interaction mediates the SUSY-breaking. This restricts considerably the parameter space of the MSSM, leaving only five parameters (free parameters and a sign), and has been widely used as a benchmark for experimental searches.

Searching for SUSY matter is a major goal of the LHC experiments. The early searches at the LHC have concentrated on the production of squarks and gluinos. These could could be copiously pair-produced in pp collisions via strong interactions. Some of the search results obtained with the 2010 data have been expressed as constrained in a given model such a mSUGRA, but the analyses in the CMS and ATLAS experiments attempt to be more "model independent" by focusing on rather inclusive searches based on characteristic event topologies expected for $R_{\rm p}$ conserving SUSY models. The pair-produced sparticles initiate a decay cascade down to ordinary particles and LSPs, leading to final states with $\not{E}_{\rm T}$, multiple jet(s) and 0, 1 or more leptons.

The modest integrated luminosity collected in 2010 has been sufficient to reach unexplored territories, beyond the sensitivity of the Tevatron experiments. This is illustrated in Fig. 21 and 22 with SUSY search results from the ATLAS experiment [44]. Similar results were obtained by the CMS experiment [46].

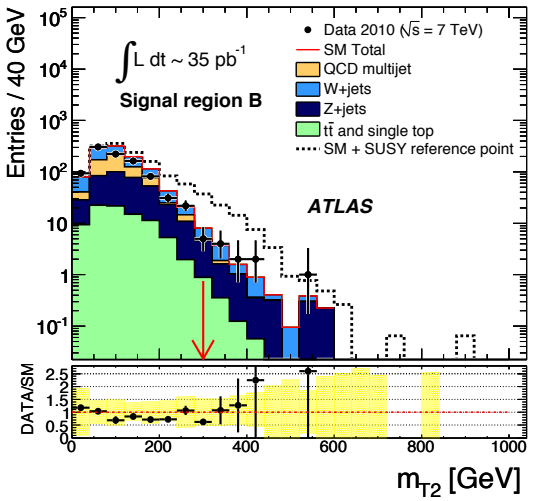

Figure 21. Distribution of the so-called [45] *"stransverse mass"* m_{T2} as obtained by ATLAS [44] in a selection targeting heavy $\tilde{q}$ pair production and requiring with $\geq$ 2 jets, with a leading jet with $p_T > 120$ GeV/c, at least another jet with $p_T > 40$ GeV/c, a $\not{E}_{\rm T} > 100$ GeV, and a smallest of the azymuthal separations between $\vec{P}_T^{miss}$ and selected jets of $\Delta\phi(\text{Jet}, \vec{P}_T^{miss})_{\rm min} > 0.4$. The distributions are shown for data and for the expected SM contributions. The red arrow indicates the signal region defined by $m_{T2} > 300$ GeV in the final selection. Also shown as a staggered dotted histogram is the contribution for a mSUGRA reference point with $m_0 = 200\,\text{GeV/c}^2$, $m_{1/2} = 190\,\text{GeV/c}^2$, $\tan\beta = 3$, $A_0 = 0$ and $\mu > 0$. Other selections targeting light $\tilde{q}\tilde{q}$, $\tilde{g}\tilde{g}$ or $\tilde{g}\tilde{q}$ production are described in Ref. [44].

6. BEYOND MINIMAL MODELS: EXTENDED, EXTRA OR EXOTICS

The SM including the Higgs mechanism (see section 5) allows to contemplate the evolution of the electromagnetic, weak and strong couplings up to very high energies (i.e. down to very small distances). Such an evolution suggest the possibility of a "Grand Unification" (GUT), a merging of the SM gauge interactions, at some GUT scale of O(10^{16}) GeV, into a single interaction characterized by a larger gauge symmetry. The presence of new heavy gauge bosons is a generic feature of many theories with extended gauge symmetries [47] such as grand unified theories or left-right symmetric models [48–50]. Resonances at the TeV scale appear in some SUSY models with additional U(1)$'$ gauge symmetries [51] and in many models concerned with an alternative to minimal Higgs mechanism for EWSB [52–54] Heavy resonances also are a generic feature of models with large or warped extra dimensions where they appear for instance as Kaluza-Klein excitations of the SM Gauge bosons [55]. Some of the early results from the searches at the LHC for new resonances are presented in the following. The search for new resonances is another major

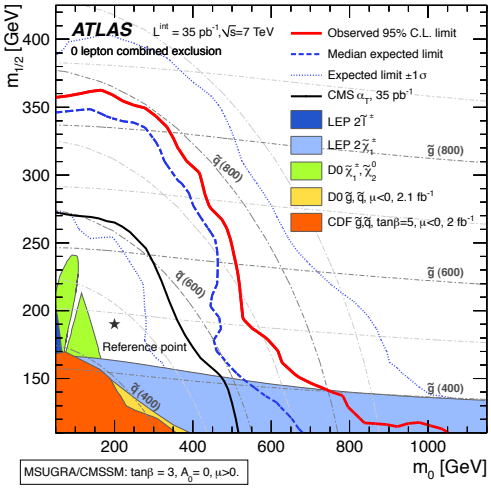

Figure 22. Exclusion limits at the 95%C.L. obtained by the ATLAS Experiment [44] in the mSUGRA/CMSSM parameter space.

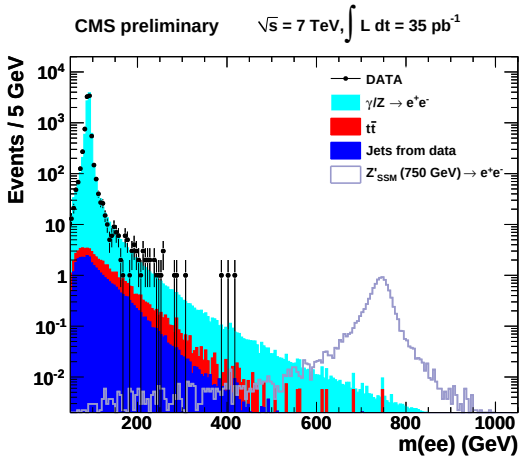

Figure 23. Invariant mass spectrum for di-electron events measured by CMS [56]. The data points are shown together with filled histograms representing the stacked expectation from SM processes: $Z/\gamma*, t\bar{t}, tW$, di-boson production, $Z \to \tau\tau$ and the multi-jet backgrounds. The open histrogram illustrates the signal expected for a Z'_{SSM} with a mass of 750 GeV.

objectives for the experiments at the LHC in Run I.

Di-leptons at the TeV Scale:

As mentioned above, many models of new physics predict the existence of narrow Z′ resonances, possibly at the TeV mass scale, that decay to a pair of charged leptons. An example of a search for TeV resonances at the LHC in the di-lepton invariant mass spectra is shown in Fig. 23. The dielectron invariant mass spectra measured [56] by CMS using their complete 2010 dataset is shown along with the expected signal from Z'_{SSM} with a mass of 750 GeV. The Z'_{SSM} from a sequential standard model (SSM) and possessing standard-model-like couplings is used here as a benchmark for illustration. The expectations from the various background sources, Z/γ^*, $t\bar{t}$, other sources of prompt leptons (tW, diboson production, $Z \to \tau\tau$) and multi-jet events are also overlaid in Fig. 23. The prediction for Drell–Yan production of Z/γ^*, is normalized to the observed $Z \to ll$ signal. Very small background contributions are expected in the signal region and the instrumental background from multi-jet background can be derived from data. All other MC predictions have been normalized to the expected cross sections.

In absence of a signal, exclusion limits at 95% C.L. have been derived and interpreted in various possible models. The Z'_{SSM} is excluded for masses below 1140 GeV. The Z'_{ψ} predicted by grand unified theories [47] is excluded for masses below 887 GeV. These results are presented in Fig. 24 in the (c_u, c_d) plane. The c_u and c_d parameters contain the information from the model-dependent Z′ couplings to fermions in the annihilation of charge 2/3 and charge −1/3 quarks. In the narrow-width approximation, the cross section for the process $pp \to Z' + X \to ll + X$ can be expressed [57,58] in terms of the quantity $c_u w_u + c_d w_d$, where w_u and w_d contain the information about PDFs for the respective annihilation at a given Z′ mass. The translation of the experimental limits into the (c_u, c_d) plane has been performed [56] in the context of both the narrow-width and finite width approximations and similar results were obtained. In Fig. 24 the limits on the Z′ mass are shown as lines in the (c_d, c_u) plane intersected by curves

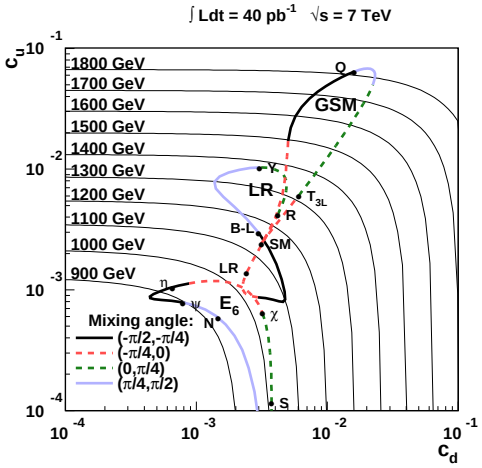

Figure 24. CMS results [56] for the lower limits on the Z′ mass at 95% C.L. in the (c_d, c_u) plane [57,58]. The c_d and c_u contain the information from the model-dependent Z′ couplings to fermions in the annihilation of d-like and u-like quarks. In this plane, the thin solid lines labeled by mass are iso-contours of cross section with constant $c_u + (w_d/w_u)c_d$, where w_d/w_u is in the range 0.5–0.6. The point labeled SM corresponds to the Z'_{SSM} and lies on the more general curve for a generalized sequential standard model (GSM) depending on a mixing angle α. Also indicated are interpretation in the E_6 model (see Ref [56] for more details).

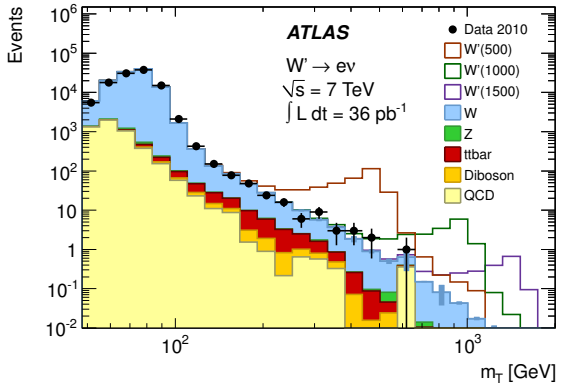

Figure 25. Transverse mass (m_T) spectrum measured for the $e\nu$ channel by the ATLAS experiment [59]. The data points are shown together with filled histograms for the stacked backgrounds. The open histograms illustrate the signal expected for a W′ of masses ranging from 500 to 1500 GeV.

from various models which specify (c_d, c_u) as a function of a model mixing parameter α. For the case of a Kaluza–Klein graviton excitations arising in the Randall-Sundrum (RS) model of extra dimensions [55], limits have been derived for two different values of the free parameters: the mass of the first graviton excitation and the coupling $k/\overline{M}_{\rm Pl}$, where k is the curvature of the extra dimension and $\overline{M}_{\rm Pl}$ is the reduced effective Planck scale. Two values of the coupling parameter that were considered. Lower mass limits of 855 and 1079 GeV are obtained for $k/\overline{M}_{\rm Pl} = 0.05$ and 0.1 respectively. For a resonance mass of 1 TeV, the widths expected for the resonances are 30, 6 and 3.5 (14) GeV for a Z'_{SSM}, Z'_{ψ}, and RS Kaluza–Klein graviton with $k/\overline{M}_{\rm Pl} = 0.05$ (0.1), respectively.

The ATLAS and CMS collaborations have also searched [59,60] for a heavy analogue of the SM W gauge boson, W′, where the particle decays leptonically to an electron and a neutrino ($W' \to e\nu$). Heavy partners of gauge bosons are predicted in many extensions to the SM, such as left-right symmetric models and supersymmetric grand unified theories [48–50]. An example of a search for W′ resonances at the LHC is provided in Fig. 25. The Transverse mass (m_T) spectrum measured for the $e\nu$ channel by the ATLAS experiment [59] using their complete 2010 dataset is shown. In absence of a signal, lower limits have been derived and are shown in Fig. 26 where LHC results are those from Tevatron experiments. The sensitivity to searches of new heavy bosons has been explored using a reference model in which the W′ is a copy of the W boson with the same left-handed fermionic couplings. Interactions with the SM gauge bosons as well as with other heavy gauge bosons such as a Z′ are excluded. As a consequence, the W′ decay modes and branching fractions are similar to those of the W boson, with the notable exception of the

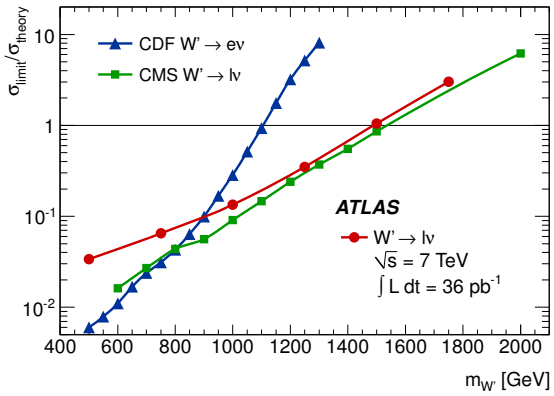

Figure 26. Normalized cross section limits ($\sigma_{limit}/\sigma_{theory}$) for a W′ as a function of the W′ mass [59]. The region above each curve is excluded at 95% C.L. The ratio $\sigma_{limit}/\sigma_{theory}$ is proportional to the square of the coupling strength. The "theory" calculation assumes that the W′ as the same couplings as the standard model W boson.

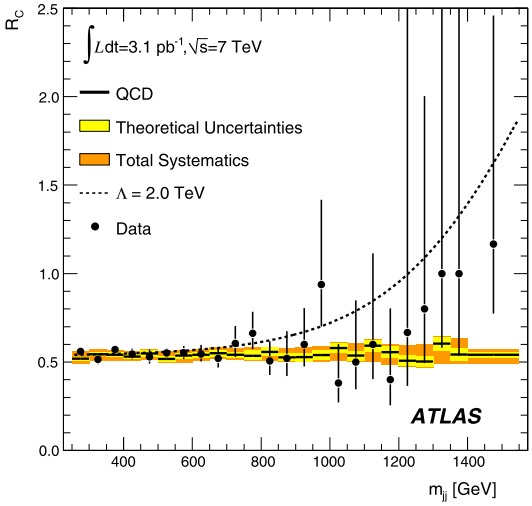

Figure 27. Di-jet centrality ratio as a fonction of the invariant mass m_{jj} measured by the ATLAS experiment [71]. Data points are compared to the QCD expectation with systematic uncertainties shown as bands. The dotted curve correspond to the expectation for QCD with a added quark contact term with $\Lambda = 2.0$ TeV.

$t\bar{b}$ channel, which opens for W′ masses beyond 180 GeV. The leptonic branching fraction is $\mathcal{B}(W' \to e\nu)$ =8.5% for all masses considered. A W′ with sequential SM couplings is excluded at 95% C.L at the LHC below 1.49 TeV. This surpasses the exclusion of masses below 1.1 TeV obtained at the Tevatron.

Di-jets in the Multi-TeV Regime:

In the SM, events with at least two high p_T jets arise in collisions involving a constituent parton of one of the incoming proton and a parton from the other proton. The scattering partons undergo showering and hadronization and manifest themselves in the detector as collimated hadronic jets. Di-jet invariant mass distributions and angular distributions provide a test of QCD in the highly perturbative regime and are sensitive to contributions from physics beyond the SM. Inclusive searches for narrow resonances in the di-jet channel have been performed by the LHC experiments [62,63] and interpreted in terms of mass constraints in various specific models that had been considered for instance in searches by the CDF experiment at the Tevatron [61]. With their early 2010 data and an integrated luminosity of only $\approx 830\,\mathrm{nb}^{-1}$, CMS [63] has set mass exclusion limits at 95% C.L. on string resonances [64], below 2.10 TeV, axigluons [65] and flavour-universal colorons [66] below 1.06 TeV, excited quarks [67] below 1.14 TeV and E6 diquarks [68] below 0.58 TeV. The reach is already comparable to the one at the Tevatron.

The sensitivity has been recently extended to the multi-TeV range using angular observables. Angular observables have been exploited by both experiments and studied as a function of the di-jet invariant mass m_{jj}. Both experiments make use of a variable χ, which is derived from the rapidities of the two leading (highest p_T) jets, and of a centrality ratio r_C. The variable χ_{jj} is related to the di-jet polar scattering angle in the parton-parton centre-of-mass frame $\chi_{jj} = (1 + |\cos\theta^*|)/(1 - |\cos\theta^*|)$, in a collinear massless-parton scattering approximation. The dijet angular distributions do not strongly depend on the details of the parton distribution functions in the proton, since the angular distributions for

the underlying processes, $qg \to qg$, $qq' \to qq'$, and $gg \to gg$, are similar. In parton-parton scattering, the angular distribution of the outgoing partons, is directly sensitive to the spin of the exchanged particle. The di-jet centrality ratio, the ratio of the number of events with the two leading (highest p_T) jets in a central pseudorapidity region over the number where both leading jets are a more forward region, is a measure the angular distribution of the di-jets and is sensitive to deviations from the SM. The χ and r_C variables are described in more details in the relevant CMS [69,70] and ATLAS [71] papers. A measurement of r_C as a fonction of the invariant mass m_{jj} as measured by the ATLAS experiment [71] is shown in Fig. 27. Using measurements of the $1/\sigma_{jj} d\sigma_{jj}/d\chi_{jj}$ differential cross sections as a function of χ_{jj}, a lower limit of $\Lambda = 5.6$ TeV has been obtained at 95% C.L. on the on the contact interaction scale for left-handed quarks.

Lepton-jet Resonances:

The viability of the SM rests on a somewhat empirical similarity between the lepton and quark sectors. The symmetry is essential in achieving an exact cancelation of chiral (triangular) anomalies. The cancelation demands that the sum of the electric charges is exactly neutralized in each generation, which happens thanks to the three quark colors. But there are no direct couplings between quarks and leptons in the SM and the theory is consistent with a separate and exact conservation of lepton and baryon numbers in all processes. Maybe the symmetry between the lepton and quark sector is an indication that leptons and quarks are connected at some fundamental level through new "lepto-quark" interactions.

Leptoquarks are colour-triplet scalar or vector bosons that carry both lepton and baryon numbers, and a fractional electromagnetic charge. They appear naturally in many theories beyond the SM such as Grand Unified Theories (GUTs) of electroweak and strong interactions [72], composite models [73], Technicolour [74] and superstring inspired E_6 models [75]. The actual searches at colliders have been mostly carried in the context of effective Lagrangian models for the leptoquark interactions [76] with leptoquarks restricted to couple to a single lepton-quark generation. A review of leptoquark phenomenology and searches can be found in [77]. There are no strong reasons for the leptoquarks to be found at the electroweak scale, if they exists. But this is not excluded. Several experiments have searched for leptoquarks, but so far no evidence has been found. The most recent limits from the D0 experiment at the Fermilab Tevatron collider exclude first-generation scalar leptoquarks with masses below 299 GeV, and second-generation scalar leptoquarks with masses below 316 GeV for $\mathcal{B} = 1$, based on proton-antiproton collisions at $\sqrt{s} = 1.96$ TeV [78].

In proton-proton collisions at the CERN Large Hadron Collider (LHC) the dominant mechanisms for pair production of scalar leptoquarks are gluon-gluon fusion and $q\bar{q}$-annihilation. The cross section depends on the strong coupling constant and the LQ mass and has been calculated at Next-to-Leading-Order (NLO) [79]; the dependence on the Yukawa coupling λ to lepton-quark pair is negligible. Leptoquarks decay to a quark and a charged lepton of the same generation with unknown branching fraction $\mathcal{B}$ and to a quark and a neutrino with branching fraction $(1 - \mathcal{B})$. A search for pair production of first-generation scalar leptoquarks decaying into electrons and jets, and of second-generation scalar leptoquarks decaying in muons and jets has been performed [80] by the CMS experiment with the $34\,\mathrm{pb}^{-1}$ of luminosity collected in 2010. Upper limits have been set on cross section $\times$ branching ratio^2 as a function of the leptoquark mass. First-generation (second-generation) leptoquarks with masses below (384 GeV) 394 GeV are excluded at a 95% confidence level for $\mathcal{B} = 1$, where $\mathcal{B}$ is the branching ratio in an electron (muon) and a quark.

7. CONCLUSION

The ATLAS and CMS experiments at the LHC collider have started in early spring 2010 to collect data at the very high pp centre-of-mass energy of 7 TeV. With integrated luminosities of up to $40\,\mathrm{pb}^{-1}$ collected in 2010, the experiments have re-visited the standard model (SM) of elec-

troweak and strong interactions and performed first measurements establishing total cross sections and some differential cross sections for the Z and W production, WW production, top quark pair and single top quark production. Complete analysis strategies have been deployed for the various production and decay channels accessible for the search of the SM Higgs boson, and of the extended Higgs sector of supersymmetric or two-Higgs doublet models. First significant results were obtained in the H→WW* channel for the Higgs boson of a SM-like model augmented with a fourth fermion family, and for the H→ $\tau\tau$ channel in minimal supersymmetric models. Constraints on the production cross section and masses of sparticles and of new resonances at the TeV scale have been established beyond the reach of previous colliders. The aim is now to collect enough data in this first run over a period of three years until fall 2012, to validate, or falsify, the SM hypothesis of the existence of a Higgs boson, the quanta of the scalar field responsible for spontaneous electroweak symmetry breaking, while extending the search for sparticles up to the TeV scale, and the search for heavy resonances in the multi-TeV range. New territories are being explored to look for the long awaited physics beyond the standard model.

REFERENCES

1. Proceedings of the ECFA "Large Hadron Collider Workshop", G. Jarlskog and D. Rein (Eds.), Aachen (4-9 October 1990), CERN Report 90-10 (December 1990) *unpublished*.
2. "The ATLAS Experiment at the CERN Large Hadron Collider", ATLAS Collab., JINST 3 (2008) S08003, 407 pp.
3. "The CMS Experiment at the CERN LHC", CMS Collab., JINST 3 (2008) S08004, 334 pp.
4. "Jets and kinematics in hadronic collisions", A. Baden, Int. J. Mod. Phys. A13 (1998) 1817-1845.
5. "Commissioning of the CMS experiment and the Cosmic Run at Four Tesla", CMS Collab., JINST 5 (2010) T03001.
6. "Studies of the performance of the ATLAS detector using cosmic-ray muons", ATLAS Collab. (December 2010) 33pp., *submitted to Eur. Phys. J. C* [arXiv:1011.6665].
7. "CMS Tracking Performance Results from Early LHC Operation", CMS Collaboration, Eur. Phys. J. C70 (2010) 1165-1192, see also CMS Physics Analysis Summary commissioning notes from 2010.
8. "Performance of the ATLAS Detector using First Collision Data", ATLAS Collaboration, JHEP 1009 (2010) 056, 64pp.
9. "Hard Interactions of Quarks and Gluons: a Primer for LHC Physics", J.M. Campbel, J.W. Houston and W.J. Stirling, Rep. Prog. Phys. 70 (2007) 89-193.
10. "QCD at the LHC", J Stirling, Talk at the "QCD at the LHC Workshop", Trento, Italy (September 2010), *unpublished*.
11. "LHC Physics Potential vs. Energy", C. Quigg, Fermilab note FN-0839-T (2009) 18pp., *unpublished* [arXiv:0908.3660].
12. "Measurement of the W → $l\nu$ and Z/$\gamma*$ → ll production cross sections in pp collisions at $\sqrt{s}$ = 7 TeV with the ATLAS detector", ATLAS Collab., JHEP 12 (2010) 60.
13. "Measurements of Inclusive W and Z Cross Sections in pp Collisions at $\sqrt{s}$ = 7 TeV, CMS Collaboration, JHEP 01 (2011) 060.
14. "Commissioning of the particle flow event reconstruction with leptons from J/ψ and W decays at 7 TeV, CMS Collaboration, PAS PFT-10-003 (July 2009) 14pp., *unpublished*.
15. "Measurements of Inclusive W and Z Cross Sections in pp Collisions at $\sqrt{s}$ = 7 TeV, CMS Collab., Physic Analysis Summary Note, PAS EWK-10-005 (March 2011) 14pp.
16. "Measurement of the production cross section for W-bosons in association with jets in pp collisions at $\sqrt{s}$ = 7 TeV with the ATLAS detector", ATLAS Collaboration, (December 2010) 26pp., *submitted to Phys. Lett. B* [arXiv:1012.5382].
17. "Measurement of the production cross section for Z/$\gamma*$ in association with jets in pp collisions at $\sqrt{s} = 7$ TeV with the ATLAS detector", ATLAS Collaboration, ATLAS-CONF-2011-001 (February 2011) 16pp.
18. "Rates of Jets Produced in Association with W and Z bosons in pp Collisions at $\sqrt{s}$ =

7 TeV", CMS Collaboration, Physic Analysis Summary Note, PAS EWK-10-012 (March 2011) 21pp.
19. "Observation of Z $\rightarrow \tau_l\tau_h$ Decays with the ATLAS Detector", ATLAS Collaboration, ATLAS-CONF-2011-010 (February 2011) 19pp.
20. "Measurement of the Inclusive Z $\rightarrow \tau^+\tau^-$ Cross Section in pp Collisions at $\sqrt{s}$ = 7 TeV", CMS Collaboration, Physic Analysis Summary Note, PAS EWK-10-013 (March 2011) 10pp.
21. "First measurement of the cross section for top-quark pair production in pp collisions at $\sqrt{s}$ = 7 TeV", CMS Collaboration, Phys. Lett. B 695 (2011) 424-443.
22. "Measurement of the top quark-pair production with ATLAS in pp collisions at $\sqrt{s}$ = 7 TeV", ATLAS Collaboration, *submitted to Eur. Phys. J. C* [arXiv:1012.1792].
23. "Measurement of the $t\bar{t}$ production cross section in $p\bar{p}$ collisions at $\sqrt{s}$ = 1.8 TeV", CDF Collab., Phys. ReV. D64 (2001) 032002; erratum-ibid. D67 (2003) 119901; "$t\bar{t}$ production cross section in $p\bar{p}$ collisions at $\sqrt{s}$ = 1.8 TeV", D0 Collab., Phys. Rev. D67 (2003) 012004; "Combination of CDF top quark pair production measurements with up to 4.6 fb^{-1}", CDF Collab., CDF Note 9913 (2009) 15 pp., *unpublished*; "Measurement of the top quark pair production cross section in the lepton + jets channel in $p\bar{p}$ collisions at $\sqrt{s}$ = 1.96 TeV", D0 Collab., (December 2010) 19pp., *unpublished* [arXiv:1101.0124] .
24. "Combination of top pair production cross sections in pp collisions at $\sqrt{s}$ = 7 TeV and comparisons with theory", CMS Collaboration, Physic Analysis Summary Note, PAS TOP-11-001 (March 2011) 8pp.
25. "Searches for Siongle Top-Quark Production with the ATLAS Detector in pp Collisions at $\sqrt{s}$ = 7 TeV", ATLAS Collaboration, ATLAS-CONF-2011-027 (February 2011) 18pp.
26. "Measurement of single-top t-channel cross section in pp collisions at $\sqrt{s}$ = 7 TeV", CMS Collaboration, Physic Analysis Summary Note, PAS TOP-10-008 (March 2010) 26pp.
27. "Measurement of the W^+W^- production cross section in pp collisions at $\sqrt{s}$ = 7 TeV with the ATLAS detector", ATLAS Collaboration, ATLAS-CONF-2011-015 (March 2011) 19pp.
28. "Measurement of W^+W^- Production and Search for the Higgs Boson in pp Collisions at $\sqrt{s}$ = 7 TeV", CMS Collaboration, (2011) 30 pp., *submitted to Phys. Lett. B* [arXiv:1102.5429].
29. "First CMS ZZ$\rightarrow$ 4μ Event", CMS Collaboration, Detector Performance Note DPS-2010/038 (November 2010) *unpublished*.
30. "Handbook of LHC Higgs Cross Sections: 1. Inclusive Observables", LHC Higgs Cross Section Working Group, S. Dittmaier et al., (January 2011) 153 pp., *unpublished* [arXiv:1101.0593].
31. CMS Collaboration, *unpublished*.
32. "ATLAS Sensitivity Prospects for Higgs Boson Production at the LHC Running at 7, 8 or 9 TeV", ATLAS Collaboration, Public Note PUB-2011-001 (November 2010) 31pp.; "Further Investigations of ATLAS Sensitivity to Higgs Boson Production in Different Assumed LHC Scenarios", ATLAS Collaboration, Public Note PUB-2011-001 (January 2011) 8pp. *unpublished*.
33. "Higgs Boson Searches using the $\sigma_H \times B(H \rightarrow WW^{(*)} \rightarrow 2l2\nu)$ Decay Mode with the ATLAS Detector at $\sqrt{s}$ = 7 TeV", ATLAS Collaboration, ATLAS-CONF-2011-005 (March 2011) 35pp.
34. "Combination of Tevatron Searches for the Standard Model Higgs Boson in W^+W^- decay Mode", CDF and D0 Collab., Phys. Rev. Lett. 104 (2010) 061802, 11pp.; "Combined Tevatron upper limit on $gg \rightarrow H \rightarrow W^+W^-$ and constraints on the Higgs boson mass in 4th-generation fermion models", CDF and D0 Collab., (May 2010) 14pp., [arXiv:1005.3216]. "Combined CDF and D0 Upper Limits on Standard Model Higgs-Boson Production with up to 6.7 fb^{-1} of Data", CDF and D0 Collab., (July 2010) 40pp.; [arXiv:1007.4587].

35. "Mass Hierarchies in Supersymmetric Theories", Edward Witten, Phys. Lett. B105 (1981) 267.
36. "Search for Neutral MSSM Higgs Boson Production via Decays to Tau Pairs in pp Collisions at $\sqrt{s} = 7$ TeV", CMS Collaboration, CMS PAS HIG-10-002 (March 2011) 11pp.
37. "Search for neutral MSSM Higgs Bosons decaying to $\tau^+\tau^-$ pairs in pp collisions at $\sqrt{s} = 7$ TeV", ATLAS Collaboration, ATLAS-CONF-2011-024 (March 2011) 22pp.
38. "Search for neutral MSSM Higgs bosons at LEP", LEP Collaborations, Eur. Phys. J. C47 (2006) 547-587.
39. "Combined CDF and D0 upper limits on MSSM Higgs boson production in τ-τ final states with up to 2.2 fb^{-1}", Tevatron New Phenomena & Higgs Working Group, (March 2010) 14 pp., *unpublished* [arXiv:1003.3363].
40. S. Glashow and S. Weinberg, Phys. Rev. D15 (1977) 1958.
41. H.E. Logan, private communication.
42. J.D. Wells, Phys. Rev. D56 (1997) 1504-1510.
43. "R-Parity-Violating Supersymmetry", M. Barbier et al., Phys. Rep. 420 (2005) 1-195.
44. "Search for squarks and gluinos using final states with jets and missing transverse momentum with the ATLAS in $\sqrt{s} = 7$ TeV proton-proton collisions", ATLAS Collaboration, (2011) 17pp., *submitted to Phys. Lett. B* [arXiv:1103.1984]
45. "Measuring masses of semiinvisibly decaying particles pair produced at hadron colliders", C.G. Lester and D.J.Summers, Phys. Lett. B463 (1999) 99; "m_{T2}: The Truth behind the glamour", A. Barr, C Lester and P. Stephens, J. Phys. G29 (2003) 2343; "Minimal Kinematic Constraints and m_{T2}", H.-C. Cheng and Z. Han, JHEP 0812 (2008) 063.
46. "Search for Supersymmetry in pp Collisions at $\sqrt{s} = 7$ TeV in Events with Two Photons and Missing Transverse Energy", CMS Collaboration (March 2011) 24pp., *submitted to Phys. Rev. Lett.* [arXiv:1103.0953].
47. "The phenomenology of extra neutral gauge bosons", A. Leike, Phys. Rep. 317 (1999) 143-250.
48. "Bounds on the mass of W_R and the $W_L - W_R$ mixing angle ζ in general $SU(2)_L \times SU(2)_R \times U(1)$ models", P. Langacker, S.U. Sankar, Phys. Rev. D40 (1989) 1569.
49. "Left-right gauge symmetry and an "isoconjugate" model of CP violation", R.N. Mohapatra and J.C. Pati, Phys. Rev. D11 (1975) 566.
50. "Exact left-right symmetry and spontaneous violation of parity", G. Senjanovic and R.N. Mohapatra, Phys. Rev. D12 (1975) 1502.
51. "The Physics of Heavy Z′ Gauge Bosons", P. Langacker, Rev. Mod. Phys. 81 (2009) 1199-1226, and references therein.
52. "CERN LHC Signatures of New Gauge Bosons in Minimal Higgsless Model", H.-J. He et al., Phys.Rev. D78 (2008) 031701.
53. "Electroweak limits on nonuniversal Z-prime bosons", R.S. Chivukula and E.H. Simmons, Phys.Rev. D66 (2002) 015006.
54. "Little Higgs Models and Their Phenomenology", M. Perelstein, Prog. Part. Nucl. Phys. 58 (2007) 247-291.
55. "An alternative to compactification", L. Randall and R. Sundrum, Phys. Rev. Lett. 83 (1999) 4690; "A large mass hierarchy from a small extra dimension", L. Randall and R. Sundrum, Phys. Rev. Lett. 83 (1999) 3370.
56. "Search for Resonances in the Dilepton Mass Distribution in pp Collisions at $\sqrt{s} = 7$ TeV", CMS Collaboration, (2011) 30 pp., *submitted to JHEP* [arXiv:1103.0981].
57. "Z′ gauge bosons at the Tevatron", M. Carena et al., Phys. Rev. D70 (2004) 093009.
58. "Z′ physics with early LHC data", E. Accomando et al., (2010) 26 pp. *unpublished* [arXiv:1010.6058].
59. "Search for High-mass States with One Lepton plus Missing Transverse Momentum in proton-proton Collisions at $\sqrt{s} = 7$ TeV", ATLAS Collaboration, (2011) 22 pp., *submitted to Phys. Lett. B* [arXiv:1103.1391]
60. "Search for a W′ Boson Decaying to a Muon and a Neutrino in pp Collisions at $\sqrt{s} = 7$ TeV", CMS Collaboration, (2011) 24 pp., *submitted to Phys. Lett. B* [arXiv:1103.0030].
61. . "Search for new particles decaying into di-

jets in proton- antiproton collisions at $\sqrt{s}$ = 1.96 TeV", CDF Collaboration, , Phys. Rev. D79 (2009) 112002.
62. "Search for New Particles in Two-Jet Final States in 7 TeV Proton-Proton Collisions with the ATLAS Detector at the LHC", ATLAS Collaboration, Phys. Rev. Lett. 105 (2010) 161801.
63. "Search for Dijet Resonances in the Dijet Mass Distribution in 7 TeV pp Collisions at CMS", CMS Collaboration, Physic Analysis Summary Note, PAS EXO-10-010 (August 2010) 16pp., *unpublished*.
64. "Dijet signals for low mass strings at the LHC", L.A. Anchordoqui et al., Phys. Rev. Lett. 101 (2008) 241803; "TeV strings and collider probes of large extra dimensions, S. Cullen, M. Perelstein, and M.E. Peskin, Phys. Rev. D62 (2000) 055012.
65. "Axigluon Production in Hadronic Collisions, J. Bagger, C. Schmidt, and S. King, Phys. Rev. D37 (1988) 1188.
66. "New Strong Interactons at the Tevatron ?", R.S. Chivukula, A.G. Cohen, and E.H. Simmons, Phys. Lett. B380 (1996) 9298.
67. "Excited Quark Production at Hadron Colliders", U. Baur, I. Hinchliffe, and D. Zeppenfeld, Int. J. Mod. Phys. A2 (1987) 1285.
68. "Low-Energy Phenomenology of Superstring-Inspired E6 Models", J.L. Hewett and T.G. Rizzo, Phys. Rep. 183 (1989) 193.
69. "Search for Quark Compositeness with the Dijet Centrality Ratio in pp Collisions at $\sqrt{s}$ = 7 TeV", CMS Collaboration, Phys. Rev. Lett. 105 (2010) 262001.
70. "Measurement of Dijet Angular Distributions and Search for Quark Compositeness in pp Collisions at $\sqrt{s}$ = 7 TeV", CMS Collab., (February 2011) 200pp., *submitted to Phys. Rev. Lett.* [arXiv:1102.2020].
71. "Search for quark contact interactions in dijet angular distributions in pp collisions at $\sqrt{s}$ = 7 TeV with the ATLAS detector", ATLAS Collaboration, Physics Letters B 694 (2011) 327345.
72. H. Georgi and S.L. Glashow, Phys. Rev. Lett. 32 (1974) 438; J.C. Pati and A. Salam, Phys. Rev. D8 (1973) 1240.
73. "Light Leptoquarks", B. Schrempp and F. Schrempp, Phys. Lett. B153 (1985) 101.
74. "Mass Without Scalars", S. Dimopoulos and L. Susskind, Nucl. Phys. B155 (1979) 237; "Technicolored Signatures", S. Dimopoulos, Nucl. Phys. B168 (1980) 69; "Dynamical Breaking of the Weak Interaction Symmetries", E. Eichten and K. Lane, Phys. Lett. B90 (1980) 125; "Technicolour", E. Farhi and L Sussking, Phys. Rep. 74 (1981) 277.
75. "Search for New Quarks Suggested by the Superstring", V. Angelopoulos et al., Nucl. Phys. B292 (1987) 59; "Low-Energy Phenomenology of Superstring Inspired E(6) Models", J.L. Hewett and T.G. Rizzo, Phys. Rep. 183 (1989) 1193, and references therein.
76. W. Buchmüller, R. Rückl and D. Wyler, Phys. Lett. B191 (1987) 442; *erratum* in Phys. Lett. B448 (1999) 320.
77. "Search for particles and forces beyond the standard model at HERA ep and Tevatron $p\bar{p}$ colliders", M. Kuze and Y. Sirois, Prog. Part. Nucl. Phys. 50 (2003) 1-62.
78. "Search for Pair Production of First-generation Leptoquarks in $p\bar{p}$ Collisions at $\sqrt{s}$ = 1.96 TeV", D0 Collaboration, Phys. Lett. B681 (2009) 224; "Search for Pair Production of Second Generation Scalar Leptoquarks in $p\bar{p}$ Collisions at $\sqrt{s}$ = 1.96 TeV", D0 Collaboration, Phys. Lett. B671 (2009) 224.
79. "Pair Production of Scalar Leptoquarks at the CERN LHC", M. Kramer et al., Phys. Rev. D71 (2005) 057503.
80. "Search for Pair Production of First-Generation Scalar Leptoquarks in pp Collisions at $\sqrt{s}$ = 7 TeV", CMS Collaboration, (December 2010) 22pp., *submitted to Phys. Rev. Lett.* [arXiv:1012.4031]. "Search for Pair Production of Second-Generation Scalar Leptoquarks in pp Collisions at $\sqrt{s}$ = 7 TeV", *idem* (December 2010) 22pp., *submitted to Phys. Rev. Lett.* [arXiv:1012.4033].

Lectures on the Kerr/CFT Correspondence

Irene Bredberg[a], Cynthia Keeler [a], Vyacheslav Lysov [a]and Andrew Strominger [a]

[a]Center for the Fundamental Laws of Nature
Harvard University
Cambridge, MA 02138 USA

We give a short introduction, beginning with the Kerr geometry itself, to the basic results, motivation, open problems and future directions of the Kerr/CFT correspondence.

1. Introduction

In the early 1970's, work by Bekenstein, Carter, Christodolou, Hawking, and many others [1–7] raised profound puzzles about the nature of black holes. One striking such puzzle was that, while macroscopic arguments gave the entropy of a black hole as one quarter of its event horizon area:

$$S = \frac{A}{4\hbar G}, \tag{1}$$

at the time no microscopic accounting for this entropy was known. It seemed imperative that we should be able to account for the black hole entropy microscopically, just as had been done in the nineteenth century for gases and liquids. Without such a microstate description, we would seem to run into serious contradictions.

This problem remained largely unsolved for more than 20 years. Then in the mid 90's string theory was used [8] to explicitly identify the missing microscopic degrees of freedom for a very particular kind of black hole. This calculation depended on many specific details of string theory. At the end of a rather lengthy computation involving numerous factors of 2, π etc., the Bekenstein-Hawking result (1) was reproduced by counting microstates. At the time, it was argued that this precise match provided indirect evidence for string theory as the correct theory of nature.

However, about a year later, it was shown [9] that in fact, any consistent, unitary quantum theory of gravity containing those particular black holes - characterized by a near-horizon region with an AdS_3 factor - as solutions must reproduce the entropy in essentially the same way. The specific details of string theory as the microscopic UV completion were not necessary. Rather, the key ingredient followed from the analysis done by Brown and Henneaux [10] in the 80's: if we find a consistent completion of quantum gravity on AdS_3 it has to be described by a 2D conformal field theory due to purely symmetry considerations. Thus, the detailed matching of the factors of 2 and π was not really a consequence of string theory but rather, it simply had to follow because string theory is a consistent theory of quantum gravity. Any other consistent theory must by necessity also reproduce the same result in the same manner.[1]

Since then, we have slowly but surely been progressing in our understanding of the relation between black holes and 2D CFTs. We started with 5D supersymmetric black holes, then proceeded to partially supersymmetric and then to the 3D nonsupersymmetric black holes with near-horizon AdS_3 geometry. Recently, our understanding has finally evolved to up the point where we can understand something about 4D Kerr black holes that we see up in the sky.

The work we are going to discuss is heavily informed by string theory, but none of it relies on the conjecture that string theory is the actual

[1]The other side of the coin here is that these general arguments imply that any consistent quantum theory of gravity must, on an AdS_3 background, behave a lot like string theory – so much so that we might reasonably call it string theory!

theory of nature, or on the stringy realizations of the AdS/CFT correspondence. Instead, all of our arguments follow from careful study of the diffeomorphism group together with some basic consistency assumptions, and do not involve any details of Planck scale physics. Indeed it would be very strange if the universal area-entropy law somehow depended on the exact microscopic details of how quantum gravity is completed in the UV!

To emphasize this point further, let us draw an analogy of the current efforts with the work of Boltzmann in the 19th century. At that time thermodynamics was understood, but people did not know much about atoms and molecules. Boltzmann wanted to explain the laws of thermodynamics by applying statistical, probabilistic reasoning to the fundamental constituents (degrees of freedom) of gases and liquids. However, he encountered a UV divergence: if a gas is treated as a continuous medium, then it has infinitely many degrees of freedom because of the existence of arbitrarily short wavelength modes. Any attempt to derive the thermodynamics of gases by applying statistical reasoning to a theory of a continuous medium, will hit the so called Rayleigh ultraviolet catastrophe in which all energy is eventually sucked into the UV modes. To avoid this problem, a consistent UV cutoff is needed. People were already talking at that time about atoms and molecules, so Boltzmann assumed that there was some theory of atoms, i.e. he assumed that there was a consistent UV cutoff for gases and liquids. He did not at all need to know what the details of this atomic cutoff were; in fact, the periodic table was not discovered until more than fifty years later. Boltzmann's mere assumption that there existed a UV cutoff at some energy scale was sufficient to derive the universal laws of thermodynamics from statistical reasoning. Of course, having a detailed microscopic theory can provide more information; for example if one wants to compute the heat capacity from first principles, one needs a detailed UV completion (that is, the actual quantum theory of atoms and molecules).

We might hope that a similar story holds for black holes. We should not need to know all the details of string theory at scales of order 10^{-38} km in order to understand why the area law (1) applies to the black hole Sagittarius A* in the center of our galaxy which is 10^7 km across! We should be able to understand the area law just from the assumption that quantum gravity has *some* consistent UV completion.

The stringy microscopic entropy analysis in [8] was akin to first computing the periodic table and then using it to compute the laws of thermodynamics. In this stringy black hole computation we had far more information than was necessary to get the area law: we had huge sets of numbers for degeneracies at any level. Only a tiny part of this information turns out to be universal. We are going to see in these lectures that this tiny universal part can be understood using universal reasoning and no assumptions about Planck scale cutoffs. This is exactly as it should be.

In these lectures we will encounter another much-studied object in theoretical physics which has a lot of universal behavior: 2D conformal field theories. Many features we know of 2D CFTs are independent of the details of a given CFT. Indeed, we will find a striking match -going far beyond the entropy formula (1) - between the universal properties of 2D conformal field theories and those of black holes.

The plan for the rest of the lectures is the following: we will start with a review of the Kerr geometry, including the Near-Horizon Extreme Kerr (NHEK) geometry. Then we will cover the asymptotic symmetry group, boundary conditions for the NHEK geometry, the CFT description of a quantum theory of gravity in NHEK and the surprising evidence for hidden conformal symmetries far from extremality. We will close with a discussion of open problems and future directions.

2. Kerr geometry

2.1. The Kerr solution

There is a famous quote from Chandrasekhar [11]

"*.... Kerr's solution has also surpassing theoretical interest: it has many properties that have the aura of the miraculous about them.* "

The first "miracle" of the Kerr story is the existence of the solution itself. It is rumored that Einstein initially believed that no non-trivial exact solution to the GR equations would ever be found in closed form. This was quickly proven wrong by Schwarzschild, but it took another 50 years to discover the Kerr solution. This solution is arguably the most complicated exact solution ever found of a nonlinear PDE describing a real physical object. In Boyer-Lindquist coordinates, it is

$$ds^2 = -\frac{\Delta}{\rho^2}\left(dt - a\sin^2\theta\, d\phi\right)^2 + \frac{\rho^2}{\Delta}dr^2 + \frac{\sin^2\theta}{\rho^2}\left((r^2+a^2)d\phi - a\, dt\right)^2 + \rho^2\, d\theta^2, \quad (2)$$

$$\Delta = r^2 - 2Mr + a^2, \quad \rho^2 = r^2 + a^2\cos^2\theta. \quad (3)$$

with $a = J/M$ where M is the mass and J is the angular momentum of the black hole.[2] The inner (r_-) and outer (r_+) horizons are defined as the two solutions to $\Delta = 0$:

$$r_\pm = M \pm \sqrt{M^2 - a^2}. \quad (4)$$

When $a = 0$, $r_+ = 2M$ and we recover the usual Schwarzschild black hole. Another interesting case is the extreme limit for which $a = M = \sqrt{J}$ and $r_\pm = M$. When $J > M^2$ the roots in the expression for the horizon radii become imaginary; there are no horizons but instead a naked ring singularity in the curvature at $r = 0$. This violates cosmic censorship. So cosmic censorship implies the angular momentum is bounded by $J \leq M^2$. Another way to understand this bound is from the formula for the angular velocity at the horizon:

$$\Omega_H = \frac{a}{2Mr_+}. \quad (5)$$

When $a = M$, the equator of the horizon is spinning at the speed of light, and so cannot spin any faster.

According to Bekenstein and Hawking, the black hole has a temperature and an entropy

$$T_H = \frac{r_+ - M}{4\pi M r_+}, \quad S = 2\pi M r_+. \quad (6)$$

[2]Here we have used units in which $G = c = 1$.

Note that if $a = M$ then $T_H = 0$, so these extreme rotating black holes are a kind of ground state. In general, the ground states of a system are easier to understand than the excited states. The fact that $T_H = 0$ in this special case hints that $a = M$, rather than the Schwarzschild case $a = 0$, describes the simplest object in the Kerr family.

2.2. Ergosphere

The Kerr geometry has an interesting ergosphere region absent in the Schwarzschild case. Lines of fixed θ, ϕ, t and varying r in the Kerr geometry are space-like as long as we are outside the event horizon $r = r_+$. If we go to $r_- < r < r_+$, then these lines become timelike, just like in the Schwarzschild case when we cross $r = 2M$. For Schwarzschild, lines with fixed r, θ, ϕ and varying t change from spacelike to timelike at the same surface $r = 2M$. However, for Kerr, these lines switch signature at the stationary limit surface, which is given by the zeros of g_{tt} and is outside of the event horizon. This surface is described by solutions to $\Delta = a^2\sin^2\theta$ and is not spherically symmetric. The region in between $r = 2M$ and the stationary limit surface is called the ergosphere.

Objects in the Kerr geometry experience a "frame-dragging" force pushing them around the black hole. In order to stay at fixed ϕ outside a Kerr black hole we actually need to move with some speed in the counterrotational direction. This speed increases as we approach the stationary limit surface, and becomes the velocity of light when we reach it. Once inside the stationary limit surface if we try to keep ϕ fixed while increasing t, we end up moving in a space-like direction. Physically it means that inside this limit surface - in the ergosphere - physical objects cannot stay at constant ϕ because they would need to move with a speed greater than light to do so. Instead, all timelike paths rotate in the same direction as the Kerr black hole.

The ergosphere is a fascinating and observable region of space-time where effects of general relativity are large. Measurements which probe the physics well inside the ergosphere near the event horizon have been made (see [12] for review). Perhaps the most-studied example is GRS1915+105

[13], a Kerr black hole surrounded by an accretion disc made up of matter which is continuously pulled in from a nearby companion star. As the matter in the accretion disc spirals inwards, energy is dissipated into thermal radiation which we observe. The frequency distribution depends on a number of factors including the gravitational redshift which gets larger closer to the horizon. The accretion disc has an innermost edge which corresponds to the existence of the so-called innermost stable circular orbit (ISCO) for geodesics in Kerr. Once matter gets closer to the black hole than the ISCO, orbits become unstable and the matter consequently free falls into the black hole rapidly and does not radiate anymore. Thus, the observed frequency spectrum encodes the location of the ISCO. This location depends on the angular momentum of the black hole and is given by a standard GR calculation. For rapidly rotating black holes, the ISCO almost coincides with the event horizon, and the maximal redshift becomes very large. Hence the maximal redshift is very sensitive to the deviation from extremality. The observation of the ISCO thus allows us to get very accurate information about J/M^2 for black holes in the sky. For example the lower bound on the ratio J/M^2 for $GRS1915+105$ is 0.98. Its mass is known to much less precision; it is estimated to be between 5 and 15 solar masses. The sky contains other candidates for rapidly rotating black holes. For example a measurement of the maximal redshift of the iron line for the supermassive black hole in the center of the nearby Seyfert galaxy MCG-6-30-15 indicates J/M^2 is greater than 0.99 [14]. Given the rapid progression of our knowledge of the sky, it is quite possible that more such near-extreme Kerr black holes will be discovered in the near future.

2.3. Killing-Yano tensor

Another amazing property of the Kerr geometry is the existence of a Killing-Yano tensor [15]. It is an antisymmetric tensor with properties similar to those of Killing vectors. For a Killing vector K_μ, we have

$$\nabla_\mu K_\nu + \nabla_\nu K_\mu = 0. \tag{7}$$

The Killing-Yano tensor satisfies

$$f_{\mu\nu} = -f_{\nu\mu}, \quad \nabla_{(\lambda} f_{\mu)\nu} = 0. \tag{8}$$

The explicit expression in Boyer-Lindquist coordinates is

$$\begin{aligned} f = a\cos\theta dr \wedge (dt - a\sin^2\theta\, d\phi) \\ - r\sin\theta\, d\theta \wedge \left(-adt + \left(r^2 + a^2\right) d\phi\right). \end{aligned} \tag{9}$$

This is yet another "miracle" of the Kerr story, since there is no obvious reason for this tensor to exist. Perhaps we will learn something about it from Kerr/CFT, whose consistency relies on the existence of this tensor. Carter used (9) to construct a symmetric tensor [16]

$$K_{\mu\nu} = f_\mu{}^\lambda f_{\lambda\nu}, \quad \nabla_{(\mu} K_{\nu\rho)} = 0 \tag{10}$$

and an extra conserved charge for geodesics:

$$Q = \dot{x}^\mu \dot{x}^\nu K_{\mu\nu}. \tag{11}$$

Consequently we have 3 constants of motion and can solve analytically for Kerr geodesics. It also allows us to separate variables for the Laplace equation in the Kerr geometry.

Despite having an explicit expression for the Killing-Yano tensor, we still do not fully understand its geometric origin. An intriguing observation has been made by Gibbons et. al. [17] relating it to a novel type of supersymmetry. The conserved Carter constant is the square of a novel supercharge (roughly $\psi^\mu f_{\mu\lambda}$) related to the Killing-Yano tensor. Of course, there is no actual supersymmetry in the usual sense for the Kerr solution.

3. NHEK=near-horizon limit of extreme Kerr

Now we turn to the near-horizon region of the extreme Kerr black hole where life simplifies dramatically. Often in physics if we can not understand a system exactly, we first explore it in a limit where things simplify. In condensed matter physics the standard trick is to take the low-energy limit where atomic/molecular details can be ignored. In the present case of black holes we will go to small radii, but small radii correspond

to high redshifts so this is also a low-energy limit. A heuristic explanation for why things simplify in the near-horizon limit is that inside the ergosphere, physical objects have to rotate around with the black hole. At the horizon of the extreme black hole, they must rotate around at the speed of light and hence only chiral (co-rotating as opposed to counter-rotating) degrees of freedom appear. Purely chiral excitations are highly constrained. This is roughly why we expect quantum gravity to simplify in this limit.

3.1. Extreme limit

In the limit $a = M$, formulae for the full Kerr geometry simplify:

$$r_\pm = a = M, \quad S = 2\pi M^2 = 2\pi J,$$
$$T_H = 0, \quad \Omega_H = \frac{a}{2Mr_+} = \frac{1}{2M}. \tag{12}$$

The metric reduces to

$$ds^2 = -\frac{\Delta}{\rho^2}\left(d\hat{t} - a\sin^2\theta\, d\hat{\phi}\right)^2 + \frac{\rho^2}{\Delta}\, d\hat{r}^2 + \frac{\sin^2\theta}{\rho^2}\left((\hat{r}^2 + a^2)\, d\hat{\phi} - a\, d\hat{t}\right)^2 + \rho^2 d\theta^2, \tag{13}$$

$$\Delta = (\hat{r} - a)^2, \quad \rho^2 = \hat{r}^2 + a^2\cos^2\theta. \tag{14}$$

3.2. Near-horizon limit

We want to study the near-horizon region of the extreme Kerr solution. This region has enhanced isometries just like the near-horizon AdS regions of various black brane solutions. We follow Bardeen and Horowitz [18] and zoom in on the region $r = M$ by introducing a scaling parameter $\lambda \to 0$. New coordinates

$$r = \frac{\hat{r} - M}{\lambda M} \tag{15}$$

$$t = \frac{\lambda\hat{t}}{2M}, \quad \phi = \hat{\phi} - \frac{\hat{t}}{2M}. \tag{16}$$

are held fixed as λ is scaled. Note that for any finite r, the original radial coordinate $\hat{r}$ is forced to be very near the horizon value M for $\lambda \to 0$. In the limit, we obtain the smooth geometry

$$ds^2 = 2\Omega^2 J\left[\frac{dr^2}{r^2} + d\theta^2 - r^2\, dt^2 + \Lambda^2(d\phi + r\, dt)^2\right], \tag{17}$$

involving two functions of θ given by

$$\Omega^2 = \frac{1 + \cos^2\theta}{2}, \quad \Lambda = \frac{2\sin\theta}{1 + \cos^2\theta}. \tag{18}$$

Formula (17) is known as the near-horizon extremal Kerr geometry (NHEK). The black hole angular momentum J appears only as an overall factor in front of the metric. Since this solution arises in the limit of a coordinate transformation of the Kerr solution, it is a solution to the Einstein equations. The metric (17) is not asymptotically flat; in fact it has very peculiar asymptotics as $r \to \infty$.

It is not hard to see that for slices of fixed polar angle θ, we have a 3D geometry which is locally a "warped" version of AdS_3. At the special value $\theta = \theta_0 : \Lambda(\theta_0) = 1$ and the local metric is exactly that of AdS_3:

$$ds^2 = 2\Omega^2 J\left[-r^2 dt^2 + \frac{dr^2}{r^2} + (d\phi + r dt)^2\right]. \tag{19}$$

Since we know that gravity on AdS_3 always has a conformal symmetry [10], this is a strong hint, which we follow up on below, of an underlying conformal symmetry for extreme Kerr.

Globally, the $\theta = \theta_0$ slice of NHEK is a quotient of AdS_3. The reason for this is that the angle ϕ is periodically identified $\phi \sim \phi + 2\pi$. We already know [19] that a quotient of AdS_3 space is related to the finite temperature partition function of the dual conformal field theory. Later we will see that the identification $\phi \sim \phi + 2\pi$ plays the same role in implying a finite temperature in the context of Kerr/CFT .

The warped AdS_3 geometries appearing at generic fixed θ are of general interest in a number of contexts [20–31] (for dS_3 cousins see [32]). They are Lorentzian analogs of the squashed S^3. The ordinary round S^3 has the isometry group $SU(2) \times SU(2)$. Of course S^3 is a Hopf fibration of S^1 over S^2 with a specific radius of the

fiber. If we deform the radius of the S^1 fiber, we break $SU(2) \times SU(2)$ down to $SU(2) \times U(1)$. Similarly, one can write quotients of AdS_3, which has isometry $SL(2,R)_R \times SL(2,R)_L$, as a Hopf-like fibration of S^1 over AdS_2 – this is essentially equation (17). Warped AdS_3 is then obtained by deforming the fiber radius and has the reduced isometry group $SL(2,R) \times U(1)$. Thus, every section of fixed θ in the NHEK geometry has $SL(2,R) \times U(1)$. This turns out to give the full isometry group of NHEK.

4. Asymptotic Symmetry Group

In order to make sense of quantum gravity on the NHEK space we must specify boundary conditions. This is our next problem. An immediate issue is that the boundary at $r \to \infty$ is rather peculiar. It does not look like the boundary of Minkowski space or that of AdS space. In order to define the theory we need to say something about the boundary conditions at this boundary.

An important notion in doing this is the so-called asymptotic symmetry group (ASG), which is made up of the allowed diffeomorphisms modulo the trivial diffeomorphisms

$$\mathrm{ASG} = \frac{\text{Allowed diffeomorphisms}}{\text{Trivial diffeomorphisms}}. \tag{20}$$

4.1. Allowed diffeomorphisms

To determine which are the allowed diffeomorphisms, we need to specify boundary conditions. Typically these will be of the form

$$g_{ab} = g^0_{ab} + \mathcal{O}(r^{-p_{ab}}) \tag{21}$$

as r approaches the boundary at infinity with g^0_{ab} being a background metric and p_{ab} a set of integers. Given the boundary conditions, the allowed diffeomorphisms ξ are diffeomorphisms for which the variation $\delta_\xi g$ of any allowed metric g results in a metric that is itself allowed. For example for 4D quantum gravity in asymptotic Minkowski space we typically demand that the metric approach the flat Minkowski metric plus $1/r$ corrections. We then are not allowed to consider diffeomorphisms which go like r[16] because this produces metric variations which do not vanish at infinity and therefore violate the boundary conditions. Note that the definition of the allowed diffeomorphisms does not require any information about dynamics.

4.2. Trivial diffeomorphisms

On the other hand, to know what the trivial diffeomorphisms are, we do need to know about the dynamics. Once dynamics are specified, for every diffeomorphism ζ there is an associated charge Q_ζ canonically constructed to obey

$$\{Q_\zeta, \Phi\}_{DB} = \mathcal{L}_\zeta \Phi \tag{22}$$

where $\{\cdot,\cdot\}_{DB}$ is the so-called Dirac bracket (the discussion at this point is classical) and Φ is any field in the theory. The Dirac bracket is a modification of the Poisson bracket designed to accommodate local symmetries and the associated constraints. For example if we have a discrete set of constraints C_i, then the Dirac bracket of two fields is defined as

$$\{A,B\}_{DB} = \{A,B\} - \{A,C_i\}\{C_i,C_j\}^{-1}\{C_j,B\} \tag{23}$$

with $\{\cdot,\cdot\}$ being an ordinary Poisson bracket. This bracket manifestly vanishes if A is itself a constraint and so preserves the constraints. In gravity the index i is continuous and the inverse matrix $\{C_i,C_j\}^{-1}$ is a nonlocal Green's function.

For local symmetries the generator of the diffeomorphism Q_ζ has the generic form

$$Q_\zeta = \int_{\text{boundary}} X + \int_{\text{bulk}} C. \tag{24}$$

Typically the bulk term vanishes due to the constraint equations (Gauss' law for electromagnetism or the $G_{0\mu}$ constraint for gravity), so the diffeomorphisms are always generated by boundary terms. The most familiar gravity example of this is the ADM mass. This generates time translations via the Dirac bracket and is the Hamiltonian of the theory. Because of the non-local nature of the Dirac bracket, it is possible for the boundary term by itself to generate a symmetry over the entire spacetime.

Returning to our discussion of the ASG and the quotient (20), a trivial diffeomorphism ζ is

one for which $Q_\zeta = 0$. For example any diffeomorphism that has compact support and vanishes at infinity is going to be trivial. The generators of the ASG can thus be thought of roughly as diffeomorphisms which are allowed by the boundary conditions but die off slowly enough at infinity to yield nonzero charges.

4.3. Discussion

In the quantum theory, the states should be annihilated by the trivial diffeomorphisms and must transform in representations of the ASG. Consequently this analysis provides us with the nontrivial symmetry group of the quantum theory.

There might appear to be much ambiguity in defining the theory because of the fact that we can start out with a large variety of boundary conditions. However, if we start with generic boundary conditions we will run into trouble if they are either too strong or too weak. Suppose we start with 4D Minkowski space and demand that the metric components fall off as $\mathcal{O}(1/\sqrt{r})$ instead of the more usual $\mathcal{O}(1/r)$. Applying (22), we will find that the generator Q is not always well-defined since the volume of the boundary goes like r^2, the integrand falls off like $r^{-3/2}$ (for some cases) and the integral (22) therefore diverges. This illustrates that the generators do not exist if we impose boundary conditions which are too weak. In the case of too strong boundary conditions, for example $\mathcal{O}(r^{-17})$, the energy is always zero and the only consistent theory is one with a single state which is flat space with no gravitons or anything. So if we make the boundary conditions too weak, the generators are not well defined and if we make them too strong, the theory becomes trivial. In all the examples we know of there is only a very small window for interesting boundary conditions. Sometimes there is more than one consistent choice, but typically very few possibilities arise.

The asymptotic symmetry group is a very important and subtle concept. It may seem like we have described a fancy mechanism to reproduce results we already know, for example that the Poincaré group is the ASG of asymptotically spatially Minkowskian gravity. Indeed, it often happens that the ASG is simply the isometry group of the vacuum. However this is not always the case. The most famous example is AdS_3 [10]. For AdS_4, the ASG is the same as the vacuum isometry group $SO(3,2)$. Naively we might assume that similarly for AdS_3 the ASG is $SO(2,2)$, but in fact there is no consistent way to define a nontrivial theory in AdS_3 with $SO(2,2)$ as the ASG. If we want to accommodate any finite energy excitations we need weaker boundary conditions - weak enough to give an ASG generated by two copies of the Virasoro algebra. The resulting theory has states transforming in representations of the 2D conformal group. Simply by analyzing the ASG, we arrive at the far-reaching conclusion that any consistent definition of quantum gravity on AdS_3 space has to be a conformal theory in this sense. This was discovered by Brown and Henneaux in the 80's. Their analysis did not provide details about what the consistent definition, if any, of quantum theory of gravity in AdS_3 should be. Indeed it was a decade later [8] before we found, using string theory and extra compact dimensions, an example of a consistent UV completion of quantum gravity in AdS_3 space.

Another highly nontrivial example is the ASG evaluated at future null infinity in asymptotically Minkowskian spaces. This is an infinite-dimensional group known as the BMS group. The full implications of this seem to be yet to be understood. Some interesting recent observations appear in [33].

5. Kerr/CFT

A lot of machinery had been developed over the years [28,34–37] to describe Dirac brackets and the Q_ζ generators. We now simply want to apply this machinery and find a consistent set of boundary conditions for NHEK. In our first analysis we impose a restriction to ensure that our boundary conditions preserve extremality, i.e.

$$\mathcal{E} = M^2 - J = 0. \tag{25}$$

We will discuss nonextremal cases later in these lectures. A motivation for studying extreme Kerr black holes first is that they are in some regards real-world analogs of the extreme black holes we have successfully analyzed in string theory, and

may be easier to understand than the general case involving nonzero energy $\mathcal{E}$. One set of consistent boundary conditions with $\mathcal{E} = 0$ has been found. In the several years which have passed since the original Kerr/CFT paper [38] was published, nobody has found another solution to this problem. This suggests they may be unique but there is no proof.

5.1. ASG for NHEK

The boundary conditions require

$$\begin{aligned} &h_{tt} = \mathcal{O}(r^2), \quad h_{t\phi} = h_{\phi\phi} = \mathcal{O}(1), \\ &h_{\phi r} = h_{\theta\theta} = h_{\theta\phi} = h_{\theta t} = \mathcal{O}(r^{-1}), \\ &\qquad h_{rr} = \mathcal{O}(r^{-3}), \quad h_{tr} = h_{\theta r} = \mathcal{O}(r^{-2}). \end{aligned} \tag{26}$$

In terms of the h the $\mathcal{E} = 0$ boundary condition is the vanishing of an ADM-like integral over the boundary. The explicit expression is given in equation (33) below with $\zeta = \partial_\tau$.

The most general diffeomorphism preserving these boundary conditions is

$$\begin{aligned} \zeta = &\left[\epsilon(\phi) + \mathcal{O}(r^{-2})\right]\partial_\phi + \left[-r\epsilon'(\phi) + \mathcal{O}(1)\right]\partial_r \\ &+ \left[C + \mathcal{O}(r^{-3})\right]\partial_\tau + \left[\mathcal{O}(r^{-1})\right]\partial_\theta \end{aligned} \tag{27}$$

where $\epsilon(\phi)$ is an arbitrary smooth function and C is an arbitrary constant. The subleading terms in (27) and leading ∂_τ term correspond to the trivial diffeomorphisms i.e they do not contribute to Q_ζ. Therefore we can take the leading part

$$\zeta(\epsilon) = \epsilon(\phi)\partial_\phi - r\epsilon'(\phi)\partial_r \tag{28}$$

as a representation of the quotient (20). In other words, this vector field generates the asymptotic symmetry group of the NHEK geometry. It is convenient to introduce a basis

$$\zeta_n \equiv \zeta(-e^{-in\phi}) = -e^{-in\phi}\partial_\phi - in\, e^{-in\phi} r\, \partial_r. \tag{29}$$

The Lie bracket[3] of the vector fields ζ_n satisfies

$$i\left[\zeta_n, \zeta_m\right] = (m-n)\zeta_{m+n}. \tag{30}$$

From (30) we learn that the asymptotic symmetry group is generated by one copy of the Virasoro algebra. There is no central charge here because this is just a classical vector field computation.

[3] $[X, Y] = \mathcal{L}_X Y - \mathcal{L}_Y X$

5.2. Central charge

Rather than studying the Lie brackets of ζ_n, we now want to consider the Dirac bracket of the charges generating the ζ_n diffeomorphisms. By construction, the Dirac bracket algebra of the charges satisfies

$$\{Q_\zeta, \Phi\}_{DB} = \mathcal{L}_\zeta \Phi. \tag{31}$$

Using the Jacobi identity, this implies that

$$\{Q_\zeta, Q_\xi\}_{DB} = Q_{[\zeta,\xi]} + c_{\zeta\xi}, \tag{32}$$

where $c_{\zeta\xi}$ is the central term. Amazingly enough, the central term in (32) can be calculated using classical gravity from the explicit expression for Q_ζ. Infinitesimal charge differences between neighboring geometries $g_{\mu\nu}$ and $g_{\mu\nu} + h_{\mu\nu}$ are given by

$$\delta Q_\zeta = \frac{1}{8\pi G}\int_{\partial\Sigma} K_\zeta(h, g) \tag{33}$$

where the integral is over the boundary of the spatial slice and

$$\begin{aligned} K_\zeta(h,g) = -\frac{1}{4}\epsilon_{\alpha\beta\mu\nu} dx^\alpha \wedge dx^\beta \Big[&\zeta^\nu D^\mu h \\ &- \zeta^\nu D_\sigma h^{\mu\sigma} + \zeta_\sigma D^\nu h^{\mu\sigma} + \frac{1}{2} h D^\nu \zeta^\mu \\ &+ \frac{1}{2} h^{\sigma\nu}(D^\mu \zeta_\sigma - D_\sigma \zeta^\mu)\Big]. \end{aligned} \tag{34}$$

This expression and its many precursors have been studied in the literature for a long time, starting with ADM back in the 50's, and so has by now been worked out in great detail. From (33) we can determine the central charge by applying it to fluctuations $h = \mathcal{L}_\xi g$ (g here is the NHEK metric) produced by the allowed diffeomorphisms. This results in a very explicit expression for the central charge:

$$c_{\xi\zeta} = \frac{1}{8\pi G}\int_{\partial\Sigma} K_\zeta(\mathcal{L}_\xi g, g). \tag{35}$$

In terms of the basis (29) one finds

$$\{Q_{\zeta_m}, Q_{\zeta_n}\}_{DB} = Q_{[\zeta_m,\zeta_n]} - iJ(m^3 + 2m)\delta_{m+n}. \tag{36}$$

The classical charges Q_ζ have units of action so we can use $\hbar$ to define a dimensionless quantity

$$\hbar L_n = Q_{\zeta_n} + \frac{3J}{2}\delta_n \tag{37}$$

and then apply the usual quantization rules to the Dirac bracket $\{\cdot,\cdot\}_{DB} \to -\frac{i}{\hbar}[\cdot,\cdot]$ for these. The quantum charge algebra turns out to be

$$[L_m, L_n] = (m-n)L_{m+n} + \frac{J}{\hbar}\, m(m^2-1)\delta_{m+n}. \tag{38}$$

From this we can read off the central charge for the NHEK geometry:

$$c = \frac{12J}{\hbar}, \tag{39}$$

where we have reinstated the factor of $\hbar$ normally set to one. This means that the $\mathcal{E} = 0$ states in NHEK with the boundary conditions (26) must form representations of one copy of the Virasoro algebra with central charge $\frac{12J}{\hbar}$ and hence in this sense comprise a (chiral half of) a 2D CFT[4].

From this analysis, we do not know if the CFT is local or unitary. We also cannot say, without an explicit microscopic construction, if the conformal symmetry persists beyond the semiclassical limit considered here. However, since Kerr black holes do exist, we do know that the structure we have found arises as a limit of a consistent physical system.

While 2D conformal symmetry often appears in critical point behavior of real-world condensed matter systems, this is the first time it has arisen in limits of observable astronomical systems. The 2D conformal symmetry arises here with a holographic connection to the 4D diffeomorphism group (note the radial $\epsilon'\partial_r$ term in (28)). This connection opens the door to adapting the beautiful insights in string theory holography to real-world black holes.

5.3. Cardy entropy

Conformal field theories have many universal properties and we would like to map these to the many universal properties of black hole dynamics. The first thing we would like to understand is whether or not there is some way for us to recover the Bekenstein - Hawking formula for black hole entropy. For the extreme Kerr geometry $S_{BH} = 2\pi J$. One would like to understand this in terms of the microstate degeneracy of a CFT at finite temperature. This is at first puzzling since we know that extreme Kerr has zero Hawking temperature. However there are two relevant conserved quantities. One of these is the energy which is conjugate to the Hawking temperature and the other is an angular momentum conjugate to the angular velocity. We are interested in counting extreme Kerr microstates which are moving at the speed of light in the near-horizon region of the black hole. Roughly speaking this means that the quantum number we are after is a linear combination of the energy and the angular momentum. Let's be specific.

In general, a black hole represents not a pure, but a mixed, state and the quantum fields around the black hole are in a thermal state. For a Schwarzschild black hole, the thermal state is weighted by the Boltzmann factor

$$e^{-\omega/T_H}. \tag{40}$$

Adding angular momentum changes this to

$$e^{-(\omega - m\Omega_H)/T_H} \tag{41}$$

with Ω_H being the angular velocity of the horizon which for extremal Kerr is $\Omega_H = 1/2M$. When we carefully take the extreme limit of Kerr, T_H goes to zero, but this does not necessarily mean that the weighting factor (41) is trivial. The reason for this is the possibility of states which have ω very near $m\Omega_H$. In the extreme limit $T_H \to 0$, we get $\omega = m\Omega_H$ states contributing to a density matrix weighted by the angular momentum m. Carefully taking the limit one finds for $T_H \to 0$

$$e^{-(\omega - m\Omega_H)/T_H} \to e^{-2\pi m} = e^{-m/T_L}. \tag{42}$$

From here we can read off the relevant temperature as $T_L = 1/2\pi$. We can also note that the angular momentum m is the eigenvalue of L_0. Using the Cardy entropy formula for a chiral CFT,

[4] We henceforth take $\hbar = 1$.

we find the entropy obeys

$$S_{cardy} = \frac{\pi^2}{3} c\, T_L = \frac{\pi^2}{3} 12 J\, T_L = 2\pi J. \qquad (43)$$

which matches the Bekenstein - Hawking entropy (6) exactly!

Note that since we do not know the exact CFT, we cannot be sure that it is in the class of unitary and modular invariant theories for which the Cardy formula is known to apply. We only know some very general properties of this CFT. In order to provide an exact description we would need to know all the microscopic laws of physics to the Planck scale and beyond. In string theory we take a top-down approach: we assume some microscopic description and that way we know everything about the dual CFT. That is not what we are doing in these lectures. Rather we are taking a bottom-up approach and must live with some uncertainty about the details of the CFT. We are trying to understand how the universal properties of black holes might follow from any consistent UV completion of the known laws of physics. We are not trying to find the completion. So rather than try to prove that the Cardy formula is applicable, we take the precise agreement of the Bekenstein-Hawking and Cardy entropy formulas resulting from our ASG analysis as the first piece of evidence both for the applicability of the Cardy formula and the physical relevance of the picture of extreme Kerr as a 2D CFT. More evidence will appear below.

Roughly speaking, the Cardy formula works when we are justified in applying statistical reasoning. It pertains to the statistical limit of 2D CFTs and hence is related to the statistical limit of black holes as studied in [39]. A sufficient, though not necessary, condition for the Cardy formula to be valid is that the temperature is large compared to the central charge. Clearly this is not the case here. It was also not the case for the stringy black holes studied in [8]. There, the temperature was just one of the charges and in the limit when the supergravity approximation was valid, the temperature was parametrically small compared to the central charge. Often, a sufficient condition for the applicability of the Cardy formula is that the temperature is large relative to the gap or lightest excitation of the theory, which means that a large number of degrees of freedom are excited. Essentially it is just a thermodynamic approximation applied to the many degrees of freedom in the CFT. We actually know that the gap for extreme Kerr must be very small. It was computed in a paper by Preskill, Schwarz, Shapere, Trivedi and Wilczek [39] two decades ago using only semiclassical reasoning. They showed that if the gap for extreme black holes is sufficiently large, the Hawking calculation would be invalid since a black hole can not radiate quanta with energies less than the gap. Therefore a large gap is inconsistent with the semiclassical Hawking calculation. This argument can provide also us with an upper bound on the size of the gap. For case of Kerr, the L_0 gap is of order $1/J$. The temperature $T_L = \frac{1}{2\pi}$ is already much larger than this, so the Cardy formula may plausibly apply. A similar story justified the string theory computations [40].

So far in our matching between gravity and the CFT, we have found agreement with just one number. However there are many generalizations of this construction in which the central charge and entropy are complicated functions of various geometrical data and the functions are matched in entirety [41–55]. Further, and qualitatively different, supporting evidence for Kerr/CFT comes from scattering amplitudes in NHEK. Kerr scattering amplitudes were computed long ago in [56–60]. They turn out to be complicated products involving ratios of four gamma functions with arguments depending on the energies and spins of the black hole and the incoming and outgoing waves . It has been shown in a variety of contexts [61–64] that these correspond exactly to the finite temperature CFT correlators! Hence the picture of extreme Kerr as a CFT holds together well.

5.4. Beyond extremality

The natural next question is how to go beyond extremality, i.e. to the case where $\mathcal{E} = M^2 - J > 0$. For infinitesimally small deviations from extremality, Castro and Larsen [65] and others [66–68] found an alternate set of boundary conditions which lead to a second copy of the Virasoro algebra. Since the conserved charge $\mathcal{E}$ derives from

an $SL(2,R)$ isometry of NHEK, the relevant Virasoro algebra is an enhancement of the $SL(2,R)$ isometry rather than the enhancement of the $U(1)$ described above.

In order to go beyond linear deviations from extremality, we need to include the effects of backreaction. The backreacted geometry is no longer asymptotically NHEK and the whole picture breaks down. It is not clear exactly what this means or how to proceed further at this point. One approach is to try to get some insight by embedding Kerr/CFT in string theory and see how the issue resolves itself in that context.[5]

We will not further explore this direction in these lectures. However in the next lecture we will find encouraging results by approaching the issue from a different angle. We simply analyze the form of the scattering amplitudes and entropy functions and find surprisingly that at low energies they take exactly the form expected for a CFT – even far from extremality! We have no a priori explanation for this "hidden" conformal symmetry but it seems to indicate more Kerr miracles still await discovery.

6. Hidden conformal symmetry for generic Kerr

6.1. Wave equation as $SL(2,R)$ Casimir

Consider the scalar Laplacian ∇^2 in the Kerr geometry. Using the Killing-Yano tensor we can construct a second-order differential operator ${f_\alpha}^\mu f^{\alpha\nu}\nabla_\mu\nabla_\nu$ which commutes with ∇^2. This allows the wave equation to be separated [16]:

$$\Phi(t,r,\theta,\phi) = e^{-i\omega t+im\phi}R(r)S(\theta). \tag{44}$$

Denoting the separation constant K_ℓ we have

$$-K_l S(\theta) = \left[\frac{1}{\sin\theta}\partial_\theta(\sin\theta\partial_\theta) - \frac{m^2}{\sin^2\theta} + \omega^2a^2\cos^2\theta\right]S(\theta), \tag{45}$$

and

$$K_l R(r) = \Big[\partial_r(\Delta\partial_r) + \frac{(2Mr_+\omega - am)^2}{(r-r_+)(r_+-r_-)} - \frac{(2Mr_-\omega - am)^2}{(r-r_-)(r_+-r_-)} + (r^2+2M(r+2M))\omega^2\Big]R(r). \tag{46}$$

Both of these equations are solved by Heun functions which are known only numerically. However, we can try to simplify the equations by going to low frequencies. The last term in (45) can be neglected if $\omega M \ll 1$ i.e. for excitation wavelengths larger than the black hole radius. In this case, the geometry can be divided into two regions

$$\begin{aligned} &\text{“Near”}: \quad r \ll \frac{1}{\omega}, \\ &\text{“Far”}: \quad r \gg M \end{aligned} \tag{47}$$

with large overlaps. We can then solve the equations (45) and (46) in both the near and far regions, and match the solutions at any value r_{match} of r in the intermediate region

$$M \ll r_{match} \ll \frac{1}{\omega}. \tag{48}$$

The fact that, in this approximation, the answer cannot depend on r_{match} implies that the solutions in the near region must behave in some special symmetric way under transformations of r_{match}. Moreover since the redshift factor depends on r, transformations of r_{match} are tied to scale transformations. This strongly hints that the near region physics should exhibit some kind of conformal symmetry arising from invariance of the full answer under shifts of the matching surface. We will see below that this is indeed the case.

In the limit $\omega M \ll 1$, the equation (45) simplifies to the spherical Laplacian and is solved in terms of spherical harmonic functions with $K_l = l(l+1)$. The radial equation (46) in the far region is solved by Bessel functions. In the

[5] Some recent progress along those lines appeared, after these lectures were given, in [69,70].

near region, the equation simplifies to

$$\left[\partial_r(\Delta\partial_r) + \frac{(2Mr_+\omega - am)^2}{(r-r_+)(r_+-r_-)} - \frac{(2Mr_-\omega - am)^2}{(r-r_-)(r_+-r_-)}\right] R(r) = l(l+1)\, R(r), \tag{49}$$

whose solutions are hypergeometric functions. In order to obtain the solution for the full geometry we need to do a matching between the two regions. The fact that the hypergeometric functions form representations of $SL(2,R)$ gives us further reason to expect some hidden conformal symmetry.

This near region $SL(2,R)$ symmetry that appears in the Laplace equation for scalar perturbations can be made explicit by introducing natural 'conformal' variables

$$\begin{aligned} w^+ &= \sqrt{\frac{r-r_+}{r-r_-}}\, e^{2\pi T_R \phi} \\ w^- &= \sqrt{\frac{r-r_+}{r-r_-}}\, e^{2\pi T_L \phi - t/2M} \\ y &= \sqrt{\frac{r-r_+}{r-r_-}}\, e^{\pi(T_R+T_L)\phi - t/4M} \end{aligned} \tag{50}$$

where

$$T_L = \frac{r_+ + r_-}{4\pi a}, \quad T_R = \frac{r_+ - r_-}{4\pi a}. \tag{51}$$

We can define the vector fields

$$\begin{aligned} H_1 &= i\partial_+ \\ H_0 &= i\left(w^+\partial_+ + \frac{1}{2} y\partial_y\right) \\ H_{-1} &= i\left(w^{+2}\partial_+ + w^+ y\partial_y - y^2\partial_-\right) \end{aligned} \tag{52}$$

and

$$\begin{aligned} \bar{H}_1 &= i\partial_- \\ \bar{H}_0 &= i\left(w^-\partial_- + \frac{1}{2} y\partial_y\right) \\ \bar{H}_{-1} &= i\left(w^{-2}\partial_- + w^- y\partial_y - y^2\partial_+\right) \end{aligned} \tag{53}$$

which obey the $SL(2,R)$ algebra

$$[H_0, H_{\pm 1}] = \mp i H_{\pm 1}, \quad [H_{-1}, H_1] = -2iH_0, \tag{54}$$

and similarly for $\bar{H}_0$ and $\bar{H}_{\pm 1}$. The $SL(2,R)$ quadratic Casimir, written in (t, r, θ, ϕ) variables, is

$$\mathcal{H}^2 = \bar{\mathcal{H}}^2 = \partial_r(\Delta\partial_r) + \frac{(2Mr_+\omega - am)^2}{(r-r_+)(r_+-r_-)} - \frac{(2Mr_-\omega - am)^2}{(r-r_-)(r_+-r_-)}\,. \tag{55}$$

As a result of this, the equation (49) for $\Phi(r)$ in the near region can be written

$$\mathcal{H}^2\Phi = \bar{\mathcal{H}}^2\Phi = l(l+1)\Phi. \tag{56}$$

This gives the solutions for Φ as representations of $SL(2,R)$ with conformal weights

$$(h_L, h_R) = (l, l). \tag{57}$$

However, although $SL(2,R)_L \times SL(2,R)_R$ is a symmetry of the near region scalar wave equation, it is broken by the extra periodic identification

$$\phi \sim \phi + 2\pi. \tag{58}$$

Under the identification (58), the conformal coordinates identify as

$$\begin{gathered} w^+ \sim e^{4\pi^2 T_R} w^+,\ w^- \sim e^{4\pi^2 T_L} w^-, \\ y \sim e^{2\pi^2(T_R+T_L)} y. \end{gathered} \tag{59}$$

This identification is generated by

$$\begin{gathered} g = e^{-4\pi^2 i T_R H_0 - 4\pi^2 i T_L \bar{H}_0}, \\ g \in SL(2,R)_L \times SL(2,R)_R, \end{gathered} \tag{60}$$

which is exactly the form of the identification for a CFT partition function at finite temperature (T_L, T_R).

We stress that the near region discussed above is not a "near-horizon" region since r can be arbitrarily large for fixed M and the conformal symmetry, although it acts on solutions of the wave equation, is not a geometric isometry!

6.2. Cardy entropy

Now let us simply suppose there is some underlying CFT at the temperatures (51) for generic Kerr. Its entropy would be given by the Cardy formula

$$S = \frac{\pi^2}{3}\, c_L T_L + \frac{\pi^2}{3}\, c_R T_R. \tag{61}$$

We only know the central charges $c_L = c_R = 12J$ for the extreme case and first order variations away from extremality. So we further assume that the central charges behave smoothly and that they do not change as we move away from the extremal case. Using (51) for the temperatures, we arrive at

$$S_{Cardy} = \frac{\pi^2}{3} 12J \left(\frac{r_+ + r_-}{4\pi a} + \frac{r_+ - r_-}{4\pi a} \right) = \frac{2\pi r_+ J}{a} = 2\pi M r_+ = S_{BH}! \quad (62)$$

Comparing this to the Bekenstein - Hawking formula (6), we see an impressive and detailed match for general M, J Kerr black holes. One can also look at the near-region low-energy scattering amplitudes. These agree precisely with those of a CFT [71] even for nonextremal Kerr. Hence the scattering amplitudes exhibit symmetries which do not come from manifest symmetries of the action. Another example of such 'hidden' symmetries which are not manifest in the action but appear in the scattering amplitudes is described in lectures at this school by N. Arkani-Hamed on 4D $\mathcal{N} = 4$ SYM theory.

Let us summarize. There is no a priori ASG or other type of argument indicating that black holes with generic values of M and J are dual to 2D CFTs. Nevertheless a phenomenological analysis of the scattering amplitudes and entropy formulae reveals that they exhibit a hidden 2D conformal symmetry: yet another 'miracle' of the Kerr story. The challenge now is to understand why this should be so.

7. Future directions

While some things have been understood at this point, there are several remaining, interrelated puzzles/questions concerning the theoretical structure of Kerr/CFT, some of which we have mentioned along the way. Related quantum gravity questions were explored in the previous Cargèse lectures [72]. These Kerr/CFT puzzles/questions include

(i) Boundary conditions are known which give either a left or a right -moving Virasoro generating the ASG. Are there boundary conditions which simultaneously give both? If not, why not?

(ii) How do we understand the fact that at finite $M^2 - J$ the NHEK region disappears?

(iii) How do we match the instability of extreme Kerr due to quantum Unruh-Starobinsky superradiance to properties of the CFT?

(iv) Where did the hidden conformal symmetry come from and why does the Cardy formula work? Is there a generalization of the standard ASG analysis which can be applied to the $r \ll \frac{1}{\omega}$ near-region to explain the hidden conformal symmetry?

(v) One might hope to match a thermal state in a nonchiral CFT with the general Kerr black hole. Such a state has three parameters: c, T_L and T_R, while Kerr has only M and J, and can therefore at best describe a subspace of the CFT states. Where does the restriction to a subspace come from? Is there a holographic dual for the generic CFT state?

Perhaps the most promising approach to addressing these questions is by embedding Kerr/CFT into string theory. Indeed many aspects of the parallel Brown-Henneaux analysis of AdS_3 were not understood until a stringy embedding was discovered. Recently (after these lectures were given), progress has been made in this direction in the context of charged spinning black holes in five dimensions with a Kaluza-Klein S^1 [69]. The structure of the corresponding NHEK geometry depends on the value of the electric charge. When the charge is pushed to its maximal value, the NHEK geometry locally approaches $AdS_3 \times S^3$. The dual at the maximality is then easily identified with standard stringy methods and has the central charge predicted by Kerr/CFT. The linearized properties away from this maximal point also agree with Kerr/CFT expectations. Even more recently [73], the dual theory has been identified for all finite submaximal values of the charge as the low energy limit of a certain wrapped D-brane configuration with nonzero charge densities, and found to be related to the so-called dipole-deformed gauge theories. One hopes that this intricate construction can be used to shed light on the general puzzles discussed above, and suggest answers which do not depend

on the details of string theory.

Of course since Kerr/CFT applies to the real world, it is not necessary to understand all aspects of its theoretical structure before attempting to find observational consequences of the symmetry. It is often the case in physics that the comparison of theory to experiment is an ingredient in understanding both! Kerr/CFT is a statement about a symmetry which applies to objects seen in the sky. At present, the observational data from those objects is good and rapidly improving. There are many observed phenomena which are not understood [13,12]. Symmetries often provide both predictions about and a useful framework for organizing the observational data. They also suggest what to look for. Analyses of black hole properties tend to focus either on the non-rotating case or small perturbations in the rotation parameter. Perhaps interesting simplifications and structures occur near extremality. This direction seems ripe for exploration in the near future.

Acknowledgements

This article was transcribed from tapes of lectures given by A. Strominger at the 2010 Cargèse School on String Theory. We are grateful to L. Baulieu, J. de Boer, M. Douglas, E. Rabinovici, P. Vanhove and P. Windey for the invitation to lecture and for organizing an exceptionally stimulating school. We would also like to thank the participants of the school for many stimulating conversations and questions.

REFERENCES

1. D. Christodoulou, Phys. Rev. Lett. **25**, 1596 (1970).
2. S. W. Hawking, "Gravitational radiation from colliding black holes," Phys. Rev. Lett. **26**, 1344 (1971).
3. J. M. Bardeen, B. Carter and S. W. Hawking, "The Four laws of black hole mechanics," Commun. Math. Phys. **31**, 161 (1973).
4. J. D. Bekenstein, "Black holes and entropy," Phys. Rev. D **7**, 2333 (1973).
5. J. D. Bekenstein, "Extraction of energy and charge from a black hole," Phys. Rev. D **7**, 949 (1973).
6. J. D. Bekenstein, "Generalized second law of thermodynamics in black hole physics," Phys. Rev. D **9**, 3292 (1974).
7. S. W. Hawking, "Particle Creation By Black Holes," Commun. Math. Phys. **43**, 199 (1975) [Erratum-ibid. **46**, 206 (1976)].
8. A. Strominger and C. Vafa, "Microscopic Origin of the Bekenstein-Hawking Entropy," Phys. Lett. B **379**, 99 (1996) [arXiv:hep-th/9601029].
9. A. Strominger, "Black hole entropy from near-horizon microstates," JHEP **9802**, 009 (1998) [arXiv:hep-th/9712251].
10. J. D. Brown and M. Henneaux, "Central Charges in the Canonical Realization of Asymptotic Symmetries: An Example from Three-Dimensional Gravity," Commun. Math. Phys. **104**, 207 (1986).
11. S. Chandrasekhar, "The Gravitational Perturbations Of The Kerr Black Hole. II. The Perturbations in the Quantities which are Finite in the Stationary State," Proc. Roy. Soc. Lond. A **358**, 441 (1978).
12. J. E. McClintock *et al.*, "Measuring the Spins of Accreting Black Holes," arXiv:1101.0811 [astro-ph.HE].
13. J. E. McClintock, R. Shafee, R. Narayan, R. A. Remillard, S. W. Davis and L. X. Li, "The Spin of the Near-Extreme Kerr Black Hole GRS 1915+105," Astrophys. J. **652**, 518 (2006) [arXiv:astro-ph/0606076].
14. L. W. Brenneman and C. S. Reynolds, "Constraining Black Hole Spin Via X-ray Spectroscopy," Astrophys. J. **652**, 1028 (2006) [arXiv:astro-ph/0608502].
15. M. Walker and R. Penrose, "On quadratic first integrals of the geodesic equations for type [22] spacetimes," Commun. Math. Phys. **18**, 265 (1970).
16. B. Carter, "Global Structure of the Kerr Family of Gravitational Fields," Phys. Rev. **174**, 1559; Comm. Math. Phys. **10**, 280.
17. G. W. Gibbons, R. H. Rietdijk and J. W. van Holten, "SUSY in the sky," Nucl. Phys. B **404**, 42 (1993) [arXiv:hep-th/9303112].
18. J. M. Bardeen and G. T. Horowitz, "The extreme Kerr throat geometry: A vacuum analog of AdS(2) x S(2)," Phys. Rev. D **60**,

104030 (1999) [arXiv:hep-th/9905099].
19. J. M. Maldacena and A. Strominger, "AdS(3) black holes and a stringy exclusion principle," JHEP **9812**, 005 (1998) [arXiv:hep-th/9804085].
20. Y. Nutku, "Exact solutions of topologically massive gravity with a cosmological constant," Class. Quant. Grav. **10**, 2657 (1993).
21. M. Gürses, "Perfect Fluid Sources in 2+1 Dimensions," Class. Quant. Grav. **11**, 2585 (1994).
22. M. Rooman and P. Spindel, "Goedel metric as a squashed anti-de Sitter geometry," Class. Quant. Grav. **15**, 3241 (1998) [arXiv:gr-qc/9804027].
23. A. Bouchareb and G. Clement, "Black hole mass and angular momentum in topologically massive gravity," Class. Quant. Grav. **24**, 5581 (2007) [arXiv:0706.0263 [gr-qc]].
24. C. P. Herzog, M. Rangamani and S. F. Ross, "Heating up Galilean holography," JHEP **0811**, 080 (2008) [arXiv:0807.1099 [hep-th]].
25. D. Anninos, "Hopfing and Puffing Warped Anti-de Sitter Space," JHEP **0909**, 075 (2009) [arXiv:0809.2433 [hep-th]].
26. D. Anninos, M. Esole and M. Guica, "Stability of warped AdS3 vacua of topologically massive gravity," JHEP **0910**, 083 (2009) [arXiv:0905.2612 [hep-th]].
27. D. Anninos, W. Li, M. Padi, W. Song and A. Strominger, "Warped AdS3 Black Holes," JHEP **0903**, 130 (2009) [arXiv:0807.3040 [hep-th]].
28. G. Compere and S. Detournay, "Semi-classical central charge in topologically massive gravity," Class. Quant. Grav. **26**, 012001 (2009) [Erratum-ibid. **26**, 139801 (2009)] [arXiv:0808.1911 [hep-th]].
29. G. Compere and S. Detournay, "Boundary conditions for spacelike and timelike warped AdS3 spaces in topologically massive gravity," JHEP **0908**, 092 (2009) [arXiv:0906.1243 [hep-th]].
30. E. D'Hoker and P. Kraus, "Charged Magnetic Brane Solutions in AdS5 and the fate of the third law of thermodynamics," JHEP **1003**, 095 (2010) [arXiv:0911.4518 [hep-th]].
31. S. Detournay, D. Israel, J. M. Lapan and M. Romo, "String Theory on Warped AdS3 and Virasoro Resonances," JHEP **1101**, 030 (2011) [arXiv:1007.2781 [hep-th]].
32. D. Anninos and T. Hartman, "Holography at an Extremal De Sitter Horizon," JHEP **1003**, 096 (2010) [arXiv:0910.4587 [hep-th]].
33. G. Barnich, C. Troessaert, "Aspects of the BMS/CFT correspondence," JHEP **1005**, 062 (2010). [arXiv:1001.1541 [hep-th]].
34. G. Barnich and F. Brandt, "Covariant theory of asymptotic symmetries, conservation laws and central charges," Nucl. Phys. B **633**, 3 (2002) [arXiv:hep-th/0111246].
35. G. Barnich, "Boundary charges in gauge theories: Using Stokes theorem in the bulk," Class. Quant. Grav. **20**, 3685 (2003) [arXiv:hep-th/0301039].
36. G. Compere, "Symmetries and conservation laws in Lagrangian gauge theories with applications to the mechanics of black holes and to gravity in three dimensions," arXiv:0708.3153 [hep-th].
37. G. Barnich and G. Compere, "Surface charge algebra in gauge theories and thermodynamic integrability," J. Math. Phys. **49**, 042901 (2008) [arXiv:0708.2378 [gr-qc]].
38. M. Guica, T. Hartman, W. Song and A. Strominger, "The Kerr/CFT Correspondence," Phys. Rev. D **80**, 124008 (2009) [arXiv:0809.4266 [hep-th]].
39. J. Preskill, P. Schwarz, A. D. Shapere, S. Trivedi and F. Wilczek, "Limitations on the statistical description of black holes," Mod. Phys. Lett. A **6**, 2353 (1991).
40. J. M. Maldacena, L. Susskind, "D-branes and fat black holes," Nucl. Phys. **B475**, 679-690 (1996). [hep-th/9604042].
41. H. Lu, J. Mei and C. N. Pope, "Kerr/CFT Correspondence in Diverse Dimensions," JHEP **0904**, 054 (2009) [arXiv:0811.2225 [hep-th]].
42. T. Azeyanagi, N. Ogawa and S. Terashima, "Holographic Duals of Kaluza-Klein Black Holes," JHEP **0904**, 061 (2009) [arXiv:0811.4177 [hep-th]].
43. T. Hartman, K. Murata, T. Nishioka and A. Strominger, "CFT Duals for Extreme Black Holes," JHEP **0904**, 019 (2009)

[arXiv:0811.4393 [hep-th]].
44. D. D. K. Chow, M. Cvetic, H. Lu and C. N. Pope, "Extremal Black Hole/CFT Correspondence in (Gauged) Supergravities," Phys. Rev. D **79**, 084018 (2009) [arXiv:0812.2918 [hep-th]].
45. H. Isono, T. S. Tai and W. Y. Wen, "Kerr/CFT correspondence and five-dimensional BMPV black holes," Int. J. Mod. Phys. A **24**, 5659 (2009) [arXiv:0812.4440 [hep-th]].
46. T. Azeyanagi, N. Ogawa and S. Terashima, "The Kerr/CFT Correspondence and String Theory," Phys. Rev. D **79**, 106009 (2009) [arXiv:0812.4883 [hep-th]].
47. J. J. Peng and S. Q. Wu, "Extremal Kerr black hole/CFT correspondence in the five dimensional Gódel universe," Phys. Lett. B **673**, 216 (2009) [arXiv:0901.0311 [hep-th]].
48. C. M. Chen and J. E. Wang, "Holographic Duals of Black Holes in Five-dimensional Minimal Supergravity," Class. Quant. Grav. **27**, 075004 (2010) [arXiv:0901.0538 [hep-th]].
49. F. Loran and H. Soltanpanahi, "5D Extremal Rotating Black Holes and CFT duals," Class. Quant. Grav. **26**, 155019 (2009) [arXiv:0901.1595 [hep-th]].
50. A. M. Ghezelbash, "Kerr/CFT Correspondence in the Low Energy Limit of Heterotic String Theory," JHEP **0908**, 045 (2009) [arXiv:0901.1670 [hep-th]].
51. H. Lu, J. w. Mei, C. N. Pope and J. F. Vazquez-Poritz, "Extremal Static AdS Black Hole/CFT Correspondence in Gauged Supergravities," Phys. Lett. B **673**, 77 (2009) [arXiv:0901.1677 [hep-th]].
52. G. Compere, K. Murata and T. Nishioka, "Central Charges in Extreme Black Hole/CFT Correspondence," JHEP **0905**, 077 (2009) [arXiv:0902.1001 [hep-th]].
53. D. Astefanesei and Y. K. Srivastava, "CFT Duals for Attractor Horizons," Nucl. Phys. B **822**, 283 (2009) [arXiv:0902.4033 [hep-th]].
54. M. R. Garousi and A. Ghodsi, "The RN/CFT Correspondence," Phys. Lett. B **687**, 79 (2010) [arXiv:0902.4387 [hep-th]].
55. T. Azeyanagi, G. Compere, N. Ogawa, Y. Tachikawa and S. Terashima, "Higher-Derivative Corrections to the Asymptotic Virasoro Symmetry of 4d Extremal Black Holes," Prog. Theor. Phys. **122**, 355 (2009) [arXiv:0903.4176 [hep-th]].
56. A. A. Starobinsky, "Amplification of waves during reflection from a rotating black hole," Zh. Exp. i Teoret. Fiz., **64**, 48 (transl. in Soviet Phys. JETP, **37**, 28).
57. A. A. Starobinsky and S. M. Churilov, "Amplification of electromagnetic and gravitational waves scattered by a rotating black hole," Zh. Exp. i Teoret. Fiz., **65**, 3.
58. S. A. Teukolsky, "Perturbations of a rotating black hole. 1. Fundamental equations for gravitational, electromagnetic and neutrino field perturbations," Astrophys. J. **185**, 635 (1973).
59. W. H. Press and S. A. Teukolsky, "Perturbations of a Rotating Black Hole. II. Dynamical Stability of the Kerr metric," Astrophys. J. **185**, 649 (1973).
60. W. H. Press and S. A. Teukolsky, "Perturbations of a Rotating Black Hole. III - Interaction of the Hole with Gravitational and Electromagnetic Radiation," Astrophys. J. **193**, 443 (1974).
61. I. Bredberg, T. Hartman, W. Song and A. Strominger, "Black Hole Superradiance From Kerr/CFT," JHEP **1004**, 019 (2010) [arXiv:0907.3477 [hep-th]].
62. M. Cvetic and F. Larsen, "Greybody Factors and Charges in Kerr/CFT," JHEP **0909**, 088 (2009) [arXiv:0908.1136 [hep-th]].
63. T. Hartman, W. Song and A. Strominger, "Holographic Derivation of Kerr-Newman Scattering Amplitudes for General Charge and Spin," JHEP **1003**, 118 (2010) [arXiv:0908.3909 [hep-th]].
64. B. Chen and C. S. Chu, "Real-time correlators in Kerr/CFT correspondence," JHEP **1005**, 004 (2010) [arXiv:1001.3208 [hep-th]].
65. A. Castro and F. Larsen, "Near Extremal Kerr Entropy from AdS_2 Quantum Gravity," JHEP **0912**, 037 (2009) [arXiv:0908.1121 [hep-th]].
66. Y. Matsuo, T. Tsukioka and C. M. Yoo, "Another Realization of Kerr/CFT Correspondence," Nucl. Phys. B **825**, 231 (2010)

[arXiv:0907.0303 [hep-th]].
67. Y. Matsuo, T. Tsukioka and C. M. Yoo, "Yet Another Realization of Kerr/CFT Correspondence," Europhys. Lett. **89**, 60001 (2010) [arXiv:0907.4272 [hep-th]].
68. J. Rasmussen, "Isometry-preserving boundary conditions in the Kerr/CFT correspondence," Int. J. Mod. Phys. A **25**, 1597 (2010) [arXiv:0908.0184 [hep-th]].
69. M. Guica and A. Strominger, "Microscopic Realization of the Kerr/CFT Correspondence," JHEP **1102**, 010 (2011) [arXiv:1009.5039 [hep-th]].
70. G. Compere, W. Song and A. Virmani, "Microscopics of Extremal Kerr from Spinning M5 Branes," arXiv:1010.0685 [hep-th].
71. A. Castro, A. Maloney and A. Strominger, "Hidden Conformal Symmetry of the Kerr Black Hole," arXiv:1004.0996 [hep-th].
72. A. Strominger, "Five Problems in Quantum Gravity," Nucl. Phys. Proc. Suppl. **192-193**, 119 (2009) arXiv:0906.1313 [hep-th].
73. Work in progress.

Time machine creation in the ultra-relativistic proton collisions

Andrey A. Bagrov[a*]

[a]Department of Theoretical Physics, Steklov Mathematical Institute,
Gubkina str. 8, Moscow, Russia, 119991

In this letter I briefly discuss the mechanism of microscopic time machines creation in the ultra-relativistic particle collisions. It is shown that in multidimensional theories of strong gravity collisions of lengthy objects (such as protons and nuclei) could lead to causality violation. Physical parameter of formed time machines have been estimated.

1. INTRODUCTION

The idea of time traveling has a long story. It was being seriously considered in theoretical physics after the renowned publication by Kurt Goedel [1] where he obtained the solution to Einstein equations which permits test particles to move along closed timelike curves (CTC). During last sixty years many other metrics with such property have been constructed. Among them we can point out the Gott time machine [2], Morris – Thorne – Yurtsever traversable wormhole [3], Wheeler wormhole [4]

However most of these solutions seem to be just toy models. They are important for our understanding of the structure of spacetime but they do not give any chance to find a way to realize the time machine in terrestrial nor cosmic conditions. Therefore experimental tests of causality violations are impossible by the present moment.

While trying to understand how the time machine can be formed we encounter three main problems:

- Most of known time machine models are stationary solutions to the equations of General Relativity. The process of their dynamical formation from some kind of initial conditions is absolutely mysterious.

- Almost all stable metrics with CTC violate the null-energy condition (NEC) which is held for usual states of matter. Involvement of exotic unknown matter is necessary for stability of the time machine.

- The Gott time machine does not violate the NEC and can be realized starting from simple initial conditions (some discussions of possible inconsistency of this metric were published [5] but I can not pay attention to them within this letter). But its existence requires extremely large amounts of energy. Therefore there is only a little chance that this time machine could exist even at early stages of the Universe evolution.

About 13 years ago the new promising paradigm of the gravitational interactions has been formulated. In the TeV-gravity models [6] our space is assumed to be embedded as a 3-brane into D-dimensional spacetime. Extra $D-4$ spatial dimensions are compactified on a manifold with inverse linear size of about few TeV. Analogous models where the dimension of spacetime is restricted to be $D=5$ also exist [7]. If one of these model is true the gravity should become much strong at energies about few TeV and more. In this case we may hope to probe some gravitational effects in high energy collisions of particles at the LHC and in cosmic rays.

*I am thankful to Prof. Irina Aref'eva and Oleg Groshev for helpful intense discussions. Especially I would like to express my deep gratitude to Marina Ivanova who managed me to believe in the possibility of time traveling and inspired me to formulate this mechanism. This work is supported by the Ministry of Science and Education of Russia (state contract 14.740.11.0710) and the non-profit "Dynasty" foundation.

One of possible gravitational effects which can be observed at the LHC and future colliders is the creation of a microscopic time machine. This idea has been discussed in several papers [8], however dynamical mechanisms of the TM appearance remains unclear. In the next section the construction similar to the Gott time machine is proposed within the framework of TeV-gravity.

2. PHYSICAL MODEL

Let us assume that our spacetime is 5-dimensional, i.e. the Randall – Sundrum model or the Dvali – Gabadadze – Porrati model is realized in our world. Also we may consider the Arkani-hamed – Dimopolous – Dvali model with an anisotropic compactification when one of compactified dimensions is much larger than others (it is well-known that the 5-dimensional ADD model is forbidden due to the phenomenological restrictions). For simplicity we may impose that the spacetime is asymptotically flat (in the RS-model it has AdS-asymptotic, but this does not change the physical picture qualitatively).

In such spacetime we can analyze a head-on collision of two protons at energies about 10TeV or more. What is the specific of their gravitational interaction? First of all we should pay attention to the fact that the proton is relatively large object, its diameter is $d_p = 1\text{fm} = 10^{-15}\text{m}$, while the de Broglie wavelength corresponding to the energy of 10TeV is about $\lambda \approx 10^{-19}\text{m}$. In comparision with such high-energy particles the proton is very large, almost infinite object.

In the rest frame of detached observer the proton is contracted in longitudinal direction due to the Lorentz transformation. The Lorentz factor in this case is approximately $\gamma \sim 10\text{TeV}/1\text{GeV} = 10^4$. Therefore in the laboratory frame the moving proton looks like almost homogenous very wide ($d_p = 10^{-15}\text{m}$) and thin ($l_p = 10^{-19}\text{m}$) disk. Its classical gravitational field is negligible in its own rest frame but significant in the rest frame of the observer due to effects of TeV-gravity. Exact expression of its metric is very complicated but near the center of disk we may neglect edge effects and consider it as a rapidly moving infinite homogenous plane in 5-dimensional spacetime. Like a point in (2+1)-dimensional spacetime [9] or a cosmic string in (3+1) dimensions [2] this object leads to appearance of a conical topological defect in (4+1) dimensions [10]:

$$ds^2 = -dt^2 + dx_\perp^2 + d\rho^2 + \rho^2 d\phi^2, \tag{1}$$

$$x_\perp = (x_1, x_2),\ \rho^2 = x_3^2 + z^2, \tag{2}$$

where (x_1, x_2) - transversal coordinates on the brane, x_3 - longitudinal brane coordinate, and z is the extra dimension. The angle variates in the range:

$$0 < \phi < \alpha, \tag{3}$$

$$\alpha = 2\pi - \delta, \tag{4}$$

$$\delta = 8\pi\gamma G_5 \frac{m_p}{S_p} = \frac{32\gamma}{M_{Pl,5}^3}\frac{m_p}{d_p^2} \tag{5}$$

Here G_5 is a 5-dimensional gravitational constant, $m_p \approx 938\text{MeV}$ is the proton mass, $G_5 = 1/M_{Pl,5}^3$. It should be note separately that there is important difference between true infinite plane and the proton. For the plane we can define the angle defect both in static (δ_0) and moving (δ) cases. They are simply related: $\delta = \gamma\delta_0$. For the proton we are not able to define the static defect.

In this approximation up to corrections of the order of $\mathcal{O}(\lambda/d_p)$ the metric of two high energy colliding protons is the 5-dimensional generalization of the Gott spacetime. It is schematically shown in the Fig. 1. Gravitational field of each proton in the laboratory frame can be represented as a flat spacetime with cut off wedge. The front side of the wedge is in the future relatively the back side. The test point falling on the front side jumps to the past. So path-tracing around both wedges can return the particle to its own past if the angle defects are large enough.

Now we can estimate what energy of protons is necessary to form closed timelike curves. In the original paper by Gott following condition for moving strings is obtained:

$$\gamma > \frac{1}{\sin\delta_0/2} \tag{6}$$

For the proton we can define formally $\delta_0 = \delta/\gamma$. In TeV-gravity models $M_{Pl,5} \approx 1\text{TeV}$. So

$$\delta_0 \approx 1.4 \cdot 10^{-6} \tag{7}$$

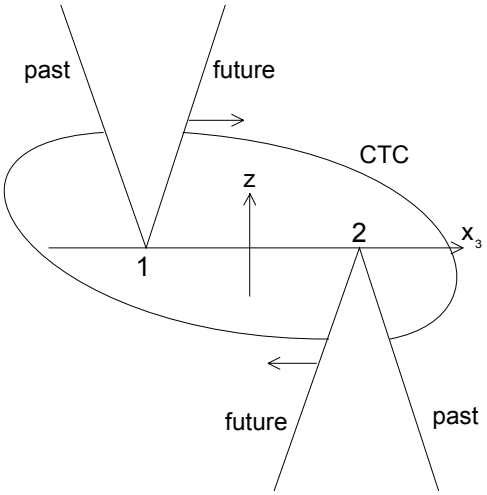

Figure 1. Each wedge represents the conical defect generated by moving proton.

The condition of time traveling is held if the Lorentz factor is

$$\gamma > 1.4 \cdot 10^6 \tag{8}$$

Unfortunately this value is much larger than one expected at the LHC. But at least it looks reasonable and we may hope to reach such energies at future colliders. Also this Lorentz factor is typical for cosmic rays.

3. POSSIBLE PHENOMENOLOGICAL SIGNATURES

We should note that CTC are localized in the bulk, and usual matter fields can not follow them. All causality violating interactions occur only via particles which may leave the brane (like a Kaluza-Klein excitations).

Path-tracing of intermediate particles leads to their multiplication and violation of energy and momentum conservation laws. Quantum conservation laws also can be violated. Therefore a lot of usually forbidden processes become possible.

But to analyze all this possibilities new approach to quantum field theory is necessary. All usual principles and paradigms is inapplicable in the case of manifolds with nontrivial topology of time.

By now we can not obtain numerical estimates on properties of these exotic processes.

REFERENCES

1. K. Godel, Rev. Mod. Phys. **21**, 447 (1949).
2. J. R. Gott, Phys. Rev. Lett. **66**, 1126 (1991).
3. M. S. Morris, K. S. Thorne and U. Yurtsever, Phys. Rev. Lett. **61**, 1446 (1988).
4. J. A. Wheeler, Phys. Rev. vol. 97, 2, 511 (1955). C. W. Misner, J. A. Wheeler, Annals of Phys., vol.2, 525 (1957)
5. S. Deser, R. Jackiw and G. 't Hooft, Phys. Rev. Lett. **68**, 267 (1992).
   S. M. Carroll, E. Farhi and A. H. Guth, arXiv:hep-th/9207037.
6. N. Arkani-Hamed, S. Dimopoulos and G. R. Dvali, Phys. Lett. B **429**, 263 (1998) [arXiv:hep-ph/9803315]. I. Antoniadis, N. Arkani-Hamed, S. Dimopoulos and G. R. Dvali, Phys. Lett. B **436**, 257 (1998) [arXiv:hep-ph/9804398].
7. L. Randall and R. Sundrum, Phys. Rev. Lett. **83**, 3370 (1999) [arXiv:hep-ph/9905221]. L. Randall and R. Sundrum, Phys. Rev. Lett. **83**, 4690 (1999) [arXiv:hep-th/9906064]. G. R. Dvali, G. Gabadadze and M. Porrati, Phys. Lett. B **485**, 208 (2000) [arXiv:hep-th/0005016].
8. I. Y. Aref'eva and I. V. Volovich, Int. J. Geom. Meth. Mod. Phys. **05**, 641 (2008) [arXiv:0710.2696 [hep-ph]].
   A. Mironov, A. Morozov and T. N. Tomaras, Facta Univ. Ser. Phys. Chem. Tech. **4**, 381 (2006) [arXiv:0710.3395 [hep-th]].
9. S. Deser, R. Jackiw and G. 't Hooft, Annals Phys. **152**, 220 (1984).
10. I. Y. Aref'eva, arXiv:1007.4777 [hep-th].

Strong coupling, discrete symmetry and flavour

James Barnard[a]

[a]Department of Mathematical Sciences, Durham University, Durham DH1 3LE, UK

Strong coupling and discrete symmetry can work together to generate the flavour structure of the Standard Model. It is proposed that the *full* UV theory has a discrete flavour symmetry, typically only associated with tribimaximal mixing in the neutrino sector. Hierarchies in the particle masses and mixing matrices emerge from multiple strongly coupled sectors that break this symmetry. This allows for a realistic flavour structure, even in models built around an underlying grand unified theory.

It is widely believed that strong coupling could explain several difficult phenomenological puzzles. Our purpose here is to revisit one of the early ideas, namely the proposal of Refs. [1–3] that strong coupling effects generate the hierarchical flavour structure observed in the quark and lepton masses and mixings. Developments since that work are encouraging a return to the subject. Firstly there is now a better understanding of the neutrino masses and mixings and a large number of well defined flavour models for the lepton sector [4]. Mostly these rely on non-abelian discrete symmetries. Strangely though, such discrete symmetries are not particularly helpful in explaining the quark sector masses and mixings. In order to accommodate the very different structures in the quark and lepton couplings, one has to have peculiar vacuum misalignments. Not only are these difficult to achieve, but also they do not sit easily with an underlying grand unified theory (GUT) structure. The second reason is that, in the interim, the AdS/CFT correspondence has given us a geometrical way to think about strong coupling. Interest in strong coupling in flavour physics has usually been drawn to models with a single confinement scale. However, the role of discrete symmetries in any of these scenarios is obscure: although it can be incorporated into the model [5,6] the underlying geometric origin is elusive.

In Ref. [7], on which these proceedings are based, our approach is governed by two principles. First we assume that strong coupling effects (for example vastly different compositeness scales) are responsible for generating hierarchies in masses and mixings. Second we believe that any discrete symmetries underlying the lepton/neutrino masses and mixings are also present in the quark sector, but are broken by the strong coupling effects. This is hard to avoid if one is interested in grand unified theories. The general picture we will explore is related to that of Ref. [3], except that instead of anarchy in the UV there is discrete symmetry. The quark sector is hierarchical because quarks are mainly composite states which feel the strong coupling whereas the leptons, especially the neutrinos, are more elementary so display a discrete symmetry.

There are various ways to think about strong coupling. In the context of $\mathcal{N} = 1$ supersymmetry Seiberg duality is a powerful tool [8]. Our initial approach in Ref. [7] is to introduce three strongly coupled SU(2) gauge groups. Each confines and produces part of a generation of Standard Model matter as bound states (in terms of the parent SU(5) theory these correspond to the **10**). The confining groups all have their own dynamics, naturally allowing an exponential hierarchy in the compositeness scales. This hierarchy appears in the superpotential when one trades bound states of the deconfined theories for properly normalised elementary fields in the dual description. Any discrete global symmetries are present in both the confined and deconfined theories, so determine the detailed structure of the coupling constants and mixing matrices. The interplay between a Z_3 permutation symmetry and an effective Z_2 symmetry (arising from the con-

finement scheme) then mimics the behaviour of the more traditional A_4 flavour symmetry. Thus tribimaximal mixing is obtained in the neutrino sector, whereas Z_3 is broken by the strong coupling in the quark sector to allow a realistic form for the quark mixing matrix.

The more geometrical way to think about strong coupling is via the AdS/CFT correspondence. One replaces each strongly coupled SU(2) gauge group with a strongly coupled CFT and consequently a slice of AdS, or warped throat. The composite quark and lepton states are localised on (or near) the infrared brane of each throat while the elementary states are localised on (or near) the ultraviolet brane. In order for there to be interactions one has to sew the three throats together at the UV end leading to a multiple throat background [9], each throat corresponding to a single generation. The Z_3 becomes a cyclical permutation symmetry of the throats. In the holographic interpretation this symmetry was spontaneously broken by the strong coupling. This can be manifest geometrically as either different bulk masses in the throats or different throat lengths [10] or both.

The picture that emerges is shown in Figure 1. It consistently represents both the field theory and the holographic approaches. An important feature is that the up quark Yukawas are composite-composite-elementary couplings, the down quark and charged leptons are composite-elementary-elementary while the neutrino couplings are elementary-elementary-elementary. This explains why the down quarks and charged leptons have similar mass hierarchies, the ups have roughly the square of the down hierarchy and the neutrinos have little or no hierarchy and large mixing. A key point elucidated by the geometric picture is what happens to the underlying GUT structure. In the traditional SU(5) theory Q, e^c, u^c sit in the antisymmetric **10** and d^c, L sit in the antifundamental $\overline{\mathbf{5}}$. The diagram clearly breaks the SU(5) structure; however it remains *approximately* intact. It is reasonable to expect such a slight splitting of wave-functions to occur since, after GUT symmetry breaking, different anomalous dimensions can arise within SU(5) multiplets.

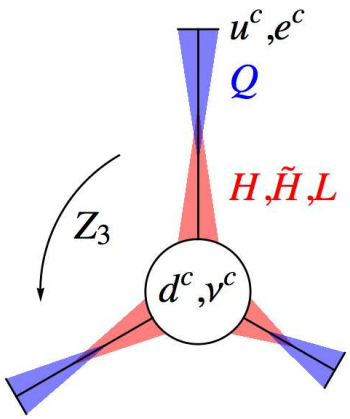

Figure 1. The triple confinement picture. Elementary states at the node feel the full discrete symmetry. Bound states are situated at the ends of "throats". The discrete symmetry is broken either by different throat lengths (shown) or by different localisations of the fields in each throat.

REFERENCES

1. R.R. Volkas and G.C. Joshi, Phys. Rept. 159 (1988) 303.
2. M.J. Strassler, Phys. Lett. B376 (1996) 119, hep-ph/9510342.
3. A.E. Nelson and M.J. Strassler, JHEP 09 (2000) 030, hep-ph/0006251.
4. G. Altarelli and F. Feruglio, (2010), 1002.0211.
5. C. Csaki et al., JHEP 10 (2008) 055, 0806.0356.
6. A. Kadosh and E. Pallante, (2010), 1004.0321.
7. S. Abel and J. Barnard, JHEP 08 (2010) 039, 1005.1668.
8. N. Seiberg, Nucl. Phys. B435 (1995) 129, hep-th/9411149.
9. G. Cacciapaglia et al., Phys. Rev. D74 (2006) 045019, hep-ph/0604218.
10. S.S.C. Law and K.L. McDonald, Phys. Rev. D82 (2010) 104032, 1008.4336.

Two-point function probes of thermalization

Alice Bernamonti[a*]

[a] Theoretische Natuurkunde, Vrije Universiteit Brussel, and International Solvay Institutes
Pleinlaan 2, B-1050 Brussels, Belgium

We present work in progress on describing the evolution towards thermality in strongly coupled gauge theories with a gravity dual. Two-point functions serve as nonlocal probes to assess thermalization.

The experimental evidence on relativistic heavy-ion collisions suggests that the products of the reaction are strongly interacting and that their near-equilibrium evolution is well described by quasi-inviscid hydrodynamics [1]. Simple strongly coupled field theories can be studied holographically through the AdS/CFT correspondence, relating gravity theories in asymptotically anti-de Sitter spacetimes (AdS) to conformal field theories (CFT) on their boundaries. A thermal field theory state is dual to a black brane in AdS, while the thermalization process is expected to correspond to black hole formation in the bulk.

Various approaches have been pursued to address holographically the thermalization dynamics at strong coupling (see for instance [2] and references therein). Here we model the equilibrating field configuration in the bulk by an infalling homogenous thin matter shell [3], and we study the onset of thermality via nonlocal probes. This contribution is based on [4] and focuses on equal-time two-point correlators of gauge invariant operators $\mathcal{O}$. We refer to [4,5] for a comprehensive analysis of different probes.

In the dual theory, two-point functions are evaluated summing over all bulk paths connecting the two endpoints. For "heavy" probes of conformal dimension $\Delta \gg 1$ in the semiclassical limit, the sum over paths can be approximated by: $\langle \mathcal{O}(\mathbf{x},t)\mathcal{O}(\mathbf{0},t)\rangle \sim \exp[-\Delta \mathcal{L}(\mathbf{x},t)]$; $\mathcal{L}(\mathbf{x},t)$ being the length of the geodesic stretching between the two boundary points [6].

Let us parametrize the $d+1$-dimensional infalling shell geometry by the Vaidya metric in Poincaré coordinates

$$ds^2 = -\left[1 - m(v) r^{-d}\right] r^2 dv^2 + 2 dv dr + r^2 d\mathbf{x}^2 \,, \quad (1)$$

where v labels ingoing null trajectories and we have set the AdS radius equal to 1. The conformal boundary of spacetime is located at $r=\infty$, where the coordinate v coincides with the asymptotic observer's time t. The mass profile of the dust shell is chosen to be

$$m(v) = (M/2)\left[1 + \tanh(v/v_0)\right] \,, \quad (2)$$

where v_0 determines the thickness of the shell falling along $v=0$. As v_0 goes to zero, the geometry outside the shell ($v>0$) is identical to that of an AdS black brane, while the metric inside the shell ($v<0$) coincides with pure AdS.

The goal is to study equal-time Wightman functions in a strongly coupled dynamical setup in the geodesic approximation. This amounts to solving for spacelike geodesics in the time-dependent geometry (1) of dimension $d=2,3,4$. The geodesic endpoints are located at $(v, r, |\mathbf{x}|) = (t_0, r_0, \pm \ell/2)$, where r_0 is a UV cut-off regularizing the infinite volume of spacetime. The geodesic equation can be solved analytically in $d=2$ in the $v_0 \to 0$ limit, and numerically otherwise.

In Fig.1 left panel (right panel) we plot the projection on the (v,r)-plane of a sample of these geodesics for fixed insertion time t_0 (spatial scale ℓ) and varying ℓ (t_0) in a 3d bulk with zero-thickness shell. For small enough ℓ or sufficiently large t_0, the geodesics extend entirely in the ther-

*Aspirant FWO; Alice.Bernamonti@vub.ac.be

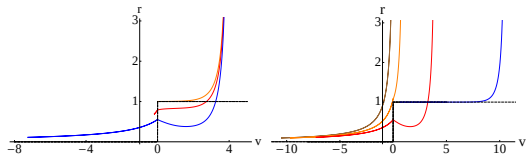

Figure 1. Geodesics in the (v, r)-plane for fixed t_0 and increasing ℓ (left panel from top to bottom), and for fixed ℓ and increasing t_0 (right panel from left to right). The apparent horizon (in black dashed) builds up to $M = 1$ at $v = 0$.

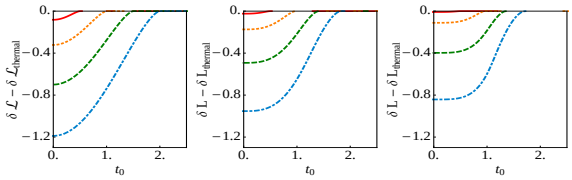

Figure 2. $\delta\mathcal{L} - \delta\mathcal{L}_{\rm thermal}$ as a function of boundary time t_0 for $d = 2$ (left), $d = 3$ (middle), and $d = 4$ (right) for a thin shell ($v_0 = 0.01$). The boundary separations are $\ell = 1, 2, 3, 4$ (from top to bottom). All quantities are in units of M.

mal black brane background. We denote the length of such geodesics $\mathcal{L}_{\rm thermal}$.

The geodesic length $\mathcal{L}$ diverges due to contributions near the boundary. Therefore, let us define a renormalized length $\delta\mathcal{L} \equiv \mathcal{L} - 2\ln(r_0/2)$ by removing the divergent part of the vacuum AdS solution. The renormalized correlator is then computed as $\langle\mathcal{O}(\mathbf{x}, t)\mathcal{O}(\mathbf{0}, t)\rangle_{ren} \sim \exp[-\Delta\delta\mathcal{L}(\mathbf{x}, t)]$. In Fig.2, we assess the approach to thermality plotting the deviation from the equilibrium result $\delta\mathcal{L} - \delta\mathcal{L}_{\rm thermal}$ as a function of t_0, for various values of ℓ. It allows to extract the time until full thermalization $\tau_{\rm th}(\ell)$ at which the curves join non-analytically the thermal ones. It turns out that in 2d $\tau_{\rm th} = \ell/2$, while it is slightly shorter than $\ell/2$ for $d = 3, 4$ field theories. In [4], it is argued that this apparent violation of causality for $d > 2$ may be related to the homogeneity of the quench. Similar results for a 2d CFT undergoing a sharp quench were also derived in [7].

As can be seen in Fig.2, complete thermalization of the correlator is first observed at short length scales. This observation is in strong contrast with the "bottom-up" scenario [8] applying to weakly coupled gauge theories. There, the gauge field thermalizes by first populating the infrared modes via gluon bremsstrahlung and then by slowly approaching the equilibrium energy distribution from the "bottom-up". From an AdS/CFT perspective, thermalization naturally proceeds "top-down" in this type of setups, with UV modes thermalizing first.

Acknowledgments: I would like to thank my collaborators: V. Balasubramanian, J. de Boer, N. Copland, B. Craps, E. Keski-Vakkuri, B. Müller, A. Schäfer, M. Shigemori, W. Staessens. This research is supported by the Belgian Federal Science Policy Office through the Interuniversity Attraction Pole IAP VI/11 and by FWO-Vlaanderen through project G011410N.

REFERENCES

1. M. Gyulassy and L. McLerran, Nucl. Phys. A **750**, 30 (2005); J. W. Harris and B. Müller, Ann. Rev. Nucl. Part. Sci. **46**, 71 (1996).
2. G. Beuf, M. P. Heller, R. A. Janik *et al.*, JHEP **0910** (2009) 043; P. M. Chesler, L. G. Yaffe, [arXiv:1011.3562 [hep-th]].
3. U. H. Danielsson, E. Keski-Vakkuri and M. Kruczenski, Nucl. Phys. B **563**, 279 (1999); S. Lin and E. Shuryak, Phys. Rev. D **78**, 125018 (2008).
4. V. Balasubramanian *et al.*, arXiv:1012.4753 [hep-th]; Same authors, in preparation.
5. V. E. Hubeny, M. Rangamani and T. Takayanagi, JHEP **0707** (2007) 062; J. Abajo-Arrastia, J. Aparicio and E. Lopez, JHEP **1011**, 149 (2010); T. Albash and C. V. Johnson, arXiv:1008.3027 [hep-th].
6. V. Balasubramanian, S. F. Ross, Phys. Rev. **D61**, 044007 (2000).
7. P. Calabrese and J. Cardy, J. Phys. A **42**, 504005 (2009).
8. R. Baier, A. H. Mueller, D. Schiff and D. T. Son, Phys. Lett. B **502**, 51 (2001).

Black Holes and Entanglement

L. Borsten[a]

[a]Theoretical Physics, Blackett Laboratory, Imperial College London
London SW7 2AZ, United Kingdom

An unexpected interplay between the seemingly disparate fields of M-theory and Quantum Information has recently come to light. We summarise these developments, culminating in a classification of 4-qubit entanglement from the physics of STU black holes. Based on work done in collaboration with D. Dahanayake, M. J. Duff, H. Ebrahim, A. Marrani and W. Rubens.

1. Introduction

The irrefutable experimental successes of quantum theory demanded a radical reappraisal of our long held notions of "physical reality". Quantum superposition reigns supreme; we reside in a fundamentally probabilistic universe. The philosophically comfortable tenets of local realism must be abandoned as phenomenologically insufficient - a direct consequence of that most quantum of phenomena, *entanglement* [1, 2]. It subsequently became apparent that, since *information* is created, stored, transformed and destroyed by physical processes, such a drastic reassessment of reality must have some profound consequences for our theories of information and computation. *Quantum Information Theory* (QIT) is the outcome [3]. It is the study of information processing systems which rely on the fundamental properties of quantum mechanics. It is anticipated that QIT may be harnessed to go beyond what is computationally achievable on any classical device. In this context entanglement is seen as a *resource* that may be created and consumed in the course of a quantum information theoretic protocol. It is essential to the emerging technologies of quantum cryptography, computation and communication. If entanglement is a resource one must address the question of its classification and quantification. It is crucial from both a technological and foundational perspective.

The other pillar of XX-century physics, Einstein's General Theory of Relativity, raises its own set of quandaries. Primarily, direct attempts at quantizing gravity using perturbative quantum field theory are plagued by uncontrollable infinities. Yet, a complete description of fundamental physics requires a consistent theory of quantum gravity. M-theory, which arose out of pioneering work on superstrings and supergravity, is a compelling framework for a unified theory of the fundamental interactions including quantum gravity. However, it is fundamentally non-perturbative and consequently remains largely mysterious, offering up only remote corners of its full structure. Just as entanglement has been central to developments in QIT, *black holes* are an important window into the non-perturbative aspects of M-theory.

For the most part these important endeavors in quantum information and gravity have led separate lives. However, this contribution centres on a curious and unexpected interplay between these seemingly disparate themes. It constitutes one corner of the *black-hole/qubit correspondence*: a relationship between the entanglement of qubits, the basic units of quantum information, and the entropy of black holes in M-theory [4].

2. Black Holes and Qubits

The entropy formula for the 8-charge (four electric plus four magnetic) STU black hole [5–7], appearing in M-theory compactified to four dimensions, is given by the 'hyperdeterminant' [8], a quantity introduced by the mathematician Cayley in 1845 [9]. Remarkably, the hyperdeterminant also shows up in the 3-tangle τ_{ABC}, which

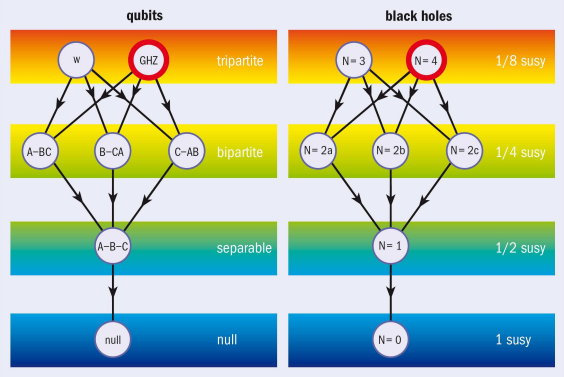

Figure 1. The classification of three qubits (left) exactly matches the classification of black holes from N wrapped branes (right). Only the GHZ state has a nonzero 3-tangle and only the N = 4 black hole has nonzero entropy.

measures the degree of tripartite entanglement shared by three qubits (Alice, Bob and Charlie) [10, 11]. A qubit is a two-state (up/down) quantum system; so three qubits can have eight different states corresponding to the eight charges of the black hole. The black hole entropy $S_{\rm BH}$ is related to the 3-tangle by [8],

$$S_{\rm BH} = \frac{\pi}{2}\sqrt{\tau_{ABC}}.$$

It was subsequently realised that there is in fact a one-to-one correspondence between the classification of 3-qubit entanglement and the classification of extremal STU black holes [4, 12]. Three qubits may be entangled in six physically distinct ways: (1) Separable A-B-C, (2a) Biseparable A-BC, (2b) Biseparable B-CA, (2c) Biseparable C-AB, (3) W and (4) GHZ (Greenberger-Horne-Zeilinger) [13, 14]. See Figure 1. Only W and GHZ have genuine three-way entanglement and only GHZ maximally violates local realism reflected in the fact that it has non-zero 3-tangle.

By embedding the STU model in type II string theory compactified on a 6-torus one obtains a microscopic interpretation of the black-hole/correspondence in terms the supersymmetric wrapping configurations of D-branes [4, 15]. Consider the type IIB theory. A subset of the black hole charges corresponds to D3-branes wrapping the internal space [16]. To relate this picture to QIT we split the 6-torus into three two 2-tori, one for each qubit. We demand that each D3-brane wraps a single circle of each 2-torus. Denoting a wrapped circle by a cross and an unwrapped circle by a nought, we identify an up (down) qubit state with xo (ox). To wrap or not to wrap; that is the qubit. Using this dictionary one finds that the supersymmetric configurations of one, two, three and four intersecting D3-branes reproduces precisely the six 3-qubit entanglement classes. See Figure 1. A fifth effective charge may be introduced while preserving supersymmetry by intersecting the fourth brane at an angle [17, 18]. This relates a well-known fact of quantum information theory, that the most general real three qubit state can be parameterized by four real numbers and an angle [19], to a well-known fact of string theory, that the most general STU black hole can be described by four D3-branes intersecting at an angle [17, 18].

Further work [4, 15, 20–30] has led to a more complete dictionary translating a variety of phenomena in one language to those in the other. It seems that we are, as yet, only glimpsing the tip of an iceberg. For example, the much more difficult problem of classifying 4-qubit entanglement has recently been addressed by invoking the black-hole/qubit correspondence [31, 32]. This is of experimental significance as 4-qubit entanglement is now achievable in the laboratory [33,34]. The stationary STU black hole solutions may be studied by performing a time-like reduction [30, 35–37]. The resulting classification of stationary black holes is related to 4-qubit entanglement via the Kostant-Sekiguchi theorem [38,39]. Our main result is that there are 31 entanglement families which reduce to nine (in agreement with [40,41]) up to permutations of the four qubits. From the black hole perspective, we find that the attractor equations, which determine the amount of supersymmetry preserved by a particular black hole solution, display a symmetry consistent with permutations of the qubits. For example, the A-GHZ state yields a set of attractor equations which are invariant under a triality corresponding to the permutation of B, C, D in the GHZ state.

I would like to thank the organisers for a wonderful school in a beautiful setting.

REFERENCES

1. Einstein, A., Podolsky, B., and Rosen, N. *Phys. Rev.* **47**(10), 777–780 (1935).
2. Bell, J. S. *Physics* **1** (1964) no. 3, 195.
3. Nielsen, M. A. and Chuang, I. L. *Quantum Computation and Quantum Information*. Cambridge University Press, New York, NY, USA, (2000).
4. Borsten, L., Dahanayake, D., Duff, M. J., Ebrahim, H., and Rubens, W. *Phys. Rep.* **471**(3–4), 113–219 (2009).
5. Duff, M. J., Liu, J. T., and Rahmfeld, J. *Nucl. Phys.* **B459**, 125–159 (1996).
6. Behrndt, K., Kallosh, R., Rahmfeld, J., Shmakova, M., and Wong, W. K. *Phys. Rev.* **D54**(10), 6293–6301 (1996).
7. Bellucci, S., Ferrara, S., Marrani, A., and Yeranyan, A. *Entropy* **10**(4), 507–555 (2008).
8. Duff, M. J. *Phys. Rev.* **D76**, 025017 (2007).
9. Cayley, A. *Camb. Math. J.* **4** (1845) 193–209.
10. Coffman, V., Kundu, J., and Wootters, W. K. *Phys. Rev.* **A61**(5), 052306 (2000).
11. Miyake, A. *Phys. Rev.* **A67**(1), 012108 (2003).
12. Kallosh, R. and Linde, A. *Phys. Rev.* **D73**(10), 104033 (2006).
13. Dür, W., Vidal, G., and Cirac, J. I. *Phys. Rev.* **A62**(6), 062314 (2000).
14. Borsten, L., Dahanayake, D., Duff, M. J., Rubens, W., and Ebrahim, H. *Phys. Rev.* **A80**, 032326 (2009).
15. Borsten, L., Dahanayake, D., Duff, M. J., Rubens, W., and Ebrahim, H. *Phys. Rev. Lett.* **100**(25), 251602 (2008).
16. Klebanov, I. R. and Tseytlin, A. A. *Nucl. Phys.* **B475**, 179–192 (1996).
17. Balasubramanian, V. In *Cargese 1997, Strings, branes and dualities*, 399–410, (1997). Published in the proceedings of NATO Advanced Study Institute on Strings, Branes and Dualities, Cargese, France, 26 May - 14 Jun 1997.
18. Bertolini, M. and Trigiante, M. *Nucl. Phys.* **B582**, 393–406 (2000).
19. Acin, A., Andrianov, A., Jane, E., and Tarrach, R. *J. Phys.* **A34**(35), 6725–6739 (2001).
20. Lévay, P. *Phys. Rev.* **D74**(2), 024030 (2006).
21. Duff, M. J. and Ferrara, S. *Phys. Rev.* **D76**(2), 025018 (2007).
22. Lévay, P. *Phys. Rev.* **D75**(2), 024024 (2007).
23. Duff, M. J. and Ferrara, S. *Phys. Rev.* **D76**(12), 124023 (2007).
24. Lévay, P. *Phys. Rev.* **D76**(10), 106011 (2007).
25. Borsten, L. *Fortschr. Phys.* **56**(7–9), 842–848 (2008).
26. Lévay, P., Saniga, M., and Vrana, P. *Phys. Rev.* **D78**(12), 124022 (2008).
27. Levay, P., Saniga, M., Vrana, P., and Pracna, P. *Phys. Rev.* **D79**, 084036 (2009).
28. Borsten, L., Dahanayake, D., Duff, M. J., and Rubens, W. *Phys. Rev.* **D81**, 105023 (2010).
29. Levay, P. and Szalay, S. (2010).
30. Levay, P. (2010).
31. Borsten, L., Dahanayake, D., Duff, M. J., Marrani, A., and Rubens, W. *Phys. Rev. Lett.* **105**, 100507 (2010).
32. Borsten, L., Duff, M., Marrani, A., and Rubens, W. (2011). * Temporary entry *.
33. Amselem, E. and Bourennane, M. *Nat. Phys.* **5**, 748–752 (2009).
34. Lavoie, J., Kaltenbaek, R., Piani, M., and Resch, K. J. *Phys. Rev. Lett.* **105**(13), 130501 Sep (2010).
35. Breitenlohner, P., Maison, D., and Gibbons, G. W. *Commun. Math. Phys.* **120**, 295 (1988).
36. Bergshoeff, E., Chemissany, W., Ploegh, A., Trigiante, M., and Van Riet, T. *Nucl. Phys.* **B812**, 343–401 (2009).
37. Bossard, G., Michel, Y., and Pioline, B. *JHEP* **01**, 038 (2010).
38. Sekiguchi, J. *J. Math. Soc. Japan* **39**(1), 127–138 (1987).
39. Collingwood, D. H. and McGovern, W. M. *Nilpotent orbits in semisimple Lie algebras*. Van Nostrand Reinhold mathematics series. CRC Press, (1993).
40. Verstraete, F., Dehaene, J., De Moor, B., and Verschelde, H. *Phys. Rev.* **A65**(5), 052112 (2002).
41. Chterental, O. and Djoković, D. Ž. In *Linear Algebra Research Advances,* Ling, G. D., editor, chapter 4, 133–167. Nova Science Publishers Inc (2007).

Reduction of type IIB on squashed Sasaki-Einstein manifolds

D. Cassani

Dipartimento di Fisica "Galileo Galilei", Università di Padova, Via Marzolo 8, 35131 Padova, Italy

We present a consistent truncation of type IIB supergravity on squashed Sasaki–Einstein manifolds, leading to half-maximal gauged supergravity in five dimensions. We comment on the holographic picture of consistency.

1. INTRODUCTION

In the context of the gauge/gravity duality, consistent truncations of 10- and 11-dimensional supergravity have proved to be powerful solution-generating tools. Since they yield a lower-dimensional model with a restricted number of degrees of freedom, consistent truncations allow to tackle several problems in a setup which is much simpler than the original theory, guaranteeing at the same time the lifting of the solutions.

Recently, there has been a revival of interest in consistent truncations, mainly motivated by the need to embed into string theory a series of lower-dimensional models providing a holographic description of certain condensed matter phenomena, such as superconductivity and quantum critical points exhibiting non-relativistic scale invariance. A crucial, non-trivial feature required by these applications is that the truncation preserve massive and/or charged Kaluza–Klein modes [1]. This can be achieved e.g. via a consistent truncation of type IIB supergravity on arbitrary squashed Sasaki–Einstein (SE) manifolds, which leads to gauged $\mathcal{N} = 4$ supergravity in five dimensions [2] (see also [3]).

2. THE REDUCTION

Locally, an SE manifold Y can be seen as a U(1) fibration over a Kähler–Einstein base $B_{\rm KE}$:

$$ds^2(Y) \,=\, ds^2(B_{\rm KE}) + \eta\otimes\eta\,, \qquad (1)$$

where η is the globally defined 1-form specifying the fibration. All 5-dimensional SE manifolds are also endowed with a real 2-form J and a complex 2-form Ω, both globally defined. These satisfy the algebraic constraints

$$\eta \lrcorner J = \eta \lrcorner \Omega = 0\,, \qquad \Omega\wedge J \,=\, \Omega\wedge\Omega \,=\, 0\,,$$
$$\Omega\wedge\overline{\Omega} \,=\, 2\,J\wedge J \,=\, 4\,\mathrm{vol}(B_{\rm KE})\,, \qquad (2)$$

as well as the differential conditions

$$d\eta \,=\, 2J\,, \qquad d\Omega = 3i\,\eta\wedge\Omega\,. \qquad (3)$$

Our ansatz for the dimensional reduction is defined by writing a general expression for the various tensor fields of type IIB supergravity in terms of these forms. In doing this, we actually consider a class of internal metrics which is more general than (1): we allow for an overall volume parameter (the "breathing mode"), as well as for a parameter modifying the relative size of the U(1) fibre with respect to the size of the Kähler–Einstein base (the "squashing mode"). Hence we are reducing on *squashed* SE manifolds.

The fact that the system of differential forms $\{\eta,\, J,\, \Omega\}$ is closed under the various operations appearing in the higher-dimensional equations of motion (exterior derivative, wedge product, Hodge star) ensures the consistency of the truncation, as it can be verified by reducing both the type IIB action and equations of motion.

An interesting extension of the universal consistent truncation outlined above can be defined for the specific SE manifold given by the $T^{1,1} = (SU(2)\times SU(2))/U(1)$ coset space [4] (see also [5]). This enhanced truncation provides the supersymmetric completion of a more limited non-supersymmetric truncation on $T^{1,1}$ [6], containing several physically relevant conifold solutions.

3. GAUGED $\mathcal{N} = 4$ SUPERGRAVITY

The 5-dimensional model stemming from the procedure described above can be understood in the framework of gauged $\mathcal{N} = 4$ supergravity [7]. In order to completely fix it, one needs to specify just a few data, namely the number of vector multiplets and the embedding tensor determining the gauging.

We find that the scalar σ-model manifold is

$$\mathcal{M}_{\rm scal} = {\rm SO}(1,1) \times \frac{{\rm SO}(5,2)}{{\rm SO}(5) \times {\rm SO}(2)}\,, \qquad (4)$$

which is consistent with an $\mathcal{N} = 4$ model with two vector multiplets. The counting and the couplings of the vector fields agree with this, though one has to take into account some complications due to the gauging. Indeed, while ungauged $\mathcal{N} = 4$ supergravity in 5 dimensions contains eight vector fields, in our model we find four vectors and four 2-forms. The latter are seen as the duals of the missing four vectors, the dualization being required by the gauging at hand.

In order to fully specify the gauging, one computes the embedding tensor mapping the gauge group generators into the generators of the global symmetry group, which in the present case is SO(1,1) × SO(5,2). This determines the various additional couplings in the lagrangian with respect to the ungauged case, including the scalar potential. The embedding tensor has components $f_{MNP} = f_{[MNP]}$ and $\xi_{MN} = \xi_{[MN]}$, where the indices $M, N, P = 1, \ldots 7$ run in the fundamental of SO(5, 2), and we find

$$\begin{aligned} &f_{125} = f_{256} = f_{567} = -f_{157} = -2, \\ &\xi_{34} = -3\sqrt{2}, \;\; \xi_{12} = \xi_{17} = -\xi_{26} = \xi_{67} = -\sqrt{2}k. \end{aligned} \qquad (5)$$

The higher-dimensional origin of the f-components is the geometric flux associated with the non-closure of the form η, while ξ_{34} can be traced back to the non-closure of Ω. The remaining non-zero ξ-components are proportional to the constant k parameterizing the internal Ramond-Ramond 5-form flux, $F_5^{\rm flux} = k\, J\wedge J\wedge\eta\,$.

By studying the commutation relations of the generators identified by the embedding tensor, one infers that the gauge group is the product of U(1) with the 3-dimensional Heisenberg group.

4. THE HOLOGRAPHIC PICTURE

The 5-dimensional scalar potential has two extrema, corresponding to AdS vacua. The first has $\mathcal{N} = 2$ susy, and lifts to the standard $\mathrm{AdS}_5 \times \mathrm{SE}_5$ solution of type IIB supergravity. The second is $\mathcal{N} = 0$, and lifts to a IIB solution with squashed internal metric, originally found by Romans.

By studying the spectrum about the susy background, we deduce that in the dual $\mathcal{N} = 1$ super Yang-Mills theory we are keeping just flavor singlets, built in terms of the gauge superfield. Since this is fermionic, we can construct just a finite number of non-vanishing combinations; these precisely match the degrees of freedom in the gravity model. We conclude that our truncation describes the large N limit of the universal gauge sector of $\mathcal{N} = 1$ super Yang–Mills theories in 4d. In the field theory, the consistency of the truncation translates into closure of the set of preserved operators under the operator product expansion.

REFERENCES

1. J. Maldacena, D. Martelli and Y. Tachikawa, JHEP **0810** (2008) 072 [arXiv:0807.1100 [hep-th]]; J. P. Gauntlett, S. Kim, O. Varela and D. Waldram, JHEP **0904** (2009) 102 [arXiv:0901.0676 [hep-th]].
2. D. Cassani, G. Dall'Agata and A. F. Faedo, JHEP **1005** (2010) 094 [arXiv:1003.4283 [hep-th]].
3. J. T. Liu, P. Szepietowski and Z. Zhao, Phys. Rev. D **81**, 124028 (2010) [arXiv:1003.5374 [hep-th]]; J. P. Gauntlett and O. Varela, JHEP **1006**, 081 (2010) [arXiv:1003.5642 [hep-th]]; K. Skenderis, M. Taylor and D. Tsimpis, JHEP **1006** (2010) 025 [arXiv:1003.5657 [hep-th]].
4. D. Cassani and A. F. Faedo, Nucl. Phys. B **843** (2011) 455 [arXiv:1008.0883 [hep-th]].
5. I. Bena, G. Giecold, M. Grana, N. Halmagyi and F. Orsi, arXiv:1008.0983 [hep-th].
6. G. Papadopoulos, A. A. Tseytlin, Class. Quant. Grav. **18** (2001) 1333-1354. [hep-th/0012034];
7. J. Schön and M. Weidner, JHEP **0605** (2006) 034 [arXiv:hep-th/0602024].

Gravitational duality in General Relativity and Supergravity theories.

F. Dehouck [a]

[a]Service de physique mathématique et interactions fondamentales.
Université Libre de Bruxelles, Campus Plaine CP-231, 1050 Bruxelles, Belgium

We quickly review the current status of gravitational duality in General Relativity. We summarize and comment some recent work on constructing dual (topological) charges and understanding how this duality acts in supergravity theories.

1. Introduction

It is a well known fact that General Relativity's equations, when reduced to three dimensions, possess an hidden $SL(2,R)$ symmetry known as Ehler's symmetry. Gravitational duality refers to an $SO(2)$ subgroup of it. In this sense, it was first understood as a symmetry of the space of solutions with a Killing vector. The famous example is the Schwarzschild solution, with mass M, that is mapped under duality to the Taub-NUT solution, with NUT charge N. Surprisingly, the story is not over as it was recently shown in [1] that the Pauli-Fierz Hamiltonian, describing the four-dimensional linearized theory, also possesses this symmetry, without any reference to the presence of Killing vectors. However, the duality is still very hypothetical at the non-linear level in the absence of Killing vectors (See also [2]).

2. Gravitational duality for linearized general relativity

In the linearized theory, gravitational duality interchanges the equation of motion with the cyclic identity. The Bianchi identity stays invariant. This is obvious when the equations are written as (see for example [3] and references therein):

$$G^{(a)}_{\mu\nu} = T^{(a)}_{\mu\nu}, \tag{1}$$

where $a = 1, 2$ describes the electric or magnetic linearized Einstein tensor and we introduced a magnetic stress-energy tensor in the cyclic identity. The Riemann tensors are related by:

$$R^{(2)}_{\mu\nu\rho\sigma} = \frac{1}{2}\epsilon_{\mu\nu\alpha\beta}R^{(1)\,\alpha\beta}{}_{\rho\sigma}, \tag{2}$$

and generic $SO(2)$ transformations of those tensors, together with rotations of the stress-energy tensors, keep the equations of motion invariant. This symmetry was made manifest at the level of the action in [1] where the existence of a generator of duality and its associated conserved Noether charge was unveiled.

This work was generalized in the presence of a cosmological constant in [4]. In this case, the duality relates the on-shell electric and magnetic parts of the Weyl tensor. One recovers the results of the asymptotically flat case in the limit $\Lambda \to 0$.

3. Existence of dual charges

As magnetic charges are by definition topological, one can not proceed through the Noether procedure to define them. In [3], we defined ten additionnal dual charges. These were postulated in analogy with the analysis of electromagnetic duality. Dual momenta were recovered by a Witten-Nester construction in [5] [1]. The twenty charges are ($8\pi G = 1$):

$$\begin{aligned} P_\mu &= \int G^{(1)}_{0\mu} d^3x^\mu, \;\; L_{\mu\nu} = 2\int G^{(1)}_{0[\mu}x_{\nu]}d^3x^\mu, \\ K_\mu &= \int G^{(2)}_{0\mu} d^3x^\mu, \;\; \tilde{L}_{\mu\nu} = 2\int G^{(2)}_{0[\mu}x_{\nu]}d^3x^\mu \end{aligned} \tag{3}$$

and we also found a way to express them as surface integrals. Looking at the Kerr-NUT solution,

[1]See also [6] and [7]

we find $P_0 = M, K_0 = N, L_{xy} = Ma, \tilde{L}_{xy} = Na$ when appropriate delta singularities are taken into account. It is clear, however, that a proper treatment of the Lorentz charges in GR should include information about non-linearities. In the common approach, usual (electric) Poincaré charges are recovered by setting the magnetic part of the Weyl tensor to zero. Allowing it to be non-zero permits to define the dual momenta at first order. However, it is not clear how relaxing this still makes sense at non-linear order. We hope to report on this in the near future [10].

In the AdS linearized case, the NUT charge can be computed using the Cotton tensor [11].

4. Supergravity

In pure $\mathcal{N} = 2$ supergravity, the charged Taub-NUT solution has a BPS bound $M^2 + N^2 = Q^2 + H^2$. This solution is supersymmetric as we computed in [5] the globally well-defined Killing spinor [2]:

$$\epsilon = \frac{1}{2}\sqrt{\frac{r-M}{R}}e^{\frac{\beta}{2}\gamma_5}\left[e^{\alpha_m\gamma_5} + ie^{-\alpha_q\gamma_5}\gamma_0\right]\epsilon_0(\theta,\phi) \quad (4)$$

where $\beta = \arctan(N/r)$, $\alpha_m = \arctan(N/M)$, $\alpha_q = \arctan(H/Q)$, $R^2 = r^2 + N^2$ and $\epsilon_0(\theta,\phi)$ are the flat space Killing spinors.

To recover the BPS bound from the supersymmetry algebra, we need to allow for K_μ. Our guess consists in complexifying it by considering the complexified Witten-Nester form. We obtain:

$$\{Q, Q^*\} = \gamma^\mu C P_\mu + \gamma_5\gamma^\mu C K_\mu - i(Q + \gamma_5 H)C \quad (5)$$

where we introduced a new supercharge Q^*. Actually, we were only able to make sense of this superalgebra when $P_\mu = \lambda K_\mu$ and in this case the new supercharge is related to the usual one by a factor γ_5, which is how the fermionic supercharge transforms when bosonic supercharges on the rhs rotate under gravitational duality. In this case, one can re-express this algebra in the usual hermitian way:

$$\{Q, Q\} = \gamma^\mu C P'_\mu - i(Q' + \gamma_5 H')C \quad (6)$$

[2] This is equivalent to the expressions given in [5] although written in a much more compact form.

This analysis shows that supersymmetry seems to be preserved under duality.

In [8], we also studied this phenomena in $\mathcal{N} = 1$ supergravity where shock pp-waves are half-BPS solutions. Under gravitational duality, pp-waves whose metrics are characterized by the knowledge of an harmonic function F are sent to supersymmetric (dual) pp-waves characterized by the conjugate harmonic function of F. The dual of the Aichelburg-Sexl pp-wave was denoted the NUT-wave.

For the gauged $\mathcal{N} = 2$ supergravity with $\Lambda < 0$, supersymmetry of the Plebanski-Demianski solution was studied in [9]. Supersymmetric solutions with NUT charge were also considered. Although electromagnetic duality is broken and also apparently the gravitational duality, the BPS bound is invariant under a mixed $U(1)$ symmetry (see also [11]).

REFERENCES

1. M. Henneaux and C. Teitelboim, Phys. Rev. D **71** (2005) 024018 [arXiv:gr-qc/0408101].
2. S. Deser and D. Seminara, Phys. Rev. D **71** (2005) 081502 [arXiv:hep-th/0503030].
3. R. Argurio and F. Dehouck, Phys. Rev. D **81**, 064010 (2010) [arXiv:0909.0542 [hep-th]].
4. B. Julia, J. Levie and S. Ray, JHEP **0511** (2005) 025 [arXiv:hep-th/0507262].
5. R. Argurio, F. Dehouck and L. Houart, Phys. Rev. D **79**, 125001 (2009) [arXiv:0810.4999 [hep-th]].
6. G. Barnich and C. Troessaert, JHEP **0901**, 030 (2009) [arXiv:0812.0552 [hep-th]].
7. G. Bossard, H. Nicolai and K. S. Stelle, Gen. Rel. Grav. **41** (2009) 1367 [arXiv:0809.5218 [hep-th]].
8. R. Argurio, F. Dehouck and L. Houart, JHEP **0901** (2009) 045 [arXiv:0811.0538 [hep-th]].
9. N. Alonso-Alberca, P. Meessen and T. Ortin, Class. Quant. Grav. **17** (2000) 2783 [arXiv:hep-th/0003071].
10. C. Compère, F. Dehouck, A. Virmani, Work in progress
11. F. Dehouck, Work in progress

Kutasov-like duality from gauge/gravity correspondence

Jérôme Gaillard[a*],

[a]Department of Physics, Swansea University, Swansea, SA2 8PP, United Kingdom

and

Departamento de Física de Partículas
Universidade de Santiago de Compostela, E-15782, Santiago de Compostela, Spain

We present a way of implementing a Kutasov-like duality in the context of gauge/gravity correspondence. It is achieved using D5-branes wrapping hyperbolic two-cycles of genus $g > 1$.

1. Introduction

The gauge/gravity correspondence [1] relates gauge theories in their large 't Hooft coupling regime and supergravity theories. Thanks to it, one can hope to get further understanding of a gauge theory by constructing and studying its string theory dual. Here the aim is to find the gravity dual of a theory exhibiting Kutasov duality [2–4]. This duality relates two four-dimensional gauge theories with $\mathcal{N} = 1$ supersymmetry: one has gauge group $SU(N_c)$, N_f fundamental chiral multiplets and one adjoint chiral superfield X with superpotential

$$W(X) = \mathrm{Tr} \sum_{l=1}^{k} g_l X^{l+1} \tag{1}$$

where k is an integer; the other theory has gauge group $SU(kN_f - N_c)$, N_f chiral superfields in the fundamental representation, N_f^2 mesons, and one adjoint chiral superfield Y. The superpotential for Y and the construction of the mesons of the second theory are related to the details of the first one. This duality has also been extended to cases with several adjoint chiral superfields [5]. In the following, we present a supergravity construction exhibiting some of the features of Kutasov duality, and we are in particular able to identify the integer k with some geometric properties of our space.

2. The supergravity construction

Field theories exhibiting Kutasov duality are $\mathcal{N} = 1$ four-dimensional gauge theories. For that reason, we consider solutions of type IIB supergravity of the form $\mathbb{R}^{1,3} \times_w X_6$ where X_6 is a six-dimensional manifold with an $SU(3)$-structure and $\times_w$ indicates a warped product. In addition, those theories have fundamental matter. Inspired by the CNP solution [6], we construct our background by wrapping D5-branes on two-cycles [7]. However, differently from CNP, we also want adjoint matter. This has been shown to come, in the gauge/gravity context, from branes wrapping Riemann surfaces of higher genus [8]. Those Riemann surfaces can be obtained by quotienting hyperbolic spaces. Our ansatz for X_6 will then be adapted from the conifold ansatz of CNP by replacing the spheres with hyperbolic spaces. We will take $X_6 \approx \mathbb{R} \times_w \mathbb{H}_2 \times_w \widetilde{SL_2}$ where there is a fibration between $\mathbb{H}_2$ and $\widetilde{SL_2}$. $\widetilde{SL_2}$ is a squashed version of the universal cover of $SL_2(\mathbb{R})$ and can be built as an $\mathbb{S}^1$ fibre bundle over $\mathbb{H}_2$. It can be parametrised by a set of three left-invariant one-forms ω_i satisfying the following relations:

$$\mathrm{d}\omega_i = -(-1)^{\delta_{i3}} \epsilon_{ijk}\, \omega_j \wedge \omega_k \tag{2}$$

*I would like to thank Eduardo Conde and Carlos Núñez for comments on the manuscript. This work was supported in part by MICINN and FEDER under grant FPA2008-01838, by the Span- ish Consolider-Ingenio 2010 Programme CPAN (CSD2007-00042) and by Xunta de Galicia (Conselleria de Educacion grant INCITE09 206 121 PR).

which differ from the ones for $\mathbb{S}^3$ by one change of sign. The metric for $\widetilde{SL_2}$ is then

$$\mathrm{d}s^2 = (\omega_1)^2 + (\omega_2)^2 + (\omega_3)^2 \tag{3}$$

3. Brane setup

In order for our construction to be dual to a theory of the type that exhibits Kutasov duality, we need two different sets of D5-branes. The first set of N_c branes will be responsible for the gauge group of the field theory. They will wrap a two-dimensional compact cycle of genus $g > 1$ to also create $g-1$ massless adjoint fermions necessary for Kutasov duality. This particular cycle will come from a combination of the two $\mathbb{H}_2$ spaces of our internal manifold (one of them being inside $\widetilde{SL_2}$), in a similar way as in [9]. That requires that one performs the same quotient on both $\mathbb{H}_2$'s.

The second set of N_f branes is wrapping a non-compact two-cycle inside the internal manifold, and it is responsible for the fundamental matter in the field theory. Since one needs to go beyond the probe approximation (which corresponds to having $N_f \ll N_c$) to study Kutasov duality, it is technically easier to smear those branes in order to be able to calculate their backreaction [10].

4. Kutasov duality on the gravity side

Doing a supersymmetry analysis on our system, we find that the BPS equations (which imply the equations of motion) are symmetric under the following change:

$$N_c \to \frac{8\mathrm{Vol}(\widetilde{SL_2})}{\mathrm{Vol}(\mathbb{H}_2)^2} N_f - N_c\,, \quad N_f \to N_f \tag{4}$$

That is exactly what one gets in Kutasov duality, calling $k = \frac{8\mathrm{Vol}(\widetilde{SL_2})}{\mathrm{Vol}(\mathbb{H}_2)^2}$. If we look at how we perform the quotients of the hyperbolic spaces, we can rewrite k as

$$k = \frac{q}{g-1} \tag{5}$$

where g is the genus of the Riemann surface and q is a rational number that depends on the details of the quotient. Note that for well-chosen quotients, k can be made integer so as to match Kutasov theories. The way in which the superpotential for the adjoint fields appears in this construction is not clearly understood. It might be in relation with the winding of the N_c colour branes around the hyperbolic two-cycles. But a deeper understanding remains to be found.

5. Conclusion

In this short note, we presented a string theory construction that is dual to a four-dimensional $\mathcal{N} = 1$ gauge theory exhibiting a Kutasov-like duality. Some features of Kutasov theories are very well captured by our solutions, such as the duality in terms of the rank of the gauge group and the number of fundamental quarks (more details in [7]). However, other points still remain to be clarified, especially the generation of the superpotential for the adjoint fields.

REFERENCES

1. J. M. Maldacena, Adv. Theor. Math. Phys. **2** (1998) 231-252. [hep-th/9711200].
2. D. Kutasov, Phys. Lett. **B351** (1995) 230-234. [hep-th/9503086].
3. D. Kutasov, A. Schwimmer, Phys. Lett. **B354** (1995) 315-321. [hep-th/9505004].
4. D. Kutasov, A. Schwimmer, N. Seiberg, Nucl. Phys. **B459** (1996) 455-496. [hep-th/9510222].
5. S. Abel, J. Barnard, JHEP **0905** (2009) 080. [arXiv:0903.1313 [hep-th]].
6. R. Casero, C. Nunez and A. Paredes, Phys. Rev. D **73**, 086005 (2006) [arXiv:hep-th/0602027].
7. E. Conde, J. Gaillard, [arXiv:1011.1451 [hep-th]].
8. J. M. Maldacena and C. Nunez, Int. J. Mod. Phys. A **16**, 822 (2001) [arXiv:hep-th/0007018].
9. M. Bertolini and P. Merlatti, Phys. Lett. B **556** (2003) 80 [arXiv:hep-th/0211142].
10. C. Nunez, A. Paredes, A. V. Ramallo, Adv. High Energy Phys. **2010** (2010) 196714. [arXiv:1002.1088 [hep-th]].

String Solutions in Sasaki-Einstein Manifolds and their marginally deformed versions

Dimitrios Giataganas[a*]

[a]National Institute for Theoretical Physics, School of Physics and Centre for Theoretical Physics, University of the Witwatersrand, Wits, 2050, South Africa

We review some recent results on string solutions in the Sasaki-Einstein manifolds and their marginally β-deformed versions. We discuss both BPS and non-BPS string solutions, some of their properties and their energy-spin relations.

1. Introduction

Lately, the quiver gauge theories have attracted increasing attention. They are $\mathcal{N} = 1$ superconformal field theories and can be obtained by placing the D3-branes at a Calabi-Yau singularity. Their gravity duals are type IIB backgrounds with the form $AdS \times Y^{p,q}$[1,2]. This duality is an interesting example of a reduced supersymmetry gauge/gravity conjecture. Aiming to understand better this toric correspondence, we study a class of string solutions in the gravity dual background which correspond to particular operators in the field theory.

The analytical study of string solutions in the (marginally deformed) Sasaki-Einstein gauge/gravity dualities is a relatively complex problem, due to the complicated background metric and the Sasaki-Einstein constraints that the solutions should satisfy. However, when looking at the BPS strings it is possible to study them by using only the toric data of the background and not the exact form of the metric. Even in the β-deformed Sasaki-Einstein backgrounds the most of the properties of the BPS quantities can be obtained in this way. Hence, it is expected to find some unique properties for these solutions in the whole class of manifolds. For the non-BPS string solutions one needs to take in account the whole metric information, and the properties of the solutions depend stronger on the particular Sasaki-Einstein manifold.

It should be noted that the marginally deformed theory we mention here, has still $\mathcal{N} = 1$ supersymmetry since the TsT deformation to the original background is done in a way that the holomorphic $(3, 0)$ form Ω which specifies the Calabi-Yau structure (together with the Kähler form) remains invariant.

In the following, we briefly review some recent analytical results for the BPS and non-BPS string solutions in these backgrounds, mainly obtained in [4–6].

2. BPS string solutions

In the undeformed background, the BPS string solutions and the relevant analysis can be found in [3]. These point-like strings move along the R-charge direction and it can be shown that they are the only BPS solutions, as expected, when imposing the Sasaki-Einstein constraints [4].

In the β-deformed background the BPS string solutions were analyzed in [6]. These are point-like strings that are localized in the space directions of AdS with global time $t = \kappa\tau$, and move in the internal manifold with the coordinates describing the motion being functions of τ. The constant κ is analogous to the energy of the string which is equal to the conformal dimension Δ of the dual operator. We can express the energy in a positive definite way in terms of the conjugate momenta and the R-charge and minimize

*The research of the author is supported by a Claude Leon postdoctoral fellowship.

it appropriately, where by taking into account the Sasaki-Einstein constraints that the solutions should satisfy, it turns out that the BPS point-like strings move in the deformed Sasaki-Einstein submanifolds where the two $U(1)$ circles shrink to zero size. In the corresponding $\mathbb{T}^3$ fibration description, the strings live on the edges of the polyhedron, where the $\mathbb{T}^3$ fibration degenerates to $\mathbb{T}^1$. It should also be mentioned that the Sasaki-Einstein constraints introduce a lower bound on the deformation parameter γ, in order for these solutions to exist. Hence, in the undeformed theory these solutions do not appear as physical since they do not satisfy these constraints.

3. Non-BPS string solutions

A wide class of non-BPS string solutions is analyzed in [4–6] where the string is localized in space directions of AdS and have time dependence similar to the point-like strings mentioned above. In the Sasaki-Einstein manifold the string is allowed to spin and extend along the three $U(1)$ directions with linear dependence on the world-sheet parameters σ and τ, and being localized appropriately in the other two directions. This allows important simplification in the equations of motion and the Virasoro constraints and makes the system in most of the cases analytically solvable.

In the undeformed background we do not find any strong specific pattern that the energy-spin relations of these string solutions follow for different ansatze. Their energy depends always on the parameter $a(p,q)$ which characterizes the manifolds, hence it depends on the particular manifold. Moreover, since the range of this parameter is constrained by the Sasaki-Einstein constraints, some of the string solutions are not valid for the whole class of $Y^{p,q}$ manifolds. Another interesting property we find for some solutions, is that when the maximum allowed value of $a(p,q)$ corresponds to the string approaching the poles of the squashed sphere in $Y^{p,q}$, their energy at this limit approaches the BPS one. Thus certain non-BPS string solutions in the whole class of Sasaki-Einstein manifolds, can become BPS in particular manifolds. This also means that by getting close to this limit by choosing specific $Y^{p,q}$ manifold, these solutions become near-BPS which are very interesting. In the field theory the corresponding operators should behave in a similar way.

By examining similar string motion in the marginally deformed $AdS \times \tilde{Y}^{p,q}$, we find that their energy-spin relation depends additionally on the deformation parameter γ of the background. It is interesting to remark here that there exist solutions where the parameter γ is bounded from below. For values of γ smaller than this lower bound, these solutions continue to exist but become complex and not physical. Hence in the deformed background there exist certain non-BPS string solutions that they do not exist in the original theory. Moreover, in some cases the string equations of motion impose an $a(p,q)$ dependence on γ, but this happens only for this particular string motion, and this constraint would be relaxed if we allow the string to extend or spin in a non-$U(1)$ direction.

It is worthy to mention that although more complicated, it is possible to find solutions of simple string configurations in the (un)deformed backgrounds where the string is additionally extended along a non-$U(1)$ direction [5].

The methodology used to find the BPS and non-BPS string solutions discussed in this note, could be extended to other similar backgrounds, where we expect that similar to the main results presented here will be obtained. For example, a short discussion on the solutions of cohomogeneity two manifolds $L^{p,q,r}$ is included in [4].

REFERENCES

1. J. P. Gauntlett, D. Martelli, J. Sparks and D. Waldram, Class. Quant. Grav. **21** (2004) 4335 [arXiv:hep-th/0402153].
2. J. P. Gauntlett, D. Martelli, J. Sparks *et al.*, Adv. Theor. Math. Phys. **8** (2004) 711-734. [hep-th/0403002].
3. S. Benvenuti and M. Kruczenski, JHEP **0610** (2006) 051 [arXiv:hep-th/0505046].
4. D. Giataganas, JHEP **0910** (2009) 087. [arXiv:0904.3125 [hep-th]].
5. D. Giataganas, JHEP **1006** (2010) 016. [arXiv:0912.3624 [hep-th]].
6. D. Giataganas, [arXiv:1010.1502 [hep-th]].

Post-ISCO Ringdown Amplitudes in Extreme Mass Ratio Inspiral

Shahar Hadar
Racah Institute of Physics, Hebrew University, Jerusalem 91904, Israel

We study the late time gravitational wave emission from an extreme mass ratio inspiralling binary system. The plunge trajectory from the innermost stable circular orbit (ISCO) is special (somewhat independent of initial conditions). We write an expression for its solution in closed-form and for the emitted waveform. In particular we extract an expression for the associated black-hole ringdown amplitudes.

This letter is based on the paper [1] and mainly states the results obtained there.

The evolution of an extreme mass ratio (EMR) Inspiral is customarily divided into two stages: an *adiabatic inspiral* where the system moves on quasi-bound orbits and slowly loses energy to gravitational waves, and a *plunge* phase where the system is set on a course of collision even when the self-force is neglected. In this limit the plunge phase simplifies to consist of geodesic motion of the projectile till it reaches the horizon of the larger BH. The ISCO is the border between the two stages, after which the compact object freely falls into the horizon, followed by merger and ringdown (through quasi-normal modes (QNM's)) into a new stationary state.

We consider the plunge trajectory that starts at the innermost stable circular orbit (ISCO) at $r_{\rm ISCO} = 3r_s$ (we use the standard Boyer-Lindquist coordinates), where r_s is the Schwarzschild radius of the large BH. This trajectory is special since the eccentricity of an orbit is known to decrease during the Keplerian regime $r >> r_s$ of the inspiral [2], thus being a "Keplerian attractor" and hence only weakly dependent on initial conditions. In the case that the inspiral has been going on for enough time for the eccentricity to be essentially radiated away by the time ISCO is reached, then the plunge trajectory will indeed start from roughly ISCO. It can be shown that this result is true, for the mass ratios we are interested in, even outside of the Keplerian regime ([3]).

First we solved *analytically* for the plunge trajectory, namely the trajectory with energy and angular momentum identical to the ISCO values

$$\begin{aligned} \tilde{E} &= \tilde{E}_{\rm ISCO} \equiv \frac{2\sqrt{2}}{3} \\ \tilde{L} &= \tilde{L}_{\rm ISCO} \equiv \sqrt{3}\, r_s \ , \end{aligned} \tag{1}$$

where $\tilde{E}_{\rm ISCO}$, $\tilde{L}_{\rm ISCO}$ are the particle's energy per unit mass and angular momentum per unit mass at ISCO. The expression for $r = r(\phi)$ is known to be especially simple and we also obtained a closed form expression for the time dependence. This is possible due to the special form of the radial effective potential in this marginally stable orbit. For example, we obtained the explicit $t-r$ dependence

$$\begin{aligned} t_p(r)/r_s &= \frac{2\, r \left(1 - \frac{12 r_s}{r}\right)}{r_s \sqrt{\chi}} + 2 \tanh^{-1}\left(\sqrt{\chi}\right) \\ &- 22\sqrt{2}\, \tan^{-1}\left(\sqrt{2\chi}\right), \end{aligned} \tag{2}$$

where $\chi := \frac{1}{2}\left(\frac{r_{\rm ISCO}}{r} - 1\right)$.

The trajectory in hand, we could write down the stress-energy tensor corresponding to the plunging projectile. Thanks to the EMR we can treat the problem in the framework of BH perturbation theory. The projectile is modeled as a point source, traveling on a geodesic in the background of the large BH (self-force effects are neglected as they make their first appearance only at higher orders in the mass ratio). The problem at leading order in the mass ratio reduces to Zerilli/Regge-Wheeler (Z/RW) [4,5] theory for radiation in the background of a Schwarzschild BH

for a given source of energy-momentum. That is, after decomposition into spherical harmonics and transforming into the tortoise coordinate $r_* = r + r_s \log(r/r_s - 1)$, the physics reduces to that of a $(1+1)$ dimensional wave equation with a potential and source term which can be be written in the frequency domain as

$$\left[\frac{\partial^2}{\partial r_*^2} + \omega^2 - V^l_{\rm Z/RW}(r)\right] \psi^{lm}_{\rm Z/RW}(r,\omega) = S^{lm}_{\rm Z/RW}(r,\omega)\ , \qquad (3)$$

where $\psi^{lm}_{\rm Z/RW}(r,\omega)$ is a specific linear function of the metric perturbations and their derivatives, $V^l_{\rm Z/RW}(r)$ is the Z/RW potential (e.g. $V^l_{\rm RW}(r) = \left(1-\frac{r_s}{r}\right)\left[\frac{l(l+1)}{r^2} - \frac{3r_s}{r^3}\right]$) and $S^{lm}_{\rm Z/RW}(r,\omega)$ is the source term, which is a specific linear function of the stress-energy tensor. We used the gauge invariant formalism of Martel-Poisson ([6]). Using our expressions for the trajectory we obtained the (time domain) source terms and Fourier transformed them into the frequency domain, obtaining closed form expressions for the frequency domain source terms, in which all frequency and r dependence is completely explicit. For example, the RW source term is given by, for $r_s < r < 3r_s$

$$\begin{aligned} S^{lm}_{\rm RW}(r,\omega) &= \frac{32\sqrt{3}\,\pi\,\tilde{m}\,r_s\left(1-\frac{r_s}{r}\right)}{r}\ B(l,m) \\ &\times\ e^{-i(\omega t_p(r) + m\phi_p(r))} \\ &\times\ \left[9i\omega\left(\left(\frac{r}{r-3r_s}\right)^3\left(1+3\left(\frac{r_s}{r}\right)^2\right)\right)\right. \\ &-\ \left. im\frac{6\sqrt{6}\,r_s\,r}{(3r_s-r)^3} + \frac{\sqrt{2}\,r^{1/2}\,(3r_s-4r)}{(3r_s-r)^{5/2}}\right] \qquad (4) \end{aligned}$$

where $B(l,m)$ is a known function of l, m. $t_p(r)$ and $\phi_p(r)$, as stressed above, are known functions. For $r \notin (r_s, 3r_s)$, $S^{lm}_{\rm RW}(r,\omega) = 0$.

We went on to calculate the radiation in the ringdown stage. We wrote the wavefunction in the time domain in terms of the frequency domain Green's function. The integration (over all frequencies) contour, then, can be deformed from the real frequency axis and into the complex plane and the residues' contributions from the poles can be collected. Finally, the ringdown waveform is given by

$$\begin{aligned} \psi^{lm}_{\rm o/e}(r,t) &= \sum_{nl} \frac{e^{i\omega_{nl}(t-r_*)}}{2\,\omega_{nl}\,\beta_{nl}} \qquad (5) \\ &\times \int_{r_s}^{3r_s} u^l_{\rm hor}(r'_*)\, S^{lm}_{\rm o/e}(r'_*,\omega_{nl})\, dr'\ , \end{aligned}$$

where the index n runs over all QNM's for a given l.

We identified the coefficient of $e^{i\omega_{nl}(t-r_*)}$ with the ringdown amplitude

$$R_{nlm} := \frac{1}{2\,\omega_{nl}\,\beta_{nl}} \int_{r_s}^{3r_s} u^l_{\rm hor}(r'_*)\, S^{lm}_{\rm o/e}(r'_*,\omega_{nl})\, dr' \qquad (6)$$

where $u^l_{\rm hor}(r'_*)$ is a homogenous solution of the Z/RW equation satisfying ingoing wave boundary conditions at the horizon, ω_{nl} is the (n,l) quasi-normal frequency and β_{nl} is a frequency dependent coefficient. This is our main result for the ringdown amplitudes.

The final expression for each post-ISCO ringdown amplitude calls for solving certain ordinary differential equations (the radial wave equations) at the QNM frequencies and performing a certain weighted radial integral over the source. These issues are being addressed numerically.

REFERENCES

1. S. Hadar and B. Kol, arXiv:0911.3899 [gr-qc].
2. P. C. Peters, Phys. Rev. **136**, B1224 (1964).
3. T. Apostolatos, D. Kennefick, E. Poisson and A. Ori, Phys. Rev. D **47**, 5376 (1993).
4. T. Regge and J. A. Wheeler, Phys. Rev. **108** (1957) 1063.
5. F. J. Zerilli, Phys. Rev. Lett. **24** (1970) 737.
6. K. Martel and E. Poisson, Phys. Rev. D **71** (2005) 104003.

Spin Field Correlators in Various Dimensions

Daniel Härtl[a]

[a]Max-Planck-Institut für Physik
Föhringer Ring 6, 80805 München, Germany

In this short note we present calculational tools allowing for the evaluation of superstring correlators involving bosons and fermions in even space-time dimensions D. We show methods for tree-level scattering as well as scattering at arbitrary loop order. This summarizes our work [1,2].

1. Introduction

Superstring amplitudes with many external legs are of considerable theoretical interest in the framework of a full-fledged superstring theory. Tree- and higher-loop amplitudes in various dimensions can be used to test multiple aspects of duality symmetries relating different string vaccua. In addition string scattering in four space-time dimensions may become relevant in describing corrections to jet cross sections from low string scale or large extra dimensions physics [3].

In the Ramond–Neveu–Schwarz (RNS) formalism of superstring theory one of the obstacles in computing scattering amplitudes is the interacting nature of the Neveu–Schwarz (NS) fermion ψ^μ and the Ramond (R) spin field S_α [4]. As these RNS fields appear in the vertex operators of the underlying super conformal field theory (SCFT) the corresponding correlation functions are difficult to obtain. The focus of this note lies on providing tools to calculate such correlators at arbitrary genus g in $D = 4, 6, 8$ and $D = 10$ space-time dimensions.

2. The RNS CFT

The operator product expansion (OPE) governs the short distance behavior of the fermions ψ^μ and the left- and right-handed spin fields $S_\alpha, S^{\dot\beta}$. The interaction between two fermions or one fermion and one spin field does not depend on the number of dimensions D. However, the conformal weights of the spin fields depend on D. According to the chiral structure of the charge conjugation matrix C we encounter different scenarios [5]:

- $D = 0 \bmod 4$ OPEs:

$$\begin{aligned} S_\alpha(z)\, S_\beta(w) &= (z-w)^{-D/8}\, C_{\alpha\beta} + \dots\,, \\ S_\alpha(z)\, S^{\dot\beta}(w) &= \frac{(\gamma^\mu\, C)_\alpha{}^{\dot\beta}}{\sqrt{2}} \\ &\quad \times (z-w)^{-D/8+1/2}\, \psi_\mu(w) + \dots\,, \end{aligned} \tag{1}$$

- $D = 2 \bmod 4$ OPEs:

$$\begin{aligned} S_\alpha(z)\, S^{\dot\beta}(w) &= (z-w)^{-D/8}\, C_\alpha{}^{\dot\beta} + \dots\,, \\ S_\alpha(z)\, S_\beta(w) &= \frac{(\gamma^\mu\, C)_{\alpha\beta}}{\sqrt{2}} \\ &\quad \times (z-w)^{-D/8+1/2}\, \psi_\mu(w) + \dots\,. \end{aligned} \tag{2}$$

From the OPEs above we can construct every RNS correlator at tree level. Note that the second equations in (1) and (2) can be inverted and every NS fermion in a correlation function can thus be replaced by two R spin fields. This can also be applied to loop calculations.

3. Loop techniques

A simple way to evaluate loop correlators is to express the RNS fields in $D = 2n$ dimensions by n copies of an $SO(2)$ spin system. The correlation function then factorizes into n $SO(2)$ correlators, which can be calculated fairly easy [6]. Generalized theta functions shifted according to some spin structure $\vec{a}, \vec{b}$ appear in the calculation. They

ensure the required periodicity of the result along the homology cycles of the g-loop string world-sheet. Additionally, the prime forms $E(z,w)$ derived from the generalized theta functions capture the short distance behavior (1) and (2).

However, making use of the $SO(2)$ spin systems it is a difficult task to give results for the RNS correlators in Lorentz covariant form. This has been achieved up to 6-point level and certain correlation functions with arbitrary many fields in [2,7] for $D = 4, 6, 8$ and $D = 10$.

4. General results

A general formula for loop correlation functions involving an arbitrary number of NS fermions and two spin fields in $D = 4$ has been proven in [7]. We find similar expressions for this type of correlators, i.e.

$$\langle \psi^{\mu_1} \dots \psi^{\mu_m} \, S_\alpha \, S_\beta \rangle^{\vec{a}}_{\vec{b}} \,,$$
$$\langle \psi^{\mu_1} \dots \psi^{\mu_n} \, S_\alpha \, S^{\dot\beta} \rangle^{\vec{a}}_{\vec{b}} \,, \qquad (3)$$

in $D = 6, 8$ and $D = 10$ dimensions [2]. Due to the chirality structure of C in $D = 4, 8$ the number m (n) has to be even (odd) for the correlation functions not to vanish. This is reversed for $D = 6, 10$.

5. $D = 4$

RNS tree-level correlators in $D = 4$ dimensions can be solved in full generality [1]. As a first step we invert the second equation in (1) and replace every NS fermion ψ^μ by two spin fields S_α and $S^{\dot\beta}$. By bosonization one can then prove that only for $D = 4$ the resulting spin field correlation function factorizes into correlators containing only right- or left-handed spin fields. A general formula for these sub-correlators has been derived by induction.

At loop-level bosonization cannot resolve the spin structure of the spin fields and therefore the factorization technique cannot be applied. However, one can still derive general expressions for the correlators of $2n$ left-handed spin fields, as well as $2n$ left-handed and two or four right-handed spin fields [7].

6. $D = 6$

In $D = 6$ dimensions a formula for the correlation functions $\langle S_{\alpha_1} \dots S_{\alpha_n} S^{\dot\beta_1} \dots S^{\dot\beta_n} \rangle^{\vec{a}}_{\vec{b}}$ at arbitrary genus g can be worked out. By replacing spin fields with fermions using (2) we find results for the correlators:

$$\langle \psi^{\mu_1} \dots \psi^{\mu_{k+l}} \, S_{\alpha_1} \dots S_{\alpha_{n-2k}} \, S^{\dot\beta_1} \dots S^{\dot\beta_{n-2l}} \rangle^{\vec{a}}_{\vec{b}}. \quad (4)$$

7. $D = 8$

In the case $D = 8$ the fermion and spin field have both conformal dimension $1/2$. This is related to the S_3 permutation symmetry of the $SO(8)$ Dynkin diagram, also referred to as triality. Therefore we can calculate a certain tree-level correlator, state the result in triality covariant form and then permute the RNS fields to find a so-far unknown correlation function. Details and examples are found in [2].

Triality does not carry over to higher genus. The different global properties of the RNS fields under transport around the world-sheet's homology cycles break this covariance. Therefore correlators, which are related by triality at tree-level, differ at loop level in the terms that depend on the spin structure, i.e. $\Theta^{\vec{a}}_{\vec{b}}$. Hence, each correlator has to be calculated separately.

8. $D = 10$

Due to the large number of index terms we are not able to find a general formula for certain correlators as it was possible in $D = 4$ and $D = 6$. Hence, every RNS correlator at tree- and loop-level has to be calculated by hand.

An easy example is the correlator of one fermion and two left left-handed spin fields,

$$\langle \psi^\mu(z_1) \, S_\alpha(z_2) \, S_\beta(z_3) \rangle^{\vec{a}}_{\vec{b}} = \frac{(\gamma^\mu \, C)_{\alpha\beta}}{(2 \, E_{12} \, E_{13})^{1/2} \, {E_{23}}^{3/4}} \times \frac{\Theta^{\vec{a}}_{\vec{b}}\big[\frac{1}{2}(\int_{z_2}^{z_1} \vec{\omega} + \int_{z_3}^{z_1} \vec{\omega})\big] \, \Theta^{\vec{a}}_{\vec{b}}\big[\frac{1}{2} \int_{z_3}^{z_2} \vec{\omega}\big]^4}{\Theta^{\vec{a}}_{\vec{b}}(0)^5} \,, \qquad (5)$$

where $\vec{\omega}$ is the period on the genus g string world-sheet and $E_{ij} \equiv E(z_i) - E(z_j)$. For $g = 0$ this reduces to the tree-level result as $\Theta^{\vec{a}}_{\vec{b}} \to 1$ and the prime form becomes $E(z,w) \to (z - w)$.

9. Conclusions

We have presented tools to calculate string scattering amplitudes in various even space-time dimensions at tree-level and to arbitrary loops. Our results can be applied to theories allowing for a CFT description, especially heterotic and superstring theories.

10. Acknowledgments

I would like to thank Stephan Stieberger and Oliver Schlotterer for collaboration on this work.

REFERENCES

1. D. Härtl, O. Schlotterer, S. Stieberger, Nucl. Phys. **B834**, 163-221 (2010). [arXiv:0911.5168 [hep-th]].
2. D. Härtl, O. Schlotterer, [arXiv:1011.1249 [hep-th]].
3. D. Lüst, S. Stieberger, T. R. Taylor, Nucl. Phys. **B808**, 1-52 (2009). [arXiv:0807.3333 [hep-th]].
4. D. Friedan, E. J. Martinec, S. H. Shenker, Nucl. Phys. **B271**, 93 (1986).
5. V. A. Kostelecky, O. Lechtenfeld, W. Lerche *et al.*, Nucl. Phys. **B288**, 173 (1987).
6. J. J. Atick, A. Sen, Nucl. Phys. **B286**, 189 (1987).
7. O. Schlotterer, JHEP **1009**, 050 (2010). [arXiv:1001.3158 [hep-th]].

Three Point Tree Level Amplitude in Superstring Theory

Ehsan Hatefi [a*]

[a]Theory Group, Physics Department, CERN CH-1211, Geneva 23, Switzerland.

In order to check exact zero result of the amplitude of three massless points (CAA) in both string theory and field theory side for $p = n$ case and to find all gauge field couplings to R-R closed string, we follow the disk level S-matrix element of one Ramond-Ramond field and two gauge field vertex operators in the world volume of BPS branes.

1. Introduction

D_p-branes are the source of Ramond-Ramond (p+1)-form fields in IIA and IIB string theories [1]. They have been studied and many properties of them have been investigated [2,3], being the center of attention both in theory and phenomenology. The stable D_p-branes (p is even in IIA and odd in IIB theory) preserve half of supersymmetry.

In fact, stability, supersymmetry, conserved Ramond-Ramond (RR) charge and having no tachyons are all properties of these type II D_p-branes. All supersymmetric D_p-branes in IIA can be generated as bound states of D_9-branes [4]. They can also be derived from K-theory [5]. At leading order, the low-energy action for fields corresponds to the dimensional reduction of a ten-dimensional U(1) super-Yang Mills theory. When derivatives of the field strengths are small on the string scale, then the action to all orders in the field strength takes the Born-Infeld form [6,7] (also see [8]). The low energy action describing the dynamics of D_p-branes consists of two parts. The first part is Born-Infeld action (for more details see [9]). In addition BI action provides the kinetic terms for the world-volume fields, it also contains the couplings of the D_p-brane to the massless Neveu-Schwarz fields in the bulk. The second part is the Wess-Zumino action, which contains the coupling of the U(N) massless world volume vectors to the closed string RR field [1,10] One method for finding these effective actions is the BSFT [11]. To study WZ couplings for BPS branes we use the second approach, which is the S-matrix method.

*ehsan.hatefi@cern.ch

2. The Three Point Superstring Scattering (CAA)

One important tool in string theory is scattering theory[12]. In this section, using the conformal field theory technique[13] we evaluate this scattering amplitude to find all couplings of one closed string RR field to two gauge fields on the world-volume of a single BPS D_p-brane with flat empty space background. A great deal of effort for the scattering amplitudes at tree level has been made [14].Some previous works on scattering that involved a Dp-brane and some other works about applications on Dp-branes can be found in [15].

To calculate a S-matrix element, one needs to choose the picture of the vertex operators appropriately. The sum of the superghost charge must be -2 for disk level amplitude. Hence, this S-matrix element is given by the following correlation function:

$$\mathcal{A}^{AAC} \sim \int dx_1 dx_2 dz d\bar{z} \langle V_A^{(-1)}(x_1) V_A^{(0)}(x_2) \times V_{RR}^{(-1/2,-1/2)}(z,\bar{z}) \rangle \quad (1)$$

Where the vertex operator and the "doubling trick" are mentioned in [16]. To find the correlator of ψ, we use Wick-like rule [17]. The only subtlety in using this formula for currents is that one must not consider the Wick-like contraction

for the two ψ's in one current [18] . One eventually finds the integrand as the following

$$\mathcal{A}^{CAA} \sim \int dx_1 dx_2 dx_3 dx_4 (P_- \not{H}_{(n)} M_p)^{\alpha\beta} I \xi_{1a} \times \xi_{2b} x_{34}^{-1/4} (x_{23}x_{24})^{-1/2} \left(a_1^a a_2^b + 2ik_{1c} I^{bac}\right)$$

where

$$\begin{aligned} I &= |x_{12}|^{-2s} |x_{13}x_{14}|^s |x_{23}x_{24}|^s |x_{34}|^{-2s}, \\ a_1^a &= ik_2^a \left(\frac{x_{32}}{x_{13}x_{12}} + \frac{x_{42}}{x_{14}x_{12}}\right) \\ a_2^b &= 2^{-1/2} x_{34}^{-3/4} (x_{23}x_{24})^{-1/2} (\gamma^b C^{-1})_{\alpha\beta} \end{aligned}$$

For finding I^{bac} see [16]. We define Mandelstam varieable as $s = -(k_1 + k_2)^2$.One can easily show that the integrand is invariant under SL(2,R) transformation. Gauge fixing this symmetry by fixing the position of the closed string vertex operator as

$$x_1 = x, \qquad x_2 = -x, \qquad x_3 = i, \qquad x_4 = -i,$$

the amplitude ultimately becomes :

$$\mathcal{A} = \mathcal{A}_1 + \mathcal{A}_2 + \mathcal{A}_3 \tag{2}$$

where

$$\begin{aligned} \mathcal{A}_1 &\sim ik_2^a (2i)^{-2s} 2^{-1/2} \xi_{1a}\xi_{2b} \mathrm{Tr}\left(P_- \not{H}_{(n)} M_p \gamma^b\right) \\ &\quad \times \int_0^\infty dx \frac{1}{x} (x^2-1)(2x)^{-2s}(x^2+1)^{2s-1} \\ \mathcal{A}_2 &\sim -k_{1c}(2i)^{-2s} 2^{1/2} \xi_{1a}\xi_{2b} \mathrm{Tr}\left(P_- \not{H}_{(n)} M_p \Gamma^{bac}\right) \\ &\quad \times \int_0^\infty dx (2x)^{-2s}(x^2+1)^{2s-1} \qquad (3) \\ \mathcal{A}_3 &\sim -k_{1c}(2i)^{-2s} 2^{1/2} \xi_{1a}\xi_{2b} (\eta^{cb} \mathrm{Tr}\left(P_- \not{H}_{(n)} M_p \gamma^a\right) \\ &\quad -\eta^{ab} \mathrm{Tr}\left(P_- \not{H}_{(n)} M_p \gamma^c\right)) \\ &\quad \times \int_0^\infty dx \frac{1}{2ix} (-x^2+1)(2x)^{-2s}(x^2+1)^{2s-1} \end{aligned}$$

So as we can see the only non vanishing integral is the second one and the result is as the following

$$\int_0^\infty dx (2x)^{-2s}(x^2+1)^{2s-1} = \frac{\pi^{1/2}\Gamma[-s+1/2]}{2\Gamma[-s+1]}$$

To compare the field theory which apparently has massless field *i.e.,* the WZ action, with the above amplitude, one must expand the amplitude such that the massless pole of the field theory survives and all other poles disappear in the form of contact terms. Note that the S-matrix element of all four point massless vertex operators in superstring theory has also been found in standard books [19,20].

3. Momentum expansion

We want to examine the limit of $\alpha' \to 0$ of the above string amplitude. Using the momentum conservation along the world volume of brane, one finds the Mandelstam variable satisfies the following constraint

$$s = -p_a p^a/2. \tag{4}$$

It has been argued in [16], generally speaking that the momentum expansion of a S-matrix element should be around $(k_i + k_j)^2 \to 0$ and/or $k_i \cdot k_j \to 0$. The amplitude must have only massless pole in the $(k_1 + k_2)^2$channel, so correct momentum expansion at the low energy limit for t-channel must be around $(k_1 + k_2)^2 \to 0$. Using the on-shell relations one can rewrite them in terms of the Mandelstam variable as $s \to 0$. Including the constraint (4), one should realize that $p_a p^a \to 0$ which is possible for D-branes. Therefore the S-matrix element can be evaluated for BPS branes. Expansion of the functions around the above point is

$$(2)^{-2s} \frac{\pi^{1/2}\Gamma[-s+1/2]}{\Gamma[-s+1]} = \pi \left(\sum_{n=-1}^{\infty} b_n (s)^{n+1}\right).$$

where some of the coefficients b_n are

$$b_{-1} = 1,\ b_0 = 0,\ b_1 = \frac{1}{6}\pi^2,\ b_2 = 2\zeta(3).$$

Note that the coefficients b_n are exactly the coefficients that appear in the momentum expansion of the S-matrix element of one RR, two gauge fields and one tachyon vertex operator [21].

4. Low Energy Field Theory

We are interested in the part of effective field theory of D-branes which includes only gauge

fields. It should be possible to extract the necessary terms from the covariant Born-Infeld action constructed as the effective D-brane action . The Born-Infeld action is an action for all orders of α' . The low energy non-abelian extension of the action was proposed to be the symmetrized trace of non-abelian generalization of Born-Infeld action (with flat background in the bulk). The non-abelian field strength and covariant derivative of the gauge field are defined respectively as

$$F^{ab} = \partial^a A^b - \partial^b A^a - i[A^a, A^b], \qquad (5)$$
$$D_a F_{bc} = \partial_a F_{bc} - i[A_a, F_{bc}].$$

where $A_a = A_a^\alpha \Lambda_\alpha$ and Λ_α are the hermitian matrices. Our conventions for Λ^α are

$$\sum_\alpha \Lambda^\alpha_{ij}\Lambda^\alpha_{kl} = \delta_{ik}\delta_{jl} \ , \quad \mathrm{Tr}\,(\Lambda^\alpha \Lambda^\beta) \ = \ \delta^{\alpha\beta}.$$

5. $p = n + 2$ **case**

Only $\mathcal{A}_2$ is non-zero. We are not interested in fixing the overall sign of the amplitudes. Taking into account the related trace, the string amplitude becomes

$$\mathcal{A}^{CAA} = \pm(\mu_p \pi^{1/2})\frac{32}{(p-2)!}k_{1c}\xi_{1a}\xi_{2b}\epsilon^{baca_1\cdots a_{p-3}} \times H_{a_1\cdots a_{p-3}}(2)^{-2s}\frac{\pi^{1/2}\Gamma[-s+1/2]}{2\Gamma[-s+1]}$$

where we normalized the amplitude by $(\mu_p 2^{1/2}\pi^{1/2})$. The above amplitude is antisymmetric upon interchanging the gauge fields. So the whole amplitude is zero for an abelian gauge group. The amplitude also satisfies the Ward identity. Since Gamma function has no tachyon/massless pole, then the amplitude has only contact terms. The leading contact term is reproduced by the following coupling

$$\frac{1}{2!}\mu_p(2\pi\alpha')^2\mathrm{Tr}\,(C_{p-3}\wedge F\wedge F). \qquad (6)$$

The non-leading order terms should correspond to the higher derivative extension of the above coupling. So the higher vertice will be

$$V(C_{p-3}, A_3, A) = \frac{\mu_p(2\pi\alpha')^2}{(p-2)!}\epsilon^{a_1\cdots a_{p+1}}H_{a_1\cdots a_{p-2}} \times\xi_{1a_{p-1}}k_{1a_p}\xi_{2a_{p+1}}\sum_{n=-1}^{\infty} b_n(\alpha' k_1.k_2)^{n+1},$$

6. $p = n$ **case**

Both $\mathcal{A}_1, \mathcal{A}_3$ in the string side are zero for this case. However we would like to do the calculations in field theory side to conclude that ,there is no any compensation of the massless pole .

$$\mathcal{A} \ = \ V^a_\alpha(C_{p-1}, A)G^{ab}_{\alpha\beta}(A)V^b_\beta(A, A_1, A_2),$$

where the vertices and propagator are

$$V^a_\alpha(C_{p-1}, A) \ = \ \frac{i\mu_p(2\pi\alpha')}{(p)!}\epsilon^{a_0\cdots a_{p-1}a} \times H_{a_0\cdots a_{p-1}}\mathrm{Tr}\,(\Lambda_\alpha),$$

$$V^b_\beta(A, A_1, A_2) = \Big[\xi^b_1(k_1-k).\xi_2 + \xi^b_2(k-k_2).\xi_1 + \xi_1.\xi_2(k_2-k_1)^b\Big](-iT_p(2\pi\alpha')^2\mathrm{Tr}\,(\lambda_1\lambda_2\Lambda_\beta)),$$

$$G^{ab}_{\alpha\beta}(A) = \frac{i\delta_{\alpha\beta}\delta^{ab}}{(2\pi\alpha')^2 T_p(s)}.$$

where the propagator is derived from the standard gauge kinetic term arising in the expansion of the Born-Infeld action. Note that the vertex $V^b_\beta(A, A_1, A_2)$ is found from the standard non abelian kinetic term of the gauge field, and also the vertex $V^a_\alpha(C_{p-1}, A)$ is found from WZ coupling $C_{p-1}\wedge F$. In the above formula k is the momentum of the off-shell gauge field. The important point is that the vertex $V^b_\beta(A, A_1, A_2)$ has no higher derivative correction as it arises from the kinetic term of the gauge field. This vertex has already been found in [16]. Considering those vertexes the amplitude becomes

$$\mathcal{A} \ = \ [\xi^b_1(k_1-k).\xi_2 + \xi^b_2(k-k_2).\xi_1 + \xi_1.\xi_2 (k_2-k_1)^b]\delta^{ab}i\mu_p(2\pi\alpha')\frac{1}{(p)!s}\mathrm{Tr}\,(\lambda_1\lambda_2) \times\epsilon^{a_0\cdots a_{p-1}a}H_{a_0\cdots a_{p-1}}$$

which of course describes apparent massless pole in field theory side .

Meanwhile there is no masslesss pole in string theory side.

7. Remarks

Probably in this case there is no massless pole at s = 0 .Perhaps we may conclude that the kinematic factor provides a compensating factor of s but we do not know how compensation can be done .

The above amplitude which is calculated in the field theory side gives zero result because $\mathrm{Tr}\,(\lambda_1\lambda_2)$ is symmetric under interchainging 1 to 2 while the quantity in square brackets is anti-symmetric so the result is zero as it appeared in the string theory side (which is quite interesting). Note that the amplitude is zero because of the above reason not because of compensating factor (which related to the contact terms). Notice that for $p = n$ case note only we do not have massless pole but also we donot have any contact terms or infact the amplitude in both string and field theory side is zero ,where shows two concrete points as the following

First ,regarding gauge fixing, upper and lower bound of the integrand in string theory have been chosen correctly .

Second,there was a masslees pole in field theory side ,however because of kinematic reasons the amplitude vanishes not because of compensating mandelstam variable. There is no inconsistency between string theory and field theory even for this particular case.

Acknowledgment

The author would like to thank G.Veneziano for very beneficial and enjoyable collaboration throughout the project. He would also like to thank his advisors Luis Álvarez-Gaumé and M.R Garousi for several valuable discussions . The author also acknowledges Lance Dixon, I.Antoniadis , C.Grojean for comments, useful suggestions and the CERN Theory Group for its hospitality. This work was supported Under the Marie Curie or the EU grant UNILHC PITN-GA-2009-237920 .

REFERENCES

1. J. Polchinski,"Dirichlet-Branes and Ramond-Ramond Charges," Phys. Rev. Lett. **75**, 4724 (1995) [arXiv:hep-th/9510017].
2. E. Witten,"Bound states of strings and p-branes," Nucl. Phys. B **460**,335 (1996) [arXiv:hep-th/9510135].
3. J. Polchinski," Lectures on D-branes," [arXiv:hep-th/9611050]
   C. P. Bachas, "Lectures on D-branes," [arXiv:hep-th/9806199].
4. P. Horava ,"Type IIA D-branes, K-theory and Matrix theory," Adv. Theor. Math. Phys. **2**,1373 (1999) [arXiv:hep-th/9812135].
5. E. Witten," D-branes and K-theory," JHEP **9812**, 019 (1998)[arXiv:hep-th/9810188].
6. J. Dai, R.G. Leigh and J. Polchinski,"New Connections Between String Theories," Mod. Phys. Lett. **A4**, 2073 (1989).
7. R. G. Leigh,"Dirac-Born-Infeld Action from Dirichlet Sigma Model," Mod. Phys. Lett. A **4**, 2767 (1989) .
8. A. A. Tseytlin,"Born-Infeld action, supersymmetry and string theory," [arXiv:hep-th/9908105].
9. R. C. Myers,"Dielectric-branes," JHEP **9912**, 022 (1999) [arXiv:hep-th/9910053].
10. M. Li,"Boundary states of D-branes and dy-strings," Nucl. Phys. **B460**, 351 (1996) [arXiv:hep-th/9510161] ; M. R. Douglas,"Branes within branes," [arXiv:hep-th/9512077]
11. P. Kraus and F. Larsen,"Boundary string field theory of the DD-bar system," Phys. Rev. D **63**, 106004 (2001) [arXiv:hep-th/0012198].
12. G. Veneziano, Nuovo Cim. A **57**, 190 (1968).
13. V. A. Kostelecky, O. Lechtenfeld, W. Lerche, S. Samuel and S. Watamura, "Conformal Techniques, Bosonization and Tree Level String Amplitudes," Nucl. Phys. B **288**,173 (1987) .
14. A. Hashimoto and I. R. Klebanov, "Scattering of strings from D-branes," Nucl. Phys. Proc. Suppl. **55B**, 118 (1997) [arXiv:hep-th/9611214] ; M. R. Garousi and R. C. Myers,"Superstring Scattering from D-Branes," Nucl. Phys. B **475**, 193 (1996) [arXiv:hep-th/9603194]. ; C. Kennedy and A. Wilkins,"Ramond-Ramond couplings on brane-antibrane systems," Phys. Lett. B **464**,

206 (1999) [arXiv:hep-th/9905195]. ; R. Medina, F. T. Brandt and F. R. Machado,"The open superstring 5-point amplitude revisited," JHEP **0207**,071 (2002) [arXiv:hep-th/0208121]. ; S. Stieberger," Open, Closed vs.Pure Open String Disk Amplitudes," [arXiv:0907.2211 [hep-th]]. ; R. H. Boels, D. Marmiroli and N. A. Obers, JHEP **1010**, 034 (2010) [arXiv:1002.5029 [hep-th]].

15. C. Bachas, "D-Brane Dynamics," Phys. Lett. **B374**, 37 (1996)[arXiv:hep-th/9511043] ; J. Polchinski,"String duality: A colloquium," Rev. Mod. Phys. **68**, 1245 (1996) [arXiv:hep-th/9607050]; ; W. Taylor,"Lectures on D-branes, gauge theory and M(atrices)," [arXiv:hep-th/9801182] ; C. Vafa,"Lectures on strings and dualities," [arXiv:hep-th/9702201] ; J. Polchinski, S. Chaudhuri and C. V. Johnson, "Notes on D-Branes," [arXiv:hep-th/9602052].
16. E. Hatefi, JHEP **1005**, 080 (2010) [arXiv:1003.0314 [hep-th]].
17. H. Liu and J. Michelson,"*-trek III: The search for Ramond-Ramond couplings," Nucl. Phys. B **614**, 330 (2001) [arXiv:hep-th/0107172].
18. M. R. Garousi and E. Hatefi, JHEP **0903**, 008 (2009) [arXiv:0812.4216 [hep-th]].
19. M. Green, J. Schwarz and E. Witten, "Superstring theory," Vol. 1, Cambridge University Press, (1987).
20. J. Polchinski, "String theory," Vol. 1 Cambridge University Press, (1998).
21. M. R. Garousi and E. Hatefi, Nucl. Phys. B **800**, 502 (2008) [arXiv:0710.5875 [hep-th]].

Heterotic domain-wall supersymmetry breaking

Johannes Held[a*],

[a]Max- Planck- Institut für Physik
Föhringer Ring 6, 80805 München, Germany

We describe briefly our new method to construct non-supersymmetric vacua in the setting of heterotic string theory compactifications with intrinsic torsion and background fluxes. This method is based on *domain-wall supersymmetry breaking* that was developed in the context of type II compactifications.

1. Introduction

During the last decade a lot of effort has been put into the understanding of string theory compactifications including background fluxes. Especially supersymmetric settings are up to now well understood (see [1] and references therein).

Nonetheless, in order to make contact to particle physics an important issue is how to incorporate supersymmetry breaking into string theory. In the setting of type II theory it is known that one can induce SUSY breaking by the inclusion of background fluxes [2]. In [3] it was possible to give clear conditions which a non-supersymmetric vacuum has to satisfy to be consistent. However, also in the heterotic case one can turn on non-trivial background fluxes and hence by duality arguments find consistent non-supersymmetric vacua [4]. This leaves open the question if these vacua can be constructed directly from the ten-dimensional heterotic supergravity action, which we answered affirmatively in [5], using the techniques of [3]. This article is a short review of this work.

2. BPS-like potential

In order to analyze non-supersymmetric vacua, we must first understand the supersymmetric case. To this end we start with the bosonic action of heterotic $\mathcal{N}=1$ supergravity up to $\mathcal{O}(\alpha')$ as given in [6]. To maintain supersymmetry in four dimensions we have to compactify this theory on a six-dimensional manifold M that admits an SU(3)-structure (for information on G-structures see [7] and references therein). Including a warp factor A the metric takes the form

$$\mathrm{d}s^2_{X_{10}} = e^{2A}\mathrm{d}s^2_{X_4} + \mathrm{d}s^2_M \ . \tag{1}$$

Using this ansatz we can rewrite the action as a four-dimensional integral over an effective potential $S = -\int_{X_4} \mathrm{d}^4x\, V$, that depends on the six dimensional metric g, the dilation ϕ, the warp factor A, and the Neveu–Schwarz three form flux H. The equations of motion for these fields imply then that X_4 has to be Minkowski, A has to be constant, and that V vanishes on-shell.

For the next step the SU(3)-structure of M is of main importance. On the one hand, it is possible to express the curvature scalar in terms of the SU(3) invariant forms J and Ω, as was done in [3]. On the other hand, also the supersymmetry conditions are expressible in terms of these forms [8] and read

$$\mathrm{d}(e^{-2\phi}\Omega) = 0 \tag{2a}$$

$$\mathrm{d}(e^{-2\phi}J\wedge J) = 0 \tag{2b}$$

$$e^{2\phi}\mathrm{d}(e^{-2\phi}J) = *H \ . \tag{2c}$$

Using these two facts one can rewrite the potential V in a BPS-like form. Meaning that it becomes a sum of terms quadratic in the supersymmetry conditions and that hence all equations of motion are satisfied as long as SUSY holds.

*I would like to thank Dieter Lüst, Fernando Marchesano, and Luca Martucci for fruitful collaboration.

3. Supersymmetry breaking

We will now break SUSY by imposing that (2a) is not satisfied anymore, but still demand that

$$\bar{\Omega} \lrcorner \mathrm{d}(e^{-2\phi}\Omega) = 0 \ . \tag{3}$$

This has two interpretations. On the one hand it means that the manifold M is not complex, although still an almost complex structure can be defined on it. On the other hand (2a) can be interpreted as a calibration condition for NS5-branes wrapping a non trivial three-cycle of M [9]. These branes appear as domain walls in four dimensions. Hence the SUSY breaking mechanism we use was dubbed *domain-wall SUSY breaking* in [3], since it is induced by non-calibrated domain-walls.

An advantage of this ansatz is that its implications remain tractable. In fact one finds that there are only few conditions to be satisfied in order to obtain consistent non-supersymmetric vacua [5]. On-shell the potential has to be zero still, which is only possible if

$$|e^{2\phi}\mathrm{d}(e^{-2\phi}\Omega)|^2 = |J \wedge \mathrm{d}\Omega|^2 \ . \tag{4}$$

is satisfied. Furthermore, the equations of motion are not any longer guaranteed by (2b), (2c), and (3) but lead to additional constraints on M. Last by $\mathcal{O}(\alpha')$ effects the SUSY breaking scale has to be much lower then the compactification scale, meaning that we indeed describe spontaneous supersymmetry breaking.

As is shown in more detail in [5], these conditions can all be satisfied for elliptic fibrations of K3, which were also considered in [4,10]. For these models we find a stabilization of the dilaton ϕ and the elliptic fiber volume. Also, one gets that the gravitino mass is inverse proportional to the volume of K3 and hence SUSY breaking is small for large base manifolds.

REFERENCES

1. M. Grana, Phys. Rept. **423** (2006) 91-158. [arXiv:hep-th/0509003].
2. S. B. Giddings, S. Kachru and J. Polchinski, Phys. Rev. D **66** (2002) 106006 [arXiv:hepth/0105097].
3. D. Lüst, F. Marchesano, L. Martucci and D. Tsimpis, JHEP **0811** (2008) 021 [arXiv:0807.4540 [hep-th]].
4. K. Becker, C. Bertinato, Y. -C. Chung *et al.*, Nucl. Phys. **B823** (2009) 428-447. [arXiv:0904.2932 [hep-th]].
5. J. Held, D. Lüst, F. Marchesano and L. Martucci, JHEP **1006** (2010) 090 [arXiv:1004.0867 [hep-th]].
6. E. A. Bergshoeff and M. de Roo, Nucl. Phys. B **328** (1989) 439.
7. P. Koerber, [arXiv:1006.1536 [hep-th]].
8. J. P. Gauntlett, D. Martelli, D. Waldram, Phys. Rev. **D69** (2004) 086002. [arXiv:hep-th/0302158].
9. L. Martucci, P. Smyth, JHEP **0511** (2005) 048. [hep-th/0507099].
10. J. -X. Fu, S. -T. Yau, J. Diff. Geom. **78** (2009) 369-428. [arXiv:hep-th/0604063].

The chiral de Rham complex and quantum non-linear sigma models

J. Källén[a]

[a]Department of Physics and Astronomy, Division of Theoretical Physics, Uppsala University
Box 516, SE-751 20 Uppsala, Sweden

In [1,2], the interpretation of the chiral de Rham complex as a formal quantization of 2d non-linear sigma models in the Hamiltonian framework was suggested and used to compute symmetry algebras for quantum models with non-flat target spaces. Here we review the construction.

1. Introduction

A 2d non-linear sigma model is a theory of maps from a two-dimensional world sheet into some target space $\mathcal{M}$. We will here describe a framework where the notion of invariance under target space coordinate transformations for supersymmetric models can be defined in the quantum setup. Carefully applying this framework allows us to compute symmetry algebras for certain non-linear sigma models. We refer to [1,2] for more details of the construction outlined below, and more references.

2. Sigma models and the chiral de Rham complex

We start with the classical theory. We work in the Hamiltonian framework. We now describe the phase space which many supersymmetric sigma models have. Consider the superloop space $\mathcal{LM} = \{S^{1|1} \to \mathcal{M}\}$. $S^{1|1}$ is a circle with one odd and one even coordinate. The superloop space is the space of embeddings of this circle into $\mathcal{M}$. The phase space of our models is the cotangent bundle $T^*\mathcal{LM}$ of the superloop space. $T^*\mathcal{LM}$ carries a natural symplectic structure, which induces a Poisson bracket given by

$$\big\{\phi^i(\sigma,\theta), S_j(\sigma',\theta')\big\} = \delta^i_j\delta(\sigma-\sigma')\delta(\theta-\theta'). \quad (1)$$

Here, (σ,θ) are coordinates on $S^{1|1}$ and $\big(\phi^i(\sigma,\theta), S_i(\sigma,\theta)\big)$, $i = 1,2\ldots,n = dim\mathcal{M}$, are local coordinates on $T^*\mathcal{LM}$. Note that S_i is odd. Let us now consider a trivial but important fact. If we make a change of coordinates on $\mathcal{M}$, with ϕ^i transforming as coordinates and S_i as one-forms:

$$\tilde{\phi}^a = f^a(\phi), \qquad \tilde{S}_a = \frac{\partial g^i}{\partial\tilde{\phi}^a}S_i, \qquad g = f^{-1}, \quad (2)$$

the Poisson bracket (1) is invariant. Hence, we can define the phase space structure in local coordinates, and then glue it around the different patches on the target manifold to construct a global object. If we formally pass from the classical to the quantum setup, (ϕ^i, S_i) are promoted to operators and the Poisson bracket (1) becomes the equal time commutator between operators. (ϕ^i, S_i) still carries the interpretation of local coordinates. Formally, under a change of coordinates, (ϕ^i, S_i) transform as in (2). One can try and ask whether the equal-time commutator is invariant under this change of coordinates. In order to ask (and answer) this question we need a formalism which makes sense of (2), when (ϕ^i, S_i) are operators. This is where the construction known as *the chiral de Rham complex* (CDR) comes into play. The CDR was introduced in [3]. Formally, it is a sheaf of supersymmetric vertex algebras over a manifold. A vertex algebra is the mathematical counterpart of a 2d conformal field theory. A summary of the aspects of vertex algebras relevant for the construction of the CDR can be found in [1], and below we will use some notions of vertex algebras without further explanations. More extensive treatments of vertex algebras are given in [4,5]. In [3], the authors consider n copies of the vertex algebra known as the $\beta\gamma-bc$

system. In superfield language, this system consists of $2n$ superfields (ϕ^i, S_i), $i = 1, 2 \dots n$. In terms of these superfields, the non-trivial operator product expansions (OPE) of the $\beta\gamma - bc$ system is written

$$[\phi^i(z,\theta), S_j(z',\theta')] = \hbar\delta^i_j\delta(z-z')\delta(\theta-\theta'). \quad (3)$$

The authors in [3] noticed that if one defines new fields $(\tilde{\phi}, \tilde{S})$ via

$$\tilde{\phi}^a = f^a(\phi), \qquad \tilde{S}_a =: \frac{\partial g^i}{\partial \tilde{\phi}^a} S_i :, \qquad g = f^{-1}, \quad (4)$$

the OPE's between the new fields $(\tilde{\phi}, \tilde{S})$ is the same as the OPE's between the original fields (ϕ, S). In (4), : : denotes the normal ordered product, which has to be used since we are multiplying fields which do not commute. With this automorphism of the $\beta\gamma - bc$ system at hand, the authors in [3] did the following construction: On each coordinate patch of $\mathcal{M}$ they attached a $\beta\gamma - bc$ system, identifying ϕ^i as coordinates and S_i as one-forms. Using (4), this local construction can be glued around to construct a global object, a sheaf of vertex algebras. Identifying the formal parameter z with the circle coordinate σ above, the resemblance between the $\beta\gamma - bc$ system and the phase space structure is striking and it is natural to interprete the OPE (3) as the equal time commutator between coordinate and momenta, and to interprete the CDR as a framework for canonical quantization of non-linear sigma models. This interpretation was made in [1]. The construction only works for the combined $\beta\gamma - bc$ system, and hence only for supersymmetric sigma models. (4) is not an automorphism when restricted to the bosonic $\beta\gamma$ system.

3. Computing symmetry algebras on curved target spaces

Classically, symmetries of a theory are described by currents, which are functionals on the phase space. Using (1), we can compute the Poisson bracket between the currents and obtain a symmetry algebra. It is an interesting question whether the symmetry algebra is preserved in the quantum theory. The CDR framework allows us to address this question for sigma models. Details of how this is done in general can be found in [2]. An example where a careful application of the CDR framework has led to an interesting result is for the sigma model defined by the action

$$S = \int d\sigma dt d\theta^- d\theta^+ g_{ij} D_+\Phi^i D_-\Phi^j. \quad (5)$$

Here g_{ij} is the metric on $\mathcal{M}$, Φ^i are N=1 superfields and $D_\pm$ are spinor derivatives. Classically, if the target space is a Kähler manifold, this model has N=(2,2) superconformal symmetry. Quantizing this model in the CDR framework and calculating the equal time commutators between the currents we find an anomaly in the N=(2,2) superconformal algebra. The anomaly vanishes if the target manifold is Calabi-Yau, with a Ricci-flat metric. This raises an interesting puzzle, since multi-loop calculations performed in the 1980's shows that the model has superconformal symmetry on a Calabi-Yau manifold, but only with a non Ricci-flat metric [6]. Understanding this mismatch is an interesting open problem.

We end by noting that the CDR is applicable to a wide range of sigma models, opening up many interesting directions of future research.

Acknowledgement: I would like to thank J. Ekstrand, R. Heluani and M. Zabzine for enjoyable collaborations.

REFERENCES

1. J. Ekstrand, R. Heluani, J. Källén, M. Zabzine, Adv.Theor.Math.Phys. 13 (2009) 1221-1254
2. J. Ekstrand, R. Heluani, J. Källén, M. Zabzine, arXiv:1003.4388 [hep-th]
3. F. Malikov, V. Schechtman, A. Vaintrob, Commun.Math.Phys. 204 (1999) 439-473
4. V. G. Kac, Vertex Algebras for Beginners, Providence, USA: AMS (1996) 141 p. (University lectures series. 10)
5. R. Heluani, V. G. Kac, Commun.Math.Phys. 271 (2007) 103-178
6. D. Nemeschansky, A. Sen, Phys.Lett. B178 (1986) 365

Some properties of Cosmic String Junctions

Johanna Karouby [a]

[a]Physics Department, McGill University,
3600 University Street, Montreal, Canada, H3A 2T8

Cosmic strings are linear concentrations of energy of macroscopic size. Since cosmic superstrings can form junctions, observing them would give some support to string theory. In the following, we study the lensing cosmic string junctions create, the shift in photons' wavelength passing through (leading to the Kaiser-Stebbins effect), and the gravitational radiation they emit.

1. Cosmic strings

Cosmic strings can be seen as linear concentrations of trapped energy : They are one dimensional topological defects [1] that form during phase transitions as the universe cools down.

1.1. The U(1) abelian string

A simple model is the U(1) abelian string when the general group which gets broken is a global U(1). We can consider a model in which the symmetry breaking is realized by means of a Higgs scalar field doublet with a "Mexican hat" potential :

$$L = \partial_\mu \overline{\phi} \partial^\mu \phi - \frac{1}{4}\lambda(\overline{\phi}\phi - \eta)^2 \quad (1)$$

where λ is a dimensionless coupling constant and η denotes the symmetry breaking amplitude of the field ϕ.

The space of ground states (vacuum manifold) is a circle of radius η. A cosmic string configuration is obtained when the field value rotates about the minimum of the potential as we move around a circle $\mathcal{C}$ in space. If this is the case, then field continuity implies that there must be a point in space on the disk bounded by the circle $\mathcal{C}$ where the field vanishes. This is a point on the defect.

1.2. Cosmic superstrings

We describe them by simply using Nambu-Goto action $S = -\mu \int d\,t\, d\,\sigma \sqrt{-|\gamma|}$, where μ is the tension of the string and γ_{mn} is the metric induced on the string $\gamma_{mn} = g_{\mu\nu}\partial_m X^\mu\, \partial_n X^\nu$. and $|\gamma|$ is its determinant. Here $m, n = \{t, \sigma\}$ are the coordinates along the string worldsheet, X^μ are the space-time coordinates and $g_{\mu\nu}$ is the space-time metric.

An important property of cosmic superstrings is that they can form junctions made of composite of F-strings and D1-branes or (D-strings).

2. Observational signatures

2.1. Lensing due cosmic strings

We derive our results in the weak field approximation and get the necessary metric to compute the lensing effect. The presence of a string creates a conical space : there is a deficit angle, $\Delta = 8\pi G\mu$ and thus, going around a cosmic string doesn't require a 360 degrees rotation but only a $(2\pi - \Delta)$ one. As a consequence, there is a lensing where we would see two exact identical images (possibly shifted with respect to each other).

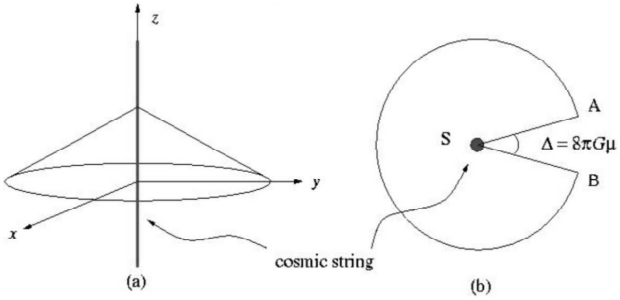

Figure 1. The metric around a cosmic string is conical

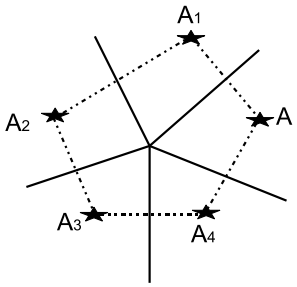

Figure 2. In this figure, the multiple lensing by N co-planar strings at a junction is sketched. The object A and its lensing counterparts $A_i, i = 1..N-1$, form a closed loop. Each image is the source for the nearby images via the enclosed string.

When looking at an object located behind a static junction of semi-infinite strings, one naturally expects multiple images to form.

Without loss of generality, we may suppose that the light rays are emitted along the negative z-direction in the y-z plane. Knowing that along each string $\mathbf{x}_i = l_i\,\vec{n}_i$, our final solution for the metric perturbation is [2]

$$h_{ab} = 4\,G\sum_i \mu_i\,(\delta_{ab} - n_{i\,a}\,n_{i\,b})\,\ln\left(\frac{r-\vec{r}\,.\,\vec{n}_i}{r_0}\right)\,, \quad (2)$$

where $r = |\mathbf{x}|$ is measured from the point of the junction and r_0 is a constant of integration.

The angle between the two light rays at their crossing point corresponds to the total deficit angle : $\Delta = |\delta\vec{v}| = 8\pi G\mu_{eff} = 8\pi G|\vec{k}\times\sum_i\vec{\mu}_i|$, where the unit vector $\vec{k}$ represents the direction of the light rays at infinity (line of sight).

2.1.1. Kaiser-Stebbins effect

Each string at the junction produces its own CMB anisotropy. The change in the CMB temperature across the i-th string is given by [2] : $\frac{\delta T}{T} = 8\pi G\,\gamma\,|\vec{v}.(\sum_i\vec{\mu}_i\times\vec{k})|$ where $\vec{v}$ is the velocity of the junction. Interestingly enough, the temperature anisotropy is different for different legs of the strings at the junction, depending on the tensions and orientations of the strings.

2.2. Gravitational radiation emitted by excited abelian cosmic strings

Radiation of gravitational waves is a generic phenomenon by the time-varying fluctuation of the metric. They are tensor perturbations that correspond to the traceless and transverse parts of the metric perturbation : $h^i_i = 0$ and $h^i_{j,i} = 0$.

Gravitational radiation would come predominantly from loop radiation : loops shrink and lose energy until they disappear. Straight cosmic strings don't produce gravitational radiation since we need the interaction of both right and left movers to enable the possibility of an emission. Here, we show that Y-junctions with an incoming wave on one of their strings do. Indeed, there will be a part reflected back at the junction and the other part will go to the 2 other strings forming the junction. When left movers and right movers will interact, gravitational radiation emission will occur.

The power emitted in direction $\mathbf{k}$ per solid angle Ω, integrating over the frequencies ω of the emitted waves, is given by

$$\frac{dE}{d\Omega} = 2G\int_0^\infty d\omega\omega^2\left[T^{\lambda\nu\,*}(k)\,T_{\lambda\nu}(k) - \frac{1}{2}|T^\lambda_\lambda(k)|^2\right]\,, \quad (3)$$

The simplest case is when the junction remains stationnary and does not not dislocate on the strings [3].

The power radiated per unit of length for a fixed junction point is :

$$\frac{dP}{d\,l} = \frac{G\mu_1^2\pi}{16}\frac{\nu_1^2}{\mu^2}\epsilon^4\kappa\,. \quad (4)$$

where $\mu \equiv \mu_1+\mu_2+\mu_3, \nu_1 \equiv \mu_2+\mu_3-\mu_1\,,\ \epsilon$ is a small number controlling the amplitude of the perturbations, and κ is the frequency of the left(right)-moving perturbations. We found the same result for a semi-infinite string attached to a rigid wall. This is not so surprising.

REFERENCES

1. "Cosmic Strings and Other Topological Defects," A. Vilenkin and E. P. S. Shellard, Cambridge University Press, 1994.
2. R. Brandenberger, H. Firouzjahi and J. Karouby, Phys. Rev. D **77**, 083502 (2008) [arXiv:0710.1636 [hep-th]].
3. R. Brandenberger, H. Firouzjahi, J. Karouby and S. Khosravi, JCAP **0901**, 008 (2009) [arXiv:0810.4521 [hep-th]].

Causality and Lifshitz Holography

Peter Koroteev [a]

[a]Department of Physics and Astronomy, University of Minnesota
116 Church Street S.E., Minneapolis, MN 55455, USA

We study signal propagation in theories with Lifshitz scaling using the gravity dual and show that backgrounds with $z < 1$ are incompatible with causality of the strongly coupled theory. We argue that causality violations in $z < 1$ theories show up in boundary correlation functions as superluminal modes.

1. Holography and anisotropic scaling

The AdS/CFT correspondence [1, 2] has been extensively used as a tool to extract properties of strongly coupled systems. Recent developments are directed towards the inventing similar techniques for strongly coupled critical points appearing in condensed matter systems [3, 4]. Although critical points show some kind of scale invariance, Lorentz symmetry is usually broken so the time coordinate can scale differently to the space coordinates $t \to \lambda^z t\,, \mathbf{x} \to \lambda\,\mathbf{x}$, where z is known as the dynamical critical exponent. Systems with dynamical scaling have been studied for a long time in condensed matter theory [5].

Consider a mean field description of massless scalar fluctuations around a critical point with dynamical exponent z. The effective Lagrangian would be

$$\mathcal{L} = (\partial_t\phi)^2 - c^2\ell^{2(z-1)}\phi(-\partial_{\mathbf{X}}^2)^z\phi\,, \tag{1}$$

where ℓ has units of length and c is the speed of light. The dispersion relation and phase velocity read

$$\omega^2 = \frac{c^2}{\ell^2}(\ell k)^{2z}\,, \quad v_{\rm ph} = \frac{\omega}{k} = c(\ell k)^{z-1}\,. \tag{2}$$

The metric proposed for a holographic description of a critical point with dynamical exponent z is [6, 7]

$$ds^2 = \frac{L^2}{r^2}\left(-\frac{\kappa^2 dt^2}{r^{2(z-1)}} + dr^2 + d\mathbf{x}^2\right)\,. \tag{3}$$

The local speed of light at a fixed value of the radial coordinate has a dependence on $1/r$ that is the same as the phase velocity in (2) with k, namely

$$c(r) = c\,\ell^{(z-1)}r^{-(z-1)}\,. \tag{4}$$

In [8] (full version of the paper) we show that the local speed of light is always related to the phase velocity at small wavelengths even in situations where there is no exact scale invariance.

2. Causality

We will now perform an analysis in the spirit of [9]. Consider a source in the field theory localized in time and in one of the spatial directions x. This will produce a planar perturbation propagating along x. In the holographic description the source is a boundary condition that will produce a shock wave-like perturbation propagating along null geodesics in both the radial and the spatial directions. We place a static probe extended in the radial direction. When the shock wave crosses a probe, it will produce a perturbation that will propagate towards the boundary along radial null geodesics producing a signal that can be interpreted as the position of the front (Fig. 2). We can find the null geodesics by solving the variational problem with Lagrangian

$$\mathcal{L} = -\frac{\kappa^2\dot{t}^2}{r^{2z}} + \frac{\dot{x}^2+\dot{r}^2}{r^2}\,, \tag{5}$$

and imposing the constraint $\mathcal{L} = 0$. Standard calculation [8] gives

$$\frac{dt}{dr} = \frac{Er^{2(z-1)}}{\kappa^2\sqrt{\frac{E^2r^{2(z-1)}}{\kappa^2} - P^2}}\,, \frac{dx}{dr} = \frac{P}{\sqrt{\frac{E^2r^{2(z-1)}}{\kappa^2} - P^2}}\,, \tag{6}$$

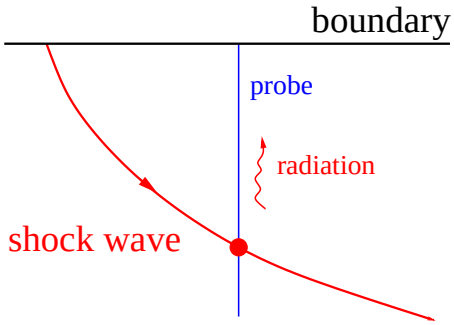

where P and E are integrals of motion. Let us assume that the initial point for the geodesic describing the shock wave is at $r = \ell$, $t = 0$, $x = 0$. In order to have a sensible solution we need the momentum to be timelike $p^2 \equiv \frac{E^2 \ell^{2(z-1)}}{\kappa^2} - P^2 > 0$. We see now a clear different qualitative behavior between $z > 1$ and $z < 1$.

For $z > 1$ the argument inside the square root in (6) is always positive, so the geodesic extends to all values of r. For $z < 1$ that argument becomes negative at a finite value of the radial coordinate, when $r_0^{1-z} = E/(\kappa|P|)$, or using $\kappa = c\ell^{z-1}$ and assuming $P > 0$,

$$\left(\frac{r_0}{\ell}\right)^{1-z} = \frac{E}{cP}. \tag{7}$$

Although the slope diverges, the values of both t and x approach a finite value, so the null geodesic is tangent to the slice of constant r at that point, and it will bounce back towards the boundary. In the above formula r_0 represents the turning point of the bulk gravitational potential.

The local speed of light at $r = \ell$ is c, that is also the speed of light of the dual theory, we can compare this value with the average velocity of the shock wave. Using (6) and (7) and assuming that $r_0 \gg \ell$ for $\rho = r/r_0$ we get

$$\frac{v_{shock}}{c} = \frac{\Delta x}{c\Delta t} \simeq z\frac{E}{cP}\,. \tag{8}$$

Since $r_0 \gg \ell$, due to (7) the latter ratio is bigger than unity, thus the shock wave travels faster than light signals at the boundary $v_S > c$. One can show that the front of radiation will coincide with the shock wave at the boundary, so its average velocity is also larger than the boundary speed of light. As was argued in [10] for asymptotically AdS spaces, whenever there is a null geodesic returning to the boundary it implies superluminal propagation one the boundary, which is totally incompatible with a holographic interpretation of a causal theory.

REFERENCES

1. Juan Martin Maldacena. The large N limit of superconformal field theories and supergravity. *Adv. Theor. Math. Phys.*, 2:231–252, 1998.
2. S. S. Gubser, Igor R. Klebanov, and Alexander M. Polyakov. Gauge theory correlators from non-critical string theory. *Phys. Lett.*, B428:105–114, 1998.
3. Sean A. Hartnoll. Lectures on holographic methods for condensed matter physics. *Class. Quant. Grav.*, 26:224002, 2009.
4. Christopher P. Herzog. Lectures on Holographic Superfluidity and Superconductivity. *J. Phys.*, A42:343001, 2009.
5. E. M. Lifshitz. On the Theory of Second-Order Phase Transitions I & II. *Zh. Eksp. Teor. Fiz.*, 11:255–269, 1941.
6. Shamit Kachru, Xiao Liu, and Michael Mulligan. Gravity Duals of Lifshitz-like Fixed Points. *Phys. Rev.*, D78:106005, 2008.
7. Peter Koroteev and Maxim Libanov. On Existence of Self-Tuning Solutions in Static Braneworlds without Singularities. *JHEP*, 02:104, 2008.
8. Carlos Hoyos and Peter Koroteev. On the Null Energy Condition and Causality in Lifshitz Holography. *Phys.Rev.*, D82:084002, 2010.
9. Diego M. Hofman and Juan Maldacena. Conformal collider physics: Energy and charge correlations. *JHEP*, 05:012, 2008.
10. Irene Amado and Carlos Hoyos-Badajoz. AdS black holes as reflecting cavities. *JHEP*, 09:118, 2008.

Scattering Amplitudes in supersymmetric Chern-Simons theory

Sangmin Lee[a]

[a]Department of Physics, University of Seoul, Seoul 130-743 Korea

We propose a contour integral formula for scattering amplitudes of the $\mathcal{N}=6$ supersymmetric Chern-Simons theory, and use it to give a formal proof for Yangian invariance of all tree level super-amplitudes.

1. INTRODUCTION

On-shell methods for computing scattering amplitudes in perturbative Yang-Mills theories have been greatly improved over the years, as explained in Z. Bern's lectures at this workshop.

One of the most remarkable recent development was the work of Arkani-Hamed *et al.* [1], where they proposed a remarkably simple contour integral formula for the tree level scattering amplitudes of planar $d=4$, $\mathcal{N}=4$ supersymmetric Yang-Mills theory.

In this short review, we propose a similar integral formula for all tree level scattering amplitudes of planar $d=3$, $\mathcal{N}=6$ supersymmetric Chern-Simons-matter theory (SCS_6), and give a formal proof of Yangian invariance. More information can be found in the original articles [2,3].

In three dimensions, null momenta can be written as bi-spinors: $p_i^{\alpha\beta}=\lambda_i^\alpha\lambda_i^\beta$. The tree level amplitudes take the simplest form when they are written as rational functions of the Lorentz invariant products $\langle ij\rangle\equiv\epsilon_{\alpha\beta}\lambda_i^\alpha\lambda_j^\beta$.

The on-shell superfield for SCS_6 involves three fermionic coordinates η^I in addition to λ^α [4], and has the expansion ($\eta^3\equiv\frac{1}{6}\epsilon_{IJK}\eta^I\eta^J\eta^K$)

$$\begin{aligned}\Phi&=\phi^4+\eta^I\psi_I+\tfrac{1}{2}\epsilon_{IJK}\eta^I\eta^J\phi^K+(\eta^3)\psi_4\,,\\ \bar\Phi&=\bar\psi^4+\eta^I\bar\phi_I+\tfrac{1}{2}\epsilon_{IJK}\eta^I\eta^J\bar\psi^K+(\eta^3)\bar\phi_4\,.\end{aligned}\qquad(1)$$

The superfields Φ and $\bar\Phi$ in (1) transform in mutually complex conjugate representations of the gauge group; a prime example is $\mathrm{U}(N)\times\mathrm{U}(N)$ gauge group [5] with Φ transforming in $(\mathbf{N},\overline{\mathbf{N}})$ and $\bar\Phi$ in $(\overline{\mathbf{N}},\mathbf{N})$. The external legs alternate between Φ and $\bar\Phi$. So, the main objects of interest are the $2k$-point color-ordered super-amplitudes

$$\mathcal{A}_{2k}(\Lambda)=\mathcal{A}_{2k}(\Lambda_1,\Lambda_2,\cdots,\Lambda_{2k}),\qquad(2)$$

where we $\Lambda_i=(\lambda^\alpha,\eta^I)_i$. By convention, we associate $\Lambda_{\mathrm{odd/even}}$ to $\bar\Phi/\Phi$.

The superconformal symmetry acting on $\mathcal{A}_{2k}$ is generated by graded quadratic products of

$$\mathcal{Z}_i^{\mathcal{A}}=(\Lambda,\partial/\partial\Lambda)_i=(\lambda^\alpha,\eta^I,\partial/\partial\lambda^\alpha,\partial/\partial\eta^I)\,.\qquad(3)$$

The bosonic generators realize the metaplectic representation for the $\mathrm{Sp}(4,\mathbb{R})\simeq\mathrm{SO}(2,3)$ conformal symmetry as well as the Clifford representation for the $\mathrm{SO}(6)$ R-symmetry.

2. CONTOUR INTEGRAL FORMULA AND YANGIAN INVARIANCE

Our proposal for the contour integral formula for the $2k$-point amplitude is [2]

$$\mathcal{A}_{2k}(\Lambda)=\int\frac{d^{k\times 2k}C}{\mathrm{vol}[\mathrm{GL}(k)]}\frac{\delta(C\cdot C^T)\,\delta(C\cdot\Lambda)}{M_1M_2\cdots M_k}\,.\qquad(4)$$

The integration variable C is a $(k\times 2k)$ matrix. The dot products denote $(C\cdot C^T)_{mn}=C_{mi}C_{ni}$, $(C\cdot\Lambda)_m=C_{mi}\Lambda_i$. M_i represents the i-th minor of C defined by

$$M_i=\epsilon^{m_1\cdots m_k}C_{m_1(i)}C_{m_2(i+1)}\cdots C_{m_k(i+k-1)}\,.\qquad(5)$$

The $\mathrm{vol}[\mathrm{GL}(k)]^{-1}$ factor is a reminder that the $\mathrm{GL}(k)$-left action on C is an exact symmetry of the integral and should be "gauge-fixed".

At the time of writing, the formula (4) has passed a number of non-trivial tests.

1. It exhibits the correct cyclic symmetry of the color-ordered super-amplitudes.
2. It has the full superconformal symmetry.
3. It reproduces the known four-point [7,8] and six-point [4] amplitudes.
4. It computes the eight-point amplitude which matches an independent computation based on a recursion relation [3].

Additional properties of the formula include

5. The integral is defined over the orthogonal Grassmannian manifold $\mathrm{OG}(k, 2k)$. [3]
6. It exhibits a Yangian symmetry, which suggests a dual superconformal symmetry [9].

We end this section with a sketch of the formal proof for Yangian invariance. We follow the methods developed in [10] for four-dimensional amplitudes. As shown in [6,4], the level one Yangian generators can be written in the bilinear form,

$$\mathcal{J}^{\mathcal{A}}{}_{\mathcal{B}} = \sum_{i<j} (-1)^{\mathcal{C}} \left(J_i^{\mathcal{A}}{}_{\mathcal{C}} J_j^{\mathcal{C}}{}_{\mathcal{B}} - J_j^{\mathcal{A}}{}_{\mathcal{C}} J_i^{\mathcal{C}}{}_{\mathcal{B}} \right) , \qquad (6)$$

where $J_i{}^{\mathcal{A}}{}_{\mathcal{B}}$ are the superconformal generators acting on the i-th particle. In terms of $\mathcal{Z}_i^{\mathcal{A}}$ defined in (3), the generators can be written as

$$\sum_{i<j} \left[\mathcal{Z}_i^{\mathcal{A}} \mathcal{Z}_{\mathcal{B}j} \mathcal{Z}_i^{\mathcal{C}} \mathcal{Z}_{\mathcal{C}j} - i \mathcal{Z}_i^{\mathcal{A}} \mathcal{Z}_{\mathcal{B}i} - (i \leftrightarrow j) \right] . \qquad (7)$$

The key insight we adopt from [10] is that $\mathcal{Z}_i^{\mathcal{C}} \mathcal{Z}_{\mathcal{C}j}$ generates an $\mathrm{O}(2k)$ action on $\{\Lambda_i\}$. Using the covariance of $\delta^{2k|3k}(C \cdot \Lambda)$, we can trade it with an inverse $\mathrm{O}(2k)$ action on the matrix C. The factors dC and $\delta(C \cdot C^T)$ are invariant under the $\mathrm{O}(2k)$ action, so we can do an integration by parts to make O_{ij} act on the denominator. Following the same steps as in [10], we can show that the quartic and quadratic terms in (7) acting on $\mathcal{A}_{2k}$ cancel each other.

3. OUTLOOK

Much work remains to be done to take full advantage of the formula (4). First, a precise prescription for the integration contour will be needed to prove that it reproduces all tree level amplitudes. The contour problem would require a closer look at the geometry of the orthogonal Grassmannian. Second, it would be nice to give an alternative proof of the Yangian invariance by rewriting the amplitude in terms of the "momentum super-twistor" variables [11,12]. Finally, it would be interesting to see how the formula can be used to address questions on loop amplitudes.

This work was initiated with inspiration from the lectures of N. Arkani-Hamed and Z. Bern and discussions with A. Lipstein during the workshop. This work was supported in part by National Research Foundation of Korea (NRF) Grants No. 2009-0072755 and 2009-0084601.

REFERENCES

1. N. Arkani-Hamed, F. Cachazo, C. Cheung and J. Kaplan, JHEP **1003**, 020 (2010) [arXiv:0907.5418 [hep-th]].
2. S. Lee, Phys. Rev. Lett. **105**, 151603 (2010).
3. D. Gang, Y.-t. Huang, E. Koh, S. Lee and A. E. Lipstein, arXiv:1012.5032 [hep-th].
4. T. Bargheer, F. Loebbert and C. Meneghelli, Phys. Rev. D **82**, 045016 (2010) [arXiv:1003.6120 [hep-th]].
5. O. Aharony, O. Bergman, D. L. Jafferis and J. Maldacena, JHEP **0810**, 091 (2008).
6. J. M. Drummond, J. M. Henn and J. Plefka, JHEP **0905**, 046 (2009).
7. A. Agarwal, N. Beisert and T. McLoughlin, JHEP **0906**, 045 (2009).
8. Y.-t. Huang and A. Lipstein, JHEP **1010**, 007 (2010).
9. Y.-t. M. Huang and A. E. Lipstein, JHEP **1011**, 076 (2010).
10. J. M. Drummond and L. Ferro, JHEP **1007**, 027 (2010) [arXiv:1001.3348 [hep-th]].
11. N. Arkani-Hamed, F. Cachazo and C. Cheung, JHEP **1003**, 036 (2010).
12. L. Mason and D. Skinner, JHEP **0911**, 045 (2009).

Dual Superconformal Symmetry of the ABJM Theory

Arthur E. Lipstein[a]

[a]California Institute of Technology, Pasadena, CA 91125, USA

We summarize the proof that all tree-level amplitudes of the ABJM theory enjoy dual superconformal symmetry. This note is based on arXiv:1008.0041 [hep-th] and arXiv:1012.5032 [hep-th].

1. Introduction

Recent studies of scattering amplitudes in the $\mathcal{N}=6$ superconformal Chern-Simons theory discovered by Aharony, Bergman, Jafferis, and Maldacena (ABJM) [1] have revealed that the ABJM theory has dual superconformal symmetry, which is inequivalent to the original superconformal symmetry and is hidden form the point of view of the action [2–4]. In section 2, I define the dual superspace and show that the four-point tree-level superamplitude has dual superconformal symmetry. In section 3, I describe a recursion relation that allows one to construct higher-point amplitudes from lower point amplitudes in the ABJM theory. In section 4, I will schematically demonstrate that the recursion relation preserves dual superconformal symmetry. Unless other wise indicated, the material in section 2 is taken from [3] and the material in sections 3 and 4 is taken from [4].

2. $\mathcal{N}=6$ Superspace

The momentum of a massless particle in three-dimensions can be written in bi-spinor form as follows

$$p^{ab}=p_\mu\sigma^{\mu ab}=\lambda^a\lambda^b \tag{1}$$

where σ^μ are the Pauli matrices and λ is a two-component spinor. Since the ABJM theory has $\mathcal{N}=6$ supersymmetry, the on-shell scattering amplitudes can be parameterized using a spinor λ^a, as well as three Grassmann-odd coordinates η^I for each external particle [2]. These Grassmann-odd coordinates transform in the fundamental representation of a U(3) subgroup of the SO(6) R-symmetry group. We shall refer to the coordinates (λ_i,η_i) as the on-shell superspace. Using Feynman diagram calculations, the four-point superamplitude of the ABJM theory was found to be

$$\mathcal{A}_4=\frac{\delta^3(P)\delta^6(Q)}{\langle 12\rangle\langle 41\rangle} \tag{2}$$

where $P^{ab}=\sum_{i=1}^4\lambda_i^a\lambda_i^b$, $Q^{aI}=\sum_{i=1}^4\lambda_i^a\eta_i^I$, and $\langle ij\rangle=\epsilon_{ab}\lambda_i^a\lambda_j^b$ [2].

The four-point superamplitude can also be written in terms of coordinates in a dual superspace which are defined as follows:

$$x_i^{ab}-x_{i+1}^{ab}=\lambda_i^a\lambda_i^b,\qquad \theta_i^{aI}-\theta_{i+1}^{aI}=\lambda_i^a\eta_i^I. \tag{3}$$

Supermomentum conservation implies that $x_1=x_5$ and $\theta_1=\theta_5$. In terms of these dual coordinates, the four-point superamplitude is given by

$$\mathcal{A}_4=\frac{\delta^3\left(x_1-x_5\right)\delta^6\left(\theta_1-\theta_5\right)}{\sqrt{\left(x_1-x_3\right)^2\left(x_4-x_2\right)^2}}. \tag{4}$$

It is straightforward to define inversion in the dual space:

$$I\left[x^{ab}\right]=\frac{x^{ab}}{x^2},\;\; I\left[\theta^{aI}\right]=\frac{x^{ab}}{x^2}\theta_b^I. \tag{5}$$

From these definitions, it follows that the four-point amplitude transforms covariantly under dual inversion:

$$I\left[\mathcal{A}_4\right]=\sqrt{x_1^2x_2^2x_3^2x_4^2}\mathcal{A}_4. \tag{6}$$

It therefore transforms in the following way under a dual conformal boost:

$$K^{ab}\mathcal{A}_4=I\left[\sum_{i=1}^4\frac{\partial}{\partial x_{iab}}I\left[\mathcal{A}_4\right]\right]=-\frac{1}{2}\sum_{i=1}^4x_i^{ab}\mathcal{A}_4. \tag{7}$$

This implies that the four-point superamplitude is invariant under the modified dual conformal boost generator $\tilde{K}^{ab} = K^{ab} + \frac{1}{2}\sum_{i=1}^{n} x_i^{ab}$, where n is the number of external particles.

By analogy with $\mathcal{N} = 4$ super Yang-Mills, we can also define dual supersymmetry generators:

$$\begin{aligned} Q_{Aa} &= \sum_{i=1}^{n} \frac{\partial}{\partial \theta_i^{Aa}}, \;\; Q_a^A \\ &= \sum_{i=1}^{n} \left(\theta^{Ab} \frac{\partial}{\partial x_i^{ab}} + \eta_i^A \frac{\partial}{\partial \lambda_i^a} \right) \end{aligned} \tag{8}$$

Note, however, that the second generator is not consistent with the second constraint in eq. (3) , i.e. $Q_a^A \left(\theta_i^{bI} - \theta_{i+1}^{bI}\right) \neq Q_a^A \left(\lambda_i^b \eta_i^I\right)$. To fix this, we must introduce three additional Grassmann-even coordinates to the dual space, which satisfy the following constraints:

$$y_i^{ab} - y_{i+1}^{ab} = \eta_i^a \eta_i^b. \tag{9}$$

Furthermore, we must modify the definition of the dual supersymmetry generator as follows:

$$\tilde{Q}_a^A = \sum_{i=1}^{n} \left(\theta^{Ab} \frac{\partial}{\partial x_i^{ab}} + \eta_i^A \frac{\partial}{\partial \lambda_i^a} + \frac{1}{2} y_i^{AB} \frac{\partial}{\partial \theta_i^{Ba}} \right) \tag{10}$$

After doing so, this generator commutes with all the constraints relating the on-shell superspace to the dual superspace. Note that all the other dual superconformal generators can be obtained by commuting the dual conformal boost generator with the dual supersymmetry generators. Furthermore, the dual supersymmetry generators reduce to ordinary supersymmetry generators when restricted to the on-shell superspace. It follows that the four-point superamplitude of the ABJM theory has dual superconformal symmetry.

3. Recursion Relation

To extend dual superconformal symmetry to all tree-level amplitudes, it is convenient to have a recursion relation that relates higher-point on-shell amplitudes to lower-point on-shell amplitudes. For quantum field theories defined in four or higher dimensions, this can be done using the BCFW recursion relation, which involves a complex deformation of two external momenta:

$$p_i \to p_i + z q_i, \;\; p_j \to p_j - z q, \tag{11}$$

where z is a complex number [5]. This deformation preserves momentum conservation since $p_i + p_j$ is invariant. Furthermore, the external momenta will remain on-shell if

$$p_i \cdot q = p_j \cdot q = q^2 = 0. \tag{12}$$

In three dimensions, the only solution to these equations is $q = 0$.

In order to generalize the BCFW approach to three-dimensions, we must allow the deformation to be nonlinear in z. The deformation can be written in terms of spinors as follows:

$$\begin{pmatrix} \lambda_i \\ \lambda_j \end{pmatrix} \to \begin{pmatrix} \frac{z+z^{-1}}{2} & -\frac{z-z^{-1}}{2i} \\ \frac{z-z^{-1}}{2i} & \frac{z+z^{-1}}{2} \end{pmatrix} \begin{pmatrix} \lambda_i \\ \lambda_j \end{pmatrix}. \tag{13}$$

One can define a similar deformation for the fermionic coordinates of the on-shell superspace, which will preserve supermomentum conservation.

After applying the deformation to an on-shell amplitude, it acquires poles in the complex parameter z. Near these poles, the amplitude factorizes into two lower-point on-shell amplitudes, which we denote $\mathcal{A}_L$ and $\mathcal{A}_R$, connected by a propagator. The poles of the amplitude in this factorization channel are therefore given by the roots of $p_f^2(z) = 0$, where f labels the factorization channel and $p_f(z)$ is the momentum in the propagator. If the amplitudes vanish at $z = 0$ and $z = \infty$, it follows that undeformed amplitude $\mathcal{A}_n(z = 1)$ is given by

$$\begin{aligned} &\mathcal{A}_n(z=1) = \\ &\frac{-1}{2\pi i} \sum_{f,i} \int d^3\eta \oint_{z=z_{i,f}} \frac{dz}{z-1} \frac{\mathcal{A}_L(z,\eta)\mathcal{A}_R(z,i\eta)}{p_f(z)^2} \end{aligned} \tag{14}$$

where the index i labels the roots of $p_f^2(z) = 0$, which we denote as $z_{i,f}$. For any channel, $p_f^2(z)$ has the form $a_f z^{-2} + b_f + c_f z^2$, so the roots are obtained by solving a quadratic equation. The amplitudes of the ABJM theory were shown to vanish at $z = 0$ and $z = \infty$ under the deformation in eq. (13), so the recursion relation above is applicable.

4. Dual Superconformal Symmetry of All Tree-Level Amplitudes

We will now argue that the recursion relation in eq. (15) is consistent with dual superconformal symmetry. Note that the dual coordinates defined in eqs. (3,9) are defined up to an overall translation in the dual superspace. We are therefore free to choose the origin of the dual superspace such that

$$x_1 = -x_n, \;\; \theta_1 = q_1 \tag{15}$$

where $q_i = \lambda_i \eta_i$. This choice is convenient because if we apply the deformation in eq (13) to legs 1 and n of an n-point amplitude, this only shifts (x_1, θ_1) in the dual space. Furthermore, the magnitude of x_1 is invariant under the shift, i.e. $x_1(z)^2 = x_1^2$.

Consider a factorization channel where $\mathcal{A}_L$ is a j-point amplitude and $\mathcal{A}_R$ is a $(n-j+2)$-point amplitude. When written in terms of dual coordinates, $\mathcal{A}_L$ is a function of $x_1(z), x_2, ..., x_j$, $\mathcal{A}_R$ is a function of $x_j, x_{j+1}, ..., x_n, x_1(z)$, and the momentum in the propagator connecting the two amplitudes is $p_f(z) = x_1(z) - x_j$. Assuming that $\mathcal{A}_L$ and $\mathcal{A}_R$ transform covariantly under dual inversion, i.e.

$$I\left[\mathcal{A}_L\right] = \sqrt{x_1^2 ... x_j^2}\mathcal{A}_L, I\left[\mathcal{A}_R\right] = \sqrt{x_j^2 ... x_n^2 x_1^2}\mathcal{A}_R, \tag{16}$$

it is not difficult to show that $\mathcal{A}_n$ computed according to eq. (15) also transforms covariantly under dual inversion,

$$I\left[\mathcal{A}_n\right] = \sqrt{x_1 ... x_n^2}\mathcal{A}_n. \tag{17}$$

This statement straightforward to prove if we choose the origin of the dual space according to eq. (15). On the other hand, since the amplitudes are invariant under dual translations, eq. (17) holds for any choice of the origin of the dual superspace. Since the four-point amplitude transforms according to eq. (17), it follows by induction that all the tree-level amplitudes of the ABJM theory have dual conformal symmetry. Moreover, since all the nontrivial dual superconformal generators can be obtained by commuting the dual conformal boost generator described in section 2 with ordinary superconformal generators, it follows that all tree-level amplitudes of the ABJM theory have dual superconformal symmetry.

5. Conclusion

I have sketched a proof that all tree-level amplitudes of the ABJM theory have dual superconformal symmetry. This suggests that the theory may have an amplitude/Wilson-loop duality and that type IIA string theory on $AdS_4 \times CP^3$ may be self-dual under some combination of bosonic and fermionic T-dualities. There are therefore many directions for future study.

Acknowledgements

I would like to thank my co-authors on the papers on which this note was based, notably Dongmin Gang, Yu-tin Huang, Eunkyung Koh, and Sangmin Lee. I would also like to thank the organizers of the Cargese Summer School "String Theory: Formal Developments and Applications" where some of the work described in this note was carried out. My work is supported in part by the US DOE grant DE-FG02-92ER40701.

REFERENCES

1. O. Aharony, O. Bergman, D. L. Jafferis and J. Maldacena, "N=6 superconformal Chern-Simons-matter theories, M2-branes and their gravity duals," JHEP **0810**, 091 (2008) [arXiv:0806.1218 [hep-th]].
2. T. Bargheer, F. Loebbert, C. Meneghelli, "Symmetries of Tree-level Scattering Amplitudes in N=6 Superconformal Chern-Simons Theory," Phys. Rev. **D82**, 045016 (2010) [arXiv:1003.6120 [hep-th]].
3. Y.-t. M. Huang and A. E. Lipstein, "Dual Superconformal Symmetry of N=6 Chern-Simons Theory," JHEP **1011**, 076 (2010) [arXiv:1008.0041 [hep-th]].
4. D. Gang, Y. t. Huang, E. Koh, S. Lee and A. E. Lipstein, arXiv:1012.5032 [hep-th].
5. R. Britto, F. Cachazo, B. Feng and E. Witten, "Direct Proof Of Tree-Level Recursion Relation In Yang-Mills Theory," Phys. Rev. Lett. **94**, 181602 (2005) [arXiv:hep-th/0501052].

Simple current extensions and the permutation orbifold.

M. Maio[a*]

[a]Nikhef, Science Park 105,
1098 XG Amsterdam, The Netherlands

We review extensions by integer spin simple currents in two-dimensional conformal field theories and their application in string theory. In particular, we study the problem of resolving the fixed points of a simple current and apply the formalism to the permutation orbifold.

1. Simple currents and fixed points

(Rational) Conformal field theories [1] not only play a special role within String Theory, but they are also interesting objects in their own right, since they appear in many other contests such as in condensed matter physics.
Standard ways are known to derive new conformal field theories from existing ones. The prototype is the *orbifold* CFT of the form G/H: given a current algebra G, one mods out its symmetry subalgebra H, leaving only H-invariant states plus twisted fields, necessary for modular invariance. Much is known about these coset models.
Another prototype example is the extension via *integer spin simple currents* (see [2] for a review). Extensions are very powerful tools in String Theory, since they allow to perform projections (e.g. GSO projection), impose constraints (such as the β-constraints in Gepner models) or implement field identifications in coset models. An extension is an orbifold-like procedure, that is possible to apply when the CFT has got *simple currents* with integer spin.
A simple current J is by definition a special field of the theory with simple fusion rules,

$$(J) \times (i) \equiv (Ji)\,,$$

having only one contribution on the r.h.s. In practice, what one does in extensions is modding out the discrete symmetry generated by $e^{2\pi i Q_J}$, being $Q_J(i)$ the monodromy charge of the field i with respect to the simple current J. One is left with zero-charge *orbits* under J of the form $(i, Ji, J^2i, \ldots, J^{N-1}i)$, for some integer N. N is called the order of J. It can happen sometimes that $Jf \equiv f$ for some field f. f will be then called a *fixed point* of J.
Fixed points are very delicate objects to handle. In the new, or *extended*, theory each fixed point gives rise to *splitted* fields, in number equal to the order of the current, on which there is a priori no control. As a consequence, the extended S matrix, $\tilde{S}$, cannot be immediately expressed in terms of the S matrix of the original theory. Instead, one has to introduce a set of new matrices, the so-called S^J matrices, one for each simple current J, in terms of which $\tilde{S}$ is parametrized as [3]:

$$\tilde{S}_{(a,i)(b,j)} = \frac{|G|}{\sqrt{|U_a||S_a||U_b||S_b|}} \sum_{J\in G} \Psi_i(J) S^J_{ab} \Psi_j(J)^\star\,.$$

In this formula, the index (a, i) labels the i^{th} field into which a is splitted; the prefactor is a group-theoretical quantity, acting as a normalization; the $\Psi_i(J)$ are the group characters acting as phases; the sum is over all the simple currents used to extend the original theory.
The S^J matrices act only on fixed points of J, i.e. $S^J_{ab} = 0$ if either a or b is not fixed by J. Moreover, modular invariance of the full $\tilde{S}$ matrix implies modular invariance of S^J:

$$S^J \cdot (S^J)^\dagger = 1\,, \qquad (S^J \cdot T^J)^3 = (S^J)^2\,.$$

Hence, in this formalism, the problem of determining the extended S matrix is equivalent to

*Based on a short talk given at the Cargese Summer School 2010.

finding the set of S^J matrices. This is known as the *fixed point resolution* problem.

2. The permutation orbifold

Theories for which the S^J matrices were already known in the past include WZW models and coset theories. Recently, the fixed point problem has been solved for the cyclic permutation orbifold, in the simplified case of two factors:

$$\mathcal{A}_{\rm perm} \equiv \mathcal{A} \times \mathcal{A}/\mathbb{Z}_2 \, .$$

the $\mathbb{Z}_2$ exchanging the two factors. $\mathcal{A}$ denotes an arbitrary CFT.

The field content of the generic permutation orbifold was already known from [4]. It consists of three kinds of fields: *diagonal*, $\phi_{(i,\chi)}$, *off-diagonal*, $\phi_{(mn)}$ with $m < n$, and *twisted*, $\phi_{\widehat{(i,\chi)}}$. Also the S matrix of this orbifold was already known from [5] in terms of the S and T matrices of the original CFT $\mathcal{A}$. We will denote it by S^{BHS}.

If one is interested in performing extensions of this cyclic orbifold, the first thing that must be asked is whether or not it admits simple currents and, in affirmative case, if the simple currents have fixed points. It turns out that the answers to both questions is yes [6–8]. Hence, one has to resolve those fixed points or, equivalently, determine the corresponding S^J matrices. One possible strategy is to give an *ansatz* for S^J which satisfies modular invariance and furthermore is subject to the following constraints:

- for the identity current, $J = 0$, S^J must reduce to S^{BHS};
- the extension by the anti-symmetric component of the identity undoes the permutation orbifold, giving back the tensor product $\mathcal{A} \times \mathcal{A}$ [6];
- the S^J must be consistent with known expressions existing for some WZW models with particular current algebras (e.g. $A(1)$, $B(n)$, $D(2n)$) [6,7].

The explicit expression for the ansatz is given in [8]. There, it is also shown that unitarity and modular invariance are satisfied. Moreover, integrality of the fusion rules has been checked numerically for very large rational CFT's, even though its proof is probably doable. All these non-trivial checks strongly suggest that this is indeed the correct answer.

Acknowledgments

Research supported by the Dutch Foundation for Fundamental Research of Matter (FOM) as part of the program STQG (String Theory and Quantum Gravity). MM would like to thank the organizers of the Cargese Summer School 2010 for their hospitality and the very motivating environment.

REFERENCES

1. A. A. Belavin, A. M. Polyakov and A. B. Zamolodchikov, "Infinite conformal symmetry in two-dimensional quantum field theory," Nucl. Phys. B **241** (1984) 333.
2. A. N. Schellekens and S. Yankielowicz, "Simple currents, modular invariants and fixed points," Int. J. Mod. Phys. A **5** (1990) 2903.
3. J. Fuchs, A. N. Schellekens and C. Schweigert, "A matrix S for all simple current extensions," Nucl. Phys. B **473** (1996) 323 [arXiv:hep-th/9601078].
4. A. Klemm and M. G. Schmidt, "Orbifolds by cyclic permutations of tensor product conformal field theories," Phys. Lett. B **245** (1990) 53.
5. L. Borisov, M. B. Halpern and C. Schweigert, "Systematic approach to cyclic orbifolds," Int. J. Mod. Phys. A **13** (1998) 125 [arXiv:hep-th/9701061].
6. M. Maio and A. N. Schellekens, "Fixed Point Resolution in Extensions of Permutation Orbifolds," Nucl. Phys. B **821** (2009) 577 [arXiv:0905.1632 [hep-th]].
7. M. Maio and A. N. Schellekens, "Complete Analysis of Extensions of $D(n)_1$ Permutation Orbifolds," arXiv:0907.3053 [hep-th].
8. M. Maio and A. N. Schellekens, "Formula for Fixed Point Resolution Matrix of Permutation Orbifolds," Nucl. Phys. B **830** (2010) 116 [arXiv:0911.1901 [hep-th]].

Soft-exactness of tree-level gluon and graviton MHV amplitudes.

David A. McGady[a]

[a]Department of Physics, Princeton University
Princeton, New Jersey 08544, USA

We discuss and present derivations of the must succinct forms for tree-level MHV gluon and MHV graviton scattering amplitudes, through appending soft-factors to lower-point MHV scattering amplitudes. For gluons, we see that the canonical spinor-helicity variables are sufficient to absorb all of the gauge redundancy needed to define transverse gluon polarization vectors. Correspondingly, the tree level gluon MHV scattering amplitudes can be cleanly and efficintly written in terms of spinor-helicity variables–and are described by the famous Parke-Taylor amplitude. However, the canonical spinor-helicity variables do not automatically enforce momentum conservation, and thus are *not* sufficiently redundant to absorb all of the differomorphism invariance that must be built into the graviton soft-factors. Nonetheless, appending graviton soft-factors to lower-point graviton MHV amplitudes yields the simplest known form for MHV graviton amplitudes. We briefly discuss new variables, better suited to describe perturbative scattering amplitudes in quantum gravity.

1. Introduction: MHV and soft factors

It is well known that tree-level gluon scattering amplitudes become very simple when expressed in terms of (kinematical) variables which encapsulate all of the physical information in the asymptotic scattering states: their momentum and their helicity.[1–3] Many different variables accomplish this goal, the simplest of which are the spinor-helicity variables, λ_α and $\tilde{\lambda}_{\dot{\alpha}}$. These variables are best suited to describe massless vectors and tensors, and are defined by:

$$\begin{aligned} &p_\mu = \sigma_\mu^{\alpha\dot{\alpha}}\lambda_\alpha\tilde{\lambda}_{\dot{\alpha}}, \qquad (1)\\ &\langle\lambda^1\lambda^2\rangle = \lambda^{1\alpha}\lambda^2{}_\alpha = \epsilon^{\alpha\beta}\lambda^1_\alpha\lambda^2_\beta = -\langle\lambda^2\lambda^1\rangle, \text{ and}\\ &[\tilde{\lambda}^1\tilde{\lambda}^2] = \tilde{\lambda}^1{}_{\dot{\alpha}}\tilde{\lambda}^{2\dot{\alpha}} = \epsilon_{\dot{\alpha}\dot{\beta}}\tilde{\lambda}^{1\dot{\alpha}}\lambda^{2\dot{\beta}} = -[\tilde{\lambda}^2\tilde{\lambda}^1]. \end{aligned}$$

The most striking example of the simplification in expressions for scattering amplitudes occurs for scattering amplitudes where 2 incoming gluons with negative helicity, 1^- and j^-, scatter into n-2 incoming gluons all of which have positive helicity, $2^+, 3^+, ..., (j-1)^+, (j+1)^+, ..., n^+$. This amplitude, discovered by Parke and Taylor[4], is

$$\mathcal{A}^{\text{MHV}}_{n\ \text{YM}} = \frac{\langle 1,j\rangle^4}{\langle 1,2\rangle ...\langle i,i+1\rangle ...\langle n,1\rangle} \qquad (2)$$

There is no known simple, one-term, form for tree-level MHV graviton scattering. The state-of-the-art is the MHV graviton super-amplitude[5],

$$\mathcal{M}^{\text{MHV}}_{n\ \text{GR}} = \frac{1}{\langle n-1,n\rangle^2}\left(\prod_{a=1}^{n-2}\frac{1}{(\langle a,n-1\rangle\langle an\rangle)^2}\right) \times \sum_{\text{trees}}\prod_{\text{edges }ab}\frac{[ab]}{\langle ab\rangle}\langle a,n-1\rangle\langle an\rangle\langle b,n-1\rangle\langle bn\rangle \qquad (3)$$

where the sum over trees contains $(n-2)^{n-4}$ terms for an n-graviton MHV process. Despite this $\sim n^n$ growth of terms, this super-amplitude is both (a) the most symmetric of all other known forms, having an explicit $S_2 \times S_{n-2}$ permutation invariance with respect to label exchange (all graviton super-amplitudes must have full S_n Bose permutation symmetry), and (b) has the fewest terms of all known forms for the amplitude.

Both amplitudes, for gluons and gravitons, can be derived through appending $n-3$ inverse soft-factors to their respective three-point MHV amplitudes.[6] This derivation highlights the need for new variables which economically encode all of the physical degrees of freedom in gravity, and offers hints towards what they might look like.

2. Soft-exactness and Parke-Taylor.

It is well known[7,8] that, based on elementary properties of the S-matrix and Lorentz-invariance, the amplitude for soft vector emission from a scattering process, $\mathcal{M}$, is given by

$$\begin{aligned}\mathcal{M} &\rightarrow \mathcal{M} \times SF(q_{\rm soft})|_{h\in\{\pm\}} \\ &= \mathcal{M} \times \sum_{i=1}^{n} \lambda_i \frac{p_\mu^i \epsilon_h^\mu(q_{\rm soft})|_{h\in\{\pm\}}}{p_\mu^i q_{\rm soft}^\mu}\end{aligned}$$

where λ_i is the corresponding coupling of the i^{th}-particle in the hard process to the soft vector.

Decomposing gluon amplitudes into color-ordered sub-amplitudes[1], we cyclically label gluons from $1,...,n$. Soft gluon, n+1, with $h = +$, enters into the region between, and only attaches to, gluons 1 and n, thus:

$$\mathrm{SF}^{\rm gluon}_{p_{n+1}\to 0} = \sum_{i=1,n} \frac{p_\mu^i \epsilon_+^\mu \left[p_{n+1(\rm soft)}\right]}{p_\mu^i p_{n+1(\rm soft)}^\mu}$$

In terms of the spinor-helicity variables, this is,

$$\mathrm{SF}^{\rm gluon}_{p_{n+1}\to 0} = \sum_{i=1,n} \frac{\langle \lambda_i \mu\rangle}{\langle \mu\lambda_{p_{n+1}}\rangle\langle\lambda_i\lambda_{p_{n+1}}\rangle},\ \epsilon^+_{\alpha\dot\alpha} = \frac{\mu_\alpha \tilde\lambda_{n+1\dot\alpha}}{\langle\mu\lambda_{n+1}\rangle}.$$

Choice of μ_α corresponds to fixing a guage. Note that, by Schouten, $|A\rangle\langle B,C\rangle + |B\rangle\langle C,A\rangle + |C\rangle\langle A,B\rangle = 0$, these two terms combine into:

$$\mathrm{SF}^{\rm gluon}_{p_{n+1}\to 0} = \frac{\langle n,1\rangle}{\langle n+1,1\rangle\langle n,n+1\rangle} \qquad (4)$$

Gluon soft-factors are thus automatically gauge-invariant. That this is manifest is entirely due to the non-trivial structure of the canonical spinor-helicity variables, λ and $\tilde\lambda$. Multiplying the n-point Parke-Taylor amplitude by this soft-factor, gives the n+1-point Parke-Taylor amplitude:

$$\frac{\langle ij\rangle^4}{\langle 12\rangle...\langle n1\rangle}\frac{\langle n,1\rangle}{\langle n+1,1\rangle\langle n,n+1\rangle} = \frac{\langle ij\rangle^4}{\langle 12\rangle...\langle n+1,1\rangle}$$

MHV scattering amplitudes, at tree-level, in (S)YM are "soft exact." In this narrow sense, the canonical spinor-helicity variables, λ and $\tilde\lambda$, are at once "big" enough to encompass all possible gauges, yet are economical enough to write consistent expressions for tree-level gluon scattering amplitudes without introducing extraneous and un-physical degrees of freedom. This is *not* the case for MHV graviton scattering, below.

3. Graviton MHV scattering amplitudes from inverse-soft-factors.

Weinberg's results are quite similar for soft gravitons attaching to a hard external line in a scattering process[7,8]. The total soft factor is,

$$\mathrm{SF}_{q\to 0} = \sum_{i=1}^{n} \frac{\epsilon^{\mu\nu}_{\rm soft}\ p_{i\mu}\ p_{i\nu}}{p_i\ q_{\rm soft}}$$

We will focus on positive helicity soft-gravitons. Graviton polarization tensors are factorized as,

$$\epsilon^+_{\alpha\dot\alpha\beta\dot\beta}(q_s) = \epsilon^+_{\alpha\dot\alpha}(q_s)\epsilon^+_{\beta\dot\beta}(q_s) = \frac{\mu_\alpha\tilde\lambda_{s\dot\alpha}}{\langle\mu\lambda_s\rangle}\frac{\mu'_\beta\tilde\lambda_{s\dot\beta}}{\langle\mu'\lambda_s\rangle}$$

Where μ_α and μ'_β are the two different reference spinors needed to define the polarization tensor, and $q_s^{\alpha\dot\alpha} = \lambda_s^\alpha\tilde\lambda_s^{\dot\alpha}$ is the soft graviton momentum.

It is convenient to gauge fix the two reference spinors to be equal to two of the physical spinor-helicity variables: $\mu \equiv \lambda_A$ and $\mu' \equiv \lambda_B$. When put in terms of the spinor-helicity variables, the Weinberg soft-factor sum, takes the form

$$\mathrm{SF}_{q\to 0} = \sum_{i=1}^{n} \frac{\langle Ai\rangle\langle Bi\rangle\langle As\rangle\langle Bs\rangle}{(\langle As\rangle\langle Bs\rangle)^2}\frac{[\tilde\lambda_s i]}{\langle\lambda_s i\rangle} \qquad (5)$$

There are several important aspects of this expression. First, the terms in the soft-factor are completely holomorphic in A and B: $\tilde\lambda_A$ and $\tilde\lambda_B$ do not enter into the expression.

Second, through gauge-fixing, two momenta, A and B, must be explicitly singled out. This breaks any possible manifest permutation invariance from S_n down to $S_{n-2}\times S_2$. Choice of a *different* pairs of reference momenta is equivalent to a different choice of gauge. In order for these gauge choices to be equivalent, the overall gravitational charges must be conserved: $\sum_i p_i = 0$.

Terms in the MHV graviton amplitude, "trees," are composed of positive helicity soft-factors appended to lower point amplitudes. Attaching a new graviton, b, to another "hard" graviton, a naively spoils the conservation of momentum: if $\sum_i p_i = 0$ before adding particle b off of particle a, then $q_a + \sum_i p_i \neq 0$, even if q_a is (component-wise) much smaller than in the other n momenta.

Because of the gauge-choice, $\mu = \lambda_A$ and $\mu' = \lambda_B$, we can deform $\tilde\lambda_A$ and $\tilde\lambda_B$, while leaving (a

sum of products of) soft-factors for positive helicity gravitons unchanged.[1] Thus, we can write the contribution to an $n \to n+1-$point MHV amplitude from adding graviton-b off of graviton-a:

$$\mathcal{M}_n^{\rm MHV} \to \mathcal{M}_n^{\rm MHV} \times \frac{\langle Aa\rangle\langle Ab\rangle\langle Ba\rangle\langle Bb\rangle}{(\langle Aa\rangle\langle Ba\rangle)^2} \times \frac{[ab]}{\langle ab\rangle}.$$

In the language of [6], this is called $g_{a\to b}$, which denotes "adding graviton-b off of graviton-a."

To build-up an $n-$point MHV amplitude, we start with three gravitons—$(1, A, B)$. The three point MHV super-amplitude is $1/(\langle n-1, n\rangle\langle 1n\rangle\langle 1, n-1\rangle)^2$, where $A = n$, $B = n-1$. We then act on $\mathcal{M}_3^{\rm MHV}$ with a series of inverse-soft-factors, of the form $\prod_{i=2}^{n-2} g_{i\to\alpha_{i-1}}$, where $k \geq \alpha_k > 0$.

This gives the term in the $n-$point MHV amplitude coming from adding particle α_1 off of particle 1, then particle 3 added off of particle $\alpha_2 \in \{1, 2\}$, then particle 4 added off of particle $\alpha_3 \in \{1, 2, 3\}$, etc. all the way upto particle n-2 added off of particle $\alpha_{n-3} \in \{1, 2, ..., n-3\}$. This defines a "tree" (graph-theory term). To get the full amplitude, one must sum over all trees. Individual "trees" are of the form:

$$\begin{aligned}
&\left\{\mathcal{M}_3(1, n-1, n)\right\} \times \prod_{k=2}^{n-2} g_{k\to\alpha_{k-1}} \\
&\left\{\frac{1}{\langle n-1,\ n\rangle^2} \times \frac{1}{\langle 1, n\rangle^2\langle 1, n-1\rangle^2}\right\} \times \\
&\prod_{k=2}^{n-2} \frac{\langle nk\rangle\langle n-1, k\rangle\langle n\alpha_{k-1}\rangle\langle n-1, \alpha_{k-1}\rangle}{\langle kn\rangle^2\langle k, n-1\rangle^2} \frac{[k\alpha_{k-1}]}{\langle k\alpha_{k-1}\rangle} \\
&= \frac{1}{\langle n-1,\ n\rangle^2} \prod_{\rm vertices} \frac{1}{\langle an\rangle^2\langle a, n-1\rangle^2} \\
&\prod_{\rm edges} \frac{[ab]}{\langle ab\rangle}\langle na\rangle\langle n-1,\ a\rangle\langle nb\rangle\langle n-1,\ b\rangle
\end{aligned}$$

Summing over all trees reproduces Eq.(3).[5,6]

4. Conservation of momentum, permutation invariance, and new variables.

This derivation treats both labels n-1 and n symmetrically, and labels 1...n-2 symmetrically. Correspondingly, it manifests only a sub-set of the full S_n permutation invariance in graviton super-amplitudes. Showing permutation invariance with respect to mixing the "reference" labels and "non-reference" labels, is done by changing the gauge: this requires momentum conservation. To go beyond, we must work with variables which enforce momentum conservation from the outset.

We define $\tilde{\lambda}_{\dot\alpha}^a \equiv \mu_{\dot\alpha}^{abc}\langle bc\rangle$: labels a- and b are implicitly summed, and $\mu_{\dot\alpha}^{abc}$ is totally antisymmetric in abc. Schouten and antisymmetry of $\mu_{\dot\alpha}^{abc}$ automatically imply momentum conservation:

$$\sum_{a=1}^{n} p_a^\mu = \frac{1}{3}\sum_{abc} \mu^{abc}\{|a\rangle\langle bc\rangle + |b\rangle\langle ca\rangle + |c\rangle\langle ab\rangle\} = 0.$$

In these variables, $\mathcal{M}_4^{\rm MHV}$ is fully S_4 invariant:

$$\mathcal{M}_4(\lambda_\alpha, \mu_{\dot\alpha}^{abc}) \quad = \quad \frac{\epsilon_{abcd}\mu^{abc}\mu^{d\alpha\beta}\langle\alpha\beta\rangle}{\prod_{1\leq ii<j\leq 4}\langle\lambda_i\lambda_j\rangle}. \qquad (6)$$

μs have their own set of gauge-redundancies: $\mu_{\dot\alpha}^{abc} \to \mu_{\dot\alpha}^{abc} + \delta\mu_{\dot\alpha}^{abc} = \mu_{\dot\alpha}^{abc} + M_{\alpha\dot\alpha}^{abcd}\lambda_d^\alpha$. For totally antisymmetric M^{abcd}s, the $\tilde\lambda$s are unchanged.[9]

Invariance with respect to the μs redundancy is equivalent to both momentum conservation and S_n-permutation invariance. However, it is unclear how to go beyond $\mathcal{M}_4^{\rm MHV}$ with the $\mu_{\dot\alpha}^{abc}$s.

Acknowledgements

I would like to thank Nima Arkani-Hamed, Jaroslav Trnka, Donal O'Connell, Henriette Elvang, Michael Kiermaier, and Jacob Bourjaily for helpful and stimulating conversations.

REFERENCES

1. L. Dixon, arXiv:hep-ph/9601359v2.
2. E. Witten, arXiv:hep-th/0312171v2.
3. N. Arkani-Hamed, F. Cachazo, and J. Kaplan, arXiv:0808.1446v2 [hep-th].
4. S. J. Parke and T. R. Taylor, *Phys. Rev. Lett.* **56**, 2459 (1986).
5. D. Nguyen, M. Spradlin, A. Volovich, and C. Wen, arXiv:0907.2276.
6. N. Arkani-Hamed and F. Cachazo, private communication.
7. S. Weinberg, *Phys. Rev.* **140** (1965) B516.
8. S. Weinberg, *Phys. Rev.* **135** (1964) B1049.
9. H. Elvang, M. Kiermaer, private communication.

[1] This is true if the soft gravitons are all in the same gauge: $\mu_i = \lambda_A$ and $\mu_i' = \lambda_B$, $\forall i \in \{\text{soft}\}$.

Simple current extensions and the permutation orbifold.

M. Maio[a*]

[a]Nikhef, Science Park 105,
1098 XG Amsterdam, The Netherlands

We review extensions by integer spin simple currents in two-dimensional conformal field theories and their application in string theory. In particular, we study the problem of resolving the fixed points of a simple current and apply the formalism to the permutation orbifold.

1. Simple currents and fixed points

(Rational) Conformal field theories [1] not only play a special role within String Theory, but they are also interesting objects in their own right, since they appear in many other contests such as in condensed matter physics.
Standard ways are known to derive new conformal field theories from existing ones. The prototype is the *orbifold* CFT of the form G/H: given a current algebra G, one mods out its symmetry subalgebra H, leaving only H-invariant states plus twisted fields, necessary for modular invariance. Much is known about these coset models.
Another prototype example is the extension via *integer spin simple currents* (see [2] for a review). Extensions are very powerful tools in String Theory, since they allow to perform projections (e.g. GSO projection), impose constraints (such as the β-constraints in Gepner models) or implement field identifications in coset models. An extension is an orbifold-like procedure, that is possible to apply when the CFT has got *simple currents* with integer spin.
A simple current J is by definition a special field of the theory with simple fusion rules,

$$(J) \times (i) \equiv (Ji)\,,$$

having only one contribution on the r.h.s. In practice, what one does in extensions is modding out the discrete symmetry generated by $e^{2\pi i Q_J}$, being $Q_J(i)$ the monodromy charge of the field i with respect to the simple current J. One is left with zero-charge *orbits* under J of the form $(i, Ji, J^2i, \ldots, J^{N-1}i)$, for some integer N. N is called the order of J. It can happen sometimes that $Jf \equiv f$ for some field f. f will be then called a *fixed point* of J.
Fixed points are very delicate objects to handle. In the new, or *extended*, theory each fixed point gives rise to *splitted* fields, in number equal to the order of the current, on which there is a priori no control. As a consequence, the extended S matrix, $\tilde{S}$, cannot be immediately expressed in terms of the S matrix of the original theory. Instead, one has to introduce a set of new matrices, the so-called S^J matrices, one for each simple current J, in terms of which $\tilde{S}$ is parametrized as [3]:

$$\tilde{S}_{(a,i)(b,j)} = \frac{|G|}{\sqrt{|U_a||S_a||U_b||S_b|}} \sum_{J\in G} \Psi_i(J) S^J_{ab} \Psi_j(J)^\star\,.$$

In this formula, the index (a, i) labels the i^{th} field into which a is splitted; the prefactor is a group-theoretical quantity, acting as a normalization; the $\Psi_i(J)$ are the group characters acting as phases; the sum is over all the simple currents used to extend the original theory.
The S^J matrices act only on fixed points of J, i.e. $S^J_{ab} = 0$ if either a or b is not fixed by J. Moreover, modular invariance of the full $\tilde{S}$ matrix implies modular invariance of S^J:

$$S^J \cdot (S^J)^\dagger = 1\,, \qquad (S^J \cdot T^J)^3 = (S^J)^2\,.$$

Hence, in this formalism, the problem of determining the extended S matrix is equivalent to

*Based on a short talk given at the Cargese Summer School 2010.

finding the set of S^J matrices. This is known as the *fixed point resolution* problem.

2. The permutation orbifold

Theories for which the S^J matrices were already known in the past include WZW models and coset theories. Recently, the fixed point problem has been solved for the cyclic permutation orbifold, in the simplified case of two factors:

$$\mathcal{A}_{\rm perm} \equiv \mathcal{A} \times \mathcal{A}/\mathbb{Z}_2 \,.$$

the $\mathbb{Z}_2$ exchanging the two factors. $\mathcal{A}$ denotes an arbitrary CFT.

The field content of the generic permutation orbifold was already known from [4]. It consists of three kinds of fields: *diagonal*, $\phi_{(i,\chi)}$, *off-diagonal*, $\phi_{(mn)}$ with $m < n$, and *twisted*, $\phi_{\widehat{(i,\chi)}}$. Also the S matrix of this orbifold was already known from [5] in terms of the S and T matrices of the original CFT $\mathcal{A}$. We will denote it by S^{BHS}.

If one is interested in performing extensions of this cyclic orbifold, the first thing that must be asked is whether or not it admits simple currents and, in affirmative case, if the simple currents have fixed points. It turns out that the answers to both questions is yes [6–8]. Hence, one has to resolve those fixed points or, equivalently, determine the corresponding S^J matrices. One possible strategy is to give an *ansatz* for S^J which satisfies modular invariance and furthermore is subject to the following constraints:

- for the identity current, $J = 0$, S^J must reduce to S^{BHS};
- the extension by the anti-symmetric component of the identity undoes the permutation orbifold, giving back the tensor product $\mathcal{A} \times \mathcal{A}$ [6];
- the S^J must be consistent with known expressions existing for some WZW models with particular current algebras (e.g. $A(1)$, $B(n)$, $D(2n)$) [6,7].

The explicit expression for the ansatz is given in [8]. There, it is also shown that unitarity and modular invariance are satisfied. Moreover, integrality of the fusion rules has been checked numerically for very large rational CFT's, even though its proof is probably doable. All these non-trivial checks strongly suggest that this is indeed the correct answer.

Acknowledgments

Research supported by the Dutch Foundation for Fundamental Research of Matter (FOM) as part of the program STQG (String Theory and Quantum Gravity). MM would like to thank the organizers of the Cargese Summer School 2010 for their hospitality and the very motivating environment.

REFERENCES

1. A. A. Belavin, A. M. Polyakov and A. B. Zamolodchikov, "Infinite conformal symmetry in two-dimensional quantum field theory," Nucl. Phys. B **241** (1984) 333.
2. A. N. Schellekens and S. Yankielowicz, "Simple currents, modular invariants and fixed points," Int. J. Mod. Phys. A **5** (1990) 2903.
3. J. Fuchs, A. N. Schellekens and C. Schweigert, "A matrix S for all simple current extensions," Nucl. Phys. B **473** (1996) 323 [arXiv:hep-th/9601078].
4. A. Klemm and M. G. Schmidt, "Orbifolds by cyclic permutations of tensor product conformal field theories," Phys. Lett. B **245** (1990) 53.
5. L. Borisov, M. B. Halpern and C. Schweigert, "Systematic approach to cyclic orbifolds," Int. J. Mod. Phys. A **13** (1998) 125 [arXiv:hep-th/9701061].
6. M. Maio and A. N. Schellekens, "Fixed Point Resolution in Extensions of Permutation Orbifolds," Nucl. Phys. B **821** (2009) 577 [arXiv:0905.1632 [hep-th]].
7. M. Maio and A. N. Schellekens, "Complete Analysis of Extensions of $D(n)_1$ Permutation Orbifolds," arXiv:0907.3053 [hep-th].
8. M. Maio and A. N. Schellekens, "Formula for Fixed Point Resolution Matrix of Permutation Orbifolds," Nucl. Phys. B **830** (2010) 116 [arXiv:0911.1901 [hep-th]].

String Vacua in Exceptional Generalized Geometry

F. Orsi[a*]

[a]Institut de Physique Theorique, CEA Saclay Orme des Merisiers 91191 Gif-sur-Yvette

In this note we outline the main results of a forthcoming publication [1], in collaboration with M. Graña. We analyze Minkowski vacua in the language of exceptional generalized geometry (EGG). Once we identify a twisted derivative operator that contains all NS and RR fluxes and transforms covariantly under the $E_{7(7)}$ U-duality group, we find the differential equations on the structures which parameterize the vector and hypermultiplet moduli spaces of $\mathcal{N}=2$ supergravity, and interpret them in terms of integrability of such structures. We pursue this analysis for both $\mathcal{N}=1$ and $\mathcal{N}=2$ vacua.

1. Introduction

One of the main advantages of study supersymmetryic backgrounds is that the compactification mechanism is restricted to specific classes of internal manifolds. When no fluxes are considered, supersymmetry can be re-stated in the Calabi-Yau condition [2]. Such manifolds separately satisfy an *algebraic* condition, namely the existence of a globally defined, nowhere vanishing internal spinor, and a *differential* one, that the spinor is covariantly constant. On the other hand fluxes, combined with the warped nature of the compactification, play a fundamental role in string theory for the possibility of fixing moduli and providing a hierarchy of scales [3]. Whenever fluxes are allowed, they backreact on the geometry yielding a deviation from the Calabi-Yau case [4].
Reformulating compactifications with fluxes in a geometric description has been very much guided by the framework of generalized geometry developed by Hitchin [5]. Generalized complex geometry (GCG) can be intuitively described as complex geometry applied to the generalized tangent bundle of the space, consisting of the sum of tangent and cotangent bundles $TM \oplus T^*M$.
The language of GCG was adopted in [6,7] to characterise $\mathcal{N}=1$ vacua, first identifying a pair of pure spinors (Φ^+, Φ^-), then by showing which kind of differential condition they should satisfy in order to describe a vacuum. The main feature of GCG is the existence of a 1-to-1 correspondence between a pure spinor and a generalized almost complex structure (GACS) defined on $TM \oplus T^*M$. In the GCG setting the NS sector of the type II string theory is absorbed as part of the geometry, while this is not the case for the RR fields.
Our interest is to study supersymmetry conditions from the point of view of exceptional generalized geometry (EGG), allowing the full flux content to be geometrized, and in particular to obtain a description of the $\mathcal{N}=2$ case independently of the $\mathcal{N}=1$. The generalized tangent bundle $TM \oplus T^*M$ should be once more enlarged in order to include the extra symmetries induced by gauge transformations of the RR fields. The analysis amounts then to interpret the susy equations in terms of integrability of the corresponding EGG algebraic structures (defined on the exceptional generalized tangent space).

2. Integrability conditions and supersymmetry

We illustrate in this section how conditions for vacua can be recast in terms of integrability of some algebraic structures, which in the cases discussed below will be a pair of compatible pure spinors. A GACS is said to be *integrable* if its associate pure spinor is closed. In each of the cases presented below the differential operator has the form of a twisted derivative under the gauge fields

*francesco.orsi@cea.fr

which are geometrized in the corresponding theory. At the end of this step by step analysis, we will interpret the GCG case as an intermediate step which naturally leads to the generalization achieved by EGG.
When considering $\mathcal{N}=2$ supersymmetry in absence of fluxes, it turns out that the condition to have a vacua can be stated as

$$d\Phi^+ = 0, \qquad d\Phi^- = 0 \tag{2.1}$$

which means that both GACS are integrable. Similarly, conditions for $\mathcal{N}=2$ supersymmetric vacua with NS only [10] are described using the criterion of twisted integrability under the H-field

$$d_H\Phi^+ = 0, \qquad d_H\Phi^- = 0 \tag{2.2}$$

being $d_H \equiv d - H\wedge = e^B d\, e^{-B}$.
The conditions for Minkowski vacua preserving $\mathcal{N}=1$ supersymmetry in the presence or NS and RR fluxes have been obtained in [7] in the language of GCG, and can alternatively be obtained from extremizing the superpotential $\mathcal{W} = z^a\mathcal{P}_a$ of the four-dimensional $N=1$ theory [11] and setting the D-term $\mathcal{D} = r^a\mathcal{P}_a$ to zero [8,9]. When sources are present, these read

$$d_H(e^{2A}\Phi'^+) = 0 \tag{2.3}$$

$$d_H(e^{A}\mathrm{Re}\Phi'^-) = 0 \tag{2.4}$$

$$d_H(e^{3A}\mathrm{Im}\Phi'^-) = *e^{3A}s(F^+) \tag{2.5}$$

where F^+ are the RR fluxes and s is an involution operator. Then $\mathcal{N}=1$ vacua require one of the pure spinors to be closed (and therefore the generalized almost complex structure associated is integrable), while RR fluxes act as a defect for integrability of the other structure.

3. Description of vacua using EGG

To take into account the complete flux content of the type II[2] theory we define a generalized connection $\mathcal{F}$, which features exterior derivatives of all the gauge fields content [13]. The twisted derivative operator has the following form

$$\mathcal{D} = \nabla + \mathcal{F}, \tag{3.1}$$

[2]We consider type IIA in this setting.

where $\mathcal{F}$ encodes the twisting of all the gauge fields as

$$\mathcal{F} = e^B e^{-\tilde{B}} e^{-C} \nabla\, e^C e^{\tilde{B}} e^{-B}\big|_{\mathbf{912}} \tag{3.2}$$

the bar denoting the projection on the **912** representation of $E_{7(7)}$, and ∇ being the ordinary Levi-Civita covariant derivative. The *algebraic* structures which play the analogous role of the pure spinors in the EGG formalism have been constructed in [12] and amount to an $SU(2)_R$ singlet L and a triplet K_a, which respectively parameterize the vector and the hypermultiplet spaces of the $\mathcal{N}=2$ supergravity theory.
The analysis of the corresponding *differential* condition lead to the EGG version of the equations (2.3-2.5) for $\mathcal{N}=1$ vacua

$$\big[\mathcal{D}(e^{2A-\phi}L)\big]|_{\mathbf{133}} = 0 \tag{3.3}$$

$$\big[\mathcal{D}(e^{A-\phi}K_1)\big]|_{\mathbf{56}} = 0 \tag{3.4}$$

$$\big[\mathcal{D}e^{3A-\phi}(K_3 + iK_2)\big]_{(1,0)}|_{\mathbf{56}} = 0 \tag{3.5}$$

where the vertical bar stands for a projection on the corresponding $E_{7(7)}$ representation.
As conjectured in [12], $\mathcal{N}=1$ supersymmetry does indeed require on one hand closure of both L (3.3) and r^aK_a (3.4), where r^a is a vector pointing in the direction of the $\mathcal{N}=1$ supersymmetry preserved. On the other hand, the structure along the complex orthogonal direction is closed upon projecting onto the holomorphic subbundle defined by L (3.5).
The equations for $\mathcal{N}=2$ vacua looks formally as (3.3)-(3.5), however the analysis reveal that the naive conjecture that all structures are closed turns out not to be true. This implies that the translation between integrability and closure is not straightforward.

REFERENCES

1. M. Graña, F. Orsi, to appear.
2. P. Candelas, G. T. Horowitz, A. Strominger and E. Witten, "Vacuum Configurations For Superstrings," Nucl. Phys. B **258** (1985) 46.
3. S. B. Giddings, S. Kachru and J. Polchinski, "Hierarchies from fluxes in string compactifications," Phys. Rev. D **66**, 106006 (2002) [arXiv:hep-th/0105097].

4. A. Strominger, "Superstrings with Torsion," Nucl. Phys. B **274** (1986) 253.; C. M. Hull, "Superstring Compactifications With Torsion And Space-Time Supersymmetry," in *Turin 1985, Proceedings, Superunification and Extra Dimensions*, 347.
C. M. Hull, "Compactifications Of The Heterotic Superstring," Phys. Lett. B **178** (1986) 357.
5. N. Hitchin, "Generalized Calabi-Yau manifolds," Quart. J. Math. Oxford Ser. **54** (2003) 281 [arXiv:math/0209099].
M. Gualtieri, "Generalized Complex Geometry," Oxford University DPhil thesis (2004) [arXiv:math.DG/0401221].
6. M. Graña, R. Minasian, M. Petrini and A. Tomasiello, "Supersymmetric backgrounds from generalized Calabi-Yau manifolds," JHEP **0408** (2004) 046 [arXiv:hep-th/0406137].
7. M. Graña, R. Minasian, M. Petrini and A. Tomasiello, "Generalized structures of N=1 vacua," JHEP **0511** (2005) 020 [arXiv:hep-th/0505212].
8. P. Koerber and L. Martucci, "From ten to four and back again: how to generalize the geometry," JHEP **0708** (2007) 059 [arXiv:0707.1038 [hep-th]].
9. D. Cassani and A. Bilal, 'Effective actions and N=1 vacuum conditions from SU(3) x SU(3) compactifications," JHEP **0709**, 076 (2007) [arXiv:0707.3125 [hep-th]].
10. C. Jeschek and F. Witt, "Generalised G(2)-structures and type IIB superstrings," JHEP **0503**, 053 (2005) [arXiv:hep-th/0412280].
11. M. Grana, J. Louis and D. Waldram, "Hitchin functionals in N = 2 supergravity," JHEP **0601**, 008 (2006) [arXiv:hep-th/0505264].
M. Grana, J. Louis and D. Waldram, "SU(3) x SU(3) compactification and mirror duals of magnetic fluxes," JHEP **0704**, 101 (2007) [arXiv:hep-th/0612237].
12. M. Graña, J. Louis, A. Sim and D. Waldram, "E7(7) formulation of N=2 backgrounds," JHEP **0907** (2009) 104 [arXiv:0904.2333 [hep-th]].
13. G. Aldazabal, E. Andres, P. G. Camara and M. Graña, "U-dual fluxes and Generalized Geometry," arXiv:1007.5509 [hep-th].

Energy–Energy Correlation in $\mathcal{N} = 4$ Supersymmetric Yang–Mills

Z. Peng[a]

[a] Institut de Physique Théorique, CEA-Saclay,
F-91191 Gif-sur-Yvette cedex, France

We outline the perturbative calculation, through next-to-leading order, of the energy-energy correlation function in $\mathcal{N} = 4$ supersymmetric Yang–Mills. We add a perturbation $H\mathcal{L}_{\mathcal{N}=4}$ to the theory, and calculate amplitudes for the decay of the scalar field H. In order to obtain a finite result for observables such as the energy-energy correlation function, we have to combine the one-loop virtual contribution and the real emission one.

1. Introduction

Next-to-leading order (NLO) calculations in gauge theory are important to collider physics. Many effective techniques were developed in recent years to perform calculations of amplitudes. We made use of these methods, especially BCFW [1,2] and unitarity [7,8,3], to advance our project.

We study $\mathcal{N} = 4$ supersymmetric Yang–Mills coupled to a massive scalar field H. The scalar is coupled to the $\mathcal{N} = 4$ multiplet via the operator $H\mathcal{L}_{\mathcal{N}=4}$. Unlike the analagous effective operator in the Standard Model, H is really just a source of momentum, and is not involved to any spontaneous symmetry breaking. We calculate the decay amplitudes of H and integrate their squares or interferences over phase space. Our ultimate aim is to compare the energy-energy correlation function at NLO with the results obtained in 'conformal collider physics' [4] and to thereby improve our understanding of the AdS/CFT correspondence.

2. Calculations of the Amplitudes

We can use the BCFW recursion relations to generate tree-level amplitudes particle type by type. Alternatively, we may use the supersymmetric recursion relations explained in [5]. We introduce two new amplitudes using Grassmann numbers η,

$$\begin{aligned} A^{\text{tree}}(H,\, 1_g^-, 2_g^-) &= -\delta^4(P_1 + P_2 - P_H)\, \langle 1\, 2\rangle^2 \\ &\quad \times \prod_{A=1}^{4} \eta_1^A \eta_2^A\,, \qquad (1) \\ A^{\text{tree}}(H,\, 1_g^+, 2_g^+) &= -\delta^4(P_1 + P_2 - P_H)[1\, 2]^2\,. \end{aligned}$$

These two amplitudes were computed using Feynmann diagrams in ref. [6]. The tree-level amplitudes for H plus four particles can be generated via supersymmetric recursion relations. Their collinear limits can be checked using splitting amplitudes [7].

For the one-loop amplitudes for H plus three particles, we used generalized unitarity [3,8].

3. Calculations of the Leading-Order Energy-Energy Correlation Function

The energy–energy correlation function is defined as follows,

$$\begin{aligned} \frac{d\Sigma}{d\cos\chi} &= \sum_{i,j} \int dPS_n |A|^2 \frac{E_i E_j}{E_{\text{total}}^2} \\ &\quad \times \delta(\cos\theta_{ij} - \cos\chi)\,, \qquad (2) \end{aligned}$$

where E_{total} is the center-of-mass energy.

We add up the squares of color-ordered three-parton amplitudes for all particle types and integrate the result over three-particle phase space in $D = 4 - 2\epsilon$ dimensions. With $u = \frac{1-\cos\chi}{2}$, $\omega = \text{Cot}^2(\chi/2)$ and taking $0 < \chi < \pi$ (thereby avoiding singular contributions at $\chi = 0, \pi$ or

$u = 0, 1$), we obtain,

$$\begin{aligned}\frac{d\Sigma}{d\cos\chi} &\propto (1-2\epsilon)((1-u)u)^{-\epsilon-1} \\ &\quad \times {}_2F_1(1-2\epsilon, 1-2\epsilon; 2-4\epsilon; u) \\ &\propto -\frac{\ln(1-u)}{(1-u)u^2} \quad (\epsilon \to 0) \\ &\propto \frac{1}{\sin^2\chi}(1+\omega)\ln\left(1+\omega^{-1}\right).\end{aligned}$$

4. Towards the NLO Energy-Energy Correlation Function

The finiteness of the full NLO correction emerges when adding the one-loop (virtual) contribution to the real emission one. The former can be obtained directly by integrating the interference of the tree and one-loop three-parton amplitudes over three-particle phase space in $D = 4-2\epsilon$ dimension.

For the real emission contribution, we hope to find several master integrals as a basis for the energy-energy correlation function. We expect to calculate these integrals in two different ways: direct integration over the four-particle D-dimensional phase space; and calculation of a corresponding loop integral followed by use of a unitarity relation. Ref. [9] explains the latter approach, and in particular how to use a unitarity relation to reproduce the following master integrals for four-particle cross section,

R_4 = 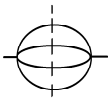 = $\int dPS_4$

R_6 = 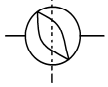 = $\int dPS_4 \frac{1}{s_{124}s_{134}}$

$R_{8,a}$ = 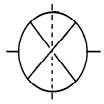 = $\int dPS_4 \frac{1}{s_{13}s_{23}s_{14}s_{24}}$

$R_{8,b}$ = 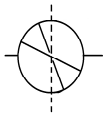 = $\int dPS_4 \frac{1}{s_{13}s_{23}s_{123}s_{234}}$

Inspired by these integrals, we choose the master integrals,

C_4 = $\int dPS_4 E_2 E_3 \delta(\cos\theta_{23} - c)$

$C_{6,a}$ = 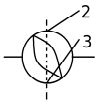 = $\int dPS_4 \frac{E_2 E_3 \delta(\cos\theta_{23} - c)}{s_{124}s_{134}}$

$C_{6,b}$ = 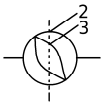 = $\int dPS_4 \frac{E_2 E_3 \delta(\cos\theta_{23} - c)}{s_{123}s_{134}}$

$C_{6,c}$ = 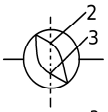 = $\int dPS_4 \frac{E_2 E_3 \delta(\cos\theta_{23} - c)}{s_{123}s_{234}}$

$C_{8,a}$ = 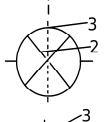 = $\int dPS_4 \frac{E_2 E_3 \delta(\cos\theta_{23} - c)}{s_{13}s_{23}s_{14}s_{24}}$

$C_{8,b}$ = 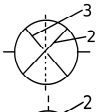 = $\int dPS_4 \frac{E_2 E_3 \delta(\cos\theta_{23} - c)}{s_{12}s_{24}s_{13}s_{34}}$

$C_{8,c}$ = 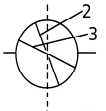 = $\int dPS_4 \frac{E_2 E_3 \delta(\cos\theta_{23} - c)}{s_{12}s_{123}s_{24}s_{234}}$

$C_{8,d}$ = 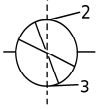 = $\int dPS_4 \frac{E_2 E_3 \delta(\cos\theta_{23} - c)}{s_{12}s_{124}s_{13}s_{134}}$

for the energy-energy correlation function. We have calculated several of these integrals, and are working on the remainder. Once we obtain expressions for them, we can write the sum of the virtual contribution and real-emission one explicitly and cancel all infrared singularities to obtain a finite result.

5. Summary

We have outlined how to calculate the energy-energy correlation function in $\mathcal{N} = 4$ supersymmetric Yang–Mills.

REFERENCES

1. R. Britto, F. Cachazo and B. Feng, Nucl. Phys. B 715, 499 (2005) [hep-th/0412308].
2. R. Britto, F. Cachazo, B. Feng and E. Witten, Phys. Rev. Lett. 94, 181602 (2005) [hep-th/0501052].

3. D. Forde, Phys. Rev. D 75: 125019 (2007) [hep-ph/0704.1835]
4. D. M. Hofman, J. Maldacena, JHEP 0805:012, (2008) [hep-th/0803.1467]
5. Andreas Brandhuber, Paul Heslop, Gabriele Travaglini, Phys. Rev. D78: 125005, (2008) [hep-th/0807.4097]
6. S.D. Badger, E. W. N. Glover, Valentin V. Khoze JHEP 0503: 023, (2005) [hep-th/0412275]
7. Z. Bern, L. J. Dixon, D. C. Dunbar and D. A. Kosower, Nucl. Phys. B **425**, 217 (1994) [hep-ph/9403226]; Nucl. Phys. B **435**, 59 (1995) [hep-ph/9409265].
8. Z. Bern, L. J. Dixon and D. A. Kosower, Nucl. Phys. B **513**, 3 (1998) [hep-ph/9708239]; Z. Bern, L. J. Dixon and D. A. Kosower, JHEP **0408**, 012 (2004) [hep-ph/0404293]; R. Britto, F. Cachazo and B. Feng, Nucl. Phys. B **725**, 275 (2005) [hep-th/0412103].
9. A. Gehrmann-De Ridder, T. Gehrmann, G. Heinrich, Nucl. Phys. B 682:265-288, (2004) [hep-ph/0311276]

Gravitational Corrections to Non-Gauge Interactions

Andreas Rodigast[a*], Theodor Schuster[a†]

[a]Institut für Physik, Humboldt-Universität zu Berlin, Newtonstraße 15, D-12489 Berlin, Germany

We compute the lowest order quantum gravitational corrections to Yukawa and φ^4 interactions.

Einstein's general relativity yields an elegant and successful description of gravity on macroscopic scales, but is—in its perturbatively quantized form—ill-suited as a fundamental theory because of its non-renormalizabillity [1]. Nevertheless, when treated as an effective field theory, perturbatively quantized Einstein gravity can be used to determine predictions of quantum gravity for energies well below the Planck scale [2].

In this context, the gravitational corrections to the running of gauge couplings are subject of an intriguing and ongoing discussion [3]. The gravitational contributions to the running of the couplings of non-gauge interactions on the other hand were neglected for a long time. In [4], we considered the lowest order quantum gravitational corrections to the Yukawa and φ^4 interactions. The masses of the matter fields naturally give dimensionful parameters which open the possibillity of logarithmically divergent gravitational contributions. Similar models were recently examined using non-standard field theory methods [5].

Our toy model consists of a massive real scalar φ and a massive Dirac fermion ψ. Both fields are minimally coupled to gravity and can interact via a Yukawa and a φ^4 interaction

$$\begin{aligned}\mathcal{L} = \sqrt{-\boldsymbol{g}}\Big[\overline{\psi}(i\boldsymbol{\not{D}} - m_\psi)\psi + \tfrac{1}{2}\boldsymbol{g}^{\mu\nu}\partial_\mu\varphi\partial_\nu\varphi \\ -\tfrac{1}{2}m_\varphi^2\varphi^2 - g\,\varphi\overline{\psi}\psi - \tfrac{\lambda}{4!}\varphi^4\Big] + \tfrac{2}{\kappa^2}\sqrt{-\boldsymbol{g}}\boldsymbol{R}\,.\end{aligned} \tag{1}$$

Here κ is the gravitational coupling, related to Newton's constant by $\kappa^2 = 32\pi\, G_{\text{Newton}}$, g is the Yukawa coupling, and λ is the φ^4 coupling constant.

*rodigast@physik.hu-berlin.de
†theodor.schuster@physik.hu-berlin.de

We expand the metric $\boldsymbol{g}_{\mu\nu}$ around the flat background $\boldsymbol{g}_{\mu\nu} = \eta_{\mu\nu} + \kappa\, h_{\mu\nu}$, with the symmetric tensor field $h_{\mu\nu}$ being the graviton and fix the gauge freedom of isomorphism transformations using the de Donder gauge condition $G_\mu = \partial^\nu h_{\mu\nu} - \frac{1}{2}\partial_\mu h^\nu{}_\nu$.

The dependence of the running couplings on the energy scale μ is determined by their β functions

$$\beta_{g_i} = \mu\frac{\mathrm{d}g_i}{\mathrm{d}\mu}\,. \tag{2}$$

We use dimensional regularization and the Minimal Subtraction scheme. Below, we only give the lowest order gravitational corrections $\sim \kappa^2$ and omit the $\mathcal{O}(\kappa^0)$ terms.

The diagrams in 1(a) lead to the following contributions to the wave function renormalizations

$$\begin{aligned} Z_\psi - 1 &= \frac{\kappa^2}{16\pi^2}\frac{1}{4}m_\psi^2\frac{2}{d-4}\,, \\ Z_\varphi - 1 &= \frac{\kappa^2}{16\pi^2}m_\varphi^2\frac{2}{d-4} \end{aligned} \tag{3}$$

and to the mass counterterms

$$\begin{aligned} Z_{m_\psi} - 1 &= \frac{\kappa^2}{16\pi^2}\frac{1}{4}m_\psi^2\frac{2}{d-4}\,, \\ Z_{m_\varphi^2} - 1 &= \frac{\kappa^2}{16\pi^2}m_\varphi^2\frac{2}{d-4}\,. \end{aligned} \tag{4}$$

These relate the renormalized and bare masses

$$m_{\psi 0} = Z_{m_\psi}Z_\psi^{-1}m_\psi\,, \quad m_{\varphi 0}^2 = Z_{m_\varphi^2}Z_\varphi^{-1}m_\varphi^2\,. \tag{5}$$

Since for both the fermion and the scalar the gravitational wavefunction renormalization (3) and the mass counterterm (4) are equal, there are

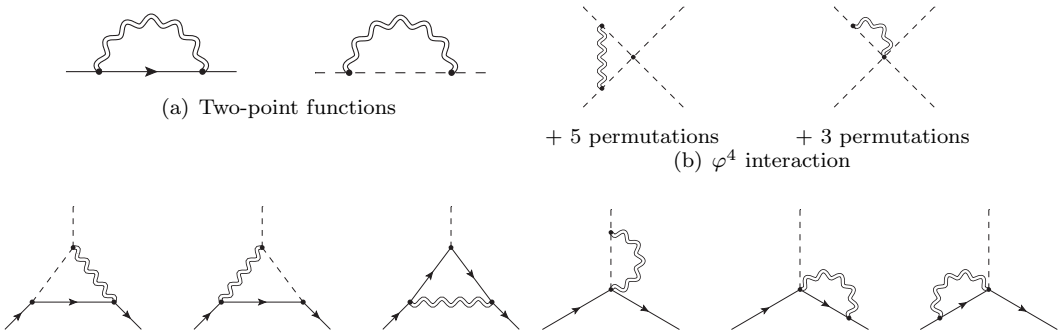

Figure 1. One-loop graphs for the order κ^2 gravitational corrections.

no gravitational corrections to the running of the masses. This cancellation is unexpected because it is not obvious how the corresponding divergences in each of the diagrams are linked. Note, that this cancellation might be absent in a different gauge, since the renormalization in gravitational systems is in general dependent on the chosen gauge [6].

To determine the renormalization of the couplings we further need the vertex renormalizations, which can be obtained from the diagrams in 1(b) and 1(c) and are given by

$$\begin{aligned} Z_{\varphi\overline{\psi}\psi} - 1 &= \frac{\kappa^2}{16\pi^2}(\tfrac{3}{4}m_\psi^2 + \tfrac{1}{4}m_\varphi^2)\frac{2}{d-4}\,, \\ Z_{\varphi^4} - 1 &= \frac{\kappa^2}{16\pi^2}4m_\varphi^2\frac{2}{d-4}\,. \end{aligned} \tag{6}$$

In dimensional regularization the renormalized and bare couplings are related by

$$\begin{aligned} g_0 &= \mu^{\frac{4-d}{2}} Z_{\varphi\overline{\psi}\psi} Z_\psi^{-1} Z_\varphi^{-\frac{1}{2}} g\,, \\ \lambda_0 &= \mu^{4-d} Z_{\varphi^4} Z_\varphi^{-2}\lambda\,. \end{aligned} \tag{7}$$

Exploiting the scale independence of the bare couplings it is no problem to compute the gravitational contributions to the β functions

$$\beta_g = -\frac{\kappa^2}{16\pi^2}(m_\psi^2 - \tfrac{1}{2}m_\varphi^2)g \tag{8}$$

$$\beta_\lambda = -\frac{\kappa^2}{4\pi^2}m_\varphi^2\lambda\,. \tag{9}$$

Hence, if the non-gravitational as well as higher order gravitational contributions are neglected we find that quantum gravity leads to the asymptotic freedom of the φ^4 interaction. The same holds for the Yukawa interaction as long as $\sqrt{2}\,m_\psi > m_\varphi$.

REFERENCES

1. G. 't Hooft, M. Veltman, *Annales Poincare Phys. Theor.* **A20** (1974) 69–94.
2. J. Donoghue, *Phys. Rev. D* **50** (1994) 6, 3874–3888.
3. S. Robinson, F. Wilczek, *Phys. Rev. Lett.* **96** (2006) 23, 231601. A. Pietrykowski, *Phys. Rev. Lett.* **98** (2007) 061801. D. Toms, *Phys. Rev. D* **76** (2007) 4, 45015; *Phys. Rev. Lett.* **101** (2008) 131301; D. Ebert, J. Plefka, A. Rodigast, *Phys. Lett. B* **660** (2008) 579–582; *JHEP* **02** (2009) 028. J. Daum, U. Harst, M. Reuter, JHEP **1001** (2010) 084.
4. A. Rodigast, T. Schuster, Phys. Rev. Lett. **104** (2010) 081301.
5. O. Zanusso, L. Zambelli, G. Vacca, R. Percacci, Phys. Lett. B **689** (2010) 90. P. Mackay, D. Toms, *Phys. Lett. B***684** (2010) 251–255.
6. I. Antoniadis, J. Iliopoulos, T. Tomaras, *Nucl. Phys. B* **267** (1986) 2, 497–508.

SUSY multiplets at first mass level in $D = 4$ superstring compactifications

O. Schlotterer[a]

[a]Max–Planck–Institut fuer Physik (Werner–Heisenberg–Institut),
Foehringer Ring 6, 80805 Munich, Germany

In this note we summarize the work presented in [1] where direct production of lightest Regge resonances is discussed in view of a low string scale scenario. Particular emphasis is put on the occurring four dimensional massive SUSY multiplets – firstly in maximally supersymmetric $\mathcal{N} = 4$ compactifications, but more importantly those $\mathcal{N} = 1$ multiplets which are universal to any superstring compactification which preserves four supercharges.

1. Introduction

The string scale $M_s = \alpha'^{-1/2}$ can be as low as a few TeV provided that some of the extra dimensions are sufficiently large [2]. In that case, resonances in lepton, quark- and gluon scattering processes due to exchange of virtual Regge excitations can potentially be observed at LHC [3–5]. Once the mass threshold M_s is crossed in the center-of-mass energies of colliding partons, one would also see the string resonance states produced directly [1].

This articles explains which of the first mass level states are universal to any four dimensional superstring compactification preserving at least $\mathcal{N} = 1$ supersymmetry in $D = 4$. Making model independent statements like ours bypasses the notorious landscape problem.

To briefly explain the index notation: vector (spinor) indices are taken as m, n, p $(A, \dot{B})$ for $SO(1, 9)$, μ, ν, λ, ρ $(\alpha, \dot{\beta})$ for $SO(1, 3)$ and i, j, k $(I, \bar{J})$ for $SO(6)$. Chiral gamma matrices in ten (four) dimensions are denoted by Γ^m (σ^μ).

2. The first mass level in ten dimensions

The first mass level of the open superstring spectrum has been known for a long time [6]. Let us briefly review the particle content in the ten dimensional uncompactified superstring:

In the Neveu Schwarz sector, 128 bosonic states remain after removing spurious solutions to the BRST constraints,

$$V^{(-1)}(B, E, k) = e^{-\phi} e^{ikX} \left(B_{mn} i\partial X^m \psi^n + E_{mnp} \psi^m \psi^n \psi^p\right) . \quad (1)$$

The symmetric and traceless wave function B_{mn} describes a massive spin two particle, and E_{mnp} represents a three form. Both tensors are transverse $k^m B_{mn} = k^m E_{mnp} = 0$ and thus fit into representation of the massive little group $SO(9)$. Terms of the form $H_m \partial\psi^m$ in (1) turn out to be spurious in ten dimensions but not in compactifications.

In the Ramond sector vertex, the spin field Θ_A contracts two vector spinor wavefunctions $\chi, \bar{\zeta}$

$$V^{(-1/2)}(\chi, \bar{\zeta}, k) = e^{-\phi/2} e^{ikX} \left(\chi^A_m i\partial X^m + \frac{\sqrt{\alpha'}}{4} \bar{\zeta}_{m\dot{B}} \psi^m \psi^n \Gamma_n^{\dot{B}A}\right) \Theta_A \quad (2)$$

whose physical degrees of freedom are Γ traceless and transverse. Hence, (2) describes a massive spin 3/2 fermion where χ and $\bar{\zeta}$ are related by a Dirac equation at mass $m = (\alpha')^{-1/2}$.

Both vertex operators are given in their canonical superghost pictures.

3. Dimensional reduction to $D = 4$

To make contact with LHC accessible scenarios, the first step is a dimensional reduction of the 256 states at the first mass level. They form an $\mathcal{N} = 1$ multiplet in ten dimensions which translates into $\mathcal{N} = 4$ from the four dimensional point

of view – provided that the internal geometry preserves all the 16 supercharges. The Lorentz group then decomposes as $SO(1,9) \to SO(1,3) \times SO(6)$.

On the bosonic side, any $SO(1,9)$ vector index can be set to spacetime values $\mu = 0,1,2,3$ or internal ones $i = 4,\ldots,9$. This easily decomposes B_{mn} and E_{mnp} as follows into scalars, vectors and tensors of $SO(1,3)$ spin $j = 0,1,2$.

- $B_{mn} \equiv 1 \times (j=2) \oplus 6 \times (j=1) \oplus 21 \times (j=0)$
- $E_{mnp} \equiv 21 \times (j=1) \oplus 21 \times (j=0)$

We have used Poincaré duality between massive $(3-p)$- and p forms in four dimensions.

For the fermions, we first of all obtain four $j = 3/2$ states, both in the fundamental $(1,0,0)$ and antifundamental $(0,0,1)$ representations of the $SU(4)$ R-symmetry group. Among the spin $j = 1/2$ Dirac fermions, eight fall into the $(1,0,0)$ or $(0,0,1)$ and another $20 \oplus 20$ into the "spin 3/2" representations $(1,1,0)$ and $(0,1,1)$ of $SU(4)_R$.

Taking everything together, this matches perfectly with the well known structure of a massive $\mathcal{N} = 4$ spin two multiplet [7]:

spin j	2	3/2	1	1/2	0
# particles	1	8	27	48	42

4. Towards $\mathcal{N} = 1$ SUSY

The spacetime SUSY charge Q can be identified with the gluino vertex at zero momentum [8]:

$$Q_A \sim \oint \frac{\mathrm{d}z}{2\pi i} e^{-\phi/2} \Theta_A \tag{3}$$

Upon dimensional reduction, the ten dimensional spin field Θ_A factorizes into $SO(1,3) \times SO(6)$ covariant constituents S and Σ of the same chirality,

$$\Theta_A = S_\alpha \otimes \Sigma^I \oplus S^{\dot\alpha} \otimes \bar\Sigma_{\bar I} \; . \tag{4}$$

A very natural way to break various supersymmetries in the compactification process lies in orbifold projections. Consider an orbifold action σ which rotates the internal worldsheet fields (X^i, ψ^i) in the Cartan Weyl basis as

$$X^{2k+2} \pm i X^{2k+3} \mapsto e^{2\pi i \phi_k} (X^{2k+2} \pm i X^{2k+3}) \; . \tag{5}$$

Bosonization techniques admit to infer the orbifold action on the internal spin fields, and it turns out that generic angles ϕ_k subject to $\phi_1 + \phi_2 + \phi_3 = 0$ preserve one out of four Σ components

$$\Sigma := \Sigma^I\big|_{\text{invariant}} \; , \quad \bar\Sigma := \Sigma_{\bar I}\big|_{\text{invariant}} \tag{6}$$

which amounts to $\mathcal{N} = 1$ in four dimensions. Note that the σ orbifold is perfectly representative for $\mathcal{N} = 1$ supersymmetric compactifications.

5. Universal $\mathcal{N} = 1$ states in $D = 4$

Vertex operators with all the conformal fields from the spacetime sector are guaranteed to remain in the spectrum of any $\mathcal{N} = 1$ compactification. Among the bosons, this applies to a spin two tensor and a complex scalar[1]:

$$V^{(-1)}(\alpha, k) \sim \alpha_{\mu\nu} i\partial X^\mu \psi^\nu e^{-\phi} e^{ikX} \tag{7}$$

$$V^{(-1)}(\Phi^\pm, k) \sim \Big[(\eta_{\mu\nu} + 2\alpha' k_\mu k_\nu) i\partial X^\mu \psi^\nu + 2\alpha' k_\mu \partial\psi^\mu \pm \frac{i\alpha'}{3} \varepsilon_{\mu\nu\lambda\rho} \psi^\mu \psi^\nu \psi^\lambda k^\rho \Big] e^{-\phi} e^{ikX} \tag{8}$$

The latter exclusively couples to gluons of $(\pm,\pm)$ helicity combination. The fact that Φ^+ propagates to Φ^- makes sure that no factorization channel shows up in vanishing four gluon amplitudes with uniform helicities $(\pm,\pm,\pm,\pm)$.

Other bosonic vertex operators involving internal $i\partial X^i, \psi^i$ generically vanish from the spectrum, but the following states survive universally

$$V^{(-1)}(\xi, k) \sim \xi_\mu \psi^\mu \sum_{k=1}^{3} \Psi^k \bar\Psi^k e^{-\phi} e^{ikX} \tag{9}$$

$$V^{(-1)}(\Omega^+, k) \sim \Psi^1 \Psi^2 \Psi^3 e^{-\phi} e^{ikX} \tag{10}$$

$$V^{(-1)}(\Omega^-, k) \sim \bar\Psi^1 \bar\Psi^2 \bar\Psi^3 e^{-\phi} e^{ikX} \tag{11}$$

with shorthands $\Psi^k := \frac{1}{\sqrt{2}}(\psi^{2k+2} + i\psi^{2k+3})$ and $\bar\Psi^k := \frac{1}{\sqrt{2}}(\psi^{2k+2} - i\psi^{2k+3})$ for the Cartan Weyl basis. Neither of them couples to gluons. In addition, there might exist additional model dependent $\mathcal{N} = 1$ states in separate SUSY multiplets which lie beyond the main focus of this article.

Among the spin fields, only $S_\alpha \Sigma$ and $S^{\dot\beta} \bar\Sigma$ are σ invariant. Two Dirac fermions of spin 3/2 and

[1] In the following, the wavefunctions $\alpha, \Phi^\pm, \ldots$ will be used as shorthands to refer to the associated states

1/2 can be formed, namely

$$V^{(-1/2)}(\chi,\bar{\zeta},k) \sim e^{-\phi/2}e^{ikX} (\chi^\alpha_\mu i\partial X^\mu - \sqrt{\alpha'}\bar{\zeta}_{\mu\dot{\beta}}\psi^\mu\psi^\nu\sigma_\nu^{\dot{\beta}\alpha})S_\alpha\Sigma \quad (12)$$

$$V^{(-1/2)}(u,\bar{v},k) \sim e^{-\phi/2}e^{ikX} u^\alpha(\sigma^\mu\bar{\sigma}^\nu)_\alpha{}^\beta\big(i\partial X^\mu k_\nu - \psi_\mu\psi_\nu/3\big)S_\beta\Sigma \quad (13)$$

as well as their relatives of reversed $SO(1,3)$ chirality, e.g. $(\chi^\alpha_\mu,\bar{\zeta}_{\mu\dot{\alpha}}) \leftrightarrow (\bar{\chi}_{\mu\dot{\alpha}},\zeta^\alpha_\mu)$ and $\Sigma \leftrightarrow \bar{\Sigma}$.[2]

Two different $\mathcal{N}=1$ multiplets are populated by the states above:

- $j=2$ multiplet with $8\oplus 8$ states $\alpha,\xi\oplus(\chi,\bar{\zeta}),(\bar{\chi},\zeta)$
- $j=1/2$ multiplet with $4\oplus 4$ states $\Phi^\pm,\Omega^\pm\oplus(u,\bar{v}),(\bar{u},v)$

6. Gauginos versus quarks

All the statements above hold for adjoint matter arising from open strings with both endpoints on the same stack of D-branes. Its adjoint Chan Paton generator T was suppressed in the vertex operators above. Chrial fermions originate from strings located at D brane intersectios. Their vertex operators can be constructed from massless gauginos via three modifications:

- T in the bifundamental representation
- adjust the vertex operator's normalization
- replace the internal spin field Σ by a boundary changing operator Ξ which can be thought of as a twist field with respect to σ

The same construction holds for fermions at the first mass level: The gaugino Regge excitations can be mapped to quark- and lepton excitations by the same steps as for the ground states.

The conformal fields Σ and Ξ give rise to the same two point functions, that is why scattering of n gluons with two gauginos yields the same disk amplitudes as for two quarks[3]. Moreover, the massive vector ξ couples universally to quarks and gauginos of opposite chirality which can again be understood from the internal CFT. But the massive $\Omega^\pm$ scalar only couples to gauginos of uniform $(\mp,\mp)$ helicity, not to chiral fermions.

[2]Numerical coefficients of (2) and (12) differ due to gamma matrix identities.

[3]This statement in fact holds to all orders in α' [5]

7. Outlook and conclusion

Any three- and four point amplitude involving one massive $\mathcal{N}=1$ state and otherwise massless ones have been computed in [1]. Selection rules for the helicity quantum numbers were derived by means of the Weyl-van-der-Waerden formalism for wave functions of massive particles up to spin $j=2$. Finally, cross sections were computed to allow for comparison with LHC data. Production and decay of higher spin excitation is pioneered in [9]. If nature is friendly enough to "choose" a low string scale, then the first experimental hints for string theory will wait around the corner.

8. Acknowledgments

I would like to thank W. Feng, D. Lüst, S. Stieberger & T. Taylor for fruitful collaboration.

REFERENCES

1. W. -Z. Feng, D. Lust, O. Schlotterer, S. Stieberger, Nucl. Phys. **B843** (2011) 570-601. [arXiv:1007.5254 [hep-th]].
2. I. Antoniadis, S. Dimopoulos, G. R. Dvali, Nucl. Phys. **B516** (1998) 70-82. [hep-ph/9710204].
3. S. Cullen, M. Perelstein, M. E. Peskin, Phys. Rev. **D62** (2000) 055012. [hep-ph/0001166].
4. D. Lust, S. Stieberger, T. R. Taylor, Nucl. Phys. **B808** (2009) 1-52. [arXiv:0807.3333 [hep-th]].
5. D. Lust, O. Schlotterer, S. Stieberger, T. R. Taylor, Nucl. Phys. **B828** (2010) 139-200. [arXiv:0908.0409 [hep-th]].
6. I. G. Koh, W. Troost, A. Van Proeyen, Nucl. Phys. **B292** (1987) 201.
7. Yu. M. Zinoviev, arXiv:hep-th/0206209.
8. D. Friedan, E. J. Martinec, S. H. Shenker, Nucl. Phys. **B271** (1986) 93.
9. O. Schlotterer, [arXiv:1011.1235 [hep-th]].

Gravity and Yang-Mills Amplitude Relations in Field Theory

Thomas Søndergaard[a]

[a]Niels Bohr International Academy and Discovery Center,
The Niels Bohr Institute, Blegdamsvej 17, DK-2100 Copenhagen, Denmark

We review some recent work in the famous Kawai-Lewellen-Tye (KLT) relations. Especially we present a compact way of writing down the general n-point relation. We also look at an extra feature of these relations which were only very recently realized, and leads to new relations among gauge-theory amplitudes.

1. Introduction

For the last couple of decades there has been an amazing development in our understanding of the structure of scattering amplitudes. Not just within quantum gravity and gauge theories individually, but also in the close connection between these seemingly different types of theories. One of the strongest manifestations of this connection appears in the famous Kawai-Lewellen-Tye (KLT) relations [1], which relate tree-level amplitudes in quantum gravity to products of color-ordered tree-level amplitudes in gauge theories. Although such relations were originally found in string theory by factorizing closed string amplitudes into products of open string amplitudes, they continue to hold in the field theory limit. The origin of these relations in field theory has long been a mystery. However, recently a purely field theoretically proof was provided [2,3], based on the recursive method of BCFW [4], forcing the relations to be true simply due to the analytical properties of scattering amplitudes. A bonus of this work was a series of new purely gauge theoretically amplitude relations [2,5].

2. KLT in field theory

Before presenting the explicit relations let us introduce a very useful function $\mathcal{S}$, that depends on k massless momenta in the following way

$$\mathcal{S}[i_1,\ldots,i_k|j_1,\ldots,j_k]_{p_1} \equiv \prod_{t=1}^{k}\left(s_{i_t 1}+\sum_{q>t}^{k}\theta(i_t,i_q)s_{i_t i_q}\right), \qquad (1)$$

where $\{i_1,\ldots,i_k\}$ and $\{j_1,\ldots,j_k\}$ are two arbitrary orderings of the k momenta. We have defined $s_{ij}\equiv(p_i+p_j)^2$, and $\theta(i_a,i_b)$ as zero if i_a comes sequentially before i_b in $\{j_1,\ldots,j_k\}$ and unity if it comes after.

In terms of this function the KLT-relations can be written as

$$\begin{aligned}(-1)^{n+1}M_n = \sum_{\alpha,\beta\in S_{n-3}} & \widetilde{A}_n(n-1,n,\alpha(2,n-2),1) \\ & \times \mathcal{S}[\alpha(2,n-2)|\beta(2,n-2)]_{p_1} \\ & \times A_n(1,\beta(2,n-2),n-1,n), \quad (2)\end{aligned}$$

where M_n is a tree-level n-point gravity amplitude, $\widetilde{A}_n$ and A_n n-point color-ordered gauge-theory amplitudes, and we have introduced the short-hand notation $\alpha(2,n-2)\equiv\{\alpha(2),\alpha(3),\ldots,\alpha(n-2)\}$ for permutations of leg $2,3,\ldots,n-2$, and likewise for $\beta(2,n-2)$. The sum is over all α and β permutations.

Using the Bern-Carrasco-Johansson (BCJ) relations [6] one can write eq. (2) in many other, but completely equivalent, ways, see [3]. Although some of these have fewer terms than eq. (2) we choose to present it in the above form because of its nice and compact n-point expression.

In fact, the BCJ-relations are close connected to the KLT-relations. The gravity amplitude is completely crossing symmetric, and therefore the right-hand-side of eq. (2) must also be crossing symmetric. This is manifest in leg $2,3,\ldots,n-2$, but not in leg 1, $n-1$ and n. Indeed permuting these legs and equating the expressions lead to BCJ-relations, something that was already apparent in [1] but not really appreciated. The con-

nection between these relations is also apparent from the following way of representing the BCJ-relations

$$0 = \sum_{\alpha \in S_{n-2}} \mathcal{S}[\beta(2,n-1)|\alpha(2,n-1)] \times A_n(1,\alpha(2,n-1),n), \qquad (3)$$

where $\beta(2,n-2)$ is just some arbitrary permutation.

For a generalization of the above results to string theory, see [7–9].

3. Quadratic gauge-theory relations

It turns out that the combination of gauge-theory amplitudes on the right-hand-side of eq. (2) is hiding another neat feature, leading to new relations among gauge-theory amplitudes.

Let A_n^k denote an N^kMHV amplitude, *i.e.* A_n^k is an n-point subamplitude with $2+k$ negative helicity gluons. Of course, to have non-vanishing amplitudes $k \in \{0,1,\ldots,n-4\}$. We do not care about the exact helicity configuration, just which helicity *sector* it belongs to.

Choosing $k \neq h$ the following identity is satisfied

$$0 = \sum_{\alpha,\beta \in S_{n-3}} A_n^k(n-1,n,\alpha(2,n-2),1) \times \mathcal{S}[\alpha(2,n-2)|\beta(2,n-2)]_{p_1} \times A_n^h(1,\beta(2,n-2),n-1,n). \qquad (4)$$

Note that in each of the A_n^k (A_n^h) amplitudes in the sum it is the same $k+2$ ($h+2$) legs that have negative helicity. Hereby we get relations among subamplitudes living in different helicity sectors.

For four points the right-hand-side is trivially zero. In order to fullfill the $k \neq h$ requirement at least one of the amplitudes must have three or four of the same helicity and thereby vanish all by itself. However, for five points we already start to get non-trivial relations, *e.g.*

$$\begin{aligned} 0 = {} & s_{12}A_5^0(1,2,3,4,5)\big[s_{13}A_5^1(4,5,2,3,1) \\ & + (s_{13}+s_{23})A_5^1(4,5,3,2,1)\big] \\ & + s_{13}A_5^0(1,3,2,4,5)\big[s_{12}A_5^1(4,5,3,2,1) \\ & + (s_{12}+s_{23})A_5^1(4,5,2,3,1)\big], \end{aligned} \qquad (5)$$

where A_5^0 is some $\overline{MHV}$ amplitude and A_5^1 an $NMHV$ (*i.e.* here $\overline{MHV}$) amplitude.

4. Conclusion

We have shown how to nicely write down the general n-point KLT-relations in field theory, along with new relations among gauge-theory amplitudes of different helicity sectors. Knowing the amplitudes for one kind of helicity sector therefore imply linear relations between amplitudes in another sector (for explicit examples see [10,11]).

With these results we might be one step closer in unraveling the mysterious connection between gravity and gauge theory.

REFERENCES

1. H. Kawai, D. C. Lewellen and S. H. H. Tye, Nucl. Phys. B **269** (1986) 1.
2. N. E. J. Bjerrum-Bohr, P. H. Damgaard, B. Feng and T. Sondergaard, Phys. Rev. D **82** (2010) 107702 [arXiv:1005.4367 [hep-th]].
3. N. E. J. Bjerrum-Bohr, P. H. Damgaard, B. Feng and T. Sondergaard, JHEP **1009** (2010) 067 [arXiv:1007.3111 [hep-th]].
4. R. Britto, F. Cachazo and B. Feng, Nucl. Phys. B **715** (2005) 499 [hep-th/0412308]; R. Britto, F. Cachazo, B. Feng and E. Witten, Phys. Rev. Lett. **94** (2005) 181602 [hep-th/0501052].
5. N. E. J. Bjerrum-Bohr, P. H. Damgaard, B. Feng and T. Sondergaard, Phys. Lett. B **691** (2010) 268 [arXiv:1006.3214 [hep-th]].
6. Z. Bern, J. J. M. Carrasco and H. Johansson, Phys. Rev. D **78**, 085011 (2008) [0805.3993 [hep-ph]].
7. N. E. J. Bjerrum-Bohr, P. H. Damgaard, T. Sondergaard and P. Vanhove, JHEP **1101** (2011) 001 [arXiv:1010.3933 [hep-th]].
8. N. E. J. Bjerrum-Bohr, P. H. Damgaard and P. Vanhove, Phys. Rev. Lett. **103**, 161602 (2009) [0907.1425 [hep-th]].
9. S. Stieberger, 0907.2211 [hep-th].
10. B. Feng and S. He, JHEP **1009** (2010) 043 [arXiv:1007.0055 [hep-th]].
11. B. Feng, S. He, R. Huang and Y. Jia, JHEP **1010** (2010) 109 [arXiv:1008.1626 [hep-th]].

Brane tilings and supersymmetric gauge theories

A. Hanany, G. Torri [a]

[a]Theoretical Physics Group, The Blackett Laboratory
Imperial College London, Prince Consort Road
London, SW7 2AZ, UK

1. Supersymmetric gauge theories

In the past 40 years, gauge theories have played a crucial role in High Energy Physics. In particular, one of their biggest successes, has been the formulation of the Standard Model from a gauge principle.

In this vast sea of theories, the class of supersymmetric gauge theories deserves special attention. In fact, the constraints that supersymmetry imposes, make a gauge theory much more well-behaved and easier to investigate from a theoretical point of view.

Furthermore, supersymmetric gauge theories are shown to arise naturally in Superstring Theory, possibly one of the preferred candidates to solve the problems that were left open by the Standard Model. In particular, the gauge degrees of freedom are brought into the theory by the open strings that are stretched between two D-branes, and are confined precisely on them. Roughly speaking, we could say that, in String Theory, supersymmetric gauge theories arise on the world-volume of D-branes. The interesting thing about this is that the structure of these gauge theories is highly sensitive to the geometry that the D-branes are probing, thus leading to a connection between the shape of space-time and the nature of the interactions of the Universe.

Studying supersymmetric gauge theories in String Theory is not only an interesting endeavour *per se*, but it could also shed some light on the fascinating duality between gauge theories and gravity conjectured by Maldacena more than 10 years ago.

In the following we will be mostly concerned about super-Yang-Mills gauge theories in $(3+1)$ dimensions, although similar considerations can be made for Chern-Simons theories in $(2+1)$ dimensions, *mutatis mutandis*.

2. Quivers

As we mentioned above, the structure of supersymmetric gauge theories is highly constrained precisely by supersymmetry. In particular, a supersymmetric lagrangian is unambiguously identified by specifying the number and types of gauge groups, the matter content and a superpotential. Furthermore, given the simplicity of the information needed to characterise a supersymmetric gauge theory, it turns out that many of them can be represented by a graph called *quiver*. This is essentially a directed graph containing arrows and nodes with the convention that:

- each node represents a gauge group $U(N)$;
- each arrow going from a node a to a different node b represents a field X_{ab} in the bifundamental representation $(\mathbf{N}, \overline{\mathbf{N}})$ of $U(N_a) \times U(N_b)$.
- each loop on a node a represents a field ϕ_a in the adjoint representation of $U(N_a)$.
- each superpotential term corresponds to a closed loop in the quiver[1];

As an example, Figure 1 shows the quiver of the well known conifold theory.

[1]However not all the loops correspond to a superpotential term!

Figure 1. Quiver of the conifold theory

The theories that can be represented by a quiver, usually called *quiver gauge theories*, constitute a class of theories which is quite easy to investigate. In fact, they are usually characterised by a very simple superpotential and they contain matter that transform in bifundamental or adjoint representations of the gauge groups.

3. Brane tilings

Another way of representing supersymmetric gauge theories is through a type of graph called *brane tiling*. It is a bi-periodic and bi-partite graph with a repeating structure which is called *fundamental domain*. In order to read off from the brane tiling the necessary information to reconstruct the lagrangian, one must keep in mind that:

- each face corresponds to a $U(N)$ gauge group;
- each edge corresponds to a bi-fundamental field;
- each node corresponds to a superpotential term;

The nice feature about brane tilings is that they allow one to write down the lagrangian of a supersymmetric gauge theory in a completely unambiguous way[2].

As an example, Figure 2 represents the brane tiling of the conifold theory.

Once a supersymmetric gauge theory is specified through a brane tiling, it is possible to investigate relevant features of this theory. In particular, through a technique called *forward algorithm*[3], it is possible to study the vacuum moduli space, i.e. the space of zero-energy solutions to the F-terms and the D-terms of the gauge theory. This algorithm also makes it easy to determine the R-charges of the operators of the theory one is studying.

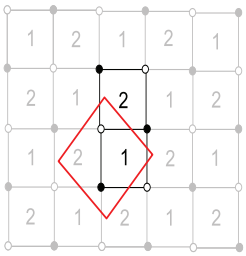

Figure 2. Tiling of the conifold theory

The brane tilings have been extensively used in the past to investigate a phenomenon called *toric duality* for D3-branes. Roughly speaking, this corresponds to the situation where two (or more) different gauge theories have the same vacuum moduli space. This duality has been shown to be equivalent to Seiberg duality.

Brane tilings seem also like a very natural setup to study the *Higgs mechanism* in for supersymmetric gauge theories. In fact, on the tiling this phenomenon is implemented simply as the removal of one or more edges. This makes it very simple also to understand how different gauge theories can be connected through the Higgs mechanism.

Finally, a very fascinating application of brane tilings is the study of supersymmetric Chern-Simons theories in $(2+1)$ dimensions. In 2008, Aharony, Bergman, Jafferis and Maldacena provided the first example of conformal field theory living on an M2-brane probing flat space. With brane tilings it has been possible to extend this

[2] With a quiver this is not quite true since not all the closed loops correspond to terms in the superpotential.

[3] The name suggests the existence of an *inverse algorithm* which, starting from a certain Calabi-Yau, gives the brane tiling of the theory that has that manifold as its vacuum moduli space.

duality to more complicated backgrounds and to investigate fascinating features of such theories.

REFERENCES

1. O. Aharony, S. S. Gubser, J. M. Maldacena, H. Ooguri and Y. Oz, Phys. Rept. **323** (2000) 183 [arXiv:hep-th/9905111].
2. I. R. Klebanov, arXiv:hep-th/0009139.
3. J. M. Maldacena, Adv. Theor. Math. Phys. **2** (1998) 231 [Int. J. Theor. Phys. **38** (1999) 1113] [arXiv:hep-th/9711200].
4. A. Hanany and K. D. Kennaway, hep-th/0503149.
5. S. Franco, A. Hanany, K. D. Kennaway, D. Vegh and B. Wecht, JHEP **0601**, 096 (2006) [arXiv:hep-th/0504110].
6. S. Franco, A. Hanany, D. Martelli, J. Sparks, D. Vegh and B. Wecht, JHEP **0601**, 128 (2006) [arXiv:hep-th/0505211].
7. I. R. Klebanov and G. Torri, arXiv:0909.1580 [hep-th].
8. A. Hanany and A. Zaffaroni, arXiv:0808.1244 [hep-th].
9. A. Hanany, D. Vegh, A. Zaffaroni, arXiv:0809.1440.
10. J. Davey, A. Hanany, N. Mekareeya and G. Torri, arXiv:0903.3234 [hep-th].
11. J. Davey, A. Hanany, N. Mekareeya and G. Torri, JHEP **0911** (2009) 028 [arXiv:0908.4033 [hep-th]].

On the Amplitude/Wilson Loop Duality in $\mathcal{N} = 6$ Chern-Simons Theory

Konstantin Wiegandt[a*],

[a]Institut für Physik, Humboldt-Universität zu Berlin, Newtonstraße 15, D-12489 Berlin, Germany

We study light-like polygonal Wilson loops in three-dimensional Chern-Simons and ABJM theory to two-loop order and find that the result is remarkably similar to that of the corresponding Wilson loop in $\mathcal{N} = 4$ SYM. We comment on the existence of a Wilson loop/scattering amplitude relation in ABJM theory.

1. Introduction

Our motivation to consider polygonal light-like Wilson loops in the 3d Chern-Simons and ABJM gauge theory [1] stems from the Wilson loop/scattering amplitude duality in $\mathcal{N} = 4$ super Yang-Mills.

In planar $\mathcal{N} = 4$ super Yang-Mills n-particle MHV scattering amplitudes $\mathcal{A}_n^{\text{MHV}} = A_n^{\text{tree}} M_n$ are related to the expectation value of the n-cusped Wilson loop operator

$$\langle W_n \rangle := \frac{1}{N} \langle 0 | \operatorname{Tr} \mathcal{P} \exp \left(i \oint_{\mathcal{C}_n} A_\mu dz^\mu \right) | 0 \rangle \,. \quad (1)$$

The contour of the n-sided polygon $\mathcal{C}_n$ is given by n points x_i $(i = 1, ..., n)$ which are related to the massless particle momenta via $x_{i+1} - x_i = p_i$. The segments of the contour are thus light-like, i.e. $(x_i - x_{i+1})^2 = p_i^2 = 0$.

The relation between the Wilson loop and the scattering amplitude is given by

$$\ln M_n = \ln W_n + \text{const} \,. \quad (2)$$

This duality was discovered in the dual $AdS_5 \times S^5$ string picture at strong gauge coupling in [2] and shown to exist also in the weak coupling regime [3, 4] with profound consequences on the symmetries of these correlators leading to a dual superconformal [4] respectively Yangian symmetry [5] of scattering amplitudes, for reviews see [10]. Moreover, there are many structural similarities of the 3d $\mathcal{N} = 6$ superconformal ABJM theory to $\mathcal{N} = 4$ super Yang-Mills, most notably the emergence of hidden integrability [11], (for reviews see [13]) in the planar limit for the spectral problem of determining anomalous scaling dimensions of local operators [15].

It was found that the expectation value of the Wilson Loop in $\mathcal{N} = 4$ super Yang-Mills is governed by an anomalous conformal Ward identity that completely fixes its form at 4 and 5 points and allows for an arbitrary function of conformal invariants starting from 6 points. This so called remainder function R_n is indeed present starting from 6 points and leads to a correction [6], [7] of the BDS Ansatz for planar gluon scattering amplitudes.

Recently, the duality has been extended to amplitudes with arbitrary helicity states by introducing a suitable supersymmetric Wilson loop [9].

2. Cusped Wilson Loops in ABJM Theory

In [8] we calculate the expectation value of the n-cusped Wilson loop operator (1) in the planar limit for light-like polygonal contours $\mathcal{C}_n$ in pure Chern-Simons and ABJM theory.

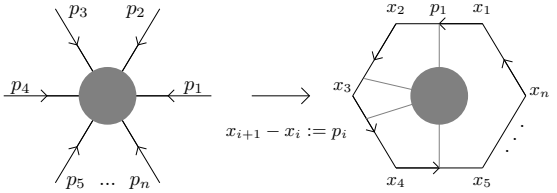

Figure 1. Duality between MHV scattering amplitudes A_n^{MHV} and Wilson loops W_n in $\mathcal{N} = 4$ super Yang-Mills.

*wiegandt@physik.hu-berlin.de

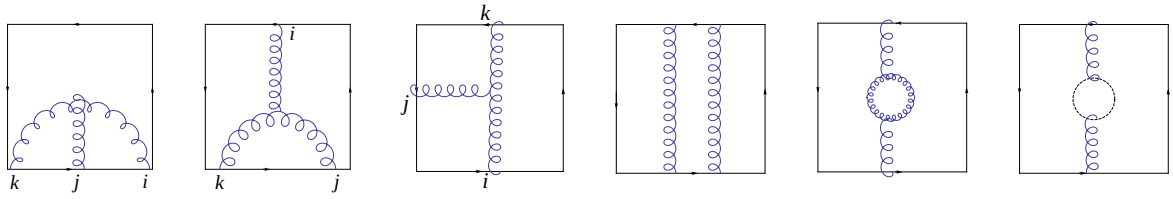

Figure 2. Planar two-loop topologies appearing in the polygonal Wilson loop in CS theory. Diagrams where one propagator is connected to a single edge or to two adjacent edges vanish in our gauge and are not displayed. In ABJM theory we additionally have bosons and fermions in the one-loop corrected gluon propagator, these contributions are similar to the one-loop diagrams in $\mathcal{N}=4$ SYM, for details see [8].

The outcome of our computations at one-loop order in pure Chern-Simons and ABJM theory is that

$$\begin{aligned}\langle W_4\rangle_{\text{1-loop}} &= 0 \quad \text{(analytically)}\,, \\ \langle W_6\rangle_{\text{1-loop}} &= 0 \quad \text{(numerically)}\,.\end{aligned} \tag{3}$$

Moreover, conformal Ward identities force $\langle W_n\rangle_{\text{1-loop}}$ to depend only on conformally invariant cross ratios of the $(x_i - x_j)^2$ and for $n = 4$ and 6 we show that these functions vanish.

At the two-loop order we compute the tetragonal Wilson-loop W_4 in pure Chern-Simons and $\mathcal{N} = 6$ superconformal Chern-Simons (ABJM theory). The result in dimensional reduction regularisation with $d = 3 - 2\epsilon$ for the correlator in ABJM theory is

$$\begin{aligned}&\langle W_4\rangle^{\text{ABJM}}_{\text{2-loop}} \\ &= -\left(\frac{N}{k}\right)^2 \Big[-\frac{1}{2}\sum_{i=1}^{4} \frac{(-\mu'^2\, x_{i,i+2}^2)^{2\epsilon}}{(2\epsilon)^2} \\ &\qquad + \frac{1}{2}\ln^2\left(\frac{x_{13}^2}{x_{24}^2}\right) + \text{const.}\Big]\end{aligned} \tag{4}$$

This is indeed of the same functional form as the one-loop result in $\mathcal{N} = 4$ super Yang-Mills theory, where one has [3]

$$\begin{aligned}&\langle W_4\rangle^{\mathcal{N}=4\ \text{SYM}}_{\text{1-loop}} \\ &= \frac{g^2 N}{8\pi^2}\Big[-\frac{1}{2}\sum_{i=1}^{4} \frac{(-\mu^2\, x_{i,i+2}^2)^{\epsilon}}{\epsilon^2} \\ &\qquad + \frac{1}{2}\ln^2\left(\frac{x_{13}^2}{x_{24}^2}\right) + \text{const.}\Big]\,.\end{aligned} \tag{5}$$

It would certainly be interesting to explore this relationship also beyond four cusps.

3. Scattering Amplitude/Wilson Loop Duality in ABJM theory

From the string perspective the scattering amplitude/Wilson loop duality in the AdS_5/CFT_4 system arises from a combination of bosonic and fermionic T-dualities under which the free $AdS_5 \times S^5$ superstring is self-dual [12]. Hence, for the existence of an analogue duality in ABJM theory one would require a similar self-duality of the $AdS_4 \times \mathbb{CP}_3$ superstring under the combined T-dualities. The problem was analysed in [16] but no T-self-duality could be found so far.

At tree-level, recent developments have uncovered Yangian and dual superconformal symmetry of the amplitudes in ABJM theory [17]. In [18] a vanishing result for the four-point one-loop amplitudes in ABJM theory was found and the authors speculated whether the two-loop scattering amplitudes in N = 6 Chern-Simons could be simply related to the one-loop N = 4 Yang-Mills amplitudes. The main result of [8] is that this picture is consistent at least up to the two-loop order.

In order to settle the question of a possible scattering-amplitude/light-like Wilson loop duality, a two-loop scattering amplitude computation in ABJM theory would be very desirable in order to compare to our result (4).

REFERENCES

1. O. Aharony, O. Bergman, D. L. Jafferis *et al.*, JHEP **0810** (2008) 091.
2. L. F. Alday, J. M. Maldacena, JHEP **0706** (2007) 064.
3. G. P. Korchemsky, J. M. Drummond, E. Sokatchev, Nucl. Phys. **B795** (2008) 385-408. A. Brandhuber, P. Heslop, G. Travaglini, Nucl. Phys. **B794** (2008) 231-243. J. M. Drummond, J. Henn, G. P. Korchemsky *et al.*, Nucl. Phys. **B795** (2008) 52-68.
4. J. M. Drummond, J. Henn, G. P. Korchemsky *et al.*, Nucl. Phys. **B828** (2010) 317-374.
5. J. M. Drummond, J. M. Henn, J. Plefka, JHEP **0905** (2009) 046.
6. J. M. Drummond, J. Henn, G. P. Korchemsky *et al.*, Phys. Lett. **B662** (2008) 456-460.
7. Z. Bern, L. J. Dixon, D. A. Kosower *et al.*, Phys. Rev. **D78** (2008) 045007.
8. J. M. Henn, J. Plefka, K. Wiegandt, JHEP **1008** (2010) 032.
9. S. Caron-Huot, [arXiv:1010.1167 [hep-th]]. L. J. Mason, D. Skinner, JHEP **1012** (2010) 018.
10. L. F. Alday, R. Roiban, Phys. Rept. **468** (2008) 153-211. J. M. Henn, Fortsch. Phys. **57** (2009) 729-822.
11. J. A. Minahan, K. Zarembo, JHEP **0303** (2003) 013.N. Beisert, M. Staudacher, Nucl. Phys. **B670** (2003) 439-463. N. Beisert, C. Kristjansen, M. Staudacher, Nucl. Phys. **B664** (2003) 131-184. I. Bena, J. Polchinski, R. Roiban, Phys. Rev. **D69** (2004) 046002.
12. N. Berkovits, J. Maldacena, JHEP **0809** (2008) 062. N. Beisert, R. Ricci, A. A. Tseytlin *et al.*, Phys. Rev. **D78** (2008) 126004.
13. A. A. Tseytlin, Comptes Rendus Physique **5** (2004) 1049-1059. A. V. Belitsky, V. M. Braun, A. S. Gorsky *et al.*, Int. J. Mod. Phys. **A19** (2004) 4715-4788. N. Beisert, Phys. Rept. **405** (2005) 1-202. N. Beisert, Comptes Rendus Physique **5** (2004) 1039-1048. K. Zarembo, Comptes Rendus Physique **5** (2004) 1081-1090. J. Plefka, Living Rev. Rel. **8** (2005) 9. J. A. Minahan, J. Phys. A **A39** (2006) 12657-12677.
14. G. Arutyunov, S. Frolov, J. Phys. A **A42** (2009) 254003.
15. J. A. Minahan, K. Zarembo, JHEP **0809** (2008) 040. N. Gromov, P. Vieira, JHEP **0901** (2009) 016.
16. P. A. Grassi, D. Sorokin, L. Wulff, JHEP **0908** (2009) 060. I. Adam, A. Dekel, Y. Oz, JHEP **0904** (2009) 120. I. Adam, A. Dekel, Y. Oz, JHEP **1010** (2010) 110.
17. T. Bargheer, F. Loebbert, C. Meneghelli, Phys. Rev. **D82** (2010) 045016. S. Lee, Phys. Rev. Lett. **105** (2010) 151603. Y. -t. Huang, A. E. Lipstein, JHEP **1011** (2010) 076. D. Gang, Y. -t. Huang, E. Koh *et al.*, arXiv:1012.5032
18. A. Agarwal, N. Beisert, T. McLoughlin, JHEP **0906** (2009) 045.

Form factors in theories with gravity duals

Alexander V. Zhiboedov[a]

[a]Department of Physics, Princeton University
Princeton, New Jersey 08544, USA

The prescription for calculating form factors at strong coupling in the theories with gravity duals was found in [1]. The use of integrability for similar objects culminated in the paper [2] where the Y-system for scattering amplitudes was found. In the paper [3] authors extended this scenario to the case of form factors in AdS_3 kinematics. Some exact solutions were present. Here we briefly review the results of [3] and later developments of the problem.

1. Form factors at strong coupling

At strong coupling form factors are given by Euclidean classical solutions of string equations of motion in AdS_5. At the boundary the solution reaches a periodic sequence of light-like lines k_i^μ. The period of the sequence is fixed by the momentum of the operator while light-like segments correspond to the momenta of particles

$$\langle k_i^{in}|\mathcal{O}(q)|k_j^{out}\rangle = e^{-\frac{\sqrt{\lambda}}{2\pi}(\text{Area})_T}\text{F}_1(1+\frac{1}{\sqrt{\lambda}}\text{F}_2)$$

where the leading term $(\text{Area})_T$ is the area of one period and it was computed in [3]. F_1 is the one loop correction and would contain information about the polarizations and the particular operator we are considering. F_2 is the two loop correction in the $1/\sqrt{\lambda}$ expansion.

2. Y-system

At strong coupling the algorithm of solving the problem was through the use of the integrability of classical strings on AdS space background. The key steps were: first, introducing the family of flat connections with an arbitrary spectral parameter $\mathcal{A}(\zeta = e^\theta)$. With this flat connection one can consider the flat section problem which allows one to introduce a set of of spectral parameter dependent cross-ratios $Y_k(\theta)$. Then one finds the set of functional equations which constraints the θ dependence of Y-functions. The system is specified with boundary conditions at $\theta \to \pm\infty$ which are obtained through WKB analysis of the flat section problem. Then one can restate these equations in integral form which happened to be of TBA form. The non-trivial part of the area then was given by the free energy of the system which depends on the set of mass parameters in which the kinematics is encoded. However it is much more convenient to have the expressions that depend only on kinematic information namely cross-ratios. It happened that after eliminating the dependence of area on mass parameters the area is given by the critical value of Yang-Yang functional.

The fact that we are dealing with periodic solutions – with the period being encoded in the monodromy Ω – can be used to truncate Y-system. For the case of AdS_3 and $2n$-gluon form factor it takes the form

$$\begin{aligned} Y_s^+ Y_s^- &= (1+Y_{s+1})(1+Y_{s-1}), \\ Y_{n-2}^+ Y_{n-2}^- &= (1+Y_{n-3})(1+\text{Tr}[\Omega]\bar{Y}+\bar{Y}^2), \\ \bar{Y}^+\bar{Y}^- &= 1+Y_{n-2}. \end{aligned}$$

This Y-system can also be used to study scattering amplitudes in periodic kinematics regime.

3. Exact solutions

In several simple cases one can solve the Y-system written above exactly. First case corresponds to the high temperature limit when all Y's

do not depend on the spectral parameter. It corresponds to the regular form factor or zig-zag solution. The Y-functions and the non-trivial part of the area in this case are

$$\begin{aligned} Y_s &= s(s+2) \\ \bar{Y} &= n-1 \\ A^{free} &= \frac{\pi}{6}(n-1). \end{aligned}$$

Another solution corresponds to 4-gluon form factor. In this case the only non-trivial Y-function takes the form $\bar{Y} = e^{Z/\zeta+\bar{Z}\zeta}$ and the non-trivial part of the area is given by the integral $\phi \in (0, \frac{\pi}{2})$

$$I = \int_{-\infty}^{\infty} dt \frac{|m|\sinh t}{2\pi \tanh(2t+2i\phi)} \log(1+e^{-2|m|\cosh t}).$$

Here $|m|$ and ϕ are related to the cross-ratio in the problem in the known way.

4. Truncation in terms of momentum twistors. AdS_5 case.

Since the truncation of the Y-system in the case of form factors is purely kinematical it is convenient to think about it in terms of target space. The boundary of AdS can be thought as submanifold $Y^2 = 0$ in the projective space. Then the i'th cusp location for the case of AdS_3 takes the form

$$Y^i_{a\dot{a}}(\zeta) = \lambda^i_a(\zeta)\tilde{\lambda}^i_{\dot{a}}(\zeta).$$

The periodicity of the contour manifests itself through the fact that $\lambda_{i+n} \propto \Omega\lambda_i$. The truncation condition used in [3] is just the identity

$$\mathrm{Tr}[\Omega]\langle\lambda^0,\lambda^1\rangle = \langle\lambda^0,\Omega\lambda^1\rangle - \langle\Omega\lambda^0,\lambda^1\rangle$$

notice that it is manifestly conformal and gauge invariant.

Written in this form it can be easily generalized to the case of AdS_5. In this case the position of the cusps are given in terms of momentum twistors

$$Y^i_{ab}(\zeta) = \lambda^i_a(\zeta)\lambda^{i-1}_b(\zeta) - \lambda^i_b(\zeta)\lambda^{i-1}_a(\zeta).$$

The periodicity is the fact that $\lambda_{i+n} \propto \Omega_s\lambda_i$. The truncation conditions take the form of manifestly conformal and gauge invariant identities

$$\mathrm{Tr}[\Omega_s]\langle\lambda_{-2},\lambda_{-1},\lambda_0,\lambda_1\rangle = \sum_{k=1}^{4}\langle\lambda_{-2},\lambda_{-1},\lambda_0,\lambda_1\rangle^{\Omega}_k \quad (1)$$

$$\begin{aligned} \mathrm{Tr}[\Omega_v]\langle\lambda_{-2},\lambda_{-1},\lambda_0,\lambda_1\rangle &= \sum_{k,j=1;k\neq j}^{4}\langle\lambda_{-2},\lambda_{-1},\lambda_0,\lambda_1\rangle^{\Omega}_{k,j} \\ \mathrm{Tr}[\Omega_v] &= \frac{1}{2}(\mathrm{Tr}[\Omega_s]^2 - \mathrm{Tr}[\Omega_s^2]) \end{aligned}$$

where, for example, $\langle\lambda_{-2},\lambda_{-1},\lambda_0,\lambda_1\rangle^{\Omega}_{1,2} = \langle\Omega_s\lambda_{-2},\Omega_s\lambda_{-1},\lambda_0,\lambda_1\rangle$ etc. The third truncation condition is the same as (1) with the change $\lambda \to \bar{\lambda}$, $\Omega_s \to \bar{\Omega}_s$. See [2] for the notations.

One can use these identities to truncate Hirota equations [2] for AdS_5. It would be nice to rewrite them in terms of Y-system as it was done for AdS_3 in [3].

5. Weak coupling analysis

From the weak coupling side form factors were studied in [4–6]. In [5] the simplicity and similarity with scattering amplitudes of the tree-level form factors of half-BPS operators was revealed. They happen to share many attractive features with the amplitudes, namely BCFW recursion relations and apparently duality with Wilson lines.

Acknowledgements

I am very grateful to Juan Maldacena for many illuminating and inspiring discussions.

REFERENCES

1. L. F. Alday, J. Maldacena, JHEP **0711**, 068 (2007). [arXiv:0710.1060 [hep-th]].
2. L. F. Alday, J. Maldacena, A. Sever, P. Vieira, J. Phys. A **A43**, 485401 (2010). [arXiv:1002.2459 [hep-th]].
3. J. Maldacena, A. Zhiboedov, JHEP **1011**, 104 (2010). [arXiv:1009.1139 [hep-th]].
4. W. L. van Neerven, Z. Phys. C **30**, 595 (1986).
5. A. Brandhuber, B. Spence, G. Travaglini *et al.*, JHEP **1101**, 134 (2011). [arXiv:1011.1899 [hep-th]].
6. L. V. Bork, D. I. Kazakov, G. S. Vartanov, [arXiv:1011.2440 [hep-th]].

List of Participants

Name	First Name	Institute
Anguelova	Lilia	University Of Cincinnati
Anous	Tarek	Harvard University
Arkani-Hamed	Nima	Ias
Bagrov	Andrey	Steklov Math. Inst.
Banerjee	Nabamita	Itf, Utrecht
Banerjee	Shamik	Harish-Chandra Institute
Barnard	James	Durham University
Benvenuti	Sergio	Imperial College
Bernamonti	Alice	Vu Brussel
Bjerrum-Bohr	Niels Emil Jannik	Niels Bohr Intl Acad, Nbi
Borsten	Leron	Imperial College, London
Bourjaily	Jacob	Princeton University
Bredberg	Irene	Harvard University
Bern	Zvi	Ucla
Cassani	Davide	University Of Padova
Closset	Cyril	U.L.B. (Bruxelles)
Compere	Geoffrey	Uc Santa Barbara
Dehouck	Francois	U.L.B. Brussels
Dumitrescu	Thomas	Princeton University
Dutta	Suvankar	Swansea University
El-Showk	Sheer	Cea Saclay
Franche	Paul	Mcgill University
Gaillard	Jerome	Swansea University
Giataganas	Dimitrios	Wits University
Green	Michael B.	Damtp
Guica	Monica	Lpthe
Green	Michael B.	Damtp
Hadar	Shahar	Hebrew University
Haertl	Daniel	Mpi For Physics, Munich
Halmagyi	Nick	Cea Saclay
Hatefi	Ehsan	Cern
Held	Johannes	Mpi For Physics
Intriligator	Kenneth	Ucsd
Johansson	Henrik	Ipht Saclay
Kallen	Johan	Uppsala University
Karouby	Johanna	Mcgill University
Katmadas	Stefanos	Itf Utrecht
Keeler	Cynthia	Harvard University
Khodaee	Sadi	Cbpf
Kiefer	Flavien	Iap
Kol	Uri	Tel Aviv University
Koroteev	Peter	University Of Minnesota

Name	First Name	Institute
Komargodski	Zohar	Ias
Lee	Sangmin	University Of Seoul
Lipstein	Arthur	Caltech
Lysov	Vyacheslav	Harvard
Maio	Michele	Nikhef
Mandal	Ipsita	Hri And Lpthe
Mcgady	David	Princeton University
Mekareeya	Noppadol	Imperial College London
Milanesi	Giuseppe	Itp Bern
Nekrasov	Nikita	IhÉs
Orsi	Francesco	Ipht/Cea Saclay
Pan	Guang	Rutgers University
Peng	Zongren	Ipht
Pioline	Boris	Lpthe
Peschanski	Robi	Ipht Saclay
Rodigast	Andreas	Humboldt-Universitaet
Schaeffer	Kevin	U Of California, Berkeley
Schlotterer	Oliver	Mpi Munich
Schuster	Frank Theodor	Humboldt-Universitaet
Sjors	Stefan	Stockholm University
Sondergaard	Thomas	The Niels Bohr Institute
Stolarski	Daniel	Uc Berkeley
Sen	Ashoke	Harish-Chandra Res. Inst. & Lpthe
Sirvois	Yves	Laboratoire Leprince-Ringuet
Son	Dam	Univ. Washington
Strominger	Andrew	Harvard
Tetsuo	Horigane	University Of Tokyo
Torri	Giuseppe	Imperial College London
Trnka	Jaroslav	Princeton University
Vanmeter	Nickolas	Harvard University
Wiegandt	Konstantin	Humboldt Univ. Berlin
Zayakin	Andrey	Lmu
Zhiboedov	Alexander	Princeton University
Zagier	Don	Bonn & Collége De France